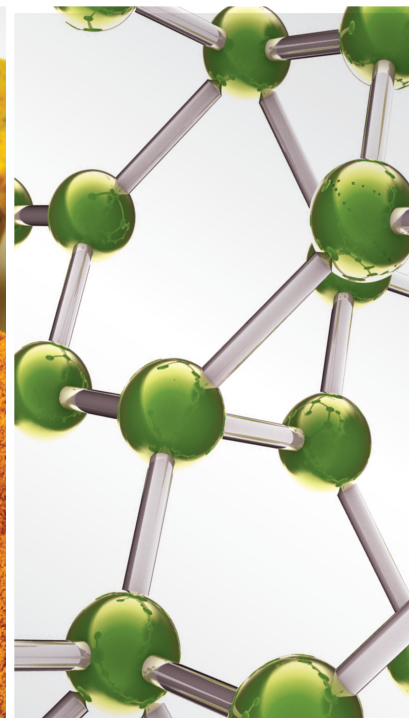
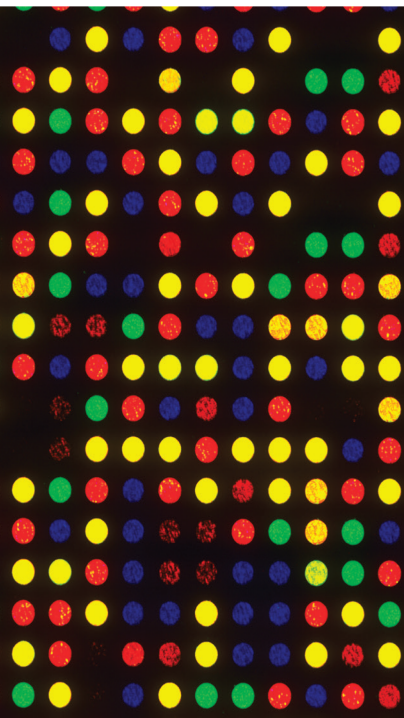


Therapies of Traditional Chinese Medicine for Cardiovascular Diseases

Lead Guest Editor: Hong Chang

Guest Editors: Yong Wang, Mingjun Zhu, Guanwei Fan, Sai-Wang Seto, and Xiao Ma





Therapies of Traditional Chinese Medicine for Cardiovascular Diseases

Evidence-Based Complementary and Alternative Medicine

Therapies of Traditional Chinese Medicine for Cardiovascular Diseases

Lead Guest Editor: Hong Chang

Guest Editors: Yong Wang, Mingjun Zhu, Guanwei
Fan, Sai-Wang Seto, and Xiao Ma



Copyright © 2021 Hindawi Limited. All rights reserved.

This is a special issue published in "Evidence-Based Complementary and Alternative Medicine." All articles are open access articles distributed under the Creative Commons Attribution License, which permits unrestricted use, distribution, and reproduction in any medium, provided the original work is properly cited.

Chief Editor

Jian-Li Gao , China






Associate Editors

Hyunsu Bae , Republic of Korea
Raffaele Capasso , Italy
Jae Youl Cho , Republic of Korea
Caigan Du , Canada
Yuewen Gong , Canada
Hai-dong Guo , China
Kuzhuvelil B. Harikumar , India
Ching-Liang Hsieh , Taiwan
Cheorl-Ho Kim , Republic of Korea
Victor Kuete , Cameroon
Hajime Nakae , Japan
Yoshiji Ohta , Japan
Olumayokun A. Olajide , United Kingdom
Chang G. Son , Republic of Korea
Shan-Yu Su , Taiwan
Michał Tomczyk , Poland
Jenny M. Wilkinson , Australia

Academic Editors

Eman A. Mahmoud , Egypt
Ammar AL-Farga , Saudi Arabia
Smail Aazza , Morocco
Nahla S. Abdel-Azim, Egypt
Ana Lúcia Abreu-Silva , Brazil
Gustavo J. Acevedo-Hernández , Mexico
Mohd Adnan , Saudi Arabia
Jose C Adsuar , Spain
Sayeed Ahmad, India
Touqeer Ahmed , Pakistan
Basiru Ajiboye , Nigeria
Bushra Akhtar , Pakistan
Fahmida Alam , Malaysia
Mohammad Jahoor Alam, Saudi Arabia
Clara Albani, Argentina
Ulysses Paulino Albuquerque , Brazil
Mohammed S. Ali-Shtayeh , Palestinian Authority
Ekram Alias, Malaysia
Terje Alraek , Norway
Adolfo Andrade-Cetto , Mexico
Letizia Angiolella , Italy
Makoto Arai , Japan

Daniel Dias Rufino Arcanjo , Brazil
Duygu AĞAGÜNDÜZ , Turkey
Neda Baghban , Iran
Samra Bashir , Pakistan
Rusliza Basir , Malaysia
Jairo Kenupp Bastos , Brazil
Arpita Basu , USA
Mateus R. Beguelini , Brazil
Juana Benedí, Spain
Samira Boulbaroud, Morocco
Mohammed Bourhia , Morocco
Abdelhakim Bouyahya, Morocco
Nunzio Antonio Cacciola , Italy
Francesco Cardini , Italy
María C. Carpinella , Argentina
Harish Chandra , India
Guang Chen, China
Jianping Chen , China
Kevin Chen, USA
Mei-Chih Chen, Taiwan
Xiaojia Chen , Macau
Evan P. Cherniack , USA
Giuseppina Chianese , Italy
Kok-Yong Chin , Malaysia
Lin China, China
Salvatore Chirumbolo , Italy
Hwi-Young Cho , Republic of Korea
Jeong June Choi , Republic of Korea
Jun-Yong Choi, Republic of Korea
Kathrine Bisgaard Christensen , Denmark
Shuang-En Chuang, Taiwan
Ying-Chien Chung , Taiwan
Francisco José Cidral-Filho, Brazil
Daniel Collado-Mateo , Spain
Lisa A. Conboy , USA
Kieran Cooley , Canada
Edwin L. Cooper , USA
José Otávio do Amaral Corrêa , Brazil
Maria T. Cruz , Portugal
Huantian Cui , China
Giuseppe D'Antona , Italy
Ademar A. Da Silva Filho , Brazil
Chongshan Dai, China
Laura De Martino , Italy
Josué De Moraes , Brazil

Arthur De Sá Ferreira , Brazil
Nunziatina De Tommasi , Italy
Marinella De leo , Italy
Gourav Dey , India
Dinesh Dhamecha, USA
Claudia Di Giacomo , Italy
Antonella Di Sotto , Italy
Mario Dioguardi, Italy
Jeng-Ren Duann , USA
Thomas Efferth , Germany
Abir El-Alfy, USA
Mohamed Ahmed El-Esawi , Egypt
Mohd Ramli Elvy Suhana, Malaysia
Talha Bin Emran, Japan
Roger Engel , Australia
Karim Ennouri , Tunisia
Giuseppe Esposito , Italy
Tahereh Eteraf-Oskouei, Iran
Robson Xavier Faria , Brazil
Mohammad Fattahi , Iran
Keturah R. Faurot , USA
Piergiorgio Fedeli , Italy
Laura Ferraro , Italy
Antonella Fioravanti , Italy
Carmen Formisano , Italy
Hua-Lin Fu , China
Liz G Müller , Brazil
Gabino Garrido , Chile
Safoora Gharibzadeh, Iran
Muhammad N. Ghayur , USA
Angelica Gomes , Brazil
Elena González-Burgos, Spain
Susana Gorzalczany , Argentina
Jiangyong Gu , China
Maruti Ram Gudavalli , USA
Jian-You Guo , China
Shanshan Guo, China
Narcís Gusi , Spain
Svein Haavik, Norway
Fernando Hallwass, Brazil
Gajin Han , Republic of Korea
Ihsan Ul Haq, Pakistan
Hicham Harhar , Morocco
Mohammad Hashem Hashempur , Iran
Muhammad Ali Hashmi , Pakistan

Waseem Hassan , Pakistan
Sandrina A. Heleno , Portugal
Pablo Herrero , Spain
Soon S. Hong , Republic of Korea
Md. Akil Hossain , Republic of Korea
Muhammad Jahangir Hossen , Bangladesh
Shih-Min Hsia , Taiwan
Changmin Hu , China
Tao Hu , China
Weicheng Hu , China
Wen-Long Hu, Taiwan
Xiao-Yang (Mio) Hu, United Kingdom
Sheng-Teng Huang , Taiwan
Ciara Hughes , Ireland
Attila Hunyadi , Hungary
Liaquat Hussain , Pakistan
Maria-Carmen Iglesias-Osma , Spain
Amjad Iqbal , Pakistan
Chie Ishikawa , Japan
Angelo A. Izzo, Italy
Satveer Jagwani , USA
Rana Jamous , Palestinian Authority
Muhammad Saeed Jan , Pakistan
G. K. Jayaprakasha, USA
Kyu Shik Jeong, Republic of Korea
Leopold Jirovetz , Austria
Jeeyoun Jung , Republic of Korea
Nurkhalida Kamal , Saint Vincent and the
Grenadines
Atsushi Kameyama , Japan
Kyungsu Kang, Republic of Korea
Wenyi Kang , China
Shao-Hsuan Kao , Taiwan
Nasiara Karim , Pakistan
Morimasa Kato , Japan
Kumar Katragunta , USA
Deborah A. Kennedy , Canada
Washim Khan, USA
Bonglee Kim , Republic of Korea
Dong Hyun Kim , Republic of Korea
Junghyun Kim , Republic of Korea
Kyungho Kim, Republic of Korea
Yun Jin Kim , Malaysia
Yoshiyuki Kimura , Japan

Nebojša Kladar , Serbia
Mi Mi Ko , Republic of Korea
Toshiaki Kogure , Japan
Malcolm Koo , Taiwan
Yu-Hsiang Kuan , Taiwan
Robert Kubina , Poland
Chan-Yen Kuo , Taiwan
Kuang C. Lai , Taiwan
King Hei Stanley Lam, Hong Kong
Fanuel Lampiao, Malawi
Ilaria Lampronti , Italy
Mario Ledda , Italy
Harry Lee , China
Jeong-Sang Lee , Republic of Korea
Ju Ah Lee , Republic of Korea
Kyu Pil Lee , Republic of Korea
Namhun Lee , Republic of Korea
Sang Yeoup Lee , Republic of Korea
Ankita Leekha , USA
Christian Lehmann , Canada
George B. Lenon , Australia
Marco Leonti, Italy
Hua Li , China
Min Li , China
Xing Li , China
Xuqi Li , China
Yi-Rong Li , Taiwan
Vuanghao Lim , Malaysia
Bi-Fong Lin, Taiwan
Ho Lin , Taiwan
Shuibin Lin, China
Kuo-Tong Liou , Taiwan
I-Min Liu, Taiwan
Suhuan Liu , China
Xiaosong Liu , Australia
Yujun Liu , China
Emilio Lizarraga , Argentina
Monica Loizzo , Italy
Nguyen Phuoc Long, Republic of Korea
Zaira López, Mexico
Chunhua Lu , China
Ângelo Luís , Portugal
Anderson Luiz-Ferreira , Brazil
Ivan Luzardo Luzardo-Ocampo, Mexico

Michel Mansur Machado , Brazil
Filippo Maggi , Italy
Juraj Majtan , Slovakia
Toshiaki Makino , Japan
Nicola Malafrente, Italy
Giuseppe Malfa , Italy
Francesca Mancianti , Italy
Carmen Mannucci , Italy
Juan M. Manzanque , Spain
Fatima Martel , Portugal
Carlos H. G. Martins , Brazil
Maulidiani Maulidiani, Malaysia
Andrea Maxia , Italy
Avijit Mazumder , India
Isac Medeiros , Brazil
Ahmed Mediani , Malaysia
Lewis Mehl-Madrona, USA
Ayikoé Guy Mensah-Nyagan , France
Oliver Micke , Germany
Maria G. Miguel , Portugal
Luigi Milella , Italy
Roberto Miniero , Italy
Letteria Minutoli, Italy
Prashant Modi , India
Daniel Kam-Wah Mok, Hong Kong
Changjong Moon , Republic of Korea
Albert Moraska, USA
Mark Moss , United Kingdom
Yoshiharu Motoo , Japan
Yoshiki Mukudai , Japan
Sakthivel Muniyan , USA
Saima Muzammil , Pakistan
Benoit Banga N'guessan , Ghana
Massimo Nabissi , Italy
Siddavaram Nagini, India
Takao Namiki , Japan
Srinivas Nammi , Australia
Krishnadas Nandakumar , India
Vitaly Napadow , USA
Edoardo Napoli , Italy
Jorddy Neves Cruz , Brazil
Marcello Nicoletti , Italy
Eliud Nyaga Mwaniki Njagi , Kenya
Cristina Nogueira , Brazil



Sakineh Kazemi Noureini , Iran
Rômulo Dias Novaes, Brazil
Martin Offenbaecher , Germany
Oluwafemi Adeleke Ojo , Nigeria
Olufunmiso Olusola Olajuyigbe , Nigeria
Luís Flávio Oliveira, Brazil
Mozaniel Oliveira , Brazil
Atolani Olubunmi , Nigeria
Abimbola Peter Oluyori , Nigeria
Timothy Omara, Austria
Chiagoziem Anariochi Otuechere , Nigeria
Sokcheon Pak , Australia
Antônio Palumbo Jr, Brazil
Zongfu Pan , China
Siyaram Pandey , Canada
Niranjan Parajuli , Nepal
Gunhyuk Park , Republic of Korea
Wansu Park , Republic of Korea
Rodolfo Parreira , Brazil
Mohammad Mahdi Parvizi , Iran
Luiz Felipe Passero , Brazil
Mitesh Patel, India
Claudia Helena Pellizzon , Brazil
Cheng Peng, Australia
Weijun Peng , China
Sonia Piacente, Italy
Andrea Pieroni , Italy
Haifa Qiao , USA
Cláudia Quintino Rocha , Brazil
DANIELA RUSSO , Italy
Muralidharan Arumugam Ramachandran,
Singapore
Manzoor Rather , India
Miguel Rebollo-Hernanz , Spain
Gauhar Rehman, Pakistan
Daniela Rigano , Italy
José L. Rios, Spain
Francisca Rius Diaz, Spain
Eliana Rodrigues , Brazil
Maan Bahadur Rokaya , Czech Republic
Mariangela Rondanelli , Italy
Antonietta Rossi , Italy
Mi Heon Ryu , Republic of Korea
Bashar Saad , Palestinian Authority
Sabi Saheed, South Africa
Mohamed Z.M. Salem , Egypt
Avni Sali, Australia
Andreas Sandner-Kiesling, Austria
Manel Santafe , Spain
José Roberto Santin , Brazil
Tadaaki Satou , Japan
Roland Schoop, Switzerland
Sindy Seara-Paz, Spain
Veronique Seidel , United Kingdom
Vijayakumar Sekar , China
Terry Selfe , USA
Arham Shabbir , Pakistan
Suzana Shahar, Malaysia
Wen-Bin Shang , China
Xiaofei Shang , China
Ali Sharif , Pakistan
Karen J. Sherman , USA
San-Jun Shi , China
Insop Shim , Republic of Korea
Maria Im Hee Shin, China
Yukihiro Shoyama, Japan
Morry Silberstein , Australia
Samuel Martins Silvestre , Portugal
Preet Amol Singh, India
Rajeev K Singla , China
Kuttulebbai N. S. Sirajudeen , Malaysia
Slim Smaoui , Tunisia
Eun Jung Sohn , Republic of Korea
Maxim A. Solovchuk , Taiwan
Young-Jin Son , Republic of Korea
Chengwu Song , China
Vanessa Steenkamp , South Africa
Annarita Stringaro , Italy
Keiichiro Sugimoto , Japan
Valeria Sulsen , Argentina
Zewei Sun , China
Sharifah S. Syed Alwi , United Kingdom
Orazio Tagliatalata-Scafati , Italy
Takashi Takeda , Japan
Gianluca Tamagno , Ireland
Hongxun Tao, China
Jun-Yan Tao , China
Lay Kek Teh , Malaysia
Norman Temple , Canada

Kamani H. Tennekoon , Sri Lanka
Seong Lin Teoh, Malaysia
Menaka Thounaojam , USA
Jinhui Tian, China
Zipora Tietel, Israel
Loren Toussaint , USA
Riaz Ullah , Saudi Arabia
Philip F. Uzor , Nigeria
Luca Vanella , Italy
Antonio Vassallo , Italy
Cristian Vergallo, Italy
Miguel Vilas-Boas , Portugal
Aristo Vojdani , USA
Yun WANG , China
QIBIAO WU , Macau
Abraham Wall-Medrano , Mexico
Chong-Zhi Wang , USA
Guang-Jun Wang , China
Jinan Wang , China
Qi-Rui Wang , China
Ru-Feng Wang , China
Shu-Ming Wang , USA
Ting-Yu Wang , China
Xue-Rui Wang , China
Youhua Wang , China
Kenji Watanabe , Japan
Jintanaporn Wattanathorn , Thailand
Silvia Wein , Germany
Katarzyna Winska , Poland
Sok Kuan Wong , Malaysia
Christopher Worsnop, Australia
Jih-Huah Wu , Taiwan
Sijin Wu , China
Xian Wu, USA
Zuoqi Xiao , China
Rafael M. Ximenes , Brazil
Guoqiang Xing , USA
JiaTuo Xu , China
Mei Xue , China
Yong-Bo Xue , China
Haruki Yamada , Japan
Nobuo Yamaguchi, Japan
Junqing Yang, China
Longfei Yang , China







Mingxiao Yang , Hong Kong
Qin Yang , China
Wei-Hsiung Yang, USA
Swee Keong Yeap , Malaysia
Albert S. Yeung , USA
Ebrahim M. Yimer , Ethiopia
Yoke Keong Yong , Malaysia
Fadia S. Youssef , Egypt
Zhilong Yu, Canada
RONGJIE ZHAO , China
Sultan Zahiruddin , USA
Armando Zarrelli , Italy
Xiaobin Zeng , China
Y Zeng , China
Fangbo Zhang , China
Jianliang Zhang , China
Jiu-Liang Zhang , China
Mingbo Zhang , China
Jing Zhao , China
Zhangfeng Zhong , Macau
Guoqi Zhu , China
Yan Zhu , USA
Suzanna M. Zick , USA
Stephane Zingue , Cameroon

Contents

Research on Effect and Mechanism of Xuefu Zhuyu Decoction on CHD Based on Meta-Analysis and Network Pharmacology

Fuguang Kui, Wenwen Gu, Fan Gao, Yuji Niu, Wenwen Li, Yaru Zhang, Lijuan Guo, Junru Wang, Zhenzhen Guo, Shihong Cen , and Gangjun Du 
Research Article (15 pages), Article ID 9473531, Volume 2021 (2021)




The Clinical Efficacy of Phytochemical Medicines Containing Tanshinol and Ligustrazine in the Treatment of Stable Angina: A Systematic Review and Meta-Analysis

Li Gao , Tong Wu , Juan Wang , Zhuoran Xiao , Chunhua Jia , and Wei Wang 
Research Article (10 pages), Article ID 8616413, Volume 2021 (2021)




***Gastrodia elata* Blume (Tianma): Hope for Brain Aging and Dementia**

Klaus Heese 
Review Article (7 pages), Article ID 8870148, Volume 2020 (2020)



Suppressive Effects of the *Gynura bicolor* Ether Extract on Endothelial Permeability and Leukocyte Transmigration in Human Endothelial Cells Induced by TNF- α

Shu-Ling Hsieh , Jyh-Jye Wang, Kuan-Hua Su, Ying-Lan Kuo, Shuchen Hsieh , and Chih-Chung Wu 
Research Article (13 pages), Article ID 9413724, Volume 2020 (2020)



Traditional Chinese Medicine for Essential Hypertension: A Clinical Evidence Map

Yan Zhang , Biqing Wang, Chunxiao Ju, Lu Liu, Ying Zhu, Jun Mei, Yue Liu , and Fengqin Xu 
Research Article (17 pages), Article ID 5471931, Volume 2020 (2020)


Literature-Based Drug Repurposing in Traditional Chinese Medicine: Reduced Inflammatory M1 Macrophage Polarization by Jisil Haebaek Gyeji-Tang Alleviates Cardiovascular Disease In Vitro and Ex Vivo

Ga-Ram Yu, Seung-Jun Lee, Da-Hoon Kim, Dong-Woo Lim, Hyuck Kim, Won-Hwan Park , and Jai-Eun Kim 
Research Article (12 pages), Article ID 8881683, Volume 2020 (2020)



Xinmailong Injection for Improvement of Cardiac Function in Patients with Heart Failure: A Systematic Review and Meta-Analysis

Yuan-long Sun, Yi-ping Li, Ting-ting Qiang, Xiao-fen Ruan , and Xiao-long Wang 
Review Article (13 pages), Article ID 6131525, Volume 2020 (2020)

Mechanisms Underlying the Cardioprotection of YangXinDingJi Capsule against Myocardial Ischemia in Rats

Miaomiao Liu, Yurun Xue, Yingran Liang, Yucong Xue, Xue Han, Ziliang Li, and Li Chu 
Research Article (16 pages), Article ID 8539148, Volume 2020 (2020)

The Efficacy and Safety of Compound Danshen Dripping Pill Combined with Percutaneous Coronary Intervention for Coronary Heart Disease





Cailan Li, Qian Li, Jiamin Xu, Wenzhen Wu, Yuling Wu, Jianhui Xie , and Xiaobo Yang 
Research Article (15 pages), Article ID 5067137, Volume 2020 (2020)

Electroacupuncture Inhibits Atherosclerosis through Regulating Intestinal Flora and Host Metabolites in Rabbit

Yuping Shen , Ze-Dong Cheng , Yi-Guo Chen , Rui sun , Xian-De Ma , Guo-liang Hou , and Rui Wang 



Research Article (10 pages), Article ID 5790275, Volume 2020 (2020)

The Protective Effect of Qishen Granule on Heart Failure after Myocardial Infarction through Regulation of Calcium Homeostasis

Xiaomin Yang , Qiyan Wang, Zifan Zeng, Qian Zhang, Fang Liu, Hong Chang, Chun Li , Wei Wang , and Yong Wang 


Research Article (11 pages), Article ID 1868974, Volume 2020 (2020)

Cardiac CaMKII δ and Wenxin Keli Prevents Ang II-Induced Cardiomyocyte Hypertrophy by Modulating CnA-NFATc4 and Inflammatory Signaling Pathways in H9c2 Cells

Na An, Yu Chen, Yanfen Xing, Honghua Wu, Xiongyi Gao, Hengwen Chen, Ke Song, Yuanyuan Li, Xinye Li, Fan Yang, Xiandu Pan, Xiaofang He, Xin Wang, Yang Li, Yonghong Gao , and Yanwei Xing 


Research Article (17 pages), Article ID 9502651, Volume 2020 (2020)

Correlation between Mitochondrial Dysfunction, Cardiovascular Diseases, and Traditional Chinese Medicine

Li Zhu, Zhigang Chen, Keli Han, Yilin Zhao, Yan Li, Dongxu Li, Xiulong Wang, Xuefang Li, Siyu Sun, Fei Lin, and Guoan Zhao 

Research Article (11 pages), Article ID 2902136, Volume 2020 (2020)

Mast Cell Degranulation and Adenosine Release: Acupoint Specificity for Effect of Electroacupuncture on Pituitrin-Induced Acute Heart Bradycardia in Rabbits

Xuezhi Wang, Meng Huang, Hongwei Yang, Di Zhang, Wei Yao, Ying Xia, and Guanghong Ding 

Research Article (15 pages), Article ID 1348914, Volume 2020 (2020)

Molecular Targets and Pathways Contributing to the Effects of Wenxin Keli on Atrial Fibrillation Based on a Network Pharmacology Approach

Yujie Zhang, Xiaolin Zhang, Xi Zhang, Yi Cai, Minghui Cheng, Chenghui Yan, and Yaling Han 

Research Article (11 pages), Article ID 8396484, Volume 2020 (2020)

Endothelium-Independent Vasodilatory Effect of Sailuotong (SLT) on Rat Isolated Tail Artery

S. Y. Yeon , S. W. Seto , G. H. H. Chan, M. Low , H. Kiat , N. Wang, J. Liu, and D. Chang 

Research Article (10 pages), Article ID 8125805, Volume 2020 (2020)


Guanxinshutong Alleviates Atherosclerosis by Suppressing Oxidative Stress and Proinflammation in ApoE^{-/-} Mice

Yingdong Lu , Yuchan Sun, Zhilin Jiang, Dandan Zhang, Hongchen Lin, Yi Qu , Chang Shang, Mingjing Zhao , and Xiangning Cui 



Research Article (13 pages), Article ID 1219371, Volume 2020 (2020)

Contents

Distribution Analysis of Salvianolic Acids in Myocardial Ischemic Pig Tissues by Automated Liquid Extraction Surface Analysis Coupled with Tandem Mass Spectrometry

Qi Qiu , Jinglin Cao, Yu Mu, Yang Lin, Yunnan Zhang, Jing Li, and Xiujin Shi
Research Article (9 pages), Article ID 8476794, Volume 2020 (2020)



Herbal Medicine (Sihogayonggolmoryeo-Tang or Chai-Hu-Jia-Long-Gu-Mu-Li-Tang) for Treating Hypertension: A Systematic Review and Meta-Analysis

Boram Lee  and Chan-Young Kwon 
Research Article (13 pages), Article ID 9101864, Volume 2020 (2020)



Yiqi Fumai Injection as an Adjuvant Therapy in Treating Chronic Heart Failure: A Meta-Analysis of 33 Randomized Controlled Trials

Heyun Nie, Shuqing Li, Meilu Liu, Weifeng Zhu , Xu Zhou , and Dongmei Yan 
Review Article (12 pages), Article ID 1876080, Volume 2020 (2020)



Five-Animal Frolics Exercise Improves Anxiety and Depression Outcomes in Patients with Coronary Heart Disease: A Single-Blind Randomized Controlled Trial

Jun Jiang, Qingbao Chi, Yuting Wang, Xue Jin , and Shui Yu 
Research Article (9 pages), Article ID 6937158, Volume 2020 (2020)

Qiju Dihuang Decoction for Hypertension: A Systematic Review and Meta-Analysis

Shuo Zhang, Xue Bai, Zhen-Lin Chen, Jia-Jia Li, Yan-Yan Chen , and Yu-Ping Tang 
Review Article (16 pages), Article ID 9403092, Volume 2020 (2020)

Network Pharmacology-Based Strategy to Investigate the Pharmacological Mechanisms of *Ginkgo biloba* Extract for Aging

Yanfei Liu , Yue Liu , Wantong Zhang, Mingyue Sun, Weiliang Weng , and Rui Gao 
Research Article (10 pages), Article ID 8508491, Volume 2020 (2020)

Research Article

Research on Effect and Mechanism of Xuefu Zhuyu Decoction on CHD Based on Meta-Analysis and Network Pharmacology

Fuguang Kui,¹ Wenwen Gu,¹ Fan Gao,¹ Yuji Niu,¹ Wenwen Li,¹ Yaru Zhang,¹ Lijuan Guo,¹ Junru Wang,¹ Zhenzhen Guo,¹ Shihong Cen^{1,2} ,² and Gangjun Du^{1,2} 

¹Institute of Pharmacy, Pharmaceutical College of Henan University, Jinming District, Kaifeng, Henan 475004, China

²School of Pharmacy and Chemical Engineering, Zhengzhou University of Industry Technology, Xinzheng, Henan 451150, China

Correspondence should be addressed to Shihong Cen; 10200053@vip.henu.edu.cn and Gangjun Du; 10200029@vip.henu.edu.cn

Received 28 July 2020; Revised 4 November 2020; Accepted 8 December 2020; Published 13 February 2021

Academic Editor: Yong Wang

Copyright © 2021 Fuguang Kui et al. This is an open access article distributed under the Creative Commons Attribution License, which permits unrestricted use, distribution, and reproduction in any medium, provided the original work is properly cited.

Xuefu Zhuyu Decoction (XFZY) is an ancient compound widely used in the treatment of coronary heart disease. However, its efficacy evaluation is not complete and its mechanism of action is not clear enough. In an attempt to address these problems, the efficacy was evaluated by meta-analysis and the mechanism was elucidated by the network pharmacology method. We systematically searched relevant studies in PubMed, Chinese National Knowledge Infrastructure Database (CNKI), Cochrane Library, Wanfang Data, and other databases from 2007 to 2019. The association between XFZY treatment and CHD was estimated by risk ratio (RR) and corresponding 95% confidence intervals (95% CIs). The compounds and the potential protein targets of XFZY were obtained from TCMSP, and active compounds were selected according to their oral bioavailability and drug similarity. The potential genes of coronary heart disease were obtained from TTD, OMIM, and GeneCards. The potential pathways related to genes were determined by GO and KEGG pathway enrichment analyses. The compound-target and compound-target-pathway networks were constructed. Molecular docking validates the component and the target. A total of 21 studies including 1844 patients were enrolled in the present meta-analysis, indicating that XFZY has a greater beneficial on total effect (fixed effect RR = 1.30; 95% CI: 1.24–1.36; $P = 0.82$; $I^2 = 0.0\%$) and electrocardiogram efficacy (fixed effect RR = 1.40; 95% CI: 1.26–1.56; $P = 0.96$; $I^2 = 0.0\%$) compared with the control group. A total of 1342 components in XFZY were obtained, among which, 241 were chosen as bioactive components. GO and KEGG analyses got top 10 significantly enriched terms and 10 enriched pathways. The C-T network included 192 compounds and 3085 targets, whereas the C-T-P network included 10 compounds, 109 targets, and 5 pathways. There was a good binding activity between the components and the targets. XFZY has the curative effect on coronary heart disease, and its mechanism is related to 10 compounds, 10 core targets, and 5 pathways.

1. Introduction

Coronary heart disease (CHD) is a leading cause of death and disability worldwide [1]. CHD is caused by narrowing or obstruction of blood vessels due to coronary atherosclerosis, myocardial ischemia, hypoxia, and necrosis. CHD has intervened effectively with the advances in cardiovascular medicine over the past decades. Despite great improvements in cardiovascular medicine, these developments now still generate to post-treat sequelae. Therefore, finding a more effective therapy method is an urgent need.

Traditional Chinese medicine (TCM), embracing centuries of knowledge and wisdom, is a medical practice [2] and has played a significant therapeutic role in various diseases [3]. Xuefu Zhuyu Decoction (XFZYD), from “Yiling Gaicuo,” is Chinese herbal formulas commonly used to treat hypertension and cardiovascular diseases in traditional Chinese medicine [4]. It consists of eleven herbs, namely, *Paeonia lactiflora* Pall (Chi Shao in Chinese); *Ligusticum chuanxiong* Hort (Chuan Xiong in Chinese); *Bupleurum chinensie* DC (Chai Hu in Chinese); *Carthamus tinctorius* L. (Hong Hua in Chinese); *Angelica sinensis* (Oliv) Diels

(Dang Gui in Chinese); *Prunus persica* (L.) Batsch (Tao Ren in Chinese); *Achyranthes bidentata* BI (Niu Xi in Chinese); *Glycyrrhiza uralensis* Fisch (Gan Cao in Chinese); *Platycodon grandifloras* (Jacq.) A. DC (Jie Geng in Chinese); *Citrus aurantium* L. (Zhi Ke in Chinese); *Rehmannia glutinosa* Libosch (Sheng Di Huang in Chinese). According to clinical view of TCM, Qi is the commander of blood. Qi stagnation causes blood stasis, which leads to CHD [5]. Studies have shown that XFZY is regulating Qi and promoting blood circulation [6]. Clinical studies have shown that XFZY is effectively ameliorative to the clinical symptoms of CHD without side effect [7]. The therapeutic effects of XFZY on atherosclerosis and hyperlipidemia were validated [8]. XFZY will improve the phlegm and blood stasis pattern in CHD [9]. XFZY is very effective in the treatment myocardial fibrosis, atherosclerosis, hypertension, unstable angina pectoris, and myocardial ischemia-reperfusion injury [10]. However, these studies are not supported by a large amount of clinical data, or incomplete. Therefore, this paper will use meta-analysis to evaluate the efficacy of XFZY on CHD through the study of a large number of clinical data. Currently, network pharmacology has shown that for complex diseases, Chinese medicine formulas have the advantages of multitarget interventions and minimal side effect [11]. Therefore, this study will also perform network pharmacology to elucidate the mechanism of XFZY on CHD.

2. Methods

The reporting of this study was guided by the Preferred Reporting Items for Systematic Reviews and Meta-Analyses checklist. The registration application for the systematic review protocol has been submitted at PROSPERO, but the registration number has not been obtained.

2.1. Literature Search. We searched the main literature database at home and abroad, namely, PubMed, PubMed Pro, Embase, Chinese Scientific Journal Database (VIP), SinoMed, Cochrane Library, CNKI, and Wanfang Data, from 2007 to 2019, identifying available studies to be included in the meta-analysis. The keywords that were used are as follows: Xuefu Zhuyu Tang, Xuefu Zhuyu Decoction, XFZY, XFZYD, coronary heart disease, and CHD. Besides, we also screened all other possible reference lists from the studies selected to identify further relevant studies and reviews (see Supplementary File 1 for further information).

2.2. Criteria for Literature Inclusion. The inclusion criteria were as follows:

- (1) Included studies were required to have enrolled patients with a clear diagnosis of coronary heart disease; no restrictions on race, age, or sex were imposed
- (2) Randomized, clinical trial

- (3) Control group for routine treatment and experimental group for XFZY on the basis of the control group
- (4) Basis of disease diagnosis is Nomenclature and Diagnostic Criteria for Ischemic Heart Disease and Guiding Principles for Clinical Research of New Chinese Medicines (trial)
- (5) The course of treatment is four weeks or more
- (6) It conforms to the ethical and moral treatment standard
- (7) The patient has no other mental illness or serious primary disease
- (8) The patient is not lactation, pregnancy, or advanced stage of disease
- (9) One or more outcome indicators of the following must be involved: (1) total therapeutic effect; (2) ECG; (3) adverse reaction; (4) angina pectoris attack frequency and duration; (5) the total effect of TCM syndromes; (6) serum lipids index; (7) blood stream change; (8) the effect of electroacupuncture acupoint; (9) vessel endothelial function and factors of vessel endothelium; (10) LVEF and PAF; (11) average hospital stay; (12) disappeared time of angina; (13) effects of decreased dose; (14) symptom improvement; (15) the total angina pectoris efficacy.

Therefore, exclusion criteria included the following:

- (1) Republished studies
- (2) Nonrandomized trials
- (3) Experiments on animals
- (4) Review
- (5) There are no clear diagnostic criteria or not meet inclusion criteria
- (6) Lack of required data for meta-analysis
- (7) Treatment duration is less than four weeks
- (8) There is no complete evaluation of efficacy

2.3. Data Extraction. Two authors searched the literature according to the established strategy, then extracted data from the included studies, and compared the results independently. Discrepancy was resolved by the third author's adjudication to avoid bias. Extracted data included author, year of publication, title of the study, diagnostic criteria, sample size, course of treatment, intervention and control measures, evaluation standard, random scheme generation, allocation hiding, blind method, incomplete result data, selective reporting, and other biases.

2.4. Quality Assessment. The Cochrane Collaboration's Bias Risk Assessment Tool was used to assess the quality of the literature. The main assessment areas are as follows: allocation concealment, random sequence generation, incomplete outcome data, blinding method for patients/researchers and outcomes assessors, selective reporting, and

other sources of bias. The results were judged as “low risk,” “high risk,” and “unclear.”

2.5. Statistical Analysis. Statistical analyses were conducted using RevMan5.3 (Review Manager 5.3). Between studies, heterogeneity of each study was assessed using I^2 tests. If high heterogeneity ($I^2 > 50\%$) was observed, random effect models were applied; otherwise, fixed effect models were used. Pooled RR with corresponding 95% CIs was used to evaluate the effect of XFZY on CHD. We used a funnel plot to determine potential publication bias.

2.6. Active Ingredients. Compounds of ten ingredients in XFZY were gathered from TCM Systems Pharmacology Database (TCMSP, a unique systems pharmacology platform designed for herbal medicines). Compounds of Sheng Di Huang were obtained from Chemistry Database (<http://www.organchem.csdb.cn/>). The ADME (absorption, distribution, metabolism, and excretion) was used to filtrating active compounds. The active components were obtained by screening for both oral bioavailability (OB) value $\geq 30\%$ and drug similarity (DL) value ≥ 0.18 .

2.7. Potential Target Identification. The targets of the active ingredients in XFZY were obtained from the TCMSP database and Chemistry Database (<http://www.organchem.csdb.cn/>).

2.8. CHD-Related Gene Targets. Retrieving the Therapeutic Target Database (TTD, <http://db.idrblab.net/ttd/>), Online Mendelian Inheritance in Man (OMIM <https://www.omim.org/>), and GeneCards (<https://www.genecards.org/>) about CHD, CHD-related gene targets were collected.

2.9. Gene Ontology (GO) and KEGG Pathway Enrichment. To seek out the biological characteristics of bioactive targets of XFZY on CHD in detail, the GO and KEGG pathway enrichment analyses of bioactive targets were conducted via DAVID 6.8 (<https://david.ncifcrf.gov/>). The top 10 significantly enriched terms and 10 significantly enriched pathways of XFZY on CHD were visualization.

2.10. Network Construction and Analysis. To further characterize the mechanism of XFZY on CHD, the C-T and C-T-P networks were constructed via Cytoscape 3.2.1. In these networks, compounds, targets, and pathways were expressed as nodes, whereas the C-T and C-T-P interactions were expressed as edges.

2.11. Molecular Docking. The bioactive component and the target with the highest degree value were selected for molecular docking. Mol2 format of molecular structure of bioactive components was obtained from the TCMSP database, and PDB format of 3D molecular structure of corresponding target genes was obtained from the RCSB PDB

database (<https://www.rcsb.org/>). LeDock software was used to dock the bioactive components with the target to obtain the docking affinity. SwissDock (<http://www.swissdock.ch/>) and Chimera 1.14 software were used to perform molecular docking visualization analysis of compounds with high docking affinity and stable conformation with target proteins.

3. Results

3.1. Search Results and Study Quality. Figure 1 schematically shows the selection procedure for eligible articles. 238 references were obtained by searching all databases, among them, 50 papers from SinoMed, 110 papers from CNKI, and 78 papers from Wanfang Data. Removed duplicates, a total of 128 papers were identified in the initial search. However, 107 articles were excluded due to irrelevant content or not up to inclusion criteria after reading the titles and abstracts (shown in Supplementary File 4). After evaluation, 21 papers qualified for detailed evaluation. A total of 1844 patients from 21 included studies, 919 control groups and 925 treatment groups, were included in this meta-analysis. The detail data extracted from these included articles are listed in Table 1. Quality assessment of 21 available studies was performed by using the Risk Assessment Tool of the Cochrane Library. The risk of inclusion literature is shown in Figure 2.

3.2. Heterogeneity Detection and Pooled Analysis. We included 21 RCTs with a total of 1844 participants. All the 21 studies, including a total of 1844 patients, reported total effect of XFZY on CHD. We used a fixed effect model to analyze results because heterogeneity was low ($I^2 < 50\%$). Meta-analysis showed that patients with XFZY had more effective than control group (Figure 3) (fixed effect RR = 1.30; 95% CI: 1.24–1.36; $P = 0.82$; $I^2 = 0.0\%$). 8 studies, including a total of 674 patients, reported electrocardiogram efficacy of XFZY on CHD. We used a fixed effect model to analyze results. Meta-analysis showed that, compared with the control group, the experimental group with XFZY was more effective than the control group (Figure 4) (fixed effect RR = 1.40; 95% CI: 1.26–1.56; $P = 0.96$; $I^2 = 0.0\%$).

3.3. Publication Bias. Funnel plots were made to evaluate publication bias. The result indicated that no clear bias in the total effect (Figure 5(a)) and electrocardiogram efficacy (Figure 5(b)).

3.4. Potential Active Moieties of XFZY. A total of 1342 chemical moieties obtained from the XFZY formula were collected from TCMSP. By ADME filtering, only 222 compounds met the principle of both oral bioavailability (OB) value $\geq 30\%$ and drug similarity (DL) value ≥ 0.18 . The number of potential active compounds from CS, CX, CH, HH, DG, TR, NX, GC, JG, and ZK was 27, 7, 17, 22, 2, 23, 20, 92, and 7, 5, respectively. 19 chemical moieties of SD were collected from the Chemistry Database (shown in

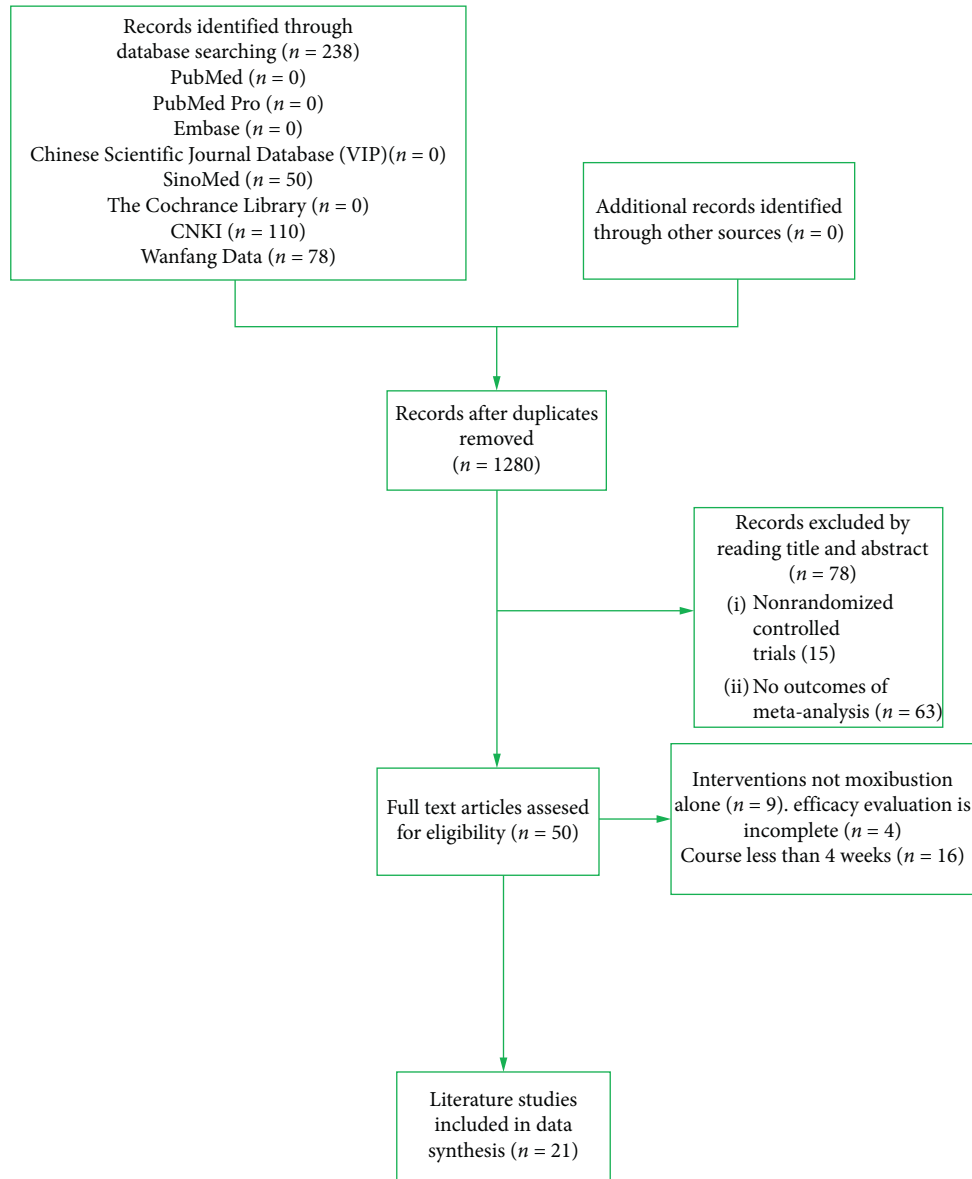


FIGURE 1: The flowchart of the study selection and exclusion criteria.

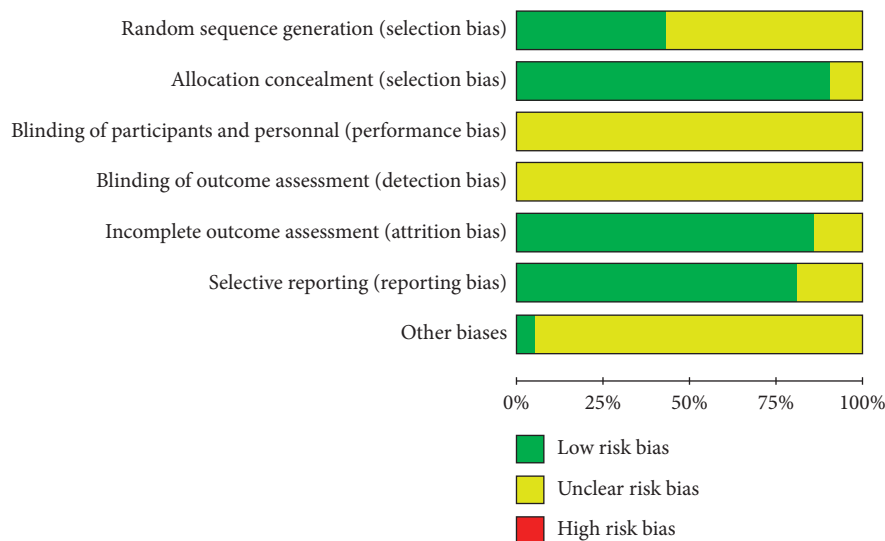
TABLE 1: The characteristics of all included studies.

Author and reference	Year	Total sample	Control/treatment	Period of treatment (day)	Drug C	T	Evaluation standard
Li Jiayun [12]	2019	108	54/54	60	(1), (4), (6)	(11)	1, 3, 9
Lu Jiansheng [13]	2018	64	32/32	60	(1), (3), (6)	(11)	1, 3, 7, 8, 11
Jiao Lixing [14]	2015	78	39/39	30	(1), (10)	(11)	1, 3, 8, 12
Zhao Dongkai [15]	2015	100	50/50	30	(14)	(11)	1, 2, 4
Huang Wenhua [16]	2018	71	35/36	30	(1), (2)	(11)	1, 4
Li Tingai [17]	2019	110	55/55	30	(1), (2), (3)③	(11)	1, 5
Fang Yuxiang [18]	2009	117	57/60	28	(1), (2)②	(11)	1, 7, 8, 13
Ying Ping [19]	2018	100	50/50	60	(1), (3), (4)	(11)	1, 6, 7
Wang Baoxin [20]	2010	58	29/29	30	(1), (8)	(11)	1, 4
Fang Jianjia [21]	2008	60	30/30	28	(2), (3)	(11)	1, 2, 14
Lin Zhijuan [22]	2015	70	30/40	30	(1), (2), (3), (9), (13)	(11)	2, 6, 15
Song Yuxin [23]	2013	82	40/42	28	(1), (6), (7), (9)	(11)	1, 2, 5, 7
Lv Xiqi [24]	2019	100	50/50	60	(1), (3), (5)	(11)	1, 7

TABLE 1: Continued.

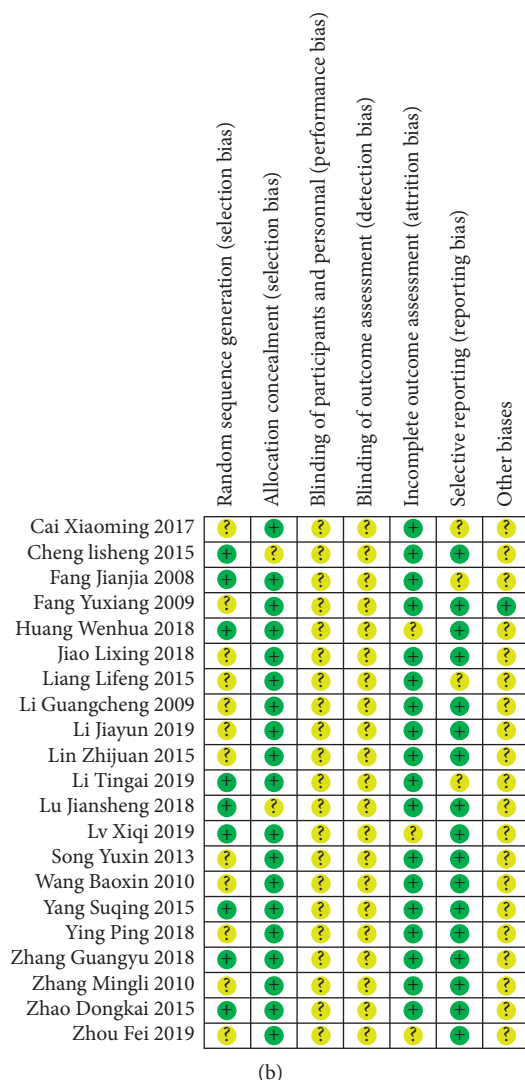
Author and reference	Year	Total sample	Control/treatment	Period of treatment (day)	Drug		Evaluation standard
					C	T	
Li Guangcheng [25]	2009	80	40/40	30	(1), (2)	(11)	1, 2, 5
Yang Suqing [26]	2015	96	48/48	28	(1), (2), (3)	(11)	1, 3, 5
Zhang Guangyu [27]	2018	92	46/46	28	(1), (3), (8)	(11)	1, 3, 4
Liang Lifeng [28]	2015	100	50/50	28	(6), (7), (9)	(11)	1, 2, 7
Cai Xiaoming [29]	2017	96	48/48	28	(6), (7), (9)	(11)	1
Zhou Fei [30]	2019	80	40/40	28	(6), (7)	(11)	1, 2, 6
Zhang Mingli [31]	2010	80	40/40	28	(2), (7), (9)	(11)	1, 2, 7
Cheng Lisheng [32]	2015	92	46/46	28	(3), (4), (10)	(11)	1, 2, 4, 7

Abbreviations: (1) aspirin; (2) nitroglycerin; (3) isosorbide dinitrate/isosorbide mononitrate; (4) metoprolol; (5) nifedipine; (6) nitrates; (7) β -blocker; (8) Betocloc; (9) calcium antagonist; (10) captopril; (11) Xuefu Zhuyu Decoction based on the control group; (12) lipid-lowering agents and pain relief drugs; (13) clopidogrel and atorvastatin; (14) Compound Salvia Tablets. 1 Total therapeutic effect; 2 ECG; 3 adverse reaction; 4 angina pectoris attack frequency and duration; 5 the total effective of TCM syndromes; 6 serum lipid index; 7 blood stream change; 8 the effect of electroacupuncture acupoint; 9 vessel endothelial function and factors of vessel endothelium; 10 LVEF and PAF; 11 average hospital stay; 12 disappeared time of angina; 13 effects of decreased dose; 14 symptom improvement; 15 the total angina pectoris efficacy.



(a)

FIGURE 2: Continued.



(b)

FIGURE 2: Risk bias graph of studies.

Supplementary File 2). The compounds were chosen as potential active moieties for further analyses.

3.5. Putative Targets for the Active Compounds of XFZY. Putative targets corresponding to 241 components were obtained from TCMSP and Chemistry Database. Removing duplicates, 163 protein targets were obtained for further analyses (shown in Supplementary File 3).

3.6. Targets of Coronary Heart Disease. In total, 6785 targets of CHD were obtained from TTD, OMIM, and GeneCards (shown in Supplementary File 5).

3.7. GO and Pathway Enrichment Analysis. DAVID 5.6 was used to perform the GO and KEGG pathway enrichment of XFZY for CHD. The top 10 significantly enriched terms are shown (Figure 6(a)), which exerted its therapeutic effects on CHD involving “response to drug,” “positive regulation of

nitric oxide biosynthetic process,” “response to hypoxia,” “positive regulation of cell proliferation,” “positive regulation of cell migration,” “response to estradiol,” “positive regulation of transcription,” “angiogenesis,” and “aging biological process.” The top 10 significantly enriched pathways of XFZY on CHD are shown (Figure 6(b)).

3.8. Network Construction and Analysis

3.8.1. Compound-Target Network (C-T Network). We performed bioactive target identification via WebGestalt (<http://webgestalt.org/>). There were 124 protein targets, which were the intersection of two parts, the targets of active compounds, and the targets of CHD, defined as bioactive targets for XFZY treating CHD. There were 192 corresponding compounds of bioactive targets. The compound-target network was constructed via Cytoscape3.2.1. The nodes represent compounds, targets, and edges which represent their interaction (Figure 7). The node color reflects

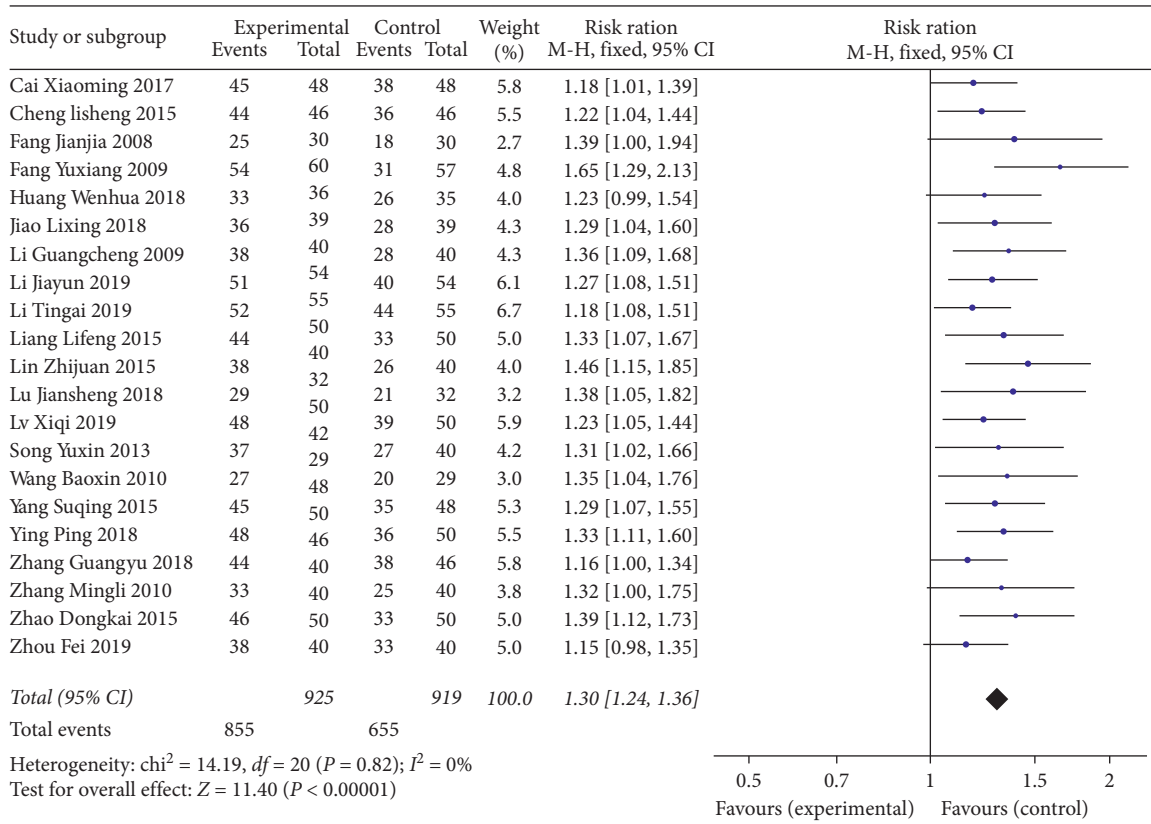


FIGURE 3: Comparison of total effect between the experimental group and the control group for coronary heart disease.

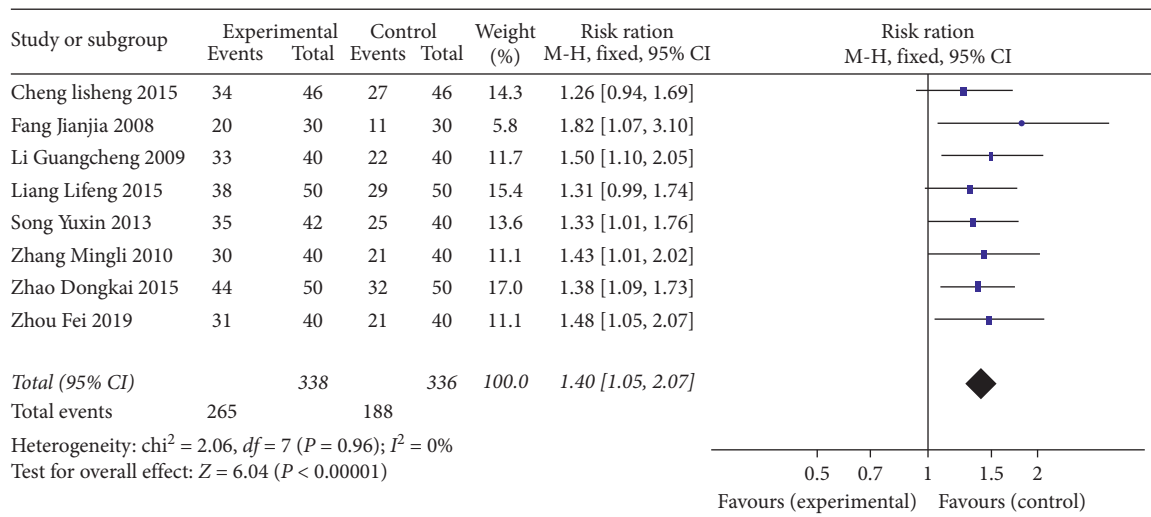


FIGURE 4: Comparison electrocardiogram efficacy between the experimental group and the control group for coronary heart disease.

the degree value. The edge thickness reflects the correlation between nodes. The result suggested that the top 10 compounds are as follows: quercetin; 7-methoxy-2-methyl isoflavone; (2R)-7-hydroxy-2-(4-hydroxyphenyl)chroman-4-one; beta-sitosterol; kaempferol; luteolin; medicarpin; formononetin; shinpterocarpin; 2-[(3R)-8,8-dimethyl-3,4-dihydro-2H-pyrano[6,5-f]chromen-3-yl]-5-methoxyphenol.

It means that these compounds may play a major role in the therapeutic effects. The top 10 targets are as follows: AR, ESR1, PTGS2, NOS2, PPARG, PIM1, DPP4, GSK3B, PRSS1, and ESR2. These targets may be the main targets of drug action. In addition, it can be seen that an effective component corresponds to multiple targets, and a target corresponds to multiple effective components.

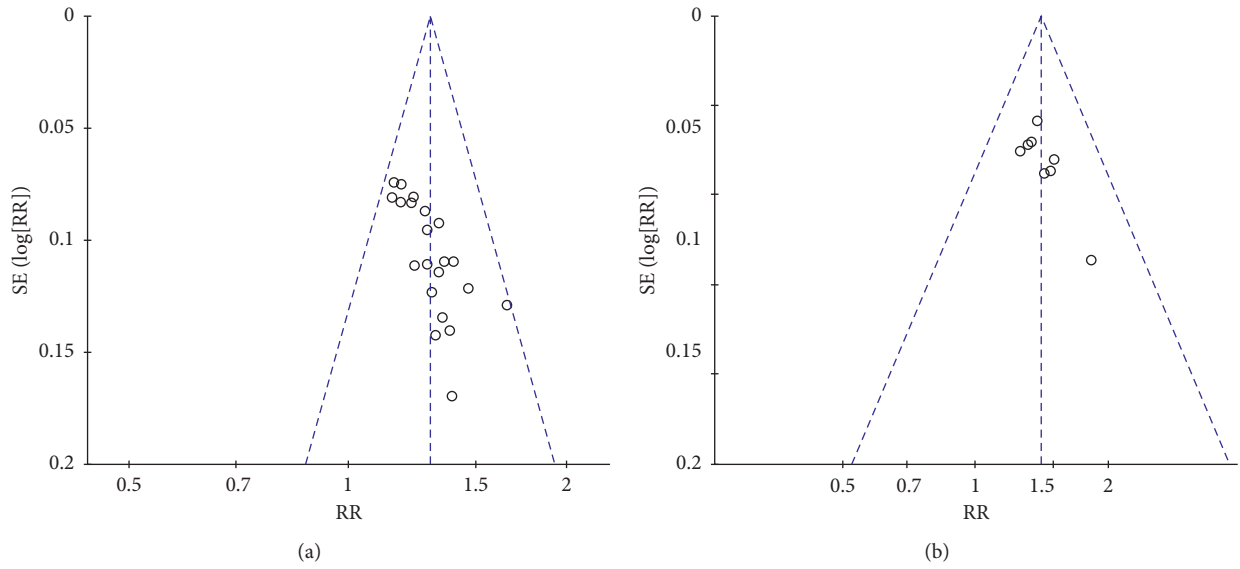


FIGURE 5: (a) The bias of the total effect in the treatment of coronary heart disease by Xuefu Zhuyu Decoction; (b) the bias of electrocardiogram efficacy in the treatment of coronary heart disease by Xuefu Zhuyu Decoction.

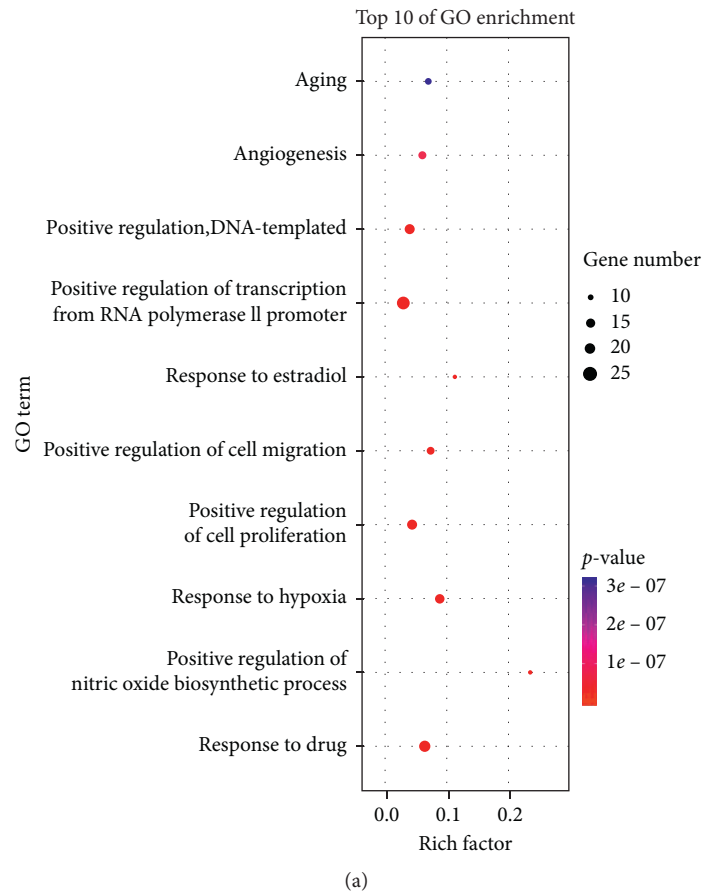


FIGURE 6: Continued.

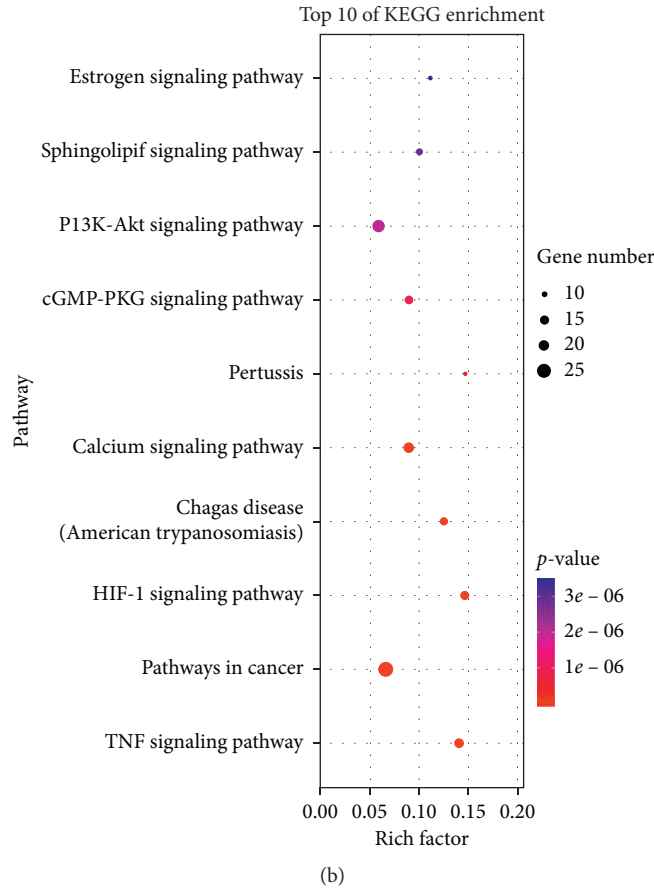


FIGURE 6: The 10 most significance of gene ontology (a) and pathway enrichment (b) analysis of therapy target genes of XFZY on CHD.

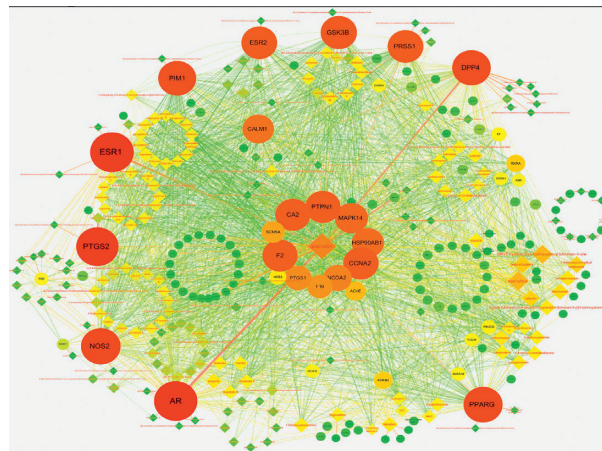


FIGURE 7: The compound-target network of XFZY on CHD. The circles represent potential protein targets, and the rhombus represents bioactive compounds. The edges represent the interactions between them, and nodes' sizes are proportional to their degree.

3.8.2. *Compound-Target-Pathway Network (C-T-P Network).* To further characterize the molecular mechanism by which XFZY on CHD, a compound-target-pathway network was performed based on all involved compounds, targets, and their corresponding significant signal pathways. Therefore, five signal pathways that may be related to CHD were

selected from the top 10 KEGG genes in the treatment of CHD by XFZY, constructing the component-target-pathway network (Figure 8). The five signal pathways are follows: TNF signaling pathway, pathways in cancer, calcium signaling pathway, HIF-1 signaling pathway, and Chagas disease (American trypanosomiasis), respectively.

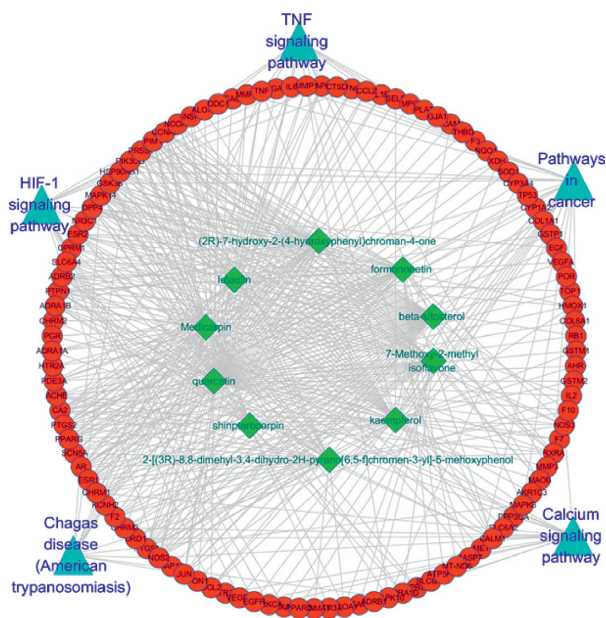


FIGURE 8: The compound-target-pathway network of XFZY on CHD. The red circles represent potential protein targets, the green rhombuses represent bioactive compounds, and the blue triangles represent signaling pathways. The edges represent the interactions between them.

3.9. Molecular Docking. For gaining docking affinity, LeDock software was used to dock quercetin; 7-methoxy-2-methyl isoflavone; (2R)-7-hydroxy-2-(4-hydroxyphenyl) chroman-4-one; beta-sitosterol; kaempferol, and other XFZY bioactive components with AR, ESR1, PTGS2, NOS2, and other targets, respectively (Table 2). The affinity of compounds and targets is greater than -4.25 kcal/mol, which indicates that the compound had a certain affinity for the protein crystal structure. Quercetin and AR, quercetin and PTGS2, kaempferol and DPP4, kaempferol and AR, luteolin and PPARG, and luteolin and DPP4 were selected for visualization with Chimera 1.14 software and SwissDock (<http://www.swissdock.ch/>) (Figure 9).

4. Discussion

TCM has obvious advantages in treating many diseases, but it also has many problems. For example, on the one hand, the clinical efficacy evaluation is incomplete or lacks a large amount of clinical data support. To solve the problem, meta-analysis was performed. Meta-analysis is a systematic, quantitative, and comprehensive statistical method based on previous research results. It is often used to evaluate intervention randomized controlled trials in evidence-based medicine, which can objectively evaluate the clinical efficacy. Therefore, in this article, we compiled the current evidence on the total effect of XFZY on CHD in 1,844 individuals from 21 studies, and electrocardiogram efficacy of XFZY on CHD in 674 individuals from 8 studies. This evidence objectively suggested that XFZY has a sound clinical effect on CHD and there are no significant adverse reactions.

In clinical practice, blood lipids are usually used as an indicator to evaluate the curative effect. Of course, it

assuredly is too limited to evaluate the effectiveness and safety of CHD in terms of total effect and electrocardiogram efficacy. Unfortunately, inclusion criteria have no other enough indicators to draw forest plot.

On the other hand, the composition of TCM is complex and the mechanism of action has not been effectively elaborated, which are the biggest bottleneck in the development and popularization of TCM. Hence, we used network pharmacology to identify major components and elucidate mechanisms of action. Network pharmacology comprehends disease as an interconnected complex biological network and cognizes the mechanisms of TCM action via network topology [33]. It is a promising approach to expound the mechanisms of TCM [34]. The results of C-T and C-T-P networks showed that quercetin; 7-methoxy-2-methyl isoflavone; (2R)-7-hydroxy-2-(4-hydroxyphenyl) chroman-4-one; beta-sitosterol; kaempferol; luteolin; medicarpin; formononetin; and shinpterocarpin; 2-[(3R)-8,8-dimethyl-3,4-dihydro-2H-pyran[6,5-f]chromen-3-yl]-5-methoxyphenol are the main ingredients at work according degree from large to small when XFZY plays curative effect and that the main targets are as follows: AR, ESR1, PTGS2, NOS2, PPARG, PIM1, DPP4, GSK3B, PRSS1, and ESR2, which mainly involves the following five signaling pathways, namely, TNF signaling pathway, pathways in cancer, calcium signaling pathway, HIF-1 signaling pathway, and Chagas disease (American trypanosomiasis).

According to the TCM prescription principles of monarch, minister, assistant, and guide, *Prunus persica* (L.) Batsch and *Carthamus tinctorius* L. are the monarch drug, *Achyranthes bidentata* BI, *Ligusticum chuanxiong* Hort, and *Paeonia lactiflora* Pall are the minister drug, *Rehmannia glutinosa* Libosch, *Angelica sinensis* (Oliv) Diels, *Citrus aurantium* L., and *Platycodon grandifloras* (Jacq.) A. DC are

TABLE 2: Molecular docking of bioactive ingredients of XFZY and corresponding targets.

Ingredient	Target name	PDB ID	Affinity (kcal/mol)
Quercetin	AR	2pir	-6.90
Quercetin	PTGS2	5f1a	-7.07
Quercetin	P1M1	2o3p	-6.27
Quercetin	NOS2	4ux6	-6.72
7-Methoxy-2-methyl isoflavone	PTGS2	5f1a	-4.88
(2R)-7-Hydroxy-2-(4-hydroxyphenyl)chroman-4-one	P1M1	2o3p	-4.59
Kaempferol	DPP4	5t4f	-5.96
Kaempferol	AR	2pir	-6.77
Kaempferol	ESR1	2i0j	-6.09
Kaempferol	PPARG	6c5t	-5.97
Luteolin	PPARG	2pob	-5.75
Luteolin	AR	2pir	-6.74
Luteolin	DPP4	5t4f	-6.01
Medicarpin	ESR1	2i0j	-4.89
Formononetin	PRSS1	1trn	-5.08
Shinpterocarpin	PPARG	6c5t	-4.53
2-[(3R)-8,8-Dimethyl-3,4-dihydro-2H-pyrano[6,5-f]chromen-3-yl]-5-methoxyphenol	DPP4	5y7k	-4.95

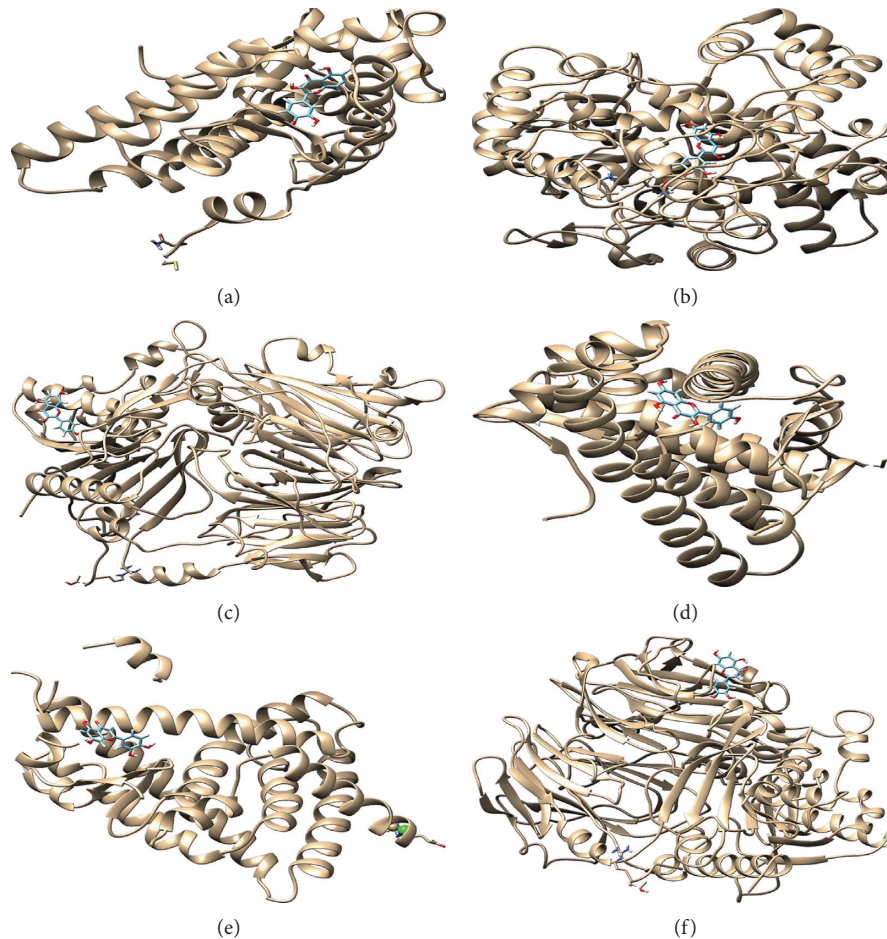


FIGURE 9: Pattern diagram of molecular docking: (a) quercetin-AR; (b) quercetin-PTGS2; (c) kaempferol-DPP4; (d) kaempferol-AR; (e) luteolin-PPARG; (f) luteolin-DPP4.

the assistant drug, and *Glycyrrhiza uralensis* Fisch is the guide drug. *Carthamus tinctorius* L. and *Prunus persica* (L.) Batsch can activate blood and dissolve stasis. *Paeonia*

lactiflora Pall, *Ligusticum chuanxiong* Hort, and *Achyranthes bidentata* BI promote stasis metabolism and excretion. *Rehmannia glutinosa* Libosch, *Platycodon grandifloras*

(Jacq.) A. DC, *Citrus aurantium* L., and *Angelica sinensis* (Oliv) Diels clear heat and activate blood, promoting circulation of Qi and blood. *Glycyrrhiza uralensis* Fisch harmonizes other medicines. In the supplemental document, we find main ingredients as follows: quercetin which originates from *Bupleurum chinensie* DC, *Glycyrrhiza uralensis* Fisch, *Achyranthes bidentata* BI, and *Carthamus tinctorius* L.; 7-methoxy-2-methyl isoflavone which originates from *Glycyrrhiza uralensis* Fisch; (2R)-7-hydroxy-2-(4-hydroxyphenyl)chroman-4-one which originates from *Glycyrrhiza uralensis* Fisch; beta-sitosterol which originates from *Paeonia lactiflora* Pall, *Carthamus tinctorius* L., *Angelica sinensis* (Oliv) Diels, *Citrus aurantium* L., *Achyranthes bidentata* BI, and *Prunus persica* (L.) Batsch; kaempferol which originates from *Bupleurum chinensie* DC, *Carthamus tinctorius* L., *Glycyrrhiza uralensis* Fisch, and *Achyranthes bidentata* BI; luteolin which originates from *Carthamus tinctorius* L. and *Platycodon grandifloras* (Jacq.) A. DC; medicarpin which originates from *Glycyrrhiza uralensis* Fisch; formononetin which originates from *Glycyrrhiza uralensis* Fisch; shinpterocarpin which originates from *Glycyrrhiza uralensis* Fisch; 2-[(3R)-8,8-dimethyl-3,4-dihydro-2H-pyrano[6,5-f]chromen-3-yl-5-methoxyphenol which originates from *Glycyrrhiza uralensis* Fisch.

Quercetin is an important flavonoid that has been normally viewed as a great antioxidant and anti-inflammatory molecule [35–37] and can prevent endothelial dysfunction and myocardial ischemia [38]. Beta-sitosterol exerted protective actions against myocardial injury [39] and is used in the treatment of hypercholesterolemia [40]. Kaempferol has antioxidant, anti-inflammatory effect [41] and protects against cardiac hypertrophy [42]. Luteolin can improve ventricular function and reduce coronary reperfusion [43] and thrombotic tendency [44]. Medicarpin and its metabolites were transported in most organs of the body [45] and can promote the publication of other ingredients. Formononetin substantially attenuates the generation of atherosclerosis [46]. 7-methoxy-2-methyl isoflavone; (2R)-7-hydroxy-2-(4-hydroxyphenyl)chroman-4-one; shinpterocarpin; and 2-[(3R)-8,8-dimethyl-3,4-dihydro-2H-pyrano[6,5-f]chromen-3-yl-5-methoxyphenol can reduce the incidence of ischemia reperfusion injuries and chronic inflammatory disease. It is well known that reducing inflammatory factor can attenuate the development of cardiac hypertrophy possibly [47]. The above ten compounds can adjust a variety of physiological activities for the treatment of coronary heart disease. The literature confirms the predicted results of network pharmacology. Generally speaking, the action of traditional Chinese medicine is consistent with the pharmacological action of its components.

The molecular docking results showed that the active components were well bound to target proteins. The affinity of quercetin and AR is -6.90 kcal/mol. The affinity of quercetin and PTGS2 is -7.07 kcal/mol. The affinity of kaempferol and DPP4 is -5.96 kcal/mol. The affinity of kaempferol and AR is -6.77 kcal/mol. The affinity of luteolin and PPARG is -5.75 kcal/mol. The affinity of luteolin and DPP4 is -6.01 kcal/mol.

Androgens work by binding to androgen receptors. Androgen is a key early event in atherosclerosis [48]. ESR1 and ESR2 mediate estrogen action. Estrogen protects against atherosclerosis [49]. PTGS2 has been linked to atherosclerosis, stroke, and other CVDs [50]. NOS2 is a subtype of NOS, which can affect the composition of NO. NO bioavailability plays a vital role in the pathophysiology of cardiovascular disease [51]. Peroxisome proliferator-activated receptor gamma (PPARG) is involved in the transcription of atherosclerosis and related diseases [52]. PIM1 has cardioprotective action [53]. The loss of DPP4 activity may affect the antithrombotic nature [54]. Manipulating GSK-3beta is a promising strategy for myocardial protection in coronary artery disease and heart failure [55]. PRSS1 is mainly involved in proteolysis and digestion.

In addition to pathways in cancer and Chagas disease (American trypanosomiasis), the pathway of Xuefu Zhuyu Decoction in the treatment of CHD is also involved in the following signaling pathways: TNF signaling pathway, calcium signaling pathway, and HIF-1 signaling pathway. TNF- α increasing ROS levels and decreasing nitric oxide production in blood vessels leads to endothelial dysfunction. It contributes also to the development of atherosclerotic plaques [56]. Dysregulation of these Ca^{2+} fluxes will lead to different heart and vascular pathologies [57]. HIF plays an essential role in the complex progression of atherosclerosis [58].

According to the literature, it is not difficult to find that the targets of network pharmacology are related to the regulation of various physiological functions such as reducing inflammatory response, sex hormone regulation, NO regulation, and calcium ion regulation. Furthermore, the pathways are mainly involving calcium regulation, arteriosclerosis development, and other biological functions.

These results will provide a reliable quality evaluation standard for the treatment of CHD by Xuefu Zhuyu Decoction. The existing TCM quality evaluation system needs more effective supplement to control the quality of compound prescription general [59]. Usually, content-based quality control is a commonly adopted method at present, which may not ensure biological activity in vivo or cannot be absorbed effectually. Network pharmacology can intuitively reflect the importance of components according degree. When evaluating the quality of traditional Chinese medicinal materials, the ingredients in the C-T network with high degree value should be considered first, rather than those with high content. For XFZY treat CHD, ten compounds, quercetin; 7-methoxy-2-methyl isoflavone; (2R)-7-hydroxy-2-(4-hydroxyphenyl)chroman-4-one; beta-sitosterol; kaempferol; luteolin; medicarpin; formononetin; shinpterocarpin; and 2-[(3R)-8,8-dimethyl-3,4-dihydro-2H-pyrano[6,5-f]chromen-3-yl-5-methoxyphenol, are suggested to selected as marker compounds for quality control. According to the importance of ingredients in the treatment of diseases, we can establish a quality control system more in line with the rules of TCM medication.

5. Conclusion

In summary, XFZY has the curative effect on coronary heart disease and its mechanism is related to 10 compounds, 10

core targets, and 5 pathways. This study may provide a novel strategy for the understanding of TCM mechanism and make a positive contribution to the standardization of quality control. However, there may still be some potential shortcomings in this study. For example, this study lacks further experiment and more clinical sample.

Data Availability

The data used to support the findings of the study are available from the corresponding author upon request

Conflicts of Interest

The authors have declared no conflicts of interest.

Authors' Contributions

Fuguang Kui and Gang Jun Du conceived and designed the experiments. Fuguang Kui, Wenwen Gu, Fan Gao, Niu Yuji, Li Wenwen, Zhang Yaru, Guo Lijuan, Wang Junru, Zhen-Zhen Guo, and Shihong Cen performed the experiments. Fuguang Kui, Gang Jun Du, Zhen-Zhen Guo, and Shihong Cen analyzed the data. Zhen-Zhen Guo and Gang Jun Du contributed reagents/materials/analysis tools. Fuguang Kui, Zhen-Zhen Guo, and Gang Jun Du wrote the paper and plotted the results.

Acknowledgments

This study was supported by the Joint Foundation of National Natural Science Foundation of China and Henan Province of China (no. U200410711). This study was supported by Youth Natural Science Foundation of Henan Province of China (no. 212300410109) and Scientific Research Foundation for Postdoctoral Science Foundation of Henan Province of China.

Supplementary Materials

Supplementary File 1: a detailed description of the methods and results of literature retrieval. Supplementary File 2: 241 compounds of XFZY, from the TCMSP database, met the principle of both oral bioavailability (OB) value $\geq 30\%$ and drug similarity (DL) value ≥ 0.18 . The number of potential active compounds from CS (*Paeonia lactiflora* Pall), CX (*Ligusticum chuanxiong* Hort), CH (*Bupleurum chinense* DC), HH (*Carthamus tinctorius* L.), DG (*Angelica sinensis* (Oliv) Diels), TR (*Prunus persica* (L.) Batsch), NX (*Achyranthes bidentata* BI), GC (*Glycyrrhiza uralensis* Fisch), JG (*Platycodon grandifloras* (Jacq.) A. DC), and ZK (*Citrus aurantium* L.) was 27, 7, 17, 22, 2, 23, 20, 92, 7, and 5, respectively. 19 chemical moieties of SD (*Rehmannia glutinosa* Libosch) were collected from the Chemistry Database. Supplementary File 3 Protein targets of 241 corresponding components were obtained from TCMSP and Chemistry Database. Supplementary File 4: literature exclusion reasons. Supplementary File 5: 6785 targets of CHD were obtained from TTD, OMIM, and GeneCards. (*Supplementary Materials*)

References

- [1] F. J. Wolters, R. A. Segufa, S. K. L. Darweesh et al., "Coronary heart disease, heart failure, and the risk of dementia: a systematic review and meta-analysis," *Alzheimer's & Dementia*, vol. 14, no. 11, pp. 1493–1504, 2018.
- [2] H. Li, J. Deng, L. Deng, X. Ren, and J. Xia, "Safety profile of traditional Chinese herbal injection: an analysis of a spontaneous reporting system in China," *Pharmacoepidemiology and Drug Safety*, vol. 28, no. 7, pp. 1002–1013, 2019.
- [3] Z. Guo, M. Meng, S. Geng et al., "The optimal dose of arsenic trioxide induced opposite efficacy in autophagy between K562 cells and their initiating cells to eradicate human myelogenous leukemia," *Journal of Ethnopharmacology*, vol. 196, pp. 29–38, 2017.
- [4] G. Zhang, G. Yang, Y. Deng et al., "Ameliorative effects of Xue-Fu-Zhu-Yu decoction, Tian-Ma-Gou-Teng-Yin and Wen-Dan decoction on myocardial fibrosis in a hypertensive rat mode," *BMC Complementary and Alternative Medicine*, vol. 16, p. 56, 2016.
- [5] T. Tao, T. He, X. Wang, and X. Liu, "Metabolic profiling analysis of patients with coronary heart disease undergoing Xuefu Zhuyu Decoction treatment," *Frontiers in Pharmacology*, vol. 10, p. 985, 2019.
- [6] G. Z. Yi, Y. Q. Qiu, Y. Xiao, and L. X. Yuan, "The usefulness of Xuefu Zhuyu tang for patients with angina pectoris: a meta-analysis and systematic review," *Evidence-Based Complementary and Alternative Medicine*, vol. 2014, Article ID 521602, , 2014.
- [7] T. Yang, X. Li, Z. Lu, X. Han, and M. Zhao, "Effectiveness and safety of Xuefu Zhuyu decoction for treating coronary heart disease angina: a systematic review and meta-analysis," *Medicine (Baltimore)*, vol. 98, no. 9, 2019.
- [8] Y. Li, K. Chen, and Z. Shi, "Effect of Xuefu Zhuyu pill on blood stasis syndrome and risk factor of atherosclerosis," *Zhongguo Zhong Xi Yi Jie He Za Zhi*, vol. 18, no. 2, pp. 71–73, 1998.
- [9] X.-Y. Lu, H. Xu, T. Zhao, and G. Li, "Study of serum metabonomics and formula-pattern correspondence in coronary heart disease patients diagnosed as phlegm or blood stasis pattern based on ultra performance liquid chromatography mass spectrometry," *Chinese Journal of Integrative Medicine*, vol. 24, no. 12, pp. 905–911, 2018.
- [10] X. Shi, H. Zhu, Y. Zhang, M. Zhou, D. Tang, and H. Zhang, "Xuefu Zhuyu decoction protected cardiomyocytes against hypoxia/reoxygenation injury by inhibiting autophagy," *BMC Complementary and Alternative Medicine*, vol. 17, no. 1, pp. 1–10, 2017.
- [11] Y.-Y. Zhang, Z.-D. Zhao, P.-Y. Kong et al., "A comparative pharmacogenomic analysis of three classic TCM prescriptions for coronary heart disease based on molecular network modeling," *ACTA Pharmacologica Sinica*, vol. 41, no. 6, pp. 735–744, 2020.
- [12] J. Li, "Application of Xuefu Zhuyu decoction in the treatment of angina pectoris and analysis of vascular endothelial function index," *Electronic Journal of Clinical Medicine*, vol. 6, no. 48, pp. 142–143, 2019.
- [13] J. Lu, "Clinical effect observation of treatment of coronary heart disease angina pectoris with Xuefu Zhuyu Decoction," *Forum of Primary Medicine*, vol. 22, no. 14, pp. 1964–1966, 2018.
- [14] L. Jiao, "Clinical experience of treating coronary heart disease angina patients with Xuefu Zhuyu decoction," *Chinese Medical Guide*, vol. 13, no. 20, pp. 198–199, 2015.

- [15] D. Zhao and Yang, "Clinical observation of 50 cases of coronary heart disease angina pectoris (heart blood stasis type) treated by jiawei Xuefu Zhuyu decoction," *China Sanatoria Medicine*, vol. 24, no. 02, pp. 150-151, 2015.
- [16] W. Huang, "Clinical observation of 36 cases of coronary heart disease angina pectoris treated by Xuefuzhuyu Decoction combined with western medicine," *Hunan Journal of Traditional Chinese Medicine*, vol. 34, no. 9, pp. 7-9, 2018.
- [17] T. Li, "Clinical observation of Xuefu Zhuyu decoction combined with western medicine in the treatment of angina pectoris of coronary heart disease," *Guangming Chinese Medicine*, vol. 34, no. 13, pp. 2052-2054, 2019.
- [18] Y. Fang, "Clinical observation of 60 cases of coronary atherosclerotic heart disease angina pectoris treated by Xuefu Zhuyu decoction combined with western medicine," *Hebei Chinese Medicine*, vol. 31, no. 5, pp. 711-712, 2009.
- [19] P. Ying, "Clinical observation of Xuefu Zhuyu decoction combined with western medicine for angina pectoris," *New Chinese Medicine*, vol. 50, no. 8, pp. 40-42, 2018.
- [20] B. Wang, "Treatment of 58 cases of coronary heart disease with Xuefu Zhuyu decoction," *Chinese Traditional Chinese Medicine Modern Distance Education*, vol. 8, no. 15, p. 34, 2010.
- [21] J. Fang, "Clinical observation of 30 cases of angina pectoris with coronary heart disease treated by Xuefu Zhuyu decoction," *Guangzhou Western Medicine*, vol. 30, no. 9, pp. 1352-1353, 2008.
- [22] Z. Lin, "Effect analysis of Xuefu Zhuyu decoction on angina pectoris of coronary heart disease," *Clinical Research of Traditional Chinese Medicine*, vol. 7, no. 26, pp. 71-72, 2015.
- [23] Y. Song, "Clinical observation on the treatment of angina pectoris by Xuefu Zhuyu decoction," *Journal of Nantong University (Medical Edition)*, vol. 33, no. 5, pp. 416-417, 2013.
- [24] X. Lv, "Therapeutic effect of Xuefu Zhuyu decoction on angina pectoris of coronary heart disease," *Heilongjiang Science*, vol. 10, no. 14, pp. 128-129, 2019.
- [25] G. Li, "Effect of Xuefu Zhuyu decoction on angina pectoris of coronary heart disease," *Henan Chinese Medicine*, vol. 29, no. 12, pp. 1226-1227, 2009.
- [26] S. Yang, "Therapeutic effect of Xuefu Zhuyu decoction on angina pectoris of coronary heart disease," *Chinese Medicine Pharmacology and Clinical Practice*, vol. 31, no. 6, pp. 144-146, 2015.
- [27] G. Zhang, "Therapeutic effect of Xuefu Zhuyu decoction on angina pectoris of coronary heart disease," *Wisdom and Health*, vol. 4, no. 27, pp. 110-111, 2018.
- [28] L. Liang and J. Li, "Therapeutic effect of Xuefu Zhuyu decoction combined with western medicine in treating coronary heart disease angina pectoris with blood stasis syndrome," *World Latest Medical Information Digest*, vol. 15, no. 82, pp. 21-22, 2015.
- [29] X. Cai, "Clinical effect analysis of Xuefu Zhuyu decoction combined with western medicine in patients with coronary heart disease angina pectoris with blood stasis syndrome," *Chinese Journal of Modern Medicine*, vol. 11, no. 5, pp. 182-183, 2017.
- [30] F. Zhou, "Effect of Xuefu Zhuyu decoction on angina pectoris of coronary heart disease with Qi deficiency and blood stasis," *Chinese Medical Forum*, vol. 34, no. 3, pp. 39-40, 2019.
- [31] M. Zhang and P. Wang, "Therapeutic effect of Xuefu Zhuyu decoction combined with western medicine in treating coronary heart disease angina pectoris with blood stasis syndrome," *Hubei Journal of Traditional Chinese Medicine*, vol. 32, no. 4, pp. 16-17, 2010.
- [32] L. Chen, "Clinical observation on the treatment of angina pectoris with coronary heart disease by Xuefu Zhuyu decoction," *Shaanxi Traditional Chinese Medicine*, vol. 36, no. 7, pp. 812-813, 2015.
- [33] W. Y. Lee, C. Y. Lee, Y. S. Kim, and C. E. Kim, "The methodological trends of traditional herbal medicine employing network pharmacology," *Biomolecules*, vol. 9, no. 8, 2019.
- [34] E. L. Berg, "Systems biology in drug discovery and development," *Drug Discovery Today*, vol. 19, no. 2, pp. 113-125, 2014.
- [35] M. R. De Oliveira, S. M. Nabavi, N. Braidly, W. N. Setzer, T. Ahmed, and S. F. Nabavi, "Quercetin and the mitochondria: a mechanistic view," *Biotechnology Advances*, vol. 34, no. 5, pp. 532-549, 2016.
- [36] F. Xue, X. Nie, J. Shi et al., "Quercetin inhibits lps-induced inflammation and ox-ldl-induced lipid deposition," *Frontiers in Pharmacology*, vol. 8, p. 40, 2017.
- [37] Y. Zhang and Y. Zhang, "Pterostilbene, a novel natural plant conduct, inhibits high fat-induced atherosclerosis inflammation via NF- κ B signaling pathway in Toll-like receptor 5 (TLR5) deficient mice," *Biomedicine & Pharmacotherapy*, vol. 81, pp. 345-355, 2016.
- [38] F. Perez-Vizcaino and J. Duarte, "Flavonols and cardiovascular disease," *Molecular Aspects of Medicine*, vol. 31, no. 6, pp. 478-494, 2010.
- [39] F. Lin, L. Xu, M. Huang et al., " β -Sitosterol protects against myocardial ischemia/reperfusion injury via targeting PPAR γ /NF- κ B signalling," *Evidence Based Complementary Alternative Medicine*, vol. 2020, Article ID 2679409, 2020.
- [40] S. Ramalingam, M. Packirisamy, M. Karuppiyah et al., "Effect of β -sitosterol on glucose homeostasis by sensitization of insulin resistance via enhanced protein expression of PPAR γ and glucose transporter 4 in high fat diet and streptozotocin-induced diabetic rats," *Cytotechnology*, vol. 72, no. 3, pp. 357-366, 2020.
- [41] I. Crespo, M. V. García-Mediavilla, B. Gutiérrez, S. Sánchez-Campos, M. J. Tuñón, and J. González-Gallego, "A comparison of the effects of kaempferol and quercetin on cytokine-induced pro-inflammatory status of cultured human endothelial cells," *British Journal of Nutrition*, vol. 100, no. 5, pp. 968-976, 2008.
- [42] H. Feng, J. Cao, G. Zhang, and Y. Wang, "Kaempferol attenuates cardiac hypertrophy via regulation of ask1/mapk signaling pathway and oxidative stress," *Planta Medica*, vol. 83, no. 10, pp. 837-845, 2017.
- [43] J.-T. Yang, L.-B. Qian, F.-J. Zhang et al., "Cardioprotective effects of luteolin on ischemia/reperfusion injury in diabetic rats are modulated by eNOS and the mitochondrial permeability transition pathway," *Journal of Cardiovascular Pharmacology*, vol. 65, no. 4, pp. 349-356, 2015.
- [44] M. G. L. Hertog, E. J. M. Feskens, D. Kromhout et al., "Dietary antioxidant flavonoids and risk of coronary heart disease: the Zutphen elderly study," *The Lancet*, vol. 342, no. 8878, pp. 1007-1011, 1993.
- [45] H. Y. Wang, T. Li, R. Ji et al., "Metabolites of medicarpin and their distributions in rats," *Molecules*, vol. 24, no. 10, 2019.
- [46] C. Ma, R. Xia, S. Yang et al., "Formononetin attenuates atherosclerosis via regulating interaction between KLF4 and SRA in apoE $^{-/-}$ mice," *Theranostics*, vol. 10, no. 3, pp. 1090-1106, 2020.
- [47] Y. Li, J. Wang, L. Sun, and S. Zhu, "LncRNA myocardial infarction-associated transcript (MIAT) contributed to

- cardiac hypertrophy by regulating TLR4 via miR-93,” *European Journal of Pharmacology*, vol. 818, pp. 508–517, 2018.
- [48] Y. Ikeda, K.-I. Aihara, S. Yoshida et al., “Androgen-androgen receptor system protects against angiotensin II-induced vascular remodeling,” *Endocrinology*, vol. 150, no. 6, pp. 2857–2864, 2009.
- [49] A. D. P. Mansur, C. C. M. Nogueira, C. M. C. Strunz, J. M. Aldrighi, and J. A. F. Ramires, “Genetic polymorphisms of estrogen receptors in patients with premature coronary artery disease,” *Archives of Medical Research*, vol. 36, no. 5, pp. 511–517, 2005.
- [50] E. Berinstein and A. Levy, “Recent developments and future directions for the use of pharmacogenomics in cardiovascular disease treatments,” *Expert Opinion on Drug Metabolism & Toxicology*, vol. 13, no. 9, pp. 973–983, 2017.
- [51] T. Fernandes, C. V. Gomes-Gatto, N. P. Pereira, Y. R. Alayafi, V. J. Das Neves, and E. M. Oliveira, “NO signaling in the cardiovascular system and exercise,” *Advances in Experimental Medicine and Biology*, vol. 1000, pp. 211–245, 2017.
- [52] W. M. We, X. Y. Wu, S. T. Li, and Q. Shen, “PPARG gene C161T CT/TT associated with lower blood lipid levels and ischemic stroke from large-artery atherosclerosis in a Han population in Guangdong,” *Neurological Research*, vol. 38, no. 7, pp. 620–624, 2016.
- [53] G. A. Borillo, M. Mason, P. Quijada et al., “Pim-1 kinase protects mitochondrial integrity in cardiomyocytes,” *Circulation Research*, vol. 106, no. 7, pp. 1265–1274, 2010.
- [54] P. A. J. Krijnen, N. E. Hahn, I. Kholová et al., “Loss of DPP4 activity is related to a prothrombogenic status of endothelial cells: implications for the coronary microvasculature of myocardial infarction patients,” *Basic Research in Cardiology*, vol. 107, no. 1, 2012.
- [55] T. Miura and T. Miki, “GSK-3 β , a therapeutic target for cardiomyocyte protection,” *Circulation Journal*, vol. 73, no. 7, pp. 1184–1192, 2009.
- [56] F. Rolski and P. Błyszczuk, “Complexity of TNF- α signaling in heart disease,” *Journal of Clinical Medicine*, vol. 9, no. 10, p. 3267, 2020.
- [57] A. Ghigo, M. Laffargue, M. Li, and E. Hirsch, “PI3K and calcium signaling in cardiovascular disease,” *Circulation Research*, vol. 121, no. 3, pp. 282–292, 2017.
- [58] T. Jain, E. A. Nikolopoulou, Q. Xu, and A. Qu, “Hypoxia inducible factor as a therapeutic target for atherosclerosis,” *Pharmacology & Therapeutics*, vol. 183, no. xxxx, pp. 22–33, 2018.
- [59] X. Wu, H. Zhang, S. Fan et al., “Quality markers based on biological activity: a new strategy for the quality control of traditional Chinese medicine,” *Phytomedicine*, vol. 44, pp. 103–108, 2018.

Research Article

The Clinical Efficacy of Phytochemical Medicines Containing Tanshinol and Ligustrazine in the Treatment of Stable Angina: A Systematic Review and Meta-Analysis

Li Gao ^{1,2}, Tong Wu ¹, Juan Wang ¹, Zhuoran Xiao ¹, Chunhua Jia ¹,
and Wei Wang ¹

¹School of Traditional Chinese Medicine, Beijing University of Chinese Medicine, Beijing, China

²St Michael's Hospital, University of Toronto, Toronto, M5B 1W8, Canada

Correspondence should be addressed to Chunhua Jia; chjia11@163.com and Wei Wang; wangwei@bucm.edu.cn

Received 12 May 2020; Revised 22 November 2020; Accepted 21 January 2021; Published 3 February 2021

Academic Editor: Sai-Wang Seto

Copyright © 2021 Li Gao et al. This is an open access article distributed under the Creative Commons Attribution License, which permits unrestricted use, distribution, and reproduction in any medium, provided the original work is properly cited.

Background. Phytochemical medicines containing tanshinol and ligustrazine are commonly used in the treatment of stable angina in China, but their clinical effectiveness and risk have not been adequately assessed. In this paper, we conducted a systematic review and meta-analysis to evaluate the clinical efficacy. **Methods.** Relevant randomized controlled trials (RCTs) of phytochemical medicines containing tanshinol and ligustrazine in the treatment of stable angina were searched in electronic databases. The search date was up to March 31, 2020, and the languages of the RCTs were limited to English and Chinese. **Results.** A total of 28 studies, including 2518 patients, were included in the meta-analysis. It was shown that the adjunctive therapy of phytochemical medicines containing tanshinol and ligustrazine was better than the conventional therapies in the improvement of stable angina according to the clinical efficacy in symptoms ($n = 2518$, $RR = 1.24$, 95% CI: 1.20 to 1.29, $P < 0.01$) and clinical efficacy in electrocardiography ($n = 1766$, $RR = 1.29$, 95% CI: 1.19 to 1.40, $P < 0.01$). **Conclusion.** The meta-analysis supported the use of phytochemical medicines containing tanshinol and ligustrazine in the treatment of stable angina. However, quality of the evidence for this finding was low due to a high risk of bias in the included studies. Therefore, well-designed RCTs are still needed to further evaluate the efficacy.

1. Introduction

Stable angina is caused by fixed blockages in coronary arteries [1]. It typically occurs during activities, and the main symptoms are chest tightness and shortness of breath, which can be alleviated after a rest or administration of sublingual nitroglycerin [2–4]. Stable angina is a chronic coronary disease compared with unstable angina; however, it seriously affects patients' lives, such as restricting daily activities [5]. Then, the treatment aims to reduce morbidity and improve symptoms.

Currently, the main treatment of stable angina is medicine, such as nitroglycerin, beta-blockers, or calcium channel blockers, which focus on decreasing heart's workload and prevent episodes [6–9]. In China, phytochemical medicines are also used by many physicians. For example,

Shao et al. [10] conducted a meta-analysis to assess the efficacy of danshen injection (main component: salvianic acid A) in the treatment of angina pectoris and concluded that it is more effective than antianginal agents alone. Yu et al. [11] and Wang et al. [12] conducted randomized controlled trials in the treatment of stable angina, respectively, and found that xinxuekang capsule (main component: steroidal saponins) had a better efficacy compared with danshen tablets. In addition, for the treatment of unstable angina, many researchers have supported different phytochemical medicines, such as puerarin injection [13], safflower yellow injection [14], and danshen chuanxiongqin injection [15].

In these phytochemical medicines, tanshinol and ligustrazine are the commonly used components. Tanshinol is also named salvianic acid A, with a molecular formula $C_9H_{10}O_5$ [16]. Ligustrazine's molecular formula is $C_8H_{12}N_2$

[17]. Tanshinol has antioxidant capacity [18]; it can attenuate oxidative stress by decreasing the expressions of FoxO3a signaling [19] and improve cardiovascular injury by scavenging reactive oxygen species [20]. In addition, tanshinol can attenuate endothelial cell apoptosis, which helps reduce the aortic atherosclerotic lesion area [21]. Ligustrazine has effects on calcium channels; the research of Ren et al. [22] showed that ligustrazine could significantly suppress calcium transient and contraction in rabbits. It was also reported that the ligustrazine exhibits an anti-inflammatory effect; as Guo et al. described, the salvia ligustrazine injection could decrease high-sensitivity C-reactive protein and interleukin-6 levels [17, 23]. Ligustrazine was also found to suppress acid-sensing ion channels and reduce ischemia-induced infarct size in rats with angina [24]. The combination of tanshinol and ligustrazine has efficacy in dilating coronary arteries, reducing blood viscosity, promoting blood circulation, and removing blood stasis through synergistic action [25–27]. Ye et al. [28] investigated the anti-inflammatory effect of danshen, chuanxiong, and their combination and found that their combination has a dual anti-inflammatory effect on macrophages and endothelial cells. All these findings provide a biological basis of tanshinol and ligustrazine in the treatment of angina.

Tanshinol and ligustrazine are the main compounds of danshen and chuanxiong. There are several phytochemical medicines whose main components are tanshinol and ligustrazine, such as danshen chuanxiongqin injection, guanxinling injection, and shenxiong glucose injection. Several systematic reviews have been conducted to evaluate the efficacy of these medicines in the treatment of angina pectoris. Jia et al. [29] analyzed eligible RCTs using guanxinling injection, Zhang et al. [15] assessed danshen chuanxiongqin injection in treating unstable angina pectoris, and Liu and Ding [30] assessed shenxiong glucose injection in the treatment of unstable angina pectoris. In addition, many randomized controlled trials have been published to support the use of danshen and chuanxiongqin in the treatment of stable angina. However, in the treatment of stable angina, no relevant meta-analysis has been conducted to assess the clinical efficacy or the risk of phytochemical medicines containing tanshinol and ligustrazine. Therefore, in this study, a meta-analysis was conducted to evaluate the efficacy of phytochemical medicines in the treatment of stable angina.

2. Methods

The protocol of this study was registered in PROSPERO with the registration number CRD42018105921.

2.1. Database and Search Strategies. The following electronic databases were searched by two independent reviewers (Gao L. and Wang J.): Web of Science, Cochrane Library, PubMed, Chinese Biomedical Literature Database, Chinese National Knowledge Infrastructure, Chinese Scientific Journal Database, and Wanfang Database. The search date was up to March 31, 2020, and the languages of the

publications were limited to English and Chinese. The following search terms were used: (tanshinol OR salvianic acid A OR β -(3,4-dihydroxyphenyl) lactic acid OR danshensu OR danshen OR radix salvia OR salvia miltiorrhiza) AND (ligustrazine OR chuanxiong OR chuanxiongzine OR tetramethylpyrazine) AND (stable angina OR angina OR angina pectoris OR stenocardia OR angor pectoris) AND (randomized controlled trial).

2.2. Inclusion Criteria. The included studies must be RCTs.

Participants: patients who were diagnosed with stable angina were included. The stable angina was diagnosed according to the criteria [31, 32], with tests such as electrocardiography (ECG), exercise ECG, and symptoms of the patients.

Interventions: interventions using phytochemical medicines containing tanshinol and ligustrazine as a main treatment were chosen. The dosages of tanshinol and ligustrazine should be described specifically.

Comparators: the control groups received conventional treatments, such as taking medicines to treat and prevent angina attacks. Placeboes were also included.

Outcomes: the primary outcome was the clinical efficacy in symptoms and ECG; the secondary outcome is adverse event.

2.3. Exclusion Criteria. The exclusion criteria in the meta-analysis included (a) non-RCTs, case studies, experience summaries, animal experiments, and unpublished or repeated studies; (b) studies that used herbal medicines as the main intervention in addition to tanshinol and ligustrazine; (c) studies that used acupuncture or cupping as combined therapies; (d) patients who were identified as unstable angina; and (e) patients who have complications of heart failure, diabetes, stroke, or some other serious organic diseases.

2.4. Data Extraction and Quality Assessment. Four reviewers (Gao L, Wu T, Jia C, and Xiao Z) independently performed the data extraction and quality assessments. Meta-analysis was conducted using RevMan 5.3 software, and the risk of bias was assessed according to the Cochrane handbook [33]. Any disagreement was resolved by discussions among all reviewers.

3. Results

3.1. Description of the Included Studies. In this meta-analysis, 1613 studies were identified through database searching. But 500 repeated studies were excluded and 882 irrelevant studies were excluded through title and abstract reviewing. The full texts of 231 studies were assessed and 203 studies were excluded, including 75 studies that used some other herbal medicines in addition to tanshinol and ligustrazine in the intervention group, 96 studies included patients with unstable angina, 2 study lacked data on the dosages of

tanshinol and ligustrazine, 1 study lacked data to judge the efficacy, and 29 studies had patients with complications. At last, a total of 28 studies [34–61] were included in the meta-analysis. The screening process is summarized in a PRISMA flow diagram (Figure 1).

Details of the 28 studies are summarized in Table 1. There were 2518 patients in total, including 1276 patients in the intervention group and 1242 patients in the control group. Sample sizes of the studies were small, and only 8 studies had sample sizes greater than 100 patients. The youngest patient in these studies was 46 years old, while most of the studies reported patients older than 60 years old. Many patients had a long course of the disease, and the longest course was 25 years. In the control group, conventional treatments were used, such as nitroglycerin, beta-blockers, and calcium channel blockers. No study used a placebo. In the intervention group, phytochemical medicines containing tanshinol and ligustrazine were used based on the control group, except that one study that used a phytochemical medicine containing tanshinol and ligustrazine alone. The uses of tanshinol and ligustrazine were in different forms, 21 studies used danshen chuanxiongqin injection (DCI), 5 studies used shenxiong glucose injection (SGI), and 2 studies used danshen injection (DI) combined with ligustrazine injection (LI). The nature of constituents is botanical. 1 ml DCI contains 0.4 mg tanshinol and 20 mg ligustrazine, 1 ml SGI contains 0.2 mg tanshinol and 1 mg ligustrazine, and 1 ml DI contains 0.2 mg tanshinol. Details of the constituents of the 28 included studies are shown in Appendix table (available here). The treatment duration lasted from 7 days to 30 days. All the studies used clinical efficacy in symptoms as the main outcome, and 18 studies used clinical efficacy in ECG.

3.2. Risk of Bias. The risk of bias was high in the included studies (Figure 2). All the studies were described using randomization, but only five of these studies [35, 38, 44, 47, 55] reported using an appropriate method of random sequence generation. None of the studies described the method for allocation concealment, blinding of participants and personnel, and blinding of the outcome assessment.

3.3. Outcome Measurements. The outcome measurements of the included studies include clinical efficacy in symptoms, clinical efficacy in ECG, and adverse events.

3.3.1. Clinical Efficacy in Symptoms. The criteria for clinical efficacy in symptoms are defined as follows [62]: effective (the frequency of angina or the amount of nitroglycerine used is reduced by more than 50%) and no effect (the frequency of angina or the amount of nitroglycerine used is reduced by less than 50%).

All the studies showed that phytochemical medicines containing tanshinol and ligustrazine have better clinical efficacy in symptoms. Since low heterogeneity was observed in the meta-analysis ($I^2 = 43%$, which is lower than 50%), a

model of fixed effects was used to calculate the pooled estimation with an analysis of the dichotomous data using relative risk (RR), including 95% confidence intervals (CIs). The total meta-analysis showed favorable effects of phytochemical medicines on clinical efficacy ($n = 2518$, $RR = 1.24$, 95% CI: 1.20 to 1.29, $P < 0.01$) compared with the control group (Figure 3).

3.3.2. Clinical Efficacy in ECG. The criteria for clinical efficacy in ECG are defined as follows [62]: effective (recovery of ST-segment depression is more than 0.05 mV, or amplitude of the inverted T wave reduces more than 50%, or the shape of T wave changes from flat to upright) and no effect (no improvements in ECG compared with before).

Since high heterogeneity was observed in the meta-analysis ($I^2 = 64%$, which is higher than 50%), a model of random effects was used. The total meta-analysis showed favorable effects of phytochemical medicines on ECG ($n = 1766$, $RR = 1.29$, 95% CI: 1.19 to 1.40, $P < 0.01$) compared with the control group (Figure 4).

3.3.3. Adverse Events (AEs). Only 10 studies reported AEs, of which 7 studies [35, 39, 40, 49, 54, 56, 59] reported that there were no AEs. In the other three studies [38, 42, 55], two studies reported AEs in the intervention group, including 2 cases of skin rash, 1 case of epigastric discomfort, 1 case of insomnia, and 1 case of tiredness, and three studies reported AEs in the control group, including 2 cases of nausea, 1 case of stomachache, 1 case of dizziness, 2 cases of skin rash, 4 cases of epigastric discomfort, 3 cases of insomnia, and 3 cases of tiredness. Other studies did not report AEs.

4. Discussion

Currently, phytochemical medicines containing tanshinol and ligustrazine have been widely utilized by physicians to treat stable angina in China. However, it is controversial since there was no systematic review to assess the therapy's clinical efficacy. Therefore, this meta-analysis aimed to evaluate the efficacy or risk of phytochemical medicines in the treatment of stable angina.

In this meta-analysis, DCI and SGI were used by most studies. Both DCI and SGI consist of tanshinol and ligustrazine. As reported, DCI and SGI have been studied in the treatment of acute myocardial infarction [63], myocardial ischemia/reperfusion injury [64], and focal cerebral ischemia [65]. In the theory of traditional Chinese medicine, angina pectoris should be treated by supplementing qi and activating blood circulation. Tanshinol and ligustrazine are extracted from danshen and chuanxiong, which are two commonly used herbs in the treatment of cardiac diseases in China.

Tanshinol is the drug used for promoting blood circulation and removing blood stasis, which can improve cardiac function by increasing coronary blood flow and slowing the heart rate down [66]. Clinical practice has proved that salvia has a curative effect on myocardial hypoxia caused by myocardial infarction, and it plays a role

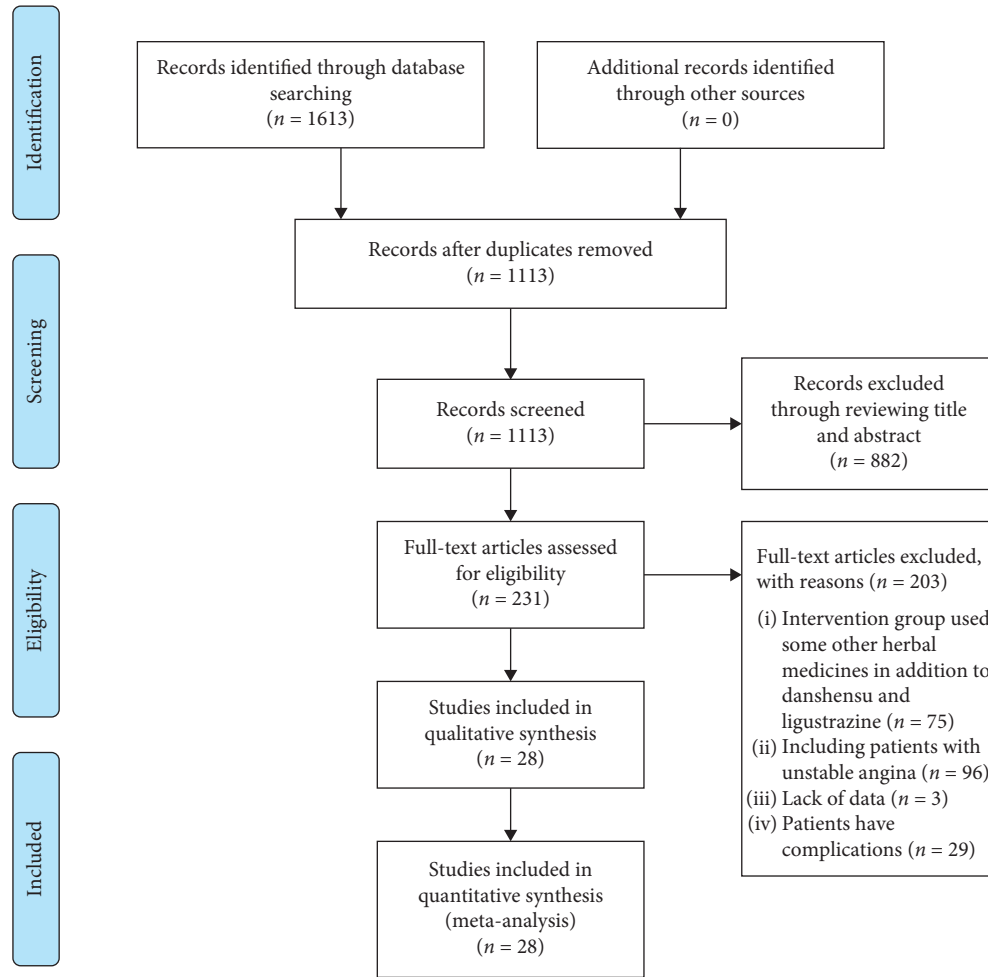


FIGURE 1: PRISMA flow diagram of the screening process.

TABLE 1: Details of the 28 included studies on phytochemical medicines containing tanshinol and ligustrazine in the treatment of stable angina.

Study	Sample size	Age (years)	Course of disease (years)	Intervention group	Control group	Treatment duration (days)	Main outcomes
Cao and Wang [34]	118 (59/59)	63.0 ± 14.0 61.5 ± 14.5	NR	DCI (10 ml) + TCR	Nifedipine 30–60 mg/d; metoprolol 100–200 mg/d; aspirin 100–300 mg/d; nitroglycerin when necessary	14	CES + ECG
Chen [35]	100 (50/50)	57.24 ± 9.64	NR	DCI (10 ml)	Aspirin 100 mg/d; atorvastatin 20 mg/d; trimetazidine 60 mg/d; nitroglycerin 10 mg/d	7	CES
Ding [36]	60 (30/30)	56–72	NR	DCI (10 ml) + TCR	Nitroglycerin	10	CES
Han [37]	60 (30/30)	64.9 ± 5.89 65.7 ± 7.93	NR	DCI (10 ml) + TCR	Nitrates; aspirin; calcium channel blockers	14	CES
He and Li [38]	70 (35/35)	48.2 ± 2.1	NR	DCI (10 ml) + TCR	Aspirin; nitrates	14	CES
Hu [39]	58 (30/28)	60 ± 8 59 ± 9	NR	DCI (10 ml) + TCR	Nitrates; beta-blockers; calcium channel blockers; aspirin	14	CES + ECG
Hua et al. [40]	70 (35/35)	64.7 ± 8.4 63.3 ± 8.3	0.5–10	DCI (10 ml) + TCR	Isosorbide mononitrate 25 mg/d; quinapril 10 mg/d; metoprolol 50 mg/d; aspirin 100 mg/d	14	CES + ECG

TABLE 1: Continued.

Study	Sample size	Age (years)	Course of disease (years)	Intervention group	Control group	Treatment duration (days)	Main outcomes
Jia [41]	76 (38/38)	62.04 ± 2.15 61.92 ± 2.13	NR	DCI (10 ml) + TCR	Aspirin 100 mg/d; atorvastatin 20 mg/d; trimetazidine 60 mg/d; isosorbide mononitrate 40 mg/d	7	CES
Lan [42]	216 (116/100)	57.6 ± 4.6 58.1 ± 5.2	7.62 ± 3.87 8.91 ± 4.28	DCI (10 ml) + TCR	Nitrates; beta-blockers; calcium channel blockers; aspirin	14	CES + ECG
Li et al. [43]	80 (40/40)	67.3 ± 6.20	3.5 ± 1.6	DCI (10 ml) + TCR	Isosorbide mononitrate 40 mg/d; metoprolol 47.5 mg/d; aspirin 100 mg/d; trimetazidine 60 mg/d	14	CES + ECG
Li and Li [44]	80 (40/40)	58.93 ± 2.07 58.42 ± 2.31	4.45 ± 1.43 4.37 ± 1.52	DCI (10 ml) + TCR	Aspirin 100 mg/d; atorvastatin 20 mg/d; trimetazidine 60 mg/d; isosorbide mononitrate 40 mg/d	7	CES
Li [45]	216 (108/108)	64.7 ± 4.8	10.6 ± 1.2	DCI (10 ml) + TCR	Aspirin; calcium channel blockers; beta-blockers; nitrates	14	CES + ECG
Liu and Li [46]	60 (30/30)	63.7 ± 7.7 64.9 ± 9.4	NR	SGI (100 ml) + TCR	Nitrates; aspirin; beta-blockers; calcium channel blockers; ACE inhibitors; ARBs	14	CES
Ma et al. [47]	80 (40/40)	NR	NR	DCI (10 ml) + TCR	Nitrates; beta-blockers; calcium channel blockers; aspirin	14	CES + ECG
Ma et al. [48]	104 (52/52)	63.74 ± 11.83 62.34 ± 10.63	NR	SGI (100 ml) + TCR	Aspirin 100 mg/d; isosorbide mononitrate 40 mg/d; metoprolol 50 mg/d; atorvastatin 20 mg/d	14	CES
Ou [49]	60 (30/30)	60.33 ± 10.04 61.21 ± 9.36	0.08–12 0.16–13	SGI (100 ml) + TCR	Nitrates; beta-blockers; calcium channel blockers; antiplatelet drug	14	CES + ECG
Pang and Liu [50]	64 (32/32)	77.2 ± 5.6	6–20	SGI (200 ml) + TCR	Antiplatelet drug; beta-blockers; statins; ACE inhibitors; ARBs; nitrates; lipid-lowering drug; hypotensor; nitroglycerin; isosorbide mononitrate 20 mg/d	14	CES + ECG
Sun [51]	80 (40/40)	72.3 ± 0.2 71.9 ± 0.4	5.2 ± 0.6 5.1 ± 0.4	DCI (5 ml) + TCR	Antiplatelet drug; thrombolytic drug; lipid-lowering drug; hypotensor; digoxin when necessary	30	CES + ECG
Tian [52]	62 (32/30)	61.68 ± 10.98 60.39 ± 9.76	NR	DCI (20 ml) + TCR	Nitrates; calcium channel blockers	14	CES
Wang and Wang [54]	62 (31/31)	46–58	3–18	DI (20 ml) + LI (80 mg) + TCR	Nitrates; beta-blockers; calcium channel blockers	14	CES + ECG
Wang and Lian [53]	105 (56/49)	51–75	1.6–25	DCI (10 ml) + TCR	Nitrates; beta-blockers; calcium channel blockers; aspirin	14	CES + ECG
Xi [55]	80 (40/40)	59.3 ± 6.4 62.4 ± 5.3	5.9 ± 0.6 4.8 ± 0.8	DCI (10 ml) + TCR	Aspirin; atorvastatin; nitroglycerin	14	CES
Xie and Zhu [56]	104 (52/52)	51–79	1.6–25	DI (20–30 ml) + LI (40–80 mg) + TCR	Nitrates; beta-blockers; calcium channel blockers; aspirin	14	CES + ECG
Xing [57]	100 (50/50)	66.2 ± 5.60	2.8 ± 1.8	DCI (10 ml) + TCR	Isosorbide mononitrate 40 mg/d; aspirin 100 mg/d	14	CES + ECG
Xiong and Wang [58]	85 (46/39)	52–71	1.6–25	DCI (10 ml) + TCR	Nitrates; beta-blockers; calcium channel blockers; aspirin	14	CES + ECG

TABLE 1: Continued.

Study	Sample size	Age (years)	Course of disease (years)	Intervention group	Control group	Treatment duration (days)	Main outcomes
Xu and Qin [59]	84 (42/42)	56.14 ± 7.40 51.20 ± 7.30	1–13 2–12	DCI (10 ml) + TCR	Nitrates; aspirin; beta-blockers; nitroglycerin when necessary	14	CES + ECG
Yu and Fang [60]	94 (47/47)	NR	NR	DCI (5–10 ml) + TCR	Antiplatelet drug; thrombolytic drug; lipid-lowering drug; hypotensor; digoxin when necessary	20	CES + ECG
Zhang [61]	90 (45/45)	68.21 ± 9.26 68.52 ± 9.39	NR	SGI (200 ml) + TCR	Antiplatelet drug; anticoagulant; ACE inhibitors; beta-blockers; calcium channel blockers; statins; nitrates	10–14	CES + ECG

NR: not reported; DCI: danshen chuanxiongqin injection; SGI: shenxiong glucose injection; DI: danshen injection; LI: ligustrazine injection; GI: guanxinning injection; TCR: treatments in the control group; ACE: angiotensin-converting enzyme; ARBs: angiotensin receptor blockers; CES: clinical efficacy in symptoms; ECG: electrocardiography.

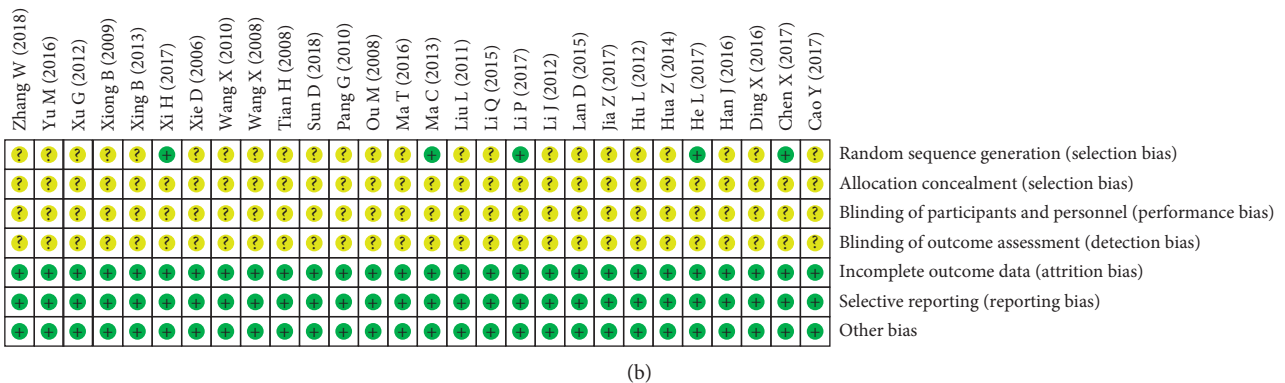
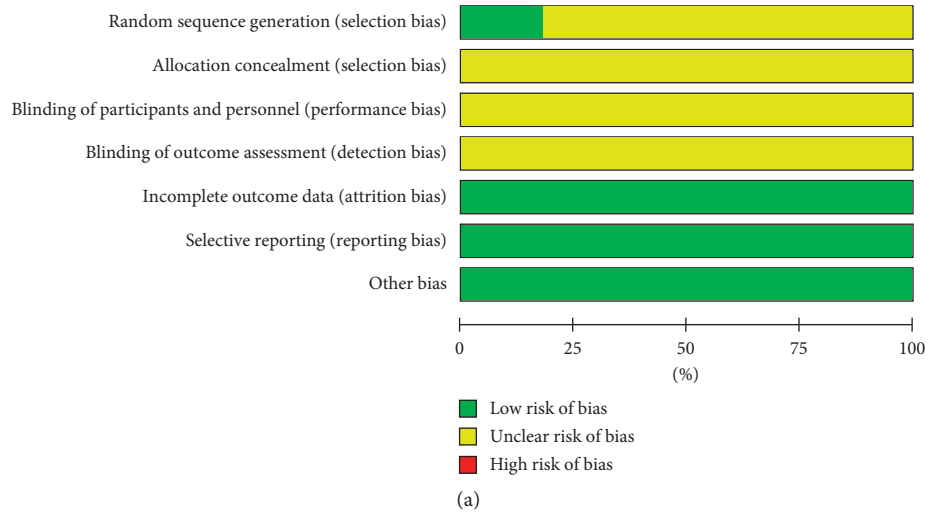


FIGURE 2: Risk of bias graph: (a) risk of bias in all included studies; (b) risk of bias summary.

in anticoagulation by dilating peripheral vessels to reduce blood pressure and improving cAMP (cyclic adenosine monophosphate) in cells [67, 68]. Ligustrazine is a kind of active alkaloid, which is effective to dilate coronary arteries and reduce coronary resistance. Ligustrazine is efficient in increasing coronary blood flow and improving myocardial oxygen supply, making it commonly to be used to inhibit platelet aggregation and depolymerize the aggregated

platelets [69, 70]. In the treatment of cardiac diseases, tanshinol and ligustrazine can promote blood circulation, dilate coronary arteries, and inhibit platelet aggregation [29, 71], which provides a rationale in the treatment of stable angina.

Heterogeneity in this meta-analysis was moderate, with clinical efficacy in symptoms of $I^2 = 43\%$, and clinical efficacy in ECG of $I^2 = 64\%$. The reasons for this may be that different

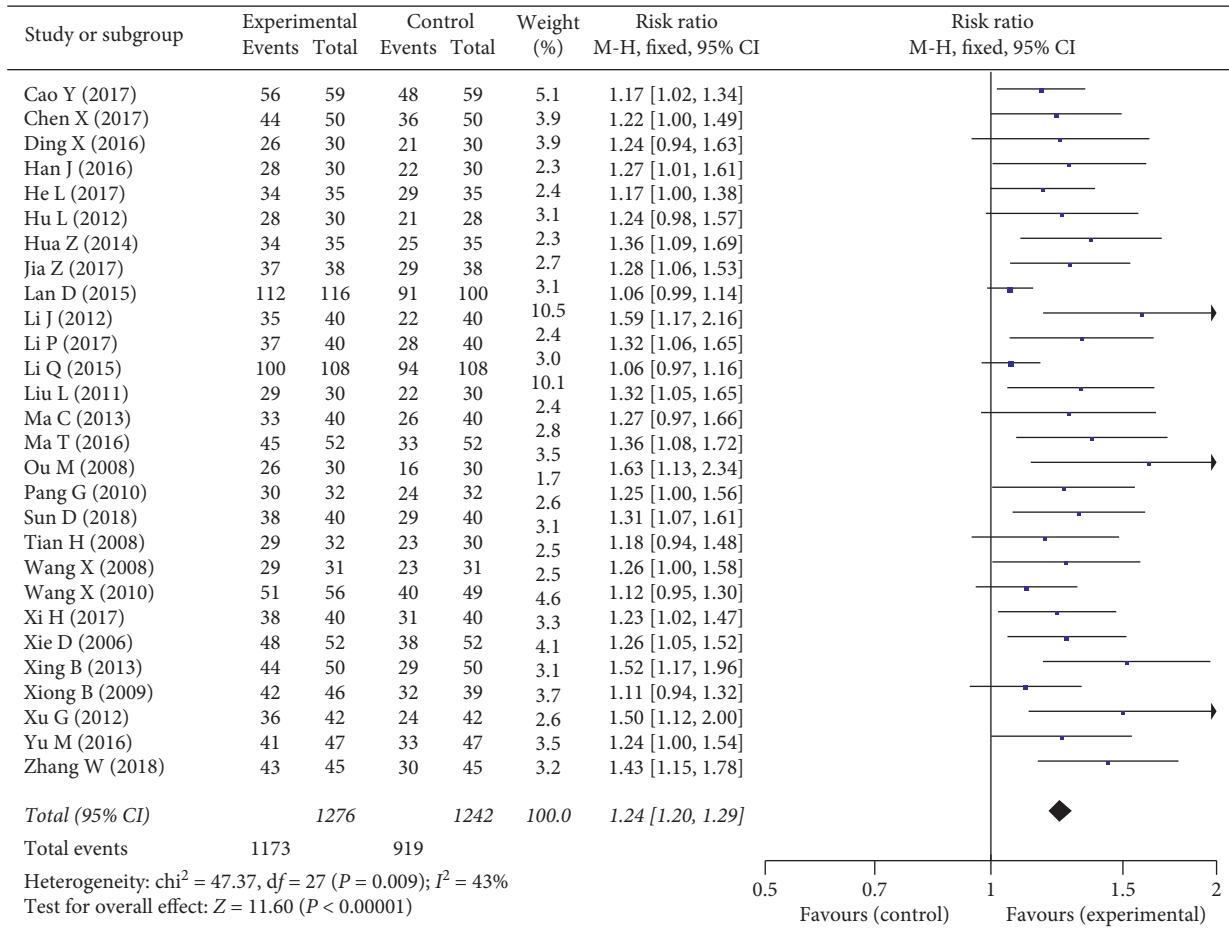


FIGURE 3: Forest plot of the clinical efficacy in symptoms of phytochemical medicines containing tanshinol and ligustrazine in the treatment of stable angina.

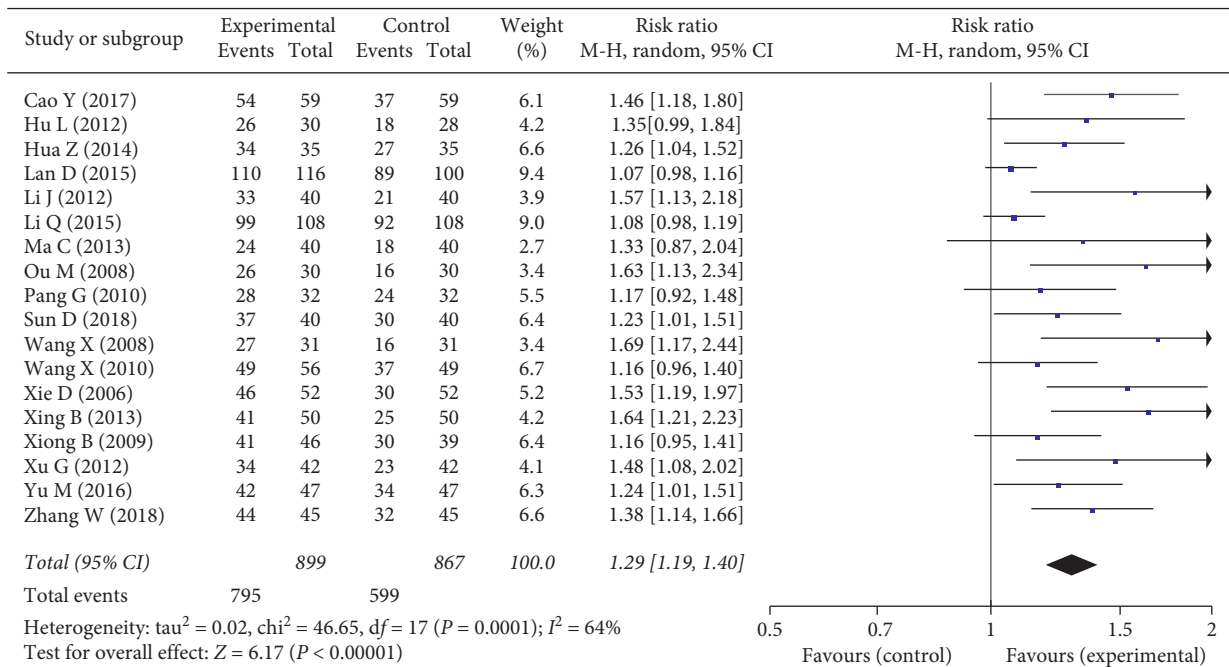


FIGURE 4: Forest plot of the clinical efficacy in ECG of phytochemical medicines containing tanshinol and ligustrazine in the treatment of stable angina.

conventional treatments were used in different control groups. Therapies in the intervention group were based on the control group; different therapies make the efficacy hard to be assessed.

The high risk of bias of the included studies makes the methodological quality for this finding low. There are several limitations to this systematic review. First, for most of the included studies, the methods for randomization, allocation concealment, and blinding were not reported clearly. Second, in the 28 included studies, only 8 studies had sample sizes greater than 100 patients, and the small sample sizes in most studies made meaningful conclusions difficult to be drawn. Third, clinical efficacy was the main outcome measurement for most studies, but a bias from the physicians may decrease the reliability and validity of the studies. Fourth, all the studies were published in China, which may limit the generalization of the findings.

5. Conclusion

In conclusion, this meta-analysis included 28 studies that used phytochemical medicines containing tanshinol and ligustrazine in the treatment of stable angina, and the results supported their clinical application. However, the studies analyzed to date are of relatively low quality. More rigorous RCTs with large sample sizes are needed to further evaluate the clinical efficacy and the adverse effects.

Abbreviations

RCTs: Randomized controlled trials
 ECG: Electrocardiography
 DCI: Danshen chuanxiongqin injection
 SGI: Shenxiong glucose injection
 DI: Danshen injection
 LI: Ligustrazine injection
 CIs: Confidence intervals
 AEs: Adverse events
 TCR: Treatments in the control group
 ACE: Angiotensin-converting enzyme
 ARBs: Angiotensin receptor blockers
 CES: Clinical efficacy in symptoms.

Data Availability

All data generated or analyzed during this study are included in this published article and its supplementary information files.

Additional Points

Highlights. (i) It was the first meta-analysis assessing the efficacy of phytochemical medicines containing tanshinol and ligustrazine in the treatment of stable angina. (ii) The clinical efficacy and safety of phytochemical medicines containing tanshinol and ligustrazine in the treatment of stable angina were comprehensively assessed. (iii) The efficacy of phytochemical medicines containing tanshinol and ligustrazine in the treatment of stable angina needed to be further evaluated.

Conflicts of Interest

The authors declare that they have no conflicts of interest.

Authors' Contributions

LG contributed to conception, acquisition, analysis, and interpretation; TW contributed to acquisition, analysis, and interpretation; JW contributed to interpretation; ZX contributed to acquisition and analysis; CJ contributed to acquisition and analysis; WW contributed to conception and interpretation. All authors drafted manuscript, revised manuscript, gave final approval, and agreed to be accountable for all aspects of work ensuring integrity and accuracy.

Acknowledgments

This study was supported by China Postdoctoral Science Foundation (Grant no. 2019M650598), Fundamental Research Funds for the Central Universities (Grant no. 2019-JYB-JS-005), National Natural Science Foundation of China (Grant no. 81874514), and National Key Research and Development Program of China (Grant no. 2017YFC1700102).

Supplementary Materials

File name: Appendix table. Title of data: summary table of the constituents of the 28 included studies. Description of data: statements of the constituents of the included studies. (*Supplementary Materials*)

References

- [1] R. Al-Lamee, D. Thompson, H.-M. Dehbi et al., "Percutaneous coronary intervention in stable angina (ORBITA): a double-blind, randomised controlled trial," *The Lancet*, vol. 391, no. 10115, pp. 31–40, 2018.
- [2] D. Tousoulis, "Editorial (hot topics: stable angina pectoris: novel therapeutic insights)," *Current Pharmaceutical Design*, vol. 19, no. 9, p. 1549, 2013.
- [3] S. V. Arnold, D. L. Bhatt, G. W. Barsness et al., "Clinical management of stable coronary artery disease in patients with type 2 diabetes mellitus: a scientific statement from the American heart association," *Circulation*, vol. 141, no. 19, 2020.
- [4] T. A. Rousan and U. Thadani, "Stable angina medical therapy management guidelines: a critical review of guidelines from the European society of cardiology and national institute for health and care excellence," *European Cardiology Review*, vol. 14, no. 1, pp. 18–22, 2019.
- [5] G. Andrikopoulos, J. Parissis, G. Filippatos et al., "Hellenic cardiovasc res S: medical management of stable angina," *Hellenic Journal of Cardiology*, vol. 55, no. 4, pp. 272–280, 2014.
- [6] M. Glezer, Y. Vasyuk, and Y. Karpov, "Efficacy of ivabradine in combination with beta-blockers versus uptitration of beta-blockers in patients with stable Angina (CONTROL-2 study)," *Advances in Therapy*, vol. 35, no. 3, pp. 341–352, 2018.

- [7] T. A. Rousan, S. T. Mathew, and U. Thadani, "Drug therapy for stable angina pectoris," *Drugs*, vol. 77, no. 3, pp. 265–284, 2017.
- [8] K. L. Gould and N. P. Johnson, "Nitroglycerine and angina," *Circulation*, vol. 136, no. 1, pp. 35–38, 2017.
- [9] W. Liao, X. Ma, J. Li et al., "A review of the mechanism of action of dantonic for the treatment of chronic stable angina," *Biomedicine & Pharmacotherapy*, vol. 109, pp. 690–700, 2019.
- [10] H. Shao, M. Li, F. Chen, L. Chen, Z. Jiang, and L. Zhao, "The efficacy of danshen injection as adjunctive therapy in treating angina pectoris: a systematic review and meta-analysis," *Heart, Lung and Circulation*, vol. 27, no. 4, pp. 433–442, 2018.
- [11] Y. N. Yu, S. Y. Hu, G. X. Li et al., "Comparative effectiveness of di'ao xin xue kang capsule and compound danshen tablet in patients with symptomatic chronic stable angina," *Scientific Reports*, vol. 4, no. 7058, 2014.
- [12] L.-Y. Wang, J.-Y. Tang, J. Liu et al., "Dynamic changes in phenotypic groups in patients with stable angina pectoris after treatment with xinxuekang capsule: a randomized controlled trial," *Current Vascular Pharmacology*, vol. 13, no. 4, pp. 492–503, 2015.
- [13] Z. Gao, B. Wei, and C. Qian, "Puerarin injection for treatment of unstable angina pectoris: a meta-analysis and systematic review," *International Journal of Clinical and Experimental Medicine*, vol. 8, no. 9, pp. 14577–14594, 2015.
- [14] D. Kong, W. Xia, Z. Zhang et al., "Safflower yellow injection combined with conventional therapy in treating unstable angina pectoris: a meta-analysis," *Journal of Traditional Chinese Medicine*, vol. 33, no. 5, pp. 553–561, 2013.
- [15] X. Zhang, J. Wu, B. Zhang, and W. Zhou, "Danshenchuanxiongqin injection in the treatment of unstable angina pectoris: a systematic review and meta-analysis," *Journal of Traditional Chinese Medicine = Chung I Tsa Chih Ying Wen pan*, vol. 36, no. 2, pp. 144–150, 2016.
- [16] Y. Wang, X. Huang, F. Qin et al., "A strategy for detecting optimal ratio of cardioprotection-dependent three compounds as quality control of Guan-Xin-Er-Hao formula," *Journal of Ethnopharmacology*, vol. 133, no. 2, pp. 735–742, 2011.
- [17] M. Guo, Y. Liu, and D. Shi, "Cardiovascular actions and therapeutic potential of tetramethylpyrazine (active component isolated from rhizoma chuanxiong): roles and mechanisms," *BioMed Research International*, vol. 2016, Article ID 2430329, 9 pages, 2016.
- [18] Y. S. Sun, H. F. Zhu, J. H. Wang, Z. B. Liu, and J. J. Bi, "Isolation and purification of salvianolic acid A and salvianolic acid B from *Salvia miltiorrhiza* by high-speed counter-current chromatography and comparison of their antioxidant activity," *Journal of Chromatography B*, vol. 877, no. 8–9, pp. 733–737, 2009.
- [19] Y. Yang, Y. Su, D. Wang et al., "Tanshinol attenuates the deleterious effects of oxidative stress on osteoblastic differentiation via Wnt/FoxO3a signaling," *Oxidative Medicine and Cellular Longevity*, vol. 2013, Article ID 351895, 18 pages, 2013.
- [20] J. Ho and C.-Y. Hong, "Salvianolic acids: small compounds with multiple mechanisms for cardiovascular protection," *Journal of Biomedical Science*, vol. 18, no. 1, p. 30, 2011.
- [21] C. Chen, G. Cheng, X. Yang, C. Li, R. Shi, and N. Zhao, "Tanshinol suppresses endothelial cells apoptosis in mice with atherosclerosis via lncRNA TUG1 up-regulating the expression of miR-26a," *American Journal of Translational Research*, vol. 8, no. 7, pp. 2981–2991, 2016.
- [22] Z. Ren, J. Ma, P. Zhang et al., "The effect of ligustrazine on L-type calcium current, calcium transient and contractility in rabbit ventricular myocytes," *Journal of Ethnopharmacology*, vol. 144, no. 3, pp. 555–561, 2012.
- [23] W. Wu, X. Yu, X.-P. Luo, S.-H. Yang, and D. Zheng, "Tetramethylpyrazine protects against scopolamine-induced memory impairments in rats by reversing the cAMP/PKA/CREB pathway," *Behavioural Brain Research*, vol. 253, pp. 212–216, 2013.
- [24] Z. G. Zhang, X. L. Zhang, X. Y. Wang, Z. R. Luo, and J. C. Song, "Inhibition of acid sensing ion channel by ligustrazine on angina model in rat," *American Journal of Translational Research*, vol. 7, no. 10, pp. 1798–1811, 2015.
- [25] X. Lv, H. Lu, M. Cao, X. Liu, and W. She, "Application of danshenchuanxiongqin injection," *Chinese Journal of Practical Internal Medicine*, vol. 29, no. S2, pp. 219–221, 2009.
- [26] R. Wang, Q. Han, Y. Jia, and J. Lv, "Effect of danshen chuanxiongqin injection on the myocardial damage of unstable angina patients undergoing percutaneous coronary intervention," *Chinese Journal of Integrated Traditional and Western Medicine*, vol. 31, no. 7, pp. 899–902, 2011.
- [27] Z. Liu, Y. Wu, X. Jiang et al., "Pharmacokinetic study of Tanshinol's impact on ligustrazine hydrochloride from *Salvia miltiorrhiza* ligustrazine hydrochloride injection in rats," *West China Journal of Pharmaceutical Sciences*, vol. 32, no. 2, pp. 182–185, 2017.
- [28] T. Ye, Y. Li, D. Xiong et al., "Combination of Danshen and ligustrazine has dual anti-inflammatory effect on macrophages and endothelial cells," *Journal of Ethnopharmacology*, vol. 266, Article ID 113425, 2021.
- [29] Y. L. Jia, S. W. Leung, M. Y. Lee, G. Z. Cui, X. H. Huang, and F. H. Pan, "The efficacy of guanxinling injection in treating angina pectoris: systematic review and meta-analysis of randomized controlled trials," *Evidence-Based Complementary and Alternative Medicine*, vol. 2013, Article ID 282707, 16 pages, 2013.
- [30] G. Liu and B. Ding, "Meta-analysis of shenqi glucose injection in the treatment of unstable angina pectoris," *Journal of Emergency in Traditional Chinese Medicine*, vol. 25, no. 2, pp. 272–275, 2016.
- [31] T. D. Fraker, S. D. Fihn, R. J. Gibbons et al., "2007 chronic angina focused update of the ACC/AHA 2002 guidelines for the management of patients with chronic stable angina," *Circulation*, vol. 116, no. 23, pp. 2762–2772, 2007.
- [32] F. H. Messerli, G. Mancina, C. R. Conti, and C. J. Pepine, "Guidelines on the management of stable angina pectoris: executive summary: the task force on the management of stable angina pectoris of the european society of cardiology," *European Heart Journal*, vol. 27, no. 23, pp. 2902–2903, 2006.
- [33] J. P. T. Higgins, D. G. Altman, P. C. Gotzsche et al., "The cochrane collaboration's tool for assessing risk of bias in randomised trials," *BMJ*, vol. 343, p. d5928, 2011.
- [34] Y. Cao and Z. Wang, "Therapeutic effect of danshen ligustrazine injection on angina pectoris," *Contemporary Medical Symposium*, vol. 15, no. 16, pp. 175–176, 2017.
- [35] X. Chen, "Clinical analysis of 50 cases of angina pectoris treated by danshen ligustrazine injection," *China Practical Medicine*, vol. 12, no. 11, pp. 145–146, 2017.
- [36] X. Ding, "Treatment of 30 cases of angina pectoris in the elderly by danshen ligustrazine injection," *For All Health*, vol. 10, no. 35, pp. 149–150, 2016.
- [37] J. Han, "Effect of danshen ligustrazine injection on angina pectoris in the elderly," *World Latest Medicine Information*, vol. 16, no. 79, p. 208, 2016.

- [38] L. He and S. Li, "Study of the effect of danshen ligustrazine injection on angina pectoris," *Cardiovascular Disease Journal of Integrated Traditional Chinese and Western Medicine (Electronic)*, vol. 5, no. 1, pp. 74-75, 2017.
- [39] L. Hu, "Observation on the therapeutic effect of danshen ligustrazine injection on angina pectoris," *Journal of Medical Forum*, vol. 33, no. 4, pp. 106-107, 2012.
- [40] Z. Hua, R. Chen, and C. Ran, "Observation on the efficacy of danshen ligustrazine injection in the treatment of angina pectoris," *Medical Aesthetics and Cosmetology*, vol. 10, pp. 24-25, 2014.
- [41] Z. Jia, "Clinical observation of danshen ligustrazine injection in treating angina pectoris in elderly patients," *Journal of Clinical Medical Literature*, vol. 4, no. 63, p. 12426, 2017.
- [42] D. Lan, "Clinical observation of danshen ligustrazine injection in treating angina pectoris," *Contemporary Medicine*, vol. 21, no. 16, pp. 154-155, 2015.
- [43] J. Li, M. Ceng, and J. Liang, "Treatment of 40 cases of stable angina pectoris in elderly patients with danshen ligustrazine injection," *World Health Digest*, vol. 9, no. 51, pp. 381-382, 2012.
- [44] P. Li and F. Li, "Clinical efficacy of danshen ligustrazine injection in the treatment of angina pectoris," *Psychological Doctor*, vol. 23, no. 14, p. 69, 2017.
- [45] Q. Li, "To explore the clinical observation of 108 cases of angina pectoris of coronary heart disease treated by dancan chuanxiongqin zhushuye," *Cardiovascular Disease Journal of Integrated Traditional Chinese and Western Medicine*, vol. 3, no. 1, pp. 79-80, 2015.
- [46] L. Liu and Z. Li, "Clinical observation on 60 cases of angina pectoris treated by shenxiong glucose injection," *Chinese Journal of Modern Drug Application*, vol. 5, no. 11, pp. 69-70, 2011.
- [47] C. Ma, P. Qu, and L. Li, "Therapeutic effect of danshen ligustrazine injection on 80 patients with angina pectoris," *China Health Care & Nutrition*, vol. 1, p. 213, 2013.
- [48] T. Ma, F. Yuan, and F. Ma, "Clinical observation on the effect of shenxiong glucose injection in treating coronary heart disease," *World Chinese Medicine*, vol. 11, no. 9, pp. 1743-1745, 2016.
- [49] M. Ou, "Clinical observation of shenxiong glucose injection in treating angina pectoris," *Modern Hospitals*, vol. 8, no. 4, pp. 46-47, 2008.
- [50] G. Pang and X. Liu, "Therapeutic effect of shenxiong glucose injection on elderly patients with angina pectoris," *Modern Journal of Integrated Traditional Chinese and Western Medicine*, vol. 19, no. 22, pp. 2764-2765, 2010.
- [51] D. Sun, "Application of danshen ligustrazine injection in the treatment of angina pectoris and analysis of symptoms," *Bao Jian Wen Hui*, vol. 5, p. 138, 2018.
- [52] H. Tian, "Therapeutic effect of danshen ligustrazine injection on stable angina pectoris," *Chinese Journal of Misdiagnosis*, vol. 8, no. 29, p. 7098, 2008.
- [53] X. Wang and H. Lian, "Therapeutic observation of danshen ligustrazine injection on angina pectoris," *Medical Journal of Chinese People's Health*, vol. 22, no. 10, p. 1257, 2010.
- [54] X. Wang and Y. Wang, "Comparison of danshen injection combined with ligustrazine and conventional drugs in treating angina pectoris," *Journal of Practical Medical Techniques*, vol. 15, no. 7, pp. 870-871, 2008.
- [55] H. Xi, "Effect of danshen ligustrazine injection on angina pectoris and its effect on plasma endothelin and carbon monoxide levels in patients," *Contemporary Medicine*, vol. 23, no. 31, pp. 84-86, 2017.
- [56] D. Xie and Y. Zhu, "Efficacy observation of danshen injection plus ligustrazine in the treatment of angina pectoris," *Journal of Practical Medical Techniques*, vol. 13, no. 11, p. 1868, 2006.
- [57] B. Xing, "Efficacy observation of danshen chuanxiong injection in the treatment of 100 patients with stable angina pectoris in the elderly," *China Health Care & Nutrition*, vol. 10, pp. 6069-6070, 2013.
- [58] B. Xiong and P. Wang, "Clinical observation on 85 cases of angina pectoris treated by danshen ligustrazine injection," *Northwest Pharmaceutical Journal*, vol. 24, no. 4, pp. 300-301, 2009.
- [59] G. Xu and L. Qin, "Clinical research of danshen and chuanxiongqin injection on angina pectoris," *Journal of Emergency in Traditional Chinese Medicine*, vol. 21, no. 4, pp. 614-615, 2012.
- [60] M. Yu and S. Fang, "Clinical curative effect observation of salvia miltiorrhiza ligustrazine injection in treating angina pectoris of coronary heart disease," *Clinical Journal of Chinese Medicine*, vol. 8, no. 6, pp. 44-45, 2016.
- [61] W. Zhang, "Therapeutic value of shenxiong glucose injection for angina pectoris," *Guide of China Medicine*, vol. 16, no. 19, pp. 52-53, 2018.
- [62] H. Ma, L. Shen, R. Gao, W. Qi, and Y. Huo, "Guidelines for the diagnosis and treatment of chronic stable angina," *Chinese Journal of Cardiology*, vol. 35, no. 3, pp. 195-206, 2007.
- [63] Z.-H. Wang, J.-H. Pan, X.-P. Ma et al., "Cardioprotective effect of Shenxiong glucose injection on acute myocardial infarction in rats via reduction in myocardial intracellular calcium ion overload," *Tropical Journal of Pharmaceutical Research*, vol. 16, no. 5, pp. 1097-1104, 2017.
- [64] W. Huang, Y. Yang, Z. Zeng, M. Su, Q. Gao, and B. Zhu, "Effect of Salvia miltiorrhiza and ligustrazine injection on myocardial ischemia/reperfusion and hypoxia/reoxygenation injury," *Molecular Medicine Reports*, vol. 14, no. 5, pp. 4537-4544, 2016.
- [65] J. Cai, R. Pan, X. Jia et al., "The combination of astragalus membranaceus and ligustrazine ameliorates micro-haemorrhage by maintaining blood-brain barrier integrity in cerebrally ischaemic rats," *Journal of Ethnopharmacology*, vol. 158, pp. 301-309, 2014.
- [66] H. B. Liu, J. Xu, Y. Peng, J. J. Zhou, and P. G. Xiao, "Targets of danshen's active components for activating blood circulation activities," *Acta Phys-Chim Sin*, vol. 26, no. 1, pp. 199-205, 2010.
- [67] W.-y. Wu and Y.-p. Wang, "Pharmacological actions and therapeutic applications of Salvia miltiorrhiza depside salt and its active components," *Acta Pharmacologica Sinica*, vol. 33, no. 9, pp. 1119-1130, 2012.
- [68] H. Y. Fan, F. H. Fu, M. Y. Yang, H. Xu, A. H. Zhang, and K. Liu, "Antiplatelet and antithrombotic activities of salvia-nolic acid A," *Thrombosis Research*, vol. 126, no. 1, pp. E17-E22, 2010.
- [69] J. Zou, P. Gao, X. Hao, H. Xu, P. Zhan, and X. Liu, "Recent progress in the structural modification and pharmacological activities of ligustrazine derivatives," *European Journal of Medicinal Chemistry*, vol. 147, pp. 150-162, 2018.
- [70] Y. Wang, H. Zhu, J. Tong, and Z. Li, "Ligustrazine improves blood circulation by suppressing platelet activation in a rat model of allergic asthma," *Environmental Toxicology and Pharmacology*, vol. 45, pp. 334-339, 2016.
- [71] Y. Sun, S. Li, and C. Quan, "Solubility of ferulic acid and tetramethylpyrazine in supercritical carbon dioxide," *Journal of Chemical & Engineering Data*, vol. 50, no. 4, pp. 1125-1128, 2005.

Review Article

Gastrodia elata Blume (Tianma): Hope for Brain Aging and Dementia

Klaus Heese 

Graduate School of Biomedical Science and Engineering, Hanyang University, 222 Wangsimni-ro, Seongdong-gu, Seoul 133791, Republic of Korea

Correspondence should be addressed to Klaus Heese; klaus@hanyang.ac.kr

Received 19 August 2020; Revised 26 October 2020; Accepted 3 November 2020; Published 28 December 2020

Academic Editor: Yong Wang

Copyright © 2020 Klaus Heese. This is an open access article distributed under the Creative Commons Attribution License, which permits unrestricted use, distribution, and reproduction in any medium, provided the original work is properly cited.

Since aging-related diseases, including dementia, represent major public health threats to our society, physician-scientists must develop innovative, interdisciplinary strategies to open new avenues for development of alternative therapies. One such novel approach may lie in traditional Chinese medicine (TCM). *Gastrodia elata* Blume (*G. elata*, tianma) is a TCM frequently used for treatment of cerebrocardiovascular diseases (CCVDs). Recent studies of *G. elata*-based treatment modalities, which have investigated its pharmacologically relevant activity, potential efficacy, and safety, have employed *G. elata* in well-characterized, aging-related disease models, with a focus on models of aging-related dementia, such as Alzheimer's disease (AD). Here, I examine results from previous studies of *G. elata*, as well as related herbal preparations and pure natural products, as prophylaxis and remedies for aging-related CCVDs and dementia. Concluding, data suggest that tianma treatment may be used as a promising complementary therapy for AD.

1. Introduction

Aging-related dementia, which is mediated by damage to brain cells induced by pathways, such as those underlying Alzheimer's disease (AD), cerebrocardiovascular diseases (CCVDs), and other neurodegenerative diseases (NDs), is causing great inquietude, anxiety, and discomposure in an aging society [1–7]. The World Health Organization (WHO) has recognized the imperative for globally coordinated research to combat dementia [8]. Much hope has been based on use of stem cell-based therapies; however, such approaches still have to overcome major challenges [9].

Thus, with dementia posing a health threat to elderly people, social awareness of healthy lifestyle choices that can prevent aging-related neuroinflammation and cognitive dysfunction has been attracting increasing attention. In particular, a healthy diet, exercise, and caloric restriction have been demonstrated to be preventive against new-onset AD and to effectively ameliorate the symptoms of AD [10, 11]. Familial (early-onset, younger than 65 years) AD is caused by genetic mutations [12–15]. However, the majority of AD cases

(~95%) is the sporadic non-inherited form, which is also referred to as late-onset (non-familial, sporadic) AD [14, 16]. Sporadic AD is likely caused by normal aging [16, 17] and its associated consequences, including oxidative stress and disturbance of protein homeostasis [13, 18–20].

Recently, many companies have stopped their AD-related clinical trials and minimized their investments in neurological studies [21]. Therefore, we need new approaches to open doors for alternative therapeutic strategies against aging-related NDs and dementia. In the past few years, alternative medicine has come into focus for the potential to provide new therapeutic measures for dementia [22–25]. Recent comparative proteomics research studies regarding AD-related TCM treatments revealed novel data that suggest that potential mechanisms of action of TCM for the prevention of AD pathogenesis involve improving the ubiquitin proteasome system (UPS, including chaperones and cochaperones (notably, heat shock proteins (HSPs) and FK506 binding proteins (FKBPs))) [20, 26]. Particularly, *G. elata* (tianma) received special attention and will therefore be discussed in more detail as follows [26].

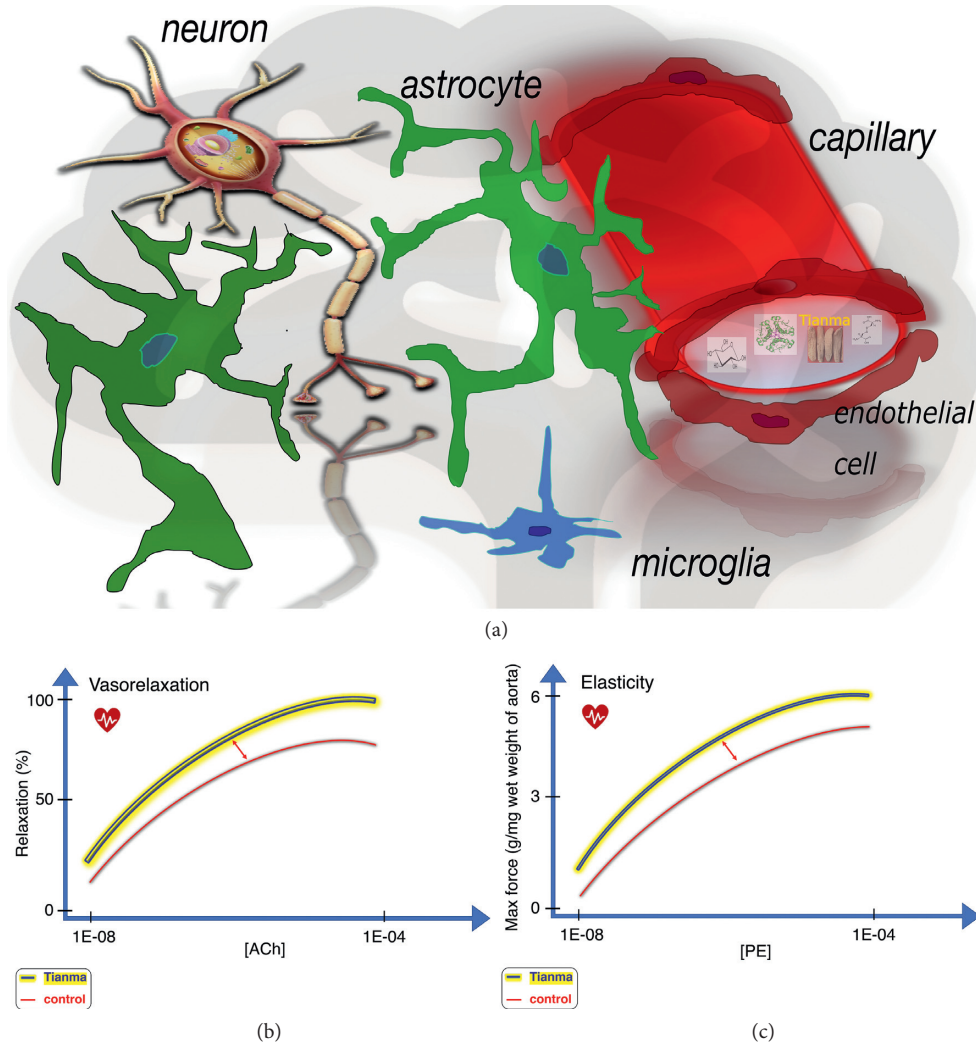


FIGURE 1: Schematic overview of tianma-mediated CCV-related activities. (a) With astrocytes serving as sensors and mediators between neural signal transmission and the vascular-dependent energy (glucose) supply, tianma can improve vascular activities and, upon uptake into the cerebrum, neuronal activities and survival and provide neuroprotection against ischemic strikes [33, 41]. (b) Quantitative data showing tianma-enhanced vasorelaxation. Elderly rats were treated with tianma for a period of three months (~ 2.5 g/kg/day), after which their thoracic aortas were isolated. Dose-response analysis with increasing level of acetylcholine- (ACh-) induced relaxation in KCl (80 mM) or phenylephrine (PE, 10^{-6} M) precontracted isolated endothelium-intact arterial rings [67]. (c) Quantitative representation of tianma-increased vascular contractile force and elasticity. Dose-response comparison of maximum contractile force in response to increasing concentration of PE in endothelium-intact thoracic aortic rings (preincubated with 80 mM K^+) in tianma-treated elderly rats and controls [67].

2. *G. Elata* (Tianma) and NDs

G. elata (tianma) is a member of the Orchidaceae family and has its origin in East Asia. Its tuber has been used in TCM for centuries [26–30], and extracts of tianma or its active ingredients convey physiological- and health-promoting features, including antitumor, memory improving, and neuroprotective activities [30–33]. Particularly, this TCM has been widely used in Asia to treat dizziness, paralysis, epilepsy [34], and hypertension [35]. Tianma has also been used in this region to overcome cognitive deficits and prevent NDs [30, 36–41], including AD [42–46], vascular dementia (VD) [33, 41], and Parkinson’s disease (PD)

[47, 48], with gastrodin and 4-hydroxybenzyl alcohol among the primary active components [48–53].

3. Tianma Mobilizes the Cerebrocardiovascular System

It is common knowledge that heart health contributed to brain health. Connections between AD, VD, diabetes mellitus (type 2, T2DM), and CCVDs have been proposed based on the strong associations between cardiovascular risk factors and AD and VD, suggesting that these diseases share common characteristics [54–57]. The risk of developing aging-related AD, VD, and CCVDs appears to

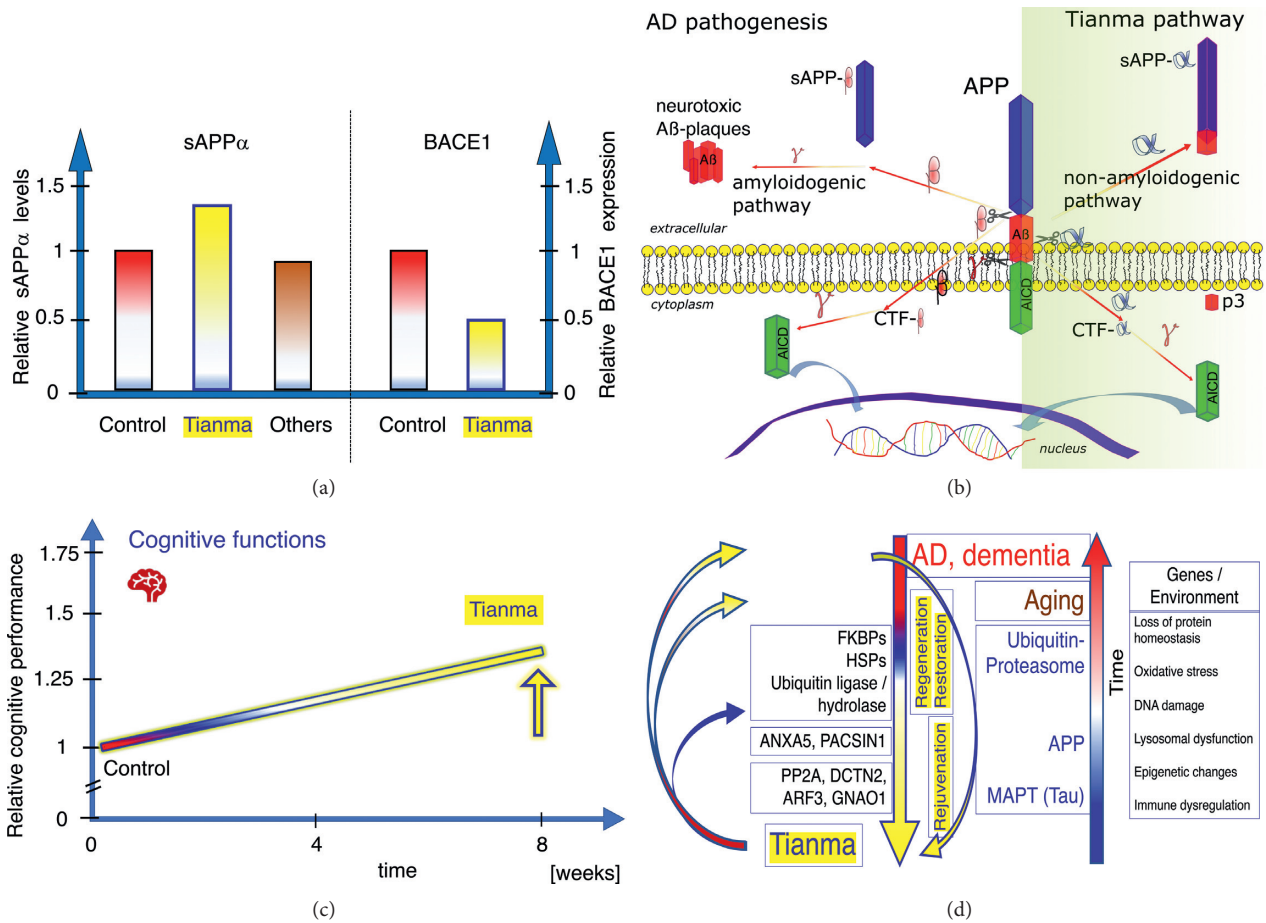


FIGURE 2: The effects of tianma on AD-related signaling and cognitive function during aging. (a) Qualitative data showing the effects of tianma and other herbs on APP processing. Estimation of soluble sAPP α level in cell culture supernatant (measured by enzyme-linked immunosorbent assay (ELISA)) and relative beta-secretase 1 (BACE1) expression (evaluated by Western blot analyses) of neuronal cells treated with tianma. Neurons were grown and treated with certain concentrations of tianma or other herbs for 24 h. Data are qualitatively represented as relative changes compared with controls. Only tianma-treated neurons showed significant increase of sAPP α level and significantly reduced BACE1 expression [44, 46]. (b) Schematic overview of the impact of tianma on APP processing. At the measured concentrations, tianma inhibits BACE1, promotes sAPP α production, suppresses amyloid beta peptide (A β) plaque formation, and reduces microtubule-associated protein tau (MAPT) phosphorylation, thereby fostering the nonamyloidogenic pathway [42, 44, 46]. (c) Qualitative data showing the effects of tianma on cognitive function. Tianma enhances memory, learning, and executive function in elderly rats during the Morris water maze, object recognition, and attention set shift tests [32, 41, 43, 46, 49]. (d) Schematic overview of the mechanisms underlying the effects of tianma on dementia. Tianma markedly improves cognitive abilities and protects against aging-related dementia, memory impairment, and neurodegeneration by restoring and rejuvenating cerebrovascular functions in elderly rats [30, 32, 33, 37, 40–44, 46, 49, 72].

be increased with a wide range of conditions and lifestyle factors, including global failure of cellular energy metabolism, hypertension, dyslipidemia, hypercholesterolemia, lower physical activity, and poor diet [22, 56, 58–66].

3.1. Tianma Enhances Acetylcholine- (ACh-) Induced Vaso-relaxation, A Measure of the Contractile Force and Elasticity of Aortic Vessels: Vasodilatory Proteomic Profile Changes in Aortic Tissue. Blood vessel tonicity is regulated by vascular smooth muscle cells which modulate contraction and relaxation. Functional aortic tissue proteomic data have demonstrated that long-term treatment with small doses of tianma regulated blood vessel tonicity by

mediating the expression of contractile proteins (e.g., actin alpha 2 (ACTA2)) and structural proteins (e.g., desmin (DES), microtubule-associated protein 4 (MAP4), PDZ, and LIM domain 1 (PDLIM1) and vinculin (VCL)), extracellular matrix proteins (ECM, e.g., elastin (ELN), fibulin 5 (FBLN5), and proline- and arginine-rich end leucine-rich repeat protein (PRELP)), and thrombotic proteins (e.g., annexin A2 (ANXA2)), thereby enhancing thoracic aortic contractile force and improving blood vessel elasticity (Figure 1) [67]. Moreover, elevated ANXA2 and reduced level of fatty acid binding protein 4 (FABP4) may prevent atherosclerosis and cardiovascular diseases [68, 69].

By inductive reasoning, tianma could likely prevent many CCVDs, such as headache, hypertension,

atherosclerosis, and stroke, by facilitating vasodilatory effects that strengthen the arterial structure. Therefore, identification of all the bioactive ingredients in tianma could help facilitate its application as an efficient therapeutic herbal medicine for treatment of CCVDs by elucidating the mechanisms by which it ameliorates these abnormal cardiovascular responses [33, 41, 54, 67, 70, 71].

4. Tianma Improves Cognitive Function during Aging-Related Dementia

Accumulating evidence indicates that tianma sharpens several cognitive functions, including memory and learning activities [30, 32, 40, 43, 49]. Moreover, neuroprotective and neuro-regenerative qualities have been attributed to tianma, particularly during aging and aging-related NDs, such as AD, PD, and VD [26, 30, 36, 38–44, 47, 72]. Specifically, pharmacologically relevant studies have demonstrated at the cellular and molecular levels that tianma could prevent AD by modulating proteolytic processing of amyloid beta precursor protein (APP), driving the nonamyloidogenic pathway (Figure 2) [41–44, 46].

5. Discussion

5.1. Aging and Dementia: Abnormal Protein Structures. In AD, accumulation of A β and hyperphosphorylated MAPT protein act as seeds for prion-like transmission of misfolded proteins to adjacent neurons, where misfolded MAPT further aggregates into neurofibrillary tangles (NFTs) [73–75]. The FKBP acts as a cochaperone in AD brains trying to prevent MAPT degradation by binding to MAPT and increasing its stability via interaction with the peptidylprolyl isomerase (PPIase) domain [76, 77]. However, downregulation of important E3-ligases (tripartite motif containing 32/37 (TRIM32/37)) and chaperone proteins, such as HSPs (e.g., HSP90), might impair hyperphosphorylated MAPT clearance [20, 37]. HSP90 and STUB1 (STIP1 (stress-induced phosphoprotein 1) homology and U-box containing protein 1, also known as carboxyl terminus of heat shock cognate 70- (HSC70-) interacting protein (CHIP)), target hyperphosphorylated MAPT for proteasomal degradation. Hyperphosphorylated MAPT loses its physiological function for axonal transport, aggregates into NFTs, and causes neuron death. In addition, the impaired UPS (consisting of the 26S proteasome, ubiquitin ligases, and ubiquitin hydrolases) and compromised function of HSPs and FKBP together impair the protein degradation pathway and promote pathophysiological conditions [20, 26, 37].

5.2. Interference Prevents Protein Misfolding during Aging and in NDs. The proposed pathomechanism underlying AD involves A β plaque formation, NFTs, and deregulation of chaperone proteins. Consequently, in AD brains, an impaired UPS system is thought to account for A β aggregation and hyperphosphorylated MAPT-mediated NFT formation, which is potentially furthered by an irregular APP intracellular domain (AICD) signaling pathway [20]. The

various protein groups modulated by tianma treatment affect the UPS system, and active tianma ingredients also target molecular chaperones and cochaperones, such as HSPs and FKBP, and modulate the actions of protein phosphate PP2A. Together, these data open new avenues for future investigations into the prophylactic effects of tianma for aging-related dementia and NDs (Figure 2(d)) [20, 26].

6. Conclusion

The human brain, with its high-level cognitive functions, requires a large degree of flexibility and adaptability for appropriate learning and memory and is very vulnerable to cerebrovascular injuries, such as ischemia or stroke, which can cause NDs and dementia. Tianma has been shown in human clinical studies to be effective against VD [40], and various pre-clinical studies have demonstrated at the molecular and cellular levels its potential as an efficacious anti-aging elixir.

Abbreviations

A β :	Amyloid beta peptide
ACh:	Acetylcholine
ACTA2:	Actin alpha 2
AD:	Alzheimer's disease
AICD:	APP intracellular domain
ANXA2:	Annexin A2
APP:	Amyloid beta precursor protein
BACE1:	Beta-secretase 1
CCVD:	Cerebrocardiovascular disease
DES:	Desmin
DM:	Diabetes mellitus
ELISA:	Enzyme-linked immunosorbent assay
ELN:	Elastin
EOAD:	Early-onset AD
FABP4:	Fatty acid binding protein 4
FBLN5:	Fibulin 5
FKBP:	FK506 binding protein
<i>G. elata</i> , tianma:	<i>Gastrodia elata</i> Blume
HSC70:	Heat shock cognate 70
HSP:	Heat shock protein
LOAD:	Late-onset (nonfamilial, sporadic) AD
MAP4:	Microtubule-associated protein 4
MAPT:	Microtubule-associated protein tau
ND:	Neurodegenerative disease
NFT:	Neurofibrillary tangles
PD:	Parkinson's disease
PDLIM1:	PDZ and LIM domain 1
PDZ:	Postsynaptic density protein (PSD95)
Dlg1:	Drosophila disc large tumor suppressor
zo-1:	zonula occludens-1 protein
LIM:	Lin11, Isl-1, Mec-3
PE:	Phenylephrine
PPIase:	Peptidylprolyl isomerase
PRELP:	

	Proline- and arginine-rich end leucine-rich repeat protein
STIP1:	Stress-induced phosphoprotein 1
STUB1:	STIP1 homology and U-box containing protein 1
TCM:	Traditional Chinese medicine
TRIM:	Tripartite motif containing
UPS:	Ubiquitin proteasome system
VCL:	Vinculin
VD:	Vascular dementia
WHO:	World Health Organization.

Conflicts of Interest

The author declares no conflicts of interest.

Acknowledgments

This study was supported by the Basic Science Research Program through the National Research Foundation of Korea (NRF), which was funded by the Ministry of Education (2019R1F1A1056445).

References

- [1] K. Nagata, T. Yamazaki, D. Takano et al., "Cerebral circulation in aging," *Ageing Research Reviews*, vol. 30, pp. 49–60, 2016.
- [2] L. Pini, M. Pievani, M. Bocchetta et al., "Brain atrophy in alzheimer's disease and aging," *Ageing Research Reviews*, vol. 30, pp. 25–48, 2016.
- [3] S. Tarantini, C. H. T. Tran, G. R. Gordon, Z. Ungvari, and A. Csiszar, "Impaired neurovascular coupling in aging and alzheimer's disease: contribution of astrocyte dysfunction and endothelial impairment to cognitive decline," *Experimental Gerontology*, vol. 94, pp. 52–58, 2017.
- [4] M. Vijayan, S. Kumar, J. S. Bhatti, and P. H. Reddy, "Molecular links and biomarkers of stroke, vascular dementia, and alzheimer's disease," *Progress in Molecular Biology and Translational Science*, vol. 146, pp. 95–126, 2017.
- [5] T. Wyss-Coray, "Ageing, neurodegeneration and brain rejuvenation," *Nature*, vol. 539, no. 7628, pp. 180–186, 2016.
- [6] T. Yang, Y. Sun, Z. Lu, R. K. Leak, and F. Zhang, "The impact of cerebrovascular aging on vascular cognitive impairment and dementia," *Ageing Research Reviews*, vol. 34, pp. 15–29, 2017.
- [7] J. P. da Costa, R. Vitorino, G. M. Silva, C. Vogel, A. C. Duarte, and T. Rocha-Santos, "A synopsis on aging-theories, mechanisms and future prospects," *Ageing Research Reviews*, vol. 29, pp. 90–112, 2016.
- [8] H. Shah, E. Albanese, C. Duggan et al., "Research priorities to reduce the global burden of dementia by 2025," *The Lancet Neurology*, vol. 15, no. 12, pp. 1285–1294, 2016.
- [9] S. Pramanik, Y. A. Sulistio, and K. Heese, "Neurotrophin signaling and stem cells-implications for neurodegenerative diseases and stem cell therapy," *Molecular Neurobiology*, vol. 54, no. 9, pp. 7401–7459, 2017.
- [10] A. M. McGrattan, B. McGuinness, M. C. McKinley et al., "Diet and inflammation in cognitive ageing and alzheimer's disease," *Current Nutrition Reports*, vol. 8, no. 2, pp. 53–65, 2019.
- [11] G. K. Bhatti, A. P. Reddy, P. H. Reddy, and J. S. Bhatti, "Lifestyle modifications and nutritional interventions in aging-associated cognitive decline and alzheimer's disease," *Frontiers in Aging Neuroscience*, vol. 11, p. 369, 2019.
- [12] D. J. Selkoe, "Alzheimer's disease: genes, proteins, and therapy," *Physiological Reviews*, vol. 81, no. 2, pp. 741–766, 2001.
- [13] K. Heese and H. Akatsu, "Alzheimer's disease-an interactive perspective," *Current Alzheimer Research*, vol. 3, no. 2, pp. 109–121, 2006.
- [14] R. E. Tanzi and L. Bertram, "New frontiers in alzheimer's disease genetics," *Neuron*, vol. 32, no. 2, pp. 181–184, 2001.
- [15] L. M. Bekris, C.-E. Yu, T. D. Bird, and D. W. Tsuang, "Review article: genetics of alzheimer disease," *Journal of Geriatric Psychiatry and Neurology*, vol. 23, no. 4, pp. 213–227, 2010.
- [16] C. Reitz and R. Mayeux, "Alzheimer disease: epidemiology, diagnostic criteria, risk factors and biomarkers," *Biochemical Pharmacology*, vol. 88, no. 4, pp. 640–651, 2014.
- [17] J. Lindsay, D. Laurin, R. Verreault et al., "Risk factors for alzheimer's disease: a prospective analysis from the Canadian study of health and aging," *American Journal of Epidemiology*, vol. 156, no. 5, pp. 445–453, 2002.
- [18] Y. Ihara, M. Morishima-Kawashima, and R. Nixon, "The ubiquitin-proteasome system and the autophagic-lysosomal system in alzheimer disease," *Cold Spring Harbor Perspectives in Medicine*, vol. 2, no. 8, p. a006361, 2012.
- [19] B. R. Troen, "The biology of aging," *Mount Sinai Journal of Medicine*, vol. 70, no. 1, pp. 3–22, 2003.
- [20] Y. A. Sulistio and K. Heese, "The ubiquitin-proteasome system and molecular chaperone deregulation in alzheimer's disease," *Molecular Neurobiology*, vol. 53, no. 2, pp. 905–931, 2016.
- [21] C. Rowland, The Washington Post, Vol. Business, 209, https://www.washingtonpost.com/business/economy/alzheimers-research-is-getting-a-reboot-at-small-companies-focused-on-the-immune-system/2019/07/03/974d8854-91e9-11e9-b58a-a6a9afaa0e3e_story.html.
- [22] E. Flanagan, D. Lamport, L. Brennan et al., "Nutrition and the ageing brain: moving towards clinical applications," *Ageing Research Reviews*, vol. 62, Article ID 101079, 2020.
- [23] Q. Yan, W. Wang, J. Weng et al., "Dissolving microneedles for transdermal delivery of huperzine A for the treatment of alzheimer's disease," *Drug Delivery*, vol. 27, no. 1, pp. 1147–1155, 2020.
- [24] A. Balan, M. A. Moga, L. Dima, S. Toma, A. Elena Neculau, and C. V. Anastasiu, "Royal jelly-A traditional and natural remedy for postmenopausal symptoms and aging-related pathologies," *Molecules*, vol. 25, no. 14, p. 3291, 2020.
- [25] X. Deng, S. Zhao, X. Liu et al., "Polygala tenuifolia: a source for anti-alzheimer's disease drugs," *Pharmaceutical Biology*, vol. 58, no. 1, pp. 410–416, 2020.
- [26] Y. A. Sulistio and K. Heese, "Proteomics in traditional Chinese medicine with an emphasis on alzheimer's disease," *Evidence-Based Complementary and Alternative Medicine*, vol. 2015, Article ID 393510, , 2015.
- [27] H.-D. Zhan, H.-Y. Zhou, Y.-P. Sui et al., "The rhizome of gastrodia elata blume-an ethnopharmacological review," *Journal of Ethnopharmacology*, vol. 189, pp. 361–385, 2016.
- [28] Y. Shou-Zhong, *The Divine Farmer's Materia Medica: A Translation of the Shen Nong Ben Cao Jing*, Blue Poppy Press, Boulder, Colo, USA, 2007.
- [29] L. Shizhen, *Bencao Gangmu: Compendium of Materia Medica*, Foreign Language Press, Beijing, China, 2006.
- [30] Y. Liu, J. Gao, M. Peng et al., "A review on central nervous system effects of gastrodin," *Frontiers in Pharmacology*, vol. 9, p. 24, 2018.

- [31] J. C. Heo, S. U. Woo, M. Son et al., "Anti-tumor activity of gastrodia elata blume is closely associated with a GTP-Ras-dependent pathway," *Oncology Reports*, vol. 18, no. 4, pp. 849–853, 2007.
- [32] Y.-M. Park, B.-G. Lee, S.-H. Park et al., "Prolonged oral administration of gastrodia elataextract improves spatial learning and memory of scopolamine-treated rats," *Laboratory Animal Research*, vol. 31, no. 2, pp. 69–77, 2015.
- [33] J. W. Xian, A. Y. Choi, C. B. Lau, W. N. Leung, C. F. Ng, and C. W. Chan, "Gastrodia and Uncaria (tianma gouteng) water extract exerts antioxidative and antiapoptotic effects against cerebral ischemia in vitro and in vivo," *Chinese Medicine*, vol. 11, p. 27, 2016.
- [34] L. M. Ojemann, W. L. Nelson, D. S. Shin, A. O. Rowe, and R. A. Buchanan, "Tian ma, an ancient Chinese herb, offers new options for the treatment of epilepsy and other conditions," *Epilepsy & Behavior*, vol. 8, no. 2, pp. 376–383, 2006.
- [35] X. Xiong, X. Yang, Y. Liu, Y. Zhang, P. Wang, and J. Wang, "Chinese herbal formulas for treating hypertension in traditional Chinese medicine: perspective of modern science," *Hypertension Research*, vol. 36, no. 7, pp. 570–579, 2013.
- [36] A. Manavalan, U. Ramachandran, H. Sundaramurthi et al., "Gastrodia elata blume (tianma) mobilizes neuro-protective capacities," *International Journal of Biochemistry and Molecular Biology*, vol. 3, no. 2, pp. 219–241, 2012.
- [37] A. Manavalan, M. Mishra, L. Feng, S. K. Sze, H. Akatsu, and K. Heese, "Brain site-specific proteome changes in aging-related dementia," *Experimental & Molecular Medicine*, vol. 45, no. 9, p. e39, 2013.
- [38] U. Ramachandran, A. Manavalan, H. Sundaramurthi et al., "Tianma modulates proteins with various neuro-regenerative modalities in differentiated human neuronal SH-SY5Y cells," *Neurochemistry International*, vol. 60, no. 8, pp. 827–836, 2012.
- [39] H. Sundaramurthi, A. Manavalan, U. Ramachandran, J.-M. Hu, S. K. Sze, and K. Heese, "Phenotyping of tianma-stimulated differentiated rat neuronal b104 cells by quantitative proteomics," *Neurosignals*, vol. 20, no. 1, pp. 48–60, 2012.
- [40] G. Du, K. Chen, W. Zhou et al., "Clinical effect of tianmacuzhi granules on senile vascular dementia," *Zhongguo Zhong Yao Za Zhi Zhongguo Zhongyao Zazhi China Journal of Chinese Materia Medica*, vol. 23, no. 11, pp. 695–698, 1998.
- [41] R. Shi, C. B. Zheng, H. Wang et al., "Gastrodin alleviates vascular dementia in a 2-VO-vascular dementia rat model by altering amyloid and tau levels," *Pharmacology*, vol. 105, no. 7–8, pp. 386–396, 2020.
- [42] M. Li and S. Qian, "Gastrodin protects neural progenitor cells against amyloid β (1-42)-induced neurotoxicity and improves hippocampal neurogenesis in amyloid β (1-42)-injected mice," *Journal of Molecular Neuroscience*, vol. 60, no. 1, pp. 21–32, 2016.
- [43] Y. Hu, C. Li, and W. Shen, "Gastrodin alleviates memory deficits and reduces neuropathology in a mouse model of alzheimer's disease," *Neuropathology: Official Journal of the Japanese Society of Neuropathology*, vol. 34, no. 4, pp. 370–377, 2014.
- [44] J.-S. Zhang, S.-F. Zhou, Q. Wang et al., "Gastrodin suppresses BACE1 expression under oxidative stress condition via inhibition of the PKR/eIF2 α pathway in alzheimer's disease," *Neuroscience*, vol. 325, pp. 1–9, 2016.
- [45] G. B. Huang, T. Zhao, S. S. Muna et al., "Therapeutic potential of Gastrodia elata Blume for the treatment of alzheimer's disease," *Neural Regeneration Research*, vol. 8, no. 12, pp. 1061–1070, 2013.
- [46] M. Mishra, J. Huang, Y. Y. Lee et al., "Gastrodia elata modulates amyloid precursor protein cleavage and cognitive functions in mice," *Bioscience Trends*, vol. 5, no. 3, pp. 129–138, 2011.
- [47] L. F. Liu, J. X. Song, J. H. Lu et al., "Tianma Gouteng Yin, a Traditional Chinese Medicine decoction, exerts neuroprotective effects in animal and cellular models of Parkinson's disease," *Scientific Reports*, vol. 5, Article ID 16862, 2015.
- [48] Y. Y. Huang, L. F. Liu, R. Q. Yue et al., "Full component analysis of Tianma-Gouteng-Yin," *Chinese Medicine*, vol. 11, p. 44, 2016.
- [49] M.-T. Hsieh, C.-R. Wu, and C.-F. Chen, "Gastrodin and p-hydroxybenzyl alcohol facilitate memory consolidation and retrieval, but not acquisition, on the passive avoidance task in rats," *Journal of Ethnopharmacology*, vol. 56, no. 1, pp. 45–54, 1997.
- [50] C.-J.-S. Lai, Y. Yuan, D.-H. Liu et al., "Untargeted metabolite analysis-based UHPLC-Q-TOF-MS reveals significant enrichment of p-hydroxybenzyl dimers of citric acids in fresh beige-scape Gastrodia elata (Wutianma)," *Journal of Pharmaceutical and Biomedical Analysis*, vol. 140, pp. 287–294, 2017.
- [51] L.-C. Lin, Y.-F. Chen, W.-C. Lee, Y.-T. Wu, and T.-H. Tsai, "Pharmacokinetics of gastrodin and its metabolite p-hydroxybenzyl alcohol in rat blood, brain and bile by microdialysis coupled to LC-MS/MS," *Journal of Pharmaceutical and Biomedical Analysis*, vol. 48, no. 3, pp. 909–917, 2008.
- [52] M. Li, Y. Du, L. Wang et al., "Efficient discovery of quality control markers for gastrodia elata tuber by fingerprint-efficacy relationship modelling," *Phytochemical Analysis*, vol. 28, no. 4, pp. 351–359, 2017.
- [53] J. H. Ha, D. U. Lee, J. T. Lee et al., "4-Hydroxybenzaldehyde from Gastrodia elata B1. is active in the antioxidation and GABAergic neuromodulation of the rat brain," *Journal of Ethnopharmacology*, vol. 73, no. 1-2, pp. 329–333, 2000.
- [54] E. Picano, R. M. Bruno, G. F. Ferrari, and U. Bonuccelli, "Cognitive impairment and cardiovascular disease: so near, so far," *International Journal of Cardiology*, vol. 175, no. 1, pp. 21–29, 2014.
- [55] A. M. Hooghiemstra, A. S. Bertens, A. E. Leeuwis et al., "The missing link in the pathophysiology of vascular cognitive impairment: design of the heart-brain study," *Cerebrovascular Diseases Extra*, vol. 7, no. 3, pp. 140–152, 2017.
- [56] U. Kumari and K. Heese, "Cardiovascular dementia-a different perspective," *The Open Biochemistry Journal*, vol. 4, pp. 29–52, 2010.
- [57] R. A. L. De Sousa, A. R. Harmer, D. A. Freitas, V. A. Mendonça, A. C. R. Lacerda, and H. R. Leite, "An update on potential links between type 2 diabetes mellitus and alzheimer's disease," *Molecular Biology Reports*, vol. 47, no. 8, pp. 6347–6356, 2020.
- [58] J. Leszek, E. V. Mikhaylenko, D. M. Belousov et al., "The links between cardiovascular diseases and alzheimer's disease," *Current Neuropharmacology*, 2020, <https://www.eurkaselect.com/184274/article>.
- [59] A. Datta, J. E. Park, X. Li et al., "Phenotyping of an in vitro model of ischemic penumbra by iTRAQ-based shotgun quantitative proteomics," *Journal of Proteome Research*, vol. 9, no. 1, pp. 472–484, 2010.
- [60] A. Datta, Q. Jingru, T. H. Khor, M. T. Teo, K. Heese, and S. K. Sze, "Quantitative neuroproteomics of an in vivo rodent

- model of focal cerebral ischemia/reperfusion injury reveals a temporal regulation of novel pathophysiological molecular markers," *Journal of Proteome Research*, vol. 10, no. 11, pp. 5199–5213, 2011.
- [61] A. Datta, H. Akatsu, K. Heese, and S. K. Sze, "Quantitative clinical proteomic study of autopsied human infarcted brain specimens to elucidate the deregulated pathways in ischemic stroke pathology," *Journal of Proteomics*, vol. 91, pp. 556–568, 2013.
- [62] A. Ahmad, V. Patel, J. Xiao, and M. M. Khan, "The role of neurovascular system in neurodegenerative diseases," *Molecular Neurobiology*, vol. 57, no. 11, pp. 4373–4393, 2020.
- [63] Z. Bartochowski, J. Conway, Y. Wallach, B. Chakkampambil, S. Alakkassery, and G. T. Grossberg, "Dietary interventions to prevent or delay alzheimer's disease: what the evidence shows," *Current Nutrition Reports*, vol. 9, no. 3, pp. 210–225, 2020.
- [64] A. C. van den Brink, E. M. Brouwer-Brolsma, A. A. M. Berendsen, and O. van de Rest, "The mediterranean, dietary approaches to stop hypertension (DASH), and mediterranean-DASH intervention for neurodegenerative delay (MIND) diets are associated with less cognitive decline and a lower risk of alzheimer's disease—a review," *Advances in Nutrition*, vol. 10, no. 6, pp. 1040–1065, 2019.
- [65] F. Pistollato, R. C. Iglesias, R. Ruiz et al., "Nutritional patterns associated with the maintenance of neurocognitive functions and the risk of dementia and Alzheimer's disease: a focus on human studies," *Pharmacological Research*, vol. 131, pp. 32–43, 2018.
- [66] V. Solfrizzi, C. Custodero, M. Lozupone et al., "Relationships of dietary patterns, foods, and micro- and macronutrients with alzheimer's disease and late-life cognitive disorders: a systematic review," *Journal of Alzheimer's Disease*, vol. 59, no. 3, pp. 815–849, 2017.
- [67] L. Feng, A. Manavalan, M. Mishra, S. K. Sze, J.-M. Hu, and K. Heese, "Tianma modulates blood vessel tonicity," *The Open Biochemistry Journal*, vol. 6, pp. 56–65, 2012.
- [68] E. C. Flood and K. A. Hajjar, "The annexin A2 system and vascular homeostasis," *Vascular Pharmacology*, vol. 54, no. 3–6, pp. 59–67, 2011.
- [69] M. Furuhashi and G. S. Hotamisligil, "Fatty acid-binding proteins: role in metabolic diseases and potential as drug targets," *Nature Reviews Drug Discovery*, vol. 7, no. 6, pp. 489–503, 2008.
- [70] I. Ferrer, "Cognitive impairment of vascular origin: neuropathology of cognitive impairment of vascular origin," *Journal of the Neurological Sciences*, vol. 299, no. 1–2, pp. 139–149, 2010.
- [71] T. Tarumi and R. Zhang, "Cerebral blood flow in normal aging adults: cardiovascular determinants, clinical implications, and aerobic fitness," *Journal of Neurochemistry*, vol. 144, no. 5, pp. 595–608, 2018.
- [72] A. Manavalan, L. Feng, S. K. Sze, J.-M. Hu, and K. Heese, "New insights into the brain protein metabolism of gastrodia elata-treated rats by quantitative proteomics," *Journal of Proteomics*, vol. 75, no. 8, pp. 2468–2479, 2012.
- [73] D. M. Walsh and D. J. Selkoe, "Amyloid β -protein and beyond: the path forward in alzheimer's disease," *Current Opinion in Neurobiology*, vol. 61, pp. 116–124, 2020.
- [74] A. A. Mamun, M. S. Uddin, B. Mathew, and G. M. Ashraf, "Toxic tau: structural origins of tau aggregation in alzheimer's disease," *Neural Regeneration Research*, vol. 15, no. 8, pp. 1417–1420, 2020.
- [75] S. A. Kent, T. L. Spires-Jones, and C. S. Durrant, "The physiological roles of tau and $A\beta$: implications for alzheimer's disease pathology and therapeutics," *Acta Neuropathologica*, vol. 140, no. 4, pp. 417–447, 2020.
- [76] L. J. Blair, J. D. Baker, J. J. Sabbagh, and C. A. Dickey, "The emerging role of peptidyl-prolyl isomerase chaperones in tau oligomerization, amyloid processing, and alzheimer's disease," *Journal of Neurochemistry*, vol. 133, no. 1, pp. 1–13, 2015.
- [77] G. Caminati and P. Procacci, "Mounting evidence of FKBP12 implication in neurodegeneration," *Neural Regeneration Research*, vol. 15, no. 12, pp. 2195–2202, 2020.

Research Article

Suppressive Effects of the *Gynura bicolor* Ether Extract on Endothelial Permeability and Leukocyte Transmigration in Human Endothelial Cells Induced by TNF- α

Shu-Ling Hsieh ¹, Jyh-Jye Wang,² Kuan-Hua Su,³ Ying-Lan Kuo,¹ Shuchen Hsieh ⁴,
and Chih-Chung Wu ⁵

¹Department of Seafood Science, National Kaohsiung University of Science and Technology, Kaohsiung 81157, Taiwan

²Department of Nutrition and Health Science, Fooyin University, Kaohsiung 83102, Taiwan

³Graduate Institute of Medical Sciences, Chang Jung Christian University, Tainan 71101, Taiwan

⁴Department of Chemistry, National Sun Yat-Sen University, Kaohsiung 80424, Taiwan

⁵Department of Food and Nutrition, Providence University, Taichung 43301, Taiwan

Correspondence should be addressed to Chih-Chung Wu; wuccmail@gmail.com

Received 26 July 2020; Revised 16 November 2020; Accepted 6 December 2020; Published 22 December 2020

Academic Editor: Sai-Wang Seto

Copyright © 2020 Shu-Ling Hsieh et al. This is an open access article distributed under the Creative Commons Attribution License, which permits unrestricted use, distribution, and reproduction in any medium, provided the original work is properly cited.

Gynura bicolor (Roxb. and Willd.) DC (*G. bicolor*) is generally used as a dietary vegetable and traditional herb in Taiwan and the Far East. *G. bicolor* exerts antioxidant and anti-inflammatory effects and regulates blood lipids and cholesterol. However, the effects of *G. bicolor* on endothelial transmigration and atherosclerosis are not clear. The present study investigated the effects of *G. bicolor* on endothelial permeability and transmigration in human endothelial cells. We prepared *G. bicolor* ether extract (GBEE) for use as the experimental material. Under TNF- α stimulation, HL-60 cell adherence to EA.hy926 cells, the shape of EA.hy926 cells, and the expression of adhesion molecules and transmigration-related regulatory molecules were analysed after pretreatment with GBEE for 24 h. GBEE inhibited leukocyte adhesion to endothelial cells, reduced intercellular adhesion molecule-1 (ICAM-1) and platelet endothelial cell adhesion molecule-1 (PECAM-1) expressions, and decreased endothelial monolayer permeability. GBEE also reduced paracellular transmigration by reducing the levels of reactive oxygen species (ROS), Src phosphorylation, and vascular endothelial-cadherin (VE-cadherin) phosphorylation. GBEE reduced transcellular migration via inhibition of Ras homolog family member A (RhoA) and Rho-associated protein kinase (ROCK) expression and phosphorylation of the ezrin-radixin-moesin (ERM) protein. Incubation of EA.hy926 cells with GBEE for 8 h and stimulation with TNF- α for 3 h reduced the phosphorylation of the inhibitor of kappa B (I κ B) and DNA-binding activity of nuclear factor- κ B (NF- κ B). These results suggest that GBEE has a protective effect against endothelial dysfunction via suppression of leukocyte-endothelium adhesion and transmigration.

1. Introduction

Gynura bicolor (Roxb. and Willd.) DC (*G. bicolor*) is widespread in South Asia and the Far East, and it is generally used as a dietary vegetable and traditional herb in Taiwan. Previous studies showed that *G. bicolor* exhibited neuro-protective [1], liver-protective [2], hypoglycaemic [3], antioxidant [4], and anticancer properties [5] and promoted iron bioavailability [6]. Our previous study found that

G. bicolor had anti-inflammatory [7] and antioxidant [8] effects and decreased serum total cholesterol, serum total triacylglycerol levels [8], and regulated immune response [9]. However, beyond its role in the regulation of blood lipids, the modification of lipoprotein levels [8] and raise antioxidative enzyme activity [9] during cardiovascular disease formation, the effects of *G. bicolor* on endothelial permeability, and leukocyte transmigration in atherosclerosis formation are not clear.

Atherosclerosis is one of the major causes of mortality worldwide, and vascular endothelial system dysfunction is an important cause of atherosclerosis [10]. Chronic pathological stimuli, such as diabetes, dyslipidaemia, inflammation, and oxidative stress, initiate endothelial dysfunction and vascular dysfunction, which lead to the development of atherosclerotic arterial disease [11]. Transmigration is the process by which leukocytes roll on the vascular endothelium, adhere to the endothelium, and invade across the endothelial cell-cell monolayer, and it occurs in the early stage of atherosclerosis formation [12]. The expression of intercellular adhesion molecule-1 (ICAM-1), vascular cell adhesion protein-1 (VCAM-1), and platelet endothelial cell adhesion molecule-1 (PECAM-1) plays an important role in transmigration. Activation of these adhesion molecules triggers the transformation of endothelial cells, changes the permeability of the endothelial cell-cell monolayer, and induces transmigration across the endothelial monolayer [13]. The transmigration of leukocytes consists of paracellular and transcellular transmigration activation [14], which are activated by oxidative stress, inflammation, and adhesion molecule activation [15]. Endothelial cell-cell junctions play an important role in transmigration. Therefore, maintaining endothelial cell-cell monolayer integrity and reducing transmigration are beneficial and have cardiovascular protective effects against atherosclerosis.

Nuclear factor- κ B (NF- κ B) is a crucial transcription factor that is involved in various physiological and pathological effects [16]. Activated NF- κ B binds to the cis-acting κ B enhancer element of target genes, such as ICAM1, E-selectin, Rho-associated protein kinase (ROCK), and Ras homolog family member A (RhoA), and activates their transcription [17]. Whether GBEE regulates these adhesion and transmigration molecules is an important issue.

The present study investigated *G. bicolor* ether extract (GBEE) mediated regulation of endothelial permeability and leukocyte transmigration in human endothelial cells. To determine the effect of GBEE on adhesion ability and endothelial cell-cell monolayer permeability, leukocyte adherence to endothelial cells, endothelial cell shape, the expression of adhesion molecules, phosphorylation of VE-cadherin, and the permeability of the endothelial cell-cell monolayer were analysed. To investigate the mechanism by which GBEE regulates the paracellular and transcellular transmigration pathways, the levels of transmigration-related regulatory molecules were measured. NF- κ B signalling was analysed to determine the regulatory effect of GBEE on transmigration and whether it occurred via the modification of NF- κ B signalling.

2. Materials and Methods

2.1. Preparation of GBEE. Fresh *G. bicolor* was purchased from the village of Yuanshan (Ilan, Taiwan) and identified by Yen Hsueh Tseng, Ph.D., based on a voucher specimen growing in the Department of Forestry, National Chung Hsieh University (NCHU, Taichung, Taiwan). A voucher specimen (TCF13549) of the newly purchased *G. bicolor* was deposited at NCHU.

To prepare GBEE, the fresh leaves of *G. bicolor* were collected, cleaned, and blended in cold water (4°C, w/w: 1/1). The homogenates were extracted with ether (v/v: 1/1) on a stir plate for 6 h at 4°C. The extract was centrifuged at 250 × g at 4°C for 10 min. The supernatant was filtered and concentrated using a rotary vacuum dryer (EYELA-Tokyo Rikakikai Co., Ltd., Tokyo, Japan) (45°C), and the concentrated product was dried in a freeze dryer at -43°C. The percentage yield of the GBEE was 0.3% (w/w).

2.2. Cell Culture and GBEE Treatment. EA.hy926 cells were established via fusion with primary human umbilical vein cells and used in this study as a model of the vascular endothelium to investigate the effects of GBEE on adhesion and transmigration in the vascular endothelial monolayer of the circulatory system. HL-60 human leukaemia cells derived from peripheral blood leukocytes and obtained using leukapheresis are widely used to study interactions of adhesion and adhesion molecules [18]. EA.hy926 and HL-60 cells were purchased from the Bioresource Collection and Research Center (BCRC, Hsinchu, Taiwan). EA.hy926 cells (at passages 40–62) and HL-60 cells (at passages 23–46) were maintained in DMEM supplemented with 10% foetal bovine serum and 1% penicillin/streptomycin at 37°C in a 5% CO₂ humidified atmosphere.

EA.hy926 cells were plated at a density of 1×10^4 per 30 mm culture dish and incubated until reaching 90% confluence. To determine the effects of GBEE on cell viability, adhesion, and transmigration, the cultured cells were pretreated with 10, 50, or 100 μ g/mL GBEE for 8 h and then stimulated with or without 10 ng/mL TNF- α (R&D Systems, Inc., Minneapolis, MN, USA) for 3 h. TNF- α was used in this study to induce oxidative stress and endothelial dysfunction [19], and the GBEE treatment time and the dose were confirmed in a series of pretests of adhesion ability and the phosphorylation of VE-cadherin, two adhesion ability, and permeability indicator, in this present study. The present study dissolved the GBEE in dimethyl sulfoxide (DMSO, Sigma-Aldrich Co., St. Louis, MO, USA), and a group treated with only DMSO was used as a control group. Groups treated with only 10 ng/mL TNF- α for the last 3 h or 100 μ g/mL GBEE for the first 8 h were used as control groups.

2.3. Cell Viability Analysis. Based on the results of our preliminary test to determine the experimental concentrations of GBEE, EA.hy926 cells were treated with 10, 50, or 100 μ g/mL GBEE for 24 h for the cell viability assay. EA.hy926 cells were pretreated with 10, 50, or 100 μ g/mL GBEE for 8 h and then stimulated with or without 10 ng/mL TNF- α for 3 h for the cell viability assay. Cell viability was evaluated using the 3-(4,5-dimethyl-2-yl)-2,5-diphenyl tetrazolium bromide (MTT, Sigma-Aldrich Co.) reduction assay, and morphological examination was performed as described by Denizot and Lang [20]. The cells were incubated with DMEM containing MTT reagent (5 μ g/mL) at 37°C for 3 h. The medium was removed, and the cells were washed twice with phosphate-buffered saline (PBS, 3.2 mM

Na_2HPO_4 , 0.5 mM KH_2PO_4 , 1.3 mM KCl, 135 mM NaCl, and pH 7.4). Formazan formation, as an indicator of cell viability, was solubilized via the addition of 1 mL of acidified isopropanol into each plate. After 15 min of extraction, the extent of formazan production was determined by reading the absorbance at 570 nm using an enzyme-linked immunosorbent assay (ELISA) reader (BioTek Instruments Inc., Winooski, VT, USA). A phase-contrast inverted fluorescence microscope was used to determine morphological changes (Olympus IX51, Olympus, Tokyo, Japan).

2.4. Adhesion Assay. An adhesion assay was performed as described by Braut-Boucher et al. [21] with modifications. EA.hy926 cells were pretreated with 10, 50, or 100 $\mu\text{g}/\text{mL}$ GBEE for 8 h and then stimulated with or without 10 ng/mL TNF- α for 3 h. The EA.hy926 cells were washed in PBS and cocultured for 1 h with HL-60 cells labelled with 10 μM 2', 7'-bis-(2-carboxyethyl)-5-(and-6)-carboxyfluorescein (BCECF, Thermo Fisher Scientific, Carlsbad, CA, USA) for 1 h. After washing in PBS, the morphology of BCECF-stained HL-60 cells was measured under an inverted fluorescence microscope (Olympus IX51, Olympus, Tokyo, Japan). The BCECF-stained cells were collected and measured fluorometrically using an ELISA reader (BMG Labtech GmbH, Offenburg, Germany) with excitation and emission wavelengths of 500 and 530 nm, respectively.

2.5. Atomic Force Microscopy (AFM) Examination. EA.hy926 cells (5×10^4 cells/30 mm plate) were seeded on cover slides in 6-well culture plates overnight and treated with 10, 50, or 100 $\mu\text{g}/\text{mL}$ GBEE for 8 h, followed by stimulation with or without 10 ng/mL TNF- α for 3 h. For AFM imaging, the attached cultured cells on slides were removed, washed three times with PBS, fixed with 4% paraformaldehyde for 20 min, and washed three times with PBS, which was exchanged with ultrapure water.

An atomic force microscope (MFP-3D, Asylum Research, Santa Barbara, CA, USA) was used to characterize the cells under ambient conditions [22]. A silicon cantilever (NanoWorld, Switzerland, Arrow FMR) with a measured spring constant of 2.8 N/m was used to image the melanoma cells. Images were collected in air using the contact mode at a scan rate of 1 Hz.

2.6. Measurement of Transepithelial Resistance (TEER). TEER is a quantitative measurement of the barrier integrity of a monolayer used to examine cell-cell integrity and permeability [23]. To measure the TEER, EA.hy926 cell monolayers (5×10^4 cells/well) were cultured on semipermeable filter (0.22 μm) inserts that served as a partition to the apical and basolateral compartments. EA.hy926 cells (5×10^4 cells/30 mm plate) were seeded on cover slides in 6-well culture plates overnight, then treated with 10, 50, or 100 $\mu\text{g}/\text{mL}$ GBEE for 8 h, followed by stimulation with or without 10 ng/mL TNF- α for 3 h. After the above treatments, one electrode was placed in the upper compartment, and another electrode was placed in the lower compartment,

with the electrodes separated by the cellular monolayer. The measurement procedure included the measurement of the resistance of the semipermeable membrane as a blank. The cell-specific resistance was measured in units of Ω . TEER values were obtained by subtracting the TEER measured at a groove in the cell culture dish from the measurement in the presence of a cell layer. These measurements were acquired using a Millicell-ERS voltohmmeter (Millipore Continental Water Systems, Bedford, MA, USA).

2.7. Analysis of the Expression of Regulatory Proteins Involved in Transmigration. EA.hy926 cells (5×10^5 /30 mm plate) were used to analyse the expression of adhesion molecules (ICAM-1 and PECAM-1), adhesion junction proteins (phosphorylation-vascular endothelial cadherin (p-cadherin) and VE-cadherin), adhesion junction regulatory proteins (p-Src, Src, Ras homolog family member A (RhoA), Rho-associated protein kinase (ROCK), and p-ezrin-radixin-moesin (ERM)), and NF- κB signalling molecules (p-I κB , I κB , cytosolic NF- κB , and nuclear NF- κB (p65)).

EA.hy926 cells were pretreated with 10, 50, or 100 $\mu\text{g}/\text{mL}$ GBEE for 8 h and stimulated with or without 10 ng/mL TNF- α for 3 h. The cells were washed twice with cold PBS and harvested using 200 μL of lysis buffer containing 10 mM Tris-HCl, 5 mM EDTA, 0.2 mM phenylmethylsulphonyl fluoride (PMSF) (Sigma-Aldrich Co.), and 20 $\mu\text{g}/\text{mL}$ aprotinin at pH 7.4. The cellular proteins were quantified following the method described by Lowry et al. [24].

Cellular protein (10 to 20 μg) from each sample was added to 10% sodium dodecyl sulphate (SDS) polyacrylamide gels [25]. After electrophoresis, the proteins were transferred to polyvinylidene difluoride membranes [26], which were incubated with antibodies against ICAM-1, PCAM-1, p-VE-cadherin, VE-cadherin, p-Src, Src, RhoA, ROCK, p-PERM, ERM, p-I κB , I κB , NF- κB , and nuclear NF- κB (p65) at 37°C for 1 h and subsequently incubated with peroxidase-conjugated secondary antibodies. Bands were visualized using hydrogen peroxide/tetrahydrochloride diaminobenzidine or an enhanced chemiluminescence detection kit (Amersham Life Science, Buckinghamshire, UK) and quantified using a ChemiDoc MP imaging system (Bio-Rad Laboratories Inc., Hercules, CA, USA).

2.8. Statistical Analysis. The data were analysed using SPSS statistical analysis software for Windows, version 20.0 (IBM, Armonk, NY, USA). One-way analysis of variance and Duncan's multiple range tests were used to evaluate the significance of differences between mean values. ^{abcd}Values were significantly different from the other groups. A *p* value less than 0.05 indicated a statistically significant difference.

3. Results

3.1. GBEE Did Not Reduce the Cell Viability of TNF- α -Induced EA.hy926 Cells. The viability of EA.hy926 cells treated with 10, 50, or 100 $\mu\text{g}/\text{mL}$ GBEE for 24 h was not significantly different from control cells (Figure 1(a)). The cell viability of EA.hy926 cells did not significantly differ

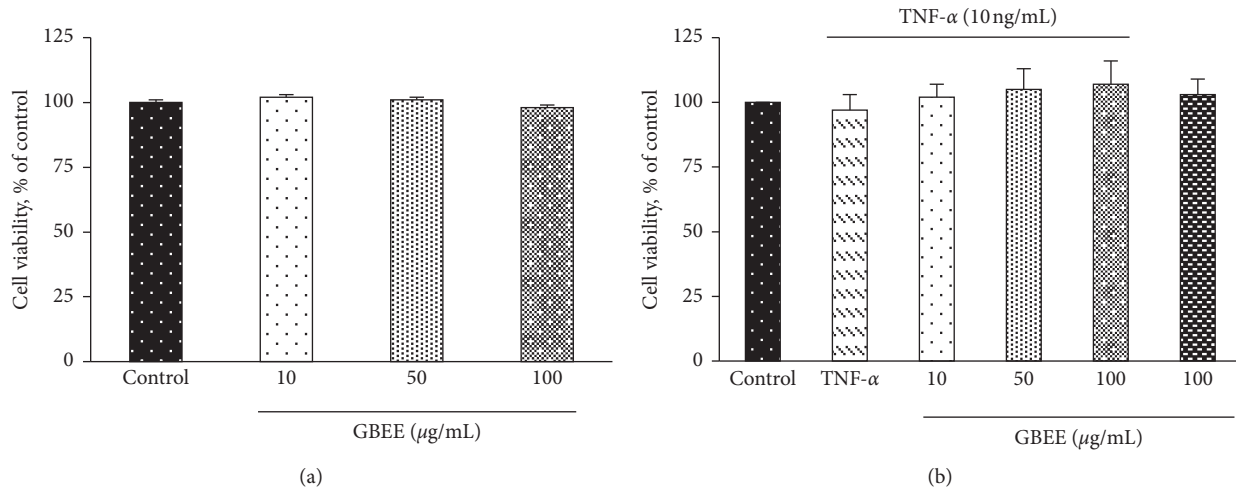


FIGURE 1: Effect of GBEE on cell viability in EA.hy926 cells. EA.hy926 cells (5×10^4 cells/30 mm plate) were seeded and cultured overnight. (a) EA.hy926 cells treated with 10, 50, or 100 µg/mL GBEE for 24 h. (b) EA.hy926 cells treated with 10, 50, or 100 µg/mL GBEE for 8 h followed by stimulation with or without 10 ng/mL TNF-α for 3 h. Values were presented as means \pm SDs ($n = 3$). ^{abcd}Values not sharing the same letter were significantly different, as shown by Duncan's test ($p < 0.05$).

between the groups treated with 10, 50, or 100 µg/mL GBEE and TNF-α (approximately 102–107%), only TNF-α (97%), and only GBEE (101%) and the control group (100%) (Figure 1(b)). Morphological examination using inverted microscopy revealed no significant differences in the cell number and cell morphology between any GBEE group and the control group (data not shown). Therefore, treatment with 10, 50, or 100 µg/mL GBEE did not affect the cell viability of EA.hy926 cells treated with TNF-α.

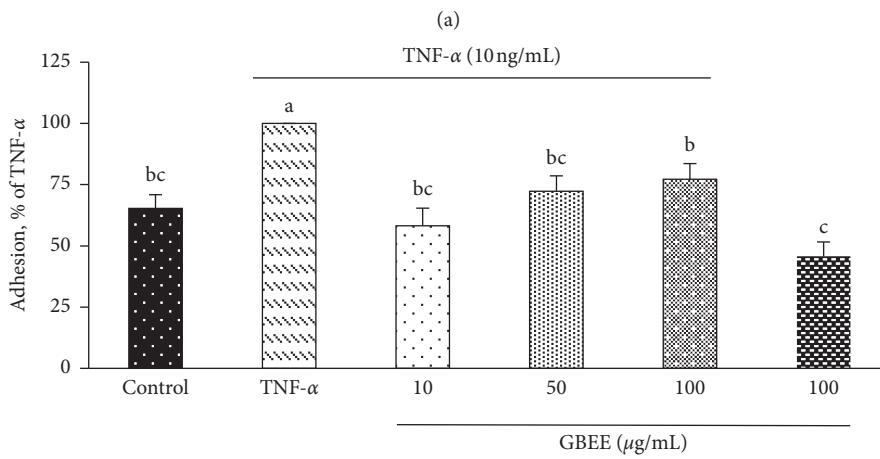
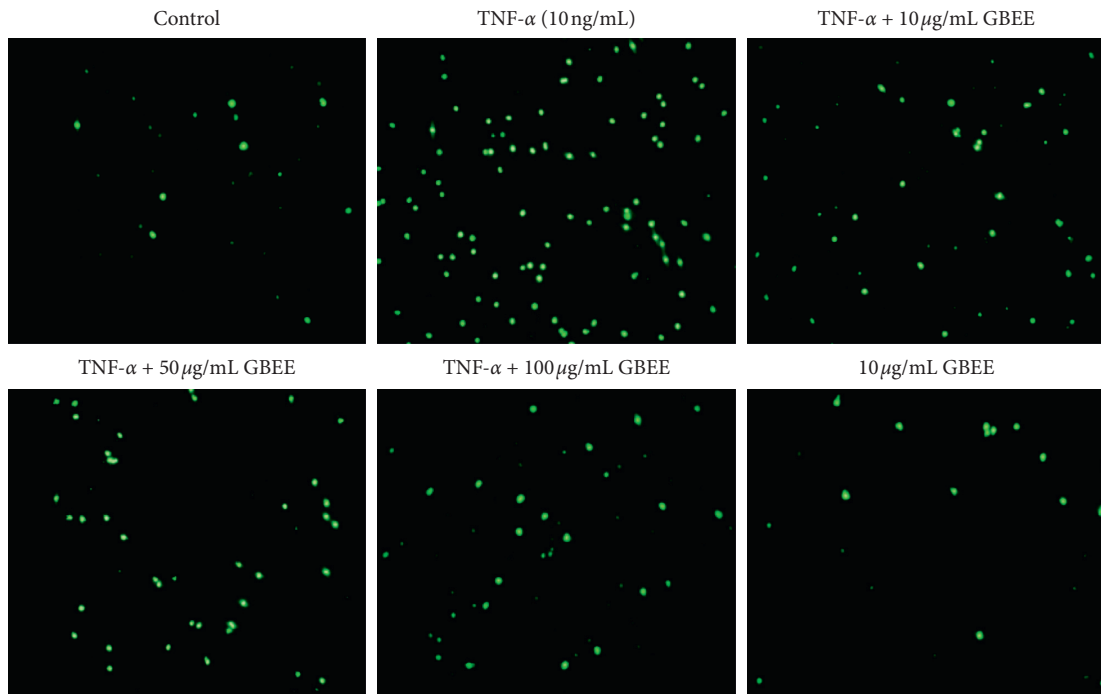
3.2. GBEE Reduced HL-60 Cell Adhesion to EA.hy926 Cells and TNF-α-Induced Changes in Cell Shape. Fluorescence microscopy examination revealed that the GBEE treatment of TNF-α-induced EA.hy926 cells significantly reduced HL-60 cell adhesion to EA.hy926 cells (Figure 2). After EA.hy926 cells were incubated with 10, 50, or 100 µg/mL GBEE for 8 h and stimulated with TNF-α for 3 h (Figures 2(a) and 2(b)), cell adhesion significantly decreased approximately 23–42% compared to the TNF-α-treated group (100%) ($p < 0.05$). These results demonstrate that GBEE decreased the ability of HL-60 cells to adhere to EA.hy926 cells and suggest that GBEE reduces leukocyte adhesion to an endothelial cell layer. Because 10, 50, or 100 µg/mL GBEE reduced the adhesion ability, the 100 µg/mL GBEE group was further used to investigate the mechanisms of cell height (morphological remodelling), cell junction protein, and gene regulation.

AFM technology was used to investigate the effects of GBEE on changes in EA.hy926 cell shape due to changes in cell-cell junctions. TNF-α-treated EA.hy926 cells, but not control cells, exhibited a flattened and partially collapsed shape (Figure 2(c)). The number of EA.hy926 cells stimulated with TNF-α and treated with 100 µg/mL GBEE was higher (86.6% compared to the control) than the number of cells in the TNF-α group (54.9% compared to the control) and exhibited a less flattened shape (Figure 2(c)).

3.3. GBEE Inhibited Changes in the Adhesion Molecule and Junction Protein Expression and Permeability in TNF-α-Induced EA.hy926 Cells. To investigate the effects of GBEE on adhesion and adhesion junctions, changes in the expression of proteins related to cell adhesion and cell junctions in EA.hy926 were examined using immunoblotting. The expression levels of ICAM-1, PECAM-1, p-VE-cadherin, and VE-cadherin in EA.hy926 cells are presented in Figure 3(a). The treatment of EA.hy926 cells with 10, 50, or 100 µg/mL GBEE and TNF-α significantly decreased approximately 49–76% and reduced PECAM-1 protein levels 27% under 100 µg/mL GBEE treatment compared to the TNF-α-treated group (100%) (Figure 2(b)). After treatment with 10, 50, or 100 µg/mL GBEE, the levels of p-VE-cadherin in EA.h926 cells were 83.6 ± 7.5 , 85.3 ± 8.2 , and $80.2 \pm 2.7\%$, respectively, of the level in the TNF-α-treated group ($p < 0.05$) (Figure 2(b)). When EA.hy926 cells were treated with 10, 50, or 100 µg/mL GBEE and TNF-α, no difference in the protein levels of VE-cadherin was observed compared with the control or TNF-α-treated groups (Figures 2(a) and 2(b)). These results indicate that GBEE suppressed the expression of this adhesion and junctional protein, and GBEE may exert an important antiadhesive effect and maintain cell junction function during TNF-α stimulation.

The effect of GBEE on the TEER of EA.hy926 cells was also examined. After treatment with 50 and 100 µg/mL GBEE, the TEER of EA.hy926 cells was $141 \pm 7\%$ and $160 \pm 8\%$, respectively (Figure 2(c)), and these values were significantly higher than those of the TNF-α-treated group (100%) ($p < 0.05$). These results demonstrated that GBEE decreased the gaps between cell-cell junctions and decreased permeability by reducing changes in the shape of EA.hy926 cells.

3.4. GBEE Regulated Paracellular and Transcellular Transmigration Regulatory Molecules in TNF-α-Induced EA.hy926 Cells. The major molecules that regulate paracellular and



(b)
FIGURE 2: Continued.

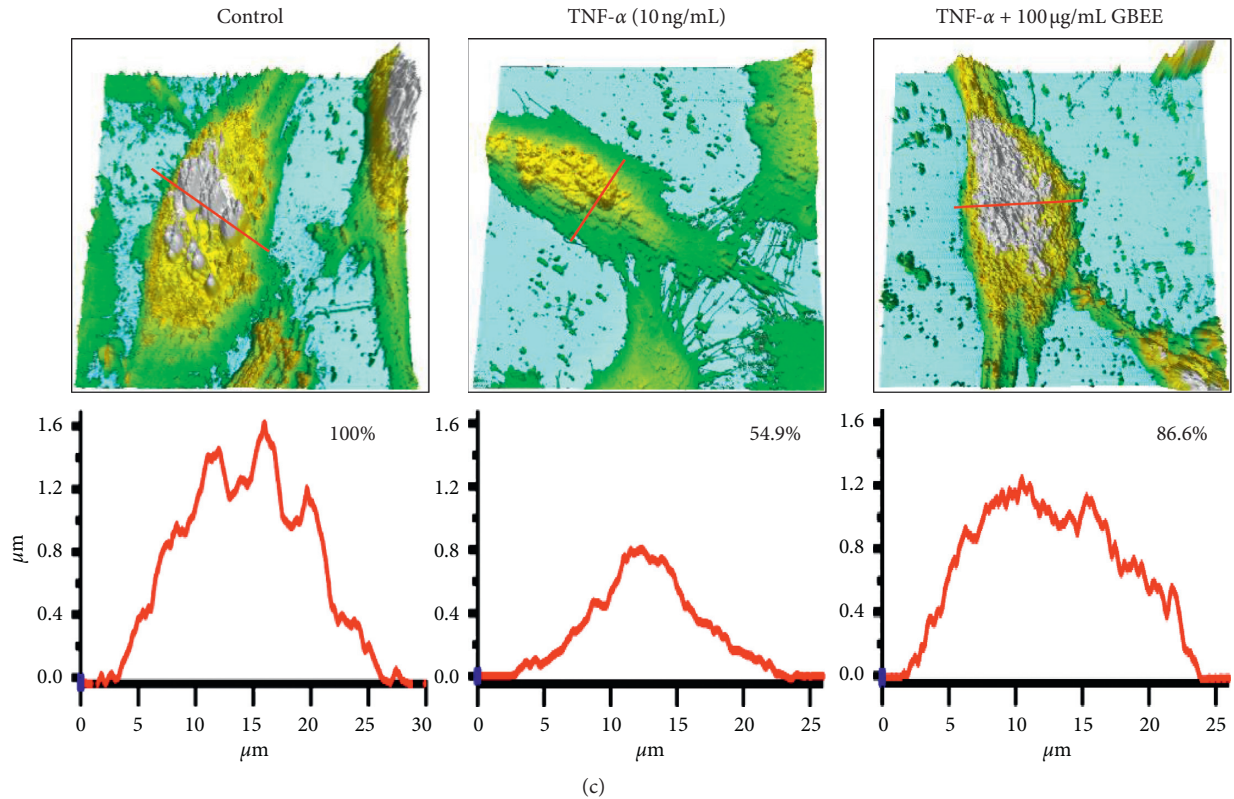


FIGURE 2: Effect of GBEE on HL-60 cell adhesion to EA.hy926 cells and analysis of TNF- α -induced changes in EA.hy926 cell height. EA.hy926 cells (5×10^4 cells/30 mm plate) were seeded, cultured overnight, and treated with 10, 50, or 100 $\mu\text{g}/\text{mL}$ GBEE for 8 h followed by stimulation with or without 10 ng/mL TNF- α for 3 h. (a) HL-60 cells were prestained with 2',7'-bis-(2-carboxyethyl)-5-(and-6)-carboxyfluorescein, and the adhesion of HL-60 cells to EA.hy926 cells was observed under a fluorescence microscope. (b) EA.hy926 cell staining was observed using a fluorescence reader with an excitation wavelength of 485 nm and an emission wavelength of 530 nm. (c) EA.hy926 cell height was observed using AFM. The height of the control cells was set at 100%. Values were presented as means \pm SDs ($n = 3$). ^{abc}Values not sharing the same letter were significantly different, as shown by Duncan's test ($p < 0.05$).

transcellular transmigration were analysed in this study. As shown in Figure 4, the levels of reactive oxygen species (ROS) in EA.hy926 cells treated with 100 $\mu\text{g}/\text{mL}$ and TNF- α decreased significantly approximately 14% compared to the TNF- α -treated group (100%) ($p < 0.05$). p-Src and RhoA protein expressions decreased significantly, 44% and 10%, respectively, compared to the TNF- α -treated group ($p < 0.05$) (Figures 3(b) and 3(c)). However, Src protein levels were not altered in cells exposed to 100 $\mu\text{g}/\text{mL}$ GBEE and TNF- α (Figures 3(b) and 3(c)). However, when EA.hy926 cells were treated with 100 $\mu\text{g}/\text{mL}$ GBEE and TNF- α , ROCK and p-ERM expressions decreased significantly (60.7 ± 53 and $70.4 \pm 12.2\%$, respectively) compared to the TNF- α -treated group ($p < 0.05$) (Figures 3(b) and 3(c)). These results showed that GBEE significantly reduced the levels of molecules that regulated paracellular and transcellular transmigration.

3.5. GBEE Reduced the Activation of NF- κ B Signalling in TNF- α -Induced EA.hy926 Cells. The results of immunoblot analysis showed that the phosphorylation of I κ B and nuclear NF- κ B levels decreased significantly, 24% and 16%, respectively, after 100 $\mu\text{g}/\text{mL}$ GBEE treatment ($p < 0.05$) (Figures 4(a) and 4(b)), but GBEE did not impact the protein

levels of cytosolic I κ B and NF- κ B in EA.hy926 cells (Figures 4(a) and 4(b)). As shown in Figure 4(c), the DNA-binding activity of nuclear NF- κ B was significantly inhibited (49%) in cells treated with 100 $\mu\text{g}/\text{mL}$ GBEE.

4. Discussion

The present study showed that GBEE had a potential protective effect against atherosclerosis via suppression of leukocyte-endothelium transmigration. Our results showed that GBEE inhibited leukocyte adhesion to endothelial cells and reduced the adhesion molecule expression and endothelial monolayer permeability. GBEE reduced the phosphorylation of VE-cadherin by inhibiting ROS levels, the phosphorylation of Src, and the paracellular transmigration of TNF- α -induced EA.hy926 cells. GBEE also decreased RhoA and ROCK levels and the phosphorylation of ERM and inhibited the transcellular transmigration of TNF- α -induced EA.hy926 cells. These novel findings show that GBEE reduces paracellular and transcellular transmigration to maintain cell-cell monolayer integrity, reduce permeability, and prevent atherosclerosis.

Leukocytes roll and adhere to the endothelium of the vasculature in the early stage of atherosclerosis [27]. When

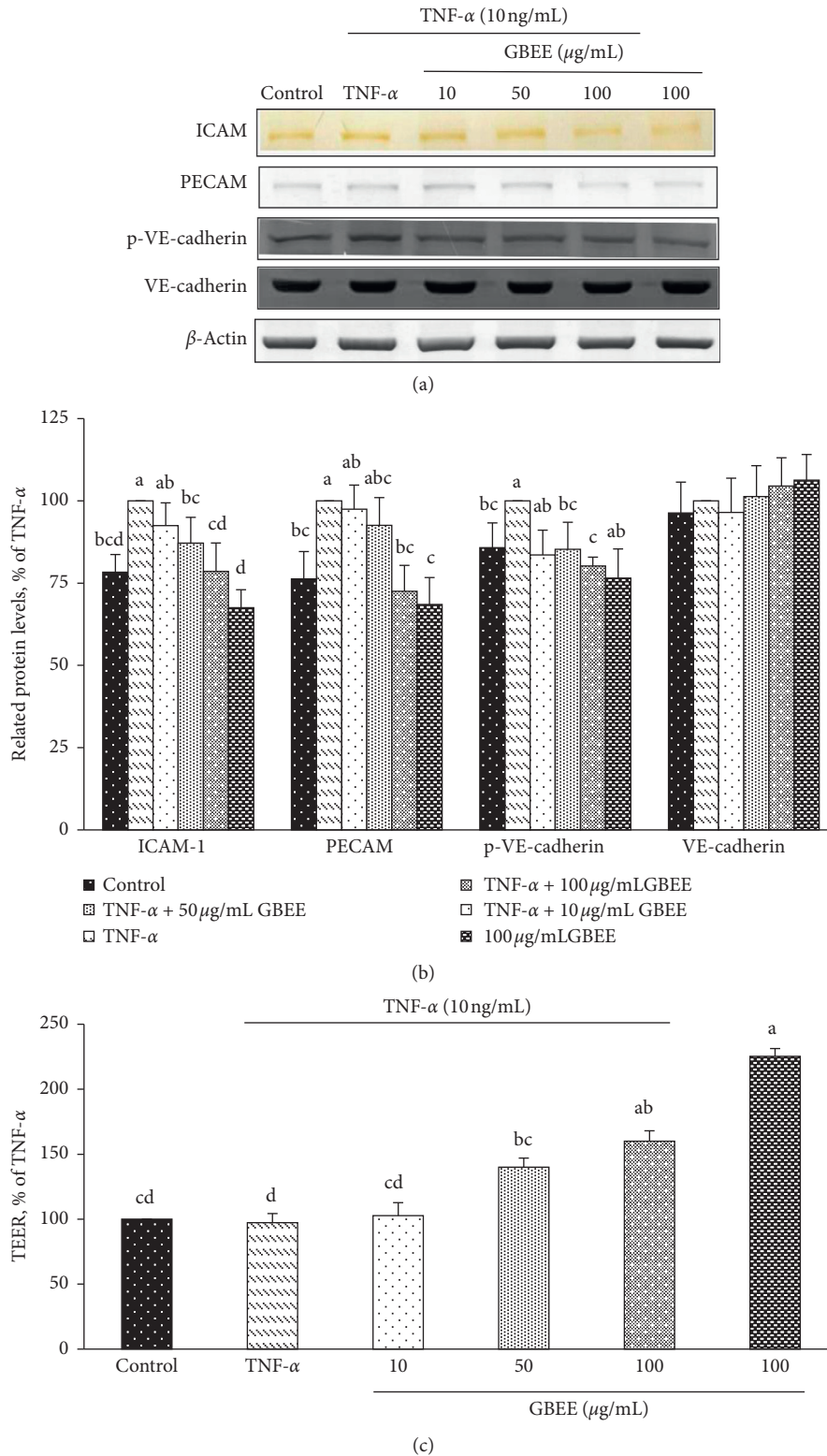


FIGURE 3: Expression levels of TNF- α -induced adhesion molecules and cell junction proteins. EA.hy926 cells (5×10^4 cells/30 mm plate) were seeded, cultured overnight, and treated with 10, 50, or 100 μ g/mL GBEE for 8 h followed by stimulation with or without 10 ng/mL TNF- α for 3 h. (a) Immunoblot assays were performed to determine the expression levels of ICAM-1, PECAM-1, p-VE-cadherin, and VE-cadherin in EA.hy926 cells. (b) Protein expression in EA.hy926 cells was quantified using densitometry. The expression levels in the control group were set at 100%. (c) The effect of GBEE on transepithelial electrical resistance in EA.hy926 cells. Values were presented as means \pm SDs ($n = 3$). ^{abc}Values not sharing the same letter were significantly different, as shown by Duncan's test ($p < 0.05$).

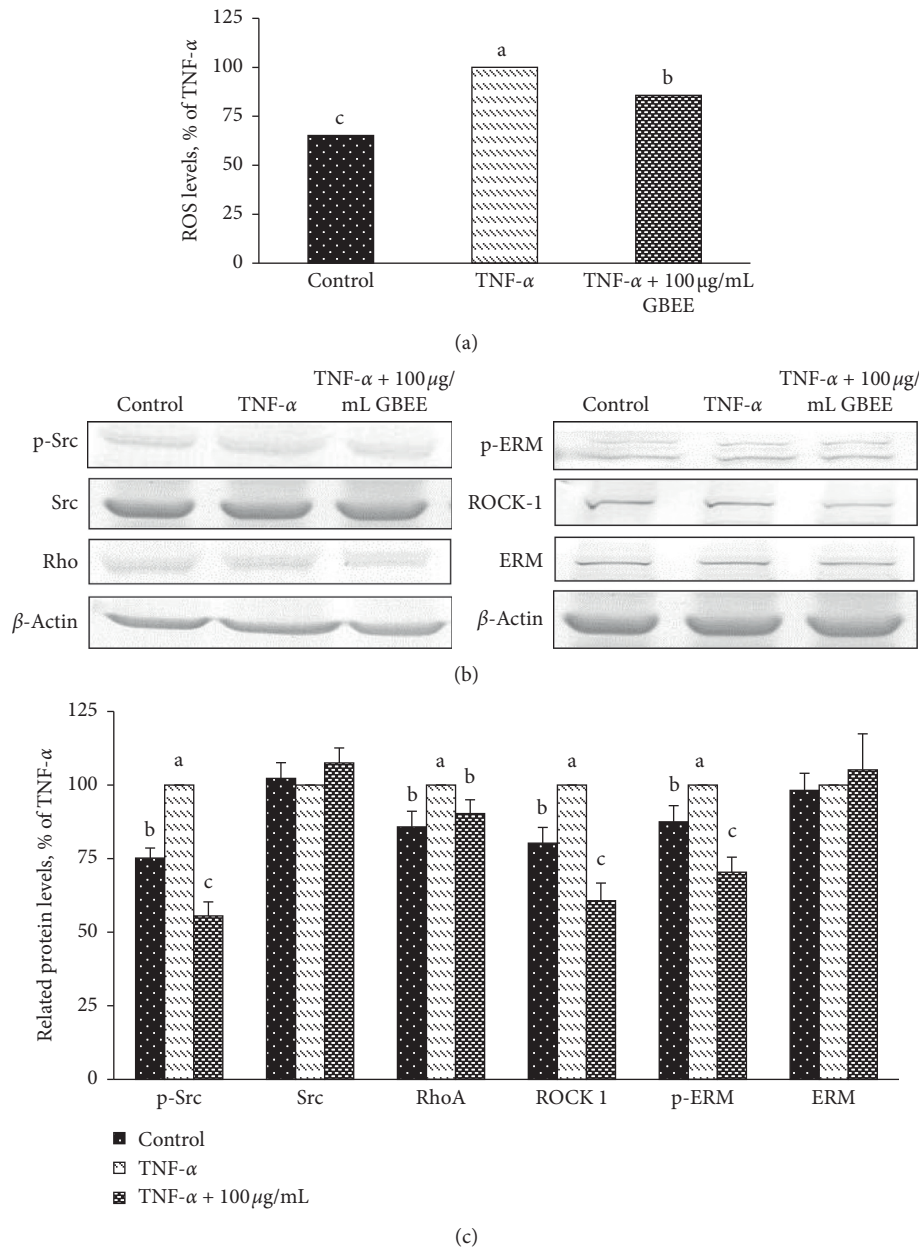


FIGURE 4: Effect of GBEE on transmigration regulatory molecules in EA.hy926 cells. EA.hy926 cells (5×10^4 cells/30 mm plate) were seeded, cultured overnight, and treated with 100 $\mu\text{g}/\text{mL}$ GBEE for 8 h followed by stimulation with or without 10 ng/mL TNF- α for 3 h. (a) The effect of GBEE on ROS levels in EA.hy926 cells was determined. (b) The expression levels of p-Src, Src, RhoA, p-ERM, ROCK, and ERM in EA.hy926 cells were determined using the immunoblot assay. (c) The protein expression in EA.hy926 cells was quantified using densitometry; expression levels in the control group were set at 100%. Values were presented as means \pm SDs ($n = 3$). ^{abc}Values not sharing the same letter were significantly different, as shown by Duncan's test ($p < 0.05$).

these leukocytes roll on the vascular endothelium, endothelial adhesion molecules, such as ICAM-1, VCAM-1, and PECAM-1, are expressed and activated, which leads to adhesion between the endothelium and leukocytes [28]. Reduced adhesion molecule expression is one mechanism of decreased leukocyte adhesion to the vascular endothelium, which reduces plaque formation. GBEE significantly inhibited ICAM-1 and PECAM-1 expressions in the present study, which led to reduced HL-60 cell adhesion to EA.hy926 cells. These findings are similar to those of a

previous study that showed that oligomeric proanthocyanidins from *Rhodiola rosea* (OPCRR) decreased the serum levels of TNF- α , IL-1 β , IL-6, ICAM-1, and VCAM-1 and enhanced IL-10 levels in atherosclerotic rats, which improved endothelial dysfunction and atherosclerosis via decreased inflammation and the expression of adhesion molecules [29]. *Sorghum bicolor* L. Moench fermented with *Aspergillus oryzae* NK (fSBE) improved blood and vascular health by decreasing the levels of VCAM-1, ICAM-1, cyclooxygenase-2, and heme oxygenase-1 [30]. Our

previous study showed that the *G. bicolor* ethanol extract decreased ICAM-1 and VCAM-1 expressions in TNF- α -induced EA.hy926 cells via potential antioxidant effects [9]. Inflammation and oxidative stress are the leading causes of atherosclerosis as a result of damage to the endothelium [11]. Oxidative stress activates redox signalling pathways, which leads to inflammatory insult [31]. An inflammatory state and the upregulation of inducible NOS (iNOS) expression lead to vascular remodelling. However, these structural changes may ultimately lead to vascular dysfunction [32, 33]. A previous study showed that GBEE reduced ROS, NO, and PGE₂ levels and increased SOD activity in *in vitro* and *in vivo* models [7, 9]. The potential antioxidant and anti-inflammatory effects of GBEE may regulate adhesion molecules and reduce adhesion.

Before leukocyte invasion and transmigration across the endothelial monolayer, the shape of monolayer endothelial cells in the vasculature is transformed [34, 35]. The shrinking, retraction, and/or flattening of endothelial cells may lead to increased cell-cell monolayer permeability and the loss of integrity and trigger transmigration [36]. AFM examination indicated that EA.hy926 cells became flat and retracted after TNF- α induction in the present study. However, cotreatment with GBEE significantly reduced this flattening in TNF- α -induced EA.hy926 cells. As known, a normal endothelial shape and higher TEER indicate tight cell-cell junctions and the integrity of the cell-cell monolayer. TEER is a widely accepted quantitative indicator of the integrity and permeability of endothelial and epithelial monolayers in cell culture models [37]. Cell-cell junctions control endothelial cell-cell monolayer integrity and regulate the ability of ions, proteins, leukocytes, and macrophages to pass through this barrier [37]. The previous report showed some of the barrier models that have been widely characterized utilizing TEER include the blood-brain barrier (BBB), gastrointestinal (GI) tract, and pulmonary models [37]. Bachinger et al. showed that there are significantly higher TEER levels than the cell control group after intestinal porcine epithelial cells (IPEC-J2) were treated with *Angelica* root extracts for 24 h [38]. In the mouse vascular endothelial cell (mMVEC) culture model, puerarin, an active compound of *Pueraria lobata* (Willd.) Ohwi, also has significantly increased the TEER levels as compared to the cell control group [39]. A previous study showed that a dietary polyphenol compound, resveratrol, reduced endothelium monolayer permeability by increasing TEER and maintaining VE-cadherin levels to prevent atherosclerosis in patients with chronic kidney disease [40]. In the present study, when EA.hy926 cells were cotreated with GBEE and TNF- α , they had a higher TEER than the TNF- α -treated control group. The above studies show the raised TEER levels in the GI tract, vascular endothelium, and epithelium cells. All can enhance intestinal and vascular barrier integrin protective cell-cell monolayer dysfunction. The results of the present study showed that GBEE improved and maintained cell-cell monolayer integrity and reduced the increased permeability of TNF- α -induced EA.hy926 cells.

GBEE improved TNF- α -induced changes in the cell shape and the permeability of the endothelial cell-cell monolayer and regulated transmigration via regulating cell-cell junctions in the present study. Changes in the shape of endothelial cells lead to changes in endothelial cell-cell junctions. Endothelial cells primarily regulate cell-cell junctions and interactions via adhesion junctions and tight junctions [41]. Adhesion junctions join cells and have various cellular physiological effects, including the establishment and maintenance of cell-cell adhesions, actin cytoskeleton remodelling, intracellular signalling, and transcriptional regulation. Tight junctions regulate cell-cell monolayer permeability and maintain a specific barrier [42]. As shown in Figure 5, ICAM-1 expression and engagement increase the phosphorylation of Src, which causes the phosphorylation of VE-cadherin [12, 43]. The phosphorylation of VE-cadherin releases adhesion junctions and tight adhesion junctions to form an open channel, which leads to the movement of leukocytes, proteins, electrolytes, and solutes across the vascular monolayer. Figure 5 also shows that GBEE significantly reduced the phosphorylation of Src, VE-cadherin, and ERM, but it did not affect the levels of these proteins. These results showed that GBEE regulated Src, VE-cadherin, and ERM by reducing the phosphorylation of these proteins and confirmed that phosphorylation played an important role in the activation of Src, VE-cadherin, and ERM (12). ROS levels increase the phosphorylation of VE-cadherin and PECAM-1 expression. Therefore, increased ROS levels enhance the opening of cell-cell junctions by decreasing PECAM-1 levels and increasing VE-cadherin activation [44]. A previous study showed that luteolin suppressed adherens junction-associated monocyte paracellular transmigration by decreasing the PECAM-1 expression in TNF- α -induced THP-1 cells [45]. Mulberry polyphenol extract, which contains high levels of polyphenolic compounds, inhibited the expression of Src and reduced the expression of RhoA to affect F-actin cytoskeleton rearrangement, which inhibited A7r5 cell migration and atherosclerosis [46]. GBEE reduced the activation of the ICAM-1 expression and significantly decreased the levels of p-Src, ROS, PECAM-1, and p-VE-cadherin in TNF- α -induced EA.hy926 cells in the present study. These results showed that GBEE reduced paracellular transmigration. GBEE also regulated transcellular transmigration by reducing RhoA, ROCK, and p-ERM expressions (Figure 5). ICAM-1 activation triggers RhoA/ROCK signalling, and ICAM-1 induction increases RhoA levels to enhance the ROCK expression in endothelial cells. The subsequent phosphorylation of ERM increases and regulates cell remodelling and transcellular transmigration. RhoA/Rho kinase-mediated actin contractility may contribute to vascular function as a mechanosensory mechanism. Phosphorylation of ERM by ROCK2 normally allows ERM to cross-link actin filaments with the plasma membrane [47]. In contrast, disruption of the endothelial barrier may lead to increased endothelial permeability and promote organ damage in various diseases [48, 49]. 18 β -Glycyrrhetic acid, the main active substance of licorice, has outstanding anti-inflammatory and antioxidant effects,

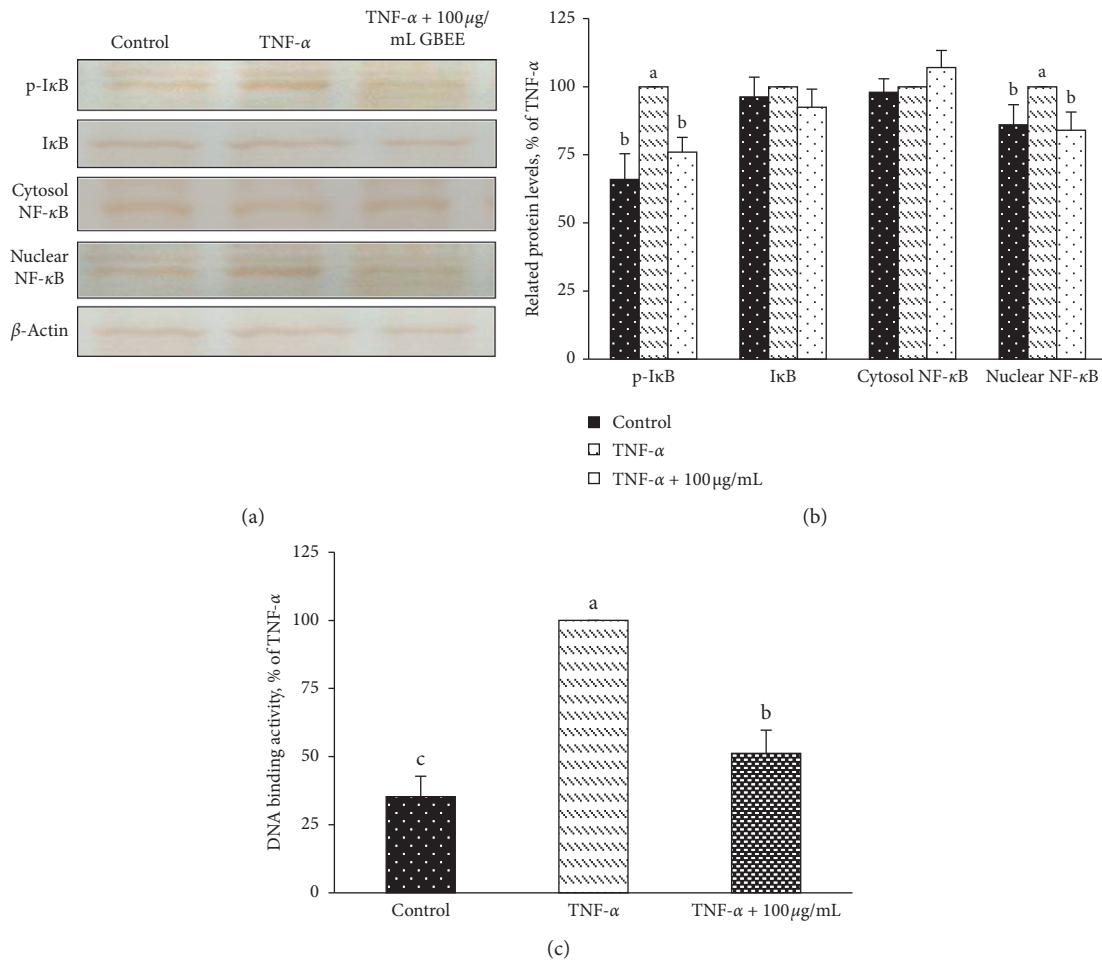


FIGURE 5: Effect of GBEE on NF- κ B signalling activation in EA.hy926 cells. EA.hy926 cells (5×10^4 cells/30 mm plate) were seeded, cultured overnight, and treated with 100 μ g/mL GBEE for 8 h followed by stimulation with or without 10 ng/mL TNF- α for 3 h. (a) Immunoblot assays were performed to determine the expression levels of p-I κ B, I κ B, cytosolic NF- κ B, and nuclear NF- κ B in EA.hy926 cells. (b) Protein expression in EA.hy926 cells was quantified using densitometry; the expression levels in the control group were set at 100%. (c) The effect of GBEE on NF- κ B DNA-binding activity in EA.hy926 cells was determined. Values were presented as means \pm SDs ($n = 3$). ^{abc}Values not sharing the same letter were significantly different, as shown by Duncan's test ($p < 0.05$).

and it inhibited pulmonary vascular remodelling by reducing the expression of RhoA and ROCK2 in pulmonary artery smooth muscle cells [50].

GBEE significantly suppressed NF- κ B signalling activation by reducing the phosphorylation of I κ B and the DNA-binding activity of NF- κ B in the present study. These suppressive effects led to a significant reduction in the expression of the cell adhesion-associated proteins ICAM1, ROCK, and RhoA in EA.hy926 cells. Our previous [7] study showed that GBEE reduced inflammation via reduced NF- κ B activation in RAW 264.7 cells. GBEE also reduced metastasis in human colorectal cancer cells via decreased NF- κ B activation [51]. NF- κ B primarily controls the adhesion- and transmigration-related regulatory molecules ICAM1, E-selectin, ROCK, and RhoA at the transcriptional level [52]. The results of the present study indicate that NF- κ B is an important cellular target of GBEE. GBEE reduction of NF- κ B signalling may be one of the important pathways in the suppression of adhesion, cell-cell monolayer permeability, and transmigration.

Notably, the acute oral toxicity study indicated that the methanol extract of *G. bicolor* has a negligible level of toxicity when administered orally and has been regarded as safe in experimental rats [5], and from a hepatotoxic assessment of pyrrolizidine alkaloids in *G. bicolor in vitro*, it is not found toxic effect [53]. Moreover, the leaves of *G. bicolor* exhibit specific colouring of dark green on the top and purple on the bottom. Lu et al. showed that the abundant plant pigments in leaves provide *G. bicolor* with its pigmentation and may have physiological effects [54]. Our previous studies showed that *G. bicolor* was rich in the chlorophyll, flavonoid, and carotenoid families of plant pigments, including gallic acid, β -carotene, rutin, anthocyanidin, myricetin, and morin [6, 7]. Bhaskar et al. also showed that flavonoid- and polyphenol-rich materials have the potential to regulate the expression of adhesion molecules [55]. However, identification of the active compounds in GBEE that regulate permeability and cell-cell monolayer integrity requires further study.

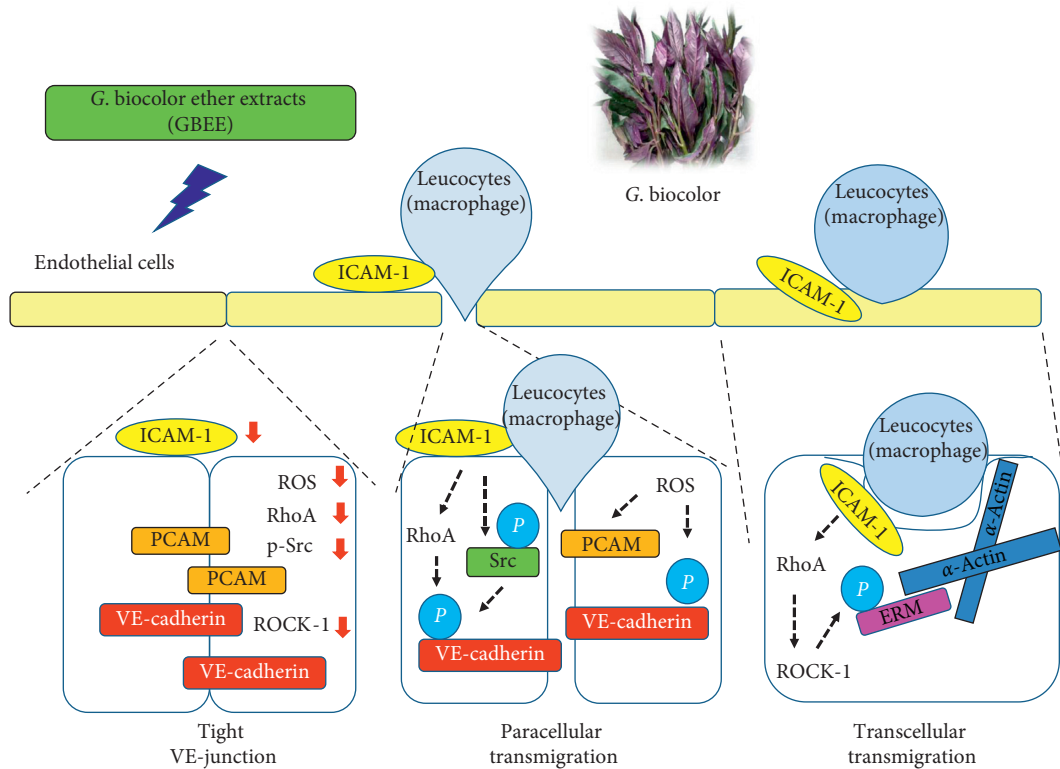


FIGURE 6: Possible mechanisms of GBEE inhibition of paracellular and transcellular transmigration in EA.hy926 cells.

5. Conclusion

The present results showed that GBEE had a potential protective effect against atherosclerosis via suppression of leukocyte-endothelium transmigration. Figure 6 shows that GBEE inhibited adhesion molecules and junction protein expression via inhibition of NF- κ B signalling and reduced leukocyte adhesion to endothelial cells ability and endothelial monolayer permeability, which led to the down-regulation of adhesion and transmigration-regulated molecular expression. GBEE reduced paracellular and transcellular transmigration to maintain cell-cell monolayer integrity, reduce permeability, and prevent endothelial dysfunction.

Data Availability

The datasets used and/or analysed during the present study are available from the corresponding author upon reasonable request.

Conflicts of Interest

The authors declare that they have no conflicts of interest.

Acknowledgments

The authors thank the Ministry of Science and Technology of Taiwan for supporting this work through grant NSC 96-2320-B-309-005-MY3.

References

- [1] Y. C. Yang, W. T. Wu, M. C. Mong, and Z. Wang, "Gynura bicolor aqueous extract attenuated H₂O₂ induced injury in PC12 cells," *Biomedicine (Taipei)*, vol. 9, pp. 38–45, 2019.
- [2] M.-C. Yin, Z.-H. Wang, W.-H. Liu, and M.-C. Mong, "Aqueous extract of gynura bicolor attenuated hepatic steatosis, glycation, oxidative, and inflammatory injury induced by chronic ethanol consumption in mice," *Journal of Food Science*, vol. 82, no. 11, pp. 2746–2751, 2017.
- [3] P. Y. Pai, M. C. Mong, Y. C. Yang, Y. T. Liu, Z. H. Wang, and M. C. Yin, "Anti-diabetic effects of gynura bicolor aqueous extract in mice," *Journal of Food Science*, vol. 84, no. 6, pp. 1631–1637, 2019.
- [4] V. Krishnan, S. Ahmad, and M. Mahmood, "Antioxidant potential in different parts and callus of *Gynura procumbens* and different parts of *Gynura bicolor*," *Biomed Research International*, vol. 2015, Article ID 147909, 2015.
- [5] W. Y. Teoh, H. P. Tan, S. K. Ling, N. Abdul Wahab, and K. S. Sim, "Phytochemical investigation of *Gynura bicolor* leaves and cytotoxicity evaluation of the chemical constituents against HCT 116 cells," *Natural Product Research*, vol. 30, no. 4, pp. 448–451, 2016.
- [6] C.-C. Wu, W.-L. Chang, C.-H. Lu, Y.-P. Chang, J.-J. Wang, and S.-L. Hsieh, "Effects of extracts from *Gynura bicolor* (Roxb. & Willd.) DC. on iron bioavailability in rats," *Journal of Food and Drug Analysis*, vol. 23, no. 3, pp. 425–432, 2015.
- [7] C.-C. Wu, C.-K. Lii, K.-L. Liu, P.-Y. Chen, and S.-L. Hsieh, "Antiinflammatory activity of gynura bicolor (紅鳳菜 *Hóng Fēng Cài*) ether extract through inhibits nuclear factor kappa B activation," *Journal of Traditional and Complementary Medicine*, vol. 3, no. 1, pp. 48–52, 2013.

- [8] S.-L. Hsieh, P.-J. Tsai, Y.-C. Liu, and C.-C. Wu, "Potential effects of antioxidant and serum cholesterol-lowering effects of *Gynura bicolor* water extracts in Syrian Hamster," *Evidence-Based Complementary and Alternative Medicine*, vol. 2020, Article ID 2907610, 2020.
- [9] C. C. Wu, Y. P. Chang, J. J. Wang et al., "Dietary administration of *Gynura bicolor* (Roxb. Willd.) DC water extract enhances immune response and survival rate against *Vibrio alginolyticus* and white spot syndrome virus in white shrimp *Litopenaeus vannamei*," *Fish and Shellfish Immunology*, vol. 42, no. 1, pp. 25–33, 2015.
- [10] K. Mc Namara, H. Alzubaidi, and J. K. Jackson, "Cardiovascular disease as a leading cause of death: how are pharmacists getting involved?" *Integrated Pharmacy Research and Practice*, vol. 8, pp. 1–11, 2019.
- [11] D. A. Chistiakov, A. N. Orekhov, and Y. V. Bobryshev, "Endothelial barrier and its abnormalities in cardiovascular disease," *Frontiers in Physiology*, vol. 6, p. 365, 2015.
- [12] M. J. Allingham, J. D. van Buul, and K. Burrige, "ICAM-1-mediated, Src- and Pyk2-dependent vascular endothelial cadherin tyrosine phosphorylation is required for leukocyte transendothelial migration," *The Journal of Immunology*, vol. 179, no. 6, pp. 4053–4064, 2007.
- [13] P. R. Clark, T. D. Manes, J. S. Pober, and M. S. Kluger, "Increased iCAM-1 expression causes endothelial cell leakiness, cytoskeletal reorganization and junctional alterations," *Journal of Investigative Dermatology*, vol. 127, no. 4, pp. 762–774, 2007.
- [14] E. S. Wittchen, "Endothelial signaling in paracellular and transcellular leukocyte transmigration," *Frontiers in Bioscience*, vol. 14, pp. 2522–2545, 2009.
- [15] A. Di, D. Mehta, and A. B. Malik, "ROS-activated calcium signaling mechanisms regulating endothelial barrier function," *Cell Calcium*, vol. 60, no. 3, pp. 163–171, 2016.
- [16] L. Tornatore, A. K. Thotakura, J. Bennett, M. Moretti, and G. Franzoso, "The nuclear factor kappa B signaling pathway: integrating metabolism with inflammation," *Trends in Cell Biology*, vol. 22, no. 11, pp. 557–566, 2012.
- [17] A. W. Orr, J. M. Sanders, M. Bevard, E. Coleman, I. J. Sarembock, and M. A. Schwartz, "The subendothelial extracellular matrix modulates NF- κ B activation by flow," *Journal of Cell Biology*, vol. 169, no. 1, pp. 191–202, 2005.
- [18] S. J. Collins, R. C. Gallo, and R. E. Gallagher, "Continuous growth and differentiation of human myeloid leukaemic cells in suspension culture," *Nature*, vol. 270, no. 5635, pp. 347–349, 1977.
- [19] X. Chen, B. Andresen, M. Hill, J. Zhang, F. Booth, and C. Zhang, "Role of reactive oxygen species in tumor necrosis factor- α induced endothelial dysfunction," *Current Hypertension Reviews*, vol. 4, no. 4, pp. 245–255, 2008.
- [20] F. Denizot and R. Lang, "Rapid colorimetric assay for cell growth and survival," *Journal of Immunological Methods*, vol. 89, no. 2, pp. 271–277, 1986.
- [21] F. Braut-Boucher, J. Pichon, P. Rat, M. Adolphe, M. Aubery, and J. Font, "A non-isotopic, highly sensitive, fluorimetric, cell-cell adhesion microplate assay using calcein am-labeled lymphocytes," *Journal of Immunological Methods*, vol. 178, no. 1, pp. 41–51, 1995.
- [22] S. Hsien, B. Y. Huang, S. L. Hsien et al., "Green fabrication of agar-conjugated Fe₃O₄ magnetic nanoparticles," *Nanotechnology*, vol. 21, no. 44, pp. 445601–445606, 2010.
- [23] P. K. Gopal, J. Prasad, J. Smart, and H. S. Gill, "In vitro adherence properties of *Lactobacillus rhamnosus* DR20 and *Bifidobacterium lactis* DR10 strains and their antagonistic activity against an enterotoxigenic *Escherichia coli*," *International Journal of Food Microbiology*, vol. 67, no. 3, pp. 207–216, 2001.
- [24] O. Lowry, N. J. Rosebrough, A. L. Farr, and R. J. Randall, "Protein measurement with Folin phenol reagent," *Journal of Biological Chemistry*, vol. 193, Article ID 265275, 1951.
- [25] H. Towbin, T. Staehelin, and J. Gordon, "Electrophoretic transfer of proteins from polyacrylamide gels to nitrocellulose sheets: procedure and some applications," *Proceedings of the National Academy of Sciences*, vol. 76, no. 9, pp. 4350–4354, 1979.
- [26] U. K. Laemmli, "Cleavage of structural proteins during the assembly of the head of bacteriophage T4," *Nature*, vol. 227, no. 5259, pp. 680–685, 1970.
- [27] W. A. Muller, "Mechanisms of transendothelial migration of leukocytes," *Circulation Research*, vol. 105, no. 3, pp. 223–230, 2009.
- [28] K. Kudo, S. Hasegawa, Y. Suzuki et al., "1 α ,25-dihydroxyvitamin D3 inhibits vascular cellular adhesion molecule-1 expression and interleukin-8 production in human coronary arterial endothelial cells," *Journal of Steroid Biochemistry and Molecular Biology*, vol. 132, no. 3–5, pp. 290–294, 2012.
- [29] Q. Zhou, X. Han, R. Li et al., "Anti-atherosclerosis of oligomeric proanthocyanidins from *Rhodiola rosea* on rat model via hypolipemic, antioxidant, anti-inflammatory activities together with regulation of endothelial function," *Phytomedicine*, vol. 51, pp. 171–180, 2018.
- [30] Y. M. Ham, H. S. Song, J. E. Kwon et al., "Effects of fermented *Sorghum bicolor* L. Moench extract on inflammation and thickness in a vascular cell and atherosclerotic mice model," *Journal of Natural Medicines*, vol. 73, no. 1, pp. 34–46, 2019.
- [31] L. Kuo and T. W. Hein, "Vasomotor regulation of coronary microcirculation by oxidative stress: role of arginase," *Frontiers in Immunol*, vol. 4, p. 237, 2013.
- [32] J. Honavar, A. A. Samal, K. M. Bradley et al., "Chlorine gas exposure causes systemic endothelial dysfunction by inhibiting endothelial nitric oxide synthase-dependent signaling," *American Journal of Respiratory Cell and Molecular Biology*, vol. 45, no. 2, pp. 419–425, 2011.
- [33] C. S. Patel, H.-W. Wilkerson, T. V. Larson, J. A. Stewart, and T. J. Kavanagh, "DIESEL particulate exposed macrophages alter endothelial cell expression of eNOS, iNOS, MCP1, and glutathione synthesis genes," *Toxicology in Vitro*, vol. 25, no. 8, pp. 2064–2073, 2011.
- [34] K. M. Stroka and H. Aranda-Espinoza, "Effects of morphology vs. cell-cell interactions on endothelial cell stiffness," *Cellular and Molecular Bioengineering*, vol. 4, no. 1, pp. 9–27, 2011.
- [35] Y. L. Dorland and S. Huvneers, "Cell-cell junctional mechanotransduction in endothelial remodeling," *Cellular and Molecular Life Sciences*, vol. 74, no. 2, pp. 279–292, 2017.
- [36] J. M. Cook-Mills and T. L. Deem, "Active participation of endothelial cells in inflammation," *Journal of Leukocyte Biology*, vol. 77, no. 4, pp. 487–495, 2005.
- [37] B. Srinivasan, A. R. Kolli, M. B. Esch, H. E. Abaci, M. L. Shuler, and J. J. Hickman, "TEER measurement techniques for in vitro barrier model systems," *Journal of Laboratory Automation*, vol. 20, no. 2, pp. 107–126, 2015.
- [38] D. Bachinger, E. Mayer, T. Kaschubek, C. Schieder, J. König, and K. Teichmann, "Influence of phytochemicals on recovery of the barrier function of intestinal porcine epithelial cells after a calcium switch," *Journal of Animal Physiology and Animal Nutrition*, vol. 103, no. 1, pp. 210–220, 2019.
- [39] D. Lian, H. Yuan, X. Yin et al., "Puerarin inhibits hyperglycemia-induced inter-endothelial junction through suppressing endothelial Nlrp3 inflammasome activation via ROS-

- dependent oxidative pathway,” *Phytomedicine*, vol. 55, pp. 310–319, 2019.
- [40] E. G. Assefa, Q. Yan, S. B. Gezahegn et al., “Role of resveratrol on indoxyl sulfate-induced endothelial hyperpermeability via aryl hydrocarbon receptor (AHR)/Src-Dependent pathway,” *Oxidative Medicine and Cellular Longevity*, vol. 2019, Article ID 5847040, 2019.
- [41] M. G. Lampugnani, M. Resnati, M. Raiteri et al., “A novel endothelial-specific membrane protein is a marker of cell-cell contacts,” *Journal of Cell Biology*, vol. 118, no. 6, pp. 1511–1522, 1992.
- [42] E. S. Harris and W. J. Nelson, “VE-Cadherin: at the front, center, and sides of endothelial cell organization and function,” *Current Opinion in Cell Biology*, vol. 22, no. 5, pp. 651–658, 2010.
- [43] G. Liu, A. T. Place, Z. Chen et al., “ICAM-1-activated Src and eNOS signaling increase endothelial cell surface PECAM-1 adhesivity and neutrophil transmigration,” *Blood*, vol. 120, no. 9, pp. 1942–1952, 2012.
- [44] I. H. Sarelius and A. J. Glading, “Control of vascular permeability by adhesion molecules,” *Tissue Barriers*, vol. 3, no. 1–2, Article ID e985954, 2015.
- [45] M. S. Kim, D. S. Kim, H.-S. Kim, S.-W. Kang, and Y.-H. Kang, “Inhibitory effects of luteolin on transendothelial migration of monocytes and formation of lipid-laden macrophages,” *Nutrition*, vol. 28, no. 10, pp. 1044–1054, 2012.
- [46] M.-H. Yu, T.-Y. Yang, H.-H. Ho, H.-P. Huang, K.-C. Chan, and C.-J. Wang, “Mulberry polyphenol extract inhibits FAK/Src/PI3K complex and related signaling to regulate the migration in A7r5 cells,” *Journal of Agricultural and Food Chemistry*, vol. 66, no. 15, pp. 3860–3869, 2018.
- [47] H. Shimokawa, S. Sunamura, and K. Satoh, “RhoA/rho-kinase in the cardiovascular system,” *Circulation Research*, vol. 118, no. 2, pp. 352–366, 2016.
- [48] H. Shimokawa, H. Tomoike, S. Nabeyama et al., “Coronary artery spasm induced in atherosclerotic miniature swine,” *Science*, vol. 221, no. 4610, pp. 560–562, 1983.
- [49] H. Shimokawa, “Primary endothelial dysfunction: atherosclerosis,” *Journal of Molecular and Cellular Cardiology*, vol. 31, no. 1, pp. 23–37, 1999.
- [50] M. Zhang, Z. Chang, P. Zhang et al., “Protective effects of 18 β -glycyrrhetic acid on pulmonary arterial hypertension via regulation of Rho A/Rho kinase pathway,” *Chemico-Biological Interactions*, vol. 311, Article ID 108749, 2019.
- [51] C.-C. Wu, P.-Y. Lai, S. Hsieh, C.-C. Cheng, and S.-L. Hsieh, “Suppression of carnosine on adhesion and extravasation of human colorectal cancer cells,” *Anticancer Research*, vol. 39, no. 11, pp. 6135–6144, 2019.
- [52] T. Collins, M. A. Read, A. S. Neish, M. Z. Whitley, D. Thanos, and T. Maniatis, “Transcriptional regulation of endothelial cell adhesion molecules: NF- κ B and cytokine-inducible enhancers,” *The FASEB Journal*, vol. 9, no. 10, pp. 899–909, 1995.
- [53] J. Chen, H. Lü, L.-X. Fang et al., “Detection and toxicity evaluation of pyrrolizidine alkaloids in medicinal plants *Gynura bicolor* and *Gynura divaricata* collected from different Chinese locations,” *Chemistry & Biodiversity*, vol. 14, no. 2, Article ID e1600221, 2017.
- [54] H. Lu, Y. Pei, and W. Li, “Studies on flavonoids from *Gynura bicolor* DC,” *Zhongguo Xian Dai Ying Yong Yao Xue*, vol. 27, pp. 613–614, 2010.
- [55] S. Bhaskar, P. R. Sudhakaran, and A. Helen, “Quercetin attenuates atherosclerotic inflammation and adhesion molecule expression by modulating TLR-NF- κ B signaling pathway,” *Cellular Immunology*, vol. 310, pp. 131–140, 2016.

Research Article

Traditional Chinese Medicine for Essential Hypertension: A Clinical Evidence Map

Yan Zhang ^{1,2,3}, Biqing Wang,^{4,2,3} Chunxiao Ju,^{4,2,3} Lu Liu,^{4,2,3} Ying Zhu,^{4,2,3} Jun Mei,^{2,3} Yue Liu ^{5,3} and Fengqin Xu ^{2,3}

¹Graduate School of China Academy of Chinese Medical Sciences, Beijing 100700, China

²Center of Geriatrics Diseases, Xiyuan Hospital, China Academy of Chinese Medical Sciences, Beijing 100091, China

³Cardiovascular Disease Team, China Center for Evidence-Based Medicine of TCM, Beijing 100091, China

⁴Graduate School of Beijing University of Chinese Medicine, Beijing 100029, China

⁵Center of Cardiovascular Diseases, Xiyuan Hospital, China Academy of Chinese Medical Sciences, Beijing 100091, China

Correspondence should be addressed to Yue Liu; liuyueheart@hotmail.com and Fengqin Xu; dr.xufengqin@outlook.com

Received 7 June 2020; Revised 14 August 2020; Accepted 11 November 2020; Published 19 December 2020

Academic Editor: Hong Chang

Copyright © 2020 Yan Zhang et al. This is an open access article distributed under the Creative Commons Attribution License, which permits unrestricted use, distribution, and reproduction in any medium, provided the original work is properly cited.

We systematically retrieved and summarised clinical studies on traditional Chinese medicine (TCM) for the prevention and treatment of essential hypertension (EH) using the evidence map. We aimed to explore the evidence distribution, identify gaps in evidence, and inform on future research priorities. Clinical studies, systematic reviews, guidelines, and pathway studies related to TCM for the prevention and treatment of EH, published between January 2000 and December 2019, were included from databases CNKI, WanFang Data, VIP, PubMed, Embase, and Web of Science. The distribution of evidence was analysed using text descriptions, tables, and graphs. A total of 9,403 articles were included, including 5,920 randomised controlled studies (RCTs), 16 guidelines, expert consensus and path studies, and 139 systematic reviews (SRs). The articles publishing trend increased over time. This study showed that the intervention time of TCM was concentrated at 4–8 weeks, mainly through Chinese herbal medicine (CHM) for the prevention and treatment of elderly hypertension and the complications. A Measurement Tool to Assess Systematic Reviews (AMSTAR) scores of the included reviews ranged from 2 to 10. Most of the SRs had a potentially positive effect ($n = 120$), mainly in 5–8 score. Primary studies and SRs show potential benefits of TCM in lowering blood pressure, lowering the TCM syndrome and symptom differentiation scores (TCM-SSD scores), improving the total effective rate, and reducing the adverse events. The adjunctive effect of TCM on improving the total effective rate, lowering the blood pressure, lowering the TCM-SSD scores, and lowering the adverse effects was only supported by low-quality evidence in this research. The evidence map was used to show the overall research on TCM for the treatment of EH; however, due to the existing problems of the primary studies, the current research conclusion needs further research with higher quality and standardisation.

1. Introduction

Hypertension has become a primary global disease and is an important global public health challenge [1]. According to literature, in 2000, 26.4% of adults worldwide suffered from high blood pressure. It is estimated that by 2025, 29.2% of people in the world will suffer from high blood pressure [2]. There is currently an upward trend of the hypertension prevalence and mortality rates among Chinese residents and it is predicted that by 2030, the annual economic burden of

cardiovascular disease deaths caused by hypertension in China will reach \$6–9 million [3]. A prospective epidemiological study of 47,000 residents in 115 urban and rural communities in China showed that the prevalence rate, awareness rate, treatment rate, and control rate of hypertension in China were 41.9%, 41.6%, 34.4%, and 8.2%, respectively, indicating that prevention, detection, treatment, and control of hypertension should be prioritised [4].

Antihypertensive therapy is currently widely used; however, its understanding, management, and control are

not well known due to the adverse effects and intolerance of antihypertensive drugs that the patients currently face [5]. Therefore, more attention must be given to complementary and alternative medical treatments. Systematic reviews (SRs) have shown that traditional Chinese medicine (TCM) has a significant effect on lowering blood pressure but there is little research on its underlying intervention mechanisms [6, 7].

As an evidence integration method, evidence mapping can integrate evidence of various study types under a research topic and comprehensively demonstrate the problems in the research topic, thereby depicting a complete picture of the research field [8–10]. Several evidence mapping reports have been published on the Chinese medical fields such as acupuncture, Tai Chi, massage, and angelica; however, they only included randomised controlled studies (RCTs) and SRs [11–14]. However, the clinical evidence for the prevention and treatment of hypertension by TCM is unclear. Therefore, this study used an evidence map to systematically find relevant literature (observational studies, RCTs, SRs, guidelines, and expert consensus) on the clinical prevention and treatment of essential hypertension, in order to better understand the distribution of evidence in this field, identify gaps in evidence, and provide potential information for priority areas.

2. Methods

2.1. Database and Search Strategies. The literature searches were conducted using PubMed, Web of Science, Embase, Chinese National Knowledge Infrastructure (CNKI), Chinese Scientific Journal Database (VIP), and WanFang data. The search was restricted from January 1, 2000, to December 31, 2019. We searched the Chinese database using “hypertension”. The retrieval subjects are limited to TCM, integrated Chinese and Western medicines, TCM internal medicine, surgery of Chinese medicine, gynaecology of Chinese medicine, paediatrics of Chinese medicine, and other TCM-related subjects. English database retrieval was divided into two parts. The search terms for the first retrieval included: (“hypertension” OR “blood pressure, high” OR “blood pressures, high” OR “high blood pressure” OR “high blood pressures”) AND (“medicine, Chinese traditional” OR “traditional Chinese medicine” OR “traditional medicine, Chinese” OR “Chinese medicine, traditional” OR “herbal medicine” OR “drugs, Chinese herbal” OR “herbal formula” OR “Chinese herbal medicine” OR “Chinese herb therapy” OR “Chinese herb” OR “herb therapy” OR “herbal remedy” OR “acupuncture”). The second retrieval search term was “hypertension” + hypertension-related formulas and non-drug therapy that frequently appeared in the meta-analysis in the Chinese database; the two retrievals were combined. The literature searched included academic journals, graduation theses, and conference papers.

2.2. Inclusion Criteria. The inclusion criteria were as follows:

- (1) Type of study: RCTs, nonrandomised controlled trials (non-RCTs), cohort studies, case-control

studies, cross-sectional studies, real-world studies (RWS), systematic reviews, meta-analyses, expert consensus, guidelines, and clinical pathway studies on TCM intervention for hypertension

- (2) Type of participants: the patients that met the diagnostic criteria of essential hypertension. There was no limitation on the age, sex, race, time of onset, and cases of the source
- (3) Type of intervention: TCM (Chinese herbal medicine (CHM) (decoction, tablet, pill, powder, granule, capsule, oral liquid, or injection), nondrug therapy (acupuncture, qigong, massage, and Baduanjin, etc.)), nursing of TCM, or above measures combined with conventional Western medicine that was used in the treatment groups. The comparison interventions were conventional Western medicine, placebo, or blank controls
- (4) Type of outcome: the main outcomes included blood pressure (BP), total effective rate, TCM syndrome and symptom differentiation (TCM-SSD) scores, and adverse events. TCM prevention and treatment, TCM syndrome type, and duration of TCM intervention

2.3. Exclusion Criteria. (1) Clinical experience, (2) clinical trial protocols, (3) meeting abstracts, (4) no full-text, (5) redundant publication, and (6) fundamental researches were excluded.

2.4. Literature Screening and Data Extraction. Four authors independently conducted the literature search, study selection, and data extraction, and 2 authors conducted it as a group. The extracted data included the following: (1) basic information: author, publication year, study object and disease, intervention measures, total sample size, and outcome indicators; (2) study type ((i) intervention study: RCTs, non-RCTs, (ii) observational study: a cohort study, case-control study, and cross-sectional study, (iii) secondary study: SRs, guidelines, and clinical pathway studies, (iv) RWS); (3) treatment categories (CPM, CHM, nursing of TCM, acupuncture, massage, TCM exercise therapy, auricular point, acupoint application, multimethod combination, and others); (4) complicating diseases (cerebral haemorrhage, cerebral infarction, angina pectoris/myocardial ischaemia, arrhythmia, diabetes/abnormal glucose metabolism, cardiac insufficiency, anxiety and depression, renal diseases, eye diseases, insomnia/sleep disorders, hyperlipidaemia, hyperuricaemia, metabolic syndrome, atherosclerosis, etc.); and (5) the duration of therapeutic intervention. Disagreements were resolved by discussion, and a consensus was reached through a third party (J. Mei).

2.5. Quality Assessment of the Included Systematic Reviews. A Measurement Tool to Assess SRs (AMSTAR), which consists of 11 items, was used to evaluate the methodological quality of all the included SRs. For each item, “Yes,” “No,”

“Can’t answer,” or “Not applicable” was assigned according to judgement criteria of AMSTAR. The number of “yes” was counted as the total AMSTAR score. A score of 4 or less was considered low quality, a score of 5 to 8 was medium quality, and a score of 9 or more was high quality [15, 16]. Based on the SRs’ clinical effectiveness, it was further divided into 4 categories: “evidence of no effect,” “unclear evidence,” “evidence of a potentially positive effect,” and “evidence of a positive effect” [13]. The category “evidence of no effect” meant that the effect of the control group is equal to or better than that of the TCM observation group. “Unclear evidence” meant that the result of a systematic review of similar contents is controversial, or the evidence is summarised as inconclusive by the original study’s author. “Evidence of a potentially positive effect” referred to the systematic review of all included clinical studies, combined results, and statistical evidence to show effectiveness but the lack of basic and auxiliary evidence made it difficult to produce positive and reliable conclusions. “Evidence of a positive effect” meant that statistics showed that TCM therapy had a significant effect and that the authors of the systematic review had no major doubts regarding the current evidence and recommend the therapy.

2.6. Data Analysis and Presentation. EXCEL 2013 was used to integrate and process the data. The data summary and analysis are shown as text and charts. The distribution of the development trend is depicted as a line chart, the distribution of category proportions as a pie chart, and the distribution of evidence as bubble plots and heatmap.

3. Results

3.1. Description of the Included Trials. The initial search retrieved 55,197 articles from the six databases. After removing duplicates, 39,162 trials were identified. After screening the titles and abstracts, 10,302 trials were retained. By browsing the full-text articles, we further excluded 899 records. In the end, 9,403 studies were reviewed, including primary studies ($n = 9,243$), systematic reviews ($n = 144$), and guidelines, expert consensus, and path studies ($n = 16$) (Figure 1).

3.2. Trends in Publication Year of Clinical Studies. A total of 9,403 studies were included from January 2000 to December 2019. The number of studies showed an overall rising trend with a peak in 2018 at home and 2015 abroad, respectively (see Figure 2). The TCM role is increasingly being suspected in the prevention and treatment of hypertension, both in China and worldwide.

3.3. Type and Scale of Clinical Studies. The clinical studies were mainly RCTs, including intervention studies (RCTs ($n = 5,920$, 63.0%), non-RCTs ($n = 2,133$, 22.7%)), observational studies ($n = 1,185$, 12.6%), RWS ($n = 5$, 0.1%), and SRs ($n = 144$, 1.5%). The minimum sample size of the RCT was 10 and the maximum was 2,110 [17]. The maximum sample size

of the observational study was 154,083 cases [18], and the sample size of the interventional study was mostly in the range of 60 to 100 cases. In RWS, the sample size ranged from 1,544 to 30,034 cases [19] (see Table 1).

3.4. Research on Syndrome and Constitution. A total of 848 clinical studies on TCM syndromes of hypertension were included, of which the syndrome distribution ranked first with a total of 162; others included hypertension syndromes and clinical indicators in young and middle-aged people ($n = 4$) [20–23], syndromes in elderly hypertension ($n = 124$), hypertension stages and grades ($n = 9$) [24], four diagnosis information and TCM syndromes ($n = 1$) [25], and TCM syndromes and clinical indicators in grade 3 hypertension ($n = 2$) [26, 27]. Regarding comorbidity, there were 2 cases of hypertension with arrhythmia, 22 cases of atherosclerosis, 9 cases of a cerebral haemorrhage, 19 cases of cerebral infarction, and 32 cases of diabetes. Studies on the correlation between syndromes and clinical indicators mainly involved indicators such as homocysteine, blood lipid, blood glucose, vascular function, and inflammation. A total of 245 studies on the TCM constitution of hypertension were included, of which there were 12 constitution and syndrome types, mainly involving the phlegm-dampness syndrome [28]. As the syndrome type and constitution articles involved more than 100 kinds of clinical indicators, only the first 36 indicators were shown (see Figure 3).

The bubble plot shows the syndrome and constitution and mainly on a wide range of hypertension and elderly patients with hypertension; however, there are few studies on prehypertension and hypertension grades.

3.5. Categories of TCM Prevention and Treatment. TCM prevention and treatment schemes are mainly divided into 10 categories, including CHM decoction ($n = 4,059$, 49.6%), Chinese patent medicine ($n = 1,916$, 23.4%), acupuncture ((electroacupuncture and meridional acupuncture) ($n = 505$, 6.2%)), massage ($n = 109$, 1.3%), auricular point and auricular acupuncture ($n = 163$, 2.0%), acupoint application ($n = 149$, 1.8%), TCM exercise therapy (Tai Chi, Baduanjin, wu qinxi) ($n = 52$, 0.6%), TCM comprehensive nursing ($n = 311$, 3.8%), multitherapy ($n = 516$, 6.3%), and others (pediluvium, fumigation, etc.) ($n = 405$, 4.9%) (Figure 4). CHM and nondrug therapies are widely used for treating hypertension.

3.6. Clinical Evaluation of the TCM Treatment Schemes. Regarding hypertension and the complications, more than 5 separate evaluations of clinical studies included 14 injections such as compound Danshen injection, astragalus injection, Shengmai injection, and Danhong injection; 12 oral CPM such as the Niu Huang Jiangya pill, Liuwei Dihuang pill, and Songling Xuemaikang capsule; and 13 types of oral CHM decoctions such as Xuefu Zhuyu decoction, Banxia Bbaizhu Tianma decoction, and Lingjiao Gouteng decoction (Figures 5 and 6). The main treatment methods included the calming liver-yang method, resolving phlegm and

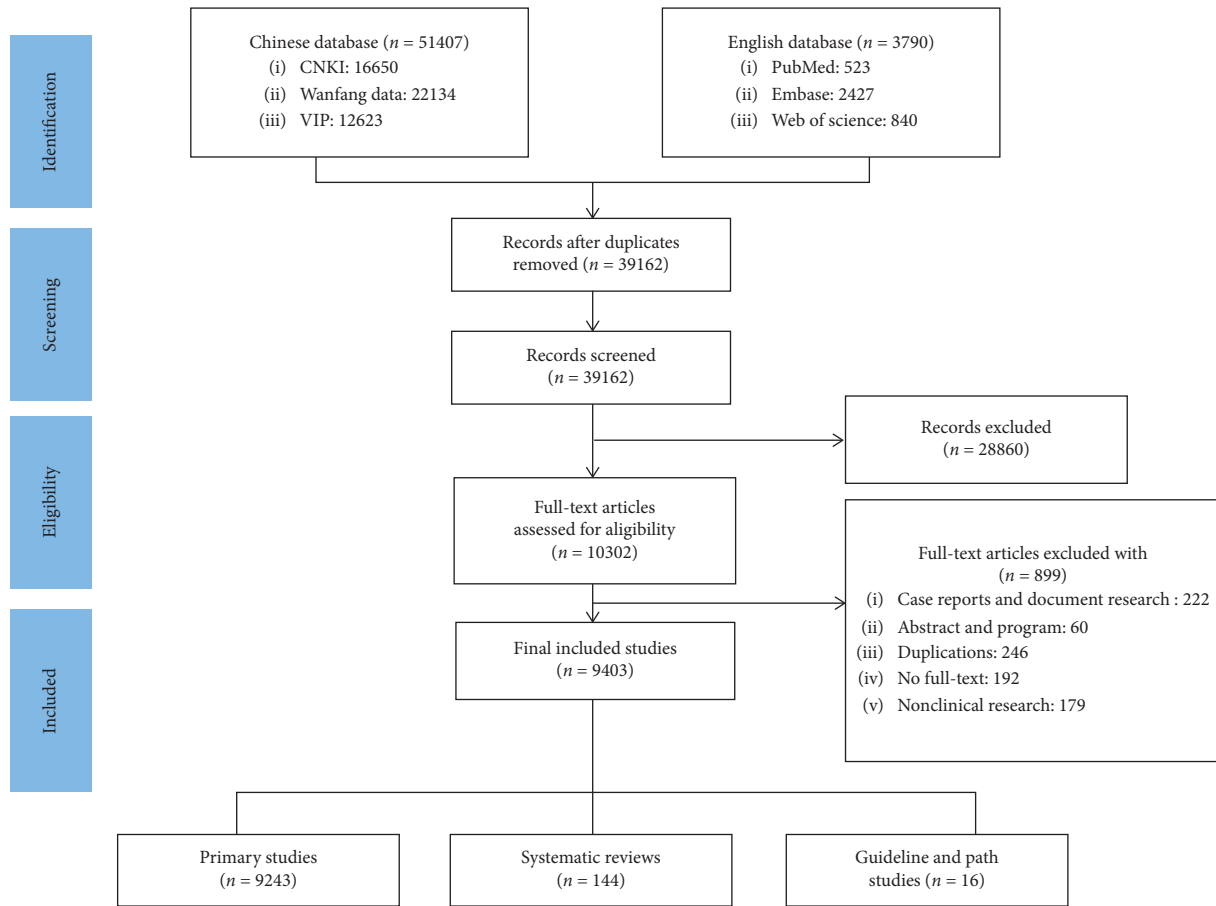


FIGURE 1: Study flow diagram.

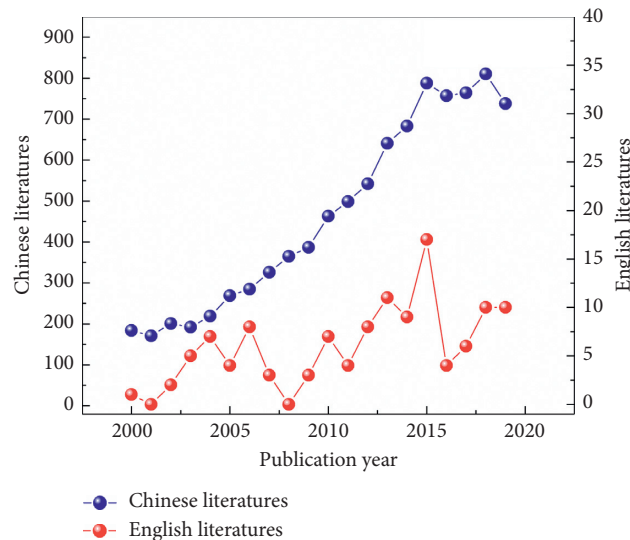


FIGURE 2: Annual trends in the clinical research literature. The blue line denotes the number of Chinese literature, and the red line denotes the number of English literature.

quenching wind, promoting blood circulation, and removal of blood stasis. The combination modes were mostly CHM decoction in combination, CHM decoction combined with CPM, and integrated Chinese and Western medicines.

The evaluation of TCM prevention and treatment schemes was divided into several types of indicators: total effective rate, BP, TCM-SSD scores, clinical symptoms, blood lipid levels, inflammatory indicators (e.g., C-reactive

TABLE 1: Clinical study scale.

Study sample size (<i>n</i>)	Number of research articles (<i>n</i> (%))		
	Intervention study	Observational study	Real-world study
$n < 60$	1252 (15.54)	41 (3.46)	0
$60 \leq n < 100$	3977 (49.38)	146 (12.32)	0
$100 \leq n < 300$	2638 (32.76)	595 (50.21)	0
$300 \leq n < 1000$	167 (2.07)	316 (26.67)	0
$n \geq 1000$	19 (0.24)	87 (7.34)	5 (100.00)
Total	8053	1185	5

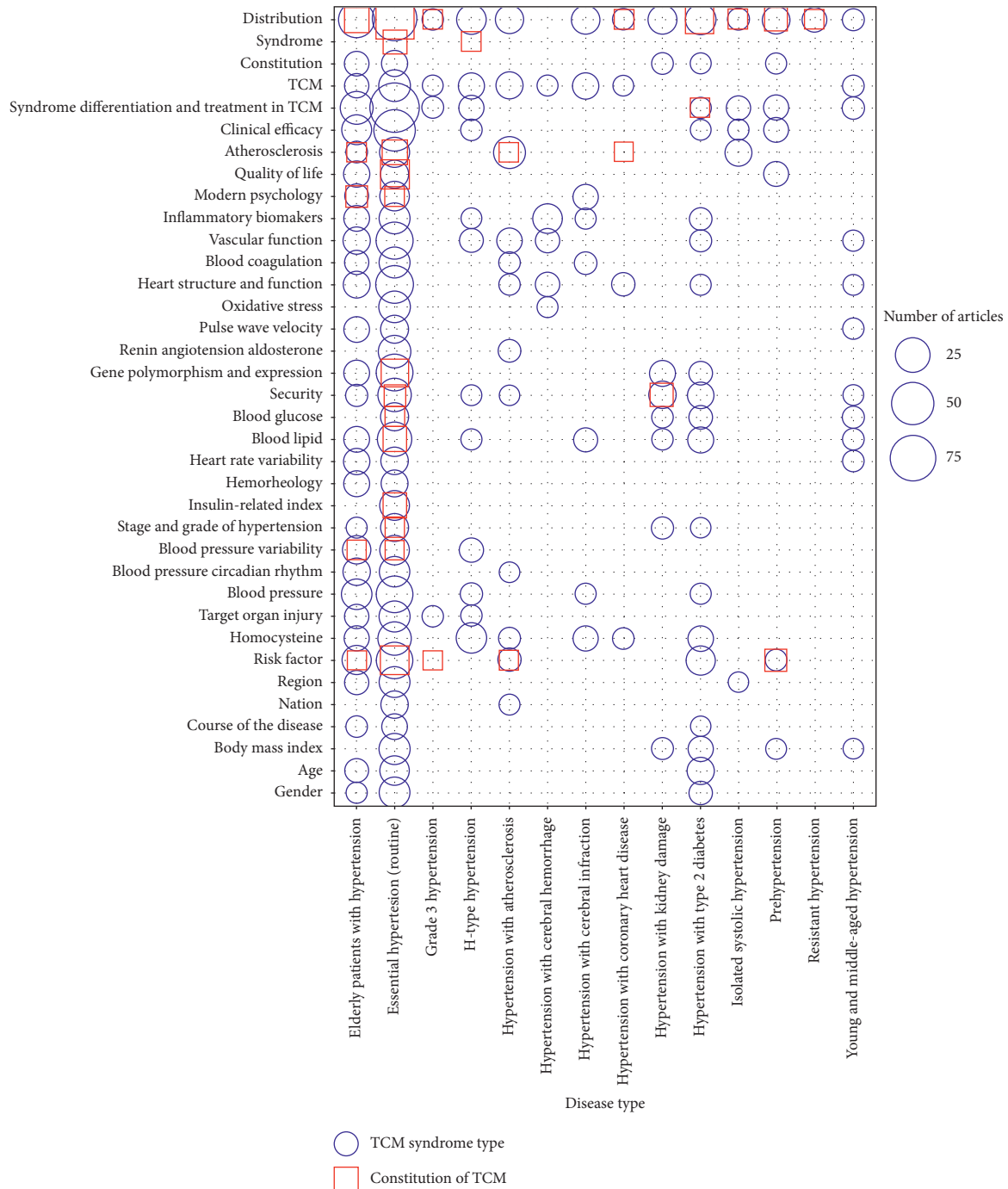


FIGURE 3: Evidence distributions of clinical studies on syndrome and constitution. Objects of study (*x*-axis) and research content (*y*-axis). The red square indicates the constitution of TCM and the blue bubbles indicate the TCM syndrome types.

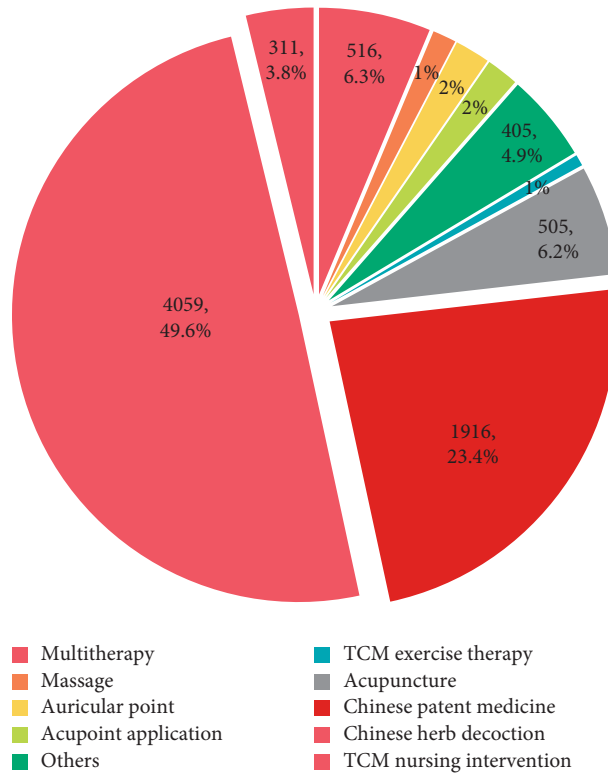


FIGURE 4: Category distribution of the prevention and treatment of hypertension by TCM.

ID	Oral Chinese medicine preparation treatment schemes	Total effective rate	Clinical symptoms	TCM-SSD scores	Blood pressure	Blood lipid	Vascular endothelium	Inflammatory biomarkers	Indicators of brain function	Blood coagulation	Hemorheology	Cardiac function index	Quality of life	Index of security
1	Banxia baizhu tianma decoction	2	67	0	95	23	3	5	1	0	1	3	0	10
2	Er-xian decoction	3	5	1	10	0	0	0	0	0	0	0	2	2
3	Compound qishao antihypertensive tablet	3	1	1	0	0	1	1	0	1	1	2	0	2
4	Guipi decoction	1	4	0	14	0	0	0	0	0	0	0	8	0
5	Jianling decoction	4	18	1	14	7	1	4	0	1	0	0	2	4
6	Jiangyabao	3	1	0	12	2	0	0	0	0	1	1	0	2
7	Jiangya yishen granula	0	1	0	2	0	0	0	0	0	0	0	0	4
8	Lingjiao gouteng decoction	2	4	0	4	2	0	0	1	0	0	0	0	3
9	Liuwei dihuang pills	2	5	0	15	2	2	2	0	1	0	0	1	8
10	Longdanxiegan decoction	1	4	0	8	0	0	0	0	0	1	1	2	3
11	Naoxintong capsule	4	3	0	10	7	3	1	4	0	5	2	1	5
12	Naoxuekang oral liquid	2	0	0	2	0	0	1	4	0	0	0	0	0
13	Niuhuangjiangya	5	6	0	11	3	2	0	0	0	2	0	0	5
14	Qijudihuang pill	4	4	0	12	3	0	1	0	0	4	0	2	2
15	Heart-protecting musk pill	8	7	1	13	4	9	3	0	1	0	11	1	10
16	Songling xuemaikang capsule	19	19	1	35	4	6	2	0	1	3	3	4	10
17	Tianmagouteng decoction	121	138	15	259	24	25	2	6	0	1	11	31	67
18	Wendan decoction	10	22	4	33	6	8	2	1	1	0	3	1	15
19	YiShen jiangya granule	0	5	1	7	1	3	0	0	0	1	1	1	3
20	Ginkgo leaf tablets	3	3	0	7	1	0	0	0	0	0	0	1	2
21	Zhenwu decoction	3	5	0	8	0	0	0	0	0	0	0	0	0
22	Zhenganxifeng decoction	36	22	4	45	4	1	1	3	0	4	0	2	17
23	Zishui pinggan decoction	3	1	3	5	1	0	0	0	0	0	0	0	0
24	Xiaoxianxiong decoction	4	3	5	3	0	0	3	0	0	0	1	0	1
25	Xuefu zhuyu decoction	10	2	2	19	6	1	1	1	0	1	2	0	0

FIGURE 5: Distribution of clinical evidence for the prevention and treatment of hypertension by oral Chinese herbal preparations. The change of “blue-white-red” colour represents the number of research literature from low to high, and numbers represent the corresponding number of literature. The evaluation index of clinical research is in x-axis and oral Chinese medicine preparation is in y-axis.

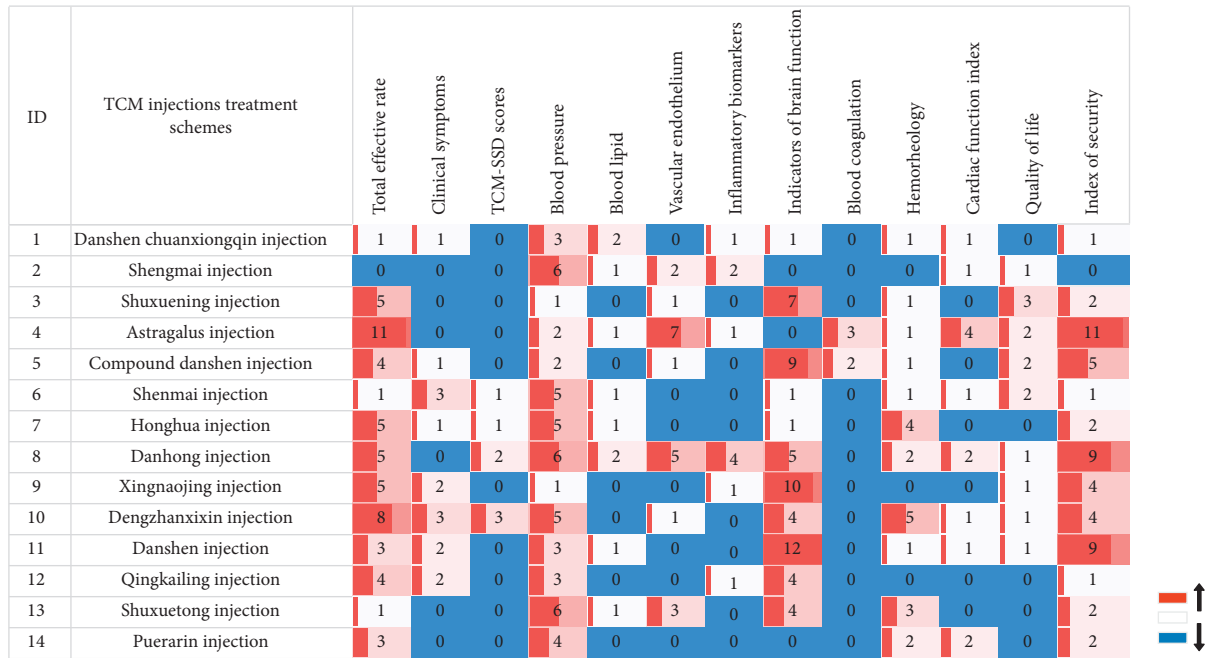


FIGURE 6: Distribution of clinical evidence on the prevention and treatment of hypertension by TCM injections. The change of “blue-white-red” colour represents the number of research literature from low to high and numbers represent the corresponding number of literature. The evaluation index of clinical research is in x-axis and traditional Chinese medicine injection is in y-axis.

protein, inflammatory factors, etc.), brain function evaluation indicators (e.g., National Institute of Health stroke scale (NIHSS), neurological function score, cerebral haematoma absorption, etc.), cardiac function indicators (such as myocardial injury markers, cardiac structure indicators, cardiac function classification, etc.), hemorheology (e.g., blood viscosity, blood flow velocity, etc.), QOL (e.g., SF-36 quality of life scale, etc.), and safety evaluation (e.g., adverse events, rebleeding event, liver and kidney function). The research evidence distribution of commonly used oral CHM preparations and traditional Chinese medicine injections for the prevention and treatment of hypertension is shown in a heatmap (Figures 5 and 6).

Studies of CHM injection and oral traditional Chinese medicine preparations showed that the evaluation indexes of hypertension were mostly related to complications. The total effective rate, BP, brain function evaluation indicators, and safety index of TCM injection had a high degree of attention, shown in red. Blood coagulation and TCM-SSD scores had low attention, shown in blue. The total effective rate, clinical symptoms, BP, and safety index of oral Chinese medicine preparation were highly relevant in the clinical studies. The indicators of blood coagulation, hemorheology, and brain function received little attention, and the research directions were generally consistent.

3.7. Investigation of the Application of TCM Prevention and Treatment Schemes. RWS found that the 30,034 hypertension patients in 16 AAA-grade hospitals were mainly treated with intravenous drugs, among which the 3 traditional Chinese medicine preparations, the Danhong injection, Shuxue Ning injection, and Ginkgo Biloba extract, were used

more than 10% of the total drugs used [19]. The Beijing Hospital found that Liuwei Dihuang pill had the highest comprehensive ranking for the use and frequency of CPM from 2008 to 2010 [29]. Regarding CHM decoction, a cohort study involving 154,083 people in Taiwan from 2003 to 2009 showed that about 80% of patients used traditional Chinese medicine at least once. Tianma Gouteng decoction and salvia miltiorrhiza were the most frequently used Chinese medicine [18]. From 1996 to 2005, the main herbal medicine types for hypertension in the Beijing area were tonify deficiency medicine, levelling liver and calming wind drugs, heat-clearing drugs, blood-activating and stasis-eliminating compound, and damp-clearing drugs [30]. Similarly, the study found that in the past 30 years, the first 5 effective treatments were activating the blood and dissolving stasis, xifeng antispasmodic, benefit qi and blood, smooth liver yang, and removal of pathogenic heat from the blood [31]. In summary, there was a consistent use of medication for hypertension prescriptions.

3.8. TCM for the Treatment of Hypertension and Complications. The current main research target is the middle-aged and elderly hypertension and mainly involves grade 1–2 hypertension. A total of 1,214 studies focussed on elderly hypertension and 42 studies focussed on the treatment of middle-aged and young patients with hypertension. A total of 2,579 studies focussed on hypertension and its complications, accounting for 27.43% of the total research. The top 3 complications were intracerebral haemorrhage ($n = 693$, 26.9%), kidney damage ($n = 397$, 15.4%), and diabetes mellitus/abnormal glucose ($n = 378$, 14.7%) (Table 2). A total of 1,309 articles commonly used intervention of

traditional Chinese medicine preparations and 1,170 articles used the analysis intervention duration, most of which were concentrated in a 4–8 week period ($n = 547$, 46.8%), of which only 3 articles of more than 42 months of intervention were present in the strongly exposed group [32–34], suggesting that the research time limit of TCM intervention in hypertension was generally shorter (Figure 7).

3.9. Evidence Quality and Evaluation of the Included Systematic Reviews. A total of 144 systematic reviews were retrieved; there were 5 overviews of SRs without analysis [35–39]. The evidence map for TCM is based on the 139 published systematic reviews, including the Chinese herbal medicine studies ($n = 92$) and nondrug therapy studies ($n = 47$). The single CHM and nondrug therapy were combined into one category, respectively. According to the types of TCM intervention, the intervention principles were divided into 23 types: acupuncture ($n = 24$), qigong ($n = 2$), Tai Chi ($n = 2$), baduanjin ($n = 4$), massage ($n = 2$), auricular point ($n = 5$), acupoint application ($n = 3$), songling xuemai kang capsule ($n = 4$), tongxinluo capsule ($n = 2$), yangxueqingnao granule ($n = 3$), tianmagouteng decoction ($n = 11$), niuhuang jiangya ($n = 4$), banxia baizhu tianma decoction ($n = 5$), buzhong yiqi decoction ($n = 2$), xuefu zhuyu decoction ($n = 2$), Promoting blood circulation and removing blood stasis injection (PBCRBSI) ($n = 3$), pinggan-qianyang treatment ($n = 2$), qiju dihuang pill ($n = 2$), compound qi ma capsule ($n = 3$), tongxinluo capsule ($n = 2$), zhengan xifeng decoction ($n = 2$), tonifying kidney herbs ($n = 8$), CHM ($n = 40$), and nondrug therapy of TCM ($n = 4$). The quality of the included reviews is shown in Figure 8.

According to the AMSTAR scale evaluation, the most qualified item, 9, had 138 SRs. However, 137 SRs did not provide the preliminary design scheme, 106 reviews did not consider the retrieval and inclusion of the grey literature, 70 SRs did not perform a comprehensive literature search, 29 SRs did not properly apply the scientific quality of the included studies to the derivation of conclusions, 31 SRs did not assess and document the scientific quality of the included studies, 138 SRs did not provide the list of included and excluded research literature, 40 SRs did not assess the likelihood of publication bias assessment, and 117 SRs did not provide a conflict of interest statement. One review met 10 criteria [40] and nine reviews met 9 criteria [6, 7, 41–47]. The authors considered these 10 systematic reviews to be of high quality. A total of 94 systematic reviews were of moderate quality and met the 8 AMSTAR criteria ($n = 19$), 7 criteria ($n = 27$), 6 criteria ($n = 27$), and 5 criteria ($n = 21$). The other 35 systematic reviews were of the lower quality and met 4 criteria ($n = 14$), 3 criteria ($n = 10$), or 2 criteria ($n = 11$).

Regarding clinical evidence with SRs, a small number of SRs had unclear evidence ($n = 16$) [40, 42, 43, 45, 47–58]. Most of the SRs had a potentially positive effect ($n = 120$) [7, 44, 46, 59–114], concentrated in 5–8 score. Three SRs were positive, concentrated in the 7–9 score. [6, 115, 116]. To summarise, most of the included SRs were based on the poor quality of primary studies and the quality of clinical efficacy of most primary outcomes was a potentially positive effect (86%).

3.10. A General Overview of the Systematic Reviews

3.10.1. CHM plus Antihypertensive Drugs versus Antihypertensive Drugs. In the 139 SRs, most of the intervention measures were CHM combined with Western medicine (77, 55.4%). Forty-three SRs (quality range = 2–8) included SBP as an outcome measure, 38 SRs (quality range = 2–9) included DBP as an outcome measure, 20 SRs (quality range = 2–8) included total effective rate as an outcome measure, and 18 SRs (quality range = 4–9) included TCM-SSD scores as an outcome measure. There are significant differences in the effect of CHM plus antihypertensive drugs for lowering SBP ($n = 35$, 81.4%) [6, 41, 43, 45, 46, 58, 61, 62, 64, 65, 67–69, 78, 80, 92, 93, 95, 96, 99, 101, 102, 114, 117–127], lowering DBP ($n = 26$, 68.4%) [6, 41, 45, 46, 58, 61, 62, 64, 68, 69, 78, 80, 93, 95, 101, 102, 119, 121–126], improving total effective rate ($n = 18$, 90.0%) [58, 76, 82, 83, 99, 103, 107, 108, 111, 112, 114, 121, 122, 126, 128–131], and lowering TCM-SSD scores ($n = 17$, 94.4%) [7, 41, 46, 48, 62, 76, 79, 94, 95, 99, 102, 112, 130, 132–135] than the antihypertensive drugs. The Xinmaitong (6 RCTs; quality = 7) and songling xuemakang capsules (4 RCTs; quality = 8), combined with antihypertensive drugs, significantly lowered the SDP and DBP and improved clinical efficacy, with low heterogeneity. Clinical evidence was the recommended level [115, 116].

3.10.2. CHM versus Antihypertensive Drugs. Among the 139 SRs, 42 SRs (27.3%) were of the CHM therapy alone. The outcome measures SBP, DBP, total effective rate, and TCM-SSD scores included 21 SRs, 20 SRs, 13 SRs, and 10 SRs, respectively. There were significant differences in the effect of CHM for lowering SBP ($n = 12$, 57.1%) [7, 45, 58, 62, 92, 93, 102, 116, 121, 127, 136, 137], lowering DBP ($n = 7$, 35.0%) [7, 45, 62, 93, 102, 116, 137], improving the total effective rate ($n = 6$, 46.1%) [55, 81, 110, 130, 138, 139], and lowering the TCM-SSD scores ($n = 9$, 90.0%) [7, 48, 62, 84, 94, 102, 112, 115, 133].

3.10.3. Nondrug Therapy plus Antihypertensive Drugs versus Antihypertensive Drugs. Of the 139 SRs, 38 SRs (27.3%) were nondrug therapy combined with Western medicine. The outcome measures of SBP, DBP, total effective rate, and TCM-SSD scores were evaluated separately in 31 SRs, 26 SRs, 17 SRs, and 6 SRs. There were significant differences in the effect of nondrug paratherapy for lowering the SBP ($n = 28$, 90.3%) [44, 53, 59, 63, 66, 71, 73, 74, 87, 91, 105, 106, 113, 140–153], lowering DBP ($n = 22$, 84.6%) [44, 53, 59, 63, 66, 71, 73, 74, 105, 140–151], improving the total effective rate ($n = 16$, 94.1%) [71, 90, 91, 113, 140, 142, 143, 145, 147, 148, 150, 152, 154–157], and lowering the TCM-SSD scores ($n = 6$, 100.0%) [70, 71, 105, 152, 156].

3.10.4. Nondrug Therapy versus Antihypertensive Drugs. Of the 139 SRs, 24 SRs (17.3%) involved nondrug therapy. The outcome measures SBP, DBP, total effective rate, and TCM-SSD scores were evaluated in 14 SRs, 12 SRs, 8 SRs, and 6 SRs, respectively. There were significant differences in the effect of nondrug therapy for lowering the SBP ($n = 6$,

TABLE 2: Distribution of research on prevention and treatment of hypertension and the complications by TCM.

Complication	Number of research articles (<i>n</i> (%))	
Cerebral haemorrhage	693	26.9
Kidney damage	397	15.4
Diabetes mellitus/abnormal glucose metabolism	378	14.7
Left ventricular dysfunction	173	6.7
Hyperlipidaemia	132	5.1
Sleep disorder	125	4.9
Angina	113	4.4
Atherosclerosis	107	4.2
Anxiety and depression	105	4.1
Cerebral infarction	76	2.9
Disease of the eyes	45	1.8
Arrhythmia	40	1.6
Hyperuricemia	27	1.1
Metabolic syndrome	22	0.9
Ventricular dysfunction	7	0.3
Hyperviscositemia	3	0.1
Others	136	5.3

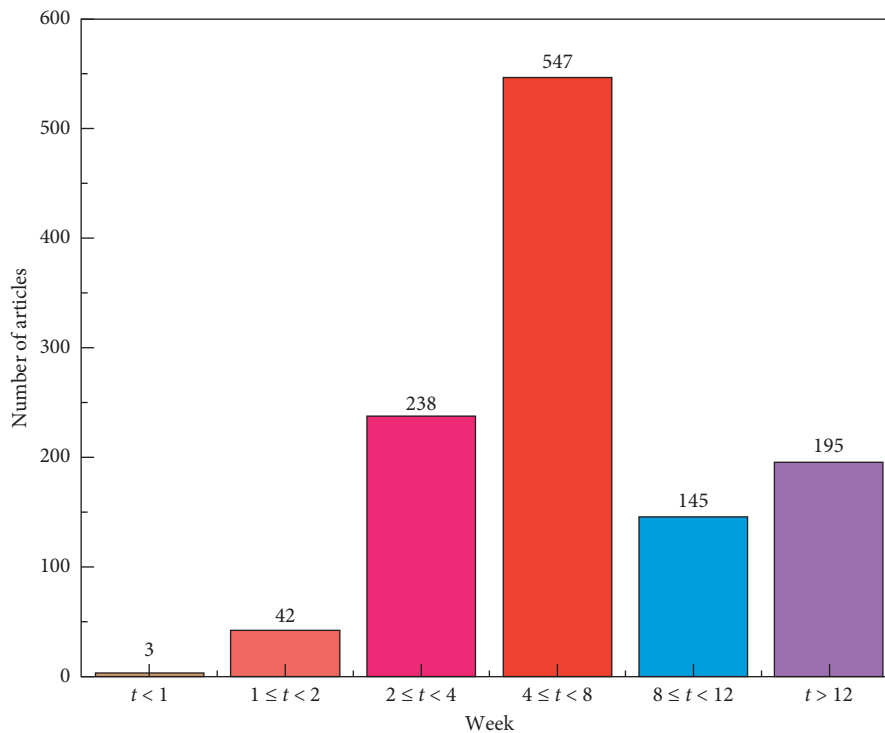


FIGURE 7: Duration distribution of TCM intervention in hypertension.

42.8%) [44, 53, 91, 105, 146, 151], lowering DBP ($n=6$, 50.0%) [44, 53, 105, 113, 141, 146], improving the total effective rate ($n=4$, 50.0%) [91, 158–160], and lowering the TCM-SSD scores ($n=5$, 83.3%) [70, 88, 105, 156, 160].

3.11. Potentially Promising Effects in High-Quality (AMSTAR ≥ 9) Literature. A total of 10 high-quality studies were retrieved, where qigong (20 RCTs), zhengan xifeng decoction (6 RCTs), Liuwei Dihuang pill (6 RCTs), and CHM (24 RCTs) were considered to have evidence of potential positive effects. Xuefu zhuyu decoction (15 RCTs) was considered

a positive effect; i.e., we are confident in estimating the research results. The SRs of acupuncture (22 RCTs), shenqi pill (4 RCTs), jianling decoction (10 RCTs), tongxinluo capsule (25 RCTs), and CHM (5 RCTs) had unclear evidence.

3.12. Blood Pressure

3.12.1. CHM versus Antihypertensive Drugs. Zhengan xifeng decoction showed a significant difference in the SBP and DBP control ($P < 0.05$; 4 RCTs) compared to antihypertensive drugs [7]. In contrast, one SR showed no significant differences [43].

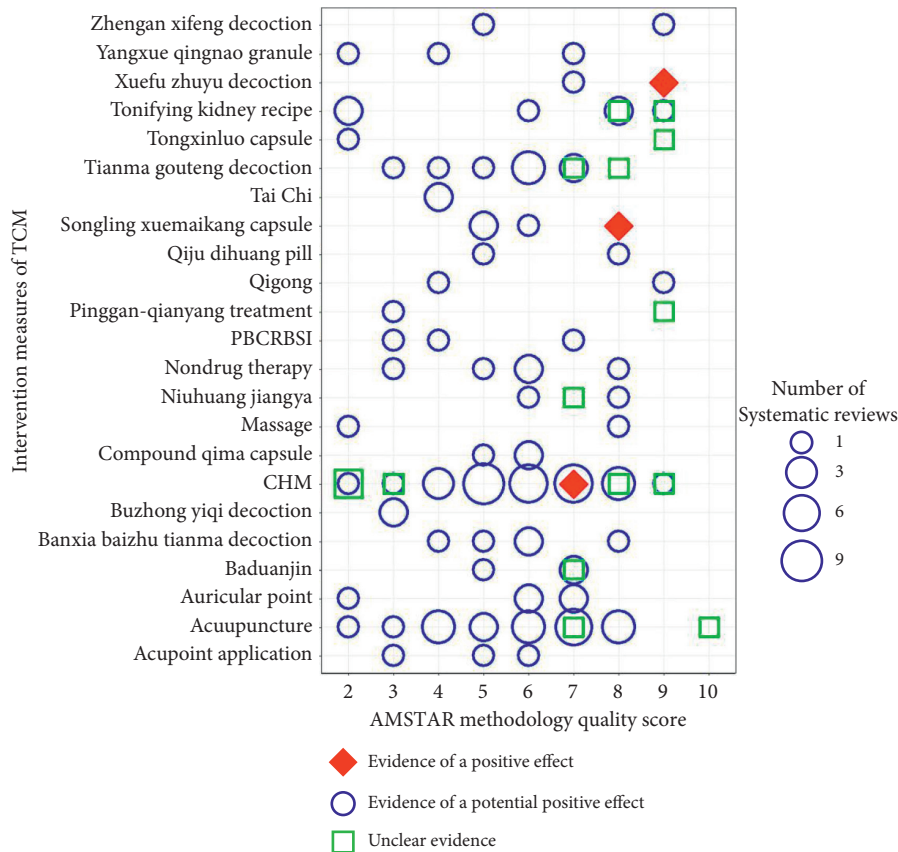


FIGURE 8: Evidence distribution diagram of systematic reviews. The plot depicts the estimated number of SRs (size of the bubble), the clinical efficacy of SRs (shape and colour of the bubble), the AMSTAR scores (x axis), and the types of TCM intervention (y axis). Green squares indicate unclear evidence of SRs, blue bubbles indicate potential evidence of SRs, and red rhombus indicate positive evidence of SRs. PBCRBSI: promoting blood circulation and removing blood stasis injection.

3.12.2. CHM plus Antihypertensive Drugs versus Antihypertensive Drugs. The pooled results of the largest review (24 RCTs, 4502 participants) showed a high number of participants with reduced blood pressure (relative risk (RR) 1.28; 95% confidence interval (CI) 1.21, 1.36, $P < 0.001$; 8 RCTs (RR: 1.12; 95% CI 1.06, 1.39, $P < 0.001$; 5 RCTs)). However, the authors cautioned evidence of a potentially positive effect due to the poor quality of the included RCTs [41]. Fifteen studies reported significant effects of xuefu zhuyu decoction combined with antihypertensive drugs (15 RCTs, 1364 participants) for lowering the blood pressure compared to the control group ($P < 0.05$). The author suggested that xuefu zhuyu decoction for hypertension should be prioritised for future preclinical and clinical studies [6]. The Liuwei Dihuang pill (6 RCTs, 555 participants) and jian ling decoction combined with antihypertensive drugs were more effective in controlling the blood pressure [43, 46]. In contrast, 2 SRs showed no significant difference [42, 47].

3.12.3. Nondrug Therapy plus Antihypertensive Drugs versus Antihypertensive Drugs. Qigong plus antihypertensive drugs significantly lowered both the SBP (WMD = -11.99 mmHg; 95% CI -15.59, -8.39, $P < 0.00001$) and DBP

(WMD = -5.28 mmHg; 95% CI -8.13, -2.42, $P = 0.0003$; 5 RCTs) compared to the antihypertensive drugs alone. Compared to no intervention, qigong significantly reduced SBP and DBP ($P < 0.05$) [44]. One Cochrane review concluded that the clinical evidence for short-term and sustained BP-lowering effect by acupuncture was unclear (quality = 10) [40].

3.13. TCM-SSD Scores

3.13.1. CHM versus Antihypertensive Drugs. One SR showed a significant effect of CHM for lowering the TCM-SSD scores compared to the antihypertensive drugs [7].

3.13.2. CHM plus Antihypertensive Drugs versus Antihypertensive Drugs. Two SRs showed a significant effect of CHM combined with antihypertensive drugs for lowering the TCM-SSD scores compared to the antihypertensive drugs [41, 46].

3.14. Adverse Events. Of the 139 SRs, there was an outcome measure of adverse effects in 77 SRs, which included gastrointestinal reaction, dizziness, headache, cough, and nausea [41, 49]. In summary, all of these SRs indicated that the side effects in the TCM adjuvant therapy group were

generally less than or lighter than those in the Western medicine group.

3.14.1. Guidelines, Consensus, and Clinical Pathway Studies.

A total of 16 papers were retrieved on the treatment of hypertension guidelines, consensus, and clinical pathway of TCM research, including the TCM treatment for hypertension and its complications and consensus ($n=10$), consensus recommendation on the application for CPM of hypertension ($n=1$) [161], the optimisation path of TCM clinical program ($n=4$), and the nursing clinical path ($n=1$) [162]. In 2019, more than 70% of the experts recommended 6 types of CPM: the Tianma Gouteng decoction, qiju dihuang capsule, jinguishenqi pill, ginkgo leaf tablets, niuhuang jiangya pill, and banxia tianma pill to help non-TCM practitioners to select appropriate CPM according to the TCM symptoms. In addition, multicentre RWS found that the 7 common syndromes under the TCM diagnosis and treatment guidelines for hypertension, including liver fire flaming upward syndrome, yin deficiency and yang hyperactive syndrome, blood stasis and internal obstruction, phlegm and dampness, deficiency of qi and blood, deficiency of kidney essence, and chong and ren imbalance, only accounted for 58.38% of the common syndromes. Further, adding the phlegm and blood stasis mutual settlement syndrome is recommended and so it cancels the chong and ren imbalance [163]. Guidelines and path research guide the treatment of EH in TCM and also guide the treatment of complications such as acute cerebral haemorrhage and depression.

4. Discussion

In this study, an evidence map was used to systematically sort the literature on hypertension in the past 20 years. Compared to the previous evidence mapping studies that only included RCTs or SRs [11–14], the current study mainly focussed on the diversified research types (observational studies, interventional studies, secondary studies, and RWS), intervention measures (CHM and nondrug therapy), and the analysis contents (TCM prevention and treatment schemes, intervention time, study outcomes, adverse reactions, etc.) has been expanded to provide a comprehensive description of the clinical problem. It shows the volume and field of available research and highlights areas where published meta-analysis has reported positive results and identified gaps in evidence.

4.1. Advantages of TCM in the Prevention and Treatment of Hypertension. For hypertension prevention and treatment by TCM, the key areas to target are lowering BP, lowering the TCM-SSD scores, improving the clinical symptoms, and protecting the target organs. The adverse events in the TCM paratherapy group were generally less than those in the control group. A total of 120 SRs found that CHM and nondrug therapy had potential active effects for the treatment of hypertension, 16 SRs showed unclear evidence, and 3 SRs showed active effects. Regarding complications, damage to the heart, brain, and kidney target organs accounted for more than 50% of the

studies, and TCM had a good effect on the dissipation of the hypertensive cerebral haematoma, stroke score, proteinuria, and left ventricular hypertrophy. Meanwhile, the evaluation of TCM clinical programs showed that TCM combined with Western medicine can enhance clinical effectiveness and reduce adverse events. Regarding clinical symptoms, it had an improved effect on the main symptoms of vertigo, headache, and systemic symptoms. Based on the study of guidelines and pathways, TCM syndromes and CPM (tianma gouteng decoction qiju dihuang capsule, jingui shenqi pill, ginkgo leaf tablets, niuhuang jiangya pill, and banxia tianma pill) have been put forward for clinical application.

4.2. Future Focus on TCM Prevention and Treatment of Hypertension. TCM intervention for prehypertension is still insufficient. At present, only 3 SRs have been published, including nondrug therapy (17 RCTs, quality=6) [160], CHM (8 RCTs, quality=5) [137], and CHM (5 RCTs, quality=8) [51]. In the future, greater focus should be placed on improving prevention and treatment during early hypertension, including prehypertension, grade 1 hypertension, and youth hypertension, and additional research should be carried out on specific clinical indicators and mechanisms. It is also important to investigate in emotion, obesity, and other hypertension risk factors by CHM and nondrug therapy.

4.3. Limitations and Implications. In general, a summary of the findings of included SRs and clinical studies showed that TCM paratherapy for EH has better efficacy and safety than the control group. The research evidence on the risk factors, quality of life, emotional and psychological, early intervention, duration of intervention, and adverse events is weak. However, there are several limitations to the present study. First, the evidence map provides only a broad overview of the research areas and cannot provide definitive answers regarding the effectiveness of an intervention. The specific control of clinical indicators requires more detailed and targeted research. Second, the evidence map did not establish the reporting guidelines and did not avoid overlap between the included studies across reviews. Third, the quality of the methodology of most SRs was low (25.2%) to moderate (67.6%), which directly influences the reliability of the results. Fourth, literature types, heterogeneity, and complex intervention measures in the included studies only elucidate the efficacy and safety at a macroscopic level.

The improvements for further evidence map are as follows [164, 165]. In terms of data sources, a complementary search of the clinical registration platform and references should be additionally conducted. Regarding content extraction, one should further focus on the retrieval according to the priority areas to further improve accuracy. To avoid unrecognised individual literature due to a large number of retrieved literature and the problem of splitting the same research results, topic selection of TCM literature should focus on specific clinical problems, avoid extensive titles, and prevent the result from being too complex for an explanation. Finally, one should review the evidence base with standard evidence synthesis methods (i.e., systematic

review), improve the methodological quality of SRs themselves, and encourage prospective registration of SRs.

5. Conclusion

The conclusion of the SRs and primary studies highlight TCM's advantages as adjunctive therapy for improving hypertension. Similarly, the development trend of CHM and nondrug therapy for the prevention and treatment of hypertension is relatively good, which reflects the diverse TCM prevention and treatment measures for hypertension. However, clinical research evidence needs to be treated with caution because of methodological flaws. In the future, studies with larger sample sizes, standardisation, and higher quality are required to provide further scientific evidence for TCM in treating hypertension.

Data Availability

The datasets used during the current study are available from the corresponding author upon reasonable request.

Conflicts of Interest

The authors declare that there are no conflicts of interest regarding the publication of this paper.

Authors' Contributions

Yue Liu and Fengqin Xu conceived the idea, designed the study, and interpreted the data together and are the cocorresponding authors. Yan Zhang, Biqing Wang, Chunxiao Ju, and Lu Liu conducted the literature searches, evaluated the risk of bias of each study, and wrote the manuscript together. Jun Mei and Ying Zhu helped to revise the manuscript.

Acknowledgments

This work was supported by the Fundamental Research Funds for the Central Public Welfare Research Institutes (ZZ13-024-4), grants of National Key R&D Program of China (2017YFC1700301), and Qihuang Scholar of "Millions of Talents Project" (Qihuang Project).

References

- [1] M. Ezzati, A. D. Lopez, A. Rodgers, S. Vander Hoorn, and C. J. Murray, "Selected major risk factors and global and regional burden of disease," *The Lancet*, vol. 360, no. 9343, pp. 1347–1360, 2002.
- [2] P. M. Kearney, M. Whelton, K. Reynolds, P. Muntner, P. K. Whelton, and J. He, "Global burden of hypertension: analysis of worldwide data," *The Lancet*, vol. 365, no. 9455, pp. 217–223, 2005.
- [3] N. Chung, S. Baek, M.-F. Chen et al., "Expert recommendations on the challenges of hypertension in Asia," *International Journal of Clinical Practice*, vol. 62, no. 9, pp. 1306–1312, 2008.
- [4] W. Li, H. Gu, K. K. Teo et al., "Hypertension prevalence, awareness, treatment, and control in 115 rural and urban communities involving 47 000 people from China," *Journal of Hypertension*, vol. 34, no. 1, pp. 39–46, 2016.
- [5] F. Guo, H. Di, W. Zhang, and R. G. Walton, "Trends in prevalence, awareness, management, and control of hypertension among United States adults, 1999 to 2010," *Journal of the American College of Cardiology*, vol. 60, no. 7, pp. 599–606, 2012.
- [6] P. Wang, X. Xiong, and S. Li, "Efficacy and safety of a traditional Chinese herbal formula xuefu zhuyu decoction for hypertension," *Medicine*, vol. 94, no. 42, Article ID e1850, 2015.
- [7] X. Xiong, X. Yang, B. Feng et al., "Zhen Gan Xi Feng decoction, a traditional Chinese herbal formula, for the treatment of essential hypertension: a systematic review of randomized controlled trials," *Evidence-based Complementary and Alternative Medicine*, vol. 2013, Article ID 982380, 9 pages, 2013.
- [8] I. M. Miake Lye, S. Hempel, R. Shanman, and P. G. Shekelle, "What is an evidence map? A systematic review of published evidence maps and their definitions, methods, and products," *Systematic Reviews*, vol. 5, no. 1, 2016.
- [9] B. Snilstveit, M. Vojtkova, A. Bhavsar, J. Stevenson, and M. Gaarder, "Evidence & gap maps: a tool for promoting evidence informed policy and strategic research agendas," *Journal of Clinical Epidemiology*, vol. 79, pp. 120–129, 2016.
- [10] M. M. Anaya, J. V. Franco Ariel, M. Ballesteros, I. Solà, G. U. Cuchí, and X. Bonfill Cosp, "Evidence mapping and quality assessment of systematic reviews on therapeutic interventions for oral cancer," *Cancer Management and Research*, vol. 11, pp. 117–130, 2019.
- [11] M. R. Solloway, S. L. Taylor, P. G. Shekelle et al., "An evidence map of the effect of Tai Chi on health outcomes," *Systematic Reviews*, vol. 5, no. 1, 126 pages, 2016.
- [12] I. M. Miake-Lye, S. Mak, J. Lee et al., "Massage for pain: an evidence map," *The Journal of Alternative and Complementary Medicine*, vol. 25, no. 5, pp. 475–502, 2019.
- [13] S. Luger, S. L. Taylor, M. R. Solloway et al., "Evidence map of acupuncture," Department of Veterans Affairs, Washington DC, USA, 2014.
- [14] H. Wei, Y. Xiao, Y. Tong et al., "Therapeutic effect of angelica and its compound formulas for hypertension and the complications: evidence mapping," *Phytomedicine*, vol. 59, Article ID 152767, 2019.
- [15] L. Monasta, G. D. Batty, A. Cattaneo et al., "Early-life determinants of overweight and obesity: a review of systematic reviews," *Obesity Reviews*, vol. 11, no. 10, pp. 695–708, 2010.
- [16] M. W. M. Lutje, M. Smeulders, H. Vermeulen, and L. W. Peute, "Effects of clinical decision-support systems on practitioner performance and patient outcomes: a synthesis of high-quality systematic review findings," *Journal of the American Medical Informatics Association*, vol. 18, no. 3, pp. 327–334, 2011.
- [17] D. Y. Peng, "The effect of traditional Chinese medicine on the prevention and treatment of hypertension in community management," *Nei Mongol Journal of Traditional Chinese Medicine*, vol. 35, no. 14, p. 165, 2016.
- [18] P. R. Yang, W. T. Shih, Y. H. Chu, P. C. Chen, and C. Y. Wu, "Frequency and co-prescription pattern of Chinese herbal products for hypertension in Taiwan: a cohort study," *BMC Complementary and Alternative Medicine*, vol. 15, p. 163, 2015.
- [19] J. H. Ma, Z. F. Wang, Y. M. Xie et al., "Study on medical pattern of traditional Chinese medicine and western medicine diagnosis and treatment of hypertension patients in 30034 cases in real world," *China Journal of Chinese Materia Medica*, vol. 39, no. 18, pp. 3435–3441, 2014.

- [20] M. H. Chen and S. W. Xie, "Investigation and analysis of clinical related factors and TCM syndrome type characteristics in 81 young patients with hypertension," *Fujian Journal of Traditional Chinese Medicine*, vol. 41, no. 1, pp. 7-8, 2010.
- [21] Y. Wu and J. B. Zhong, "Clinical characteristics and efficacy of 105 young patients with essential hypertension," *Beijing Journal of Traditional Chinese Medicine*, vol. 36, no. 3, pp. 213-216, 2017.
- [22] S. S. Ye, "Study on the correlation between heart rate variability, left ventricular mass index and traditional chinese medicine syndrome," M. S. thesis, Guangxi University of Chinese Medicine, Nanning, China, 2018.
- [23] M. H. Chen, "Analysis of clinical related factors and syndrome characteristics of 81 young patients with hypertension," in *Proceedings of the 11th Annual Conference of Heart Disease Branch of Chinese Society of Traditional Chinese Medicine*, Hangzhou, Zhejiang, China, 2009.
- [24] Z. Zhao, "The study of the relationship between hypertension TCM syndrome and duration, classification and risk factors of hypertension," M.S. thesis, Guangzhou University of Chinese Medicine, Guangzhou, China, 2015.
- [25] M. Pang, Y. Zhang, and C. Wang, "Study on the correlation between the four diagnosis information of traditional Chinese medicine and syndrome factors in 150 patients with hypertension," *Liaoning Journal of Traditional Chinese Medicine*, vol. 39, no. 4, pp. 606-608, 2012.
- [26] L. An, "Study on features of tcm syndromes and target organs disfunction of the 3 grade hypertension and related factors," D.S. thesis, Shandong University of Traditional Chinese Medicine, Jinan, China, 2012.
- [27] C. F. Shen, "Clinical research on TCM syndrome factor in hypertension of rank 3," Nanjing University of Chinese Medicine, M.S. Thesis, 2007.
- [28] Y. Tang, "Clinical research for the dampness constitution hypertensive patients' degree of atherosclerosis and related risk factors," Heilongjiang University of Chinese Medicine, M.S. thesis, 2013.
- [29] B. H. Zhang, S. Q. Gao, and D. X. Fu, "Analysis of utilization of antihypertensive Chinese patent medicine in Beijing hospital of Ministry of health during 2008-2011," *Evaluation and Analysis of Drug-Use in Hospitals of China*, vol. 13, no. 2, pp. 133-136, 2013.
- [30] Z. D. Zou, N. Liu, P. Guo et al., "Analysis on clinical treatment in hypertension by traditional Chinese medicine for 10 years in Beijing," *China Journal of Chinese Materia Medicine*, vol. 32, no. 15, pp. 1569-1572, 2007.
- [31] F. C. Si and S. X. Li, "Analysis on Chinese medicine medication of essential hypertension in recent 30 years," *Journal of Medical Research*, vol. 39, no. 3, pp. 46-49, 2010.
- [32] L. J. Gao, W. F. Cui, S. F. Wang et al., "Effect of traditional Chinese medicine jiangyabao on arteriosclerosis in middle-aged and elderly patients with essential hypertension," *Chinese Journal of Gerontology*, vol. 38, no. 15, pp. 3587-3589, 2018.
- [33] W. F. Cui, X. H. Fan, S. F. Wang et al., "Effect of long-term use of jiangyabao series of Chinese patent medicines on the outcome of hypertension: a cohort study," *Chinese General Practice*, vol. 22, no. 1, pp. 101-105, 2019.
- [34] W. F. Cui, L. K. Wang, Y. Y. Pan et al., "The effect of prescription of jiangyabao series on cardiovascular and cerebrovascular risk in the treatment of essential hypertension," *Chinese Journal of Gerontology*, vol. 38, no. 17, pp. 4097-4099, 2018.
- [35] M. S. Lee, J.-I. Kim, and E. Ernst, "Is cupping an effective treatment? An overview of systematic reviews," *Journal of Acupuncture and Meridian Studies*, vol. 4, no. 1, pp. 1-4, 2011.
- [36] J. Wang and X. Xiong, "Outcome measures of Chinese herbal medicine for hypertension: an overview of systematic reviews," *Evidence-based Complementary and Alternative Medicine*, vol. 2012, Article ID 697237, 7 pages, 2012.
- [37] Y. Wang, Y. F. Liu, Z. Wang et al., "Traditional Chinese medicine treatment for essential hypertension from 2015 to 2019: an overview of systematic reviews," *Chinese Journal of Evidence-Based Medicine*, vol. 19, no. 12, pp. 1460-1469, 2019.
- [38] Y. T. Yang, L. Ma, X. X. Yang et al., "Traditional Chinese medicine for essential hypertension: an overview of systematic reviews," *Chinese Journal of Evidence-Based Medicine*, vol. 14, no. 9, pp. 1070-1076, 2014.
- [39] X. D. Tan, Y. J. Pan, W. B. Jiang et al., "Acupuncture therapy for essential hypertension: an overview of systematic reviews," *Chinese Journal of Evidence-Based Medicine*, vol. 10, no. 7, pp. 794-799, 2018.
- [40] J. Yang, J. Chen, M. Yang et al., "Acupuncture for hypertension," *Cochrane Database of Systematic Reviews*, vol. 2018, no. 11, Article ID D8821, 2018.
- [41] J. Zhao, "Preliminary clinical observation of a randomized, controlled, double-blind trial of songling xuemakang capsule in the treatment of essential hypertension (grade 1)," M. S. Thesis, Beijing University of Chinese Medicine, Beijing, China, 2017.
- [42] X. Xiong, X. Li, Y. Zhang, and J. Wang, "Chinese herbal medicine for resistant hypertension: a systematic review," *BMJ Open*, vol. 5, no. 1, Article ID e5355, 2015.
- [43] X. Xiong, P. Wang, X. Li, and Y. Zhang, "The effect of Chinese herbal medicine jian ling decoction for the treatment of essential hypertension: a systematic review," *BMJ Open*, vol. 5, no. 2, Article ID e6502, 2015.
- [44] X. Xiong, P. Wang, X. Li, and Y. Zhang, "Qigong for hypertension a systematic review," *Medicine*, vol. 94, no. 1, Article ID e3521, 2015.
- [45] J. Wang, X. Xiong, and W. Liu, "Chinese patent medicine tongxinluo capsule for hypertension: a systematic review of randomised controlled trials," *Evidence-based Complementary and Alternative Medicine*, vol. 2014, Article ID 187979, 14 pages, 2014.
- [46] J. Wang, K. Yao, X. Yang et al., "Chinese patent medicine Liu Wei di Huang Wan combined with antihypertensive drugs, a new integrative medicine therapy, for the treatment of essential hypertension: a systematic review of randomized controlled trials," *Evidence-based Complementary and Alternative Medicine*, vol. 2012, Article ID 714805, 7 pages, 2012.
- [47] X. Xiong, P. Wang, X. Li, and Y. Zhang, "Shenqi pill, a traditional Chinese herbal formula, for the treatment of hypertension: a systematic review," *Complementary Therapies in Medicine*, vol. 23, no. 3, pp. 484-493, 2015.
- [48] X. Xiong, P. Wang, and S. Li, "Meta-analysis of the effectiveness of traditional Chinese herbal formula Zhen Wu decoction for the treatment of hypertension," *BMJ Open*, vol. 5, no. 12, Article ID e7291, 2015.
- [49] J. Wang, B. Feng, X. Yang et al., "Tianma Gouteng Yin as adjunctive treatment for essential hypertension: a systematic review of randomized controlled trials," *Evidence-based Complementary and Alternative Medicine*, vol. 2013, Article ID 706125, 18 pages, 2013.

- [50] D.-Z. Li, Y. Zhou, Y.-N. Yang et al., "Acupuncture for essential hypertension: a meta-analysis of randomized sham-controlled clinical trials," *Evidence-based Complementary and Alternative Medicine*, vol. 2014, Article ID 279478, 7 pages, 2014.
- [51] J. Wang, B. Feng, X. Yang, W. Liu, and X. Xiong, "Chinese herbal medicine for the treatment of prehypertension," *Evidence-based Complementary and Alternative Medicine*, vol. 2013, Article ID 493521, 9 pages, 2013.
- [52] H. S. Ding and X. F. Zhou, "Meta-analysis of the antihypertensive effect of 442 cases of TCM decoction," *Practical Journal of Clinical Medicine*, vol. 9, no. 4, pp. 192–194, 2012.
- [53] J. Qian and Z. Z. Sun, "Systematic evaluation of ba duan jin in the adjuvant treatment of hypertension," *Chinese Journal of Ethnomedicine and Ethnopharmacy*, vol. 27, no. 8, pp. 52–57, 2018.
- [54] H. Wang, H. C. Shang, J. H. Zhang et al., "Niu Huang jiangya preparation for treatment of essential hypertension: a systematic review," *Liaoning Journal of Traditional Chinese Medicine*, vol. 5, pp. 649–652, 2008.
- [55] Z. Q. Zhi, "Meta-analysis of the clinical efficacy of traditional Chinese medicine in the treatment of hypertension," *Chinese Medicine Modern Distance Education of China*, vol. 15, no. 7, pp. 57–58, 2017.
- [56] Y. P. Wu and J. G. Zhang, "Meta-analysis of the antihypertensive effect of traditional Chinese medicine on essential hypertension," *Lishizhen Medicine and Materia Medica Research*, vol. 23, no. 9, pp. 2360–2361, 2012.
- [57] Y. Ren, A. H. Ou, and X. Z. Lin, "Meta-analysis of a randomized controlled trial of traditional Chinese medicine in the treatment of essential hypertension," *Shaanxi Journal of Traditional Chinese Medicine*, vol. 7, pp. 794–796, 2006.
- [58] J. Wang, "Systematic evaluation of gastrodia elata hooteng decoction in the treatment of hypertension," M.S. thesis, Shaanxi University of Traditional Chinese Medicine, Xi'an, China, 2013.
- [59] J. Wang, X. Xiong, and W. Liu, "Acupuncture for essential hypertension," *International Journal of Cardiology*, vol. 169, no. 5, pp. 317–326, 2013.
- [60] X. Tan, Y. Pan, W. Su et al., "Acupuncture therapy for essential hypertension: a network meta-analysis," *Annals of Translational Medicine*, vol. 7, no. 12, p. 266, 2019.
- [61] X. Gong, X. Yang, W. Liu et al., "Banxia baizhu tianma decoction for essential hypertension: a systematic review of randomized controlled trials," *Evidence-based Complementary and Alternative Medicine*, vol. 2012, p. 10, Article ID 271462, 2012.
- [62] J. Wang, X. Xiong, G. Yang et al., "Chinese herbal medicine Qi Ju di Huang Wan for the treatment of essential hypertension: a systematic review of randomized controlled trials," *Evidence-based Complementary and Alternative Medicine*, vol. 2013, p. 10, Article ID 262685, 2013.
- [63] X. Yang, H. Zhao, and J. Wang, "Chinese massage (Tuina) for the treatment of essential hypertension: a systematic review and meta-analysis," *Complementary Therapies in Medicine*, vol. 22, no. 3, pp. 541–548, 2014.
- [64] X. Xiong, P. Wang, L. Duan et al., "Efficacy and safety of Chinese herbal medicine Xiao Yao San in hypertension: a systematic review and meta-analysis," *Phytomedicine*, vol. 61, Article ID 152849, 2019.
- [65] H.-C. Liu, J.-Q. Ju, Y.-L. Li et al., "Efficacy of Chinese herbal medicine on health-related quality of life (SF-36) in hypertensive patients: a systematic review and meta-analysis of randomized controlled trials," *Complementary Therapies in Medicine*, vol. 23, no. 3, pp. 494–504, 2015.
- [66] X. Ma, H. Hu, J. Li et al., "Is acupuncture effective for hypertension? A systematic review and meta-analysis," *PLoS One*, vol. 10, Article ID e01270197, 2015.
- [67] Y. Cao, L.-t. Liu, and M. Wu, "Is Chinese herbal medicine effective for elderly isolated systolic hypertension? A systematic review and meta-analysis," *Chinese Journal of Integrative Medicine*, vol. 23, no. 4, pp. 298–305, 2017.
- [68] J. Wang, X. Yang, B. Feng et al., "Is yangxue qingnao granule combined with antihypertensive drugs, a new integrative medicine therapy, more effective than antihypertensive therapy alone in treating essential hypertension?" *Evidence-based Complementary and Alternative Medicine*, vol. 2013, Article ID 540613, 8 pages, 2013.
- [69] J. Lan, Y. Zhao, F. Dong et al., "Meta-analysis of the effect and safety of berberine in the treatment of type 2 diabetes mellitus, hyperlipemia and hypertension," *Journal of Ethnopharmacology*, vol. 161, pp. 69–81, 2015.
- [70] X.-J. Yan, P.-Q. Wang, and S.-J. Li, "Blood-letting therapy for hypertension: a systematic review and meta-analysis of randomized controlled trials," *Chinese Journal of Integrative Medicine*, vol. 25, no. 2, pp. 139–146, 2019.
- [71] N. Hou, Y. Huang, R. H. Chen, and Z. X. Zhang, "Meta analysis of the clinical efficacy of moxibustion in the treatment of essential hypertension," *Shi Zhen Guo Yi Guo Yao*, vol. 30, no. 10, pp. 2519–2524, 2019.
- [72] X. Y. Chen, J. Y. Zhao, G. Q. Zhang et al., "Meta analysis of the effect of baduanjin on blood pressure in patients with hypertension," *China Medical Herald*, vol. 15, no. 24, pp. 137–140, 2018.
- [73] J. H. Lin and R. Li, "Systematic evaluation and meta-analysis of the efficacy of badan jinlian in the treatment of essential hypertension with conventional regimens," *Journal of Guangzhou University of Traditional Chinese Medicine*, vol. 34, no. 5, pp. 774–780, 2017.
- [74] Z. S. Chen, L. W. Zheng, C. C. Yang et al., "Effects of baduanjin exercise on patients with hypertension: a meta-analysis," *Nursing Journal of Chinese People's Liberation Army*, vol. 35, no. 10, pp. 1–8, 2018.
- [75] M. Zhu and Y. L. Li, "Systematic evaluation of the effect of pinellia atractylodes rhizome gastrodia elata decoction and its addition and reduction prescription on serum lipid level in patients with hypertension associated with hyperlipidemia," *Journal of Changchun University of Traditional Chinese Medicine*, vol. 29, no. 6, pp. 980–982, 2013.
- [76] M. Zhu, J. Q. Ju, and Y. L. Li, "Systematic review of randomized controlled trials of banxia baizhu tianma decoction on essential hypertension with phlegm-dampness pattern," *Journal of Shandong University of Traditional Chinese Medicine*, vol. 38, no. 2, pp. 105–108, 2014.
- [77] J. Juan, "Clinical efficacy evaluation of acupoint selection based on syndrome differentiation and meridians in the treatment of essential hypertension," D. S. thesis, Chengdu University of TCM, Chengdu, China, 2015.
- [78] J. X. Zou, W. P. Wang, and L. T. Lou, "An meta analysis of the treatment of hypertension by method of invigorating kidney and promoting blood circulation," *Henan Traditional Chinese Medicine*, vol. 39, no. 11, pp. 1737–1743, 2019.
- [79] X. Z. Lu, "Systematic evaluation of kidney-tonifying prescription in the treatment of essential hypertension," M.S. thesis, Shandong University of Chinese Medicine, Jinan, China, 2017.

- [80] J. H. Liang, M. Chen, Y. H. Cai et al., "The efficacy of bushen yixin tablets with western medicine for the treatment of hypertension: meta analysis and systematic review," *Chinese Journal of Integrative Medicine on Cardio-/Cerebrovascular Disease*, vol. 15, no. 19, pp. 2372–2376, 2017.
- [81] M. Shi and Y. H. Zhang, "Systematic evaluation of invigorating kidney-qi therapy for deficiency of kidney-qi syndrome in essential hypertension," *Shandong Journal of Traditional Chinese Medicine*, vol. 31, no. 4, pp. 236–238, 2012.
- [82] C. J. Song and X. Zhuang, "Meta-analysis of the antihypertensive effect of buzhong yiqi decoction on qi-deficiency hypertension," *Hunan Journal of Traditional Chinese Medicine*, vol. 34, no. 2, pp. 118–119, 2018.
- [83] X. B. Wang and L. Xiao, "Meta analysis of modified buzhong yiqi decoction for treating hypertension," *Shanxi Journal of Traditional Chinese Medicine*, vol. 32, no. 9, pp. 46–48, 2016.
- [84] L. Liu and Y. L. Li, "Systematic review on treatment of essential hypertension from spleen and kidney deficiency," *China Journal of Traditional Chinese Medicine and Pharmacy*, vol. 26, no. 8, pp. 700–703, 2011.
- [85] Q. Wang, "Meta analysis of efficacy and safety of danshen injection in the treatment of hypertensive cerebral hemorrhage," M.S. thesis, Zhejiang University, Hangzhou, China, 2012.
- [86] Q. X. Song, D. Z. Cui, and Z. Wang, "Systematic evaluation of the effect of danhong injection on renal function in hypertensive patients with renal damage," *Shandong Medical Journal*, vol. 57, no. 25, pp. 78–80, 2017.
- [87] X. Meng, Q. Zhang, Y. J. Zhang et al., "Meta-analysis of the clinical efficacy of auricular apex bloodletting in the treatment of hypertension," *Guiding Journal of Traditional Chinese Medicine and Pharmacy*, vol. 25, no. 14, pp. 120–124, 2019.
- [88] H. H. Zhang, X. Y. Wang, and J. H. Song, "Meta-analysis of the therapeutic effect of ear buries on primary hypertension nursing," *Scientific & Technical Information of Gansu*, vol. 46, no. 2, pp. 89–90, 2017.
- [89] H. L. Zhang, Q. L. Chen, M. Zhang et al., "Auricular pressure therapy for mild-to-moderate essential hypertension: a meta-analysis trials," *Chinese Journal of Integrative Medicine on Cardio-/Cerebrovascular Disease*, vol. 14, no. 17, pp. 1966–1970, 2016.
- [90] Y. N. Shi, H. M. Guan, and Q. H. Sun, "Meta analysis of clinical effect of ear acupoint application adjuvant therapy for hypertension patients," *Nursing Research of China*, vol. 31, no. 18, pp. 2229–2232, 2017.
- [91] Q. Q. Liu, X. C. Liu, J. Liu et al., "Auricular acupuncture for essential hypertension: a systematic review," *Asia-Pacific Traditional Medicine*, vol. 12, no. 21, pp. 38–43, 2016.
- [92] Z. M. Zhao, W. Ren, P. J. Du et al., "Depressor effect of compound qima capsule on hypertension: a meta-analysis," *Chinese Manipulation & Rehabilitation Medicine*, vol. 9, no. 24, pp. 47–52, 2018.
- [93] Z. M. Zhao, N. N. Xia, and W. Ren, "Meta-analysis of the self-controlled study on intervention of compound qima capsule on blood pressure and blood lipid in patients with hypertension," *Clinical Journal of Chinese Medicine*, vol. 11, no. 30, pp. 18–24, 2019.
- [94] Z. M. Zhao, N. N. Xia, J. P. Du et al., "Safety and TCM curative efficacy of compound qi ma capsule for hypertension: a meta analysis," *Traditional Chinese Drug Research and Clinical Pharmacology*, vol. 30, no. 5, pp. 614–621, 2019.
- [95] D. M. De and X. M. Fang, "Meta-analysis of the integrated treatment of traditional Chinese and western medicine and the therapeutic effect of western medicine on hypertension," *Chinese Journal of Integrative Medicine on Cardio-/Cerebrovascular Disease*, vol. 11, no. 5, pp. 518–521, 2013.
- [96] P. P. Sun and X. Jin, "Meta-analysis of the effect of puerarin on hypertension," *Journal of Qiqihar University of Medicine*, vol. 38, no. 13, pp. 1492–1497, 2017.
- [97] W. Guo, "Auxiliary effect of safflower injection for essential hypertension in China: a systematic review," *Journal of Liaoning University of Traditional Chinese Medicine*, vol. 15, no. 9, pp. 109–111, 2013.
- [98] W. Guo, "Systematic evaluation of radix astragali injection in the treatment of renal damage in essential hypertension," *Journal of Shandong University of Traditional Chinese Medicine*, vol. 37, no. 5, pp. 375–377, 2013.
- [99] Y. J. Zhao, X. H. Su, and Y. Y. Guo, "Systematic evaluation and meta-analysis of the efficacy and safety of the randomized controlled clinical trial of activating blood circulation and removing blood stasis in the treatment of essential hypertension," *Chinese Journal of Integrative Medicine on Cardio-/Cerebrovascular Disease*, vol. 15, no. 12, pp. 1417–1427, 2017.
- [100] A. Li, "Clinical safety evaluation of representative expectorant containing pinellia chinensis based on meta-analysis," M.S. thesis, Beijing University of Chinese Medicine, Beijing, China, 2019.
- [101] H. Yu, "Clinical evaluation of chinese patent medicine in the treatment of essential hypertension based on meta-analysis and data mining," D.S. thesis, China Academy of Chinese Medical Sciences, Beijing, China, 2019.
- [102] J. H. Ma, "Based on meta-analysis and clinical study of songling xuemai kang, the therapeutic effect of pinggan method on hypertension was evaluated," D.S. thesis, China Academy of Chinese Medical Sciences, Beijing, China, 2018.
- [103] S. S. Zhang, "A meta-analysis of the treatment of hypertension with longdan xiegang decoction based on a randomized controlled trial," M.S. thesis, Shandong University of Traditional Chinese Medicine, Jinan, China, 2016.
- [104] Y. W. Song, "A meta-analysis of the treatment of hypertension with bezoar antihypertensive prescription based on a randomized controlled trial," M.S. thesis, Shandong University of Traditional Chinese Medicine, Jinan, China, 2016.
- [105] C. Y. Ma, "A meta-analysis of acupuncture therapy for hypertension based on randomized controlled trials," M.S. thesis, Shandong University of Traditional Chinese Medicine, Jinan, China, 2016.
- [106] H. Chen, "Establishment of evidence system for acupuncture treatment of essential hypertension based on reticular analysis," D.S. thesis, Nanjing University of Chinese Medicine, Nanjing, China, 2019.
- [107] W. F. Cui, B. C. Wang, J. M. Fan et al., "A meta analysis of jiang ya Bao in treatment of essential hypertension," *Clinical Journal of Traditional Chinese Medicine*, vol. 27, no. 6, pp. 849–850, 2015.
- [108] X. Y. Cui, X. Z. Ma, and Q. Y. Qiu, "Systematic evaluation of intervention of jingui shenqi pills in hypertension," *Chinese Journal of Information on Traditional Chinese Medicine*, vol. 25, no. 7, pp. 87–91, 2018.
- [109] D. Y. De, Z. J. Zhi, and D. G. Liu, "Meta analysis of the effect of traditional Chinese medicine nursing intervention in elderly hypertension community," *Clinical Journal of Traditional Chinese Medicine*, vol. 29, no. 7, pp. 1036–1039, 2017.

- [110] H. Yu, J. Mei, P. Zhang et al., "Systematic evaluation of the efficacy and safety of bezoar antihypertensive Chinese patent medicine in the treatment of essential hypertension," *Beijing Journal of Traditional Chinese Medicine*, vol. 38, no. 5, pp. 487–491, 2019.
- [111] W. J. Xu and Y. L. Li, "Systematic review of clinical evidence about calm the liver and subdue yang therapy on the hypertension disease with syndrome of upper hyperactivity of liver yang," *China Journal of Traditional Chinese Medicine and Pharmacy*, vol. 27, no. 3, pp. 736–739, 2012.
- [112] J. Q. Ju, Y. L. Li, and C. H. Yang, "Systematic review of clinical efficacy and safety of qiju dihuang pills in treating essential hypertension," *Journal of Shandong University of Traditional Chinese Medicine*, vol. 37, no. 5, pp. 363–367, 2013.
- [113] W. Xiao, W. C. Zhang, and X. F. Chen, "Analysis of the effect of qigong exercise in the treatment of hypertension meta," *Journal of Jiangxi University of Traditional Chinese Medicine*, vol. 27, no. 2, pp. 49–56, 2015.
- [114] H. Yu, J. Mei, P. Zhang et al., "Efficacy and safety of qingnao jiangya patent medicine in the treatment of primary hypertension: a systematic review," *Chinese Journal of Integrative Medicine on Cardio-Cerebrovascular Disease*, vol. 17, no. 7, pp. 961–966, 2019.
- [115] X. X. Lang, "Meta analysis of the treatment of hypertension by song ling xue mai kang capsule based on the randomized controlled trial," M.S. thesis, Shandong University of Traditional Chinese Medicine, Jinan, China, 2016.
- [116] L. Chen, "Meta analysis of the treatment of by using the randomized controlled trials of the xinmaitong capsule," M.S. thesis, Shandong University of Traditional Chinese Medicine, Jinan, China, 2016.
- [117] S. H. Han, "Antihypertensive effect and quality of life evaluation of combination of Chinese and western medicine in the treatment of senile hypertension," M.S. thesis, China Academy of Chinese Medical Sciences, Beijing, China, 2011.
- [118] Y. Cao, "Meta-analysis of the efficacy of traditional Chinese medicine in elderly patients with simple systolic hypertension," M.S. thesis, Beijing University of Chinese Medicine, Beijing, China, 2017.
- [119] X. Lu and J. C. Jiang, "Meta-analysis of clinical efficacy of Chinese medicine in treatment of insulin resistance (IR) of hypertension," *Chinese Archives of Traditional Chinese Medicine*, vol. 37, no. 2, pp. 460–465, 2019.
- [120] D. N. Dong and C. H. Yang, "Effects of Chinese medicine on elderly isolated systolic hypertension :a meta-analysis," *Liaoning Journal of Traditional Chinese Medicine*, vol. 39, no. 5, pp. 812–815, 2012.
- [121] J. Dai, "Traditional Chinese medicine for essential hypertension: a systematic review," *Journal of China Traditional Chinese Medicine Information*, vol. 2, no. 36, pp. 22–24, 2010.
- [122] W. L. Hu, R. Tang, L. J. Lu et al., "A systematic review on songlingxuemaikang capsule combined ARB for treating hypertension," *China Pharmaceuticals*, vol. 23, no. 4, pp. 22–25, 2014.
- [123] M. Guo, "Meta analysis on the treatment of essential hypertension with rhizoma gastrodia corydalis combined with amlodipine besylate," M.S. thesis, University of Jinan, Jinan, China, 2016.
- [124] B. Q. Lu, Y. H. Ge, X. F. Wu et al., "Systematic Review and meta analysis of tian-ma-gou-teng-yin combined with nifedipine in the treatment of essential hypertension," *Nei Mongol Journal of Traditional Chinese Medicine*, vol. 35, no. 12, pp. 52–54, 2016.
- [125] Q. Y. Zhou, K. Q. Ma, Y. X. Guo et al., "Meta-analysis of tianma gouteng decoction combined with angiotensin-converting enzyme inhibitors for treating primary hypertension," *Chinese Journal of Experimental Traditional Medical Formulae*, vol. 21, no. 4, 2015.
- [126] W. Liu, F. Y. Zhu, R. Yuan et al., "Efficacy and safety of tongxinluo capsule for hypertension: a systematic review," *Beijing Journal of Traditional Chinese Medicine*, vol. 34, no. 3, pp. 196–201, 2015.
- [127] J. Q. Ju, Y. L. Li, and Z. Z. Shen, "Efficacy of zhengan xifeng decoction treating essential hypertension: a systematic review," *Journal of Emergency in Traditional Chinese Medicine*, vol. 23, no. 6, pp. 1060–1063, 2014.
- [128] J. H. Liang, C. G. Chen, and X. T. Jiang, "Efficacy of wenxin granule and metoprolol in the treatment of hypertensive heart disease complicated with ventricular premature meta analysis and trial sequential analysis," *Chinese Journal of Integrative Medicine on Cardio-Cerebrovascular Disease*, vol. 17, no. 2, pp. 161–169, 2019.
- [129] S. H. Luo, L. J. Zhao, Y. Li et al., "Systematic evaluation of the efficacy of TCM syndrome differentiation or combination of western medicine in the treatment of hypertensive left ventricular hypertrophy," *Traditional Chinese Medicine Journal*, vol. 16, no. 6, 2017.
- [130] Y. Q. Zhao, "Meta-analysis of the clinical efficacy of gastrodia gastrodiae hooteng decoction plus or minus in the treatment of hyperactivity of liver yang in patients with hypertension," M. S. thesis, Shaanxi University of Traditional Chinese medicine, Xianyang, China, 2017.
- [131] W. Guo, W. Guo, and Y. Liu, "Systematic evaluation of a randomized controlled trial of gastrodia elata hooteng decoction in the treatment of primary hypertension with hyperactivity of liver yang," *Shandong Journal of Traditional Chinese Medicine*, vol. 32, no. 11, pp. 794–796, 2013.
- [132] J. Zhao, J. H. Du, G. L. Wang et al., "Meta-analysis on randomized controlled trials of Chinese herbal medicine treating essential hypertension," *China Journal of Traditional Chinese Medicine and Pharmacy*, vol. 33, no. 3, pp. 922–926, 2018.
- [133] Q. Wang and S. X. Xi, "Meta-analysis on randomized controlled trials of Chinese herbal medicine treating essential hypertension," *China Journal of Traditional Chinese Medicine and Pharmacy*, vol. 19, no. 9, pp. 345–349, 2013.
- [134] X. N. An, "Meta analysis of efficacy and safety of traditional Chinese medicine in the treatment of early and middle stage renal damage in hypertension," M. S. thesis, Beijing University of Chinese Medicine, Beijing, China, 2019.
- [135] S. F. Chen, T. Li, M. L. Li et al., "Xuefu Zhuyu recipe for the treatment of essential hypertension: a systematic review and meta-analysis," *Tianjin Journal of Traditional Chinese Medicine*, vol. 36, no. 9, pp. 882–890, 2019.
- [136] J. Chen, Y. Liu, and J. C. Zhang, "Meta analysis of effect of Chinese medicine on inflammatory response in hypertensive patients," *Journal of Medical Research*, vol. 42, no. 6, pp. 48–51, 2013.
- [137] H. J. Liu, Q. Xu, and X. H. Liu, "Effect of Chinese herbal medicine on blood pressure in pre-hypertensive cases: a meta-analysis," *World Chinese Medicine*, vol. 11, no. 11, pp. 2441–2443, 2016.
- [138] Q. Q. Wu, "Meta-analysis of the clinical efficacy of wendan decoction and pinellia atractylodia rhizome decoction in the treatment of hypertension," *Traditional Chinese Medicinal Research*, vol. 28, no. 8, pp. 72–74, 2015.

- [139] H. S. Ding, "Meta analysis of traditional chinese medicine of lowering blood pressure deficiency," M. S. thesis, North Sichuan Medical College, Nanchong, China, 2011.
- [140] W. W. Li, X. Y. Zhang, and S. S. Luo, "Meta-analysis of the clinical efficacy of acupoint application of traditional Chinese medicine in the treatment of hypertension," *The Journal of Practical Medicine*, vol. 31, no. 19, pp. 3237–3240, 2015.
- [141] Q. Tian, "Clinical study on the treatment of primary hypertension with hyperactivity of liver yang by acupuncture at yuanluo and acupoint," D. S. thesis, Guangzhou University of Chinese Medicine, Guangzhou, China, 2014.
- [142] T. Zhu and L. Ding, "Meta analysis of acupuncture on fengchi and quchi acupoint in the treatment of primary hypertension," *Clinical Journal of Traditional Chinese Medicine*, vol. 30, no. 3, pp. 461–465, 2018.
- [143] Y. Y. Chen, J. B. Zhai, T. Shi et al., "Meta-analysis of the clinical efficacy of acupuncture at renying point in the treatment of essential hypertension," *Journal of New Chinese Medicine*, vol. 49, no. 1, pp. 184–188, 2017.
- [144] J. P. Zhang, "Study on fMRI brain function connection in patients with primary hypertension by acupuncture at taixi point," M. S. thesis, Southern Medical University, Guangzhou, China, 2017.
- [145] R. Zhao, L. X. Fu, and J. Xiong, "The effect of acupuncture therapy on essential hypertension: a systematic review of long-term effect," *Journal of Clinical Acupuncture and Moxibustion*, vol. 27, no. 3, pp. 46–51, 2011.
- [146] L. L. Zhang, H. Kang, C. Yang et al., "Effect of acupuncture for hypertension and frequency of acupoints," *Liaoning Journal of Traditional Chinese Medicine*, vol. 40, no. 10, pp. 2115–2119, 2013.
- [147] W. Guo, Q. W. Pei, W. L. Dong et al., "A systematic review of the literature on the combination of acupuncture and medicine in the treatment of essential hypertension," *Journal of Shandong University of Traditional Chinese Medicine*, vol. 37, no. 2, pp. 99–100, 2013.
- [148] Q. Zhao, H. S. Li, M. Q. Ji et al., "Systematic review and meta-analysis of efficacy and safety of massage in treatment of essential hypertension," *Journal of Traditional Chinese Medicine*, vol. 59, no. 18, pp. 1568–1573, 2018.
- [149] K. Y. Liu, N. H. Zhu, and J. X. Peng, "Meta-analysis of intervention effect of TCM nursing in elderly hypertension community," *Clinical Journal of Traditional Chinese Medicine*, vol. 29, no. 9, pp. 1454–1458, 2017.
- [150] H. G. Li and X. Z. Wen, "Systematic evaluation of tai chi in the treatment of essential hypertension," *Science & Technology Echnology of Stationery & Sporting Goods*, vol. 7, pp. 35–37, 2011.
- [151] L. Cai and X. Li, "Meta-analysis of curative effect of taichi on primary hypertension," *Clinical Journal of Traditional Chinese Medicine*, vol. 28, no. 10, pp. 1425–1428, 2016.
- [152] Y. J. Zhang, Z. J. Li, and Y. Gao, "Meta-analysis on efficacy of acupuncture and acupuncture combined with medicine in treatment for mild to moderate essential hypertension," *Liaoning Journal of Traditional Chinese Medicine*, vol. 41, no. 9, pp. 1802–1806, 2014.
- [153] Y. X. Qian, "Systematic evaluation of the efficacy and safety of acupuncture in the treatment of essential hypertension," *Journal of North Pharmacy*, vol. 10, no. 3, pp. 72–74, 2013.
- [154] G. Y. Zhang, S. P. Ou, and Q. D. Zhou, "Meta-analysis of clinical effect of acupoint sticking supplementary therapy of fructus evodiae on hypertension," *Chinese Journal of Basic Medicine in Traditional Chinese Medicine*, vol. 24, no. 12, pp. 1757–1761, 2018.
- [155] M. W. Sun, C. Wang, and S. J. Wang, "Meta analysis on yongquan point sticking therapy for high blood pressure," *Journal of Liaoning University of Traditional Chinese Medicine*, vol. 19, no. 11, pp. 136–138, 2017.
- [156] F. S. Liu, C. Q. Guo, and X. F. Jin, "Acupuncture for mild-to-moderate essential hypertension: a meta-analysis of randomized clinical trials," *Chinese Journal of Basic Medicine in Traditional Chinese Medicine*, vol. 18, no. 4, pp. 421–423, 2012.
- [157] X. M. Chen, N. Q. Shao, X. Ma et al., "Meta analysis and evaluation system of non-drug therapy about traditional Chinese medicine in treatment of essential hypertension," *Jilin Journal of Traditional Chinese Medicine*, vol. 36, no. 9, pp. 887–890, 2016.
- [158] S. Han, L. D. Zhang, L. Y. Gu et al., "Meta-analysis of acupuncture and tianma gouteng decoction in treatment of hypertension," *Journal of Practical Traditional Chinese Internal Medicine*, vol. 33, no. 11, pp. 5–8, 2019.
- [159] Z. H. Tang, "Systematic evaluation of acupuncture treatment of essential hypertension," M. S. thesis, Chengdu University of TCM, Chengdu, China, 2011.
- [160] Y. R. Ouyang, C. Y. Huang, W. W. Fu et al., "Meta-analysis of external therapy of traditional Chinese medicine for high-normal blood pressure," *Journal of Yunnan University of Traditional Chinese Medicine*, vol. 42, no. 2, pp. 31–38, 2019.
- [161] X. J. Valaskatgis, "Consensus recommendations on the clinical application of chinese patent drugs in hypertension," in Proceedings of 2011 Annual Conference of Heart Disease Branch of Chinese Association of Traditional Chinese Medicine and Annual Meeting of Cardiovascular Diseases Committee of Beijing Association of Traditional Chinese Medicine, Beijing, China, pp. 232–237, 2011.
- [162] X. F. Yong and X. F. Yong, "Influence of traditional Chinese medicine clinical nursing pathway on blood pressure level and negative emotion of hypertensive patients," *Today Nurse*, vol. 25, no. 2, pp. 132–135, 2018.
- [163] L. Y. Wang, Y. Li, X. J. Han et al., "Applicability analysis of TCM diagnosis and treatment guideline for hypertension in the real world," *China Journal of Traditional Chinese Medicine and Pharmacy*, vol. 29, no. 10, pp. 3250–3252, 2014.
- [164] M. Chen, Y. Xiao, Y. Liu et al., "The quality analysis of literature retrievals of systematic reviews for traditional Chinese medicine," *Journal of Evidence-Based Medicine*, vol. 8, no. 1, pp. 42–52, 2015.
- [165] J. Zhang, Y. Li, B. Zhang et al., "Evidence-based traditional Chinese medicine research: Beijing declaration," *Journal of Evidence-Based Medicine*, vol. 13, no. 2, pp. 91–92, 2020.

Research Article

Literature-Based Drug Repurposing in Traditional Chinese Medicine: Reduced Inflammatory M1 Macrophage Polarization by Jisil Haebaek Gyeji-Tang Alleviates Cardiovascular Disease In Vitro and Ex Vivo

Ga-Ram Yu,¹ Seung-Jun Lee,¹ Da-Hoon Kim,¹ Dong-Woo Lim,² Hyuck Kim,^{1,3}
Won-Hwan Park ,¹ and Jai-Eun Kim ²

¹Department of Diagnostics, College of Korean Medicine, Dongguk University, Dongguk-Ro 32, Goyang 10326, Republic of Korea

²Department of Pathology, College of Korean Medicine, Dongguk University, Dongguk-Ro 32, Goyang 10326, Republic of Korea

³Institute of Korean Medicine, Dongguk University, Dongguk-Ro 32, Goyang 10326, Republic of Korea

Correspondence should be addressed to Won-Hwan Park; diapwh@dongguk.ac.kr and Jai-Eun Kim; iamkimjaieun@daum.net

Received 20 August 2020; Revised 13 November 2020; Accepted 24 November 2020; Published 7 December 2020

Academic Editor: Xiao Ma

Copyright © 2020 Ga-Ram Yu et al. This is an open access article distributed under the Creative Commons Attribution License, which permits unrestricted use, distribution, and reproduction in any medium, provided the original work is properly cited.

Relatively high proportions of proinflammatory M1-like macrophages in tissues may lead to vascular impairment and trigger numerous diseases including atherosclerosis-related cardiovascular disease (CVD). Jisil Haebaek Gyeji-tang (JHGT), a polyherbal decoction, is traditionally used to treat various human ailments including chest pain, angina, and myocardial infarction. In the present study, we investigated the anti-inflammatory effects of JHGT on lipopolysaccharide- (LPS-) stimulated M1 macrophage polarization generated via the mitogen-activated protein kinases (MAPKs) pathway in RAW 264.7 mouse macrophages. The reducing power of JHGT was also investigated using DAF-FA DA in a zebrafish model. JHGT significantly reduced inflammatory mediator levels, including iNOS, COX2, TNF- α , IL-6, and IL-1 β , as compared with LPS-stimulated controls in vitro and ex vivo. Furthermore, JHGT suppressed the ERK1/2, JNK, and p38 MAPK pathways and reduced p-I κ B α levels and the nuclear translocation of NF- κ B in RAW 264.7 cells. In addition, treatment with JHGT significantly reduced the NO levels in LPS-treated zebrafish larva ex vivo. Our findings show the potent anti-inflammatory properties of JHGT are due to its suppression of MAPK signaling, NF- κ B translocation, and M1 macrophage polarization.

1. Introduction

Inflammation is complex physiological response to noxious stimuli, such as physical or chemical injuries, or infections including exogenous pathogens such as bacterial lipopolysaccharide (LPS) [1, 2]. However, excessive, uncontrolled proinflammatory responses can cause severe vascular damage and result in atherosclerosis-related cardiovascular diseases (CVD) [3]. Atherosclerosis is the result of a proinflammatory response of arterial walls and can give rise to macrophage polarization via plaque rupture or tissue erosion [4, 5]. The incidence of atherosclerosis-related CVD are steadily increasing in developing and developed

countries, and they remain the leading cause of mortality worldwide [6].

Macrophages are the major antigen-presenting cells (APCs) and are well-known to provide crucial molecular alarm signals, which include proinflammatory cytokines, after pathogen invasion [7, 8]. Resident macrophages are activated by stimulation of toll-like receptor (TLR; a primary LPS receptor) to produce proinflammatory cytokines and initiate inflammation in lesions [9, 10]. When inflammatory responses occur in blood vessels, macrophages are polarized into proinflammatory M1 and anti-inflammatory M2 types, and the proinflammatory M1 form predominates in atherosclerotic plaque [11]. Several studies have provided

compelling evidence that the presence of a high proportion of M1-type macrophages promotes atherosclerosis [12–14]. Macrophages polarization is also caused by mitochondrial dysfunction, and this too results in excessive productions of inflammatory cytokines and mediators such as interleukins (ILs), tumor necrosis factor- α (TNF- α), nitric oxide (NO), inducible nitric oxide synthase (iNOS), and cyclooxygenase 2 (COX2) [15, 16]. On contrary to this, M2 phenotype can secrete anti-inflammatory factors such as IL-10 and tumor growth factor β (TGF- β) and promote tissue remodeling and repairing through collagen formation in CVD events. Therefore, the balance between the M1 and M2 macrophage phenotypes is viewed as a therapeutic target for inflammatory response-related CVD.

Traditional Chinese medicine (TCM) has more than 2,000 years of history, is based on natural products, and is now viewed as attractive safe medicines that provide multicomponent-based and multitargeting therapies. Recently, researchers and clinical practitioners in TCM have begun to look into the CVD in molecular concepts, eventually to enhance its diagnosis and treatment [17, 18]. CVD are strongly associated with characteristics of metabolic syndrome, such as obesity, diabetes, and dyslipidemia. In a previous study, we demonstrated that literature-based herbal digestive Sochewan have pharmacological properties and that repurposing of alternative medicine may result in treatments for metabolic syndrome and chronic inflammatory diseases [19]. Also, our another study supports the notion that polyherbal prescription Jwa Kum Whan have potential for the treatment and prevention of metabolic syndrome [20]. Emerging evidences suggest that the promising effect of TCM on CVD is not only on high expectation values but also according to the medicinal effects [21, 22]. However, the key regulatory mechanism responsible for the atheroprotective properties of TCM is not fully understood.

The treatment of chest pain with Jisil Haebaek Gyeji-tang (JHGT) is mentioned in the most famous TCM classic Gum-Gue-Yo-Lak (櫃櫃要略), which states JHGT be administered when “the chest is frustrated and pain is present under the armpits or at the bottom of the heart,” that is, when the symptoms of vascular inflammation-related arteriosclerosis are manifest [23]. Novel approaches are required to treat inflammatory disease, and efforts are being made to discover natural product-derived modulators of macrophage polarization of the treatment of atherosclerosis-related CVD. In a recent study, we reported the protective effects of two similar Gum-Gue-Yo-Lak prescriptions on LPS-stimulated M1 macrophage polarization-induced vascular inflammation [24]. In the present study, we extended our studies by investigating the molecular mechanism responsible for the inhibitory effect of JHGT on the LPS-induced M1 polarization of murine bone marrow-derived macrophages and RAW264.7 cells. In addition, we explored the biological test of NO reduction in LPS-induced zebrafish's larva and confirmed that JHGT treatment could significantly inhibit NO secretion, which might be realized by affecting the regulation of macrophages polarization. Our findings highlighted the anti-inflammatory effects of JHGT, as well as

determined the important role of macrophages polarization in the atherosclerosis-related CVD.

2. Materials and Methods

2.1. Chemicals. Fetal bovine serum (FBS) and penicillin/streptomycin solution were purchased from Invitrogen (Carlsbad, CA, USA) and Dulbecco's Modified Eagle's Medium (DMEM) and RPMI 1640 medium from Hyclone (Logan, UT, USA). Lipopolysaccharide (LPS) and other reagents were obtained from Sigma Chemicals (St. Louis, MO, USA). Mouse recombinant IFN gamma was supplied by GenScript (Piscataway, NJ, USA). ELISA kits for IL-1 β , IL-6, and TNF- α were obtained from R&D Systems (Minneapolis, MN, USA). Primary antibodies for lamin B, iNOS, COX2, and β -actin and horseradish peroxidase- (HRP-) conjugated secondary antibodies were purchased from Santa Cruz (Dallas, TX, USA). Primary antibodies, including phosphor-extracellular signal-regulated kinases (p-ERK), phosphor-c-Jun N-terminal kinases (p-JNK), phosphor-p38 mitogen-activated protein kinases (p-p38), p-I κ B- α , and p-NF- κ B (p-p65) were obtained from Cell Signaling Technology (Beverly, MA, USA). The oligonucleotide primers used in real-time qPCR were supplied by Macrogen (Seoul). DAF-FM DA (4-amino-5-methylamino-2',7'-difluoro-fluorescein diacetate) was supplied by Sigma Chemicals (St. Louis, MO, USA).

2.2. Herbal Formula Preparation. The prescription used in this study was prepared by subjecting a JHGT herbal mixture (Fructus Ponciri Seu Aurantii Immaturus: Bulbus Allii Macrostemi: Ramulus Cinnamomi: Cortex Magnoliae Officinalis: Fructus Trichosanthis = 45 g: 300 g: 40 g: 160 g: 25 g) to aqueous reflux extraction at 95°C for 3 h as described in an original text. The herbal mixture was purchased from Human herb (Gyeongsangbuk-do, South Korea). The hot water extract obtained was filtered and concentrated using a rotary evaporator (Buchi, Flawil, Switzerland) at 95°C and freeze-dried to obtain JHGT (3.51%, w/w), as previously described with slight modification [25]. Voucher specimens were deposited at the Institute of Korean Medicine, Dongguk University (DG-DIA017 W).

2.3. Animals and Culture Cells. Bone marrow-derived macrophages were isolated from 8-week-old C57BL/6J male mice obtained from Orient Bio (Gyeonggi-do, South Korea). Cells were isolated as previously described [26]. Briefly, mice were anesthetized with a Zoletil and Rompun mixture, and upper and lower parts of femurs were excised. RPMI 1640 medium was then passed through femur segments (from top to bottom) using a syringe, and the cells were obtained by centrifuging the cell suspension at 3,000 rpm for 8 min. Macrophages were then plated in RPMI-1640 containing 10% FBS in 6-well cell culture plates, incubated until 90 confluent, differentiated with the recombinant mouse macrophage colony stimulating factor (M-CSF) (20 ng/mL) for 72 h, and treated with LPS for another 48 h to induce M1 polarization. The protocols used in animal experiments were

approved beforehand by the Ethics Committee of Dongguk University (IACUC-2020-030-1).

RAW264.7 cells (a murine macrophage cell line) were purchased from the Korea Cell Line Bank (KCLB, Seoul). Cells were cultured in DMEM supplemented with 10% FBS containing 100 U/mL penicillin and 100 $\mu\text{g}/\text{mL}$ streptomycin at 37°C in a humidified 5% CO₂ environment.

2.4. Cell Viability Assay. Cell viabilities were determined using the EZ-Cytox cell viability assay kit (Daeil Lab Service, Seoul) according to the manufacturer's instructions with slight modification [27]. Briefly, mouse bone marrow-derived macrophages or RAW264.7 cells were maintained at 70–80% confluence and then seeded at a density of 1.2×10^5 cells/mL in 96-well plates. After 24 h of incubation, the medium was changed to FBS-free DMEM containing serially diluted JHGT (0–200 $\mu\text{g}/\text{mL}$). After incubation for another 24 h, 10 μl of EZ-Cytox reagent was added to each well, and cells were incubated at 37°C in the humidified 5% CO₂ incubator for 1 h. Optical densities (ODs) were measured at 450 nm using a microplate reader (VersaMax, Molecular Devices, CA, USA).

2.5. Nitrite Assay. Griess reagent was used to investigate the inhibitory effect of JHGT on LPS-induced nitrite levels, as we previously described [28]. Briefly, RAW264.7 cells were seeded in triplicate on 6-well culture plates at 1.2×10^5 cells/mL and incubated at 37°C in the humidified 5% CO₂ incubator for 24 h. Cells were then pretreated with various concentrations of JHGT in the absence or presence of LPS (1 $\mu\text{g}/\text{mL}$) for 24 h. Supernatants were collected and mixed with Griess reagent. ODs were measured at 570 nm, and nitrite concentrations were calculated using a standard curve.

2.6. Preparation of Nuclear and Cytosolic Fraction. Nuclear and cytosolic proteins were separated using the Nuclear and Cytoplasmic Extraction Reagents kit from Thermo Fisher Scientific. Briefly, RAW 264.7 macrophages were seeded on 60 mm cell culture dishes at 1.2×10^5 cells/mL and pretreated with JHGT at 25–100 $\mu\text{g}/\text{mL}$ for 1 h. Cells were then stimulated with LPS (1 $\mu\text{g}/\text{mL}$) for 24 h. The nuclear translocation of NF- κB from cytoplasm was assessed by Western blot.

2.7. Immunoblot Assay. Protein levels of iNOS, COX2, MAPKs (ERK1/2, JNK, and p38), NF- κB (I $\kappa\text{B}\alpha$ and p65), lamin B, and β -actin were determined by Western blotting as previously described with slight modification [29]. Briefly, cells were washed with ice-cold DPBS and lysed with radio immunoprecipitation assay buffer (Thermo Fisher Scientific, Rockford, IL, USA) containing protease inhibitor and phosphatase inhibitor cocktail (GenDEPOT, Barker, TX, USA). Protein concentrations were measured using the BCA kit (Thermo Fisher Scientific). Protein lysates (30 μg) were loaded into 10% SDS-PAGE gels, electrophoresed, and transferred to PVDF membranes at 100 V for 70 min using an electrophoretic transfer cell (Bio-Rad, Hercules, CA,

USA). Membranes were blocked with 5% BSA in TBS/T (containing 0.1% Tween 20) for 1 h, and blots were incubated with primary antibodies (diluted at 1:1500 in TBS/T containing 3% BSA) at 4°C overnight with gentle shaking. After washing with TBS/T, membranes were incubated with secondary antibodies (diluted at 1:3000 in TBS/T) at room temperature for 2 h. Blots were detected using a Western blot imaging system (Fusion Solo, Vilber Lourmat, Collégien, France), and proteins were visualized using a chemiluminescent ECL buffer (Super Signal West Pico, Thermo Fisher Scientific).

2.8. Quantitative Real-Time Polymerase Chain Reaction. The expression levels of proinflammatory mediators were determined by quantitative real-time polymerase chain reaction (qPCR). Total RNA was isolated from RAW264.7 cells and bone marrow macrophages using TRIzol reagent (Thermo Fisher Scientific) according to the manufacturer's instructions [30]. Briefly, reverse transcription was performed using AccuPower RT PreMix (Bioneer, Daejeon, South Korea) and oligo deoxythymine (dT) 18 primers (Invitrogen, Carlsbad, CA, USA). Amplification of primer-specific binding cDNA was performed using a LightCycler 480 PCR system (Roche, Basel, Switzerland). Reactants include 10 μL of SYBR Green Master mixture (Roche, Switzerland), 8 μL of ultrapure water, 10 pmol/ μL of primer, and 1 μL of templated cDNA. Amplification was performed using the following schedule: denaturation at 95°C for 10 min, followed by 45 amplification cycles (denaturation at 95°C for 10 s and annealing at 50–60°C for 5 min). Threshold cycle values (Ct value) were used to quantify PCR products. The primers used were as follows: iNOS forward, 5'-GAGACAGGGAAGTCTGAAGCAC-3', reverse, 5'-CCAGCAGTAGTTGCTCCTCTTC-3'; COX2 forward, 5'-GCGACATACTCAAGCAGGAGCA-3', reverse, 5'-AGTGGTAACCGCTCAGGTGTTG-3'; TNF- α forward, 5'-AAGCCTGTAGCCCACGTCGTA-3', reverse, 5'-GGCACCCTAGTTGTTGTCTTTG-3'; IL-1 β forward, 5'-CTGAACTCAACTGTGAAATGCCA-3', reverse, 5'-AAAGGTTTGAAGCAGCCCT-3'; IL-6 forward, 5'-CCACTTCACAAGTCGGAGGCTTA-3', reverse, 5'-GCAAGTGCATCATCGTTGTTTCATAC-3', and β -actin forward 5'-GCAAGTGCTTCTAGGCGGAC-3', and reverse 5'-AAGAAAGGGTGTAACACG-CAGC-3' (β -actin was used as the internal control). Results were normalized by dividing the Ct values of genes by that of β -actin. Data were acquired using Roche LightCycler 480 software (Roche Applied Science, USA).

2.9. Immunofluorescence Assay. To follow the nuclear localization of NF- κB , RAW264.7 cells were grown on Lab-Tek II chamber slides (Nalge Nunc, IL, USA) as previously described with slight modification [31]. Briefly, cells were fixed in 4% formaldehyde for 10 min, permeabilized with 0.1% Triton X-100 for 10 min at room temperature, blocked with 1% BSA for 1 h, and labeled with 2 $\mu\text{g}/\text{mL}$ of primary antibody for 3 h. NF- κB in cytoplasm and nuclei was detected by treating cells with PBS containing 2 $\mu\text{g}/\text{mL}$ of FITC and 0.2%

BSA for 45 min. Nuclei were stained with DAPI (Vector Laboratories, CA, USA) and observed and photographed under a fluorescence microscope (BX50, Olympus, Japan).

2.10. ELISA Analysis. Concentrations of inflammatory cytokines, that is, IL-1 β , IL-6, and TNF- α in cell culture supernatants, were quantified using Quantikine ELISA kits (R&D Systems, Inc. Minneapolis, MN, USA) as according to the manufacturer's instructions [32]. Briefly, RAW264.7 cells were seeded at 1.2×10^5 cells/mL in 24-well plates and pretreated with JHGT at 25, 50, and 100 $\mu\text{g/mL}$ for 1 h. Cells were then stimulated with LPS (1 $\mu\text{g/mL}$) for 24 h. Culture media were then collected, and the concentrations of IL-1 β , IL-6, and TNF- α were measured using an ELISA kit.

2.11. Nitrite Determination in Zebrafish. Synchronized zebrafish embryos were collected, pipetted at 20 embryos/well into six-well plates containing 2 mL of embryo medium E2 buffer (5 mM NaCl, 0.17 mM KCl, 0.33 mM MgSO₄, 0.33 mM CaCl₂, and 5% methylene blue) at 7–9 h post-fertilization, and incubated with or without of JHGT (100 $\mu\text{g/mL}$) for 1 h. Embryos were then stimulated with LPS (10 $\mu\text{g/mL}$) for 24 h at 28.5°C and transferred to fresh embryo medium E2 buffer. NO levels in LPS-stimulated zebrafish were measured using the fluorescent probe dye, 4-amino-5-methylamino-2',7'-difluorofluorescein diacetate (DAF-FM DA), which reacts with NO to produce highly fluorescent triazole derivatives. After 7 h in embryo medium E2 buffer, LPS-stimulated zebrafish larvae were transferred into 96-well plates and treated with DAF-FM DA solution (2.5 μM) for 1 h in the dark at 28.5°C, rinsed in fresh embryo medium, and fixed in 4% formaldehyde. The fluorescence intensities of individual larvae were assessed using a fluorescence microscope (BX50, Olympus, Japan) [33]. LPS-stimulated zebrafish larvae were transferred into 96-well plates and treated with DAF-FM DA solution (2.5 μM) for 1 h in the dark at 28.5°C. Following incubation, zebrafish larvae were rinsed in fresh zebrafish embryo medium and fixed in 4% formaldehyde solution prior to observation. The fluorescence intensity of individual zebrafish larvae was quantified using a fluorescence microscope (BX50, Olympus, Japan).

2.12. Statistical Analyses. Experimental data were analyzed using GraphPad Prism version 5.0 software (GraphPad, La Jolla, CA, USA). Standard curves were constructed using Excel and PowerPoint (Microsoft, Redmond, WA, USA). Analysis of variance and one-way ANOVA with Dunnett's multiple comparison tests were used to determine the significances of differences between samples. Results are presented as means \pm SDs, and *P* values of <0.05 were considered statistically significant.

3. Results

3.1. Effects of JHGT on RAW264.7 Viability and NO Production. To evaluate the effect of JHGT, RAW 264.7 cell viabilities were measured using the EZ-Cytox assay kit. Cells

were incubated with various concentrations of JHGT (6.25, 12.5, 25, 50, 100, or 200 $\mu\text{g/mL}$) for 24 h, and the cell viabilities observed were 98.51, 97.28, 96.5, 95.81, 94.33, and 88.64%, respectively (Figure 1(a)). When mouse macrophages were pretreated with JHGT and then stimulated with LPS, JHGT dose-dependently reduced LPS-induced NO production (Figure 1(b)). Subsequent experiments were performed using JHGT at concentrations of 25, 50, or 100 $\mu\text{g/mL}$.

3.2. JHGT Inhibited iNOS and COX2 Expressions in LPS-Stimulated RAW264.7 Cells. Because iNOS is stimulated under inflammatory conditions and produces NO, we assessed the expressions of iNOS and COX2 in LPS-stimulated macrophages pretreated with JHGT. JHGT pretreatment significantly and dose-dependently inhibited the LPS-induced production of iNOS and obviously suppressed COX2 protein levels (Figures 2(a) and 2(b)). Furthermore, JHGT pretreatment at 50 or 100 $\mu\text{g/mL}$ significantly reduced the LPS (1 $\mu\text{g/mL}$) induced up-regulations of the iNOS and COX2 genes (Figures 2(c) and 2(d)).

3.3. JHGT Reduced LPS-Induced Proinflammatory Cytokine Increases in RAW264.7 Cells. ELISA and qPCR were used to investigate the effects of JHGT on proinflammatory cytokine levels. Pretreatment with JHGT at 50 or 100 $\mu\text{g/mL}$ significantly inhibited LPS-induced increases in TNF- α , IL-1 β , and IL-6 in RAW 264.7 cells (Figures 3(a)–3(c)). qPCR results confirmed that JHGT markedly suppressed the gene expressions of TNF- α , IL-1 β , and IL-6 in LPS-stimulated RAW 264.7 cells (Figures 3(d)–3(f)).

3.4. JHGT Regulated MAPK Activity in LPS-Stimulated RAW 264.7 Cells. Several studies have suggested that MAPK signal cascades, such as those of ERK1/2, JNK, and p38 MAPKs, play important roles in the inflammatory responses induced by LPS in macrophages [34, 35]. Western blot analysis was used to confirm the inhibitory effect of JHGT on the activations of MAPK signals by LPS. At 1 $\mu\text{g/mL}$, LPS markedly increased the phosphorylations of ERK1/2, JNK, and p38 MAPK, and pretreatment with JHGT inhibited these effects of LPS (Figure 4(a)) and dose-dependently reduced the phosphorylation of JNK (Figure 4(b)).

3.5. JHGT Suppressed the Nuclear Translocation of NF- κ B in RAW 264.7 Cells. Western blot showed that JHGT significantly inhibited the LPS-induced phosphorylations of NF- κ B (Figures 5(a)–5(c)) and I κ B- α (Figure 5(b)), and when JHGT pretreated RAW 264.7 cells were stimulated with LPS, immunofluorescence microscopy showed that JHGT reduced the LPS-induced nuclear translocation of p65 (Figure 5(d)). However, JHGT (100 $\mu\text{g/mL}$) alone had no obvious effect on translocation of p65.

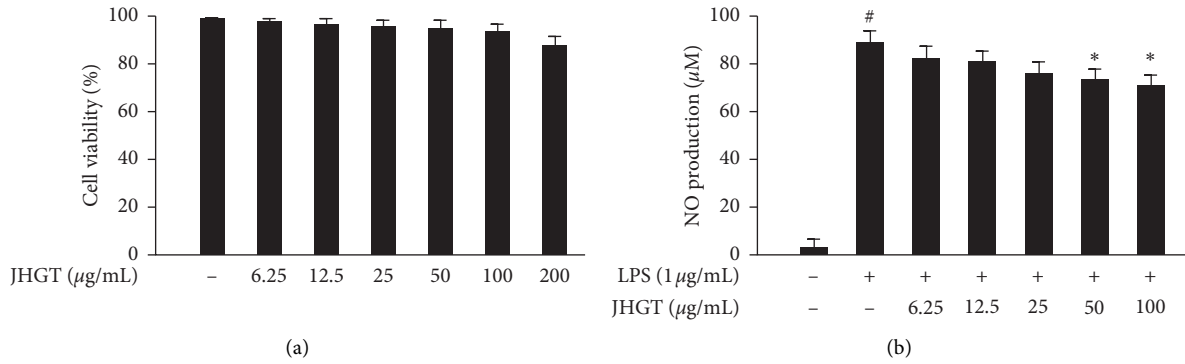


FIGURE 1: Effect of JHGT on RAW264.7 cell viability and NO production. (a) RAW264.7 cells were incubated for 24 h with JHGT at 0–200 µg/mL. Cell viabilities were measured using an EZ-Cytox assay kit. Results are expressed in percentages of nontreated controls. (b) RAW264.7 cells were pretreated with JHGT for 1 h and then cotreated with JHGT and LPS (1 µg/mL) for 24 h. NO concentrations were measured using Griess reagent. Results are presented as the means ± SDs of three different experiments. [#]*P* < 0.01 versus nontreated controls, and ^{*}*P* < 0.05 and ^{**}*P* < 0.01 versus LPS-treated controls.

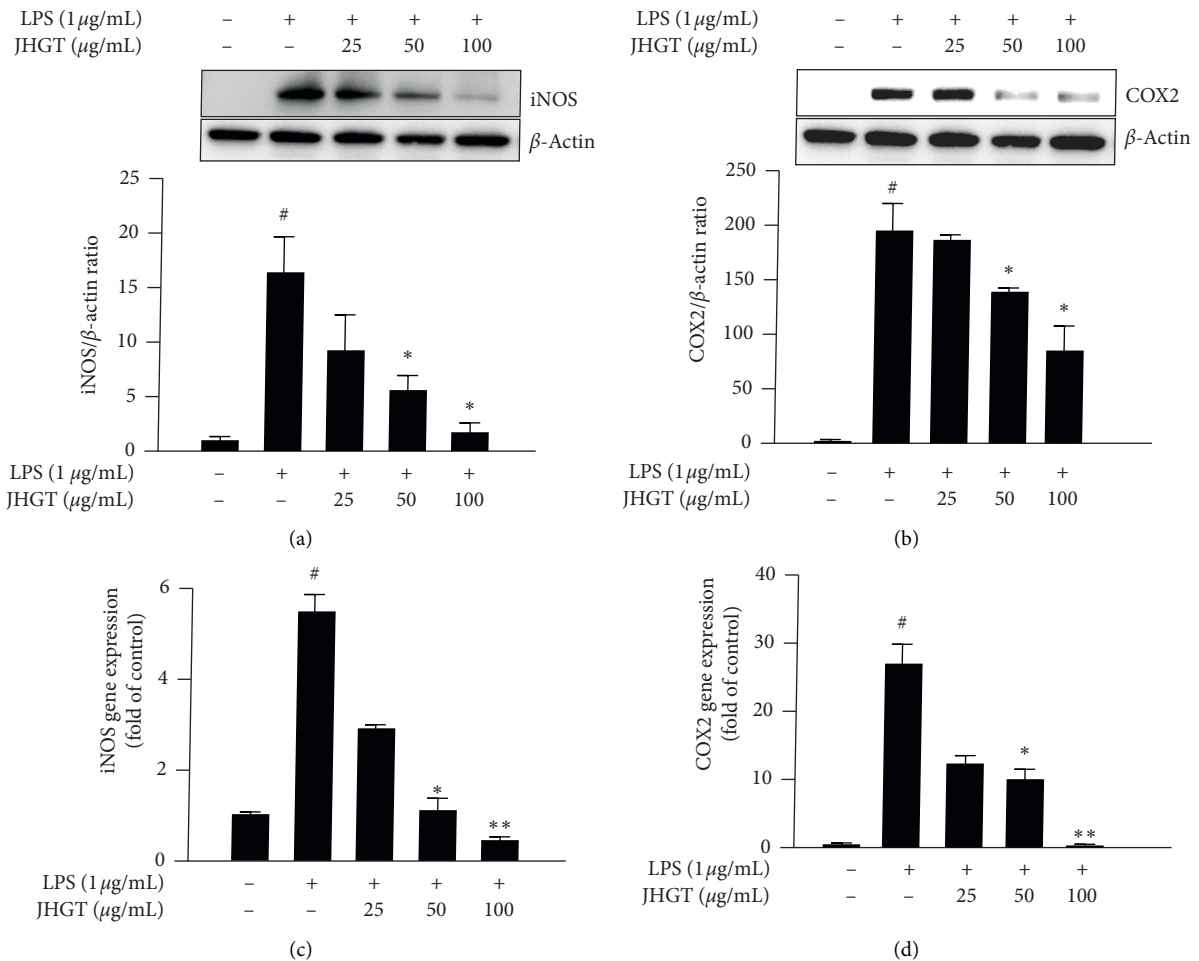


FIGURE 2: JHGT inhibited LPS-induced upregulations of iNOS and COX2 in RAW264.7 cells. RAW264.7 cells were pretreated with JHGT for 1 h and then treated with LPS (1 µg/mL) for 24 h. (a-b) Relative expressions of inflammatory iNOS and COX2 by Western blot. (c-d) Relative gene expression levels of iNOS and COX2 by real-time PCR. qPCR data were normalized by dividing the Ct values of genes by that of β-actin. Results are presented as the means ± SDs of three different experiments. [#]*P* < 0.01 versus nontreated normal controls, and ^{*}*P* < 0.05 and ^{**}*P* < 0.01 versus LPS-treated controls.

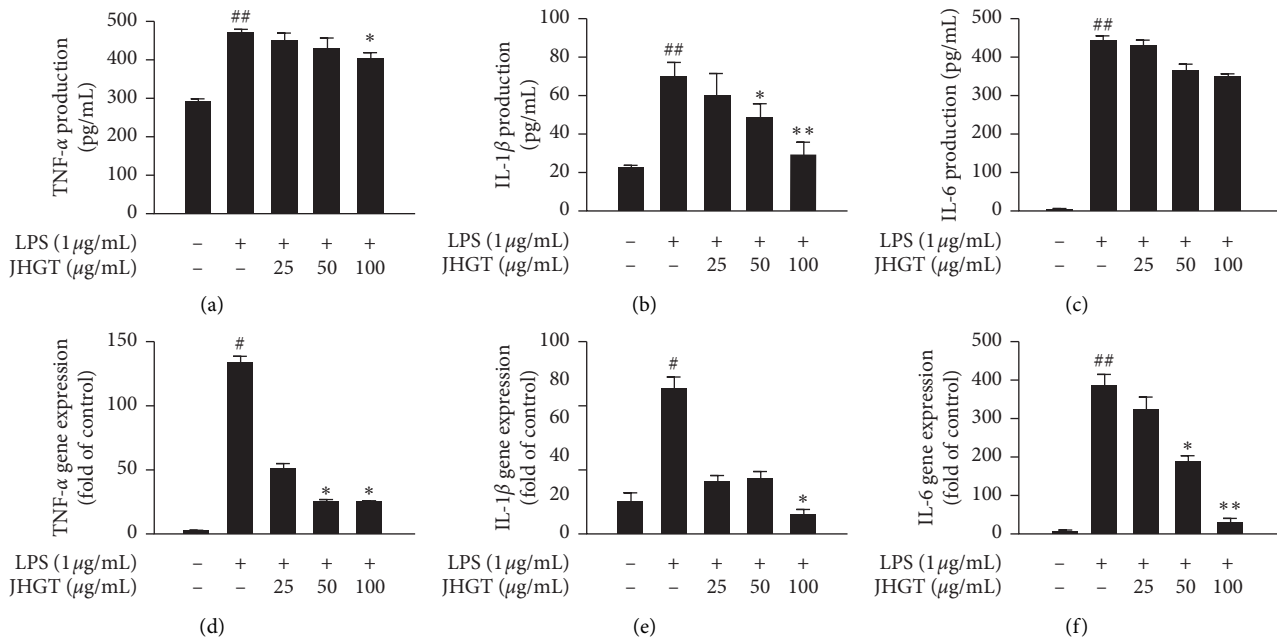


FIGURE 3: JHGT reduced LPS-induced increases in proinflammatory cytokine levels in RAW264.7 cells. Cells were pretreated with JHGT for 1 h and then treated with LPS (1 μg/mL) for 24 h. (a–c) Relative expressions of TNF-α, IL-1β, and IL-6 as determined by ELISA. (d–f) Relative expressions of TNF-α, IL-1β, and IL-6 as determined by qPCR. Results are presented as the means ± SDs of three different experiments. ^{##} $P < 0.01$ versus nontreated normal controls, and ^{*} $P < 0.05$ and ^{**} $P < 0.01$ versus LPS-treated controls.

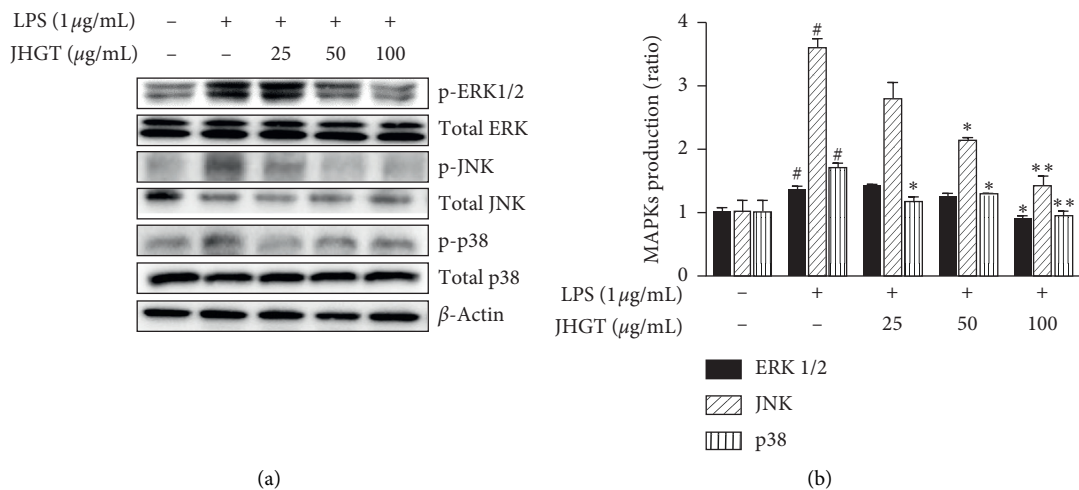


FIGURE 4: JHGT regulated MAPK activity in LPS-stimulated RAW 264.7 cells. Cells were pretreated with JHGT for 1 h and then treated with LPS (1 μg/mL) for 24 h. (a) Relative MAPK expressions as determined by Western blot. (b) Band intensities were measured by densitometry and normalized versus the intensities of total forms and β-actin. Results are presented as the means ± SDs of three different experiments. ^{##} $P < 0.01$ versus normal nontreated controls, and ^{*} $P < 0.05$ and ^{**} $P < 0.01$ versus LPS-treated controls.

3.6. JHGT Inhibited Inflammatory Mediator Responses Induced by LPS Plus $INF\gamma$ Cotreatment and Regulated M1 Polarization in Mouse Bone Marrow-Derived Macrophages. To investigate the influence of JHGT on inflammatory mediators and M1 polarization, we used mouse bone marrow-derived macrophages. Cells were treated with 15 or 25 μg/mL of JHGT in the absence or presence of LPS (1 μg/mL) plus $INF\gamma$ (20 ng/mL) for 24 h (Figure 6(a)). Cotreatment with $INF\gamma$ and LPS potentially induced M1 inflammatory

mediators, but pretreatment with JHGT at 25 μg/mL significantly reduced the mRNA levels of iNOS, COX2, TNF-α, IL-1β, and IL-6 (Figures 6(b)–6(f)).

3.7. JHGT Decreases NO Production in Zebrafish. Zebrafish are often used as an *in vivo* model because like mammals, they have innate and acquired immune systems. We investigated whether JHGT inhibits LPS-induced NO

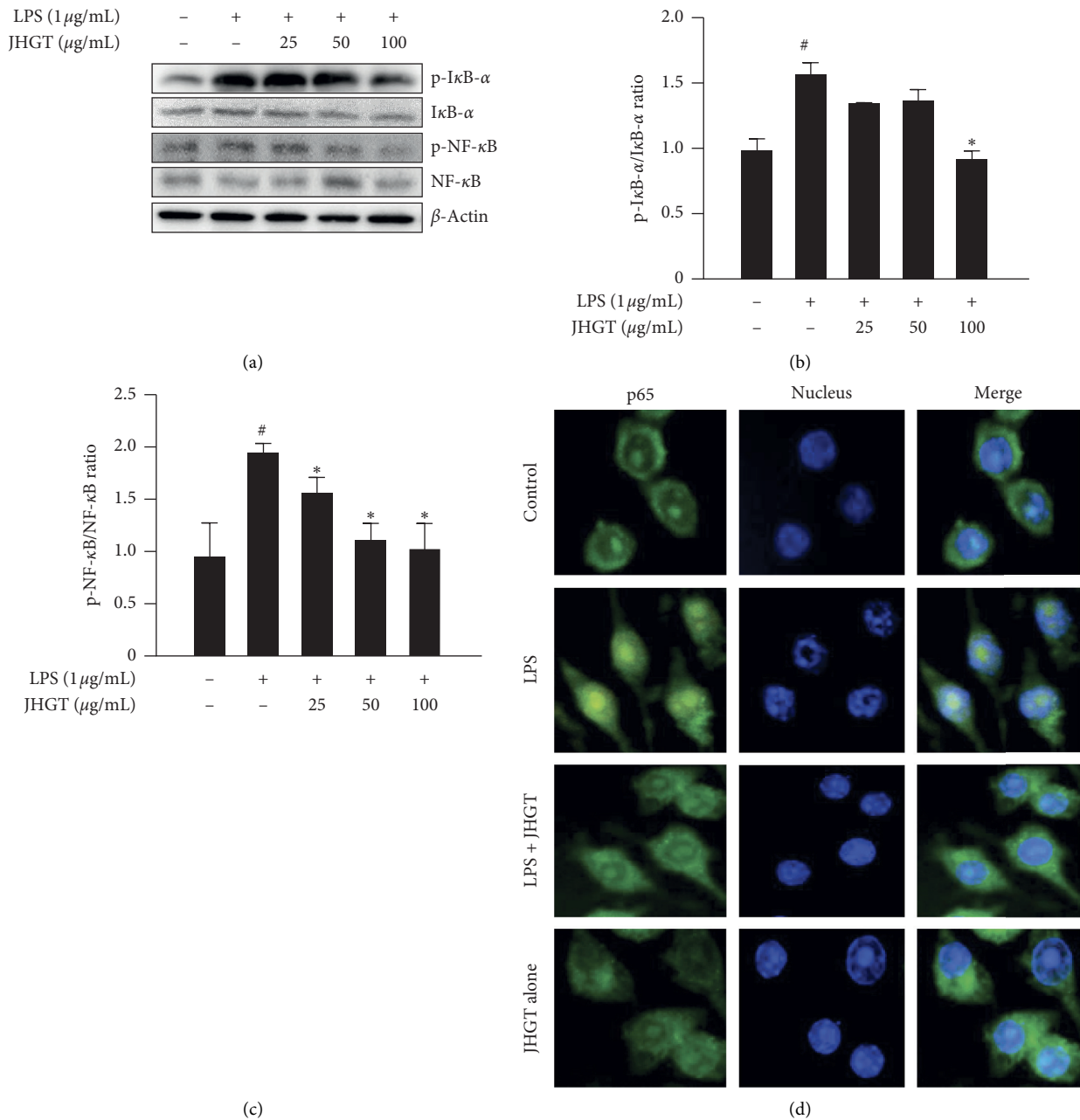


FIGURE 5: JHGT suppressed NF-κB signal translocation in RAW 264.7 cells. Cells were pretreated with JHGT for 1 h and then treated with LPS (1 μg/mL) for 24 h. (a) Relative phosphorylations of intracellular NF-κB and IκBα and their total protein levels as determined by Western blot. (b–d) The nuclear translocation of NF-κB (p65) was visualized by immunofluorescence microscopy. Results are presented as the means ± SDs of three different experiments. ^{##}*P* < 0.01 versus normal nontreated controls, and ^{*}*P* < 0.05 and ^{**}*P* < 0.01 versus LPS-treated controls.

production in zebrafish using the fluorescent probe DAF-FM (Figure 7(a)). LPS treatment stimulated NO production by 241% in zebrafish, and JHGT pretreatment significantly reduced this LPS-induced increase in NO production (Figure 7(b)).

4. Discussion

“Geum-Gwe-Yo-Ryak (檣匱要略),” the oldest pharmacological Bible, recorded to Kwaru Haebak Paekju (KHP), Kwaru Haebak Banha (KHB), and Jisil Haebak Gyeji-tang

(JHGT), treated for chest pains in Chapter 9 [36]. In particular, KHP, KHB, and JHGT were constitutional to two same herbs, that is, *Trichosanthes kirilowii* Maxim. (*Trichosanthes Fructus*) and *Allium macrostemon* Bunge. (*Allii Macrostemonis Bulbus*). *A. macrostemon*, a major constituent of JHGT, has been reported to have a therapeutic effect on acute myocardial ischemia via reducing inflammatory responses [37]. Furthermore, *A. macrostemon* and *T. kirilowii* are among the top 10 natural products for the treatment of coronary artery diseases [38]. Recently, a study

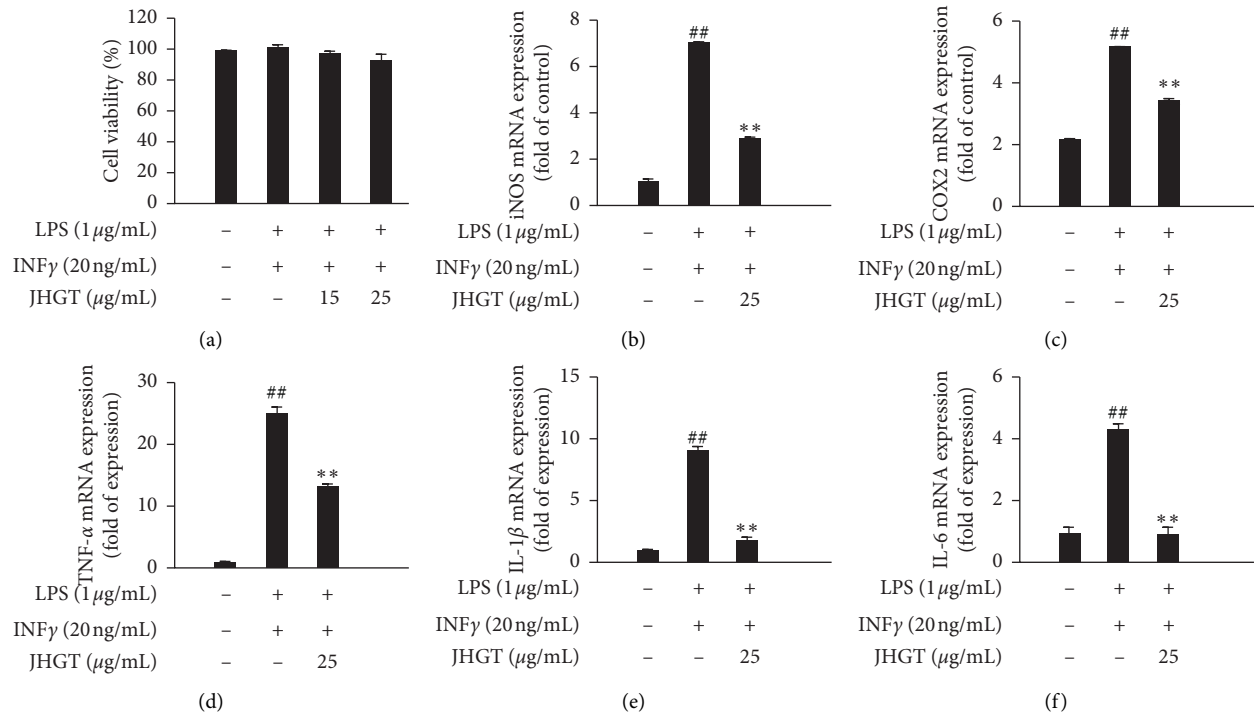


FIGURE 6: JHGT inhibited inflammatory mediator inductions by LPS plus INF γ cotreatment and regulated M1 polarization responses in mouse bone marrow macrophages. (a) Cytotoxic effect of JHGT on M1 polarized from bone marrow-derived macrophages. Cells were incubated with various concentrations of JHGT for 24 h. Results are expressed as percentages of nontreated controls. (b–f) Relative gene expression levels in bone marrow-derived M1-like macrophages as determined by real-time PCR. Results are presented as the means \pm SDs of three different experiments. ## $P < 0.01$ versus normal nontreated controls, and * $P < 0.05$ and ** $P < 0.01$ versus LPS plus INF γ cotreated controls.

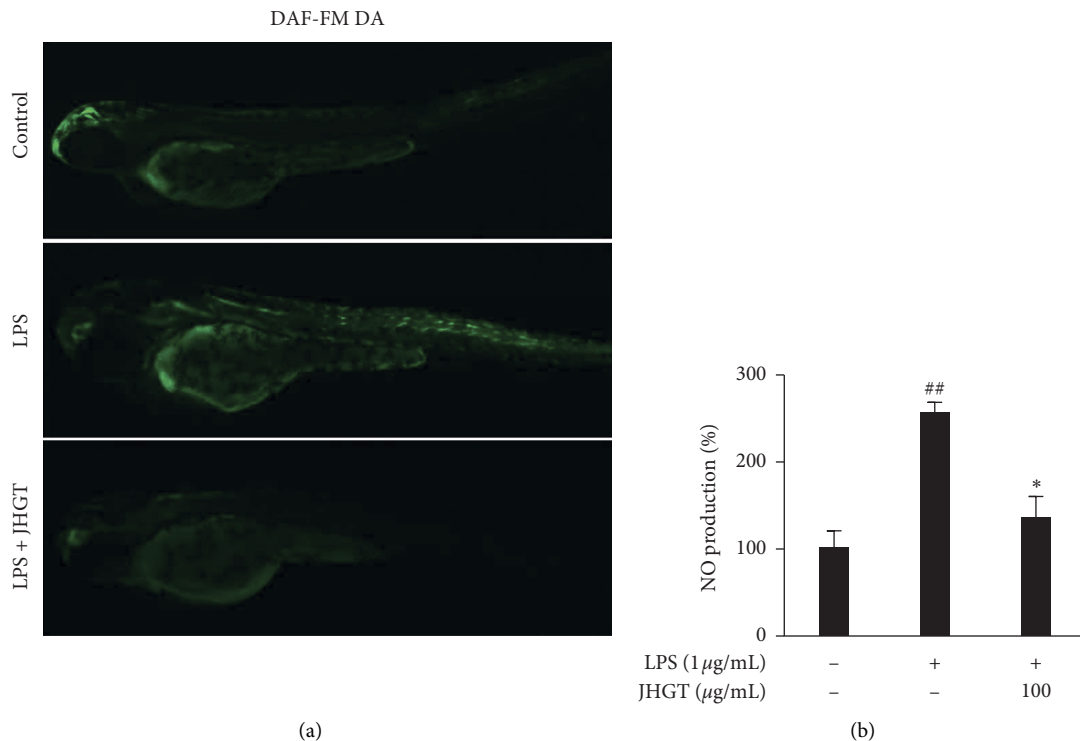


FIGURE 7: Effect of JHGT on LPS-induced NO production in zebrafish embryos. Zebrafish embryos were pretreated with JHGT (100 μ g/mL) for 1 h and then exposed to LPS (10 μ g/mL) for 24 h. (a) NO levels were measured using DAF-FM-DA. (b) Results were quantified using Image J software and are presented as the means \pm SDs of three different experiments. ## $P < 0.01$ versus normal nontreated controls, and * $P < 0.05$ versus LPS-treated controls.

undertaken by our group showed that both KHP and KHB alleviate LPS-induced inflammatory responses in RAW264.7 cells. In a previous study, we also found that these prescriptions have beneficial effects on atherosclerotic-related CVD lesions, which are known to be regulated by macrophage polarization [24].

Cinnamomi cassia Presl. (Cinnamomi Ramulus), which was another JHGT constitutional herb, has been treated with the literature-based weak chest pain or prodromal symptoms. *C. cassia* is well known and commonly used in TCM, and it has also been reported to have a wide range of pharmacological properties, that is, to reduce oxidative stress and inflammation and protect the cardiovascular system [36, 39, 40]. Furthermore, *C. cassia* contains many known anti-inflammatory compounds such as cinnamaldehyde, cinnamyl acetate, and cinnamyl alcohol, which reduce the mRNA expressions of inflammatory cytokines (e.g., IL-1 β , IL-6, and TNF- α) in LPS-induced RAW 264.7 macrophages [41, 42].

Nitric oxide (NO) is an important free radical and is induced by endotoxins such as LPS. Under inflammatory conditions, iNOS generates excessive nitric oxide (NO) in blood vessels, which in turn, increases tissue levels of inflammatory mediators such as COX2, TNF- α , IL-1 β , and IL-6 [43]. IL-6 is well known to enhance inflammatory signal transduction, which leads to the upregulations of proinflammatory signals such as ERK1/2, JNK, and p38 kinase [44]. Therefore, reducing NO production is regarded as one of the best ways of preventing the progression of treating inflammatory diseases such as atherosclerosis-related CVD. Our results show that JHGT significantly decreases NO levels in LPS-induced RAW264.7 cells, and our ex vivo results show that JHGT reduces NO levels in INF- γ plus LPS cotreated mouse bone marrow-derived macrophages. In addition, in vitro results show that JHGT dose-dependently and significantly downregulated levels of inflammatory mediators, including COX2, TNF- α , IL-1 β , and IL-6.

In the context of inflammatory response in macrophages, LPS can also activate inflammatory cell signal pathways via MAPKs and NF- κ B [45]. MAPKs are well-known serine/threonine protein kinases and are responsible for signal transduction under various proinflammatory conditions [46]. Furthermore, nuclear factor kappa B (NF- κ B) is modulated by inflammatory mediators, and this is followed by activation of the MAPK signaling pathway [47, 48]. Modulation of DNA binding activity of NF- κ B is regulated by the phosphorylation and degradation of I κ B [49]. Therefore, blocking these MAPK and NF- κ B cell signaling cascades offers a potential means for treating inflammation-related atherosclerotic development. We also investigated the effects of JHGT on the MAPK signaling pathway and nuclear translation of NF- κ B in LPS-stimulated macrophages. When RAW264.7 cells were treated with LPS (1 μ g/mL), the phosphorylations of ERK, JNK, and p38 MAPK and the nuclear translocation of p65 increased, but pretreatment with JHGT significantly reduced these effects.

Polarized macrophages may be of M1 (proinflammatory) or M2 (anti-inflammatory) type, and M1 macrophages play a critical role in adaptive immune response in blood vessels [50].

However, excessive, uncontrolled proinflammatory response causes mitochondrial dysfunction and endothelial damage and results in an imbalance of macrophages polarization toward the M1 phenotype [51]. Previous study has suggested that unmoderated macrophage M1 polarization complicates inflammatory responses and leads to atherosclerosis-related CVD [52]. Several pioneering studies suggested that immoderated macrophage M1 polarization complicates inflammatory responses, which leads to CVD-related atherosclerosis [53, 54]. In the present study, we found that CD86 acted as a marker of M1 macrophage polarization (data not shown). CD86 is expressed on activated APCs (antigen-presenting cells) in response to pathogens and leads to the stimulation of proinflammatory cell signaling pathways such as those controlled by MAPK and NF- κ B. Furthermore, interferon gamma (INF γ) and LPS act synergistically on macrophages and ultimately trigger M1 macrophage polarization. In the present study, using CD86 as a marker, JHGT pretreatment was found to significantly reduce the proportion RAW264.7 cells and bone marrow-derived murine macrophages exhibiting the M1 phenotype. These observations indicate that JHGT reinforces the anti-inflammatory pathway and causes the repolarization of macrophages of the M1 phenotype under pathogen-induced inflammatory conditions.

Animal research studies support that the zebrafish (*Danio rerio*) model provides a valuable means for studying human disease and discovering new drugs. Recently, the zebrafish was found to share 70% functional similarity to humans at the gene level [55, 56]. We observed by fluorescence microscopy that JHGT strongly reduced NO levels in our LPS-induced zebrafish larva model ex vivo. The probable explanation of this result is ex vivo study macrophages driven by repolarization; thus, we suggest further experiments be undertaken to identify the molecular mechanism of atherosclerosis-related CVD and the way JHGT influences this mechanism.

5. Conclusions

In summary, our findings provide insight into the possible repositioning of a traditional medication for the treatment of atherosclerosis-related CVD. Importantly, JHGT was found to reduce M1 macrophage polarization, which appeared to be responsible for its anti-inflammatory activities. These results suggest that JHGT be considered a potential treatment for atherosclerosis-related CVD.

Abbreviations

NO:	Nitric oxide
LPS:	Lipopolysaccharide
IL-1 β :	Interleukin-1 beta
TNF- α :	Tumor necrosis factor alpha
iNOS:	Inducible nitric oxide synthase
COX2:	Cyclooxygenase 2
MAPKs:	Mitogen-activated protein kinases
NF- κ B:	Nuclear factor kappa B
CD86:	Cluster differentiation 86
INF γ :	Interferon gamma.

Data Availability

The data used to support the findings of this study are included within the article.

Conflicts of Interest

The authors declare that they have no conflicts of interest.

Authors' Contributions

Won-Hwan Park, Jai-Eun Kim, and YGR performed animal surgery, cell experiments, quantitative assay, and generated the figures. LSJ and KDH also performed the animal surgery and analyzed Western blot data. LDW and KH conceived and designed the experiments. PWH analyzed the data and revised the manuscript. KJE supervised the project and contributed to the final draft of the paper. All authors read and approved the final manuscript.

Acknowledgments

This work was supported by Basic Science Research Program through the National Research Foundation of Korea by the Ministry of Education (Grant no. 2018R1D1A1B07048467).

References

- [1] D. P. Hajjar and A. M. Gotto, "Biological relevance of inflammation and oxidative stress in the pathogenesis of arterial diseases," *The American Journal of Pathology*, vol. 182, no. 5, pp. 1474–1481, 2013.
- [2] N. Shibata and C. K. Glass, "Regulation of macrophage function in inflammation and atherosclerosis," *Journal of Lipid Research*, vol. 50, pp. S277–S281, 2009.
- [3] P. H. Black and L. D. Garbutt, "Stress, inflammation and cardiovascular disease," *Journal of Psychosomatic Research*, vol. 52, no. 1, pp. 1–23, 2002.
- [4] J. Boyle, "Macrophage activation in atherosclerosis: pathogenesis and pharmacology of plaque rupture," *Current Vascular Pharmacology*, vol. 3, no. 1, pp. 63–68, 2005.
- [5] J. L. Stöger, M. J. Gijbels, S. van der Velden et al., "Distribution of macrophage polarization markers in human atherosclerosis," *Atherosclerosis*, vol. 225, no. 2, pp. 461–468, 2012.
- [6] K. S. Reddy and S. Yusuf, "Emerging epidemic of cardiovascular disease in developing countries," *Circulation*, vol. 97, no. 6, pp. 596–601, 1998.
- [7] M. P. Murtaugh and D. L. Foss, "Inflammatory cytokines and antigen presenting cell activation," *Veterinary Immunology Immunopathology*, vol. 87, no. 3–4, pp. 109–121, 2002.
- [8] N. Fujiwara and K. Kobayashi, "Macrophages in inflammation," *Current Drug Targets-Inflammation Allergy*, vol. 4, no. 3, pp. 281–286, 2005.
- [9] X. H. Xu, P. K. Shah, E. Faure et al., "Toll-like receptor-4 is expressed by macrophages in murine and human lipid-rich atherosclerotic plaques and upregulated by oxidized LDL," *Circulation*, vol. 104, no. 25, pp. 3103–3108, 2001.
- [10] M. Salagianni, I. E. Galani, A. M. Lundberg et al., "Toll-like receptor 7 protects from atherosclerosis by constraining "inflammatory" macrophage activation," *Circulation*, vol. 126, no. 8, pp. 952–962, 2012.
- [11] M. de Gaetano, D. Crean, M. Barry, and O. Belton, "M1-and M2-type macrophage responses are predictive of adverse outcomes in human atherosclerosis," *Frontiers in Immunology*, vol. 7, p. 275, 2016.
- [12] J. Khallou-Laschet, A. Varthaman, G. Fornasa et al., "Macrophage plasticity in experimental atherosclerosis," *PLoS One*, vol. 5, no. 1, Article ID e8852, 2010.
- [13] S. Yang, H.-Q. Yuan, Y.-M. Hao et al., "Macrophage polarization in atherosclerosis," *Clinica Chimica Acta*, vol. 501, pp. 142–146, 2020.
- [14] Y. V. Bobryshev, E. A. Ivanova, D. A. Chistiakov, N. G. Nikiforov, and A. N. Orekhov, "Macrophages and their role in atherosclerosis: pathophysiology and transcriptome analysis," *BioMed Research International*, vol. 2016, Article ID 9582430, 13 pages, 2016.
- [15] J. Van den Bossche, J. Baardman, N. A. Otto et al., "Mitochondrial dysfunction prevents repolarization of inflammatory macrophages," *Cell Reports*, vol. 17, no. 3, pp. 684–696, 2016.
- [16] F. O. Martinez, A. Sica, A. Mantovani, and M. Locati, "Macrophage activation and polarization," *Frontiers in Bioscience: A Journal Virtual Library*, vol. 13, p. 453, 2008.
- [17] L. D. Karaliedde and C. T. Kappagoda, "The challenge of traditional Chinese medicines for allopathic practitioners," *American Journal of Physiology-Heart Circulatory Physiology*, vol. 297, no. 6, pp. H1967–H1969, 2009.
- [18] J. Zhang, H. Meng, Y. Zhang et al., "The therapeutical effect of Chinese medicine for the treatment of atherosclerotic coronary heart disease," *Current Pharmaceutical Design*, vol. 23, no. 34, pp. 5086–5096, 2017.
- [19] D.-W. Lim, H. Kim, Y.-M. Kim, Y.-W. Chin, W.-H. Park, and J.-E. Kim, "Drug repurposing in alternative medicine: herbal digestive Sochehwan exerts multifaceted effects against metabolic syndrome," *Scientific Reports*, vol. 9, no. 1, pp. 1–12, 2019, <https://www.researchgate.net/deref/https%3A%2F%2Fwww.nature.com%2Farticles%2F41598-019-45099-x>.
- [20] D.-W. Lim, H. Kim, S.-J. Lee, G.-R. Yu, J.-E. Kim, and W.-H. Park, "Jwa Kum Whan attenuates nonalcoholic fatty liver disease by modulating glucose metabolism and the insulin signaling pathway," *Evidence-Based Complementary Alternative Medicine*, vol. 2019, Article ID 4589810, 10 pages, 2019.
- [21] J. Fang, P. J. Little, and S. Xu, "Atheroprotective effects and molecular targets of tanshinones derived from herbal medicine danshen," *Medicinal Research Reviews*, vol. 38, no. 1, pp. 201–228, 2018.
- [22] P. Hao, F. Jiang, J. Cheng, L. Ma, Y. Zhang, and Y. Zhao, "Traditional Chinese medicine for cardiovascular disease: evidence and potential mechanisms," *Journal of the American College of Cardiology*, vol. 69, no. 24, pp. 2952–2966, 2017.
- [23] E.-A. Jung, Y.-K. Kim, D.-H. Kim, S.-I. Lee, and N.-J. Kim, "Studies on the development of antihyperlipidemic drugs from oriental herbal medicines (III)-antihyperlipidemic effects of gamigwaruhaebaekwhanggum-tang and its constituent herbal medicines *in vitro*," *Korean Journal of Pharmacognosy*, vol. 32, no. 1, pp. 22–30, 2001.
- [24] C.-H. Son, S.-M. Lee, G.-R. Yu et al., "Effects of [Geum-Gwe-Yo-Ryak (檉匾要略)] prescription for chest pain including kwaruhaebaekbanha-tang and kwaruhaebaekpaekju-tang on macrophage polarization," *Journal of Korean Medicine*, vol. 40, no. 2, pp. 51–62, 2019, <https://www.researchgate.net/deref/https%3A%2F%2Fdx.doi.org%2F10.13048%2Fjkm.19016>.
- [25] J. Seung-Ho, K. Kang-Beom, K. In-Su et al., "Protective effects of jisilhaebaekgyeji-tang and constituents extract on cultured rat myocardial cell treated by XO/HX," *Journal of Physiology*

- & *Pathology in Korean Medicine*, vol. 17, no. 4, pp. 952–957, 2003.
- [26] A. H. Fortier and L. A. Falk, “Isolation of murine macrophages,” *Current Protocols in Immunology*, vol. 11, no. 1, pp. 14.11. 11–14.11. 19, 1994.
- [27] C. H. Jin, Y. K. So, S. N. Han, and J.-B. Kim, “Isoegomaketone upregulates heme oxygenase-1 in RAW264. 7 cells via ROS/p38 MAPK/Nrf2 pathway,” *Biomolecules Therapeutics*, vol. 24, no. 5, pp. 510–516, 2016.
- [28] L. Schmölz, M. Wallert, and S. Lorkowski, “Optimized incubation regime for nitric oxide measurements in murine macrophages using the Griess assay,” *Journal of Immunological Methods*, vol. 449, pp. 68–70, 2017.
- [29] S. H. Lee, C. H. Kwak, S. K. Lee et al., “Anti-inflammatory effect of ascochlorin in LPS-stimulated RAW 264.7 macrophage cells is accompanied with the down-regulation of iNOS, COX-2 and proinflammatory cytokines through NF- κ B, ERK1/2, and p38 signaling pathway,” *Journal of Cellular Biochemistry*, vol. 117, no. 4, pp. 978–987, 2016.
- [30] M. Kobori, M. Yoshida, M. Ohnishi-Kameyama, and H. Shinmoto, “Ergosterol peroxide from an edible mushroom suppresses inflammatory responses in RAW264. 7 macrophages and growth of HT29 colon adenocarcinoma cells,” *British Journal of Pharmacology*, vol. 150, no. 2, pp. 209–219, 2007.
- [31] X.-Y. Yang, S.-X. Cai, W.-J. Zhang et al., “Semi-vioxanthin isolated from marine-derived fungus regulates tumor necrosis factor- α , cluster of differentiation (CD) 80, CD86, and major histocompatibility complex class II expression in RAW264. 7 cells via nuclear factor- κ B and mitogen-activated protein kinase signaling pathways,” *Biological and Pharmaceutical Bulletin*, vol. 31, no. 12, pp. 2228–2233, 2008.
- [32] S.-S. Wong, H.-R. Zhou, M. Marin-Martinez, K. Brooks, and J. Pestka, “Modulation of IL-1 β , IL-6 and TNF- α secretion and mRNA expression by the trichothecene vomitoxin in the RAW 264.7 murine macrophage cell line,” *Food Chemical Toxicology*, vol. 36, no. 5, pp. 409–419, 1998.
- [33] J.-H. Hwang, K.-J. Kim, S.-J. Ryu, and B.-Y. Lee, “Caffeine prevents LPS-induced inflammatory responses in RAW264. 7 cells and zebrafish,” *Chemico-biological Interactions*, vol. 248, pp. 1–7, 2016.
- [34] Y.-W. Ki, J. H. Park, J. E. Lee, I. C. Shin, and H. C. Koh, “JNK and p38 MAPK regulate oxidative stress and the inflammatory response in chlorpyrifos-induced apoptosis,” *Toxicology Letters*, vol. 218, no. 3, pp. 235–245, 2013.
- [35] S. O. Abarikwu, “Kolaviron, a natural flavonoid from the seeds of *Garcinia kola*, reduces LPS-induced inflammation in macrophages by combined inhibition of IL-6 secretion, and inflammatory transcription factors, ERK1/2, NF- κ B, p38, Akt, pc-JUN and JNK,” *Biochimica et Biophysica Acta (BBA)*, vol. 1840, no. 7, pp. 2373–2381, 2014.
- [36] C. Zhang, L. Fan, S. Fan et al., “*Cinnamomum cassia* Presl: a review of its traditional uses, phytochemistry, pharmacology and toxicology,” *Molecules*, vol. 24, no. 19, p. 3473, 2019.
- [37] E. Lee, S.-G. Kim, N.-Y. Park et al., “KOTMIN13, a Korean herbal medicine alleviates allergic inflammation *in vivo* and *in vitro*,” *BMC Complementary Alternative Medicine*, vol. 16, no. 1, p. 169, 2016.
- [38] W. Zhou and Y. J. Wang, “A network-based analysis of the types of coronary artery disease from traditional Chinese medicine perspective: potential for therapeutics and drug discovery,” *Journal of Ethnopharmacology*, vol. 151, no. 1, pp. 66–77, 2014.
- [39] J.-C. Liao, J.-S. Deng, C.-S. Chiu et al., “Anti-inflammatory activities of *Cinnamomum cassia* constituents *in vitro* and *in vivo*,” *Evidence-Based Complementary Alternative Medicine*, vol. 2012, Article ID 429320, 12 pages, 2012.
- [40] S. Rahman, H. Begum, Z. Rahman, F. Ara, M. J. Iqbal, and A. K. M. Yousuf, “Effect of cinnamon (*Cinnamomum cassia*) as a lipid lowering agent on hypercholesterolemic rats,” *Journal of Enam Medical College*, vol. 3, no. 2, pp. 94–98, 2013, <https://www.researchgate.net/deref/http%3A%2F%2Fdx.doi.org%2F10.3329%2Fjemc.v3i2.16132>.
- [41] H. Cao, J. F. Urban, and R. A. Anderson, “Cinnamon polyphenol extract affects immune responses by regulating anti- and proinflammatory and glucose transporter gene expression in mouse macrophages,” *The Journal of Nutrition*, vol. 138, no. 5, pp. 833–840, 2008.
- [42] M. E. Kim, J. Y. Na, and J. S. Lee, “Anti-inflammatory effects of trans-cinnamaldehyde on lipopolysaccharide-stimulated macrophage activation via MAPKs pathway regulation,” *Immunopharmacology Immunotoxicology*, vol. 40, no. 3, pp. 219–224, 2018.
- [43] R. Au, T. Al-Talib, A. Au, P. Phan, and C. Frondoza, “Avocado soybean unsaponifiables (ASU) suppress TNF- α , IL-1 β , COX-2, iNOS gene expression, and prostaglandin E2 and nitric oxide production in articular chondrocytes and monocyte/macrophages,” *Osteoarthritis Cartilage*, vol. 15, no. 11, pp. 1249–1255, 2007.
- [44] P. Ma, H.-T. Liu, P. Wei et al., “Chitosan oligosaccharides inhibit LPS-induced over-expression of IL-6 and TNF- α in RAW264. 7 macrophage cells through blockade of mitogen-activated protein kinase (MAPK) and PI3K/Akt signaling pathways,” *Carbohydrate Polymers*, vol. 84, no. 4, pp. 1391–1398, 2011.
- [45] R. L. Tiwari, V. Singh, and M. K. Barthwal, “Macrophages: an elusive yet emerging therapeutic target of atherosclerosis,” *Medicinal Research Reviews*, vol. 28, no. 4, pp. 483–544, 2008.
- [46] B. Kaminska, “MAPK signalling pathways as molecular targets for anti-inflammatory therapy—from molecular mechanisms to therapeutic benefits,” *Biochimica et Biophysica Acta (BBA)*, vol. 1754, no. 1–2, pp. 253–262, 2005.
- [47] L. Tornatore, A. K. Thotakura, J. Bennett, M. Moretti, and G. Franzoso, “The nuclear factor kappa B signaling pathway: integrating metabolism with inflammation,” *Trends in Cell Biology*, vol. 22, no. 11, pp. 557–566, 2012.
- [48] I. Rahman, J. Marwick, and P. J. B. p. Kirkham, “Redox modulation of chromatin remodeling: impact on histone acetylation and deacetylation, NF- κ B and pro-inflammatory gene expression,” *Biochemical Pharmacology*, vol. 68, no. 6, pp. 1255–1267, 2004.
- [49] F. E. Chen and G. J. O. Ghosh, “Regulation of DNA binding by Rel/NF- κ B transcription factors: structural views,” *Oncogene*, vol. 18, no. 49, pp. 6845–6852, 1999.
- [50] Y.-C. Liu, X.-B. Zou, Y.-F. Chai, and Y.-M. Yao, “Macrophage polarization in inflammatory diseases,” *International Journal of Biological Sciences*, vol. 10, no. 5, p. 520, 2014.
- [51] M. J. López-Armada, R. R. Riveiro-Naveira, C. Vaamonde-García, and M. N. Valcárcel-Ares, “Mitochondrial dysfunction and the inflammatory response,” *Mitochondrion*, vol. 13, no. 2, pp. 106–118, 2013.
- [52] B. N. Brown, B. D. Ratner, S. B. Goodman, S. Amar, and S. F. Badyal, “Macrophage polarization: an opportunity for improved outcomes in biomaterials and regenerative medicine,” *Biomaterials*, vol. 33, no. 15, pp. 3792–3802, 2012.

- [53] M. Peled and E. A. Fisher, "Dynamic aspects of macrophage polarization during atherosclerosis progression and regression," *Frontiers in Immunology*, vol. 5, p. 579, 2014.
- [54] S. Colin, G. Chinetti-Gbaguidi, and B. Staels, "Macrophage phenotypes in atherosclerosis," *Immunological Reviews*, vol. 262, no. 1, pp. 153–166, 2014.
- [55] G. Kari, U. Rodeck, A. P. J. C. P. Dicker, and Therapeutics, "Zebrafish: an emerging model system for human disease and drug discovery," *Clinical Pharmacology*, vol. 82, no. 1, pp. 70–80, 2007.
- [56] K. Howe, M. D. Clark, C. F. Torroja et al., "The zebrafish reference genome sequence and its relationship to the human genome," *Nature*, vol. 496, no. 7446, pp. 498–503, 2013.

Review Article

Xinmailong Injection for Improvement of Cardiac Function in Patients with Heart Failure: A Systematic Review and Meta-Analysis

Yuan-long Sun,^{1,2} Yi-ping Li,^{1,2} Ting-ting Qiang,^{1,2} Xiao-fen Ruan ^{1,2}
and Xiao-long Wang ^{1,2}

¹Cardiovascular Department, Shuguang Hospital of Shanghai University of Traditional Chinese Medicine, Shanghai 201203, China

²Cardiovascular Research Institute of Traditional Chinese Medicine, Shuguang Hospital of Shanghai University of Traditional Chinese Medicine, Shanghai 201203, China

Correspondence should be addressed to Xiao-fen Ruan; ruanxiaofeng@shutcm.edu.cn and Xiao-long Wang; wangxiaolong@shutcm.edu.cn

Received 28 June 2020; Revised 16 October 2020; Accepted 28 October 2020; Published 19 November 2020

Academic Editor: Sai-Wang Seto

Copyright © 2020 Yuan-long Sun et al. This is an open access article distributed under the Creative Commons Attribution License, which permits unrestricted use, distribution, and reproduction in any medium, provided the original work is properly cited.

Background. Insect drugs have great potential for treating cardiovascular diseases. Xinmailong (XML) injection, a bioactive composite extracted from *Periplaneta americana* (a species of cockroach), was widely used in treating heart failure in China. This meta-analysis aimed to assess the efficacy and safety of XML injection for the improvement of cardiac function in HF. **Materials and Methods.** Online literature search for relevant studies was performed using databases including PubMed, EMBASE, Cochrane Library, CNKI, and Wanfang. Left ventricular ejection fraction (LVEF), six-minute walk test (6MWT), and brain natriuretic peptide (BNP) were selected as target outcomes. The analysis was performed using Stata 12.0, and sources of heterogeneity were explored by subgroup analysis and metaregression. **Results.** 32 studies were included in this meta-analysis after meeting the inclusion/exclusion criteria. The results demonstrated that additional use of XML improved LVEF (WMD = 5.82, 95% CI: 5.52–7.13, $P < 0.00001$) and 6MWT (WMD = 51.48, 95% CI: 35.83–67.13, $P < 0.00001$) and reduced BNP (WMD = -172.84, 95% CI: -205.79 to -139.89, $P < 0.00001$). The results of subgroup analyses and metaregression suggested that XML injection has more cardiac function improvement for middle-aged HF patients than youth, and greater LVEF and 6MWT improvement were associated with higher average age. **Conclusions.** XML plus conventional treatment demonstrated a significant effect in reducing cardiac dysfunction in HF patients, and age is a potential factor of higher efficacy. Given the heterogeneity and bias of the included RCTs, large, prospective, rigorous trials are still needed.

1. Introduction

Heart failure (HF) is a global healthcare issue, defined as a severe and terminal-stage symptom after heart disease, and has high patient mortality [1, 2]. HF induces structural, neurohumoral, cellular, and molecular dysfunctions and leads to several organ and system dysfunction resulting in complex clinical manifestations [3]. About 12% of individuals over 80 have HF [4]. As of 2015, 8.9% of Chinese population over 35 years of age have HF [5].

Insect drugs, a type of traditional Chinese medicine (TCM), have great potential for the treatment of several

cardiovascular diseases. Insect extracts are rich sources of pharmacopeias occurring naturally and have great scientific and medical value [6]. In the TCM theory system, insect drugs have the effect of activating blood circulation and removing blood stasis, which fits the TCM pathogenesis of HF.

Xinmailong injection (XML, commercialized by the Yunnan Teng Yao Pharmaceutical Co., Ltd, China) is a kind of Chinese patent medicine made by extracting effective substances from *Periplaneta americana* (a species of cockroach) with modern technology [7]. As a kind of insect drug, fresh adult *P. americana* bodies were dried and processed into powder for the treatment of disease. The *P. americana*

powder has a history of applying for thousands of years that can be traced back to the Ming Dynasty (A.D. 1578). It was recorded in the “Compendium of Materia Medica” for its therapeutic effects of promoting blood circulation, detoxification, and urination [8].

Extracts of *P. americana* have many effects, such as promoting wound healing, antitumor activity, and treating HF and gastrointestinal ulcers. Research studies obtained the chemical compounds from *P. americana*, which were polyhydric alcohols, organic acids, alkaloids [9], divinyl sulfide, noradrenaline, ketone compounds [10, 11], adenosine, inosine, protocatechuic acid, and pyroglutamate acid [12]. These extracts play a specific role in the treatment of diseases with their function of antibacterial, antiviral, and antitumor activity and enhancement of immune function [8]. XML injection as a medicine has a positive inotropic activity, improves microcirculation, dilates pulmonary vessels, induces diuresis, has antiarrhythmia function, and inhibits free radical damage [13].

XML injection has achieved beneficial curative effects in clinical studies and can improve HF patients’ cardiac function [14]. However, few studies systematically evaluate the effectiveness of XML injection and the quality of researches. Therefore, we performed this systematic review of available randomized controlled trials to evaluate the efficacy of XML on the improvement of cardiac function in HF patients. Left ventricular ejection fraction (LVEF), six-minute walk test (6MWT), and brain natriuretic peptide (BNP) were three typical indicators of measuring cardiac functions and were selected as target outcomes in this review. We performed several subgroup analyses and meta-regression to find out the facts that caused the heterogeneity among articles.

2. Materials and Methods

The present meta-analysis was performed based on the Preferred Reporting Items for Systematic Reviews and Meta-Analyses (PRISMA) guidelines 2015 statement [15, 16] and was registered on PROSPERO (CRD42020163716).

2.1. Database and Literature Search Strategies. Online literature search for relevant studies was performed using five databases, which included PubMed, EMBASE, Cochrane Library, Chinese National Knowledge Infrastructure (CNKI), and Wanfang. Studies were reviewed and selected by two experienced investigators. Relevant data were extracted by an additional two independent investigators. Any discrepancies in data extraction or literature review were resolved by consensus or by consulting a third reviewer. All relevant data from the literature review were extracted from the aforementioned databases from inception to April 2020.

The following keywords were searched in various combinations (Xinmailong OR XML OR Xin Mai Long OR XMLI OR Xinmailong Injection) AND (heart failure OR HF OR cardiac failure OR Chronic Heart Failure OR CHF) AND (randomized controlled trial OR RCT).

2.2. Inclusion Criteria. All patients from the selected studies met the internationally accepted criteria for the diagnosis of HF. Only human studies for random clinical trials (RCTs) were considered. No etiology, ethnic group, severity, or course of disease were considered as exclusion criteria. In the experiment group, XML injection plus conventional therapy was considered as a treatment strategy. On the basis of the conventional therapy of western medicine, patients in the control group had placebo or not. Measurable outcomes were LVEF, 6MWT, and BNP.

2.3. Exclusion Criteria. The exclusion criteria were (1) non-RCTs; (2) animal studies, mechanistic studies, case reports, and reviews; (3) patients with acute heart failure and severe liver and kidney disease; (4) use of other TCM formulas; (5) studies with unacceptable trial designs and inappropriate statistical methods; and (6) duplicate publications.

2.4. Data Extraction and Quality Assessment. Clinical data and adverse events were collected and cross-checked by two independent investigators. Any disagreements were resolved through discussion or by consulting a third investigator. The following data were extracted from studies: patient characteristics, details, differences in intervention between the control and experimental groups, outcome measures, and results from the items listed in the inclusion criteria. Methodological quality was assessed based on the Cochrane Handbook. The included RCTs were assessed for (1) random sequence generation, (2) allocation concealment, (3) blinding of participants and personnel, (4) blinding of outcome assessments, (5) selective outcome reporting, (6) incomplete outcome data, and (7) other potential sources of bias [17].

2.5. Data Synthesis. Effect-size calculations and meta-analytical statistics were performed using Stata 12.0 obtained from its official website (<http://www.stata.com>). Weighted mean differences (WMD) with 95% CI were expressed for continuous variables and were analyzed using the inverse-variance method. Heterogeneity across the trials was evaluated using the Cochran Q test and the Higgins I² test [18]. Only fixed-effect models were used for both dichotomous and continuous variables, unless the results of pooled analyses showed significant heterogeneity ($P < 0.10$ and $I^2 > 50\%$). A random-effect model was used for significant heterogeneity. Potential publication bias was assessed by Begg’s and Egger’s tests [19]. A 2-tailed P value of less than 0.05 was set for statistical significance. Subgroup analyses and meta-regression were performed for sensitivity analysis. Meta-regression sensitivity analyses were performed using the “metareg” macro available in the Stata statistical package. Gender, average age, age section, pattern identification, duration time, course of disease, publication year, and sample size were set as the covariances of meta-regression analyses.

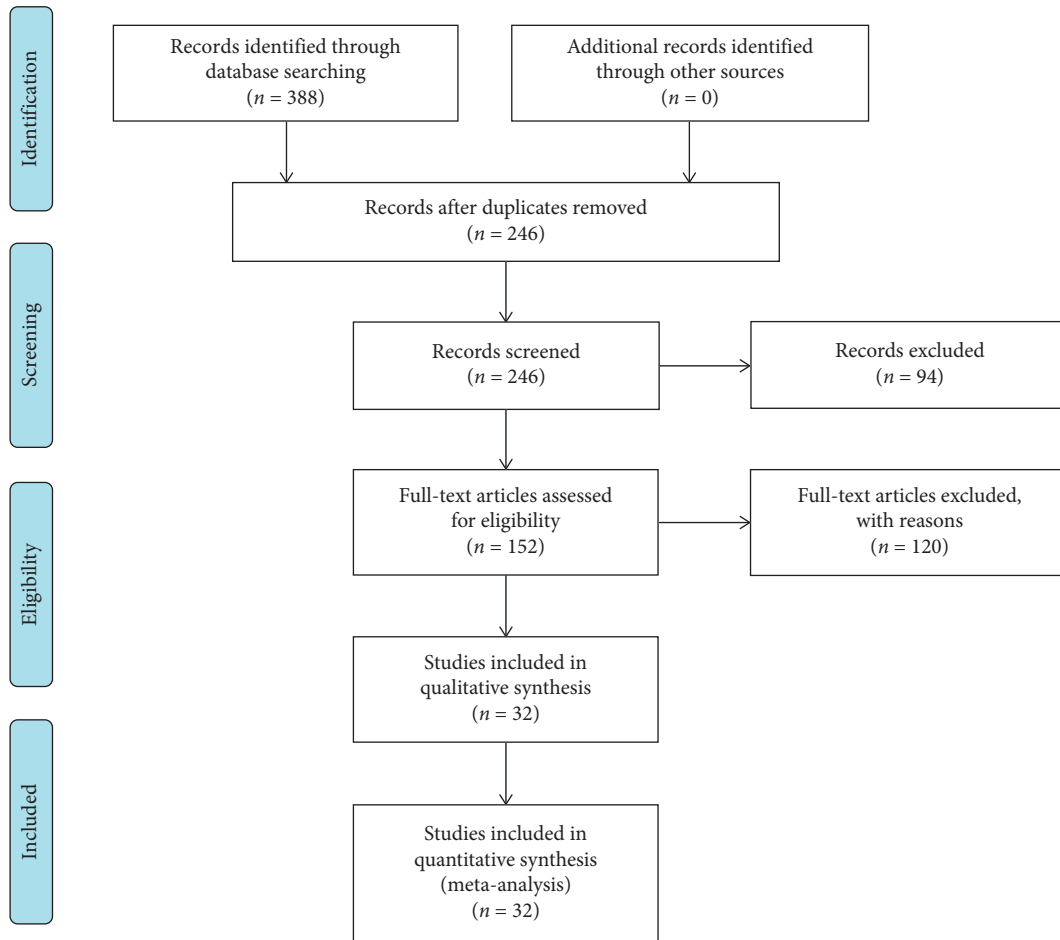


FIGURE 1: Flowchart depicting publication search criteria and selection.

3. Results

3.1. Description of Selected Studies. 388 potentially eligible publications were retrieved after the primary search from the eight databases. Of which 32 RCTs were included for the meta-analysis (Figure 1). Except for one selected study that was published in English, the rest studies were published in Chinese. All selected studies were conducted in China and included 3730 patients. Characteristics of the included studies are listed in Table 1.

As shown in Table 2, all 32 selected studies mentioned random sequence generation and no selective reporting bias and 9 studies mentioned allocation sequence and concealment using random number tables. Three studies cited blinding of participants and personnel, and no study mentioned blinding of outcome assessments. 4 studies reported patient attrition; among these, 2 studies reported no dropouts and 2 studies mentioned attrition rates.

3.2. Results of Outcomes

3.2.1. Left Ventricular Ejection Fraction (LVEF). Twenty-seven studies reported the LVEF level; the results showed significant increase in LVEF in HF patients with

XML injection (WMD = 5.82, 95% CI: 5.52–7.13, $P < 0.00001$) (Figure 2). Subgroup analyses showed significantly higher LVEF improvement ($P = 0.006$) in HF patients of middle age (WMD = 7.7, 95% CI: 5.6–9.79) than those of youth (WMD = 4.11, 95% CI: 2.61–5.62) (Table 3). However, there was no significant difference ($P = 0.88$) between studies performing TCM pattern identification (WMD = 5.68, 95% CI: 3.83–7.53) and those not performing TCM pattern identification (WMD = 5.87, 95% CI: 4.38–7.36). There was no publication bias according to Begg's test ($P = 0.505$) and Egger's test ($P = 0.109$) (Table 4).

3.2.2. Six-Minute Walk Test (6MWT). Fifteen studies reported the 6MWT; the results showed significant increase in 6MWT in HF patients with XML injection (WMD = 51.48, 95% CI: 35.83–67.13, $P < 0.00001$) (Figure 3). Subgroup analysis indicated that XML injection has more 6MWT improvement for HF patients of middle age (WMD = 77.39, 95% CI: 58.94–95.84) than those of youth (WMD = 34.58, 95% CI: 21.26–47.89, $P < 0.0002$ for between subgroups) (Table 3), but similar increase in pattern identification (WMD = 60.6, 95% CI: –1.01 to 122.21 for pattern identification and WMD = 48.88, 95% CI: 34.52–63.24 for non-pattern identification, $P = 0.72$ for between subgroups). No

TABLE 1: Characteristics of the selected studies.

Study	Indication	NYHA	Sample size (E/C)	Mean age (year)	Male/female (E/C)	Course of disease (year)	Intervention	Duration (day)	Endpoints
Chen 2012 [20]	CHF	III-IV	47/53	69.3 ± 6.9	NA	5.7 ± 1.2	5 mg/kg bid	5	LVEF, BNP
Du et al. 2016 [21]	CHF	II-IV	49/49	49-79	53/45	NA	5 mg/kg bid	10	LVEF, BNP, 6MWT
Guo and Ren 2016 [22]	CHF	II-IV	52/52	E: 69 ± 8 C: 68 ± 5	E: 26/26 C: 28/24	E: 8.3 ± 6.0 C: 8.3 ± 6.1	6 ml bid	10	6MWT, LVEF, BNP
Han et al. 2012 [23]	CHF	II-IV	25/21	E: 65 ± 7 C: 68 ± 6	E: 15/10 C: 13/8	NA	5-10 mg/kg bid	14	LVEF, 6MWT
Han and Gu 2016 [24]	CHF	NA	136/147	E: 79 ± 11 C: 77 ± 12	E: 109/27 C: 122/25	NA	4 ml bid	14	LVEF, BNP
Han and Liu 2018 [25]	CHF	II-IV	56/56	E: 72.5 ± 11.4 C: 74.3 ± 12.7	E: 38/18 C: 36/20	NA	5 mg/kg bid	10	LVEF
He 2017 [26]	CHF	II-IV	47/48	E: 70.8 ± 7.6 C: 69.6 ± 7.9	E: 23/24 C: 23/25	NA	5 mg/kg bid	15	LVEF, 6MWT
Li and Li 2015 [27]	CHF	II-IV	35/30	E: 62 ± 10 C: 58 ± 8	E: 20/15 C: 18/12	NA	8 ml bid	15	LVEF
Li 2016 [28]	CHF	I-IV	24/24	E: 63.3 ± 5.8 C: 63.7 ± 5.2	E: 16/8 C: 15/9	E: 7.6 ± 6.5 C: 7.9 ± 6.3	5 mg/kg bid	14	BNP, LVEF
Li et al. 2018 [29]	HF	II-III	100/100	E: 58.9 ± 7.2 C: 58.4 ± 7.1	E: 52/48 C: 54/46	E: 3.4 ± 1.4 C: 3.4 ± 1.5	5 mg/kg bid	5	BNP
Liu HL 2018 [30]	CHF	II-IV	80/42	E: 67 ± 8 C: 68 ± 10	E: 38/42 C: 32/48	NA	5 mg/kg bid	5	LVEF, 6MWT
Liu et al. 2018 [31]	CHF	II-IV	46/46	E: 60.3 ± 4.0 C: 61.0 ± 4.3	E: 25/21 C: 27/19	E: 7.9 ± 1.4 C: 8.0 ± 1.3	4 ml bid	14	BNP, LVEF
Liu et al. 2018 [32]	CHF	II-IV	60/60	E: 62-84 C: 63-85	E: 31/29 C: 30/30	NA	5 mg/kg bid	10	BNP
Quan and Miao 2017 [33]	CHF	II-IV	46/48	E: 67.6 ± 10.5 C: 65.8 ± 11.4	E: 35/16 C: 38/13	E: 37.8 ± 7.5 C: 39.6 ± 8.6	5 mg/kg bid	10	LVEF, 6MWT
Shen et al. 2017 [34]	CHF	II-IV	58/58	E: 62.8 ± 7.1 C: 61.6 ± 7.8	E: 34/24 C: 36/22	E: 8.3 ± 7.5 C: 8.1 ± 7.8	4 ml bid	14	6MWT, LVEF
Shi et al. 2016 [35]	HF	NA	58/58	E: 56.2 ± 8.74 C: 55.6 ± 9.18	E: 28/30 C: 29/29	NA	5 mg/kg bid	5	BNP
Teng and Wang 2017 [36]	CHF	II-III	40/40	E: 75.5 ± 3.8 C: 73.4 ± 3.7	E: 22/18 C: 23/17	E: 1.7 ± 0.5 C: 1.5 ± 0.3	5 mg/kg bid	5	LVEF
Wang et al. 2012 [37]	CHF	III-IV	24/26	NA	NA	NA	10	LVEF, 6MWT, BNP	
Wu et al. 2017 [38]	HF	NA	48/42	E: 54.05 ± 3.96 C: 56.13 ± 4.87	E: 28/20 C: 31/11	E: 6.33 ± 0.94 C: 6.01 ± 0.33	5 mg/kg bid	10	BNP
Wu and Yang 2015 [39]	HF	III-IV	50/50	E: 70 ± 7.5 C: 71 ± 7.1	E: 30/20 C: 29/21	NA	5 mg/kg bid	10	BNP
Xu and Xu 2016 [40]	CHF	NA	76/76	NA	E: 50/26 C: 48/28	NA	5 mg/kg bid	14	LVEF, 6MWT
Xue et al. 2015 [41]	CHF	II-III	120/115	E: 63.1 ± 9.80 C: 63.9 ± 9.01	E: 69/46 C: 60/60	E: 2.07 C: 2.37	5 mg/kg bid	5	LVEF, 6MWT
Xue et al. 2019 [14]	CHF	II-III	50/50	E: 63.8 ± 9.46 C: 64.3 ± 7.78	E: 29/21 C: 27/23	2.48 ± 2.25 C: 1.90 ± 1.65	5 mg/kg bid	16	LVEF, 6MWT, BNP
Yang et al. 2012 [42]	CHF	III-IV	57/53	E: 79 ± 10 C: 78 ± 11	E: 46/11 C: 44/9	NA	4 ml bid	14	LVEF, BNP
Yang et al. 2017 [43]	CHF	II-IV	33/33	E: 60.2 ± 5.8 C: 61.1 ± 4.5	E: 18/15 C: 19/14	E: 3.9 ± 1.2 C: 3.9 ± 1.0	5-10 mg/kg bid	14	LVEF
Yuan et al. 2015 [44]	CHF	I-IV	54/34	E: 51.5 ± 5.6 C: 52.3 ± 6.0	E: 30/24 C: 19/15	E: 2.5 ± 2.3 C: 2.8 ± 3.1	5 mg/kg bid	5	6MWT

TABLE 1: Continued.

Study	Indication	NYHA	Sample size (E/C)	Mean age (year)	Male/female (E/C)	Course of disease (year)	Intervention	Duration (day)	Endpoints
Zhao et al. 2014 [45]	CHF	II-IV	30/30	E: 41-78 C: 40-76	E: 13/17 C: 16/14	NA	5 mg/kg bid	14	LVEF, 6MWT
Zhao et al. 2010 [46]	CHF	IV	131/112	NA	NA	NA	5-10 mg/kg bid	14	LVEF, BNP
Jiang et al. 2019 [47]	HF	/	52/56	E: 63.1 ± 7.2 C: 62.7 ± 7.6	E: 29/23 C: 31/25	E: 7.87 ± 4.2 C: 7.57 ± 5.7	5 mg/kg bid	10	6MWT, LVEF
Li 2019 [48]	CHF	II-IV	200/60	E: 63.79 ± 8.82 C: 62.96 ± 9.34 E: 57.43 ± 6.45	E: 131/69 C: 40/20	E: 9.06 ± 2.42 C: 8.96 ± 2.25	8 ml qd	14	LVEF
Liu and Zhao 2019 [49]	CHF	I-IV	42/42	C: 56.55 ± 5.94 E: 68.85 ± 6.20	E: 25/17 C: 20/22	NA	5-10 mg/kg bid	5	LVEF
Zhang and Zhao 2019 [50]	CHF	II-IV	47/46	C: 56.55 ± 5.94 E: 68.85 ± 6.20 C: 69.03 ± 6.31	E: 27/20 C: 28/18	NA	5 mg/kg bid	14	LVEF

NYHA, New York Heart Association; E, experimental group; C, control group; CHF, chronic heart failure; HF, heart failure, NA, not applicable; BNP, brain natriuretic peptide; 6MWT, 6-minute walk test; LVEF, left ventricular ejection fraction; IVST, interventricular septal thickness.

TABLE 2: Risk of bias.

Study	Random sequence generation	Allocation concealment	Blinding of participants and personnel	Blinding of outcome assessment	Incomplete outcome data	Selective reporting	Other bias
Chen 2012 [20]	+	/	/	/	/	+	/
Du et al. 2016 [21]	+	/	/	/	/	+	/
Guo and Ren 2016 [22]	+	+	/	/	/	+	/
Han et al. 2012 [23]	+	/	/	/	/	+	/
Han and Gu 2016 [24]	+	/	/	/	/	+	/
Han and Liu 2018 [25]	+	/	/	/	/	+	/
He 2017 [26]	+	/	/	/	/	+	/
Li and Li 2015 [27]	+	/	/	/	/	+	/
Li 2016 [28]	+	+	/	/	/	+	/
Li et al. 2018 [29]	+	+	/	/	/	+	/
Liu et al. 2018 [30]	+	/	/	/	/	+	/
Liu 2018 [31]	+	/	/	/	/	+	/
Liu et al. 2018 [32]	+	/	/	/	/	+	/
Quan and Miao 2017 [33]	+	+	/	/	+	+	/
Shen et al. 2017 [34]	+	/	+	/	/	+	/
Shi et al. 2016 [35]	+	/	/	/	/	+	/

TABLE 2: Continued.

Study	Random sequence generation	Allocation concealment	Blinding of participants and personnel	Blinding of outcome assessment	Incomplete outcome data	Selective reporting	Other bias
Teng and Wang 2017 [36]	+	+	/	/	/	+	/
Wang et al. 2012 [37]	+	/	/	/	-	+	/
Wu et al. 2017 [38]	+	+	/	/	/	+	/
Wu and Yang 2015 [39]	+	/	/	/	/	+	/
Xu and Xu 2016 [40]	+	/	/	/	/	+	/
Xue et al. 2015 [41]	+	+	+	/	-	+	/
Xue et al. 2019 [14]	+	+	+	/	+	+	/
Yang et al. 2012 [42]	+	/	/	/	/	+	/
Yang et al. 2017 [43]	+	/	/	/	/	+	/
Yuan et al. 2015 [44]	+	/	/	/	/	+	/
Zhao et al. 2014 [45]	+	/	/	/	/	+	/
Zhao et al. 2010 [46]	+	/	/	/	/	+	/
Jiang et al. 2019 [47]	+	/	/	/	/	+	/
Li 2019 [48]	+	/	/	/	/	+	/
Liu and Zhao 2019 [49]	+	/	/	/	/	+	/
Zhang and Zhao 2019 [50]	+	+	/	/	/	+	/

+, low risk; -, high risk; /, unclear risk.

publication bias was observed in the 6MWT of HF patients ($P = 0.451$ for Begg's test and $P = 0.209$ for Egger's test) (Table 4).

3.2.3. Brain Natriuretic Peptide (BNP). Sixteen studies reported the BNP; the results showed that BNP level in the XML plus conventional therapy group was significantly higher compared to conventional therapy alone (WMD = -172.84, 95% CI: -205.79 to -139.89, $P = 0.00001$) (Figure 4). For the subgroup analysis based on age section, significantly higher BNP decrease was observed in middle-aged HF patients than young patients (WMD = -301.54, 95% CI: -405.38 to -197.71 for middle-aged and WMD = -156.7, 95% CI: -201.26 to -112.15 for youth, $P = 0.01$ for between subgroups) (Table 3). No significant difference was observed in subgroup analysis based on pattern identification (WMD = -243.87, 95% CI: -426.98 to -60.76 for pattern identification and WMD = -159.1, 95% CI: -193.3 to -124.89 for nonpattern identification, $P = 0.37$ for between subgroups). The results of Begg's test ($P = 0.137$) and Egger's test ($P = 0.014$)

indicated potential publication bias in the BNP level (Table 4).

3.2.4. Metaregression Results. The results of metaregression (Table 5) suggested that the age section and average age could be two main sources that contributed to the heterogeneity of LVEF and 6MWT. Unfortunately, gender, pattern identification, duration time, course of the disease, publication year, and sample size showed no significant effect on LVEF and 6MWT, and none of these indicators listed had a statistically significant effect on the BNP level. The significant regression effect of age section (adj $R^2 = 26.75\%$, $P = 0.013$ for LVEF; adj $R^2 = 69.25\%$, $P = 0.003$ for 6MWT) met the results of subgroup analyses, which further indicated that middle-aged HF patients with XML administration could have higher LVEF and 6MWT improvement than the youth. The metaregression results based on average age (adj $R^2 = 16.54\%$, $P = 0.049$ for LVEF; adj $R^2 = 36.39\%$, $P = 0.048$ for 6MWT) suggested that greater LVEF and 6MWT improvements were associated with higher average age (Figure 5).

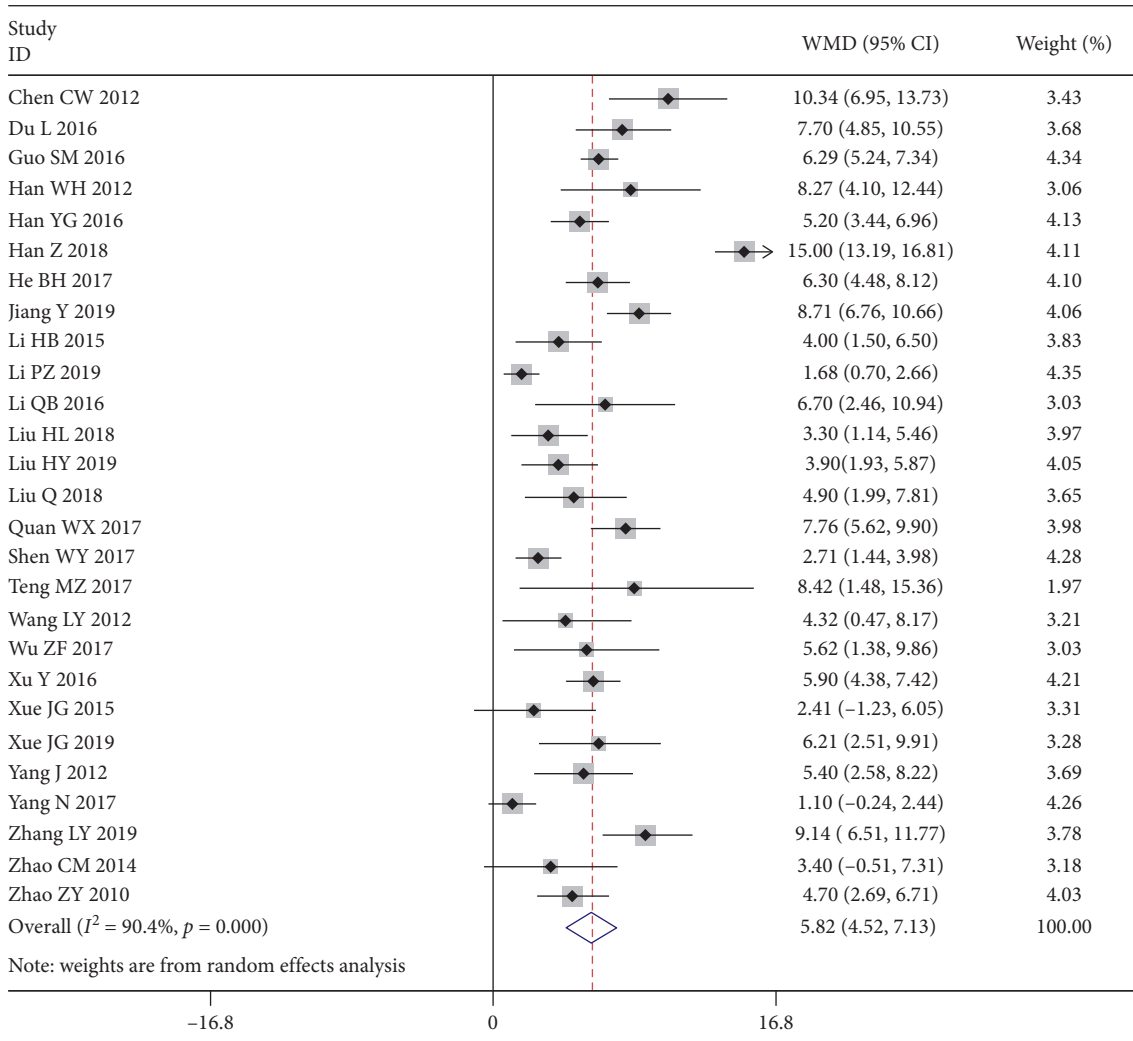


FIGURE 2: Forest plot of LVEF in patients administered XML plus conventional therapy versus conventional HF therapy alone.

3.2.5. Adverse Events. 16 out of the 32 studies investigated adverse events. 10 of these studies reported no obvious adverse events, while the remaining 6 studies mentioned details of adverse events. As shown in Table 6, 7 adverse events were observed between the experimental and control groups. These included cutaneous pruritus (3/0), palpitation (1/4), dizziness (2/0), headaches (0/1), nausea (2/1), leukocytosis (0/2), and hypotension (1/0). All symptoms reported were resolved during study observation, and no deaths related to XML administration were reported.

4. Discussion

4.1. Summary of Main Results. XML injection is a bioactive composite extracted from *P. americana*. The injection form can avoid people's visual aversion and improve the utilization ratio of bioavailability for its advanced extraction process. XML injection has been widely used in China for decades. Studies provided evidences to support XML as an effective administration to HF patients that XML injection can mitigate epirubicin-induced cardiotoxicity via activating

the PI3K/Akt signaling pathway and inhibiting the Erk1/2 and P38 MAPK signaling pathways [51]. XML can also activate *T*-type calcium channels and inhibit $\text{Na}^+/\text{K}^+ - \text{ATPase}$ to increase intracellular calcium levels when treating HF [52]. Besides, the pharmacological research on XML has been carried out continuously and many components and functions of XML are being explored [12]. Despite its treatment effects on HF, it can also repair damaged skin and treat gastric ulcers [8].

This systematic review provided evidence that additional XML injection treatment demonstrates better therapeutic effects than conventional treatment on improving cardiac function in patients with HF evidenced by the increase in LVEF and 6MWT and reduction in BNP. Subgroup analyses provided evidence that the age section is a source of causing significant differences between groups. Under XML injection administration, the cardiac function of middle-aged patients showed better improvement than young patients (average > 65 as middle aged, average < 65 as youth). Further metaregression demonstrated that age section and average age showed significant heterogeneity in LVEF and 6MWT and

TABLE 3: Mean difference of cardiac function of HF patients with XML injection administration in different subgroup analyses.

	LVEF				6MWT				BNP			
	N	WMD (95% CI)	I ² (%)	P value for between-group difference	N	WMD (95% CI)	I ² (%)	P value for between-group difference	N	WMD (95% CI)	I ² (%)	P value for between-group difference
Overall	27	5.82 (4.52, 7.13)	90		15	51.48 (35.83, 67.13)	88		16	-172.84 (-205.79, -139.89)	94	
Subgroups												
Age section	0.006				0.0002				0.01			
Youth	11	4.11 (2.61, 5.62)	83		6	34.58 (21.26, 47.89)	61		5	-156.70 (-201.26, -112.15)	88	
Middle age	11	7.70 (5.60, 9.79)	90		5	77.39 (58.94, 95.84)	77		6	-301.54 (-405.38, -197.71)	97	
Pattern identification	0.88				0.72				0.37			
Yes	4	5.68 (3.83, 7.53)	33		3	60.60 (-1.01, 122.21)	87		3	-243.87 (-426.98, -60.76)	97	
No	23	5.87 (4.38, 7.36)	90		12	48.88 (34.52, 63.24)	84		13	-159.10 (-193.30, -124.89)	94	

LVEF, left ventricular ejection fraction; 6MWT, six-minute walk test; BNP, brain natriuretic peptide; WMD, weighted mean difference; CI, confidence interval.

TABLE 4: Publication bias.

	Number of studies	Begg's P value	Egger's P value
LVEF	27	0.505	0.109
6MWT	12	0.451	0.209
BNP	16	0.137	0.014

LVEF, left ventricular ejection fraction; 6MWT, six-minute walk test; BNP, brain natriuretic peptide.

greater improvement of LVEF and 6MWT was connected to a higher age. The above evidences lead to the conclusion that XML injection may be more suitable for middle-aged patients and its efficiency increases by age, while it has a considerable improvement in HF patients of all age ranges.

The pattern identification presented no potential heterogeneity in both subgroup analysis and metaregression, indicating XML injection, as a single-substance extract, has fixed therapeutic efficacy on HF without pattern identification, unlike other Chinese patent drugs that focus on TCM syndromes. Unfortunately, the rest covariances (gender, duration time, course of disease, publication year, and sample size) may contribute no significance to the heterogeneity.

4.2. Adverse Events. No obvious adverse reactions of Xinmailong injection were found before marketing. With the expansion of users after marketing, many adverse reactions have been reported gradually. In previous reviews, the incidence of adverse reactions was 7.6% [53]. The most common symptoms are pruritus, slight blood pressure rise, nausea, and vomiting. In this review, adverse effects of XML injection were also collected from included studies, of which

2 studies mentioned skin itching [14, 36], each study mentioned hypertension [37] and nausea [36]. Other studies also described palpitation, dizziness, headache, and leukocytosis of HF patients during XML administration. There is no case of liver and kidney function damage in the clinical study of Xinmailong. On the contrary, there is a protective effect of XML injection on the early renal function damage caused by grass carp bile [54] and extracts of *P. americana* have a protective effect on liver damage, liver fibrosis, and hepatitis [55]. Although all the adverse reactions mentioned above can be relieved by rest or slowing down the intravenous drip, no lethal events or major adverse cardiovascular events were observed. XML seemed to be generally safe for HF treatment, but the evidence is still insufficient to make a decisive conclusion on safety. Attentions are still needed in practical application, as the safety of TCM herbal injections has been increasingly concerned by both medical workers and the public.

4.3. Limitations. Study limitations in this review were mostly due to the risk of bias [56] of included studies. Many studies have no description of the necessary process of clinical trials, and therefore the evaluation of these studies

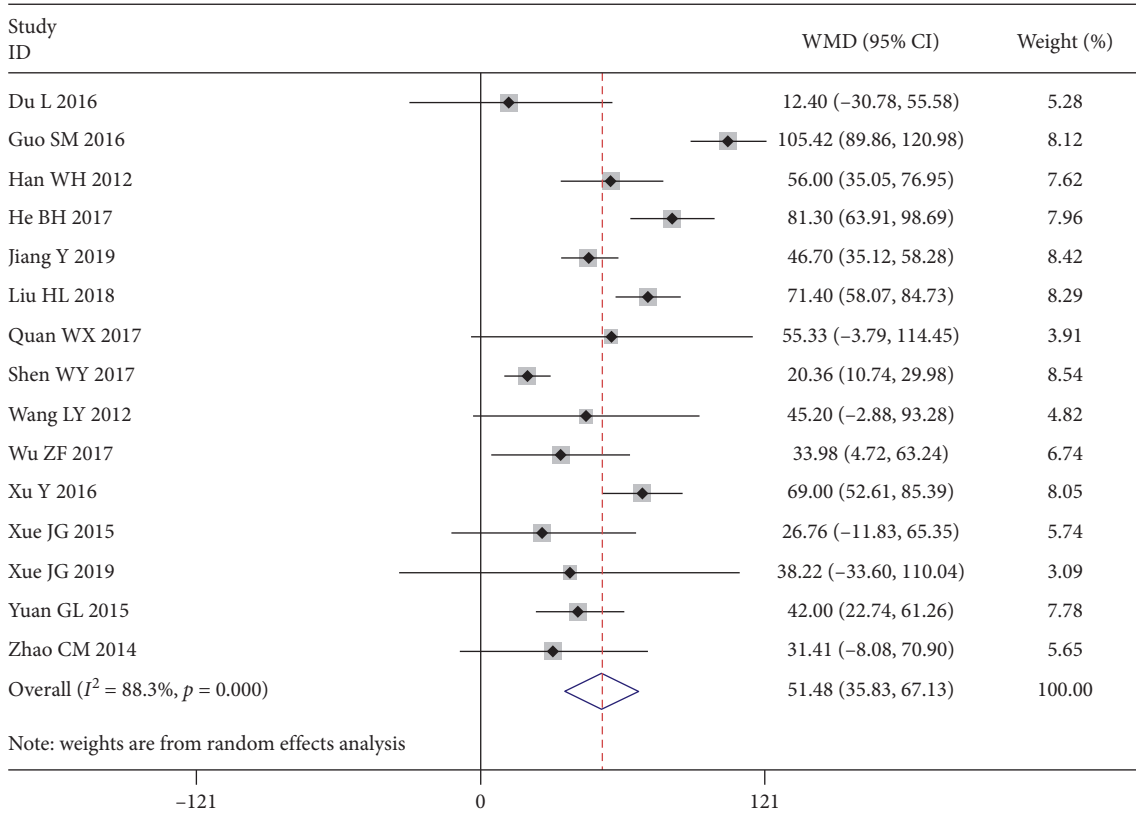


FIGURE 3: Forest plot of 6MWT in patients administered XML plus conventional therapy versus conventional HF therapy alone.

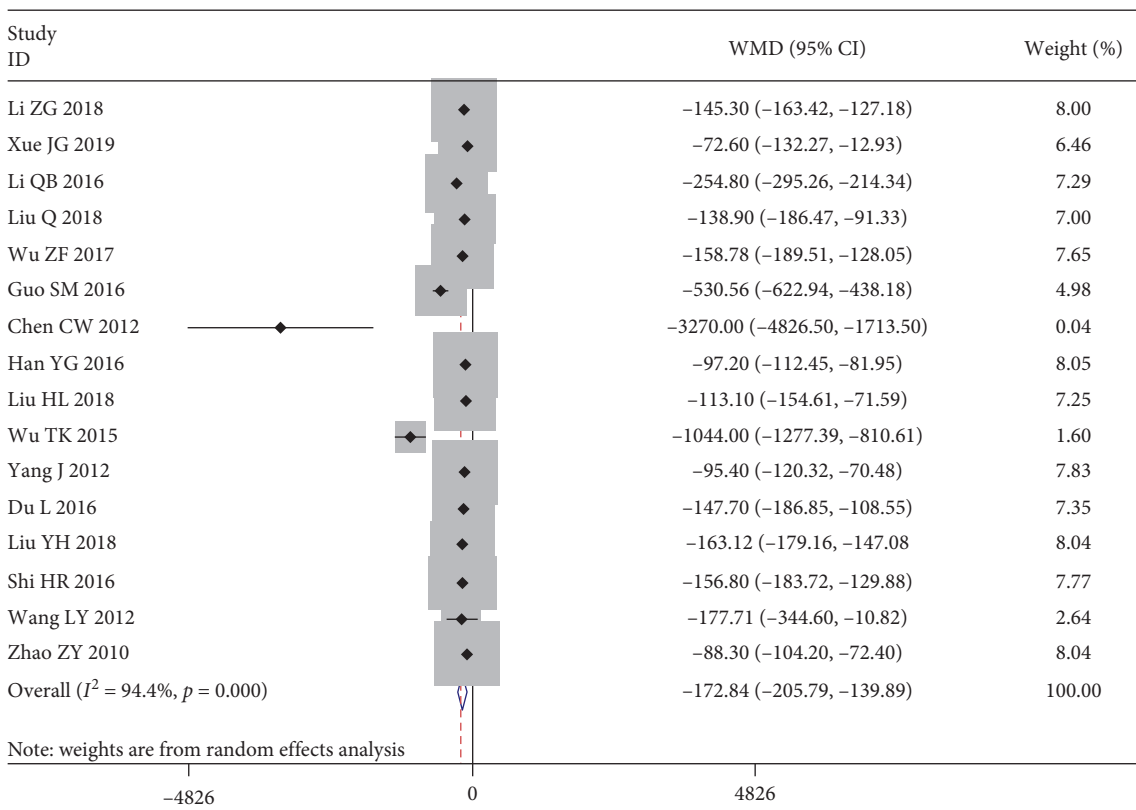


FIGURE 4: Forest plot of BNP level in patients administered XML plus conventional therapy versus conventional HF therapy alone.

TABLE 5: Metaregression analysis of association between covariates and cardiac function of HF patients with XML injection administration.

	LVEF					6MWT					BNP				
	N	P value	Tau ²	I ² (%)	Adj R ² (%)	N	P value	Tau ²	I ² (%)	Adj R ² (%)	N	P value	Tau ²	I ² (%)	Adj R ² (%)
Gender	22	0.727	9.304	92.03	-4.89	12	0.447	656.7	88.15	-0.47	12	0.573	61293	93.91	-8.69
Age section	22	0.013	7.121	87.36	26.75	11	0.003	192.5	70.52	69.25	11	0.340	98464	95.34	-3.05
Average age	22	0.049	8.114	89.25	16.54	11	0.048	398.2	86.05	36.39	11	0.737	117450	95.15	-22.93
Pattern identification	27	0.890	8.442	90.55	-3.97	15	0.300	508	84.71	8.82	16	0.924	53996	94.60	-12.45
Duration time	27	0.436	8.202	89.67	-1.02	16	0.836	558.2	87.91	-8.62	16	0.549	54559	93.98	-13.62
Course of disease	13	0.421	7.450	89.28	-1.03	8	0.686	812	92.87	-7.69	7	0.456	20608	93.53	27.79
Publication year	27	0.884	8.464	90.61	-4.24	15	0.805	603.6	89.07	-8.36	16	0.683	55437	93.69	-15.45
Sample size	27	0.255	8.014	89.78	1.31	15	0.865	600.2	89.11	-7.75	16	0.484	49753	92.83	-3.62

LVEF, left ventricular ejection fraction; 6MWT, six-minute walk test; BNP, brain natriuretic peptide.

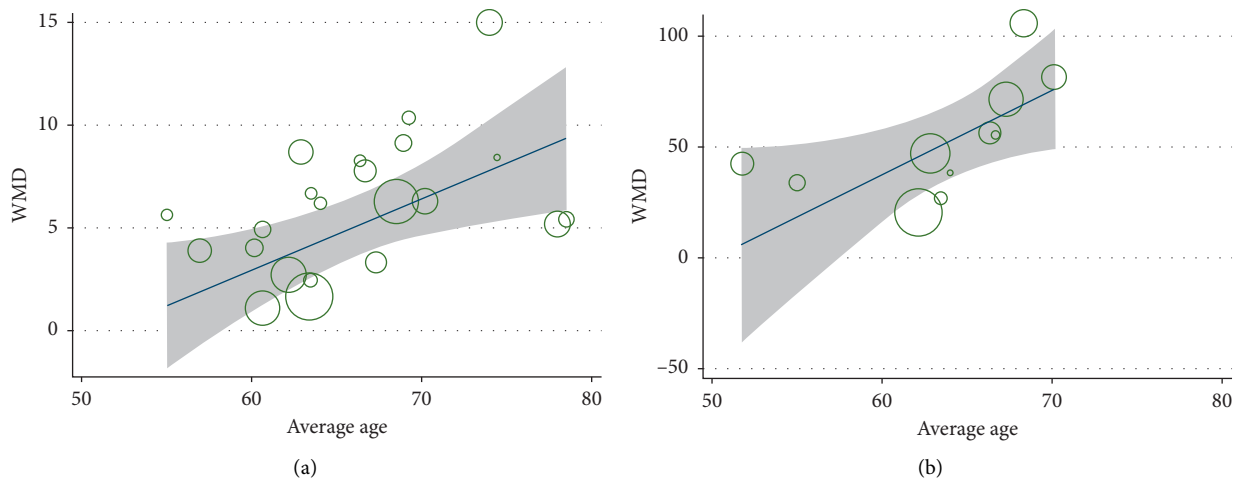


FIGURE 5: Metaregression bubble plot of correlation between WMD of (a) LVEF and (b) 6MWT and average age.

TABLE 6: Incidence rates for adverse events.

Items	No. of studies	No. of adverse events		References
		XML	Control	
Cutaneous pruritus	2	3	0	Xue et al. 2019 [14], Teng and Wang 2017 [36]
Palpitation	2	1	4	Han and Liu 2018 [25], Du et al. 2016 [21]
Dizziness	2	2	0	Du et al. 2016 [21], Zhao et al. 2010 [46]
Headache	1	0	1	Zhao et al. 2010 [46]
Nausea	1	2	1	Teng and Wang 2017 [36]
Leukocytosis	1	0	2	Xue et al. 2019 [14]
Hypotension	1	1	0	Wang et al. 2012 [37]

related to unclear risk of bias. Besides, current research studies focus on the total effect of XML injection, while paying less attention to comprehensive assessment based on basic data collection of different types of patients, which brought difficulty to follow up subgroup analyses and metaregression analysis. Studies in the future could be designed with an emphasis on confirmation and further exploration of age grouping, as average age had been explored to be a source of heterogeneity.

Concerning data extraction, the included trials used different diagnostic and measurement criteria for HF patients. These different measurement criteria and the use of

different instruments affect study comparisons and hence the meta-analysis. Treatment based on pattern identification is a key characteristic of TCM [57]. Application of Chinese patent medicines without the implementation of TCM pattern identification could be a matter of heterogeneity and subsequently reduce the reliability of meta-analysis results. Subgroup analyses in this review, unfortunately, found no heterogeneity based on pattern identification. Further studies are needed for conducting patient selection in which pattern identification is classified.

The results of Begg's and Egger's tests demonstrated no significant asymmetry and suggested no potential

publication bias in this review [58]. Future clinical studies investigating XML treatment for HF should be designed with appropriate controls and better study designs using large patient cohorts, multicenter and prospective. Heterogeneity within the study should be addressed and include appropriate subgroup classification.

5. Conclusion

This review demonstrated that combinational use of XML and conventional treatment may demonstrate better therapeutic effects on improving cardiac function in patients with HF, and age is a potential factor of higher efficacy. Study limitations included the low quality of the selected trials. Additional large, multicenter, prospective clinical trials are warranted to validate our findings.

Data Availability

The data used to support this systematic review are included within the article.

Conflicts of Interest

The authors declare that there are no conflicts of interest regarding the publication of this paper.

Authors' Contributions

Wang XL, Ruan XF, and Sun YL proposed the meta-analysis and designed the study. Qiang TT, Li YP, and Ruan XF performed publication review. Li YP, Sun YL, and Wang XL performed data extraction and analysis. Sun YL wrote the manuscript.

Acknowledgments

The authors would like to thank the authors of the selected XML clinical trials for performing their work investigating HF treatment strategies. This work was financially supported by the National Natural Science Foundation of China (Nos. 81573647 and 81403352) and the Three-Year Foundation Project of Further Development of Traditional Chinese Medicine in Shanghai (ZY(2018–2020)-CCCX-2003-07).

References

- [1] A. P. Ambrosy, G. C. Fonarow, J. Butler et al., "The global health and economic burden of hospitalizations for heart failure," *Journal of the American College of Cardiology*, vol. 63, no. 12, pp. 1123–1133, 2014.
- [2] E. J. Benjamin, S. S. Virani, C. W. Callaway et al., "Heart disease and stroke statistics—2018 update: a report from the American heart association," *Circulation*, vol. 137, no. 12, p. E493, 2018.
- [3] P. A. Heidenreich, N. M. Albert, L. A. Allen et al., "Forecasting the impact of heart failure in the United States," *Circulation: Heart Failure*, vol. 6, no. 3, pp. 606–619, 2013.
- [4] J. Huang, "Epidemiological characteristics and prevention strategies of heart failure in China," *Chinese Journal of Heart and Heart Rhythm*, vol. 3, no. 2, pp. 81–82, 2015.
- [5] G. Maheedhar, K. Muhammad, and J. Orvar, "Heart failure," *South Dakota Medicine the Journal of the South Dakota State Medical Association*, vol. 68, no. 9, pp. 403–409, 2015.
- [6] U. Bushra, B. Rabia, K. B. Ali, Z. Sarwat, and F. Fehmida, "Potential uses of venom proteins in treatment of HIV," *Protein and Peptide Letters*, vol. 25, no. 7, pp. 619–625, 2018.
- [7] S. Bhattacharjya, I.-W. Kim, J. H. Lee et al., "De novo transcriptome analysis and detection of antimicrobial peptides of the American cockroach *Periplaneta americana* (linnaeus)," *PLoS ONE*, vol. 11, p. 5, 2016.
- [8] C. Zeng, Q. Liao, Y. Hu, Y. Shen, F. Geng, and L. Chen, "The role of *Periplaneta americana* (blattodea: blattidae) in modern versus traditional Chinese medicine," *Journal of Medical Entomology*, vol. 56, no. 6, pp. 1522–1526, 2019.
- [9] H. Wang, Y. Ye, W. Wan et al., "Xinmailong modulates platelet function and inhibits thrombus formation via the platelet alphaIIb beta3-mediated signaling pathway," *Frontiers in Pharmacology*, vol. 10, p. 923, 2019.
- [10] C. X. Jiao, C. G. Zhang, and G. M. Liu, "Gas chromatography–mass spectrometry of the volatile components in the *Periplaneta americana* alcohol extraction of water-soluble ingredients," *Lishizhen Medicine and Materia Medica Research*, vol. 23, no. 1, pp. 2797–2798, 2012.
- [11] C. X. Jiao, C. G. Zhang, G. M. Liu, and S. N. Li, "Establishment of HPLC fingerprint of Xinmailong injection," *Traditional Chinese Patent Medicines*, vol. 33, no. 1, pp. 1648–1652, 2011.
- [12] J. Qi, J. Yu, Y. Tan et al., "Mechanisms of Chinese Medicine Xinmailong's protection against heart failure in pressure-overloaded mice and cultured cardiomyocytes," *Scientific Reports*, vol. 7, no. 1, Article ID 42843, 2017.
- [13] L. Zhang, "Pharmacological effect and clinical effect of Xinmailong injection," *Herald of Medicine*, vol. 20, no. 4, p. 250, 2001.
- [14] J. Xue, Y. Xu, Y. Deng et al., "The efficacy and safety of Xinmailong injection in patients with chronic heart failure: a multicenter randomized double-blind placebo-controlled trial," *The Journal of Alternative and Complementary Medicine*, vol. 25, no. 8, pp. 856–860, 2019.
- [15] L. Shamseer, D. Moher, M. Clarke et al., "Preferred reporting items for systematic review and meta-analysis protocols (PRISMA-P) 2015: elaboration and explanation," *Bmj*, vol. 349, no. jan02 1, p. g7647, 2015.
- [16] S. Upadhaya, S. Madala, R. Baniya, K. Saginala, and J. Khan, "Impact of acetylsalicylic acid on primary prevention of cardiovascular diseases: a meta-analysis of randomized trials," *European Journal of Preventive Cardiology*, vol. 26, no. 7, pp. 746–749, 2019.
- [17] F. Fang, Y. Zhang, J. Tang et al., "Association of corticosteroid treatment with outcomes in adult patients with sepsis," *JAMA Internal Medicine*, vol. 179, no. 2, pp. 213–223, 2019.
- [18] J. Higgins, "Measuring inconsistency in meta-analyses," *Bmj*, vol. 327, no. 7414, pp. 557–560, 2003.
- [19] G. D. S. Egger, M. Schneider, and C. E. Minder, "Bias in meta-analysis detected by a simple, graphical test," *Bmj*, vol. 315, no. 7109, pp. 629–634, 1997.
- [20] C. W. Chen, "Clinical observation of Xinmailong injection in the treatment of chronic congestive heart failure," *Journal of Qiqihar Medical University*, vol. 33, no. 18, pp. 2461–2462, 2012.
- [21] L. Du, Y. Wu, W. Li, F. Hu, G. Y. Ge, and X. N. Sun, "Clinical effect of Xinmailong injection on chronic heart failure and its effect on cardiac function and BNP," *Chinese Journal of Integrative Medicine on Cardio-Cerebrovascular Disease*, vol. 14, no. 22, pp. 2656–2658, 2016.

- [22] S. M. Guo and J. M. Ren, "Effects of different doses of Xinmailong injection on cardiac function and plasma B-type natriuretic peptide in elderly patients with chronic heart failure," *Herald of Medicine*, vol. 35, no. 01, pp. 54–57, 2016.
- [23] W. H. Han, G. Li, S. . i. Wang, X. X. He, and S. J. Yang, "Clinical observation of Xinmailong injection in the treatment of senile chronic heart failure," *Chinese Journal of Cardiovascular Rehabilitation Medicine*, vol. 21, no. 04, pp. 422–424, 2012.
- [24] Y. Han and H. Gu, "Effect and significance of conventional therapy combined with Xinmailong injection on chronic heart failure," *Guide of China Medicine*, vol. 14, no. 20, pp. 10–12, 2016.
- [25] Z. Han and Y. Liu, "Clinical observation of Xinmailong injection in the treatment of 56 cases of senile chronic heart failure with slow arrhythmia," *China Pharmaceuticals*, vol. 27, no. 05, pp. 55–57, 2018.
- [26] B. H. He, "Effect of furosemide and Xinmailong injection on left ventricular ejection fraction and blood lactic acid in patients with heart failure," *Chinese Journal of Cardiovascular Rehabilitation Medicine*, vol. 26, no. 05, pp. 529–533, 2017.
- [27] H. B. Li and D. D. Li, "Clinical observation of Xinmailong injection in the treatment of chronic heart failure," *Hebei Medical Journal*, vol. 37, no. 05, pp. 713–714, 2015.
- [28] Q. B. Li, "Clinical effect of Xinmailong injection on 48 cases of chronic heart failure," *Journal of Gannan Medical University*, vol. 36, no. 03, pp. 419–420, 2016.
- [29] Z. G. Li, G. F. Ma, J. Yang, Q. Q. Zhang, and S. X. Geng, "Effect of Xinmailong injection combined with bisoprolol on hemodynamics and serum hs-CRP, BNP and VEGF in patients with coronary heart disease and heart failure," *Chinese Journal of Integrative Medicine on Cardio-Cerebrovascular Disease*, vol. 16, no. 4, pp. 393–397, 2018.
- [30] H. L. Liu, R. B. Zhang, and H. Y. Wang, "Effect of Xinmailong on cardiac function and exercise tolerance in patients with ischemic cardiomyopathy and heart failure," *The Journal of Medical Theory and Practice*, vol. 31, no. 15, pp. 2209–2211, 2018.
- [31] Q. Liu, "Clinical observation of Xinmailong combined with atorvastatin in the treatment of chronic heart failure," *Acta Medicinæ Sinica*, vol. 31, no. 05, pp. 96–99, 2018.
- [32] Y. H. Liu, X. . l. Gao, X. K. Zhang, M. Xie, Y. N. Liu, and S. Q. Cui, "Effect of torasemide combined with Xinmailong injection on VEGF, BNP, NGAL and ICAM-1 in patients with chronic heart failure," *Shaanxi Medical Journal*, vol. 47, no. 10, pp. 1322–1324, 2018.
- [33] W. Quan and Y. Miao, "Clinical observation of Xinmailong injection in the treatment of chronic heart failure," *Chinese Journal of New Clinical Medicine*, vol. 10, no. 04, pp. 353–356.
- [34] W. Shen, Y. Li, and S. Yang, "Effect of Xinmailong injection on cardiac function and NT-proBNP in patients with coronary heart disease and heart failure," *Chinese Journal of Integrative Medicine on Cardio-Cerebrovascular Disease*, vol. 15, no. 07, pp. 833–835, 2017.
- [35] H. R. Shi, Y. P. Feng, X. Q. Yang, J. W. Song, and X. Lu, "Effect of Xinmailong injection on BNP, hsCRP and VEGF in patients with coronary heart disease and heart failure," *Chinese Journal of Integrative Medicine on Cardio-Cerebrovascular Disease*, vol. 14, no. 02, pp. 168–170, 2017.
- [36] M. Teng and X. Wang, "Clinical observation of Xinmailong injection combined with trimetazidine in the treatment of chronic heart failure of coronary heart disease (qiyang deficiency syndrome)," *China Pharmacy*, vol. 28, no. 26, pp. 3705–3707, 2017.
- [37] L. Y. Wang, M. H. Hu, X. H. Zhang, L. W. Ma, and L. P. Ren, "Clinical observation on the improvement of heart function in patients with chronic heart failure of coronary heart disease," *Chinese Journal of Integrative Medicine on Cardio-Cerebrovascular Disease*, vol. 10, no. 11, p. 1380, 2012.
- [38] Z. Wu, W. Chen, and X. Liu, "Effect of Xinmailong injection on serum BNP, hsCRP and VEGF in patients with coronary heart disease and heart failure," *Chinese Archives of Traditional Chinese Medicine*, vol. 35, no. 09, pp. 2433–2435, 2017.
- [39] T. Wu and H. Yang, "Clinical effect of Xinmailong injection on ischemic cardiomyopathy with heart failure," *Medical Journal of Chinese People's Health*, vol. 27, no. 04, pp. 74–108, 2015.
- [40] Y. Xu and F. Z. Xu, "Clinical effect of Xinmailong injection on chronic heart failure," *Chinese Journal of Integrative Medicine on Cardio-Cerebrovascular Disease*, vol. 14, no. 20, pp. 2413–2414, 2016.
- [41] J. G. Xue, X. L. Wang, Y. Xu et al., "A multicenter randomized controlled study of Xinmailong injection in the treatment of chronic heart failure (Syndrome of deficiency of both qi and Yang and internal obstruction of blood stasis)," *Chinese Journal of Integrated Traditional and Western Medicine*, vol. 35, no. 07, pp. 796–800, 2015.
- [42] J. Yang, G. H. Chen, B. Jiang, and X. Q. Yang, "Clinical observation of Xinmailong injection in 110 elderly patients with chronic heart failure," *China Medical Herald*, vol. 9, no. 14, pp. 93–99, 2012.
- [43] N. Yang, H. Wang, and D. Si, "Clinical observation of Xinmailong injection combined with dopamine in the treatment of chronic heart failure," *Drugs and Clinic*, vol. 32, no. 05, pp. 796–799, 2017.
- [44] G. L. Yuan, Y. Q. Zhao, X. T. Li, and M. Yang, "Clinical observation of Xinmailong injection in the treatment of chronic heart failure," *Hebei Journal of Traditional Chinese Medicine*, vol. 37, no. 10, pp. 1545–1548, 2015.
- [45] C. M. Zhao, X. Z. Wang, Y. H. Guo, X. M. Zhang, and H. J. Li, "Effect of Xinmailong on serum MMP-9 in patients with heart failure," *Chinese Journal of Gerontology*, vol. 17, no. 02, pp. 173–176, 2014.
- [46] Z. Y. Zhao, Z. Qi, X. E. Cui, F. An, and J. Wang, "Clinical study on the treatment of chronic heart failure with Xinmailong injection," *Journal of Logistics University of PAP(Medical Sciences)*, vol. 19, no. 02, pp. 120–122, 2010.
- [47] Y. Jiang, S. Li Bao, Y. P. Tang, M. Zhou, T. T. Li, and J. X. Chu, "Clinical study of Xinmailong injection in the treatment of chronic heart failure in the elderly," *China Pharmaceuticals*, vol. 28, no. 15, pp. 53–55, 2019.
- [48] P. Z. Li, "Effects of Xinmailong injection combined with standard regimen on cardiac function and short-term prognosis in patients with chronic heart failure," *Chinese Journal of Integrative Medicine on Cardio-Cerebrovascular Disease*, vol. 17, no. 17, pp. 2618–2621, 2019.
- [49] H. Y. Liu and Y. H. Zhou, "Effect of Xinmailong injection on chronic heart failure and its influence on NT-proBNP, hs CRP and PCT in serum," *Chinese Journal of Gerontology*, vol. 39, no. 15, pp. 3610–3613, 2019.
- [50] L. Y. Zhang and Z. L. Zhou, "Effects of Xinmailong injection on cardiac function and vascular endothelial function in elderly patients with chronic heart failure," *Journal of Qiqihar Medical University*, vol. 40, no. 06, pp. 703–704, 2019.
- [51] H. Li, Y. Mao, Q. Zhang et al., "Xinmailong mitigated epirubicin-induced cardiotoxicity via inhibiting autophagy," *Journal of Ethnopharmacology*, vol. 192, pp. 459–470, 2016.

- [52] Z. Li, S. Li, L. Hu et al., "Mechanisms underlying action of Xinmailong injection, a traditional Chinese medicine in cardiac function improvement," *African Journal of Traditional, Complementary and Alternative Medicines*, vol. 14, no. 2, pp. 241–252, 2017.
- [53] Z. Q. Liu, H. B. Liu, and B. L. Wang, "Meta analysis of the safety of Xinmailong injection in the treatment of heart failure," *China Pharmacy*, vol. 29, no. 22, pp. 3152–3157, 2018.
- [54] J. Wu, R. Nui, and C. Dong, "Effects of Xinmailong Xiangdan and Shenmai Injection on early kidney damage induced by toxin of grass carp bile," *Zhong Xi Yi Jie He Xue Bao*, vol. 2, no. 1, pp. 33–35, 2004.
- [55] Q. J. Li, Z. G. Wang, Q. Liu, Y. Xie, and H. L. Hu, "Research status of *Periplaneta americana* with analyses and prospects of key issues," *Zhongguo Zhong Yao Za Zhi*, vol. 43, no. 7, pp. 1507–1516, 2018.
- [56] H. Riaz, S. U. Khan, H. Rahman et al., "Effects of high-density lipoprotein targeting treatments on cardiovascular outcomes: a systematic review and meta-analysis," *European Journal of Preventive Cardiology*, vol. 26, no. 5, pp. 533–543, 2019.
- [57] H. Liu, Y. Yan, P. Pang et al., "Angong Niu Huang Pill as adjuvant therapy for treating acute cerebral infarction and intracerebral hemorrhage: a meta-analysis of randomized controlled trials," *Journal of Ethnopharmacology*, vol. 237, pp. 307–313, 2019.
- [58] A. Walther, J. Breidenstein, and R. Miller, "Association of testosterone treatment with alleviation of depressive symptoms in men," *JAMA Psychiatry*, vol. 76, no. 1, pp. 31–40, 2018.

Research Article

Mechanisms Underlying the Cardioprotection of YangXinDingJi Capsule against Myocardial Ischemia in Rats

Miaomiao Liu,¹ Yurun Xue,¹ Yingran Liang,¹ Yucong Xue,¹ Xue Han,^{1,2} Ziliang Li,³
and Li Chu^{1,4} 

¹School of Pharmacy, Hebei University of Chinese Medicine, Shijiazhuang 050200, Hebei, China

²Hebei Higher Education Institute Applied Technology Research Center on TCM Formula Preparation, Shijiazhuang 050091, China

³School of Basic Medicine, Hebei University of Chinese Medicine, Shijiazhuang 050200, Hebei, China

⁴Hebei Key Laboratory of Integrative Medicine on Liver-Kidney Patterns, Shijiazhuang 050200, Hebei, China

Correspondence should be addressed to Li Chu; chuli0614@126.com

Received 30 July 2020; Revised 26 August 2020; Accepted 20 October 2020; Published 17 November 2020

Academic Editor: Hong Chang

Copyright © 2020 Miaomiao Liu et al. This is an open access article distributed under the Creative Commons Attribution License, which permits unrestricted use, distribution, and reproduction in any medium, provided the original work is properly cited.

Background. YangXinDingJi (YXDJ) capsule is one of traditional Chinese medicines (TCMs) derived from Zhigancao decoction, which is usually used for the treatment of cardiovascular disease in China. **Aim of the Study.** Cardiovascular events are one of the leading causes of death worldwide. Myocardial ischemia (MI) severely reduces myocyte longevity and function. The YangXinDingJi (YXDJ) capsule has been used in the treatment of clinical cardiac disease in China. Nevertheless, the underlying cellular mechanisms for the benefits to heart function resulting from the use of this capsule are still unclear. The aim of this study was to evaluate the protective effects of the YXDJ on isoprenaline-induced MI in rats and to clarify its underlying myocardial protective mechanisms based on L-type calcium channels and myocardial contractility. **Materials and Methods.** Rats were randomly divided into five groups with ten rats in each group: (1) control; (2) ISO-induced model; (3) high-dose YXDJ (2.8 g/kg/day intraperitoneally for five days), (4) low-dose YXDJ (1.4 g/kg/day for five days); and (5) verapamil ($n = 10$ in each group). Isoproterenol (ISO) was injected subcutaneously for two consecutive days to induce the rat model of MI. Heart and biochemical parameters were obtained. The patch-clamp technique was used to observe the regulatory effects of YXDJ on the L-type calcium current (I_{Ca-L}) in isolated cardiomyocytes. An IonOptix MyoCam detection system was used to observe the contractility of YXDJ on isolated cardiomyocytes. **Results.** YXDJ caused a significant improvement in pathological heart morphology and alleviated oxidative stress and inflammatory responses. Exposure to YXDJ caused a decrease in blockade of I_{Ca-L} in a concentration-dependent manner. **Conclusions.** The results indicate that YXDJ significantly inhibited inflammatory cytokine expressions, oxidative stress, and L-type Ca^{2+} channels, and decreased contractility in isolated rat cardiomyocytes. These findings may be relevant to the cardioprotective efficacy of YXDJ.

1. Introduction

As a fatal disease, ischemic heart disease (IHD) has become one of the most serious health problems both in developing and developed countries [1, 2]. Prolonged ischemia can lead to reperfusion injury to cardiac myocytes, which may include varying degrees of cell death and myocardial edema [3]. Several factors are known to increase the risk for myocardial ischemia (MI); for example,

beta-adrenergic stimulation is thought to exacerbate ongoing myocardial infarction [4]. Isoprenaline (ISO), a nonselective β -adrenoceptor agonist, is widely used to induce MI in experimental rat models of cardiac disease. In these models, activation of the adrenergic system causes severe stress in the myocardium by inducing an increase in the L-type Ca^{2+} channel (LTCC) activity [5].

In the occurrence and maintenance of MI, a number of mechanisms are involved that cause an imbalance of

intracellular Ca^{2+} . LTCCs are the main routes for calcium entry into cardiac myocytes, which is responsible for initiating contraction in the heart [6, 7]. LTCCs (also known as voltage-gated calcium channels, $\text{Ca}_v1.2$ channels, and dihydropyridine receptors) can respond to small changes in membrane potential [8]. This allows LTCC to create a “calcium window” that provides a small, sustained influx of Ca^{2+} into the cell that can activate the contractile mechanism [9]. Membrane depolarization via the action potential leads to the opening of L-type channels, which leads to heart contractions during systole [10]. Plasma membrane influx of Ca^{2+} by LTCCs leads to Ca^{2+} -induced Ca^{2+} release, which in turn regulates cardiac contractility. Oxidative stress can cause some cellular defects such as decreasing of the sarcolemmal Ca^{2+} ATPase pump and Na^+ - K^+ ATPase activities. These alterations lead to a decrease in the Ca^{2+} effluxes and an increase in the Ca^{2+} influxes, respectively [11].

Studies on the association of Ca^{2+} increase with an increase in oxidative stress have been contradictory, and the sequence of events remains controversial. The increase in cytosolic Ca^{2+} concentration is induced by reactive oxygen species (ROS) [12]. An increase in Ca^{2+} is a constant feature of pathological states associated with oxidative stress [13]. It has been found that myocardial ischemia is related to inflammatory response and oxidative stress [14, 15]. Oxidative stress is an imbalance between ROS and antioxidants and is actually the imbalance between the generations of ROS and body antioxidant defense systems that associated with many noncommunicable diseases, such as cancer, heart disease, and diabetes [16]. Excessive ROS causes oxidative damage to important cellular components such as DNA, protein, and lipid membranes. In MI, hypoxia and reoxygenation occur, which may induce the excessive production of ROS in cardiac tissues [17]. Free radicals are typically scavenged by antioxidant enzymes including superoxide dismutase (SOD) and malondialdehyde (MDA), and previous studies have suggested that the antioxidant activities of these enzymes may be reduced in patients following MI or in those with ischemic heart disease [18, 19]. After an MI, inflammatory response occurs, and macrophage infiltration gradually increases. In addition, recent research suggests that MI injury is a result of an increased expression of inflammatory cytokines [20]. Expression and release of inflammatory cytokines such as interleukin (IL)-6, tumor necrosis factor (TNF)- α , and several chemokines contribute to upregulation of cell-adhesion molecules, cardiac functional depression, and apoptosis [21].

Traditional Chinese medicine (TCM) has been widely used in clinical treatment of heart disease in China [22]. Zhigancao decoction is a TCM that originated from “*shang han lun*” written by Zhang Zhongjing in the Eastern Han Dynasty [23]. The therapeutic effects of Zhigancao decoction medicated serum are comparable to routinely used antiarrhythmic medicines. Long-term use in patients has also demonstrated good tolerance to the drug in patients [24]. YangXinDingJi capsule (YXDJ) evolved from the Zhigancao decoction, which is composed of *Radix ophiopogonis*, *Rehmannia*, licorice, ginger, red ginseng, jujube, donkey hide gelatin, black sesame, and cinnamon twig (see Table 1).

This prescription was approved by the China Food and Drug Administration (license no. Z19991082) and is used in the treatment of palpitations caused by heart syndrome. According to previous research, the main constituents in YXDJ capsule, including liquiritin, glycyrrhizic acid, cinnamic acid, and cinnamic aldehyde, were analyzed by the HPLC analysis method using a Diamonsil C18 column and the results showed good linear relationships. The ranges of liquiritin, glycyrrhizic acid, cinnamic acid, and cinnamic aldehyde were 1.00–80.24 $\mu\text{g}/\text{mL}$ ($r = 0.9990$), 2.52–100.70 $\mu\text{g}/\text{mL}$ ($r = 0.9997$), 0.50–40.40 $\mu\text{g}/\text{mL}$ ($r = 1.0000$), and 0.66–52.96 $\mu\text{g}/\text{mL}$ ($r = 1.0000$), respectively [25]. A recent clinical trial confirmed its effectiveness for improving symptoms and reducing angina pectoris and complications along with few adverse effects [26]. However, the precise mechanism underlying the cellular Ca^{2+} homeostasis of YXDJ protects against cardiac remains poorly understood. We hypothesized that YXDJ plays a role in myocardial protection by regulating Ca^{2+} homeostasis, reducing oxidative stress, suppressing inflammatory cytokine expressions, and reducing cytoplasmic myocardial concentration.

In this paper, we evaluated the LTCC current ($I_{\text{Ca-L}}$) changes with respect to relieving oxidative stress of YXDJ in cardiomyocytes. Further study on the cellular mechanisms of YXDJ will not only contribute to a better understanding of the efficacies in clinical treatments but also provide experimental evidence for rational applications.

2. Materials and Methods

2.1. Reagents. YangXinDingJi capsule (batch no. 06720021241, 0.5 g/capsule, approval number: Z19991082) was acquired from Yongfeng Pharmaceutical Co., Ltd. (Shijiazhuang, China). ISO was acquired from Amylet Scientific Inc. (Michigan, USA). Verapamil was acquired from Hefeng Pharmaceutical Co., Ltd. (Shanghai, China). Unless otherwise stated, other chemical reagents were obtained from Sigma-Aldrich (St. Louis, MO, USA). All solvents used were of analytical grade.

2.2. Animals. A total of 100 adult male Sprague-Dawley rats weighing 200 ± 20 g are used in this study. The rats were provided by the Experimental Animal Center of Hebei Province. Thirty-eight rats were used for patch clamp to record Ca^{2+} currents, twelve rats were used to detect cell shortening, and fifty rats were used for experiment in vivo. Male adult SD rats (200 ± 20 g) were exposed to an environment of $22 \pm 2^\circ\text{C}$, and humidity was $55 \pm 5\%$ with a 12 h light-12 h dark cycle and adequate food and water supplies. All studies were performed in conformity with the guidelines for care and standard experimental animals' study ethical protocols and approved by the Ethics Committee for Animal Experiments of Hebei University of Chinese Medicine.

2.3. Induction of Myocardial Ischemia Injury. After acclimatization to laboratory conditions, fifty male SD rats were randomly assigned into five experimental groups ($n = 10$ per group): (1) control group (CON); (2) ISO-induction group

TABLE 1: Description of YangXinDingJi capsule.

Chinese name	Latin name	Family	Scientific name	Plant part	%	Origin (China)
Dihuang	<i>Radix et Rhizoma Rhei</i>	Polygonaceae	<i>Rehmannia glutinosa</i> (Gaertn.) DC.	Rhizome	37	Si Chuang
Dazao	<i>Fructus Jujubae</i>	Rhamnaceae	<i>Ziziphus jujuba</i> Mill.	Fruit	14	Hebei
Maidong	<i>Ophiopogonis Radix</i>	Liliaceae	<i>Ophiopogon japonicus</i> (Thunb.) Ker Gawl.	Root	13	Guang Dong
Zhigancao	<i>Radix Glycyrrhizae Preparata</i>	Leguminosae	<i>Glycyrrhiza glabra</i> L.	Rhizome	9	Gan Su
Heizhima	<i>Sesami Semen Nigrum</i>	Pedaliaceae	<i>Sesamum indicum</i> L.	Seed	7	Hu Bei
Guizhi	<i>Ramulus Cinnamomi</i>	Lauraceae	<i>Cinnamomum cassia</i> (L.) J. Presl	Branch	6	Guang Dong
Shengjiang	<i>Rhizoma Zingiberis Recens</i>	Zingiberaceae	<i>Zingiber officinale</i> Roscoe	Rhizome	6	Hebei
Ejiao	<i>Asini Corii Colla</i>	Equidae	<i>Equus asinus</i> L.	Hide gelatin	4	Shan Dong
Hongshen	<i>Radix Ginseng Rubra</i>	Araliaceae	<i>Panax ginseng</i> CA Mey.	Rhizome	4	Ji Lin

(ISO); (3) verapamil treatment group (VER); (4) high-dose YXDJ (YXDJ_H); and (5) low-dose YXDJ (YXDJ_L). The CON and ISO groups were gavaged with distilled water. YXDJ_H and YXDJ_L groups were gavaged with YXDJ (2.8 and 1.4 g/kg/day, respectively). The VER group was intraperitoneally injected with verapamil (2 mg/kg/day). After seven days of continuous administration, rats were subcutaneously injected with ISO for two consecutive days (85 mg/kg/day, except in the CON group). At the end of the experiment, the rats were anesthetized with sodium pentobarbital (40 mg/kg) and hearts were removed and examined as described below.

2.4. Electrocardiogram. At the end of the experimental period, the anesthetized rats were examined by electrocardiogram (ECG). The needle electrodes were linked to the rat's right arm, front arms, and left leg. ECGs were recorded with needle electrodes and a BL-420S Biological Data Acquisition & Analysis System (Chengdu TEM Technology Co., Ltd., China).

2.5. Myocardium Histopathology. The animal hearts were dissected rapidly and fixed in 4% paraformaldehyde. The heart tissues obtained from rats were embedded in paraffin and sectioned into 4- μ m slices. The heart tissues were processed for sectioning and staining by standard histological methods. The results were observed under a microscope (Leica DM4000B, Solms, Germany).

2.6. Ultrastructural Examination by Transmission Electron Microscopy. Rats were anesthetized, and the hearts were quickly removed. Heart tissues were cut into small pieces (approximately, 1 mm³). These pieces were then rapidly fixed with 2.5% glutaraldehyde in 0.1 mol/L sodium phosphate buffer (pH 7.4) at 4°C for 3 h and then fixed again with 1% osmium tetroxide at 4°C for 1 h. After dehydration with a graded ethanol series, the thin sections were cut with a Leica EM UC6 (Leica Co, Austria) ultramicrotome. A sample was embedded in epon812, and the section was viewed and photographed on a Hitachi 7650 transmission electron microscope (TEM) from (Hitachi, Japan) at 80 kV.

2.7. Serum Preparation for Detection of CK, LDH, SOD, and MDA. Blood was obtained from rats that had been anesthetized at the end of 7 days of treatment. Serum was pipetted and saved at -20°C following centrifugation at 3000 rpm at 4°C for 10–15 min. CK and LDH, SOD activity, and MDA levels were determined by standard commercial kits (Jiancheng, Nanjing, China) according to the manufacturer's instructions.

2.8. Detection of Intracellular ROS. Dihydroethidium (DHE) oxidation is commonly used as a method for monitoring cellular production of ROS. The fluorescence of DHE probe was used to evaluate ROS production in heart tissues. We studied quantitative changes in DHE oxidation products. ROS generation was labeled with the red fluorescence, and visualized and analyzed using a high-content screening system. All experiments were repeated at least three times.

2.9. Inflammation Assay. After centrifugation, serum was collected. IL-6 and TNF- α levels in serum were determined to examine the relationship between the cardioprotective effects of YXDJ and inflammatory cytokine levels. Serum level of IL-6 was calculated from the kit standards and expressed as pg/mL, and TNF- α was expressed as pg/mL.

2.10. Detection of Calcium Concentration in Myocardial Tissues. The Ca²⁺ concentration was determined in heart tissue. Myocardial tissues were placed in a buffered solution (m/V = 1 : 9). The homogenate was centrifuged at 1000 rpm at 4°C for 10 min to remove cell debris, and the supernatant was saved for all downstream biochemical analyses. Ca²⁺ concentrations were evaluated by Coomassie Brilliant Blue staining with a commercial kit (Jiancheng, Nanjing, China).

2.11. Isolation of Cardiomyocytes. Single myocardial cells were obtained via enzymolysis. Rats were intraperitoneally injected with 500 IU/kg heparin and anesthetized with 40 mg/kg sodium pentobarbital. The heart was quickly removed from the rat, placed on a Langendorff instrument for perfusion with an oxygenated free calcium Tyrode's solution, which contained (mM) NaH₂PO₄ 0.33, NaCl 135, KCl

5.4, glucose 10, MgCl₂ 1.0, and HEPES 10 (pH adjusted to 7.4 with 3 M NaOH). After clearance of the blood, the enzyme solution containing 4 g/L taurine, 10 g/L bovine serum albumin (Roche, Basel, Switzerland), and 4 g/L collagenase type II (GIBCO, Invitrogen, Carlsbad, CA, USA) was perfused for 15 to 25 min at 37°C until the heart was soft. After perfusion, the heart was placed into Krebs buffer (KB) and the heart tissue was dissected into small pieces. The cardiomyocytes were preserved in KB solution (bubbled with O₂) at a temperature of 23–25°C for up to 1 to 2 h before the experiment.

2.12. Electrophysiological Techniques. Inward Ca²⁺ currents were recorded from rat myocytes. Whole-cell L-type Ca²⁺ currents were recorded using the conventional patch-clamp technique, as previously described [27]. Pipettes of 4 to 6 MΩ resistance were pulled from borosilicate glass (Kimax 51, KIMBLE Glass Inc.) Microelectrodes had resistances of 4 to 6 MΩ and were lightly fire polished and filled with an intracellular solution containing MgCl₂ 2.0 mM, glucose 10 mM, CaCl₂ 1.8 mM, TEA-Cl 140 mM, HEPES 10 mM, and TTX 10 μM (pH 7.4). Seventy to ninety percent of the series resistance was compensated. Cells were bathed in a potassium-free extracellular solution that contained (in mM) 140 NaCl, 5.4 CsCl, 2.5 CaCl₂, 0.5 MgCl₂, 11 glucose, and 5.5 HEPES (pH 7.4). YXDJ capsule was dissolved in distilled water before, and then dissolved in extracellular solution when patch clamp is used to record Ca²⁺ currents at the following concentration of 100–500 μg/mL. Whole-cell patch-clamp experiments were carried out at room temperature (20–25°C). For all experiments, the holding potential was –80 mV and currents were elicited by a 200-msec depolarizing pulse. Data were analyzed using the pCLAMP (Axon Instruments, Inc.).

2.13. Measurements of Cell Shortening. Ventricular myocytes were placed at the bottom of the glass chamber, and the normal Tyrode's solution flowed at a speed of 1 mL/min. Cell activity could be observed with an inverted microscope and a detection system placed on the glass chamber. Cell shortening at 500 μg/mL of YXDJ was measured to determine the effects of YXDJ on myocardial contractility. Myocytes with clear edges were selected to measure cell shortening before and after MI. The contractions of ventricular myocytes were assessed with an IonOptix MyoCam detection system (IonOptix, Milton, MA, USA).

2.14. Statistical Analysis. The steady-state activation and inactivation curves of I_{Ca-L} were fitted by Boltzmann functions. These conductances were normalized to their individual maximal conductance. All the values are represented as mean ± standard error of the mean (SEM) and were analyzed by one-way analysis of variance (ANOVA). The statistical differences among different groups were analyzed by Student's *t*-test. *P* values of <0.05 were considered significant.

3. Result

3.1. Effects of YXDJ on Electrocardiography. Analysis of electrocardiography patterns was done to determine the actions of YXDJ on ISO-induced MI animals. As shown in Figures 1(a) and 1(b), the obvious reduction in the J-point elevation and heart rate was achieved in the YXDJ groups at both the high and low doses compared to ISO (*P* < 0.05; *P* < 0.01). Compared with CON, the heart rate and J-point of ISO-induced rats were evidently elevated.

Figure 1(c) shows sample ECG tracings from the experimental rats. The ECG of the CON group was normal. In the ISO group, the amplitude of the R wave decreased and the ST interval increased, suggesting that ISO induced a reduction in the amplitude of ECG waves and an increase in frequency. The YXDJ group and VER group showed a recovered R wave amplitude and ST interval.

3.2. Effects of YXDJ on the Pathological Changes of Rat Hearts. The biochemical alterations mentioned above could be correlated with the histological changes in the heart, as shown in Figure 2. According to the hematoxylin and eosin (H&E) staining of the heart tissue, the heart tissue showed the normal histology of the CON group, which was composed of a natural muscle fibril structure. However, H&E staining showed that ISO-induced structural alterations in the myocardium in which cardiomyocytes appeared smaller, cardiac muscle fiber was disorganized, and vestigial infiltrating inflammatory cells were present. The damage in the YXDJ and VER administration groups was lower than that in the ISO group.

3.3. Effects of YXDJ on the Myocardial Mitochondrion Ultrastructure. Mitochondrial ultrastructure was observed by TEM. As shown in Figure 3, the ultrastructure of the cardiac muscle from rats of the CON and VER groups was identical. However, myocardial mitochondria from the ISO group suffered substantial structural damage, including disordered mitochondrial distribution with disarranged and obscure crista and vacuoles within the matrix accompanying by disrupted sarcomere and myofilament. Noticeably, YXDJ pretreated alleviated these deleterious effects of mitochondrial ultrastructure induced by MI injury.

3.4. Effects of YXDJ on Cardiac Marker Enzymes. Cardiac markers in blood are the mainstay for cardiac damage diagnosis. As shown in Figure 4, a significant increase in cardiac markers was noted after ISO induction (*P* < 0.05) compared with the CON group. The serum CK and LDH activities of rats in the VER- and YXDJ-treated groups were significantly lower than those in the ISO group (*P* < 0.05, *P* < 0.01).

3.5. Effects of YXDJ on SOD and MDA in Serum. To investigate the antioxidative effects of YXDJ, the action of YXDJ on ISO-induced SOD activity and MDA levels were detected. The activity of SOD in serum, as shown in Figure 5, ISO

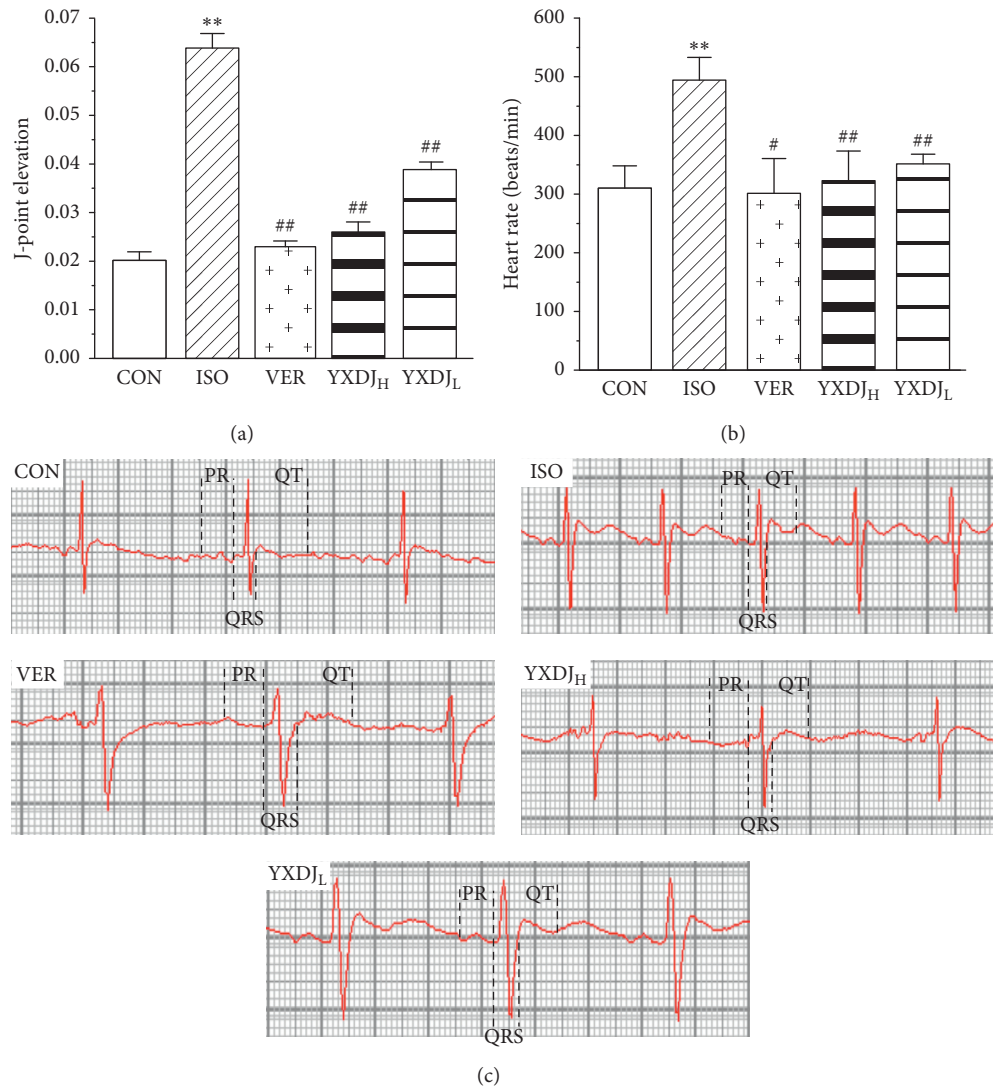


FIGURE 1: Actions of YangXinDingJi (YXDJ) on the electrocardiogram (ECG): (a) statistical analysis of J-point elevation, (b) heart rate, and (c) representative ECG tracings. Values represent the mean \pm SE, for 10 rats in each group. ** $P < 0.05$ versus control (CON); # $P < 0.05$, ## $P < 0.01$ versus isoproterenol (ISO).

group rats was markedly lower than that of the CON rats ($P < 0.05$). However, after treatment with YXDJ (2.8 and 1.4 g/kg/day) and VER, the activity of SOD evidently increased ($P < 0.05$; $P < 0.01$). MDA content was significantly higher in the ISO group than in the CON group ($P < 0.05$). Meanwhile, compared with the ISO-induced rats, the MDA levels significantly reduced after treatment with YXDJ (2.8 and 1.4 g/kg/day) and VER ($P < 0.05$).

3.6. Effects of YXDJ on ROS Release. The effect of YXDJ on the ISO-induced MI was evaluated with fluorescence of a dihydroethidium probe, specifically for assessing myocardial tissue ROS. As shown in Figure 6, VER obviously caused a reduction in the production of ROS. ROS evaluation revealed similar results in animals treated with YXDJ at both high and low doses ($P < 0.05$; $P < 0.01$). The results implied that YXDJ could cause a reduction in ISO-induced oxidative stress.

3.7. Effects of YXDJ on IL-6 and TNF- α . To further evaluate and validate the protective function of YXDJ during MI injury, we measured the levels of IL-6 and TNF- α in serum. The levels of TNF- α and IL-6 were significantly increased after ISO induction. Preprocessing by YXDJ caused a decrease in the expressions of IL-6 and TNF- α as shown in Figures 7(a) and 7(b) ($P < 0.01$). However, serum IL-6 and TNF- α concentrations in VER and high-dose YXDJ groups remained higher than those in the low-dose YXDJL group.

3.8. Effects of YXDJ on Calcium Concentration. As shown in Figure 8, ISO induction of MI resulted in a significant increase in the Ca²⁺ concentration of the heart tissue relative to the CON. However, compared with the ISO group, the YXDJ group and VER group were significantly decreased ($P < 0.05$).

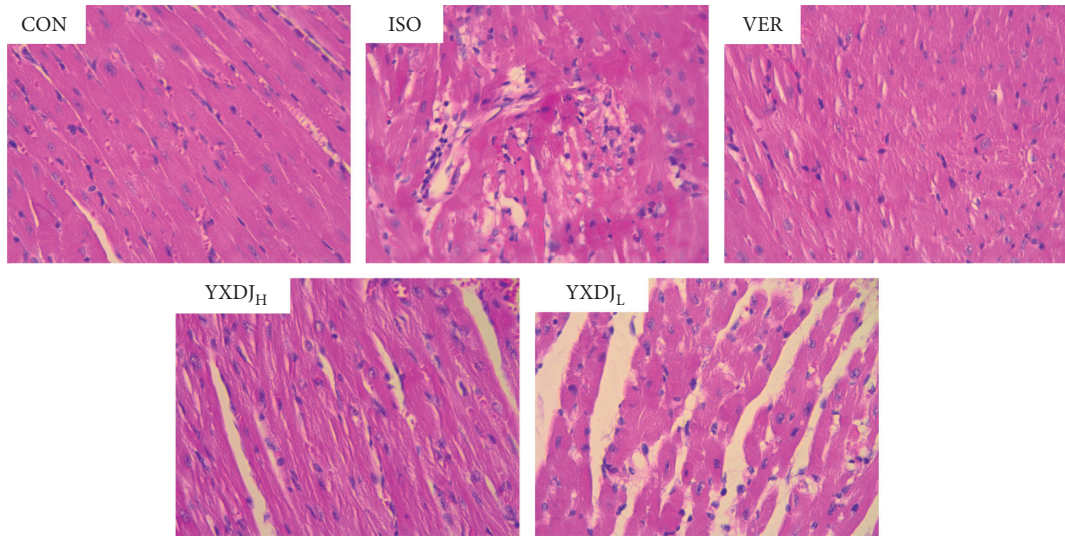


FIGURE 2: Effects of YXDJ on hematoxylin and eosin (H&E) staining. Representative microscopic photographs of hearts stained with H&E (magnification: 400x). The myocardial tissues obtained from the CON, ISO, verapamil (VER), and high- and low-dose YXDJ groups. Scale bar: 50 μ m.

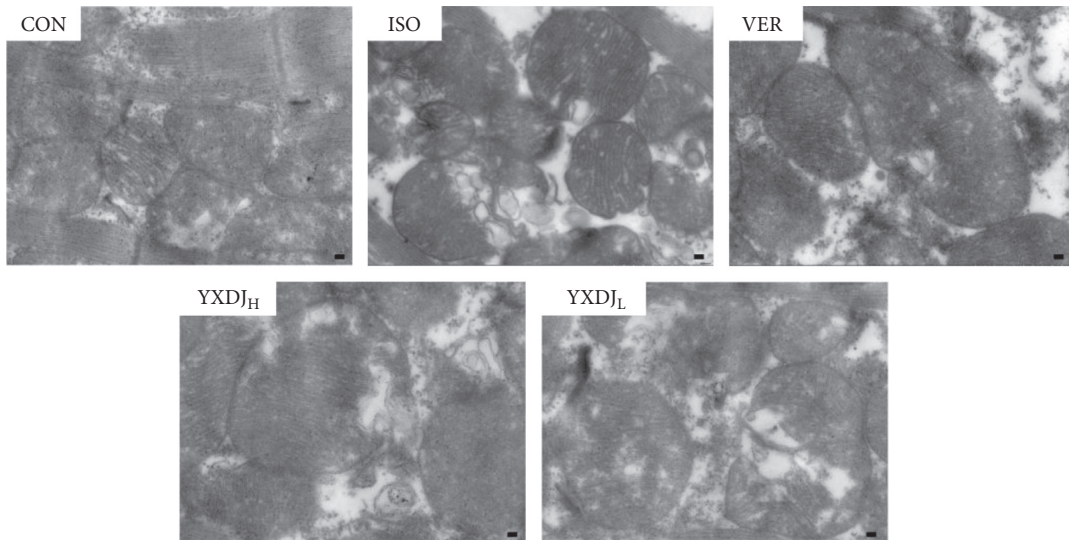


FIGURE 3: Actions of YXDJ on ultrastructural changes. The ultrastructure of cardiac tissues was detected by TEM from the ventricle of the CON, ISO, VER, and high- and low-dose YXDJ groups (magnification: 15000x). Scale bar: 1.0 μ m.

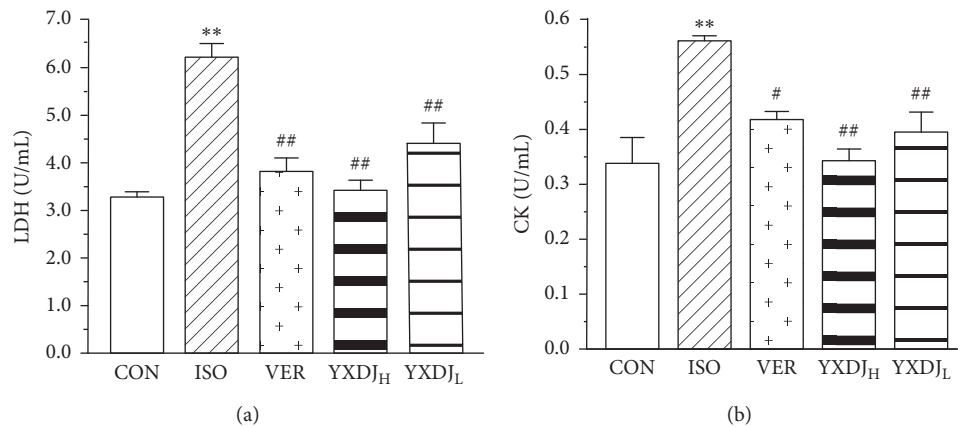


FIGURE 4: Actions of YXDJ on cardiac marker enzymes. Sera were analyzed for (a) lactate dehydrogenase (LDH) and (b) creatine kinase (CK). Values represent the mean \pm SE, for 10 rats in each group. ** $P < 0.05$ versus CON; # $P < 0.05$, ## $P < 0.01$ versus ISO.

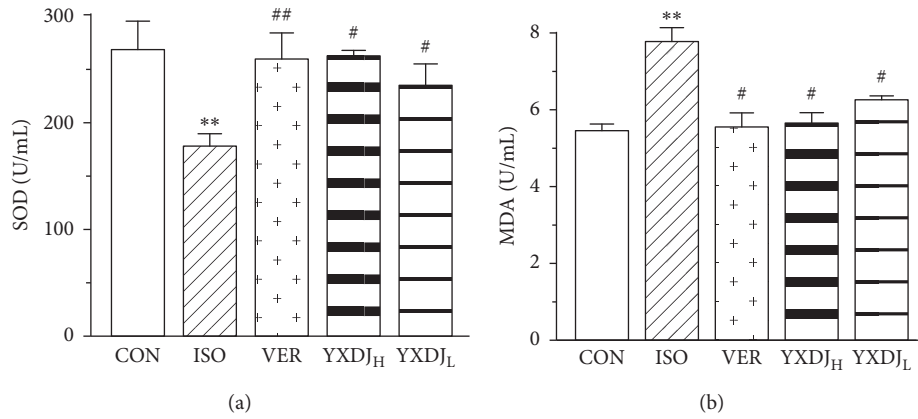


FIGURE 5: Actions of YXDJ on the superoxide dismutase (SOD) activity (a) and malondialdehyde (MDA) levels (b). Values represent the mean \pm SE, for 10 rats in each group. ** $P < 0.05$ versus CON; # $P < 0.05$, ## $P < 0.01$ versus ISO.

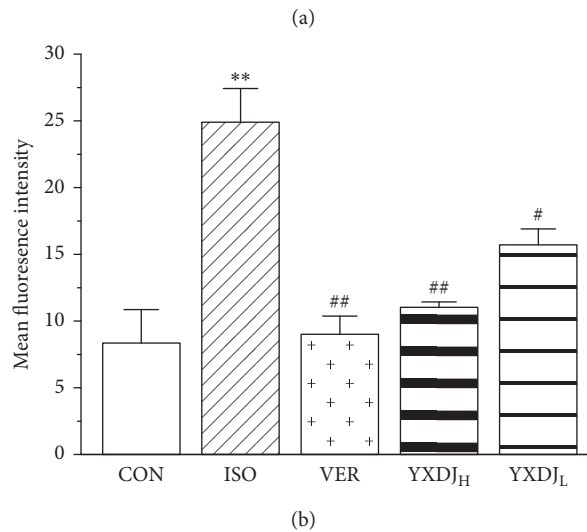
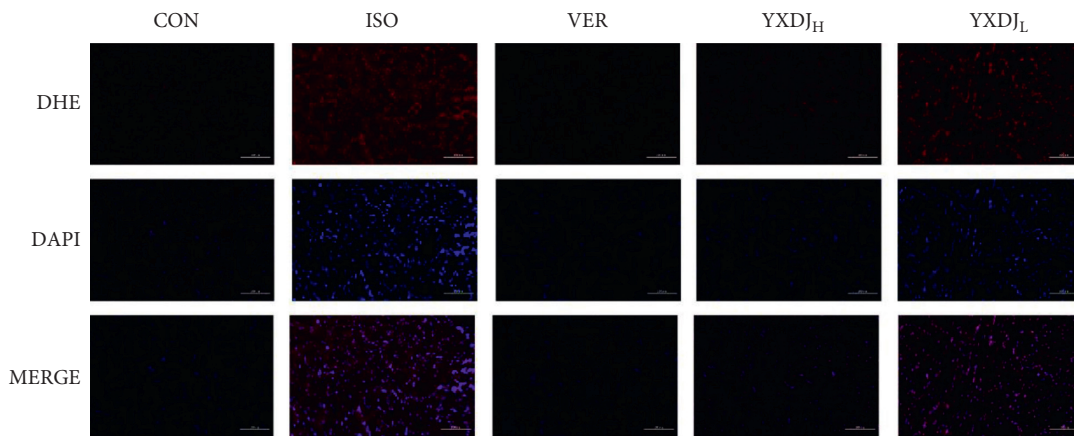


FIGURE 6: Actions of YXDJ on production of reactive oxygen species (ROS). Representative sections from the cardiac of the CON, ISO, VER, and high- and low-dose YXDJ groups. ROS generation was monitored by dihydroethidium staining. Values represent the mean \pm SE. ** $P < 0.05$ versus CON; # $P < 0.05$, ## $P < 0.01$ versus ISO. Scale bar: 100 μ m.

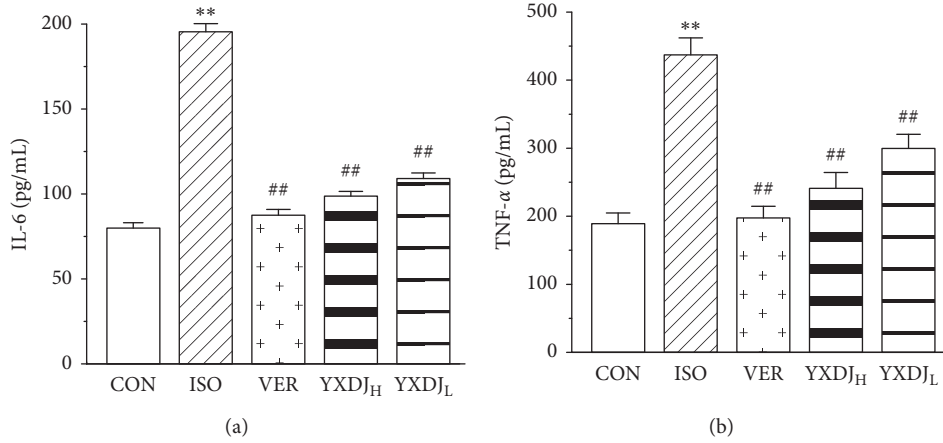


FIGURE 7: Effects of YXDJ on the expression of interleukin (IL)-6 and tumor necrosis factor (TNF)-α in ISO-induced myocardial infarction (MI): (a) the expression of IL-6 in serum; (b) the expression of TNF-α in serum. Values represent the mean ± SE, for 10 rats in each group. ***P* < 0.05 versus CON; #*P* < 0.05, ##*P* < 0.01 versus ISO.

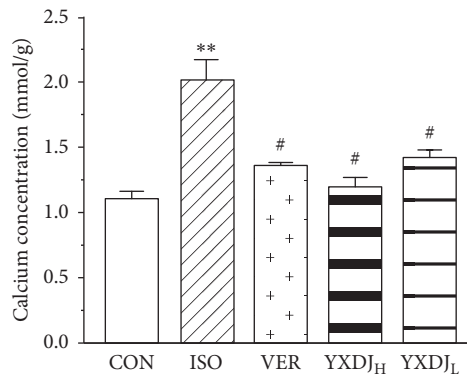


FIGURE 8: Actions of YXDJ on the Ca²⁺ concentrations. Values represent the mean ± SE, for 10 rats in each group. ***P* < 0.05 versus CON; #*P* < 0.05, ##*P* < 0.01 versus ISO.

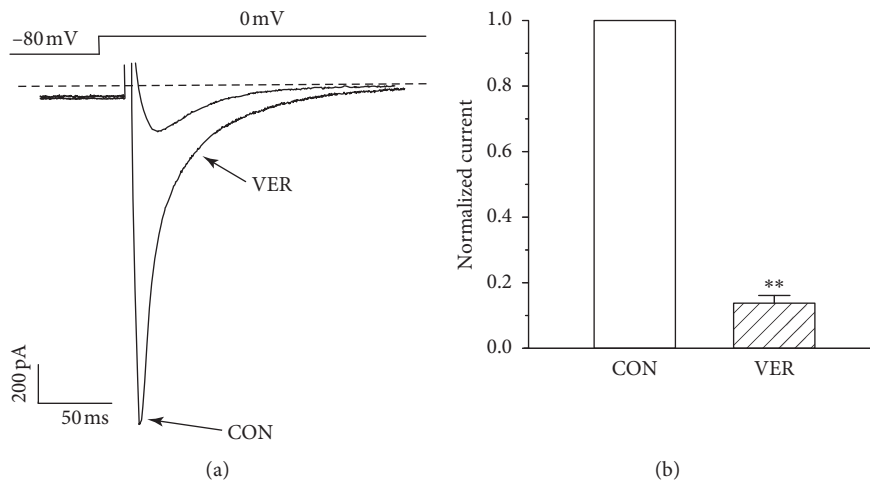


FIGURE 9: Confirmation of I_{Ca-L} in myocardial cells: (a) representative trace of after treatment by VER (0.1 mM); (b) summary data of (a). Values represent the mean ± SE, for 7 cells in each group. ***P* < 0.05 versus CON.

3.9. Reduction of I_{Ca-L} and Cell Shortening by YXDJ

3.9.1. Confirmation of I_{Ca-L} . As shown in Figure 9, VER (0.1 mM), as a specific I_{Ca-L} blocker, caused an almost complete abolishment of the currents, indicating that these currents were Ca^{2+} currents ($P < 0.01$).

3.9.2. Effects of YXDJ on I_{Ca-L} of Normal and Ischemic Myocyte Cell. As Figures 10(a)–10(c) show, I_{Ca-L} decreased after treatment with 500 $\mu\text{g}/\text{mL}$ YXDJ with an inhibition rate of 52.0% in normal ventricular myocytes ($P < 0.05$). However, the I_{Ca-L} was almost impossible to recover after washing out with the external solution. As shown in Figures 10(d)–10(f), after the 500 $\mu\text{g}/\text{mL}$ YXDJ treatment, I_{Ca-L} was significantly reduced, and the inhibition rate was 47.21% in ischemic ventricular myocytes ($P < 0.05$); however, the I_{Ca-L} was almost impossible to recover, after washing out with the external solution.

3.9.3. Dose Dependence of YXDJ on I_{Ca-L} . The time course of the peak I_{Ca-L} was progressively decreased by increasing doses of YXDJ (100, 200, 300, 400, and 500 $\mu\text{g}/\text{mL}$) or VER. As shown in Figure 11, different concentrations of YXDJ were used in the current traces induced by the test potential from -80 to 0 mV. The inhibition rates of YXDJ at 100–500 $\mu\text{g}/\text{mL}$ (in 100 $\mu\text{g}/\text{mL}$ increments) were $7.25\% \pm 0.94\%$, $18.57\% \pm 0.89\%$, $32.25\% \pm 0.47\%$, $44.63\% \pm 1.69\%$, and $48.75\% \pm 1.11\%$, respectively.

3.9.4. Effects of YXDJ on I-V Relationship. As shown in Figure 12, the effects of YXDJ (300 and 500 $\mu\text{g}/\text{mL}$) and 0.1 mM VER on the I-V relationship of the I_{Ca-L} are depicted. The current was generated from -60 to 60 mV. After the application of YXDJ, I-V curves shifted upward, indicating that YXDJ has a concentration-/time-dependent effect on inhibition of I_{Ca-L} . However, the peak potential of I_{Ca-L} and activated potential were markedly unchanged over the measured time period.

3.9.5. Effects of YXDJ on Steady-State Activation and Inactivation of I_{Ca-L} . As shown in Figure 13, different concentrations of YXDJ (300 and 500 $\mu\text{g}/\text{mL}$) affected steady-state activation and inactivation of I_{Ca-L} . YXDJ at 300 and 500 $\mu\text{g}/\text{mL}$ did not change the inactivation and activation of I_{Ca-L} . The $V_{1/2}$ value for activation of 0, 300, and 500 $\mu\text{g}/\text{mL}$ YXDJ was -2.24 ± 0.87 mV/7.30 \pm 0.73, -1.95 ± 0.77 mV/8.01 \pm 0.63, and -1.82 ± 0.98 mV/8.25 \pm 0.79, respectively. The $V_{1/2}$ value for inactivation caused by 0, 300, and 500 $\mu\text{g}/\text{mL}$ YXDJ was -26.10506 ± 0.28256 mV/4.76285 \pm 0.23397, -26.94475 ± 0.41879 mV/4.96567 \pm 0.36614, and -30.21752 ± 0.12523 mV/5.77407 \pm 0.1198, respectively. These data suggest that YXDJ did not alter the activation and inactivation of cardiac Ca^{2+} gating properties ($P > 0.05$). There were no significant differences between values of $V_{1/2}$ in the presence and absence of YXDJ for the normalized inactivation and activation.

3.9.6. Effects of YXDJ on Myocyte Shortening. The representative cell shortening recordings before and after administration of YXDJ are shown in Figure 14. The results indicate that 500 $\mu\text{g}/\text{mL}$ YXDJ caused a significant inhibition of cell shortening by $44.4\% \pm 3.89\%$.

4. Discussion

The goal for this study was to determine whether the YangXinDingJi capsule (YXDJ) was efficacious in protecting against MI by regulating calcium homeostasis. MI causes cardiac tissue damage via reduced levels of nutrients and oxygen due to a temporary decrease or shortage of blood supply. The cardiac muscle disease has partially been reported, and some authors proved an alteration of calcium homeostasis, especially in L-type voltage-gated calcium channel (VGCC) expression and regulation. TCM as therapy for MI has better prospects because of its components and targets [28].

In China, TCM has been considered an alternative and adjuvant approach for preventing cardiovascular disease (CVD) and ischemia injury [29, 30]. While, Zhigancao decoction is a Chinese herbal prescription generally used to treat arrhythmia and palpitation in clinics. YXDJ is a Chinese patent medicine, which was derived from Zhigancao decoction. It is used to treat heart disease in clinics. Although the capsule has been shown to be clinically effective, its protective mechanism on the heart is still unclear. In this paper, we investigated the regulation effect of calcium homeostasis and possible mechanism of YXDJ on ISO-induced MI. However, clinical studies are limited because of the difficulty in obtaining human myocardial samples from myocardial ischemia consumers. In experimental studies, myocardial ischemia models were replicated in animals comparable to what occurs in the human model.

Measurement of cardiac markers in blood is the mainstay for diagnosis of acute myocardial infarction [31]. Therefore, CK and LDH were used as biochemical indicators for detecting changes in ISO-induced MI. As shown in Figure 4, CK and LDH activities decreased after treatment with YXDJ. Meanwhile, as Figure 2 shows, ISO-induced histopathological changes in animal hearts showed that cardiomyocytes appeared smaller, cardiac muscle fibers were disorganized, and vestigial infiltrating inflammatory cells were present. After treatment with YXDJ and VER, histopathological sections show similarly normal structures, slight edema, a small number of inflammatory cardiomyocytes, and clear transverse fringes. The ultrastructure of the myocardium was also changed as shown in Figure 3. Myocardial mitochondria from the ISO group suffered substantial structural damage, and some mitochondria were fused, swollen, or cristae. However, the morphological changes in the YXDJ and VER groups showed significant improvements. In this study, the results of histopathology and cardiac marker enzymes showed that YXDJ caused a significant decreased in ISO-induced myocardial ischemic injury.

Isoprenaline (ISO) is a nonselective β -adrenoceptor agonist, and it is widely accepted that ISO injection can

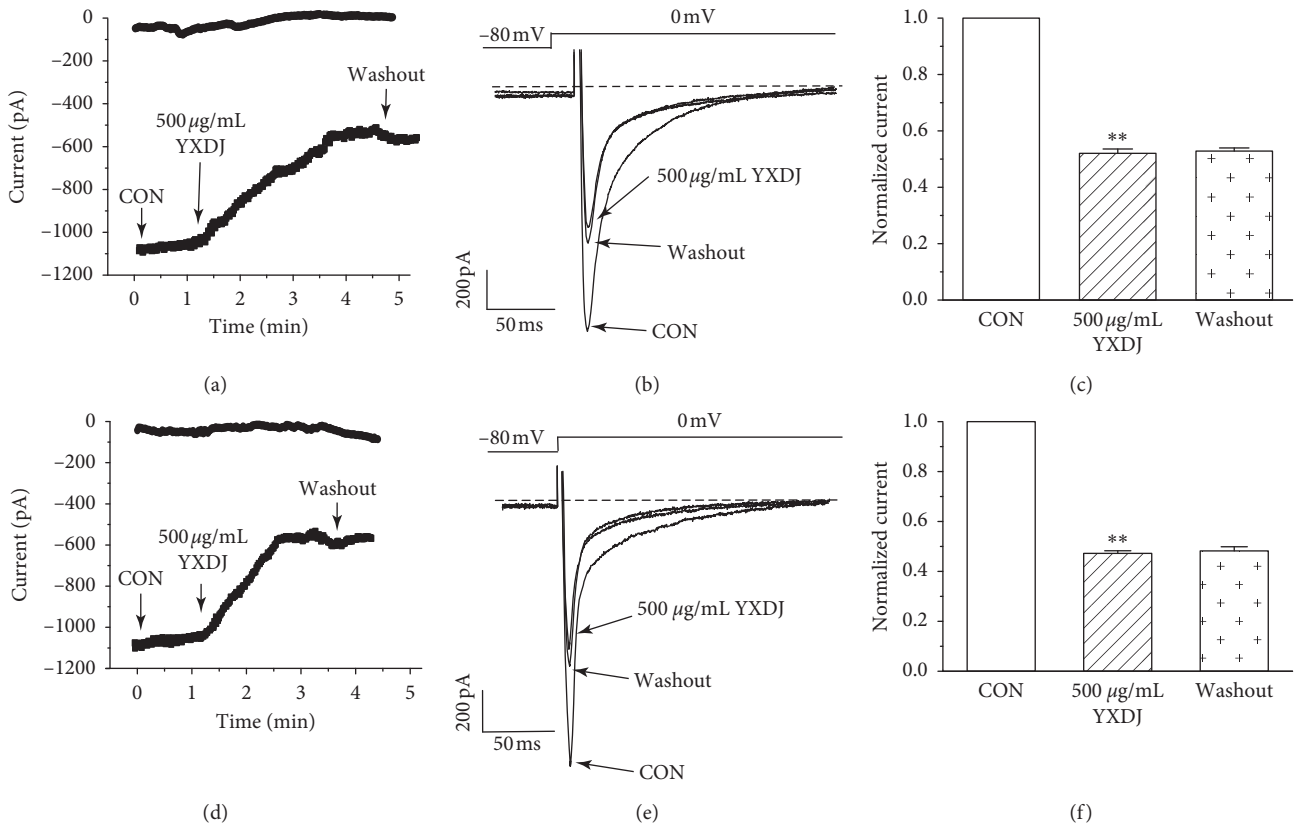


FIGURE 10: Actions of YXDJ capsule on I_{Ca-L} of healthy and ischemic cardiomyocytes. Actions of YXDJ capsule on I_{Ca-L} of healthy myocardial cells (a–c) and ischemic myocardial cells (d–f). YXDJ capsule I_{Ca-L} under control conditions, 500 $\mu\text{g}/\text{mL}$ YXDJ, and washout. Values represent the mean \pm SE for 7 cells in each group. ** $P < 0.05$ versus CON.

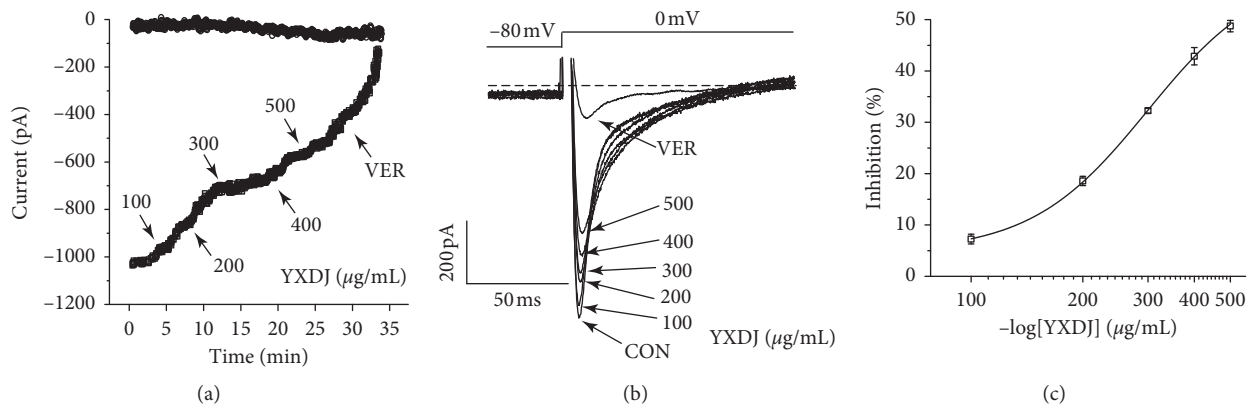


FIGURE 11: Actions of YXDJ capsule at different concentrations on I_{Ca-L} : (a) time course of exposure to 100–500 $\mu\text{g}/\text{mL}$ (in 100 $\mu\text{g}/\text{mL}$ increments) and 0.1 mM VER; (b) example of current traces of I_{Ca-L} recorded during exposure to 100–500 $\mu\text{g}/\text{mL}$ and 0.1 mM VER; (c) concentration-response curve representing the percent inhibitory of YXDJ. Values represent the mean \pm SE, for 7 cells in each group. ** $P < 0.05$ versus CON.

readily induce MI in animals [30, 32]. Stimulated β -adrenergic receptors may induce intracellular Ca^{2+} overload, inflammation, and accumulation of ROS leading to cardiac problems. In addition, the overloading of Ca^{2+} can induce arrhythmias and myocardial ischemia [33, 34]. Thus,

blocking the Ca^{2+} channels and reducing the Ca^{2+} overload will benefit the treatment of arrhythmias and myocardial ischemic. Our study demonstrates that ISO induction caused MI and arrhythmias, which causes changes in ECGs, such as tachycardia and J-point elevation, while treatment with

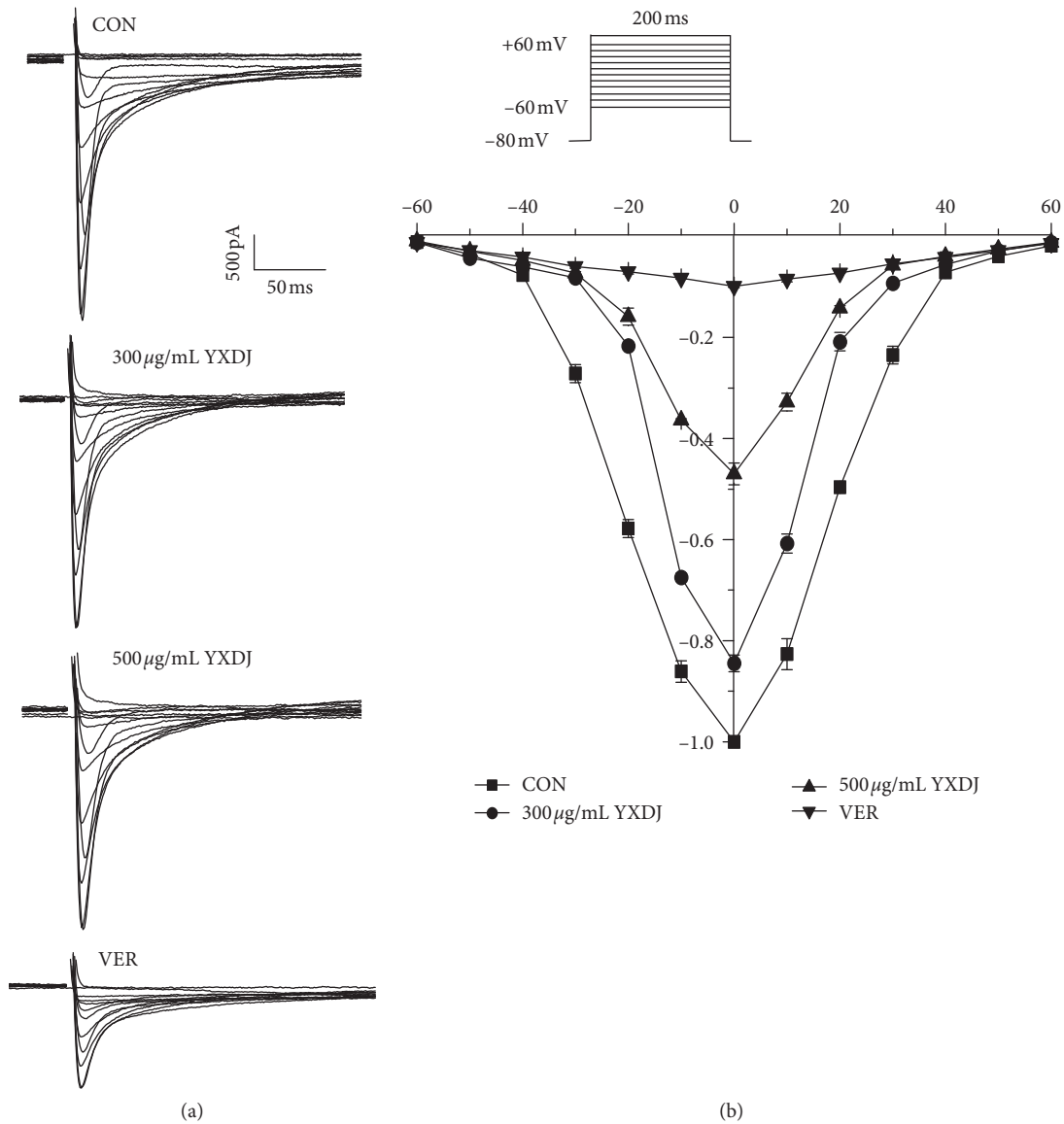


FIGURE 12: Actions of YXDJ capsule on the I-V relationship: (a) representative I_{Ca-L} current recordings and (b) the I-V relationship for I_{Ca-L} under the treatment of Con (\square), YXDJ at 300 $\mu\text{g/mL}$ (\circ), YXDJ at 500 $\mu\text{g/mL}$ (Δ), and VER at 0.1 mM (∇). Values represent the mean \pm SE for 7 cells in each group.

YXDJ could alleviate tachycardia and reduce J-point elevation. Therefore, YXDJ treatment can reduce the incidence of cardiac arrhythmias and MI in rats.

MI induced by ISO is mediated by vasospasticity, combined with increased oxygen demand due to its positive inotropic effect, and is related to the oxidative stress. Antioxidant activity is one of the key mechanisms of anti-MI efficacy. There are many kinds of free radicals, and ROS is closely associated with oxidative stress [35]. At the same time, some data have shown that Ca^{2+} activates the ROS-scavenging enzymes, such as SOD and MDA [36]. As shown in Figures 5 and 6, SOD activities, MDA concentrations, and intracellular ROS were detected. The oxidative stress injury in the ISO-induced group was more serious than other groups. After YXDJ treatment, the production of ROS in cardiomyocytes and MDA concentration were obviously

reduced, and the activity of SOD was obviously increased. These results indicate that YXDJ can alleviate the oxidative stress response by causing improvements in SOD activity and MDA levels. Therefore, the mechanism of YXDJ in alleviating myocardial ischemic might be related to inhibition of oxidative stress-related reactions. The anti-MI properties of YXDJ were then assessed by studying different inflammatory markers. As shown in Figure 7, evaluation of inflammatory markers showed that ISO induced an obvious increase in TNF- α and IL-6 levels. Pretreatment with YXDJ and VER led to a decreased in the TNF- α and IL-6 levels, suggesting that the anti-inflammatory properties were associated with its cardioprotective effects of YXDJ.

Ca^{2+} is thought to play a significant role in controlling the prooxidant-antioxidant balance. An increase of cytosolic Ca^{2+} concentration is due to ROS, and Ca^{2+} increase is a

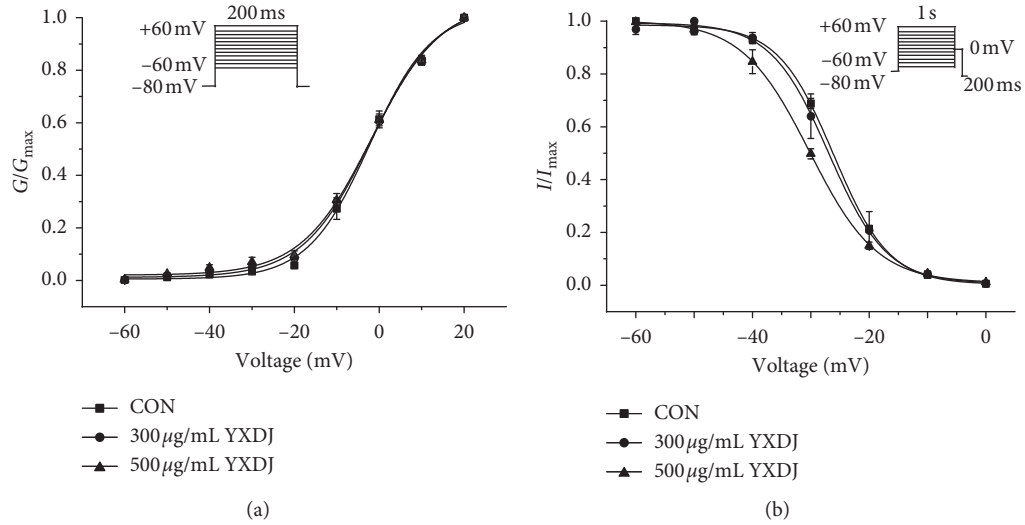


FIGURE 13: Actions of YXDJ capsule on steady-state activation and inactivation of I_{Ca-L} : (a) steady-state activation curves and (b) steady-state inactivation of I_{Ca-L} are shown under the treatment of CON (\square), YXDJ at 300 $\mu\text{g/mL}$ (\circ), and YXDJ at 500 $\mu\text{g/mL}$ (\triangle). Values represent the mean \pm SE for 7 cells in each group.

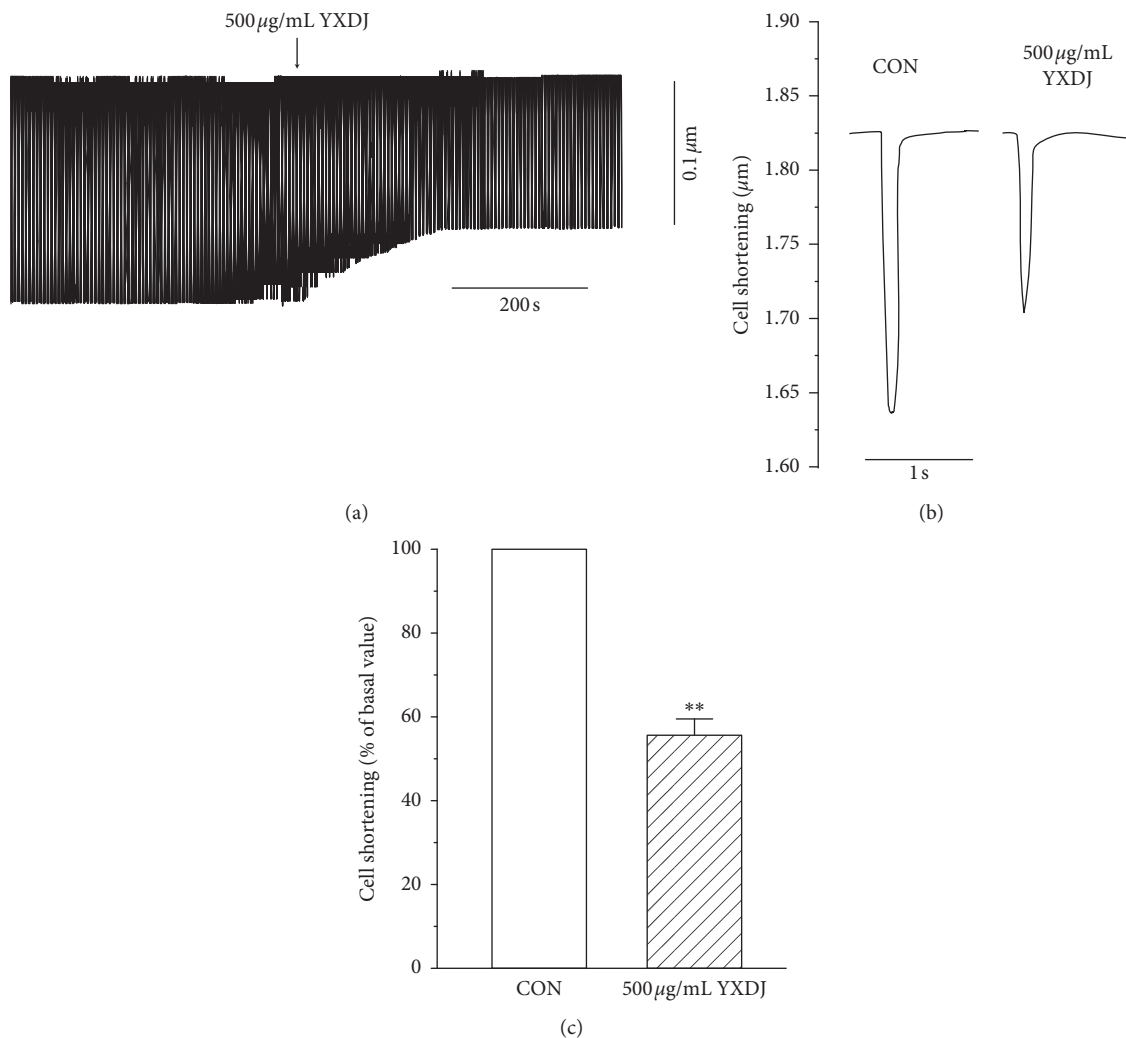


FIGURE 14: Actions of YXDJ capsule on cell shortening: (a) time parameters of cell shortening recordings; (b) exemplary traces of cell shortening under the CON and with 500 $\mu\text{g/mL}$ YXDJ; (c) summary results of (b). Values represent the mean \pm SE for 7 cells in each group. ** $P < 0.05$ versus CON.

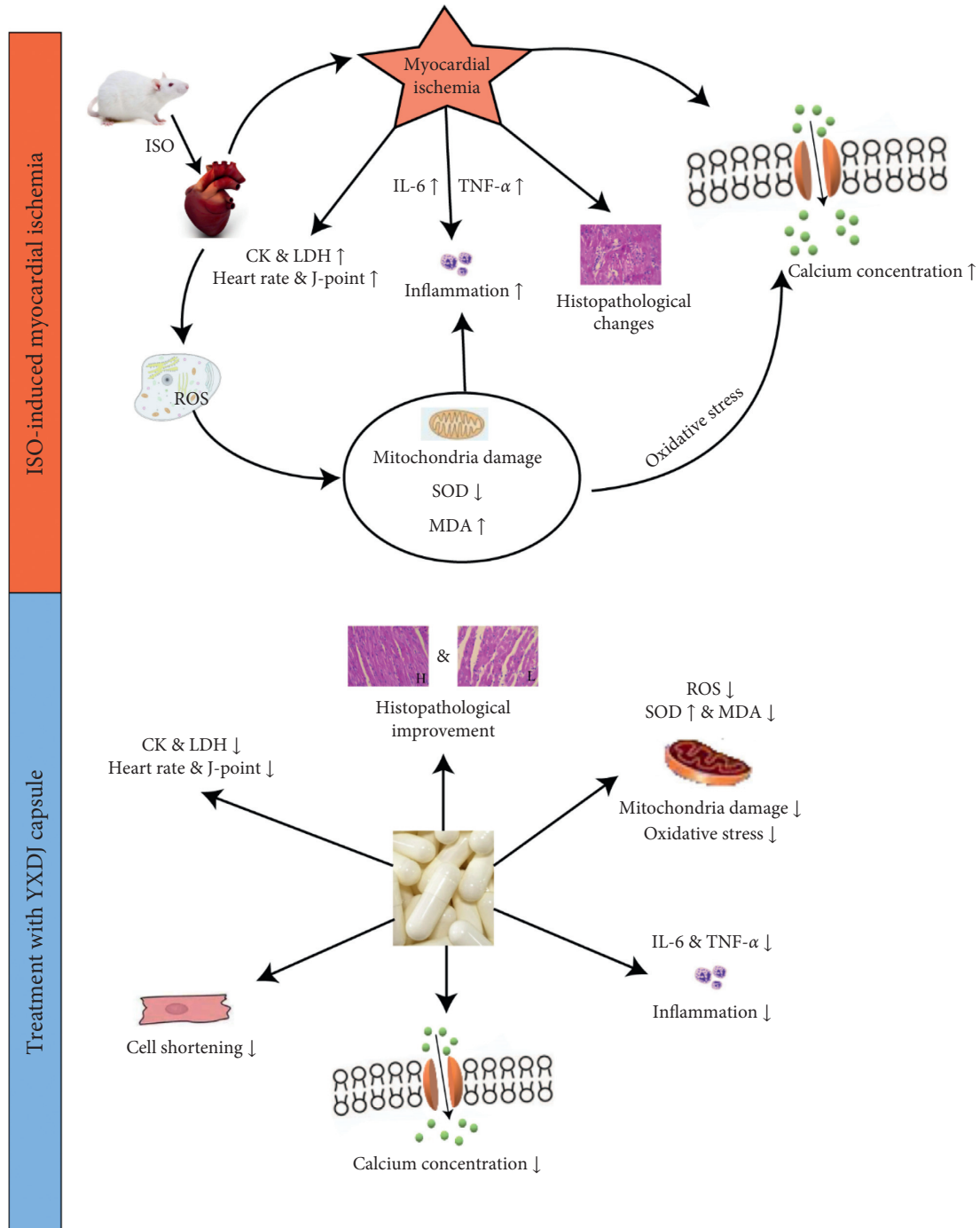


FIGURE 15: Cardioprotective effects of YXDJ capsule on ISO-induced MI.

constant feature of pathological states associated with oxidative stress [37]. We tested the effects of YXDJ on heart tissues and found that it caused a reduction in the calcium concentration. Therefore, the effects of YXDJ on Ca^{2+} channels and intracellular conditions were investigated using the whole-cell patch-clamp technique.

The results show that YXDJ led to a reduction in the I_{Ca-L} . As shown in Figure 11, YXDJ caused a reduction in I_{Ca-L} in a concentration-dependent manner with an IC_{50} of 299.26 $\mu\text{g}/\text{mL}$. Furthermore, I_{Ca-L} was also reduced by YXDJ at 500 $\mu\text{g}/$

mL in both ischemic ventricular and healthy ventricular myocytes. However, the I_{Ca-L} reverse potential and I-V relationship remained unchanged. The heart is an excitable organ, driven by excitation-contraction (EC) coupling that undergoes spontaneous force generation and relaxation cycles. A unique feature of EC coupling is the timely circulation of cytoplasmic calcium under control of a large group of proteins, including Na^+/Ca^{2+} exchanger (NCX), phospholamban-regulated Ca^{2+} -ATPase (SERCA), and ryanodine receptor (RyR) [38]. The process of Ca^{2+} induced Ca^{2+} release

(CICR) is caused by Ca^{2+} inflow that triggers Ca^{2+} release from the sarcoplasmic reticulum (SR). However, CICR provides the necessary signal to initiate mechanical shortening of the cell contraction mechanism and can lead to several-fold increase in cytosolic Ca^{2+} concentration [39]. Nevertheless, the mechanisms for altering calcium homeostasis have still not been clearly established. The function of calcium channel antagonists is to reduce the entering rate of Ca^{2+} and turn off the calcium channel. Calcium antagonists are introduced into the therapeutic armory because of their specific effects on oxygen consumption, myocardial contractility and myocardial blood supply. In this present study, patch-clamp methods were used to examine excitation-contraction (EC) coupling, and we found that YXDJ had a significant inhibitory effect on $I_{\text{Ca-L}}$. It seems that YXDJ could be used as a cardioprotective agent to inhibit $I_{\text{Ca-L}}$ and reduce myocardial contractility. These results suggest that YXDJ caused the $I_{\text{Ca-L}}$ inhibition primarily by reducing the Ca^{2+} current amplitude.

In addition, contractility was inhibited by YXDJ. This result can be explained by the process of myocardial contraction. Contraction is related not only to intracellular Ca^{2+} concentration but also to intracellular proteins that are involved in contraction. We utilized an IonOptix MyoCam detection system to examine the impact of YXDJ on rat ventricular myocytes. In this study, YXDJ significantly reduced the Ca^{2+} contractility, which may be related to the inhibition of $I_{\text{Ca-L}}$. Furthermore, the present study focused on the effect of YXDJ in the of MI rats. To investigate the mechanism through which YXDJ exerts antiarrhythmic effect, it is necessary to study the related ion channels. However, the L-type Ca^{2+} channel is involved in the predominant mechanism responsible for the influx of Ca^{2+} in cardiac cells. We found that YXDJ can inhibit LTCC reducing calcium ions released, thereby reducing free intracellular Ca^{2+} and inhibiting cell shortening. This series of studies reveal that YXDJ can effectively reduce calcium overload and effectively relieve arrhythmias and myocardial ischemia.

Our data suggest that YXDJ could inhibit the increase in Ca^{2+} concentration via a decrease in the extracellular Ca^{2+} influx. Sufficient evidence links YXDJ to cardioprotection via inhibition of $I_{\text{Ca-L}}$ and myocardial contractility.

5. Conclusion

The results demonstrated the cardioprotective effects of YXDJ in ISO-induced MI (see Figure 15). The mechanism may be related to regulating oxidative stress, anti-inflammatory effects, and reduction of calcium inflow via LTCC inhibition. These results provide the basis for further understanding the molecular mechanism of the beneficial effects of YXDJ on IHD.

Abbreviations

CK: Creatine kinase
CVD: Cardiovascular disease
DHE: Dihydroethidium

ECG: Electrocardiogram
H&E: Hematoxylin and eosin
IC₅₀: Concentration required to inhibit transport by 50%
I_{Ca-L}: L-type calcium current
IHD: Ischemic heart disease
IL-6: Interleukin-6
LTCC: L-type Ca^{2+} channel
ISO: Isoproterenol
LDH: Lactate dehydrogenase
MDA: Malondialdehyde
MI: Myocardial ischemia
NCX: $\text{Na}^+/\text{Ca}^{2+}$ exchanger
ROS: Reactive oxygen species
RyR: Ryanodine receptor
SOD: Superoxide dismutase
TNF- α : Tumor necrosis factor- α
TCM: Traditional Chinese medicine
TEM: Transmission electron microscope
YXDJ: YangXinDingJi capsule.

Data Availability

The data used to support the findings of this study are available from the corresponding author upon request.

Ethical Approval

This study was approved by the Ethics Committee for Animal Experiments of Hebei University of Chinese Medicine (approved number: DWLL2020004 and date: Jan. 9, 2020).

Conflicts of Interest

The authors declare that there are no conflicts of interest.

Authors' Contributions

Li Chu, Xue Han, and Ziliang Li designed the research; Miaomiao Liu, Xue Han, and Yurun Xue performed the experiments; Miaomiao Liu, Yingran Liang, Yucong Xue, and Yurun Xue analyzed the data; Miaomiao Liu, Li Chu, and Ziliang Li wrote the manuscript; and Li Chu revised the manuscript.

Acknowledgments

This work was supported by the Research Foundation of Hebei University of Chinese Medicine (KTZ2019043 and YTZ2019003).

References

- [1] H. Thomas, J. Diamond, A. Vieco et al., "Global atlas of cardiovascular disease 2000–2016: the path to prevention and control," *Global Heart*, vol. 13, no. 3, pp. 143–163, 2018.
- [2] K. Chaudhuri, D. Kaye, J. Headrick et al., "Myocardial ischemia-reperfusion injury, antioxidant enzyme systems, and selenium: a review," *Current Medicinal Chemistry*, vol. 14, no. 14, pp. 1539–1549, 2007.

- [3] A. Caliskan, C. Yavuz, O. Karahan et al., "Iloprost reduces myocardial edema in a rat model of myocardial ischemia reperfusion," *Perfusion*, vol. 29, no. 3, pp. 260–264, 2014.
- [4] A. P. Waldenström, Å. C. Hjalmarson, and L. Thornell, "A possible role of noradrenaline in the development of myocardial infarction: an experimental study in the isolated rat heart," *American Heart Journal*, vol. 95, no. 1, pp. 43–51, 1978.
- [5] Z. Nichtova, M. Novotova, E. Kralova, and T. Stankovicova, "Morphological and functional characteristics of models of experimental myocardial injury induced by isoproterenol," *General Physiology and Biophysics*, vol. 31, no. 2, pp. 141–151, 2012.
- [6] H. M. Stankovicova and L. C. Hool, "The L-type Ca^{2+} channel: a mediator of hypertrophic cardiomyopathy," *Channels*, vol. 11, no. 1, pp. 5–7, 2017.
- [7] H. M. Viola, P. G. Arthur, and L. C. Hool, "Evidence for regulation of mitochondrial function by the L-type Ca^{2+} channel in ventricular myocytes," *Journal of Molecular and Cellular Cardiology*, vol. 46, no. 6, pp. 1016–1026, 2009.
- [8] M. F. Navedo, G. C. Amberg, V. S. Votaw, and L. F. Santana, "Constitutively active L-type Ca^{2+} channels," *Proceedings of the National Academy of Sciences of the United States of America*, vol. 102, no. 31, pp. 11112–11117, 2005.
- [9] P. Santana, C. E. Van Hove, J. van Langen et al., "Contribution of transient and sustained calcium influx, and sensitization to depolarization-induced contractions of the intact mouse aorta," *BMC Physiology*, vol. 12, no. 1, p. 9, 2012.
- [10] D. M. Bers, "Ca regulation in cardiac muscle," *Medicine and Science in Sports and Exercise*, vol. 23, no. 10, pp. 1157–1162, 1991.
- [11] A. W. Harman and M. J. Maxwell, "An evaluation of the role of calcium in cell injury," *Annual Review of Pharmacology and Toxicology*, vol. 35, no. 1, pp. 129–144, 1995.
- [12] X. Yang, Y. Chen, Y. Li et al., "Effects of Wenxin Keli on cardiac hypertrophy and arrhythmia via regulation of the calcium/calmodulin dependent kinase II signaling pathway," *Biomed Research International*, vol. 2017, Article ID 1569235, 12 pages, 2017.
- [13] S. Abdoul-Azize, C. Buquet, J.-P. Vannier, and I. Dubus, "Pyr3, a TRPC3 channel blocker, potentiates dexamethasone sensitivity and apoptosis in acute lymphoblastic leukemia cells by disturbing Ca^{2+} signaling, mitochondrial membrane potential changes and reactive oxygen species production," *European Journal of Pharmacology*, vol. 784, pp. 90–98, 2016.
- [14] M. A. Dubus, E. Tseliou, B. Sun et al., "Therapeutic efficacy of cardiosphere-derived cells in a transgenic mouse model of non-ischaemic dilated cardiomyopathy," *European Heart Journal*, vol. 36, no. 12, pp. 751–762, 2015.
- [15] X. Cheng, B. Li, Y. Zhao et al., "Protective effects of antioxidants on chronic intermittent hypoxia-induced cardiac remodeling in mice," *Zhonghua Xin Xue Guan Bing Za Zhi*, vol. 42, no. 11, pp. 944–950, 2014.
- [16] D. P. Jones, "Redefining oxidative stress," *Antioxid Redox Signal*, vol. 8, no. 9–10, pp. 1865–1879, 2006.
- [17] R. Rodrigo, M. Libuy, F. Feliú, and D. Hasson, "Oxidative stress-related biomarkers in essential hypertension and ischemia-reperfusion myocardial damage," *Disease Markers*, vol. 35, no. 6, pp. 773–790, 2013.
- [18] A. Hasson, H. H. Hughie, and P. A. Lucchesi, "Regulation of hypertrophic and apoptotic signaling pathways by reactive oxygen species in cardiac myocytes," *Antioxidants & Redox Signaling*, vol. 5, no. 6, pp. 731–740, 2003.
- [19] H. Katsumi, M. Nishikawa, H. Yasui, F. Yamashita, and M. Hashida, "Prevention of ischemia/reperfusion injury by hepatic targeting of nitric oxide in mice," *Journal of Controlled Release*, vol. 140, no. 1, pp. 12–17, 2009.
- [20] H.-W. Yamashita, H.-J. Liu, H. Cao, Z.-Y. Qiao, and Y.-W. Xu, "Diosgenin protects rats from myocardial inflammatory injury induced by ischemia-reperfusion," *Medical Science Monitor*, vol. 24, pp. 246–253, 2018.
- [21] G. Qiao, O. Dewald, and N. Frangogiannis, "Inflammatory mechanisms in myocardial infarction," *Current Drug Target -Inflammation & Allergy*, vol. 2, no. 3, pp. 242–256, 2003.
- [22] P. Hao, F. Jiang, J. Cheng, L. Ma, Y. Zhang, and Y. Zhao, "Traditional Chinese medicine for cardiovascular disease: evidence and potential mechanisms," *Journal of the American College of Cardiology*, vol. 69, no. 24, pp. 2952–2966, 2017.
- [23] W. Ma, X. Xiong, B. Feng, R. Yuan, F. Chu, and H. Liu, "Classic herbal formula Zhigancao decoction for the treatment of premature ventricular contractions (PVCs): a systematic review of randomized controlled trials," *Complementary Therapies in Medicine*, vol. 23, no. 1, pp. 100–115, 2015.
- [24] J. Yuan, Y. Lu, H. Yan et al., "Application of the myocardial tissue/silicon substrate microelectrode array technology on detecting the effect of Zhigancao decoction medicated serum on cardiac electrophysiology," *International Journal of Clinical and Experimental Medicine*, vol. 8, no. 2, pp. 2017–2023, 2015.
- [25] H.-X. Wang, L.-F. Li, R. An, X.-M. Cheng, C.-H. Wang, and X.-H. Wang, "Simultaneous determination of four constituents in Yangxin Dingji capsules by HPLC," *Chinese Traditional Patent Medicine*, vol. 39, no. 1, pp. 98–101, 2017.
- [26] X. Zhao, "Curative efficacy of Yangxindingji capsule in treatment of coronary heart disease and effects on cardiovascular events," *Chinese Journal of Microcirculation*, vol. 28, no. 3, pp. 31–34, 2018.
- [27] A. E. Belevych, C. Sims, and R. D. Harvey, "ACh-induced rebound stimulation of L-type Ca^{2+} current in guinea-pig ventricular myocytes, mediated by Gbetagamma-dependent activation of adenylyl cyclase," *Journal of Physiology*, vol. 536, no. 3, pp. 677–692, 2001.
- [28] F. Liu, Z.-Z. Huang, Y.-H. Sun et al., "Four main active ingredients derived from a traditional Chinese medicine Guanxin Shutong capsule cause cardioprotection during myocardial ischemia injury calcium overload suppression," *Phytotherapy Research*, vol. 31, no. 3, pp. 507–515, 2017.
- [29] J.-Y. Li, Q. Li, Z.-Z. Ma, and J.-Y. Fan, "Effects and mechanisms of compound Chinese medicine and major ingredients on microcirculatory dysfunction and organ injury induced by ischemia/reperfusion," *Pharmacology & Therapeutics*, vol. 177, pp. 146–173, 2017.
- [30] Y. C. Fan, L. Yan, C. S. Pan et al., "The contribution of different components in QiShenYiQi pills(R) to its potential to modulate energy metabolism in protection of ischemic myocardial injury," *Frontiers in Physiology*, vol. 9, p. 389, 2018.
- [31] A. H. B. Wu, M. Panteghini, F. S. Apple, R. H. Christenson, F. Dati, and J. Mair, "Biochemical markers of cardiac damage: from traditional enzymes to cardiac-specific proteins. IFCC subcommittee on standardization of cardiac markers (S-SCM)," *Scandinavian Journal of Clinical and Laboratory Investigation*, vol. 59, no. sup230, pp. 74–82, 1999.
- [32] O. E. Panteghini, "Cardiac hypertrophy induced by sustained β -adrenoreceptor activation: pathophysiological aspects," *Heart Failure Reviews*, vol. 12, no. 1, pp. 66–86, 2007.
- [33] Y. Xing, Y. Gao, J. Chen et al., "Wenxin-Keli regulates the calcium/calmodulin-dependent protein kinase II signal

- transduction pathway and inhibits cardiac arrhythmia in rats with myocardial infarction,” *Evidence-Based Complementary and Alternative Medicine*, vol. 2013, Article ID 464508, 15 pages, 2013.
- [34] Y. Chen, Y. Li, L. Guo et al., “Effects of Wenxin Keli on the action potential and L-type calcium current in rats with transverse aortic constriction-induced heart failure,” *Evidence-Based Complementary and Alternative Medicine*, vol. 2013, Article ID 572078, 12 pages, 2013.
- [35] H. Inafuku, Y. Kuniyoshi, S. Yamashiro et al., “Determination of oxidative stress and cardiac dysfunction after ischemia/reperfusion injury in isolated rat hearts,” *Annals of Thoracic and Cardiovascular Surgery*, vol. 19, no. 3, pp. 186–194, 2013.
- [36] A. E. D. Arakaki, M. A. Ilian, J. D. Morton, L. Vanhanen, J. R. Sedcole, and R. Bickerstaffe, “Effect of calcium chloride, zinc chloride, and water infusion on metmyoglobin reducing activity and fresh lamb color,” *Journal of Animal Science*, vol. 83, no. 9, pp. 2189–2204, 2005.
- [37] L. Vanhanan, S. Amoroso, A. Pannaccione et al., “Apoptosis induced in neuronal cells by oxidative stress: role played by caspases and intracellular calcium ions,” *Toxicology Letters*, vol. 139, no. 2-3, pp. 125–133, 2003.
- [38] G. Gong, X. Liu, and W. Wang, “Regulation of metabolism in individual mitochondria during excitation-contraction coupling,” *Journal of Molecular and Cellular Cardiology*, vol. 76, pp. 235–246, 2014.
- [39] J. L. Greenstein, R. Hinch, and R. L. Winslow, “Mechanisms of excitation-contraction coupling in an integrative model of the cardiac ventricular myocyte,” *Biophysical Journal*, vol. 90, no. 1, pp. 77–91, 2006.

Research Article

The Efficacy and Safety of Compound Danshen Dripping Pill Combined with Percutaneous Coronary Intervention for Coronary Heart Disease

Cailan Li,¹ Qian Li,^{2,3} Jiamin Xu,⁴ Wenzhen Wu,⁴ Yuling Wu,⁴ Jianhui Xie ^{2,3},
and Xiaobo Yang ^{2,3}

¹Department of Pharmacology, Zunyi Medical University, Zhuhai Campus, Zhuhai 519041, China

²State Key Laboratory of Dampness Syndrome of Chinese Medicine,

The Second Affiliated Hospital of Guangzhou University of Chinese Medicine, Guangzhou 510120, China

³Guangdong Provincial Key Laboratory of Clinical Research on Traditional Chinese Medicine Syndrome, The Second Affiliated Hospital of Guangzhou University of Chinese Medicine, Guangzhou 510120, China

⁴The Second School of Medicine, Guangzhou University of Chinese Medicine, Guangzhou 510120, China

Correspondence should be addressed to Jianhui Xie; xiejianhui888@hotmail.com and Xiaobo Yang; yangxiaobo39358517@hotmail.com

Received 30 July 2020; Revised 9 October 2020; Accepted 21 October 2020; Published 17 November 2020

Academic Editor: Mingjun Zhu

Copyright © 2020 Cailan Li et al. This is an open access article distributed under the Creative Commons Attribution License, which permits unrestricted use, distribution, and reproduction in any medium, provided the original work is properly cited.

Objective. Compound Danshen dripping pill (CDDP) is a well-known Chinese patent medicine, which is commonly used for the treatment of coronary heart disease (CHD) in China. This study is aimed at systematically assessing the clinical efficacy of CDDP for CHD patients. **Methods.** Eight databases were retrieved for eligible research studies from the founding date to April 20, 2020. Risk ratio (RR) was used to assess major adverse cardiac events (MACE) and adverse reactions, and mean difference (MD) was adopted to evaluate the hemorheology and blood lipid indexes, vascular endothelial function, cardiac function, and inflammation. **Result.** Twenty randomized controlled trials involving 2574 participants with CHD were included. The results indicated that, compared with percutaneous coronary intervention (PCI) alone, the combination of CDDP with PCI treatment remarkably reduced MACE (RR = 0.53, 95% confidence interval (CI) (0.44, 0.65), $P < 0.00001$). Moreover, hemorheology and blood lipid parameters and inflammatory mediators of CHD patients were also dramatically mitigated after the combined therapy ($P < 0.01$). In addition, vascular endothelial function and cardiac function were prominently improved by this combination ($P < 0.001$). However, there was no significant difference in adverse reactions between the two groups ($P > 0.05$). **Conclusion.** Evidence from the meta-analysis demonstrated that CDDP combined with PCI treatment prominently reduced the incidence of MACE, improved cardiovascular functions, and inhibited inflammation in CHD patients. Therefore, CDDP combined with PCI treatment could be an effective and safe therapeutic method for CHD patients.

1. Introduction

Coronary heart disease (CHD) is one of the most serious heart diseases that threaten human health [1]. It is characterized by coronary atherosclerosis lesions aroused by myocardial ischemia, hypoxia or necrosis, stenosis, occlusion of the lumen, and inflammation [2]. The World Health

Organization (WHO) divides CHD into five categories: asymptomatic myocardial ischemia, angina pectoris, myocardial infarction, ischemic cardiomyopathy, and sudden death [3]. In recent years, in order to keep up with the continuous updating of the concept of diagnosis and treatment of CHD and facilitate the formulation of treatment strategies, two kinds of syndromes were proposed

clinically, namely, chronic myocardial ischemia syndrome and acute coronary syndrome (ACS) [4, 5]. CHD is one of the major causes of death worldwide, accounting for about one-third of all deaths [6].

The treatment of CHD mainly includes lifestyle change, drug therapy, percutaneous coronary intervention (PCI), and surgical operation [7]. At present, PCI has been the most common method for the treatment of CHD, which can effectively alleviate coronary artery stenosis or occlusion, rebuild coronary artery blood flow, and improve coronary artery blood circulation, with less trauma and obvious clinical effect [8]. However, PCI is an invasive operation, which very easily leads to vascular endothelial injury [9]. After PCI treatment, there was a high incidence of adverse cardiovascular events such as recurrent angina pectoris, coronary restenosis, acute myocardial infarction, malignant arrhythmia, and sudden death, which reduces the therapeutic effect of PCI treatment for CHD patients [10]. Therefore, how to improve the short-term efficacy and long-term prognosis of CHD patients with PCI treatment has become the direction clinical workers should strive for.

According to the basic theory of traditional Chinese medicine, the etiology and pathogenesis of CHD are associated with blood stasis. Therefore, promoting blood circulation and removing blood stasis are an important treatment for CHD. Compound Danshen dripping pill (CDDP) is a famous Chinese patent medicine approved by China Food and Drug Administration (CFDA), which has been widely used in various cardiocerebrovascular diseases [11, 12]. CDDP is prepared from *Salvia miltiorrhiza*, *Panax notoginseng*, and *Borneolum* with modern techniques [13]. The main function of CDDP is promoting blood circulation to remove blood stasis and regulating qi-flowing for relieving pain [14]. In recent years, CDDP is frequently used to treat CHD sufferers combined with PCI [15]. However, most of the clinical researches could not provide sufficient evidence for the small sample sizes, and systematic evidence is lacking and urgently needed to prove the efficacy and safety. Therefore, this meta-analysis was conducted by systematically evaluating the effectiveness of CDDP combined with PCI for CHD compared with PCI therapy alone, in order to provide a scientific basis for this combination treatment.

2. Materials and Methods

2.1. Search Strategy. This meta-analysis was conducted according to the PRISMA statement [16]. Randomized controlled trials (RCTs) were independently searched and retrieved by two investigators (Cailan Li and Qian Li) in the following databases from the founding date to April 20, 2020: PubMed, Embase, the Cochrane Library, Web of Science (WOS), China National Knowledge Infrastructure (CNKI), China Biology Medicine disc (CBMdisc), Wanfang data, and VIP medicine information system (VMIS). In the literature retrieval, the following search terms were used in combination: (“compound Danshen dripping pill” OR “Fufang Danshen diwan”) AND (“coronary heart

disease” OR “CHD” OR “coronary artery disease” OR “CAD”) AND (“percutaneous coronary intervention” OR “PCI”).

2.2. Inclusion Criteria. Based on the suggestions of several specialists, the inclusion criteria were established as follows: (1) participants were diagnosed with CHD by the cardiovascular disease diagnostic criteria determined by the Chinese Medical Society (CMA) or American Heart Association (AHA) in RCTs [17, 18]; (2) all researches mentioned were described as RCTs; (3) CDDP served as the only Chinese patent medicine in RCTs; (4) sufferers in the experimental group were treated with the combined therapy of CDDP and PCI-based treatment, whereas sufferers in the control group only received PCI therapy; (5) outcome measurements of each research included at least one of the following indices: major adverse cardiac events (MACE) including recurrent angina, coronary restenosis, acute myocardial infarction, malignant arrhythmia, cardiac failure, cardiogenic shock and sudden cardiac death, hemorheology indices including whole blood viscosity (WBV), plasma viscosity (PV), hematocrit (HCT), erythrocyte aggregation index (EAI), and fibrinogen (FIB) level, vascular endothelial function indicators involving endothelin (ET), flow mediated dilation (FMD), and nitric oxide (NO), blood lipid parameters including total cholesterol (TC), triglyceride (TG), high density lipoprotein cholesterol (HDL-C), and low density lipoprotein cholesterol (LDL-C), cardiac function indicators including left ventricular ejection fraction (LVEF), left ventricular end diastolic diameter (LVEDD), and cardiac index (CI), inflammatory mediators including high-sensitivity C-reactive protein (Hs-CRP), tumor necrosis factor-alpha (TNF- α), interleukin-6 (IL-6) and interleukin-8 (IL-8), and adverse reactions. Among these indices, MACE is the primary indicator, and the others belong to the secondary indicators.

2.3. Exclusion Criteria. If they demonstrated any one of the following, researches could be ruled out: (1) they were case report, editorials, and irrelevant clinical trials; (2) studies were not RCTs or diagnostic criteria were not clear; (3) the intervention of CHD patients was not conformed; (4) for the researches with data duplication, the late published study was regarded as data fraud and rejected if the authors could not be reached.

2.4. Data Extraction and Quality Evaluation. Information of eligible researches containing author names, publication year, sample size, intervention methods, outcome measurements, etc. was abstracted and is summarized in Table 1. In light of the Cochrane Handbook for Systematic Reviews of Interventions, quality assessment of included studies was independently conducted by two authors (Cailan Li and Jiamin Xu) using the risk of bias table from Review Manager 5.3 [39]. There were seven kinds of biases including random sequence generation (selection bias), allocation concealment

TABLE 1: Characteristics of the included studies.

Study ID	T/C	Intervention	Control	CDDP dosage	Duration	Outcome measures
Wang et al. [19]	15/33	CDDP + control	PCI + conventional treatment	10 pills, t.i.d.	1 month	MACE; CF indexes
Qiu and Zhong [20]	32/30	CDDP + control	PCI + conventional treatment	10 pills, t.i.d.	3 months	CF indexes
Chen, 2008 [21]	30/30	CDDP + control	PCI + conventional treatment	10 pills, t.i.d.	3 months	BL and CF indexes
Xuan et al. [22]	50/50	CDDP + control	PCI + conventional treatment	10 pills, t.i.d.	3 weeks	VEF and CF indexes
Zhao et al. [23]	83/77	CDDP + control	PCI + conventional treatment	10 pills, t.i.d.	3 months	HR indexes
Li et al. [24]	252/248	CDDP + control	PCI + conventional treatment	10 pills, t.i.d.	1 month	MACE; CF indexes
Tian et al. [25]	44/40	CDDP + control	PCI + conventional treatment	10 pills, t.i.d.	3 months	MACE; BL indexes
Xia [26]	15/15	CDDP + control	PCI + conventional treatment	10 pills, t.i.d.	2 months	BL indexes
Tang and Zhang [27]	44/44	CDDP + control	PCI + conventional treatment	10 pills, t.i.d.	6 months	MACE; HR indexes
Yao et al. [28]	30/30	CDDP + control	PCI + conventional treatment	10 pills, t.i.d.	3 months	HR indexes
Li and Wang [29]	42/42	CDDP + control	PCI + conventional treatment	10 pills, t.i.d.	3 months	MACE; HR indexes
Fang et al. [30]	60/60	CDDP + control	PCI + conventional treatment	10 pills, t.i.d.	3 months	CF and inflammation indexes
Zhang [31]	76/84	CDDP + control	PCI + conventional treatment	10 pills, t.i.d.	3 months	MACE; CF indexes
Chen et al. [32]	60/60	CDDP + control	PCI + conventional treatment	10 pills, t.i.d.	1 month	BL and inflammation indexes
Li [33]	40/40	CDDP + control	PCI + conventional treatment	10 pills, t.i.d.	3 months	Inflammation indexes; ARs
Tian et al. [34]	79/79	CDDP + control	PCI + conventional treatment	10 pills, t.i.d.	1 month	MACE; VEF indexes; ARs
Wu and Xu [35]	97/97	CDDP + control	PCI + conventional treatment	10 pills, t.i.d.	1 month	VEF and inflammation indexes
Ji et al. [36]	67/69	CDDP + control	PCI + conventional treatment	10 pills, t.i.d.	1 week	MACE; CF indexes
Su [37]	75/75	CDDP + control	PCI + conventional treatment	10 pills, t.i.d.	2 months	CF indexes
Wang et al. [38]	90/90	CDDP + control	PCI + conventional treatment	10 pills, t.i.d.	2 months	CF and inflammation indexes

T, trial group; C, control group; CDDP, compound Danshen dripping pill; PCI, percutaneous coronary intervention; t.i.d., three times a day; MACE, major adverse cardiac events; HR, hemorheology; VEF, vascular endothelial function; BL, blood lipid; CF, cardiac function; conventional treatment referred to some Western medicines mainly including nitrates, β -blockers, calcium channel blockers, statins, and platelet inhibitors.

(selection bias), blinding of participants and personnel (performance bias), blinding of outcome assessment (detection bias), incomplete outcome data (attrition bias), selective reporting (reporting bias), and other bias. Each term was judged with three grades: low risk of bias, unclear, and high risk of bias. "Low risk of bias" indicates the description of methods or procedures was adequate or correct, while "high risk of bias" represents inadequate or incorrect description. When inadequate information was shown in the study and we could not definitely judge "high risk" or "low risk," the item was judged as "unclear." Discrepancies about data abstraction and research assessment were settled by mutual discussion or consultation to a third reviewer (Jianhui Xie).

2.5. Statistical Analysis. Review Manager 5.3 (Cochrane Collaboration) was used to analyze the abstracted data from the eligible researches [39]. Outcome measures including MACE and adverse reactions were considered as dichotomous variables and presented as the risk ratio (RR) with 95% confidence interval (CI), the indices of hemorheology, vascular endothelial function, blood lipid, cardiac function, and inflammation being continuous variables that presented as the mean difference (MD) with 95% CI. The chi-squared test was employed to check the heterogeneity among researches, and I^2 statistic was used for showing the size of heterogeneity. A fixed-effect model was adopted to analyze data with low heterogeneity ($P \geq 0.1$ and $I^2 \leq 50\%$), and data with high heterogeneity ($P < 0.1$ or $I^2 > 50\%$) was evaluated

by a random-effect model [40]. The risk of publication bias in the included researches was revealed by a funnel plot.

3. Results

3.1. Study Selection. There were one hundred and twenty-five potential records from Chinese databases identified in the first review, and no related record was retrieved in English databases. Sixty-four duplicated records were removed due to the intersection of database coverage. A total of 61 records were obtained for title or abstract examination, and 22 records were dropped by reason of unrelated topics. Thirty-nine records were reserved to check full text. According to the full-text inspection, 19 studies were excluded for the following reasons: 3 researches were not RCTs, diagnosis in 7 studies was not clear, 5 trials mentioned improper interventions, and 4 articles, respectively, showed same data with another article. In final, there were twenty researches [19–38] included in the meta-analysis (Figure 1).

3.2. Study Characteristics and Quality Assessment. Twenty eligible researches including 2574 sufferers were all published in Chinese databases from 2003 to 2019. The experimental group contained 1281 sufferers, and the control group contained 1293 sufferers. The age of all the sufferers ranged from 20 to 80. All the included trials were RCTs with a comparison between the combined therapy of CDDP and PCI treatment and PCI treatment only. In all studies, the dose of CDDP was 10 pills each time, three times a day by oral administration. And most studies reported that the duration of treatment lasted for 3 months or so. Obvious difference was not found between the two groups in basic information (Table 1).

The methodological quality of the eligible studies was assessed by the Cochrane risk of bias evaluation and showed to be universally low. Eleven [19, 21–23, 25, 27–30, 32, 34] of the included trials showed the allocation sequence generation without giving the specific random method, and seven studies [24, 26, 31, 33, 35–37] indicated that they were randomly grouped according to the random number table method. All the included researches did not describe allocation concealment, blinding of participants, and outcome assessment. Nine trials [19, 24, 25, 27, 29, 31, 34–36] were at low risk of attrition bias for providing a complete outcome data. Five researches [21, 27, 29, 33, 34] reporting the result of detailed indices showed a low risk of reporting bias. The risk of bias graph is shown in Figure 2.

3.3. Major Adverse cardiac events. Eight [19, 24, 25, 27, 29, 31, 34, 36] of 20 researches compared the incidence of MACE between CDDP combined with PCI treatment and single PCI treatment. A meta-analysis of the 8 studies adopting a fixed-effect model indicated that the combination therapy of CDDP and PCI treatment markedly reduced the incidence of MACE compared to single PCI treatment in treating CHD (RR = 0.53, 95% CI (0.44, 0.65), $P < 0.00001$). No statistically significant heterogeneity

($P = 0.34$, $I^2 = 9\%$) was found among individual studies (Figure 3).

Furthermore, subgroup analysis was performed based on different cardiac events. There were, respectively, four [25, 27, 31, 34], three [25, 27, 34], three [25, 29, 34], five [19, 24, 25, 31, 36], four [24, 29, 31, 34], two [24, 31], and four [24, 29, 34, 36] trials comparing the incidence of recurrent angina, coronary restenosis, acute myocardial infarction, malignant arrhythmia, cardiac failure, cardiogenic shock, and sudden cardiac death between the experimental and control groups. The results of subgroup analysis showed that CDDP could significantly reduce the incidence of recurrent angina (RR = 0.20, 95% CI (0.09, 0.46), $P = 0.0001$), coronary restenosis (RR = 0.29, 95% CI (0.12, 0.72), $P = 0.008$), malignant arrhythmia (RR = 0.63, 95% CI (0.50, 0.80), $P = 0.0002$), and cardiac failure (RR = 0.45, 95% CI (0.24, 0.83), $P = 0.01$), and there was no difference about the incidence of acute myocardial infarction (RR = 0.42, 95% CI (0.14, 1.23), $P = 0.11$), cardiogenic shock (RR = 1, 95% CI (0.31, 3.26), $P = 0.99$), and sudden cardiac death (RR = 0.83, 95% CI (0.35, 1.94), $P = 0.66$) between the experimental and control groups (Figure 3).

3.4. Hemorheology Indices. WBV, PV, HCT, EAI, and FIB were the indices of blood rheology measured in the eligible researches. There were four trials [23, 27–29] mentioned WBV (high shear). No heterogeneity was found among individual researches ($P = 0.76$, $I^2 = 0\%$), so a fixed-effect model was used to conduct a meta-analysis which showed that CDDP combined with PCI treatment markedly reduced WBV (high shear) (MD = -0.4, 95% CI (-0.51, -0.29), $P < 0.00001$; Figure 4(a)). Three trials [23, 27, 29] compared WBV (middle and low shear) between the experimental and control groups. Significant heterogeneity was, respectively, found among individual researches ($P = 0.001$, $I^2 = 85\%$; $P = 0.005$, $I^2 = 81\%$), and a random-effect model was adopted to carry out the meta-analysis. The pooled results showed that the combination of CDDP and PCI treatment significantly decreased WBV (middle shear) (MD = -0.86, 95% CI (-1.31, -0.41), $P = 0.0002$; Figure 4(b)) and WBV (low shear) (MD = -0.87, 95% CI (-1.46, -0.27), $P = 0.0004$; Figure 4(c)).

There were, respectively, four studies [23, 27–29] that reported PV and two studies [23, 27] that reported HCT and EAI. No heterogeneity was, respectively, found among individual researches ($P = 0.87$, $I^2 = 0\%$; $P = 0.84$, $I^2 = 0\%$; $P = 0.48$, $I^2 = 0\%$), and a fixed-effect model was adopted to carry out the meta-analysis. The pooled results showed that the combination of CDDP and PCI treatment significantly decreased PV (MD = -0.26, 95% CI (-0.3, -0.21), $P < 0.00001$; Figure 4(d)) and EAI (MD = -0.41, 95% CI (-0.55, -0.28), $P < 0.00001$; Figure 4(f)), and there was no difference about HCT between the experimental and control groups (MD = 0.67, 95% CI (-0.98, 2.33), $P = 0.43$; Figure 4(e)).

Three studies [23, 27, 29] reported the level of FIB in blood plasma. Significant heterogeneity was observed among individual researches ($P < 0.0001$, $I^2 = 90\%$) and then a

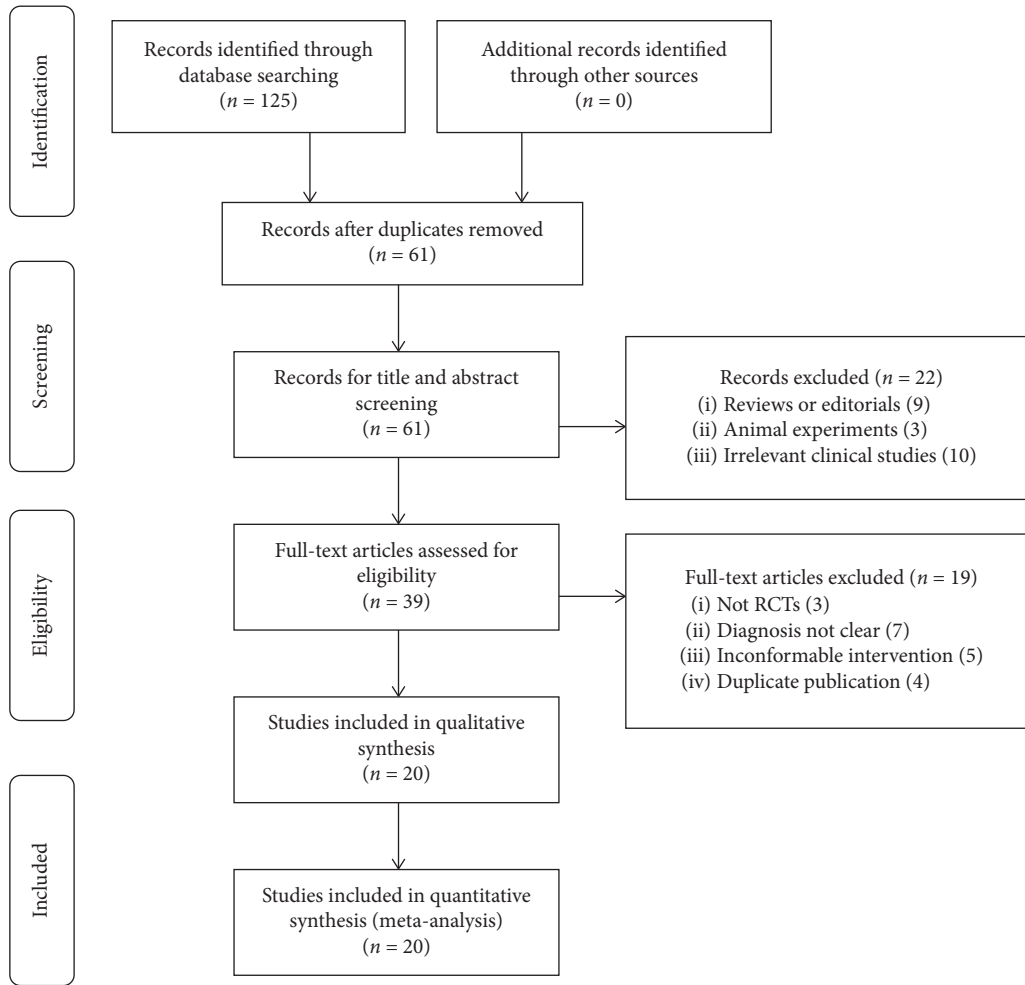


FIGURE 1: Flow diagram of study searching and screening for the meta-analysis.

Author (Year)	Zhao et al., 2010	Zhang, 2017	Yao et al., 2015	Xuan et al., 2008	Xia, 2014	Wu and Xu, 2018	Wang et al., 2019	Wang et al., 2003	Tian et al., 2018	Tian et al., 2011	Tang and Zhang, 2015	Su, 2019	Qiu and Zhong, 2007	Li et al., 2011	Li and Wang, 2016	Li, 2018	Ji et al., 2019	Fang et al., 2017	Chen et al., 2018	Chen, 2008	
Random sequence generation (selection bias)	?	+	?	?	+	+	-	?	?	?	?	+	-	+	?	+	+	?	?	?	?
Allocation concealment (selection bias)	?	?	?	?	?	?	?	?	?	?	?	?	?	?	?	?	?	?	?	?	?
Blinding of participants and personnel (performance bias)	?	?	?	?	?	?	?	?	?	?	?	?	?	?	?	?	?	?	?	?	?
Blinding of outcome assessment (detection bias)	?	?	?	?	?	?	?	?	?	?	?	?	?	?	?	?	?	?	?	?	?
Incomplete outcome data (attrition bias)	?	+	-	?	?	+	?	+	+	+	+	?	-	+	+	?	+	?	?	?	?
Selective reporting (reporting bias)	-	?	?	?	?	?	-	?	+	?	+	?	?	?	+	+	?	?	?	?	+
Other bias	?	?	?	?	?	?	?	?	?	?	?	?	?	?	?	?	?	?	?	?	?

FIGURE 2: Methodological quality assessment for the risk of bias in the included studies.

random-effect meta-analysis was conducted to indicate that there was no difference about FIB between the experimental and control groups (MD = 0.22, 95% CI (-0.75, 1.19), $P = 0.66$; Figure 4(g)).

3.5. *Vascular Endothelial Function Indices.* ET, FMD, and NO were the indices of vascular endothelial function measured in the included studies. There were, respectively, three [22, 34, 35], two [22, 35], and two [22, 34] studies

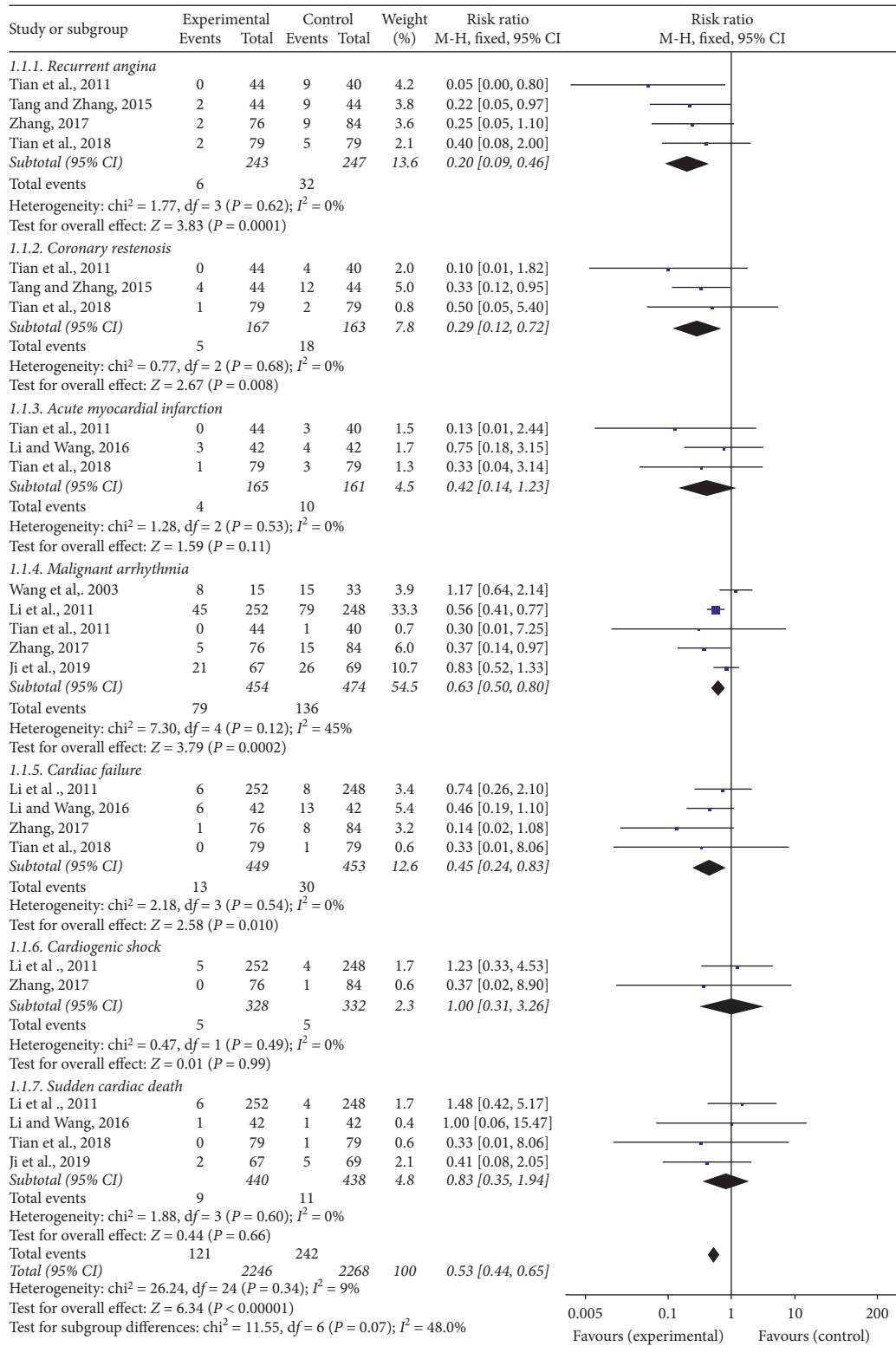
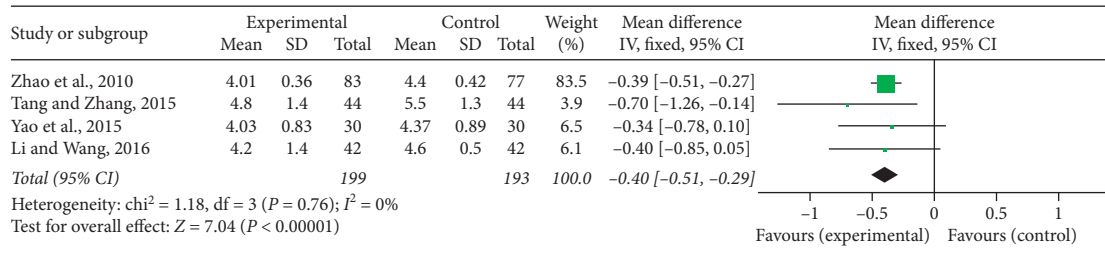


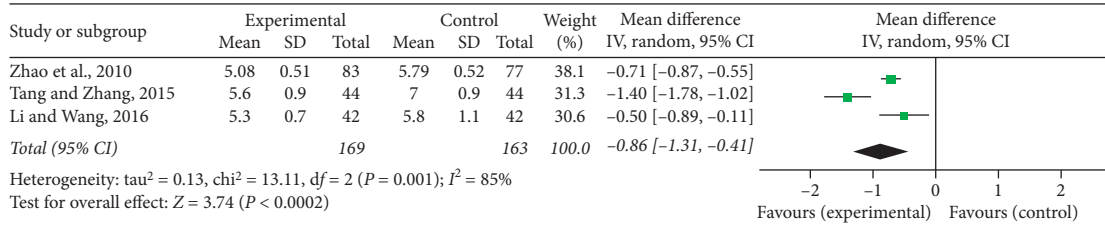
FIGURE 3: Forest plot of major adverse cardiac events of CDDP plus PCI treatment compared to PCI treatment alone for CHD patients. I^2 and P are the criterion for the heterogeneity test, \blacklozenge pooled risk ratio, \blacksquare risk ratio, and 95% CI.

reporting ET, FMD, and NO. Significant heterogeneity was, respectively, found among individual studies ($P < 0.00001$, $I^2 = 99\%$; $P < 0.00001$, $I^2 = 99\%$; $P = 0.001$, $I^2 = 90\%$), and a

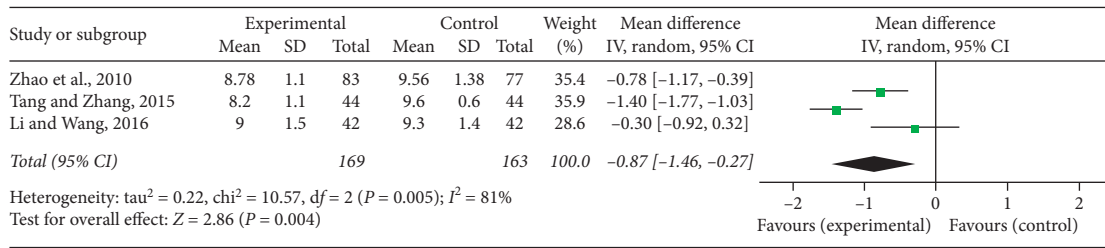
random-effect model was adopted to carry out the meta-analysis. The pooled results showed that the combination of CDDP and PCI treatment significantly decreased ET



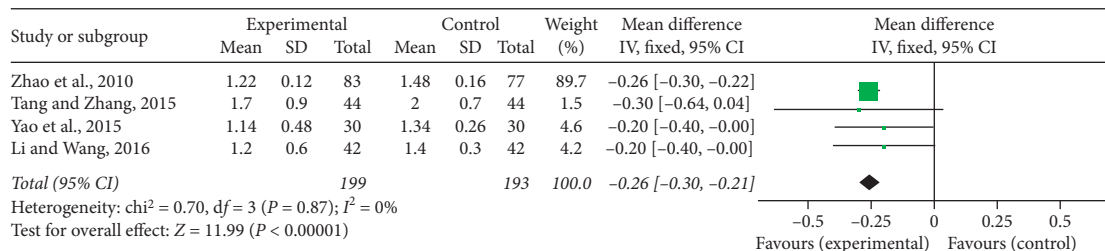
(a)



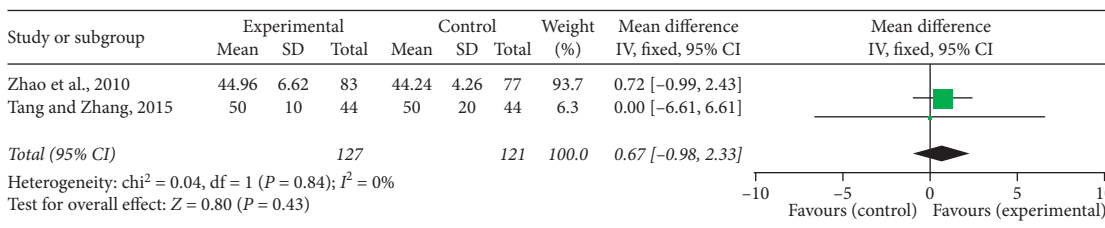
(b)



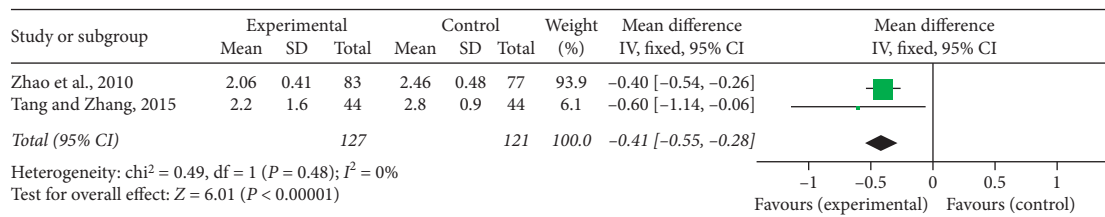
(c)



(d)

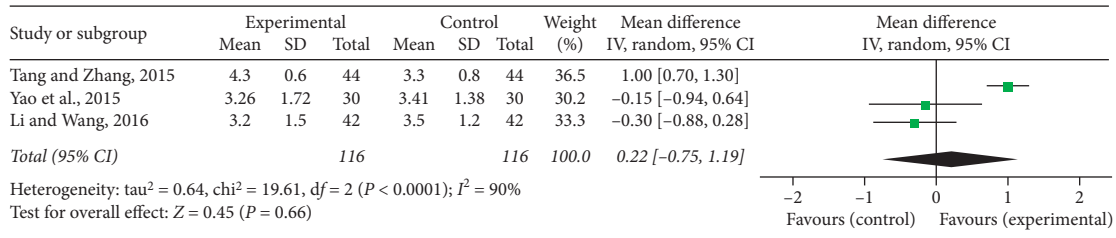


(e)



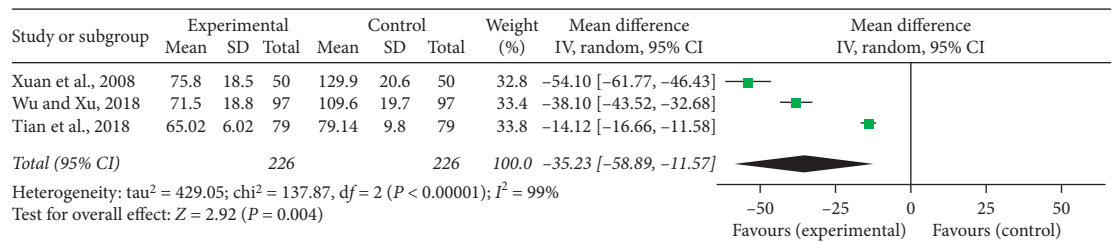
(f)

FIGURE 4: Continued.

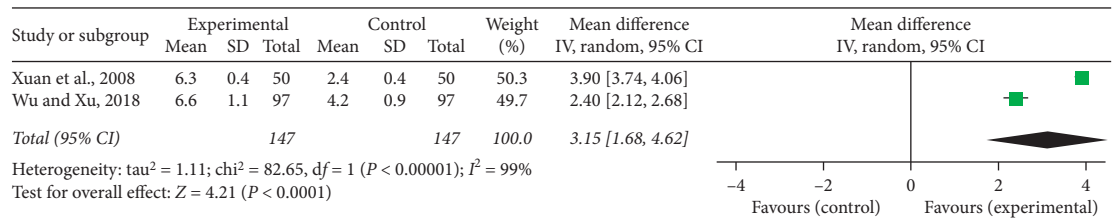


(g)

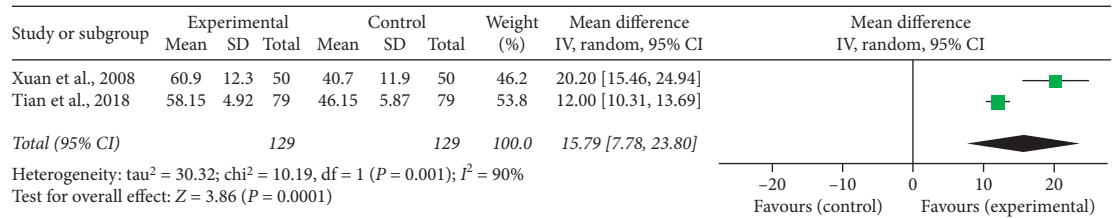
FIGURE 4: Forest plot of comparison in two groups for hemorheology indices. (a)-(c) Whole blood viscosity (high, middle, and low shear); (d) plasma viscosity; (e) hematocrit; (f) erythrocyte aggregation index; (g) fibrinogen level. I² and P are the criterion for the heterogeneity test, ◆ pooled mean difference, -■- mean difference, and 95% CI.



(a)



(b)



(c)

FIGURE 5: Forest plot of comparison in two groups for vascular endothelial function indices. (a) Endothelin; (b) flow mediated dilation; (c) nitric oxide. I² and P are the criterion for the heterogeneity test, ◆ pooled mean difference, -■- mean difference, and 95% CI.

(MD = -35.23, 95% CI (-58.89, -11.57), P = 0.004; Figure 5(a)) and improved FMD (MD = 3.15, 95% CI (1.68, 4.62), P < 0.0001; Figure 5(b)) and NO (MD = 15.79, 95% CI (7.78, 23.8), P = 0.0001; Figure 5(c)).

3.6. Blood Lipid Indices. TC, TG, HDL-C, and LDL-C were the indices of blood lipid measured in the included studies. There were four studies [21, 25, 26, 32] that reported TC, TG, HDL-C, and LDL-C. Significant heterogeneity was, respectively, found among individual researches (P < 0.00001, I² = 88%; P < 0.00001, I² = 95%; P < 0.00001, I² = 87%; P < 0.00001, I² = 88%), and a random-effect model was adopted to carry out the meta-analysis. The pooled results

showed that CDDP combined with PCI treatment significantly decreased TC (MD = -0.32, 95% CI (-0.53, -0.11), P = 0.003; Figure 6(a)) and LDL-C (MD = -0.38, 95% CI (-0.59, -0.18), P = 0.0002; Figure 6(d)), and there was no difference about TG (MD = -0.23, 95% CI (-0.48, 0.02), P = 0.07; Figure 6(b)) and HDL-C (MD = 0.15, 95% CI (-0.03, 0.33), P = 0.11; Figure 6(c)) between the experimental and control groups.

3.7. Cardiac Function Indices. LVEF, LVEDD, and CI were the indices of cardiac function measured in the included studies. There were nine [19-22, 24, 31, 36-38] and five [20, 22, 24, 30, 36] studies which reported LVEF and

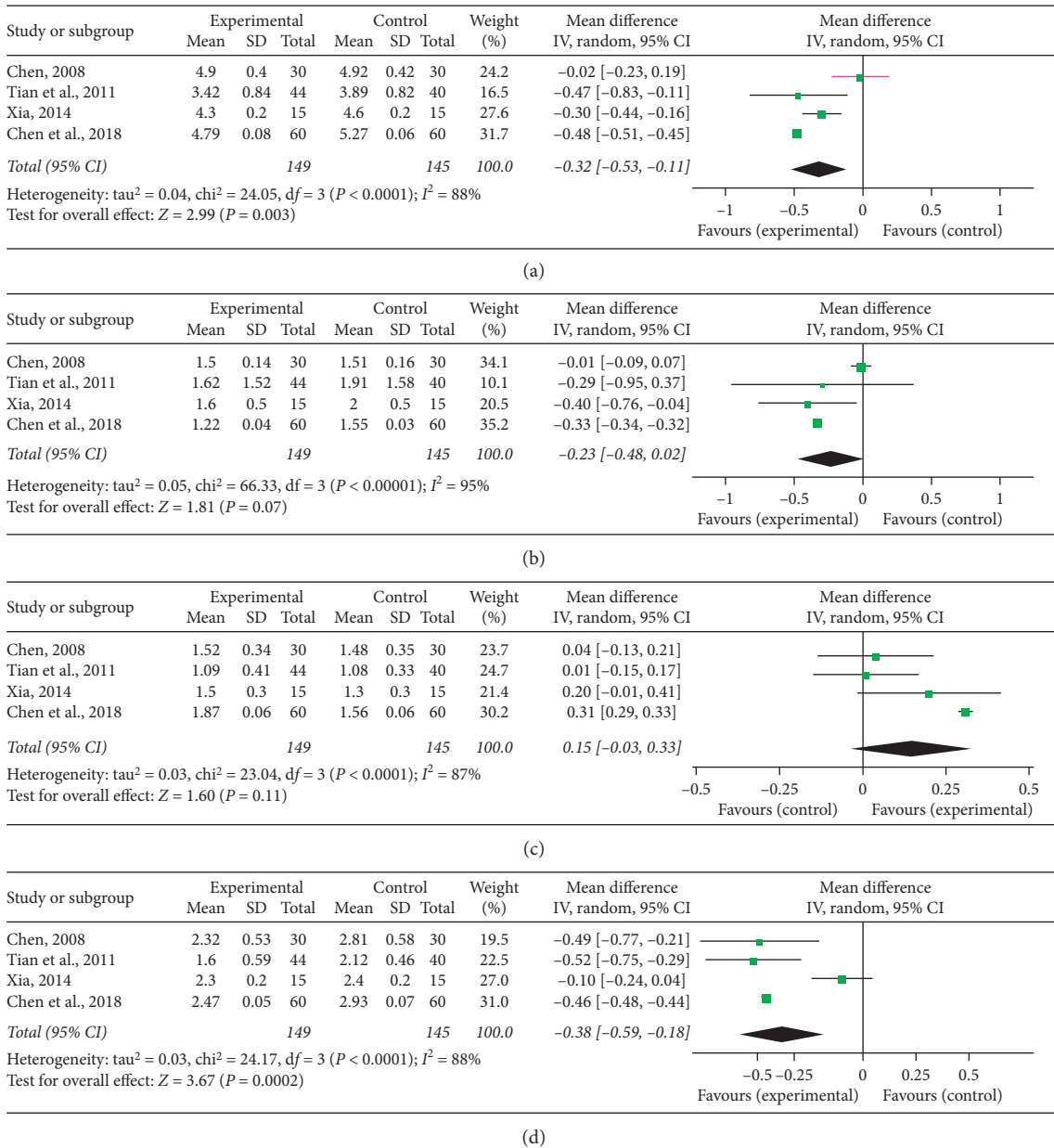


FIGURE 6: Forest plot of comparison in two groups for blood lipid indices. (a) Total cholesterol; (b) triglyceride; (c) high density lipoprotein cholesterol; (d) low density lipoprotein cholesterol. I² and P are the criterion for the heterogeneity test, ◆ pooled mean difference, ■ mean difference, and 95% CI.

LVEDD. Significant heterogeneity was, respectively, found among individual studies (P = 0.02, I² = 57%; P < 0.0001, I² = 85%), and a random-effect model was adopted to carry out the meta-analysis. The pooled results showed that CDDP combined with PCI treatment significantly improved LVEF (MD = 3.46, 95% CI (2.15, 4.77), P < 0.0001; Figure 7(a)) and decreased LVEDD (MD = -2.5, 95% CI (-3.93, -1.08), P = 0.0006; Figure 7(b)). Two studies [20, 38] recorded the detection of CI. There was no heterogeneity (P = 0.86, I² = 0%) and a fixed-effect model was adopted to carry out the meta-analysis. The pooled result showed that the combination therapy of CDDP and PCI treatment significantly improved CI compared to single

PCI treatment (MD = 1.11, 95% CI (0.8, 1.43), P < 0.00001; Figure 7(c)).

3.8. *Inflammatory Mediators Production.* Hs-CRP, TNF- α , IL-6, and IL-8 were the indices of inflammation measured in the included studies. Two studies [21, 33] mentioned the investigation on Hs-CRP. No statistically significant heterogeneity (P = 0.34, I² = 0%) was detected in the meta-analysis and a fixed-effect model was used. An OR with 95% CI was adopted to present the comparison of Hs-CRP between the experimental and control groups (MD = -0.74, 95% CI (-1.05, -0.42), P < 0.00001; Figure 8(a)). It indicated

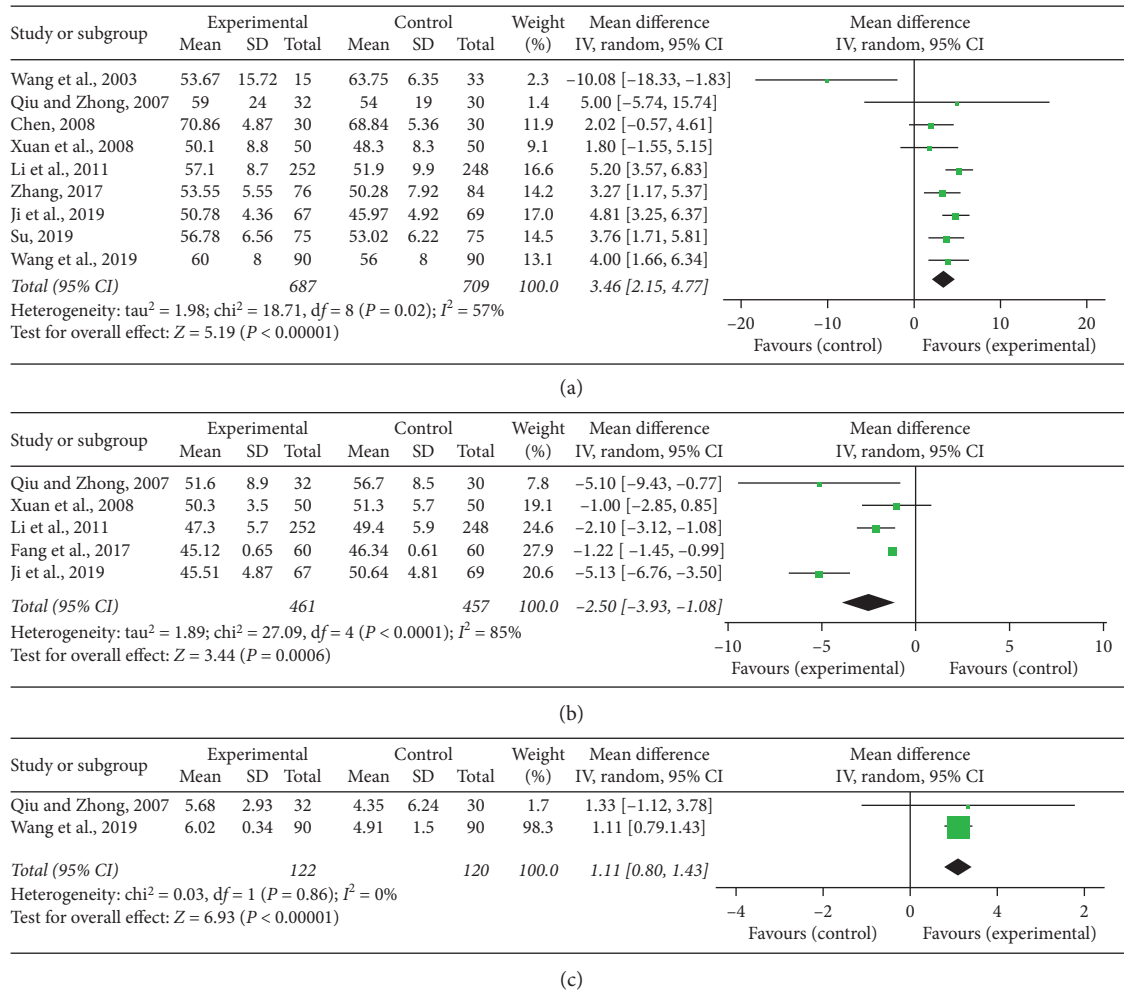


FIGURE 7: Forest plot of comparison in two groups for cardiac function indices. (a) Left ventricular ejection fraction; (b) left ventricular end diastolic diameter; (c) cardiac index. I^2 and P are the criterion for the heterogeneity test, \blacklozenge pooled mean difference, \blacksquare mean difference, and 95% CI.

that CDDP could significantly decrease Hs-CRP for CHD patients. There were three [32, 33, 38], five [30, 32, 33, 35, 38], and three [30, 32, 35] studies that reported TNF- α , IL-6, and IL-8. Significant heterogeneity was respectively, found, among individual researches ($P < 0.00001$, $I^2 = 94\%$; $P < 0.00001$, $I^2 = 88\%$; $P = 0.02$, $I^2 = 75\%$), and a random-effect model was adopted to carry out the meta-analysis. The pooled results showed that CDDP combined with PCI treatment significantly improved TNF- α (MD = -4.35, 95% CI (-5.99, -2.71), $P < 0.00001$; Figure 8(b)), IL-6 (MD = -6.76, 95% CI (-7.84, -5.68), $P < 0.00001$; Figure 8(c)), and IL-8 (MD = -1.87, 95% CI (-2.09, -1.66), $P < 0.00001$; Figure 8(d)).

3.9. Adverse Reaction. Two [21, 28] of the included researches reported that no obvious adverse reaction occurred during treatment, and two [33, 34] recorded the incidence of adverse reactions. The adverse reactions consisted of gastrointestinal intolerance, dizziness, phlebitis, and pruritus. No heterogeneity ($P = 0.89$, $I^2 = 0\%$) was found among

individual studies, and a fixed-effect model was used to perform the meta-analysis. The pooled RR with 95% CI showed that there was no difference about the incidence of adverse reactions between the experimental and control groups (RR = 1.13, 95% CI (0.45, 2.81), $P = 0.8$; Figure 9).

3.10. Publication Bias. Funnel plot was employed to evaluate the publication bias. The publication bias was checked for MACE. As shown in Figure 10, the plots were basically symmetric, indicating that there was no obvious publication bias.

4. Discussion

4.1. Overview. Cardiovascular disease (CVD) is induced by more and more risk factors including improvement of people's living standards, changes in people's living habits, aging of population, and the constantly changing environment [41, 42]. The morbidity and mortality of CVD remain high, and the burden of prevention and treatment of CVD is

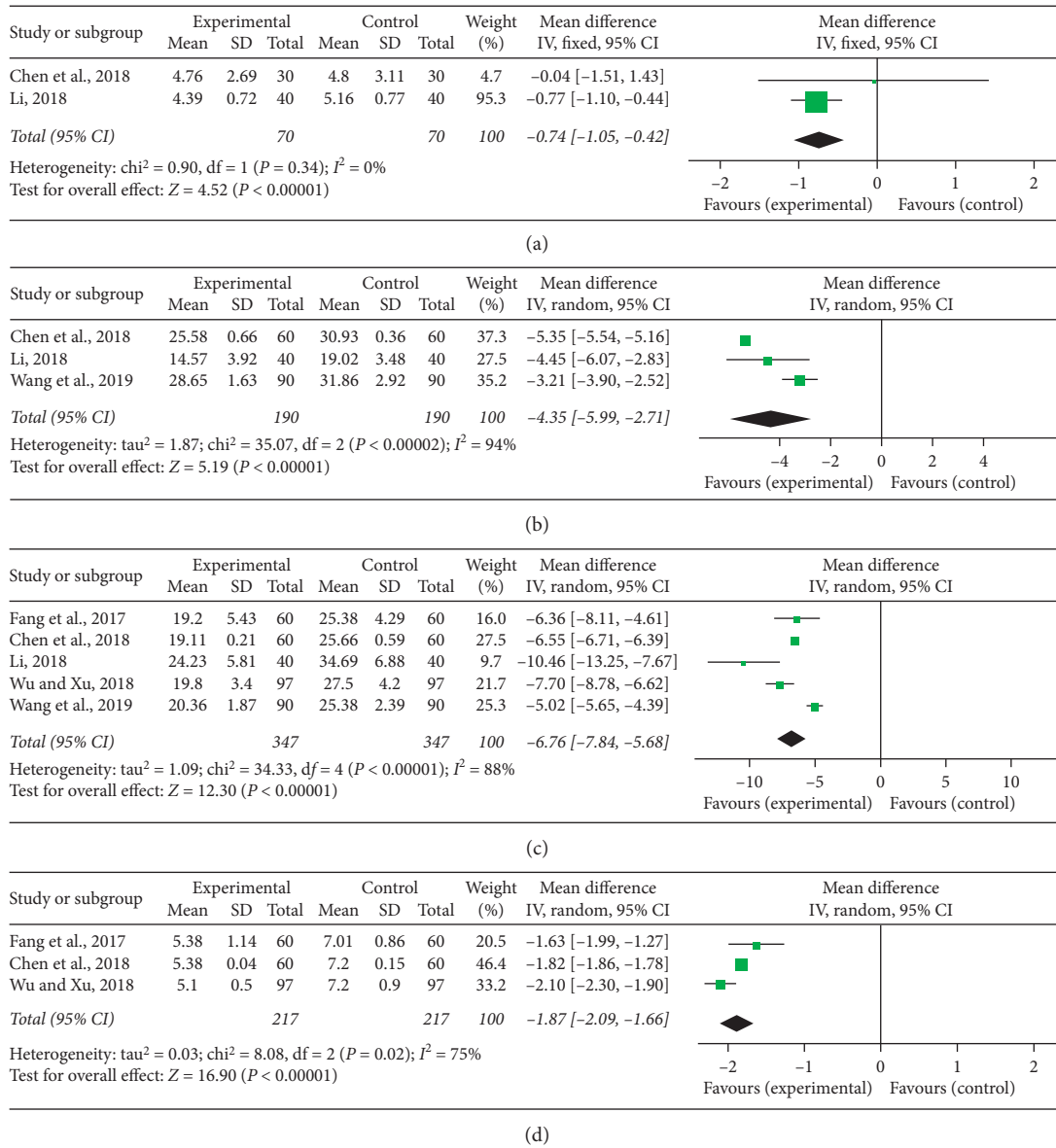


FIGURE 8: Forest plot of comparison in two groups for inflammatory indices. (a) High-sensitivity C-reactive protein; (b) tumor necrosis factor-alpha; (c) interleukin-6; (d) interleukin-8. I^2 and P are the criterion for the heterogeneity test, \blacklozenge pooled mean difference, $-\blacksquare-$ mean difference, and 95% CI.

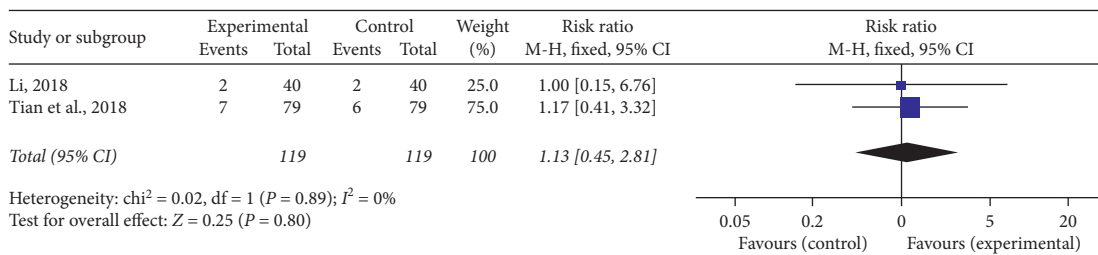


FIGURE 9: Forest plot of adverse reactions of CDDP plus PCI treatment compared to PCI treatment alone for CHD patients. I^2 and P are the criterion for the heterogeneity test, \blacklozenge pooled risk ratio, $-\blacksquare-$ risk ratio, and 95% CI.

increasing [43]. It has become an important public health issue for human health. CHD is one of the most common and harmful CVD, characterized by high disability rate,

mortality rate, and many complications, and seriously threatens public health [44]. Therefore, the researches on the treatment of CHD are of great significance to human health.

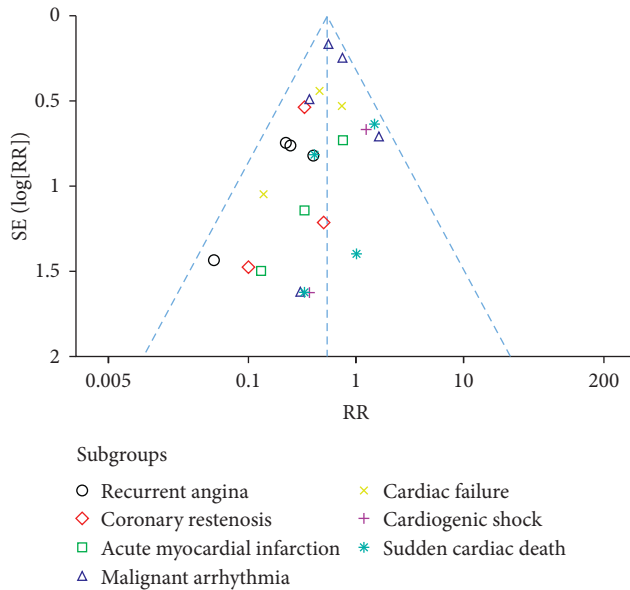


FIGURE 10: Funnel plot for the publication bias of major adverse cardiac events.

At present, PCI has become one of the main means for treating CHD because of its good therapeutic effect [45]. However, there has been a high incidence of adverse cardiovascular events in CHD patients after PCI treatment [46]. Given the circumstances, more effective and safe treatment is urgently needed for CHD patients in China and even the world.

Chinese clinicians have been looking for better treatments for CHD over the years. Traditional Chinese medicine (TCM) has been used to treat CHD for more than two thousand years. The therapeutic effect of Chinese traditional medicines for treating CHD is not bad and even stronger than some western medicines, and Chinese traditional medicines are characterized by little toxicity and side effect. Therefore, the application prospect of Chinese traditional medicines in CHD is great [47]. Along with the development of modern pharmaceutical technologies, oral preparations and injections for the prevention and treatment of CHD based on classical TCM prescriptions or theories have sprung up in large numbers [48].

CDDP is an excellent Chinese patent medicine developed by modern pharmaceutical technology based on the basic theory of TCM. Compared with the original tablet, CDDP has many advantages including small dosage, outstanding therapeutic effect, fewer side effects, and reduced gastrointestinal irritation [49]. Therefore, it is a commonly used Chinese medicine preparation in clinical practice in China. At present, Phase III clinical trial of CDDP has been completed in the United States. Then Tianjin Tasly Pharmaceutical Co., Ltd., will submit a new drug application to Food and Drug Administration [50]. CDDP is prepared from *Salviae miltiorrhizae*, *Panax notoginseng*, and *Borneolum*, and its major active constituents are tanshinol, protocatechuic aldehyde, salvianolic acid B, notoginsenoside, and so on [51]. Modern pharmacological studies have

shown that these components are related to some effects, such as regulating lipid metabolism, improving vascular function, and inhibiting thrombosis [52]. CDDP have been widely used in the treatment of various CVD for many years [53]. However, there is lack of a comprehensive and systematic evaluation of CDDP for the treatment of CHD after PCI according to general international standards. Therefore, this study is aimed at providing an internationally recognized systematic assessment of the efficacy and safety of CDDP for treating CHD patients after PCI treatment.

This meta-analysis for the first time systematically assessed the clinical effect and safety of CDDP for treating CHD patients after PCI treatment. The incidence of MACE was used to evaluate the efficacy of CDDP combined with PCI treatment for CHD patients. Compared with PCI treatment alone, CDDP combined with PCI treatment was associated with remarkably lower MACE ($P < 0.00001$). Hemorheology indices, including WBV, PV, HCT, EAI, and FIB, were used to study the fluidity and deformability of blood in CHD participants. Compared with PCI treatment alone, CDDP combined with PCI treatment was associated with significantly lower WBV, PV, and EAI ($P < 0.01$). It indicated that CDDP contributed to improving the antithrombotic and anticoagulation effects. ET, FMD, and NO were used to evaluate vascular endothelial function in CHD patients. Our analysis results showed that, compared with PCI treatment alone, CDDP combined with PCI treatment was associated with significantly lower ET and higher FMD and NO ($P < 0.01$). Moreover, TC, TG, HDL-C, and LDL-C were used to assess the blood lipid in CHD patients. Results demonstrated that CDDP combined with PCI treatment significantly decreased the levels of TC and LDL-C in comparison with PCI treatment alone ($P < 0.01$). LVEF, LVEDD, and CI were used to estimate cardiac function in CHD patients. Compared with PCI treatment alone, CDDP combined with PCI treatment was associated with significantly lower LVEDD and higher LVEF and CI ($P < 0.001$). In addition, Hs-CRP, TNF- α , IL-6, and IL-8 were applied to evaluate inflammation state in CHD patients after PCI. Results suggested that, compared with PCI treatment alone, CDDP combined with PCI treatment was associated with significantly lower Hs-CRP, TNF- α , IL-6, and IL-8 ($P < 0.00001$). However, there was no difference about adverse reactions between the experimental and control groups ($P = 0.8$). It could be only temporarily concluded that CDDP is relatively safe without increasing the incidence of adverse reactions before including more eligible studies.

4.2. Limitations. Although comprehensive search and strict methodologies were employed to screen researches and investigate the therapeutic effect and safety associated with CDDP treatment, several potential limitations still existed in this meta-analysis that should be considered. Firstly, although an overall retrieval strategy was adopted to reduce the publication bias as far as possible, there was still a certain degree of selective bias that our meta-analysis only searched the Chinese and English databases and no reference was

made to researches published in other languages. Secondly, all the eligible trials were conducted in China and most participants were Chinese. However, it is necessary to include some diverse population samples into the study to achieve more abundant and reliable results. Thirdly, the methodological quality in most of the eligible researches showed to be poor. Eleven of the 20 trials only referred to “randomization” but did not point out the specific random method. And all the included researches did not report allocation concealment and blinding method. Fourthly, we did not contact the authors using phone call or e-mail for more details of the included trials. Fifthly, there was statistically significant heterogeneity detected in several outcomes, such as FIB, ET, FMD, and NO. It is relatively difficult to study the heterogeneity in the outcomes of continuous variables. We were unable to perform a subgroup analysis for the small number of researches providing these outcomes and also failed to detect the sources of the heterogeneity after performing sensitivity analysis. It can be concluded that the heterogeneity came from two or more factors, such as gender, age, and duration of treatment. Finally, drug safety is significant to develop alternative medicines for health care. However, only two of the included researches reported adverse reactions.

4.3. Direction for the Future. According to our study, CDDP combined with PCI treatment is more effective for CHD patients compared with single PCI treatment. Therefore, this combination therapy regimen is recommended for widespread clinical use. Meanwhile, in consideration of the limitations existing in this meta-analysis, high-quality and large-scale RCTs, with good experimental design and methodological quality, are needed to investigate the clinical effect and safety of CDDP for CHD in the future.

5. Conclusion

The results showed that CDDP combined with PCI treatment remarkably reduced the incidence of MACE in CHD patients. Meanwhile, this combination improved blood rheology, vascular endothelial function, and cardiac function, decreased blood lipid, and exhibited anti-inflammatory effects. However, our findings must be interpreted with care for the limitations existing in this meta-analysis. Other rigorous and large-scale RCTs are in need to confirm these results.

Abbreviations

CDDP:	Compound Danshen dripping pill
CHD:	Coronary heart disease
CI:	Cardiac index
CVD:	Cardiovascular disease
EAI:	Erythrocyte aggregation index
ET:	Endothelin
FIB:	Fibrinogen
FMD:	Flow mediated dilation
HCT:	Hematocrit
HDL-C:	High density lipoprotein cholesterol

Hs-CRP:	High-sensitivity C-reactive protein
IL-6:	Interleukin-6
IL-8:	Interleukin-8
LDL-C:	Low density lipoprotein cholesterol
LVEDD:	Left ventricular end diastolic diameter
LVEF:	Left ventricular ejection fraction
MACE:	Major adverse cardiac events
NO:	Nitric oxide
PCI:	Percutaneous coronary intervention
PV:	Plasma viscosity
RCTs:	Randomized controlled trials
TC:	Total cholesterol
TCM:	Traditional Chinese medicine
TG:	Triglyceride
TNF- α :	Tumor necrosis factor-alpha
WBV:	Whole blood viscosity.

Data Availability

The data used to support the findings of this study are included within the article.

Conflicts of Interest

All authors declared that there are no conflicts of interest.

Authors' Contributions

Cailan Li, Jianhui Xie, and Xiaobo Yang conceived and designed the experiments. Cailan Li, Qian Li, Jiamin Xu, Wenzhen Wu, and Yuling Wu conducted the experiments. Cailan Li, Qian Li, and Jiamin Xu analyzed the data. Jianhui Xie and Xiaobo Yang contributed reagents/materials/analysis tools. Cailan Li, Qian Li, and Jiamin Xu wrote the paper. Jianhui Xie and Xiaobo Yang revised the paper.

Acknowledgments

This work was financially supported by the National Natural Science Foundation of China (Nos. 81673845 and 82003771), Science and Technology Planning Project of Guangdong Province (Nos. 2016A020226036 and 2017B030314166), Special Project of State Key Laboratory of Dampness Syndrome of Chinese Medicine (No. SZ2020ZZ03), Provincial Natural Science Foundation of Guangdong (No. 2019A1515010638), Science and Technology Research Project of Guangdong Provincial Hospital of Chinese Medicine (No. YN2018ZD02), and Guizhou Science and Technology Foundation of China (No. QKHPTRC[2018] 5772-021).

References

- [1] A. Bechthold, H. Boeing, C. Schwedhelm et al., “Food groups and risk of coronary heart disease, stroke and heart failure: a systematic review and dose-response meta-analysis of prospective studies,” *Critical Reviews in Food Science and Nutrition*, vol. 59, no. 7, pp. 1071–1090, 2019.

- [2] M. J. Pencina, A. M. Navar, D. Wojdyla et al., "Quantifying importance of major risk factors for coronary heart disease," *Circulation*, vol. 139, no. 13, pp. 1603–1611, 2019.
- [3] A. M. Navar, "The evolving story of triglycerides and coronary heart disease risk," *Journal of the American Medical Association*, vol. 321, no. 4, pp. 347–349, 2019.
- [4] M. De Hert, J. Detraux, and D. Vancampfort, "The intriguing relationship between coronary heart disease and mental disorders," *Dialogues in Clinical Neuroscience*, vol. 20, no. 1, pp. 31–40, 2018.
- [5] S. Kachur, V. Chongthammakun, C. J. Lavie et al., "Impact of cardiac rehabilitation and exercise training programs in coronary heart disease," *Progress in Cardiovascular Diseases*, vol. 60, no. 1, pp. 103–114, 2017.
- [6] F. Sanchis-Gomar, C. Perez-Quilis, R. Leischik, and A. Lucia, "Epidemiology of coronary heart disease and acute coronary syndrome," *Annals of Translational Medicine*, vol. 4, no. 13, pp. 1–12, 2016.
- [7] P. H. Wirtz and R. Von Kanel, "Psychological stress, inflammation, and coronary heart disease," *Current Cardiology Reports*, vol. 19, no. 11, p. 111, 2017.
- [8] N. V. K. Pothineni, S. Subramany, K. Kuriakose et al., "Infections, atherosclerosis, and coronary heart disease," *European Heart Journal*, vol. 38, no. 43, pp. 3195–3201, 2017.
- [9] G. Veronesi, H. Tunstall-Pedoe, M. M. Ferrario et al., "Combined effect of educational status and cardiovascular risk factors on the incidence of coronary heart disease and stroke in European cohorts: implications for prevention," *European Journal of Preventive Cardiology*, vol. 24, no. 4, pp. 437–445, 2017.
- [10] S. F. Su, M. Y. Chang, and C. P. He, "Social support, unstable angina, and stroke as predictors of depression in patients with coronary heart disease," *Journal of Cardiovascular Nursing*, vol. 33, no. 2, pp. 179–186, 2018.
- [11] X. Y. Li, "Recommendations on the clinical use of compound danshen dripping pills," *Chinese Medical Journal*, vol. 130, no. 8, pp. 972–978, 2017.
- [12] Y. F. Tian, L. Y. Li, R. Wang, and L. X. Ji, "A survey of cardioprotective effects of compound danshen dripping pills," *Acta Chinese Medicine and Pharmacology*, vol. 33, pp. 60–61, 2005.
- [13] Q. Li, "Research progress and clinical application of compound danshen dripping pills," *China Journal of Traditional Chinese Medicine and Pharmacy*, vol. 33, no. 7, pp. 2989–2991, 2018.
- [14] L. Xiao, "Research progress in pharmacological action and clinical application of compound danshen dripping pills," *World Chinese Medicine*, vol. 10, no. 7, pp. 1117–1123, 2015.
- [15] X. Huang, G. J. Kou, and B. H. Wang, "The clinical research progress of compound danshen dripping pill," *Lishizhen Medicine and Materia Medica Research*, vol. 27, no. 5, pp. 1187–1190, 2016.
- [16] D. Moher, A. Liberati, J. Tetzlaff, and D. G. Altman, "Preferred reporting items for systematic reviews and meta-analyses: the prisma statement," *Annals of Internal Medicine*, vol. 151, pp. 332–336, 2009.
- [17] E. Braunwald, E. M. Antman, J. W. Beasley et al., "ACC/AHA guidelines for the management of patients with unstable angina and non-ST-segment elevation myocardial infarction," *Journal of the American College of Cardiology*, vol. 36, no. 3, pp. 970–1062, 2000.
- [18] D. Y. Li and L. K. Ma, "Progress in diagnosis and treatment of acute coronary syndrome," *International Journal of Geriatric Psychiatry*, vol. 28, pp. 173–177, 2007.
- [19] H. Wang, F. Wang, Y. Z. Lin, J. Lu, G. M. Xu, and L. Liu, "Clinical observation of trimetazidine and compound Danshen dripping pills on percutaneous coronary intervention of coronary heart disease," *Shaanxi Medical Journal*, vol. 32, no. 3, pp. 252–254, 2003.
- [20] Y. Q. Qiu and Y. M. Zhong, "Effects of compound danshen dripping pills on elderly patients with acute myocardial infarction undergoing emergent interventional therapy of coronary artery," *Evaluation and Analysis of Drug-Use in Hospitals of China*, vol. 7, no. 5, pp. 376–377, 2007.
- [21] Y. J. Chen, *Therapeutic Effect of Compound Danshen Dripping Pills on Coronary Heart Disease after PCI*, pp. 14–20, Guangzhou University of Chinese Medicine, Guangzhou, China, 2008.
- [22] C. H. Xuan, H. B. Sun, and D. Z. Ding, "Effect of compound danshen dripping pills on myocardial microcirculation of coronary heart disease patients after percutaneous coronary intervention," *Lishizhen Medicine and Materia Medica Research*, vol. 19, no. 11, pp. 2797–2798, 2008.
- [23] R. Z. Zhao, Q. C. Fan, and B. Shi, "Effect of compound danshen dripping pills on hemorheology after PCI in patients with coronary heart disease," *Chinese Journal of New Drugs*, vol. 19, no. 2, pp. 130–132, 2010.
- [24] G. P. Li, X. T. Zheng, H. Z. Wang et al., "Clinical effect of compound danshen dripping pills on percutaneous coronary intervention of acute ST-segment elevation myocardial infarction," *Chinese Journal of Interventional Cardiology*, vol. 19, no. 1, pp. 24–28, 2011.
- [25] C. M. Tian, S. X. Li, and Y. X. Lv, "Therapeutic effect of compound danshen dripping pills and trimetazidine on coronary restenosis in patients with myocardial infarction after percutaneous coronary intervention," *Chinese Community Doctors*, vol. 13, no. 9, p. 168, 2011.
- [26] X. P. Xia, "Clinical observation of compound danshen dripping pills on coronary restenosis in patients with coronary heart disease after percutaneous coronary intervention," *Journal of Today Health*, vol. 13, no. 4, pp. 125–126, 2014.
- [27] Y. Tang and H. Zhang, "Clinical research of compound danshen dripping pills in preventing and curing coronary heart disease with restenosis after percutaneous coronary intervention," *Journal of Community Medicine*, vol. 13, no. 21, pp. 16–19, 2015.
- [28] Y. L. Yao, B. Yang, H. Kang, Y. M. Zhang, and Z. Y. He, "Effect of compound danshen dripping pills on hemorheology in acute coronary syndrome patients before and after percutaneous coronary intervention," *Chinese Journal of Multiple Organ Diseases in The Elderly*, vol. 14, no. 9, pp. 678–682, 2015.
- [29] M. H. Li and J. Wang, "Effect of compound danshen dripping pills on hemorheology in patients with coronary heart disease after PCI," *Chinese Medicine Modern Distance Education of China*, vol. 14, no. 4, pp. 61–62, 2016.
- [30] F. Fang, S. Y. Gan, G. R. Feng, H. Yu, and X. N. Zhang, "Effects of long-term use of compound danshen dripping pills on left ventricular remodeling and inflammatory factors in elderly patients with acute myocardial infarction after PCI," *Progress in Modern Biomedicine*, vol. 17, no. 3, pp. 544–546, 2017.
- [31] Y. Y. Zhang, *Influence of Compound Danshen Dripping Pills on PCI Efficacy in Patients with Acute ST-Segment Elevation Myocardial Infarction*, pp. 3–8, Shanxi Medical University, Shanxi, China, 2017.
- [32] H. Chen, D. M. Wei, L. Yu, G. Yin, J. S. Li, and X. N. Yang, "Effect of compound danshen dripping pills on serum inflammatory factors and T cell subset in elderly patients with

- acute myocardial infarction after PCI,” *Chinese Journal of Gerontology*, vol. 38, no. 11, pp. 2586–2588, 2018.
- [33] D. F. Li, “Clinical effect of compound danshen dripping pills and atorvastatin on improving inflammatory response and myocardial perfusion in patients with acute myocardial infarction after PCI,” *Prevention and Treatment of Cardio-Cerebral-Vascular Disease*, vol. 18, no. 6, pp. 500–502, 2018.
- [34] L. G. Tian, L. X. Zhang, C. Ji, Z. Y. Yuan, and J. Y. Liu, “Effects of alprostadil and compound danshen dripping pills on vascular endothelial function and cardiovascular adverse events in patients with coronary heart disease after PCI,” *Chinese Journal of Integrative Medicine on Cardio-Cerebrovascular Disease*, vol. 16, no. 24, pp. 3680–3682, 2018.
- [35] N. T. Wu and L. Q. Xu, “Effect of compound danshen dripping pills and statins on contrast-induced nephropathy and vascular function in patients with coronary heart disease after PCI,” *Journal of Hunan University of Chinese Medicine*, vol. 38, no. 3, pp. 335–338, 2018.
- [36] Y. Q. Ji, Z. X. Li, and J. M. Zuo, “Clinical observation of compound danshen dripping pills in the treatment of acute myocardial infarction after percutaneous coronary intervention,” *Journal of Critical Care in Internal Medicine*, vol. 25, no. 3, pp. 243–245, 2019.
- [37] X. S. Su, “Effects of compound danshen dripping pills on brain natriuretic peptide level and ventricular remodeling after percutaneous coronary intervention in patients with acute myocardial infarction,” *Chinese Journal of Practical Medicine*, vol. 46, no. 12, pp. 110–114, 2019.
- [38] R. T. Wang, M. X. Wu, and K. Y. Wang, “Effect of compound danshen dripping pills on expression of miR-1 in serum after percutaneous coronary intervention in patients with acute myocardial infarction,” *Chinese Journal of Integrated Traditional and Western Medicine in Intensive and Critical Care*, vol. 26, pp. 302–305, 2019.
- [39] A. D. Furlan, A. Malmivaara, and R. Chou, “Updated method guideline for systematic reviews in the cochrane back and neck group,” *Spine*, vol. 40, no. 21, pp. 1660–1673, 2015.
- [40] J. P. T. Higgins and S. G. Thompson, “Quantifying heterogeneity in a meta-analysis,” *Statistics in Medicine*, vol. 21, no. 11, pp. 1539–1558, 2002.
- [41] M. Kivimäki and A. Steptoe, “Effects of stress on the development and progression of cardiovascular disease,” *Nature Reviews Cardiology*, vol. 15, no. 4, pp. 215–229, 2018.
- [42] X. Ma, Y. X. Yang, N. A. Chen et al., “Meta-analysis for clinical evaluation of xingnaojing injection for the treatment of cerebral infarction,” *Frontiers in Pharmacology*, vol. 8, pp. 1–12, 2017.
- [43] C. J. Lagranha, T. L. A. Silva, S. C. A. Silva et al., “Protective effects of estrogen against cardiovascular disease mediated via oxidative stress in the brain,” *Life Sciences*, vol. 192, pp. 190–198, 2018.
- [44] S. S. Khan, H. Ning, J. T. Wilkins et al., “Association of body mass index with lifetime risk of cardiovascular disease and compression of morbidity,” *Journal of the American Medical Association Cardiology*, vol. 3, no. 4, pp. 280–287, 2018.
- [45] O. Kahkonen, P. Kankkunen, H. Miettinen, M. L. Lamidi, and T. Saaranen, “Perceived social support following percutaneous coronary intervention is a crucial factor in patients with coronary heart disease,” *Journal of Clinical Nursing*, vol. 26, no. 9, pp. 1264–1280, 2019.
- [46] S. Kodera, H. Morita, A. Kiyosue, J. Ando, and I. Komuro, “Cost-effectiveness of percutaneous coronary intervention compared with medical therapy for ischemic heart disease in Japan,” *Circulation Journal*, vol. 83, no. 7, pp. 1498–1505, 2019.
- [47] K. J. Zhang, Q. Zheng, P. C. Zhu et al., “Traditional Chinese medicine for coronary heart disease: clinical evidence and possible mechanisms,” *Frontiers in Pharmacology*, vol. 10, pp. 1–22, 2019.
- [48] X. Yang, T. He, S. Han et al., “The role of traditional Chinese medicine in the regulation of oxidative stress in treating coronary heart disease,” *Oxidative Medicine and Cellular Longevity*, vol. 2019, p. 13, 2019.
- [49] X. G. Hu, “The difference between compound danshen dripping pills and compound danshen tablets,” *Chinese Community Doctors*, vol. 36, no. 12, p. 116, 2020.
- [50] Y. L. Xu, “Tasly compound danshen dripping pill has completed phase III clinical trial of US Food and drug administration,” *Tianjin Journal of Traditional Chinese Medicine*, vol. 34, no. 2, pp. 74–75, 2017.
- [51] J. Zhang, “Determination of six components in compound danshen dripping pills by HPLC-UV-ELSD,” *Herald of Medicine*, vol. 33, no. 10, pp. 1375–1379, 2014.
- [52] Y. Zou, “Advances in pharmacological effects and metabolism of compound danshen dripping pills,” *Chinese Journal of Clinical Rational Drug Use*, vol. 11, no. 3, pp. 162–163, 2018.
- [53] L. Y. Peng, “Pharmacological and clinical study of compound danshen dripping pills in cardiovascular diseases,” *China Health Industry*, vol. 17, no. 19, pp. 186–188, 2013.

Research Article

Electroacupuncture Inhibits Atherosclerosis through Regulating Intestinal Flora and Host Metabolites in Rabbit

Yuping Shen ¹, Ze-Dong Cheng ², Yi-Guo Chen ¹, Rui sun ¹, Xian-De Ma ¹,
Guo-liang Hou ¹ and Rui Wang ¹

¹Department of Acupuncture and Moxibustion, Liaoning University of Traditional Chinese Medicine, Shenyang, China

²Liaoning University of Traditional Chinese Medicine,

Ministry of Education Key Laboratory of Visceral Phenomenon Theory and Application in Traditional Chinese Medicine, Shenyang, China

Correspondence should be addressed to Ze-Dong Cheng; 893554622@qq.com and Yi-Guo Chen; cyg05@hotmail.com

Received 28 April 2020; Revised 28 September 2020; Accepted 18 October 2020; Published 31 October 2020

Academic Editor: Mingjun Zhu

Copyright © 2020 Yuping Shen et al. This is an open access article distributed under the Creative Commons Attribution License, which permits unrestricted use, distribution, and reproduction in any medium, provided the original work is properly cited.

Background and Objective. As a recommended option for 43 diseases by the World Health Organization, electroacupuncture is also being used to treat some others in China. Diet-related intestinal flora imbalance can induce atherosclerosis. This study aims to evaluate how electroacupuncture copes with atherosclerosis through regulating intestinal flora. **Methods.** In this study, general rabbit conditions, vascular histology, metabolites, and intestinal flora structures were analyzed. Integrated analysis of metabolomics and 16S rRNA sequencing were performed. All the rabbits were randomly divided into four groups. The rabbit model of atherosclerosis was established. The histopathological change in the common carotid artery was assessed by HE staining and the structural change in the flora by 16S rRNA sequencing. HPLC-TOF-MS and Agilent MPP 12.1 were integrated to identify and screen out differential metabolites. Correlational analyses of every differential metabolite with intestinal flora were integrated on Omicshare platform. **Results.** Atherosclerotic rabbits showed obvious changes in general conditions, significant fibrous cap and necrotic center on carotid artery, abnormal intestinal bacteria structure, and metabolites levels. Electroacupuncture improved the conditions, reduced lipid deposition on the carotid artery wall, diversified intestinal flora, and normalized host metabolism. Integrated analysis showed that 149 altered metabolites were related to 22 intestinal flora, among which eight intestinal floras and 21 metabolites have relationships with atherosclerosis. **Conclusion.** Electroacupuncture can effectively reverse atherosclerosis through manipulating the structural feature of intestinal flora to influence the host metabolites. The possible mechanisms involved activating signal pathways through host metabolites or affecting the activity of cardiovascular-related enzymes, or regulating host lipid metabolism directly.

1. Introduction

Harboring microbes with metabolic functions, intestinal flora is critical to human health. Species spectrum analysis based on 16S rRNA sequencing has comprehensively explored the role of intestinal flora, mainly its structure, in disease development [1]. Besides, metabolomics has been increasingly applied to unravel the functions of human microbiota [2]. Metabolomic analysis focuses on the endogenous metabolites of a biological system, in a holistic view that also appears in Traditional Chinese Medicine (TCM) [3]. Recent years have seen its breakthrough in

dealing with cardiovascular disease. These technologies enable us to study on the relationship between intestinal flora and chronic diseases.

In the recent decade, the relationship between intestinal flora and chronic cardiovascular diseases has become a hot topic. The incidence and mortality from atherosclerosis have declined in some countries [4]. It is clear that the intestinal flora can metabolize dietary L-carnitine and choline into trimethylamine, a substance further transformed into trimethylamine-N-oxide (TMAO) in the liver. TMAO can increase cholesterol deposition in vascular cells and accelerate the formation of foam cells and subsequent

atherosclerosis plaques. However, atherosclerosis is caused by complex factors, and the relationships between metabolites and intestinal flora remain to be discovered. Therefore, in this research, we focused on the intestinal flora associated metabolites that participates in atherosclerosis.

Therapeutic methods for atherosclerosis vary. Acupuncture has emerged as a new clinical option for atherosclerosis in China. Some clinical studies showed that acupuncture can decrease carotid intimal thickness (IMT) and Crouse scores in phlegm dampness constitution carotid atherosclerosis with unique advantages [5]. Another clinical study showed that acupuncture combined with intravenous administration of alprostadil achieve better effect than simple intravenous administration of alprostadil for lower limb atherosclerosis of early diabetes mellitus [6]. In animal experiments, acupuncture has the same effect. A study showed that electroacupuncture at Quchi (LI-11), Zhongwan (CV-12), and Fenglong (ST-4) could regulate HDL-C, LDL-C, and atherosclerosis index [7]. Our previous studies [8] showed that electroacupuncture could reduce the atherosclerotic plaques, regulate the abnormal changes of blood lipid [9], and hemorheology in rabbits [10], and point stimulation can optimize the structure of intestinal flora [11]. A study has also found that electroacupuncture can modulate the status of intestinal flora [12]. Intestinal flora is known to have relationship with atherosclerosis, but the mechanism needs more evidence. Therefore, we designed this research to illustrate how electroacupuncture regulates rabbit intestinal flora to reverse the development of atherosclerosis.

2. Materials and Methods

2.1. Animals and Ethical Approval. A total of 24 male New Zealand white rabbits (weighing 2.5 ± 0.5 kg, aged 2–3 months) were kept under standardized conditions (light from 6 am to 6 pm, temperature 18–20°C, relative humidity 50–70%), with free access to food and water. Rabbits were supplied by the Jinan Jinfeng Experimental Animal Company. The certification number is SCXK(Lu)2014-0006. All animal procedures were approved by the Local Ethical Review Panel of the Liaoning University of TCM (Ethical Inspection, No. 21000092017018). After experiment, animals were euthanized with air needle injection.

2.2. Reagents. High-fat diet, consisting of 1% cholesterol, 3% lard, 10% egg yolk powder, and 86% common ingredients, was processed into pellet feed by Qianmin Animal Feed Processing Center in Yuhong District, Shenyang, China. Other materials included atorvastatin calcium tablets (code: 9H0285991, Beijing Jialin Pharmaceutical Co., Ltd.); penicillin sodium (code: H13020657, North China Pharmaceutical Co., Ltd.); disposable sterile PTCA balloon dilatation catheter (2.0×15 mm, Beijing Demarc Co., Ltd.); needles (diameter 0.32 mm, length 15 mm, Suzhou Global Co., Ltd.); electroacupuncture apparatus (Suzhou medical products Co., Ltd.); HPLC-grade methanol (Merck, Darmstadt, Germany); distilled water (Mill-Q ultrapure water

machine, Millipore, USA); HPLC-grade formic acid (Tianjin Kermel Chemical Company, Tianjin, China). Pipettes, EP tubes, 10% urethane, heparin, injection bottles, pipette tips, and oil red O dye were provided by Liaoning University of the TCM laboratory.

2.3. Model Establishment. After one week of adaptive feeding, the rabbits were randomly divided into five groups: control group (normal rabbits, $n=6$) and model group (atherosclerotic rabbits, $n=6$), AC group (atherosclerotic rabbits + atorvastatin, $n=6$), and EA group (atherosclerotic rabbits + electroacupuncture, $n=6$). From beginning to the end, the control group was fed with standard diet without any treatment. In model, AC, and EA groups, after four week's high-fat diet (120 g per day), carotid artery balloon injury was made. Then, the high-fat diet was continued for another four weeks.

2.4. Balloon Injury. After 12 h of fasting and water deprivation, rabbits were anesthetized with 10% urethane 3 ml/kg through the ear vein. The skin was cut to expose subcutaneous tissue at midline of neck. The right carotid artery and the right external carotid artery were dissected. After injection of 200 μ /kg heparin at the ear vein, the right external carotid artery was blocked at distal end. The proximal end was separated, and then a small hole was made at the right external carotid artery. A 3.0×20 mm PTCA balloon catheter was inserted into the right carotid artery through a point about 4–5 cm to the right external carotid artery incision. Under 5–6 atmospheres, the saline was used to fill balloon. This process was repeated for three times and each time thirty seconds. The inserted catheter was pulled out, and the right external carotid artery was ligated. Meanwhile, intramuscular injection of 1,000,000 units of penicillin was administered after surgery for three days to prevent infection. After the balloon injury, the control group was fed with normal diet while the others with high-fat diet.

2.5. Experimental Treatment. After model establishment, atorvastatin calcium tablets (1 mg/kg/d) were added into high-fat diet in the AC group for four weeks. The EA group was treated with electroacupuncture therapy for four courses.

2.6. Electroacupuncture. Acupoints Neiguan (PC-6), Zusanli (ST-36), and Guanyuan (BL-26) were stimulated with sterile acupuncture needles. The needle was inserted by 0.2–0.3 cm for PC-6, 0.5–0.8 cm for ST-36, and 0.3–0.5 cm for BL-26. PC-6 was located in the gap of radius and ulna, on the line connecting the rasceta with the ulnar side of the biceps tendon, and 1/6 to the midpoint of the rasceta. ST-36 was located at 2/5 of the line connecting the navel and symphysis pubis. BL-26 was located at the upper 1/5 to the intersection of lateral calf, about 1.2 cm below the fibular head, 1 cm behind the posterior tibial crest. According to the rabbit's tolerance and local muscle twitching, the electroacupuncture apparatus was powered with rarefaction wave, 1 mA

consuming current, and 2 Hz frequency. This therapy was performed once a day, 20 minutes per treatment, six days per course, and with an interval of one day after a course.

2.7. Sample Collection. At the end of the treatments, all groups were anesthetized with 10% urethan (3 ml/kg) through ear vein. Two milliliters of blood were drawn for metabolomics. After euthanasia, partial fragment of the right carotid artery and fresh feces were collected. The plasma samples and feces were stored in fridge at -80°C . Excess tissues of the right carotid arteries were eliminated and fixed with 10% neutral formalin.

2.8. General Conditions. The general conditions were graded and scored (Table 1). The scores of every rabbits in each group before and after the study were compared [13, 14].

2.9. Histopathology Analysis

2.9.1. HE Staining. The right carotid artery was embedded by paraffin was transversely sectioned (thickness of $5\ \mu\text{m}$, 4 sections per artery) and HE stained. After sealing, the pathological changes in arterial tissue were observed and photographed using a digital microscope.

2.9.2. Red Oil Staining. After 24 h of fixation, parts of carotid arteries were washed by PBS water for 3 times. The carotid artery was cut longitudinally and immersed in the oil red dye for 1 h. The artery tissue was washed with 75% ethanol, until the fatty plaque turned red and other parts turned milky white. Then, the artery tissue was washed with distilled water for three times and fixed with needles.

2.10. Plasma Sample Preparation. All plasma samples were unfrozen at room temperature before HPLC-TOF-MS analysis. In HPLC-TOF-MS analysis, every $200\ \mu\text{L}$ of plasma was mixed with $600\ \mu\text{L}$ of methanol. After vortex-mixing for 2 min, the mixture was centrifuged (7,500 rpm, 15 min, 4°C) to precipitate the proteins. The supernatant was transited into an EP tube with a proper pipette and dried by nitrogen concentration. The samples were dissolved with $100\ \mu\text{L}$ of methanol and centrifuged again (2,000 rpm, 2 min, 4°C). Finally, $90\ \mu\text{L}$ of supernatant was transferred into an autosampler vials with a proper pipette.

2.11. Data Processing and Multivariate Analysis. The mass data were analyzed with Agilent Qualitative Analysis software, Mass Hunter Qualitative analysis software (MHQ, USA) within molecular feather extraction (MFE) and with Agilent MPP software (version 12.1, Agilent Corporation, USA) for alignment and normalization. Using PCA analysis, the metabolites with variable importance in the projection (fold change > 2) and the P values of one-way ANOVA ($P < 0.01$) were selected as potential biomarkers. The potential markers were identified by MPP software with ID Browsers and contrasted in available biochemical databases,

KEGG and National center for biotechnology information (NCBI).

2.12. HPLC-TOF-MS Analysis. The Agilent 1290 HPLC system (Agilent Corporation, USA), Agilent Time of flight Mass Spectrometer equipped with electrospray ionization, and Agilent Poroshell 120 SB-C18 column ($100\ \text{mm} \times 4.6\ \text{mm}$ i.d., $2.7\ \mu\text{m}$, Agilent Corp, USA) were used for t HPLC-MS analysis. The column temperature was kept at 35°C , the flow rate of the mobile phase at $0.4\ \text{ml/min}$, and the injection volume at $4\ \mu\text{L}$. Mobile phase consisted of 0.1% formic acid in water (A) and methanol (B). The column was eluted with 100% B first, then 20% A and 80% B for 10.00 min, and 100% B for 20.00 min. The parameters for HPLC-TOF-MS analysis were set as follows: ion source of: –ESI, capillary voltage of 3500 V, gas temperature of 250°C , drying gas of $9\ \text{L/min}$, nebulizer of 45 psig, and fragmentor voltage of 125 V. An injection with a needle of automatic-washing mode was employed on the autosampler.

2.13. Analysis of Intestinal Flora Structure and Multiomics Union. 16S rRNA sequencing was performed by Shanghai Personal Biotechnology Co., Ltd. Multiomics union analysis was performed by Guangzhou Genedenovo Biotechnology Co., Ltd.

3. Results

3.1. General Condition Score. During the first week, rabbits were in good condition, and there was no significant difference between groups ($P > 0.05$). However, after modeling, the rabbits gradually showed decreased activity, loss of appetite, diarrhea, dark ear color, and general body lightening. But, the general condition of the rabbits treated with atorvastatin or electroacupuncture was better. The general condition score is shown in Figure 1.

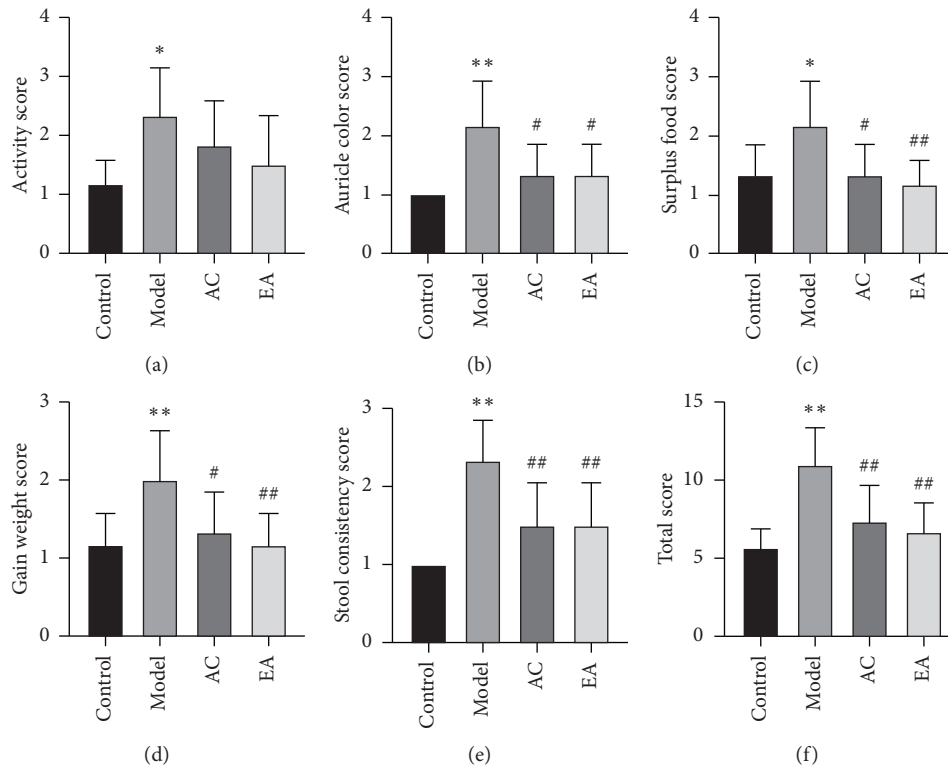
3.2. Histopathological Results

3.2.1. HE Staining Results. The aorta tissues (Figure 2) in the control group showed uniform vascular, integrated endothelium, smooth vascular wall without lipid deposition, no foam cell accumulation, and atherosclerotic plaques. In contrast, the tissues in the model group showed obvious fibrous cap and necrotic center, indicating that the atherosclerotic models had been successful established. In AC and EA groups, the thickness of the vascular wall, the level of inflammatory cells, the infiltration of foam cells, and the plaque area decreased after atorvastatin or electroacupuncture.

3.2.2. Red Oil Staining Results. Red oil staining results were showed the changes of atherosclerosis plaque size. After staining, the normal carotid artery tissue in the control group was milky white, while in the model group the lipid deposited on the endothelium, showing orange red (Figure 3). The orange red areas in the AC and EA groups were smaller than those in the model group.

TABLE 1: Scores of conditions.

Score	Activity	Auricle color	Surplus food (g)	Weight	Stool consistency
1	Active move, lively	Ruddy	<60	Gained >0.8 kg	Round and smooth
2	Active move, not lively	Pale	60–100	Gained <0.8 kg	Diarrhea, amount less than 10 ml
3	Inactive	Gloomy	>100	Lose weight	Diarrhea, amount more than 10 ml

FIGURE 1: General condition scores. * $P < 0.05$ vs. control, ** $P < 0.01$ vs. control. # $P < 0.05$ vs. model, and ## $P < 0.01$ vs. model.

3.3. Intestinal Flora Structure. The top ten most abundant of intestinal flora were visualized. Different color means different flora, and the length of each color column means the abundance of corresponding flora. The results showed that, on family level, the abundances of intestinal flora in different groups were different (Figure 4). ACE and Simpson indexes were used to show abundance and diversity (Table 2).

3.4. Metabolic Analysis Results. Low-molecular weight metabolites were separated completely in 20 min. The results of ANOVA using MPP software and principal component analysis (PCA) are shown in Figure 5. Obviously, the metabolites in different groups showed differences. The dimensional patterns in AC and EA groups were closer to that in the control group, which meant the metabolites in these three groups are similar. Actually, 222 metabolites showed statistic difference. Compared with control group, there were 70 metabolites upregulated and 151 metabolites downregulated. Compared with the model group, 117 metabolites in AC group and 84 metabolites in EA group were upregulated, while 86 metabolites in AC group and 136 metabolites in EA group were downregulated. The 132 metabolites in AC group and 129 metabolites in EA group showed the

same tendency with control group, which indicated that electroacupuncture not only regulated the structure of intestinal flora but also the production of host metabolites.

3.5. Integration of Metabolomics and 16S rRNA Sequencing. The results of O2PLS analysis are shown in the Figure 6(a). The dots represent bacterium or metabolites. The greater the absolute value in the coordinates, the greater the degree of association between this element and another omics. Among the 222 metabolites with differential levels, 149 metabolites showed relationships with 22 intestinal flora ($P < 0.05$) (Figure 6(b)). According to the *Method for diagnosing heart disease through bacterial metagenomic analysis* [15], the changes of Thermogemmatissporaceae, Flavobacteriaceae, Verrucomicrobiaceae, S24-7, Lachnospiraceae, Bifidobacteriaceae, Turicibacteraceae, Veillonellaceae, Rumino-coccaceae, and Clostridiales could be used in the diagnosis of cardiovascular disease, including atherosclerosis. These 10 families of intestinal bacterium were definitely related to 45 metabolites. According to KEGG, Lipid MAP, METLIN, and HMDB databases, 21 metabolites have been confirmed to be associated with the development of atherosclerosis. In this study, electroacupuncture regulated the 8 intestinal bacteria

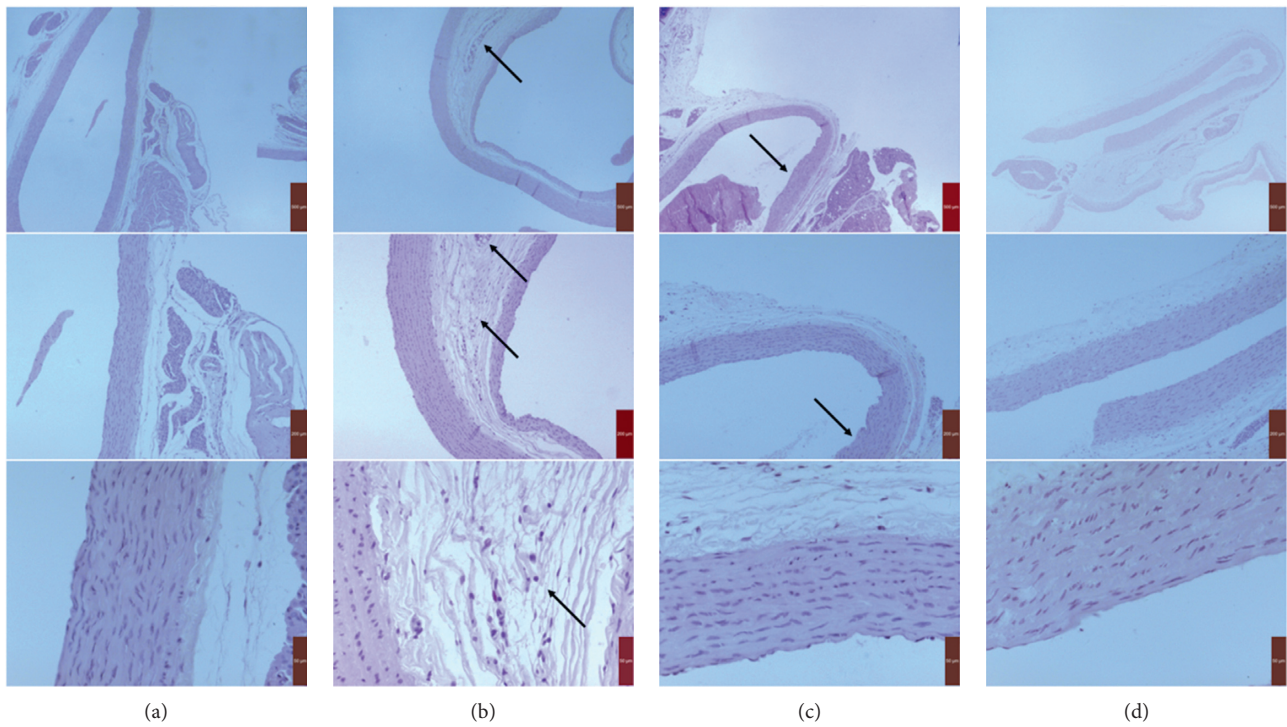


FIGURE 2: HE staining of atherosclerotic plaques ($\times 40$, $\times 100$, and $\times 400$). (a) Control group. (b) Model group. (c) AC group. (d) EA group.

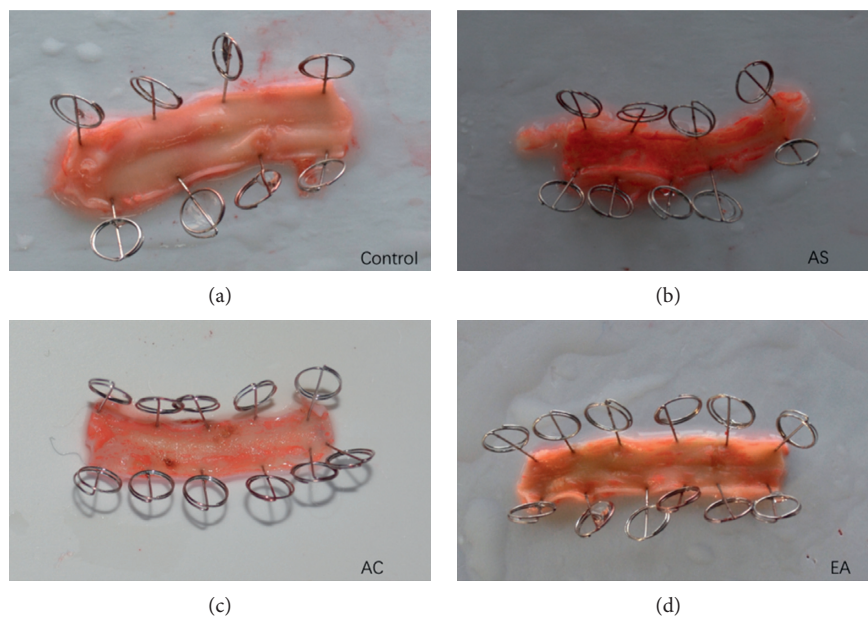


FIGURE 3: Oil red O staining of atherosclerotic plaque size.

TABLE 2: Alpha index of intestinal flora. * $P < 0.05$ vs. control, ** $P < 0.01$ vs. control, and ## $P < 0.05$ vs. model.

Group	ACE	Simpson
Control	1466.1383 \pm 165.9871	0.9826 \pm 0.0066
Model	1050.4783 \pm 141.9394*	0.9548 \pm 0.0276**
AC	1305.4950 \pm 134.5323#	0.9789 \pm 0.0042#
EA	1308.0183 \pm 75.8283#	0.9768 \pm 0.0082#

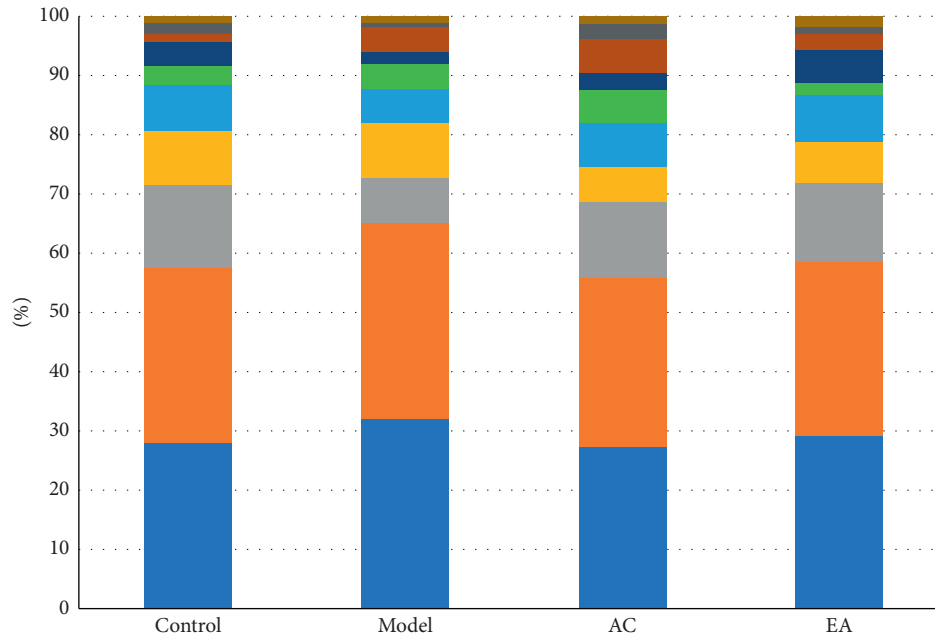


FIGURE 4: Intestinal flora abundance on family level.

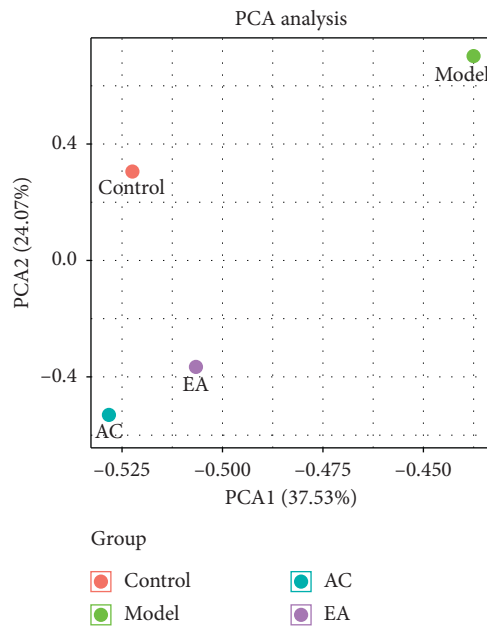


FIGURE 5: PCA of metabolites in different groups.

to influence 21 host metabolites to reverse atherosclerosis (Figure 6(c)).

4. Discussion

TCM holds that atherosclerosis develops with the stagnant *qi* and blood, usually caused by vascular phlegm and stasis. At present, the mechanism of atherosclerosis is not fully understood, but it is certain that the occurrence and development of atherosclerosis are closely related to the abnormal metabolic function of organism. The intestinal flora parasitizes in the intestines of animals and participates in the

metabolic processes of the host. Intestinal flora has become a new therapeutic target for various metabolic diseases [16].

In previous study, three relevant findings that can support the use of electroacupuncture as an intervention to treat atherosclerosis. Firstly, point stimulation could change the structural features of intestinal flora [11]. Secondly, electroacupuncture has a good regulatory effect on myocardial ischemia diseases [17]. Thirdly, electroacupuncture could increase the concentration of drugs in specific viscera, which means electroacupuncture combined with drugs will achieve synergistic effect and improve drug efficacy. Besides, it has shown that stimulating PC-6 can benefit the coronary blood flow [18], stimulating ST-36 can decrease blood lipid [19] and stimulating BL-36 can optimize the structure of intestinal flora [20]. This is the mainly reason that why we choose electroacupuncture as the intervention in this study.

4.1. General Condition and TCM. According TCM theory, atherosclerosis is caused by the combination of phlegm, blood stasis, and toxin. In human body, atherosclerosis will develop with some signs and symptoms, like chest tightness, asthma, fatigue, obesity, or emaciation. In rabbits, fur, ear color, activity, weight gain, and feces condition are important indices, for example, the auricle color could be related with blood stasis. In this study, those symptoms worsen after modeling and relieve after treatment.

4.2. Changes in Histopathology. In this study, electroacupuncture reduced atherosclerosis plaque in EA groups. Favorable morphological changes confirmed the anti-atherosclerotic effect of electroacupuncture. This incidence verified the antiatherosclerotic effect of electroacupuncture for atherosclerosis qualitatively.

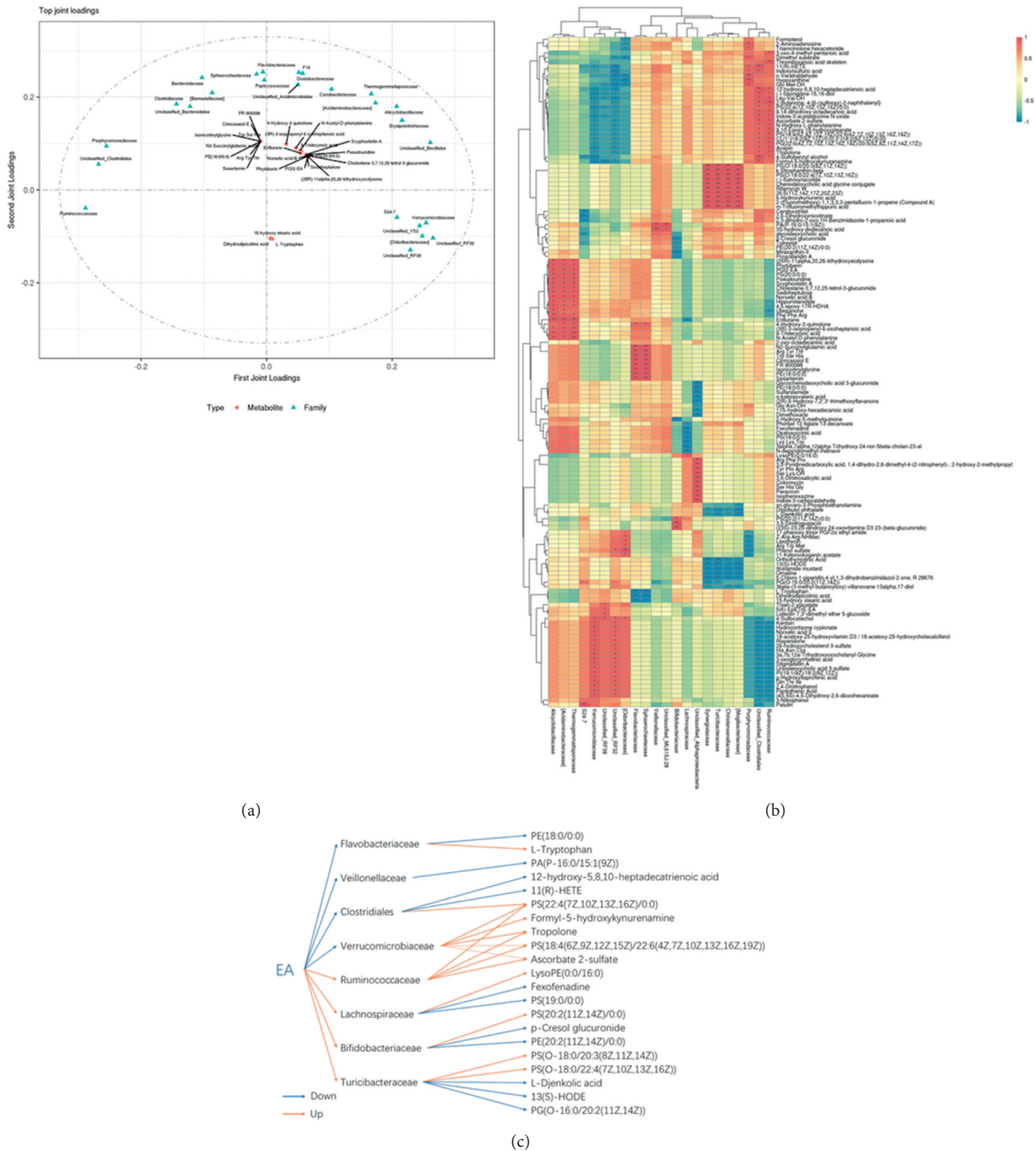


FIGURE 6: (a) Integrated metabolomics and 16S rRNA sequencing. * $P < 0.05$; ** $P < 0.01$. (b) O2PLS analysis. (c) Possible methods.

4.3. Structural Feature Changes in Intestinal Flora by Electroacupuncture. Normal intestinal flora maintains homeostasis. Drug may decrease the probiotics, enrich the pathogenic bacteria or opportunistic bacterium [21], and overturn the structural features of intestinal flora [22]. In this study, the differences of the structural features of intestinal flora were obvious, suggesting that the occurrence of atherosclerosis may be related to abnormal structural features of the intestinal flora, and electroacupuncture can regulate this state.

4.4. Metabolites in Plasma Were Different between Groups. In the present study, 16S rRNA sequencing showed that either of atherosclerosis, atorvastatin application, and electroacupuncture could change intestinal flora structural features. In order to determine whether this change has an impact on the host, this study selected non-targeted metabolomics to test plasma metabolites. Our results showed that either of atherosclerosis lesions, atorvastatin application, and electroacupuncture could change plasma metabolism levels among the groups. The

PCA patterns in model and control groups were different, which indicated that atherosclerosis had bad effect on the metabolism of the body. Interestingly, the PCA pattern in the EA group was different to that in model group, but similar to that in the control group, which demonstrates that electroacupuncture could have some therapeutic effect on this metabolic abnormality. And, some of 222 differentially produced metabolites were directly related to atherosclerosis: Ascorbate 2-sulfate [23, 24], hypoxanthine [25], Hippurate [26], 13(S)-HODE [27], inositol [28], 6-keto-PGF 1α [29], N-acetylneuraminic acid [30], ubiquinone [31], glucuronide [32], L-tryptophan [33], 15(S)-HETE [34], etc. However, the current evidence is still unable to confirm whether these metabolic changes were caused by intestinal flora or not, so it was necessary to perform integrated analysis of two omics.

4.5. Almost 67% Differential Metabolites Were Related to Intestinal Flora. The integrated analysis of omics showed that 67% of 222 differential plasma metabolites were closely related to 22 intestinal flora, suggesting that intestinal flora is not only an important participant in the development of atherosclerosis but also a medium for electroacupuncture to treat atherosclerosis.

The host metabolites can be influenced by electroacupuncture through intestinal flora to activate some signal pathway. Taking Turicibacteriaceae as an example, electroacupuncture can increase its abundance in atherosclerotic rabbits, decrease the metabolites 13(S)-HODE and L-Djenkolic acid in plasma, and then eliminate the atherosclerotic plaque. L-djenkolic acid [35] could produce oxygen ion to trigger low-density lipoprotein oxidation reaction, which will accelerate the formation of atherosclerotic plaque. 13(S)-HODE is a kind of trans-unsaturated fatty acid, which is harmful to the cardiovascular system; however, the fact is that 13(S)-HODE is negatively correlated with Turicibacteriaceae, but its level in the plasma is high. The reason may be that one metabolite may be affected by multiple intestinal flora. 13(S)-HODE is also affected by Christensenellaceae and (Mogibacteriaceae). 13(S)-HODE is a ligand in the PPAR signal pathway existing in adipocytes. Peroxisome proliferator-activated receptors (PPARs) are nuclear hormone receptors that can be activated by fatty acids and their derivatives, including three major members: PPAR α , PPAR β/δ , and PPAR γ . A lot of evidence showed that atorvastatin lowers lipid level through activating PPARs. This is why 13(S)-HODE is higher after electroacupuncture. Moreover, we can speculate that electroacupuncture may also relieve atherosclerosis by employing the intestinal flora to regulate the levels of host metabolites and then activate PPARs.

Host metabolites can be affected by electroacupuncture through intestinal flora to adjust the activity of cardiovascular-related enzymes, Tropolone, for instance, a kind of catechol-O-methyltransferase (COMT) inhibitor. COMT has been implicated in both depression and cardiovascular disease (CVD). A study showed that high COMT activity genotype Val158-Met, associated with activity of COMT, can increase the risk of

CVD [36]. Moreover, Hinokitiol, a derivative of Tropolone, can mediate p-JNK and p-PLC γ 1 signaling pathways to achieve antiatherosclerotic plaque effects [37]. In this study, electroacupuncture can upregulate Ruminococcaceae and downregulate Verrucomicrobiaceae to upregulate Tropolone in plasma, which indicated that electroacupuncture may inhibit the activity of COMT by upregulating Tropolone through intestinal flora to prevent CVD.

Electroacupuncture also can influence host lipids through intestinal flora to adjust lipid metabolism, such as PS(22:4(7Z, 10Z, 13Z, 16Z)/0:0), LysoPE(0:0/16:0), PA(P-16:0/15:1(9Z)), PS(O-18:0/20:3(8Z, 11Z, 14Z)), PS(O-18:0/22:4(7Z, 10Z, 13Z, 16Z)), and PG(O-16:0/20:2(11Z, 14Z)). They belong to glycerophospholipid category, and electroacupuncture can adjust them through intestinal flora.

This study has some limitations. Firstly, the range of the mass-to-charge ratio that can be predicted by HPLC/ESI-TOF-MS is 100 to 1500, so beyond this range, molecular information cannot be captured. Secondly, the metabolomics in this study is nontargeted and metabolites cannot be accurately quantified. Therefore, the results of this study need to be verified by more experiments.

5. Conclusion

Electroacupuncture can effectively reverse atherosclerosis through manipulating the structural feature of intestinal flora to influence the host metabolites. The possible mechanisms involved activating the signal pathways through metabolites, or affecting the activity of cardiovascular-related enzymes, or regulating host lipid metabolism directly.

Data Availability

The data used to support the article are available in the article.

Disclosure

Zedong-Cheng is the co-first author.

Conflicts of Interest

The authors declared no potential conflicts of interest with respect to the research, authorship, and/or publication of this article.

Authors' Contributions

YC and ZC designed the experiment. XM, RW, and RS performed the animal experiment and histopathology analysis and biochemical tests. YS performed metabolomics analysis and paper writing. GH and YS reviewed and edited the manuscript.

Acknowledgments

The authors are very grateful to Prof. Xiansheng-Meng for assistance with the metabolomics. They are grateful to Shanghai Personal Biotechnology Co., Ltd, for assisting in 16S rRNA sequencing and grateful to Guangzhou Gene Denovo Biotechnology Co., Ltd, for assisting in integrated analysis. This paper is from the National Natural Science Foundation of China (No.81674078) and the Open Fund of Ministry of Education Key Laboratory of Visceral Phenomenon Theory and Application of Liaoning University of Traditional Chinese Medicine (zyzx1708).

Supplementary Materials

All data that involved in this manuscript have been uploaded. (*Supplementary Materials*)

References

- [1] Y. K. Chan, M. S. Brar, P. V. Kirjavainen et al., "High fat diet induced atherosclerosis is accompanied with low colonic bacterial diversity and altered abundances that correlates with plaque size, plasma A-FABP and cholesterol: a pilot study of high fat diet and its intervention with *Lactobacillus rhamnosus* GG (LGG) or telmisartan in ApoE^{-/-} mice," *BMC Microbiology*, vol. 16, no. 1, p. 264, 2016.
- [2] J. Chong and J. Xia, "Computational approaches for integrative analysis of the metabolome and microbiome," *Metabolites*, vol. 7, no. 4, p. 62, 2017.
- [3] M. X. Chen, S.-Y. Wang, C.-H. Kuo, and I.-L. Tsai, "Metabolome analysis for investigating host-gut microbiota interactions," *Journal of the Formosan Medical Association*, vol. 118, no. 1, pp. S10–S22, 2019.
- [4] W. Herrington, B. Lacey, P. Sherliker, J. Armitage, and S. Lewington, "Epidemiology of atherosclerosis and the potential to reduce the global burden of atherothrombotic disease," *Circulation Research*, vol. 118, no. 4, pp. 535–546, 2016.
- [5] H. Liang, L. Meng, Y. Yuan et al., "Clinical observation on the treatment of carotid atherosclerosis in phlegm dampness constitution," *Guangdong Medical Journal*, vol. 39, no. 13, pp. 2070–2073, 2018.
- [6] P. Liang, A. Wei, and Z. Gu, "Effects of acupuncture at stellate ganglion on lower limb atherosclerosis of early diabetes mellitus," *Zhongguo Zhen Jiu*, vol. 36, no. 5, pp. 476–480, 2016.
- [7] G. X. Zhang, J. L. Miao, Z. Y. Zhang, H. J. Wang, and L. X. Ji, "Regulation effects of electroacupuncture with different acupoint combinations on blood lipid in rats with hyperlipemia," *Zhongguo Zhen Jiu*, vol. 34, no. 9, pp. 894–897, 2014.
- [8] Z. Cheng, Y. Ning, and R. Wang, "Effects of electroacupuncture on expression of CD36 in peritoneal macrophages of rabbits with atherosclerosis," *Zhongguo Zhen Jiu*, vol. 38, no. 2, pp. 179–184, 2018.
- [9] H. Luo and Z. Cheng, "Effects of Electroacupuncture on blood lipid and hemorheology in atherosclerotic rabbits," *Liaoning Journal of Traditional Chinese Medicine*, vol. 45, no. 8, pp. 1761–1790, 2018.
- [10] S. H. Zhang and Z. D. Cheng, "Effects of electroacupuncture on CYP7A1 expression in liver of rabbits with atherosclerosis," *Zhongguo Zhen Jiu*, vol. 39, no. 1, pp. 59–64, 2019.
- [11] S. Wang, Z. Cheng, D. Jin, and Y. Chen, "Moxibustion at Front-Mu point of abdomen for intestinal dysbacteriosis in rats," *Journal of Acupuncture and Tuina Science*, vol. 9, no. 1, pp. 21–25, 2011.
- [12] J. Xu, X. Zheng, K.-K. Cheng et al., "NMR-based metabolomics reveals alterations of electro-acupuncture stimulations on chronic atrophic gastritis rats," *Scientific Reports*, vol. 7, no. 1, Article ID 45580, 2017.
- [13] G. C. Mcmillan, J. H. Whiteside, and G. L. Duff, "The effect of undernutrition on cholesterol atherosclerosis in the rabbit," *Journal of Experimental Medicine*, vol. 99, no. 3, pp. 261–274, 1954.
- [14] D. C. Cavallini, R. Bedani, L. Q. Bomdespacho, R. C. Vendramini, and E. A. Rossi, "Effects of probiotic bacteria, isoflavones and simvastatin on lipid profile and atherosclerosis in cholesterol-fed rabbits: a randomized double-blind study," *Lipids Health Disease*, vol. 8, no. 1, 2009.
- [15] Y. Jin, *Method for Diagnosing Heart Disease through Bacterial Metagenomic Analysis*, <https://kns.cnki.net/kcms/detail/detail.aspx?FileName=CN110392741A&DbName=SCPD2019>, 2019.
- [16] Y. Qi, S. Kim, E. M. Richards, M. K. Raizada, and C. J. Pepine, "Gut microbiota: potential for a unifying hypothesis for prevention and treatment of hypertension," *Circulation Research*, vol. 120, no. 11, pp. 1724–1726, 2017.
- [17] S. Wang, L. Ren, L. Jia et al., "Effect of acupuncture at Neiguan (PC 6) on cardiac function using echocardiography in myocardial ischemia rats induced by isoproterenol," *Journal of Traditional Chinese Medicine*, vol. 35, no. 6, pp. 653–658, 2015.
- [18] P. Li, K. F. Pitsillides, S. V. Rendig, H.-L. Pan, and J. C. Longhurst, "Reversal of reflex-induced myocardial ischemia by median nerve stimulation: a feline model of electroacupuncture," *Circulation*, vol. 97, no. 12, pp. 1186–1194, 1998.
- [19] E. L. W. Santos, B. H. M. Dias, A. C. R. d. Andrade et al., "Effects of acupuncture and electroacupuncture on estradiol-induced inflammation and oxidative stress in health rodents," *Acta Cirurgica Brasileira*, vol. 28, no. 8, pp. 582–588, 2013.
- [20] Z. Cheng, Y. Chen, and T. Zhang, "Effect of mild moxibustion on intestinal flora of chronic fatigue rats," *Chinese Journal Infarction Traditional Chinese Medicine*, vol. 20, no. 1, pp. 45–63, 2013.
- [21] M. Y. Yoon and S. S. Yoon, "Disruption of the gut ecosystem by antibiotics," *Yonsei Medical Journal*, vol. 59, no. 1, pp. 4–12, 2018.
- [22] G. A. Weiss and T. Hennot, "Mechanisms and consequences of intestinal dysbiosis," *Cellular and Molecular Life Sciences*, vol. 74, no. 16, pp. 2959–2977, 2017.
- [23] E. Hayashi, J. Yamada, M. Kunitomo, M. Terada, and M. Sato, "Fundamental studies on physiological and pharmacological actions of L-ascorbate 2-sulfate. V. On the hypolipidemic and antiatherosclerotic effects of L-ascorbate 2-sulfate in rabbits," *The Japanese Journal of Pharmacology*, vol. 28, no. 1, pp. 61–72, 1978.
- [24] F. J. Finamore, R. P. Feldman, and G. E. Cosgrove, "L-ascorbic acid, L-ascorbate 2-sulfate, and atherogenesis," *International Journal for Vitamin and Nutrition Research*, vol. 46, no. 3, pp. 275–285, 1976.
- [25] H. M. Ryu, Y. J. Kim, E. J. Oh et al., "Hypoxanthine induces cholesterol accumulation and incites atherosclerosis in apo-lipoprotein E-deficient mice and cells," *Journal of Cellular and Molecular Medicine*, vol. 20, no. 11, pp. 2160–2172, 2016.
- [26] M. Huang, R. Wei, Y. Wang, T. Su, P. Li, and X. Chen, "The uremic toxin hippurate promotes endothelial dysfunction via the activation of Drp1-mediated mitochondrial fission," *Redox Biology*, vol. 16, pp. 303–313, 2018.

- [27] K. Zha, C. Zuo, A. Wang et al., "LDL in patients with sub-clinical hypothyroidism shows increased lipid peroxidation," *Lipids in Health and Disease*, vol. 14, no. 1, p. 95, 2015.
- [28] I. De Meyer, W. Martinet, C. E. Van Hove et al., "Inhibition of inositol monophosphatase by lithium chloride induces selective macrophage apoptosis in atherosclerotic plaques," *British Journal of Pharmacology*, vol. 162, no. 6, pp. 1410–1423, 2011.
- [29] J. Wang, L. Wang, H. Yang et al., "Prevention of atherosclerosis by Yindan Xinnaotong capsule combined with swimming in rats," *BMC Complementary and Alternative Medicine*, vol. 15, no. 1, p. 109, 2015.
- [30] P. Hou, S. Hu, J. Wang et al., "Exogenous supplement of N-acetylneuraminic acid improves macrophage reverse cholesterol transport in apolipoprotein E-deficient mice," *Lipids in Health and Disease*, vol. 18, no. 1, p. 24, 2019.
- [31] I. Zeb, N. Ahmadi, J. Kadakia et al., "Aged garlic extract and coenzyme Q10 have favorable effect on inflammatory markers and coronary atherosclerosis progression: a randomized clinical trial," *Journal of Cardiovascular Disease Research*, vol. 3, no. 3, pp. 185–190, 2012.
- [32] Y. Kawai, " β -Glucuronidase activity and mitochondrial dysfunction: the sites where flavonoid glucuronides act as anti-inflammatory agents," *Journal of Clinical Biochemistry and Nutrition*, vol. 54, no. 3, pp. 145–150, 2014.
- [33] M. J. Forteza, K. A. Polyzos, R. Baumgartner et al., "Activation of the regulatory T-cell/indoleamine 2,3-dioxygenase Axis reduces vascular inflammation and atherosclerosis in hyperlipidemic mice," *Frontiers in Immunology*, vol. 9, p. 950, 2018.
- [34] V. Kundumani-Sridharan, E. Dyukova, D. E. Hansen, and G. N. Rao, "12/15-Lipoxygenase mediates high-fat diet-induced endothelial tight junction disruption and monocyte transmigration: a new role for 15(S)-hydroxyeicosatetraenoic acid in endothelial cell dysfunction," *Journal of Biological Chemistry*, vol. 288, no. 22, pp. 15830–15842, 2013.
- [35] J. W. Heinecke, H. Rosen, L. A. Suzuki, and A. Chait, "The role of sulfur-containing amino acids in superoxide production and modification of low density lipoprotein by arterial smooth muscle cells," *The Journal of Biological Chemistry*, vol. 262, no. 21, pp. 10098–10103, 1987.
- [36] A. Almas, Y. Forsell, V. Millischer, J. Möller, and C. Lavebratt, "Association of Catechol-O-methyltransferase (COMT Val158Met) with future risk of cardiovascular disease in depressed individuals—a Swedish population-based cohort study," *BMC Medical Genetics*, vol. 19, no. 1, p. 126, 2018.
- [37] P.-S. Yang, M.-J. Wang, T. Jayakumar et al., "Antiproliferative activity of Hinokitiol, a Tropolone derivative, is mediated via the inductions of p-JNK and p-plc γ 1 signaling in PDGF-BB-stimulated vascular smooth muscle cells," *Molecules*, vol. 20, no. 5, pp. 8198–8212, 2015.

Research Article

The Protective Effect of Qishen Granule on Heart Failure after Myocardial Infarction through Regulation of Calcium Homeostasis

Xiaomin Yang ¹, Qiyan Wang,¹ Zifan Zeng,² Qian Zhang,³ Fang Liu,⁴ Hong Chang,⁵ Chun Li ⁶, Wei Wang ³ and Yong Wang ¹

¹School of Life Sciences, Beijing University of Chinese Medicine, Beijing 100029, China

²State Key Laboratory of Bioactive Substances and Function of Natural Medicine, Institute of Materia Medica, Peking Union Medical College and Chinese Academy of Medical Sciences, Beijing 100050, China

³College of Chinese Medicine, Beijing University of Chinese Medicine, Beijing 100029, China

⁴School of Chinese Materia Medica, Beijing University of Chinese Medicine, Beijing 100029, China

⁵Traditional Chinese Medicine College, North China University of Science and Technology, Tangshan, Hebei 063210, China

⁶Modern Research Center for Traditional Chinese Medicine, School of Chinese Materia Medica, Beijing University of Chinese Medicine, Beijing 100029, China

Correspondence should be addressed to Chun Li; lichun19850204@163.com, Wei Wang; wangwei@bucm.edu.cn, and Yong Wang; doctor_wangyong@163.com

Received 5 June 2020; Revised 26 August 2020; Accepted 22 September 2020; Published 23 October 2020

Academic Editor: Ester Pagano

Copyright © 2020 Xiaomin Yang et al. This is an open access article distributed under the Creative Commons Attribution License, which permits unrestricted use, distribution, and reproduction in any medium, provided the original work is properly cited.

Qishen granule (QSG) is a frequently prescribed traditional Chinese medicine formula, which improves heart function in patients with heart failure (HF). However, the cardioprotective mechanisms of QSG have not been fully understood. The current study aimed to elucidate whether the effect of QSG is mediated by ameliorating cytoplasmic calcium (Ca^{2+}) overload in cardiomyocytes. The HF rat model was induced by left anterior descending (LAD) artery ligation surgery. Rats were randomly divided into sham, model, QSG-low dosage (QSG-L) treatment, QSG-high dosage (QSG-H) treatment, and positive drug (diltiazem) treatment groups. 28 days after surgery, cardiac functions were assessed by echocardiography. Levels of norepinephrine (NE) and angiotensin II (AngII) in the plasma were evaluated. Expressions of critical proteins in the calcium signaling pathway, including cell membrane calcium channel $\text{CaV}1.2$, sarcoendoplasmic reticulum ATPase 2a (SERCA2a), calcium/calmodulin-dependent protein kinase type II (CaMKII), and protein phosphatase calcineurin (CaN), were measured by Western blotting (WB) and immunohistochemistry (IHC). Echocardiography showed that left ventricular ejection fraction (EF) and fractional shortening (FS) value significantly decreased in the model group compared to the sham group, and illustrating heart function was severely impaired. Furthermore, levels of NE and AngII in the plasma were dramatically increased. Expressions of $\text{CaV}1.2$, CaMKII, and CaN in the cardiomyocytes were upregulated, and expressions of SERCA2a were downregulated in the model group. After treatment with QSG, both EF and FS values were increased. QSG significantly reduced levels of NE and AngII in the plasma. In particular, QSG prevented cytoplasmic Ca^{2+} overload by downregulating expression of $\text{CaV}1.2$ and upregulating expression of SERCA2a. Meanwhile, expressions of CaMKII and CaN were inhibited by QSG treatment. In conclusion, QSG could effectively promote heart function in HF rats by restoring cardiac Ca^{2+} homeostasis. These findings revealed novel therapeutic mechanisms of QSG and provided potential targets in the treatment of HF.

1. Introduction

Heart failure remains one of the major threats to people's health, although great progress has been made in the understanding of HF pathophysiology and advances in its therapeutic strategies [1]. It poses the entire medical community a tremendous challenge to further explore HF pathogenesis and the treatment approaches. In recent decades, the maintenance of cardiac calcium homeostasis in HF development has been extensively investigated due to its roles in HF progress [2, 3]. Of note, cardiac calcium overload is so essential that it is considered as the attractive target for treating HF. Therefore, the calcium channel blockers in the management of HF has gained a great interest worldwide [4, 5].

Changes of calcium concentration in cardiomyocytes determine the contractility of the heart, thus to influence the heart function. Free calcium ions are mainly distributed in the extracellular fluid such as blood and intracellular organelles such as sarcoplasmic reticulum. However, it is the cytosolic Ca^{2+} concentration that directly determines the myocardial contractility. During cardiac excitation-contraction coupling, calcium concentration in the cytosol increases approximately 10-fold because extracellular Ca^{2+} flows into the cardiomyocyte via the cardiac cell membrane calcium channel CaV1.2 and triggers more Ca^{2+} release from the sarcoplasmic reticulum membranes [6, 7]. Relaxation occurs when Ca^{2+} is pumped back into the SR by SERCA2a [8, 9]. In the failing heart, cytosolic calcium is overload due to excessive calcium entry from the extracellular fluid and SR or reduced calcium efflux from the cytosol. Abnormally activated CaV1.2 or reduced expression of SERCA2a leads to accumulation of Ca^{2+} in the cytosol, which prevents relaxation and further impairs contractility due to depletion of the Ca^{2+} available for release during systole [10, 11].

Furthermore, CaMKII and CaN in the cytosol are two of the most important calcium-dependent signaling proteins, which can bind with the increasing Ca^{2+} in the cytosol, thus to induce cardiac hypertrophy and remodeling directly [12–14]. Cytosolic calcium overload during HF could be induced by excessive activation of two core signaling pathways, including the β -adrenergic signaling pathway and renin-angiotensin-aldosterone pathway [15, 16]. Activation of the β -adrenergic pathway by NE activates the protein kinase A (PKA) and CaMKII and subsequently phosphorylates CaV1.2 , which results in an increase of cytosolic calcium entry from the extracellular fluid [17]. Meanwhile, phosphorylation of the ryanodine receptor isoform 2 by PKA leads to diastolic leakage of calcium from the SR during heart failure [18]. Moreover, activation of AngII in HF can facilitate calcium flow into the myocardial cells by changing the permeability of CaV1.2 , and increase cytosolic calcium ions by promoting the release of calcium from SR, which finally lead to myocardial fibrosis [19].

Traditional Chinese medicine (TCM) has been applied in the treatment and prevention of HF for thousands of years. Qishen granule, one of the most widely prescribed herbal formulae, is composed of six herbs, including *Radix Astragali Mongolici*, *Salvia miltiorrhiza Bunge*, *Flos*

Lonicerae, *Scrophularia*, *Radix Aconiti Lateralis Preparata*, and *Radix Glycyrrhizae*. This formulae is widely manufactured in China in accordance with the China Pharmacopoeia standard of quality control. The fingerprint of QSG was analyzed by HPLC-IT-TOF-MS, and the typical chromatograms were reported as we described before [20]. Our previous studies have demonstrated that QSG has a definite effect in improving heart function. Study based on network pharmacology predicted that the calcium signaling pathway was one of the most potential drug targets of QSG [21]. However, whether its efficacy is related to amelioration of abnormal accumulation of Ca^{2+} in the cytosol remains poorly defined.

In this study, we aim to investigate the underlying pharmacological mechanisms of QSG in the HF model. The effects of QSG on calcium transfer proteins and calcium/calmodulin-dependent enzymes were studied. The HF model was induced by ligation of the left anterior descending coronary artery in rats. This study will provide insight into the therapeutic mechanisms of QSG and provide the experimental basis for its clinical application.

2. Materials and Methods

2.1. Herbs Preparation. QSG were composed of 460 g *Radix Astragali Mongolici*, 230 g *Salvia miltiorrhiza Bunge*, 160 g *Flos Lonicerae*, 160 g *Scrophularia*, 140 g *Radix Aconiti Lateralis Preparata*, and 90 g *Radix Glycyrrhizae*. These herbs were purchased from Beijing Tong Ren Tang Chinese Medicine Co., Ltd. (Beijing, China) and prepared in the traditional Chinese medicine preparation department of Beijing China-Japan Friendship Hospital. The major extraction steps were performed as described previously [20]. Briefly, herbs were extracted by water for three times. Then, the water extract was concentrated and precipitated by ethanol. The sediment was dried and screened over an 80-mesh sieve for crushing. After preparation, the extracted QSG was enriched by 4 times. The fingerprint spectrum was further established by the high-performance liquid chromatography (HPLC) method in our previous studies [20, 22]. The major components are formononetin, tanshinone IIA, tanshinone I, cryptotanshinone, and harpagoside [23]. The Chinese herbs were identified by Professor Jian Ni, School of Chinese Materia Medica, Beijing University of Chinese Medicine. The voucher specimens (Voucher numbers: HQ-2016-007; DQ-2016-008; JYH-2016-009; XS-2016-010; FZ-2016-011; and GC-2016-012) were submitted to Department of Chinese Medicine Teaching and Research, School of Traditional Chinese Medicine, Beijing University of Chinese Medicine.

2.2. Animal Grouping and Induction of Acute Myocardial Infarction (AMI). Sixty male Sprague-Dawley (SD) rats (weighted 220 ± 10 g) were randomly divided into five groups including sham-operated, model, QSG-low dosage treatment, QSG-high dosage treatment, and positive drug (diltiazem) treatment groups. Rats were purchased from Beijing Si Bei Fu Biotechnology Co., Ltd. (Beijing, China). Studies were performed with the approval of the Animal

Care Committee of Beijing University of Chinese Medicine. The rats were regularly fed for one week before surgery.

Models of HF after AMI were induced by left anterior descending artery ligation surgeries. The operational procedure has been described in our previous study [21]. Briefly, left thoracotomies of the rats were performed after anaesthetized via intraperitoneal injection by 1% pentobarbital sodium at the dosage of 50 mg/kg. LAD coronary arteries were then ligated with 5-0 polypropylene sutures. After ligation, the thoraxes were closed, and the rats were given sodium penicillin for 3 continuous days to prevent the potential inflammation. Rats in the sham group received the same procedure except that the coronary arteries were not ligated. A total of 25 rats died within 24 hrs after the surgery due to lethal arrhythmias or acute pump failure. 7 rats in each group were reserved for further research, and they were all analyzed at the end of study. From the second day after surgery, rats were treated with drugs or water via oral gavage for 28 consecutive days. QSG-L and QSG-H treatment groups received QSG at the raw dosage of 9.33 g/kg or 18.66 g/kg per day, respectively. The positive group received diltiazem at the dosage of 37.5 mg/kg per day. QSG and diltiazem were dissolved in water. Animals in the sham and model groups were given a gavage of normal water. After 28 days, cardiac functions were assessed by echocardiography. The rats were anaesthetized using 1% pentobarbital sodium at the dosage of 50 mg/kg via intraperitoneal injection, then blood samples were collected through abdominal aorta puncture, and hearts were harvested. The tissues were stored in the liquid nitrogen or 4% paraformaldehyde for further use.

2.3. Measurement of Cardiac Functions. Cardiac functions were assessed by echocardiography after rats were anaesthetized at 28 days after surgery. By using a Vevo 2100 (Visual Sonics Inc, Toronto, Ontario, Canada) and a PST 65A sector scanner (8 MHz probe), two dimensional images were generated at a frame rate of 300–500 frames/s. The parameters of cardiac functions include left ventricular ejection fraction, fractional shortening, left ventricular internal dimension-systole (LVID; s), and left ventricular internal dimension-diastole (LVID; d).

2.4. Morphometric Analysis. The new harvested hearts were crosscut 5 mm below the ligature. The upper parts of hearts were fixed in 4% paraformaldehyde for 72 hrs. After that, heart tissues were embedded in paraffin and sectioned into 5 μ m slices. Masson's staining was applied to evaluate the degree of myocardial fibrosis.

2.5. Measurement of Plasma Indicators. Level of norepinephrine in plasma was measured by enzyme-linked immunosorbent assay (ELISA) (ST-360 microplate reader, Shanghai Ke Hua Co., Ltd., Shanghai, China). Blood was left at room temperature for 30 min and then centrifuged for 10 min at 3000g. The upper plasma was collected for measurement. Level of angiotensin II in plasma was measured by radioimmunoassay (RIA) (DFM-96 radioimmunoanalyzer, Hefei Zhong Cheng electromechanical

Co., Ltd., Hefei, China). The blood was homogenized on ice in saline containing an enzyme inhibitor (0.30 M EDTA-Na 10 μ L, 0.34 M 8-hydroxyquinoline 10 μ L, and 0.32 M dimercaptopropanol 5 μ L per mL blood). The homogenate was centrifuged at 3000g for 10 min, and then, the supernatant was used for determination. Norepinephrine and angiotensin II were both determined in Beijing Zhong Tong Lan Bo Clinical Laboratory (Beijing, China). Each assay was performed following respective instructions. Standards at a series of concentrations were run in parallel with the samples. The concentrations in the samples were calculated in reference to the corresponding standard curves.

2.6. Measurement of Indicators by Western Blotting. Cardiac tissues were lysed using RIPA buffer (50 mM Tris-HCl pH 7.4, 150 mM NaCl, 1% NP-40, and 0.1% SDS) containing a protease inhibitor cocktail. Total proteins were extracted from these homogenates, and protein concentrations were measured by a protein assay kit. After boiling for 5 min, equal amounts of protein extracts (50 μ g) were separated by 10% sodium dodecyl sulphate- (SDS-) polyacrylamide gel electrophoresis (Bio-Rad, CA, U.S.A.) and transferred onto PVDF membranes electrophoretically. The membranes then were blocked with 5% nonfat dry milk in Tris buffered saline (20 mM Tris, pH 7.6, and 137 mM NaCl) with 0.1% Tween 20 followed by incubation with primary antibodies. Primary antibodies employed included mouse monoclonal anticalcium channel L type DHPR alpha 2 subunit (CaV1.2, ab2864, Abcam, UK), rabbit monoclonal anti-SERCA2 ATPase (SERCA2a, ab137020, Abcam, UK), rabbit monoclonal anti-CaMKII delta (CaMKII, ab181052, Abcam, UK), rabbit monoclonal anticalcineurin A (CaN, ab52761, Abcam, UK), and mouse monoclonal anti-glyceraldehyde-3-phosphate dehydrogenase (GAPDH, ab8245, Abcam, UK). After incubation with the primary antibodies, the membranes were washed for 3 times, and then incubated with the secondary antibodies (SA00001-1 or SA00001-2, Proteintech Group, Inc., U.S.A.). The membranes were treated with ECL Plus Western blotting detection reagent for 1 min at room temperature. The bands in the membrane were visualized and analyzed using UVP BioImaging Systems. Protein expressions were normalized by the GAPDH band densities.

2.7. Measurement of Indicators by IHC. IHC was performed by using immunohistochemistry kits (Wuhan Service Biotechnology Co., Ltd., Wuhan, China). Briefly, histological sections were deparaffinized in xylene, rehydrated in alcohol gradient, and then rinsed in water. Following antigen retrieval, the sections were treated with 3% hydrogen peroxide to block endogenous peroxides and incubated with 3% bovine serum albumin to block nonspecific staining. The slides were then incubated with primary antibody (mouse monoclonal anticalcium channel L type DHPR alpha-2 subunit, CaV1.2, ab2864, Abcam, UK) overnight at 4°C. The immunoreaction was achieved with the secondary antibody (the goat antimouse antibody, SA00001-1, Proteintech Group, Inc., U.S.A.) and developed with 3,3'-diaminobenzidine tetrahydrochloride (DAB). After they were stained by hematoxylin for 3 min, the slides were dehydrated

by graded ethanol and xylene and mounted with rhamsan gum. The immunostaining results were observed under the optical microscope and photographed. Positive area was specific stained brown–yellow. The proportion of positive area to total tissue area represented CaV1.2 expressions.

2.8. Statistical Analysis. Statistical analyses were performed by the one-way analysis of variance (ANOVA) test using SPSS 17.0 software. $P < 0.05$ was considered statistically significant. Data were presented as mean \pm standard deviation (mean \pm SD).

3. Results

3.1. QSG Could Restore Heart Function and Ameliorate Myocardial Fibrosis in HF Rats after AMI. Parameters of cardiac functions were detected by echocardiography. Representative *M*-mode frames are shown in Figure 1(a). Values of EF and FS in the model group decreased by 68.90% ($P < 0.001$) and 74.63% ($P < 0.001$) compared with those in the sham group. Meanwhile, LVID; s and LVID; d in the model group increased significantly by 185.03% ($P < 0.001$) and 61.13% ($P < 0.001$) as compared with those in the sham group. EF and FS values in the QSG-L group were upregulated by 44.47% ($P < 0.05$) and 65.17% ($P < 0.05$), respectively, compared with those in the model group. In the QSG-H group, EF and FS values were upregulated by 67.32% ($P < 0.01$) and 65.17% ($P < 0.01$). Diltiazem treatment also improved the function and ventricular structure (Figure 1(b)). The values of EF, FS, LVID; s, and LVID; d, are shown in Table 1.

Masson staining was applied to assess the degree of myocardial fibrosis. As shown in Figure 1(c), there was little interstitial collagen deposition in the sham group. However, extensive collagen deposition, as indicated by blue stains, was observed in the model group. In the QSG-L, QSG-H, and diltiazem groups, collagen deposition was inhibited as compared with the model group.

3.2. Effects of QSG on Plasma Indicators of NE and AngII in HF Rats after AMI. The increase of plasma indicators NE and AngII could reflect the alteration of cardiac functions and influence the calcium level in cardiac myocytes. Compared with the sham group, the levels of NE (Figure 2(a)) and AngII (Figure 2(b)) of the model group were increased by 79.76% ($P < 0.01$) and 55.43% ($P < 0.001$), respectively. After treatment with QSG-L, the plasma levels of NE and AngII were decreased by 48.76% ($P < 0.01$) and 62.86% ($P < 0.001$), respectively, as compared with the model group. QSG-H treatment decreased NE and AngII by 60.70% ($P < 0.001$) and 58.13% ($P < 0.001$). The positive drug diltiazem also downregulated the plasma levels of NE and AngII. These results suggested that QSG had a cardioprotective effect under ischemic stimulus and had the potential role of reducing the calcium level in cardiac myocytes.

3.3. Effects of QSG on Expressions of CaV1.2 and SERCA2a in HF Rats after AMI. CaV1.2 was assessed by immunohistochemistry and Western blot. Integrated optical density (IOD) and expression of CaV1.2 in the model group were increased by 86.87% ($P < 0.001$) and 43.61% ($P < 0.001$) compared with the sham group. After treatment with QSG-L and QSG-H, the IOD of CaV1.2 were decreased by 23.34% ($P < 0.001$) and 33.46% ($P < 0.001$) respectively, and the protein levels were decreased by 20.41% ($P > 0.05$) and 41.19% ($P < 0.001$), respectively, indicating that QSG-L and QSG-H could reduce the flow of extracellular calcium into the cytoplasm of cardiac myocytes. The positive control drug diltiazem also significantly suppressed the expression of CaV1.2 (Figures 3(a) and 3(b)).

Expression of SERCA2a in the model group was downregulated significantly by 202.74% ($P < 0.001$) compared with the sham group. Treatment with QSG-L and QSG-H upregulated expressions of SERCA2a by 101.09% ($P < 0.05$) and 163.83% ($P < 0.001$), respectively, as compared with the model group. In diltiazem treatment group, the expression of SERCA2a was upregulated by 104.98% ($P < 0.05$) compared with that in the model group (Figure 3(c)).

3.4. Effects of QSG on Expressions of CaMKII and CaN in HF Rats after AMI. To further confirm the effect of QSG on the calcium signaling pathway, levels of CaMKII and CaN were determined. Expressions of CaMKII and CaN were evaluated by WB. The protein level of CaMKII in the model group was upregulated by 48.86% ($P < 0.01$) compared with the sham group. In QSG-L and QSG-H group, the expressions of CaMKII were downregulated by 44.50% ($P < 0.01$) and 68.16% ($P < 0.001$), respectively, compared with the model group. Diltiazem also downregulated the expression of CaMKII ($P < 0.05$), but the effect of diltiazem on CaMKII was milder than that of QSG-L and QSG-H groups (Figure 4(a)). Expression of CaN in the model group was increased by 55.33% ($P < 0.001$) compared with the sham group. Treatment with QSG-L and QSG-H downregulated expressions of CaN by 29.88% ($P < 0.05$) and 71.34% ($P < 0.001$), respectively, as compared with the model group. In diltiazem treatment group, expression of CaN was downregulated by 53.16% ($P < 0.001$) compared with those in the model group (Figure 4(b)).

4. Discussion

Traditional Chinese medicine has been widely used in the prevention and treatment of HF for thousands of years. QSG is a patent formula of TCM and has been shown to be effective in treating HF [24, 25]. In this study, by applying the rat model of heart failure after myocardial infarction, we investigated the pharmacological mechanisms of QSG in the treatment of myocardial infarction. Our major findings are as follows: (1) QSG could effectively improve the cardiac functions and ameliorate myocardial fibrosis in rats after AMI. (2) The therapeutic effects of QSG may be mediated by ameliorating cytoplasmic Ca^{2+} overload in the cardiac cells,

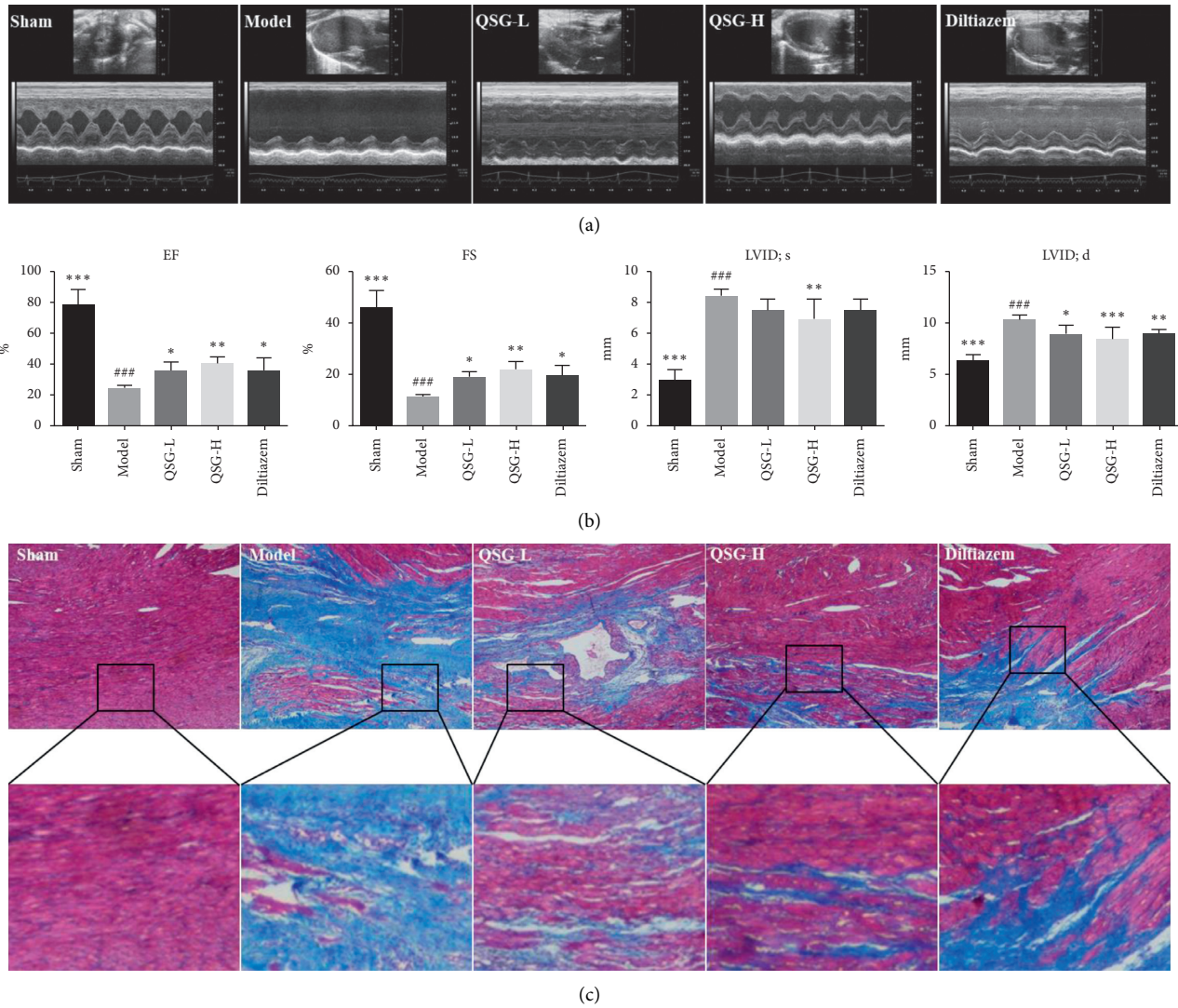


FIGURE 1: QSG could restore heart function and ameliorate myocardial fibrosis in HF rats after AMI. (a) Representative images of 2D echocardiogram in sham, model, QSG-L, QSG-H, and diltiazem groups. (b) Echocardiographic measurements of EF, FS, LVID; s, and LVID; d. QSG-L and QSG-H improved left ventricular EF and FS. (c) Masson staining indicated that QSG-L and QSG-H preserved cardiomyocyte structure and inhibited myocardial fibrosis. ## $P < 0.01$ and ### $P < 0.001$ vs. the sham group; * $P < 0.05$, ** $P < 0.01$, and *** $P < 0.001$ vs. the model group.

TABLE 1: Indicators of heart functions tested by echocardiography in different groups of rats.

Group	Sham	Model	QSG-L	QSG-H	Diltiazem
EF (%)	78.726 ± 9.228	24.483 ± 1.787	35.372 ± 5.861	40.965 ± 3.756	36.075 ± 7.323
FS (%)	46.033 ± 5.735	11.640 ± 0.691	19.497 ± 1.681	21.579 ± 2.976	19.576 ± 3.149
LVID; d (mm)	2.983 ± 0.628	8.502 ± 0.362	7.552 ± 0.599	6.895 ± 1.147	7.517 ± 0.702
LVID; d (mm)	6.432 ± 0.457	10.364 ± 0.394	9.014 ± 0.759	8.493 ± 1.050	8.943 ± 0.373

Data are presented as mean ± standard deviation (mean ± SD).

manifested by downregulation of cell membrane calcium channel CaV1.2 and upregulation of the SERCA2a. (3) CaMKII and CaN were inhibited by QSG treatment, which provided further evidence that QSG protected cardiac functions through the calcium signaling pathway.

Calcium signaling pathway plays a critical role in the process of heart failure. Calcium influx is also considered to

account for many detrimental effects of traditional inotropic drugs, such as glycosides digoxin [26]. Imbalance of calcium homeostasis in the cardiomyocytes not only directly interferes myocardial contraction and relaxation through calcium/calmodulin-dependent proteins but also exacerbates the heart failure process by interacting with other pathophysiological factors such as the β -adrenergic signaling

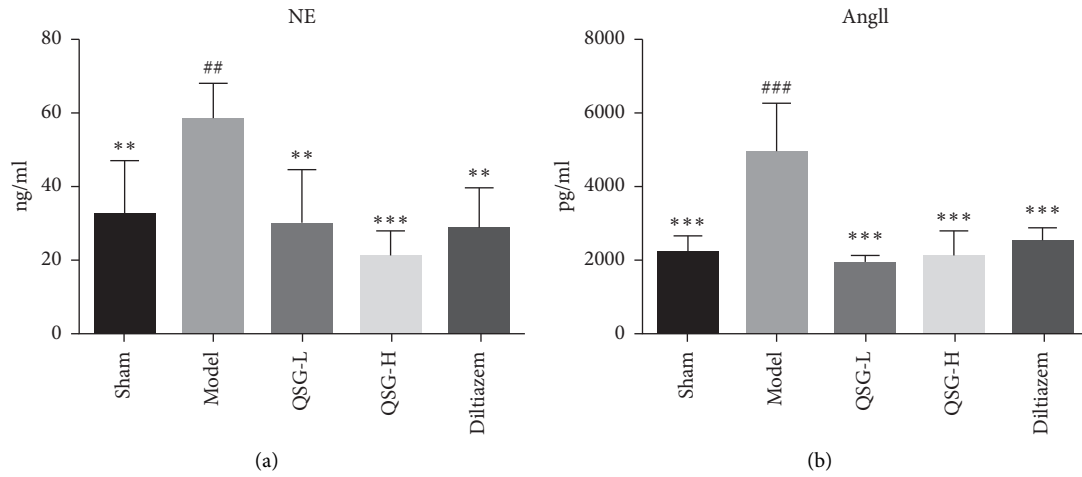


FIGURE 2: Effects of QSG on plasma indicators NE and AngII in HF rats after AMI. Plasma levels of NE (a) and AngII (b) in the five groups of rats were detected, respectively, by ELISA and RIA. QSG-L and QSG-H could decrease NE and AngII levels compared with the model group. Diltiazem had an effect similar to QSG-L and QSG-H groups. ## $P < 0.01$ and ### $P < 0.001$ vs. the sham group; * $P < 0.01$, *** $P < 0.001$ vs. the model group.

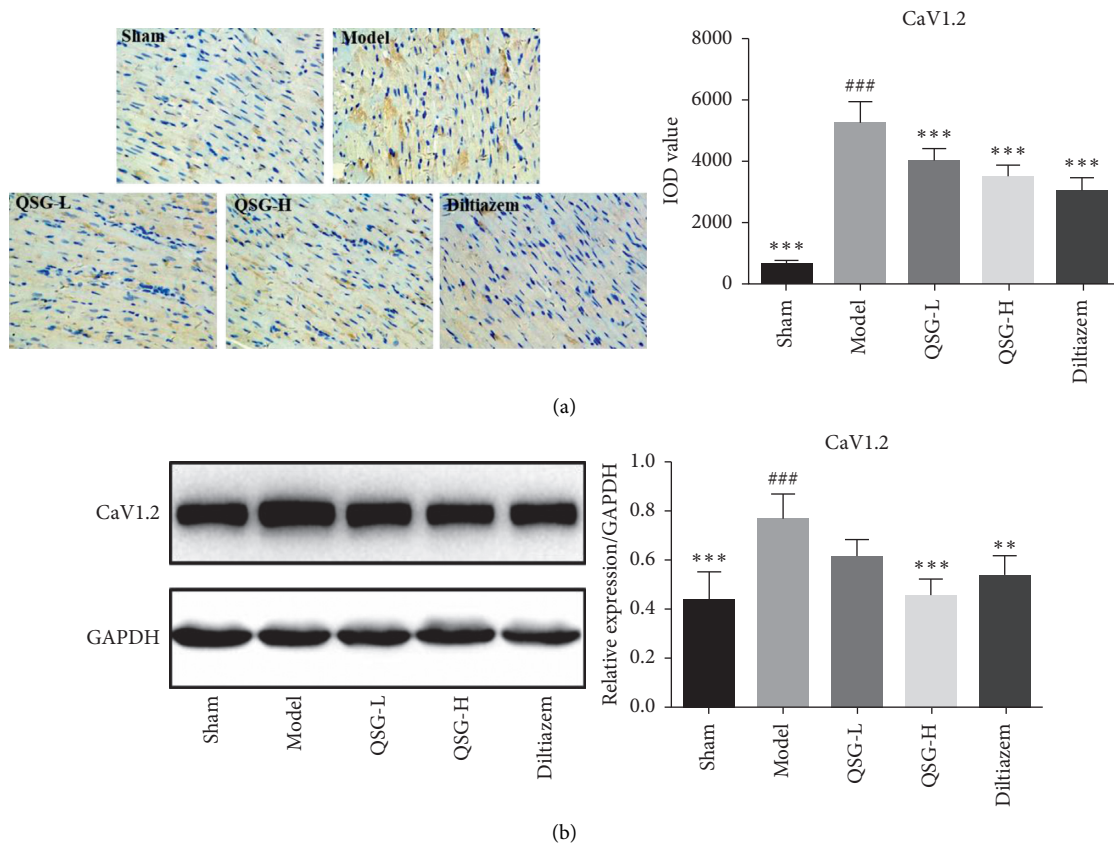
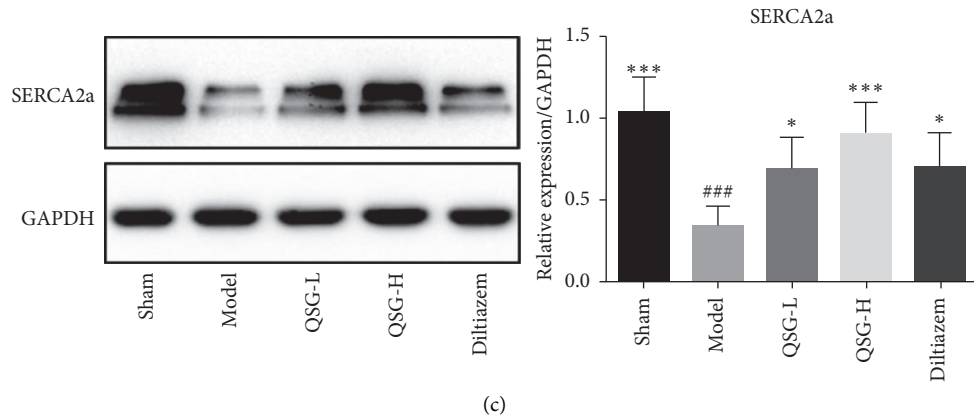
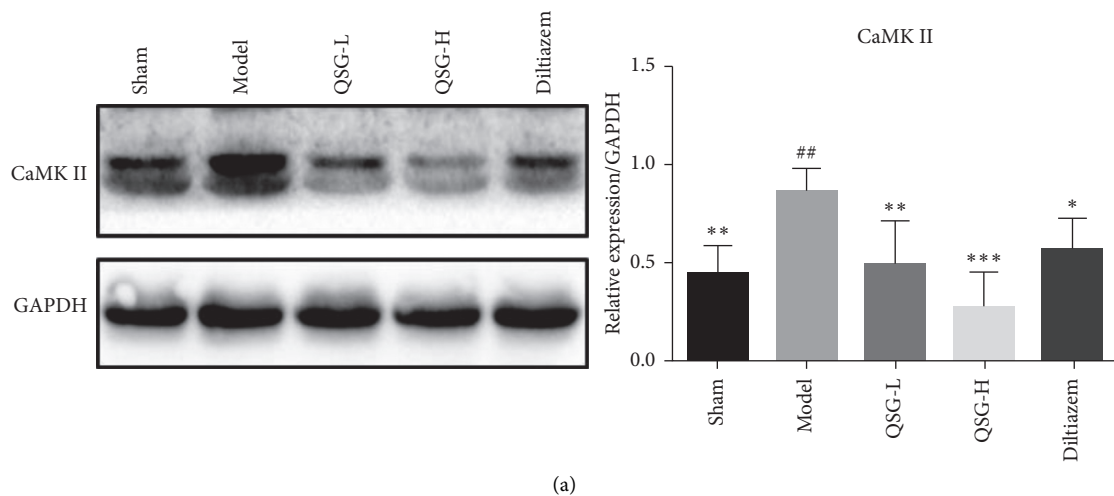


FIGURE 3: Continued.

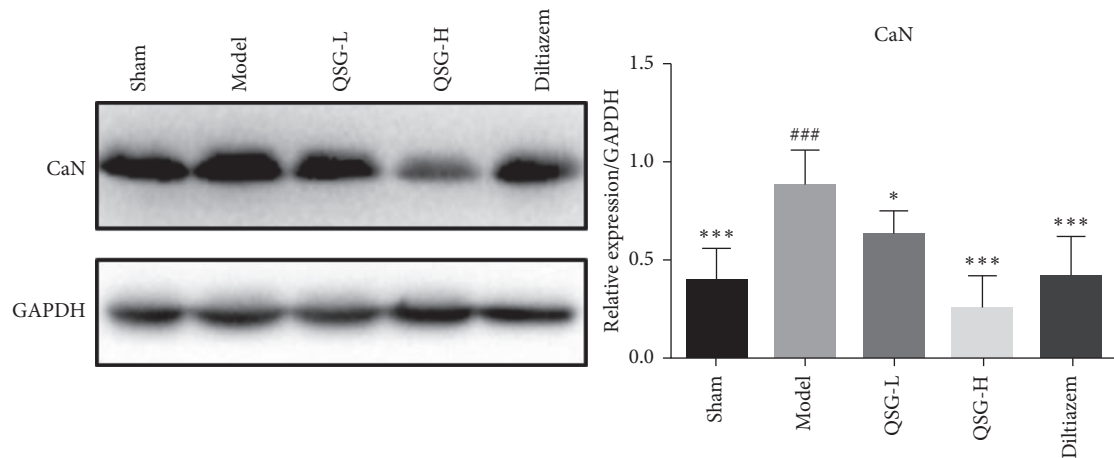


(c)

FIGURE 3: Effects of QSG on expressions of CaV1.2 and SERCA2a in HF rats after AMI. (a) Immunohistochemistry images of CaV1.2 and quantitative results in the heart tissues of rats in different groups. (b) WB bands of CaV1.2 and its quantitative results in the heart tissues of rats. (c) WB bands of SERCA2a and its quantitative results in the heart tissues of rats. IHC and WB results showed that the expression of CaV1.2 in the model group was upregulated compared with the sham group. QSG-L and QSG-H could decrease levels of CaV1.2 compared with the model group. Western blot showed that the expression of SERCA2a in the model group was downregulated compared with the sham group. QSG-L and QSG-H could increase protein levels of SERCA2a significantly compared with the model group. ### $P < 0.001$ vs. the sham group; * $P < 0.05$, ** $P < 0.01$, and *** $P < 0.001$ vs. the model group.



(a)



(b)

FIGURE 4: Effects of QSG on expressions of CaMKII and CaN in HF rats after AMI. (a) WB bands of CaMKII and its quantitative results in heart tissues of rats. (b) WB bands of CaN and its quantitative results in heart tissues of rats. Western blot showed that the expressions of CaMKII and CaN in the model group were upregulated compared with the sham group. QSG-L and QSG-H could decrease levels of CaMKII and CaN compared with the model group. ## $P < 0.01$ and ### $P < 0.001$ vs. the sham group; * $P < 0.05$, ** $P < 0.01$, and *** $P < 0.001$ vs. the model group.

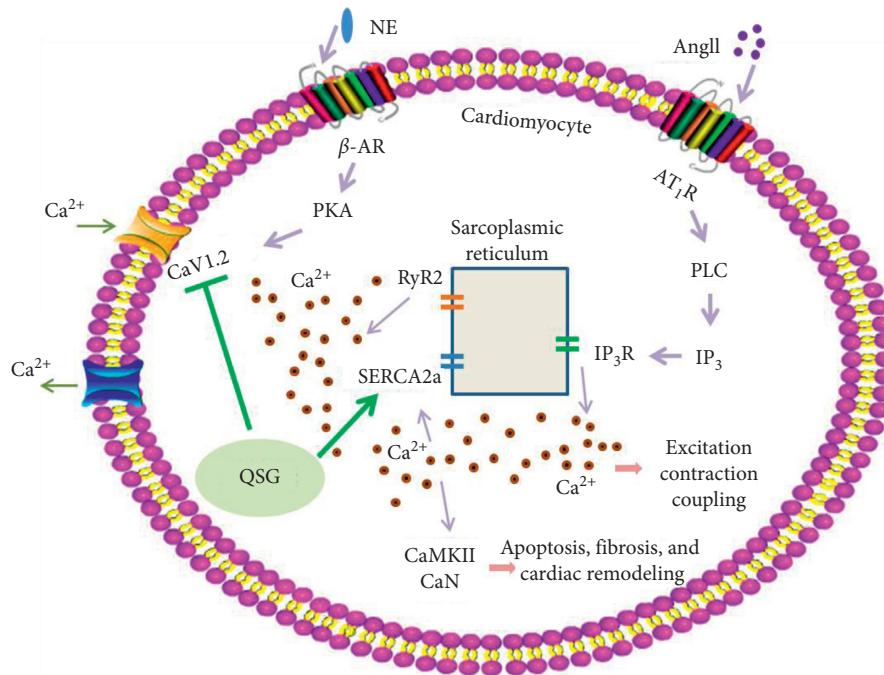


FIGURE 5: Potential mechanism of QSG efficacy on HF rats. QSG improved heart function and decreased cardiac remodeling by regulating the calcium signaling pathway. QSG ameliorated cytoplasmic Ca^{2+} overload in the cardiac cells, manifested by downregulation of CaV1.2 and upregulation of the SERCA2a and further confirmed by inhibition of CaMKII and CaN after QSG treatment.

pathway and renin-angiotensin-aldosterone system (RAAS) [27–30]. These pathophysiological changes were also confirmed by our experimental results. Heart function and the structure in HF rats after AMI were severely impaired, as illustrated by decreased EF and FS values and increased degrees of myocardial fibrosis in the model group compared to the sham group. In addition, expressions of critical channel proteins in the calcium signaling pathway were altered. Expression of CaV1.2 was upregulated, while SERCA2a was downregulated, and the levels of NE and AngII in the plasma were increased. These changes could inevitably lead to cytosolic Ca^{2+} overload by promoting extracellular Ca^{2+} influx and reducing the flow of cytoplasmic Ca^{2+} back into SR. Furthermore, Ca^{2+} overload in the cytosol would abnormally activate calcium/calmodulin-dependent protein kinase and protein phosphatase or upregulate their expressions. Our results showed that the expressions of CaMKII and CaN were definitely upregulated in the model group compared to the sham group. Our results were consistent with other studies which reported that the pathological changes of these molecules were found in HF. For example, it was reported that phosphorylation of CaV1.2 was increased during heart failure, and altered expression or mutation of CaV1.2 channels at Ser1700 caused reduced contractile function, cardiac hypertrophy, and heart failure [31, 32]. Furthermore, microdomain-targeted remodeling of CaV1.2 properties could influence calcium homeostasis and might contribute to ventricular arrhythmogenesis in the settings of HF-associated remodeling [33]. During heart failure, the expression of cardiac SERCA2a was downregulated, and the activity of SERCA2a was inhibited by its modulator, phospholamban [11]. It has been demonstrated

that CaMKII δ contributes to mitochondrial dysfunction and the transition from hypertrophy to HF [34]. In addition to inducing HF, CaMKII could further aggravate cytoplasmic Ca^{2+} overload by phosphorylating CaV1.2 at Ser1512/Ser1570 and ryanodine receptor 2 (RyR2) at Ser2030/Ser2814 [35, 36]. CaN dephosphorylates and induces the translocation of cytoplasmic NFAT to the nucleus and subsequently activates the transcription of prohypertrophic target genes [37]. Studies have showed that the responses of calcineurin and its substrates depend upon its composition of specific subcellular domains [38]. During heart failure, elevated levels of NE in the blood activated PKA and lead to hyperphosphorylation of CaV1.2, which further enhanced Ca^{2+} induced Ca^{2+} release through CaV1.2 and RyR2, and resulted in a significant decrease in SERCA2a protein and activity [39, 40]. In addition, AngII was shown to reduce calcium transient amplitudes and cardiomyocyte contractile function in a rat model of HF [41]. AngII was also found to promote CaN- β -mediated calcium influx in cardiomyocytes, which resulted in the upregulation of the expression of ANP and cardiac hypertrophy [42].

In recent decades, calcium-handling proteins become the attractive targets of drugs research and development in HF therapies. For example, vepoloxamer, a rheologic agent, improved left ventricular function in dogs with advanced heart failure by inhibiting Ca^{2+} entry into cardiomyocytes [43]. Zacopride, an inward rectifier potassium channel agonist, alleviated cardiac hypertrophy and failure via alterations in calcium dyshomeostasis in rats [44]. As shown in our results, QSG significantly improved the EF and FS value and ameliorated myocardial fibrosis in HF rats after AMI. Moreover, CaMKII and

CaN, the critical enzymes activated by high Ca^{2+} concentrations in the cytoplasm, were inhibited by QSG treatment. Studies have showed that inhibition of CaMKII suppressed diastolic Ca^{2+} waves, thus improving cardiac function in isoproterenol-challenged HF myocytes [45]. Excessive and sustained activation of CaN in the heart leads to fundamental changes in a number of substrates that often act in a feed-forward fashion, which contributes to pathological hypertrophic remodeling and accelerates cardiac decline [38]. In addition to QSG, several other traditional medicines were also found to act by inhibiting activities of CaMKII and CaN. For example, the YiQi-FuMai powder injection significantly attenuated HF and improved the cardiac function by downregulating phosphorylation of CaMKII [46]. Buckwheat rutin exhibited an inhibitory effect on AngII-induced hypertrophy in cultured neonatal rat cardiomyocytes via Ca^{2+} antagonism action, thus blocking the CaN-dependent signal pathway [47]. Furthermore, our results showed that QSG downregulated CaV1.2 and upregulated SERCA2a, which would reduce the excessive extracellular calcium influx and promote the cytosolic calcium back into the SR, thus partly preventing cytosolic Ca^{2+} overload in the cardiac cells. Levels of NE and AngII in the plasma decreased in the QSG group compared with the model group, which was beneficial to ameliorate cytosolic Ca^{2+} overload, as chronic activation of the sympathetic nervous system and RAAS are thought to be main reasons of defective Ca^{2+} handling in failing hearts. The pharmacological mechanisms of QSG in the treatment of HF might be mediated by downregulating CaV1.2 and upregulating SERCA2a, as shown in Figure 5. Similar with our findings, many studies have shown that therapies targeting the abovementioned critical molecules in the calcium signaling pathway were beneficial for treating HF [48–51]. Inhibition of L-type calcium channel reversed the susceptibility of atrial fibrillation in isoproterenol-induced HF mouse [48]. Gene-based therapies targeting SERCA2a led to improvements in calcium homeostasis and excitation-contraction coupling [50]. A novel pyrimidine-based CaMKII inhibitor was found to have the ability of increasing SR Ca^{2+} accumulation, and thus improving cardiomyocyte function effectively [49]. CaN inhibition in mice was shown to attenuate pathological cardiac hypertrophy [51].

5. Conclusions

QSG has regulatory effects on the calcium signaling pathway in cardiomyocytes of rats with heart failure, and the effects are mainly mediated by activating SERCA2a and inhibiting CaV1.2, CaMKII, and CaN. This study provides further insight into the therapeutic mechanism of QSG and proposes new strategies in the management of cardiovascular diseases by TCM.

Data Availability

The datasets used and analyzed during this study are available from the corresponding author upon reasonable request.

Conflicts of Interest

The authors declare that there are no conflicts of interest regarding the publication of this article

Authors' Contributions

Xiaomin Yang, Qiyan Wang, and Zifan Zeng contributed equally to this work.

Acknowledgments

This study was financially supported by the grants from the National Natural Science Foundation of China (81673802, 81530100, and 81822049), the Construction Project of Beijing Supporting Central Universities-Youth Talents Program (YETP0790), the Fundamental Research Funds for the Central Universities (2017-JYB-JS-020), Beijing Nova Program (Z171100001117028), and Scientific Research Program by Hebei Chinese Medicine Bureau (2018177).

References



- [1] S. S. Virani, A. Alonso, E. J. Benjamin et al., "Heart disease and stroke statistics-2020 update: a report from the American heart association," *Circulation*, vol. 141, no. 9, pp. e139–e596, 2020.
- [2] P. Djousse, "Noncoding RNAs in cardiovascular diseases," *Current Opinion in Cardiology*, vol. 34, no. 3, pp. 241–245, 2019.
- [3] P. Yampolsky, M. Koenen, M. Mosqueira et al., "Augmentation of myocardial I(f) dysregulates calcium homeostasis and causes adverse cardiac remodeling," *Nature Communications*, vol. 10, no. 1, p. 3295, 2019.
- [4] N. Mahon and W. J. McKenna, "Calcium channel blockers in cardiac failure," *Progress in Cardiovascular Diseases*, vol. 41, no. 3, pp. 191–206, 1998.
- [5] C. K. Lam, L. Tian, N. Belbachir et al., "Identifying the transcriptome signatures of calcium channel blockers in human induced pluripotent stem cell-derived cardiomyocytes," *Circulation Research*, vol. 125, no. 2, pp. 212–222, 2019.
- [6] D. M. Bers, "Cardiac sarcoplasmic reticulum calcium leak: basis and roles in cardiac dysfunction," *Annual Review of Physiology*, vol. 76, no. 1, pp. 107–127, 2014.
- [7] D. Sato, R. E. Dixon, L. F. Santana, and M. F. Navedo, "A model for cooperative gating of L-type Ca^{2+} channels and its effects on cardiac alternans dynamics," *PLoS Computational Biology*, vol. 14, no. 1, Article ID e1005906, 2018.
- [8] D. Jeong, J. Yoo, P. Lee et al., "miR-25 tough decoy enhances cardiac function in heart failure," *Molecular Therapy*, vol. 26, no. 3, pp. 718–729, 2018.
- [9] C. Quan, M. Li, Q. Du et al., "SPEG controls calcium reuptake into the sarcoplasmic reticulum through regulating SERCA2a by its second kinase-domain," *Circulation Research*, vol. 124, no. 5, pp. 712–726, 2019.
- [10] J. Ouyang, J. Cao, X. Jiang, L. Xu, and Y. Wang, "Kv4.3 expression reverses ICa remodeling in ventricular myocytes of heart failure," *Oncotarget*, vol. 8, no. 61, pp. 104037–104045, 2017.
- [11] Y. Zhang, L. Jiao, L. Sun et al., "LncRNA ZFAS1 as a SERCA2a inhibitor to cause intracellular Ca^{2+} overload and contractile

- dysfunction in a mouse model of myocardial infarction,” *Circulation Research*, vol. 122, no. 10, pp. 1354–1368, 2018.
- [12] K. Pan and H. Chen, “MiR-625-5p inhibits cardiac hypertrophy through targeting STAT3 and CaMKII,” *Human Gene Therapy Clinical Development*, vol. 30, no. 4, pp. 182–191, 2019.
- [13] T. Tenma, H. Mitsuyama, M. Watanabe et al., “Small-conductance Ca^{2+} -activated K^+ channel activation deteriorates hypoxic ventricular arrhythmias via CaMKII in cardiac hypertrophy,” *American Journal of Physiology-Heart and Circulatory Physiology*, vol. 315, no. 2, pp. H262–h272, 2018.
- [14] S. Tsutsui, N. Lozano-Vidal, M. D. López-Maderuelo, L. J. Jiménez-Borreguero, Á. L. Armesilla, and J. M. Redondo, “Cardiomyocyte calcineurin is required for the onset and progression of cardiac hypertrophy and fibrosis in adult mice,” *The FEBS Journal*, vol. 286, no. 1, pp. 46–65, 2019.
- [15] R. Kamada, H. Yokoshiki, H. Mitsuyama et al., “Arrhythmogenic β -adrenergic signaling in cardiac hypertrophy: the role of small-conductance calcium-activated potassium channels via activation of CaMKII,” *European Journal of Pharmacology*, vol. 844, pp. 110–117, 2019.
- [16] D. d. S. Soares, G. H. Pinto, A. Lopes et al., “Cardiac hypertrophy in mice submitted to a swimming protocol: influence of training volume and intensity on myocardial renin-angiotensin system,” *American Journal of Physiology-Regulatory, Integrative and Comparative Physiology*, vol. 316, no. 6, pp. R776–r782, 2019.
- [17] H. Yu, C. Yuan, R. E. Westenbroek, and W. A. Catterall, “The AKAP Cypher/Zasp contributes to β -adrenergic/PKA stimulation of cardiac $\text{CaV}1.2$ calcium channels,” *Journal of General Physiology*, vol. 150, no. 6, pp. 883–889, 2018.
- [18] S. O. Marx, S. Reiken, Y. Hisamatsu et al., “PKA phosphorylation dissociates FKBP12.6 from the calcium release channel (ryanodine receptor): defective regulation in failing hearts,” *Cell*, vol. 101, no. 4, pp. 365–376, 2000.
- [19] S. Mathieu, N. El Houry, K. Rivard, P. Paradis, M. Nemer, and C. Fiset, “Angiotensin II overstimulation leads to an increased susceptibility to dilated cardiomyopathy and higher mortality in female mice,” *Scientific Reports*, vol. 8, no. 1, p. 952, 2018.
- [20] K. Xia, Q. Wang, C. Li, Z. Zeng, Y. Wang, and W. Wang, “Effect of QSKL on MAPK and RhoA pathways in a rat model of heart failure,” *Evidence-Based Complementary and Alternative Medicine*, vol. 2017, Article ID 3903898, 13 pages, 2017.
- [21] Y. Wang, Z. Liu, C. Li et al., “Drug target prediction based on the herbs components: the study on the multitargets pharmacological mechanism of qishenkeli acting on the coronary heart disease,” *Evidence-Based Complementary and Alternative Medicine*, vol. 2012, Article ID 698531, 10 pages, 2012.
- [22] Y. Wang, W. Lin, C. Li et al., “Multipronged therapeutic effects of Chinese herbal medicine qishenyiqi in the treatment of acute myocardial infarction,” *Frontiers in Pharmacology*, vol. 8, p. 98, 2017.
- [23] Q. Zhang, J. Shi, D. Guo et al., “Qishen Granule alleviates endoplasmic reticulum stress-induced myocardial apoptosis through IRE-1-CRYAB pathway in myocardial ischemia,” *Journal of Ethnopharmacology*, vol. 252, Article ID 112573, 2020.
- [24] Y. Li, S. Wang, Z. Zhao et al., “Clinical assessment of complementary treatment with Qishen Yiqi dripping pills on ischemic heart failure: study protocol for a randomized, double-blind, multicenter, placebo-controlled trial (CACT-IHF),” *Trials*, vol. 14, no. 1, p. 138, 2013.
- [25] R. Huang, Y.-C. Cui, X.-H. Wei et al., “A novel traditional Chinese medicine ameliorates fatigue-induced cardiac hypertrophy and dysfunction via regulation of energy metabolism,” *American Journal of Physiology-Heart and Circulatory Physiology*, vol. 316, no. 6, pp. H1378–h1388, 2019.
- [26] E. D. Cummings and H. D. Swoboda, *Digoxin Toxicity*, StatPearls Publishing LLC., Treasure Island, FL, USA, 2020.
- [27] M. Luo and M. E. Anderson, “Mechanisms of altered Ca^{2+} handling in heart failure,” *Circulation Research*, vol. 113, no. 6, p. 690, 2013.
- [28] M. T. Mora, J. M. Ferrero, L. Romero, and B. Trenor, “Sensitivity analysis revealing the effect of modulating ionic mechanisms on calcium dynamics in simulated human heart failure,” *PLoS One*, vol. 12, no. 11, Article ID e0187739, 2017.
- [29] A. Babick, D. Chapman, S. Zieroth, V. Elimban, and N. S. Dhalla, “Reversal of subcellular remodelling by losartan in heart failure due to myocardial infarction,” *Journal of Cellular and Molecular Medicine*, vol. 16, no. 12, pp. 2958–2967, 2012.
- [30] E. D. Fowler, M. J. Drinkhill, R. Norman et al., “Beta1-adrenoceptor antagonist, metoprolol attenuates cardiac myocyte Ca^{2+} handling dysfunction in rats with pulmonary artery hypertension,” *Journal of Molecular and Cellular Cardiology*, vol. 120, pp. 74–83, 2018.
- [31] L. Yang, D.-F. Dai, C. Yuan et al., “Loss of β -adrenergic-stimulated phosphorylation of $\text{CaV}1.2$ channels on Ser1700 leads to heart failure,” *Proceedings of the National Academy of Sciences*, vol. 113, no. 49, pp. E7976–E7985, 2016.
- [32] O. M. Koval, X. Guan, Y. Wu et al., “ $\text{CaV}1.2$ beta-subunit coordinates CaMKII-triggered cardiomyocyte death and afterdepolarizations,” *Proceedings of the National Academy of Sciences*, vol. 107, no. 11, pp. 4996–5000, 2010.
- [33] J. L. Hund, A. Bhargava, T. O’Hara et al., “Microdomain-specific modulation of L-type calcium channels leads to triggered ventricular arrhythmia in heart failure,” *Circulation Research*, vol. 119, no. 8, pp. 944–955, 2016.
- [34] B. D. Punjabi, H. Ling, A. S. Divakaruni et al., “Mitochondrial reprogramming induced by CaMKII δ mediates hypertrophy decompensation,” *Circulation Research*, vol. 116, no. 5, pp. e28–39, 2015.
- [35] A. Miyamoto, A. Welling, S. Fischer et al., “Facilitation of murine cardiac L-type $\text{CaV}1.2$ channel is modulated by calmodulin kinase II-dependent phosphorylation of S1512 and S1570,” *Proceedings of the National Academy of Sciences*, vol. 107, no. 22, pp. 10285–10289, 2010.
- [36] A. E. Belevych, S. E. Sansom, R. Terentyeva et al., “MicroRNA-1 and -133 increase arrhythmogenesis in heart failure by dissociating phosphatase activity from RyR2 complex,” *PLoS One*, vol. 6, no. 12, Article ID e28324, 2011.
- [37] O. F. Bueno, E. van Rooij, J. D. Molkenin, P. A. Doevendans, and L. J. De Windt, “Calcineurin and hypertrophic heart disease: novel insights and remaining questions,” *Cardiovascular Research*, vol. 53, no. 4, pp. 806–821, 2002.
- [38] V. Parra and B. A. Rothermel, “Calcineurin signaling in the heart: the importance of time and place,” *Journal of Molecular and Cellular Cardiology*, vol. 103, pp. 121–136, 2017.
- [39] J. G. Ryall, J. D. Schertzer, K. T. Murphy, A. M. Allen, and G. S. Lynch, “Chronic β 2-adrenoceptor stimulation impairs cardiac relaxation via reduced SR Ca^{2+} -ATPase protein and activity,” *American Journal of Physiology-Heart and Circulatory Physiology*, vol. 294, no. 6, pp. H2587–H2595, 2008.
- [40] M. Lei, X. Wang, Y. Ke, and R. J. Solaro, “Regulation of Ca^{2+} transient by PP2A in normal and failing heart,” *Frontiers in Physiology*, vol. 6, p. 13, 2015.

- [41] F. Hohendanner, D. Bode, U. Primessnig et al., "Cellular mechanisms of metabolic syndrome-related atrial decompensation in a rat model of HFpEF," *Journal of Molecular and Cellular Cardiology*, vol. 115, pp. 10–19, 2018.
- [42] Y. Pieske, Y. Zhou, Z. Cao et al., "miR-155 functions downstream of angiotensin II receptor subtype 1 and calcineurin to regulate cardiac hypertrophy," *Experimental and Therapeutic Medicine*, vol. 12, no. 3, pp. 1556–1562, 2016.
- [43] H. N. Sabbah, K. Zhang, R. C. Gupta, and M. Emanuele, "Effects of intravenous infusion of vepoloxamer on left ventricular function in dogs with advanced heart failure," *Cardiovascular Drugs and Therapy*, vol. 34, no. 2, pp. 153–164, 2020.
- [44] Q. H. Liu, X. Qiao, L. J. Zhang et al., "I(K1) channel agonist zacopride alleviates cardiac hypertrophy and failure via alterations in calcium dyshomeostasis and electrical remodeling in rats," *Frontiers in Pharmacology*, vol. 10, p. 929, 2019.
- [45] A. E. Belevych, H. T. Ho, I. M. Bonilla et al., "The role of spatial organization of Ca²⁺ release sites in the generation of arrhythmogenic diastolic Ca²⁺ release in myocytes from failing hearts," *Basic Research in Cardiology*, vol. 112, no. 4, p. 44, 2017.
- [46] Y. Zhang, L. Zhang, Y. Zhang et al., "YiQiFuMai powder injection attenuates coronary artery ligation-induced heart failure through improving mitochondrial function via regulating ROS generation and CaMKII signaling pathways," *Frontiers in Pharmacology*, vol. 10, p. 381, 2019.
- [47] J. X. Chu, G. M. Li, X. J. Gao, J. X. Wang, and S. Y. Han, "Buckwheat rutin inhibits AngII-induced cardiomyocyte hypertrophy via blockade of CaN-dependent signal pathway," *Iranian Journal of Pharmaceutical Research: IJPR*, vol. 13, no. 4, pp. 1347–1355, 2014.
- [48] M. X. Zhang, J. K. Zheng, W. W. Wang et al., "Exchange-protein activated by cAMP (EPAC) regulates L-type calcium channel in atrial fibrillation of heart failure model," *European Review for Medical and Pharmacological Sciences*, vol. 23, no. 5, pp. 2200–2207, 2019.
- [49] S. Neef, A. Steffens, P. Pellicena et al., "Improvement of cardiomyocyte function by a novel pyrimidine-based CaMKII-inhibitor," *Journal of Molecular and Cellular Cardiology*, vol. 115, pp. 73–81, 2018.
- [50] W. J. Park and J. G. Oh, "SERCA2a: a prime target for modulation of cardiac contractility during heart failure," *BMB Reports*, vol. 46, no. 5, pp. 237–243, 2013.
- [51] E. N. Olson and J. D. Molkentin, "Prevention of cardiac hypertrophy by calcineurin inhibition: hope or hype?" *Circulation Research*, vol. 84, no. 6, pp. 623–632, 1999.

Research Article

Cardiac CaMKII δ and Wenxin Keli Prevents Ang II-Induced Cardiomyocyte Hypertrophy by Modulating CnA-NFATc4 and Inflammatory Signaling Pathways in H9c2 Cells

Na An,^{1,2} Yu Chen,³ Yanfen Xing,⁴ Honghua Wu,⁵ Xiongyi Gao,¹ Hengwen Chen,¹ Ke Song,² Yuanyuan Li,² Xinye Li,^{1,6} Fan Yang,¹ Xiandu Pan,^{1,6} Xiaofang He,² Xin Wang,² Yang Li,⁷ Yonghong Gao ,² and Yanwei Xing ¹

¹Guang'anmen Hospital, Chinese Academy of Chinese Medical Sciences, Beijing 100053, China

²Key Laboratory of Chinese Internal Medicine of Ministry of Education, Dongzhimen Hospital Affiliated to Beijing University of Chinese Medicine, Beijing 100700, China

³Fujian Health College, Fuzhou 350101, China

⁴Shanxi University of Chinese Medicine, Jinzhong 030619, China

⁵Tianjin State Key Laboratory of Modern Chinese Medicine, Tianjin Key Laboratory of TCM Chemistry and Analysis Institute of Traditional Chinese Medicine, Tianjin University of Traditional Chinese Medicine, Tianjin 300193, China

⁶Beijing University of Chinese Medicine, Beijing, China

⁷Department of Cardiology, General Hospital of People's Liberation Army, Beijing 100853, China

Correspondence should be addressed to Yonghong Gao; gaoyh7088@163.com and Yanwei Xing; xingyanwei12345@163.com

Na An, Yu Chen, Yanfen Xing, and Honghua Wu contributed equally to this work.

Received 26 July 2020; Revised 18 August 2020; Accepted 20 September 2020; Published 23 October 2020

Academic Editor: Hong Chang

Copyright © 2020 Na An et al. This is an open access article distributed under the Creative Commons Attribution License, which permits unrestricted use, distribution, and reproduction in any medium, provided the original work is properly cited.

Previous studies have demonstrated that calcium-/calmodulin-dependent protein kinase II (CaMKII) and calcineurin A-nuclear factor of activated T-cell (CnA-NFAT) signaling pathways play key roles in cardiac hypertrophy (CH). However, the interaction between CaMKII and CnA-NFAT signaling remains unclear. H9c2 cells were cultured and treated with angiotensin II (Ang II) with or without silenced CaMKII δ (siCaMKII) and cyclosporine A (CsA, a calcineurin inhibitor) and subsequently treated with Wenxin Keli (WXKL). Patch clamp recording was conducted to assess L-type Ca²⁺ current (I_{Ca-L}), and the expression of proteins involved in signaling pathways was measured by western blotting. Myocardial cytoskeletal protein and nuclear translocation of target proteins were assessed by immunofluorescence. The results indicated that siCaMKII suppressed Ang II-induced CH, as evidenced by reduced cell surface area and I_{Ca-L}. Notably, siCaMKII inhibited Ang II-induced activation of CnA and NFATc4 nuclear transfer. Inflammatory signaling was inhibited by siCaMKII and WXKL. Interestingly, CsA inhibited CnA-NFAT pathway expression but activated CaMKII signaling. In conclusion, siCaMKII may improve CH, possibly by blocking CnA-NFAT and MyD88 signaling, and WXKL has a similar effect. These data suggest that inhibiting CaMKII, but not CnA, may be a promising approach to attenuate CH and arrhythmia progression.

1. Introduction

Cardiomyocyte hypertrophy (CH) is an adaptive response to the pathological stimuli that maintain normal cardiac function. CH is a prerequisite marker of heart failure (HF)

and usually occurs after myocardial infarction and stress overload. Although the initially adaptive response can maintain cardiac output, sustained hypertrophic growth can lead to a pathological state that leads to decreased compliance, HF, and sudden death [1–5]. Therefore, CH remains

a major threat in the population, and it is necessary to elucidate the pivotal molecular mechanisms involved in CH that can ameliorate pathological CH responses. Different signaling molecules have been considered as causes of myocardial hypertrophy, including nuclear factor of activated T cells (NFAT), calcium-/calmodulin- (CaM-) dependent protein kinase II (CaMKII), and β -adrenergic receptors [6].

Calcineurin (CaN), a calcium- and CaM-dependent serine/threonine phosphatase, is a well-established mediator of β -adrenergic-induced CH [7, 8]. CaN consists of two subunits: the catalytic subunit (CnA) and a regulatory Ca^{2+} -binding subunit (CnB) [9, 10]. It is generally known that CaN plays an influential role in regulating pathological hypertrophy. The constitutive activation of CaN and its downstream target, NFAT, are thought to play an important role in abnormal CH [11, 12]. Moreover, it is known that CaMKII phosphorylates many vital signaling factors that are related to initiating abnormal hypertrophy [13]. Transgenic overexpression of the splice variants CaMKII δ b (located in the nucleus) and CaMKII δ c (located in the cytosol) promotes CH and dilated cardiomyopathy, respectively. However, the complete pathological molecular mechanism is not fully understood, which hinders the development of improved treatments for CH [14, 15]. Ca^{2+} -dependent signaling through CaMKII and CaN has been suggested to contribute to adverse CH [16]. However, the interaction between CaMKII and CnA-NFAT signaling for CH remains unclear.

Wenxin Keli (WXKL) is the first Chinese medicine approved by the Chinese state for its antiarrhythmic effects; the medicine can tonify q_i , supply y_{in} , promote blood circulation, and remove blood stasis according to the theory of traditional Chinese medicine. The main components of WXKL consist of *Nardostachys jatamansi* (D.Don) DC (Gansong), *Codonopsis pilosula* (Franch.) Nannf (Dangshen), *Panax notoginseng* (Burkill) F.H.Chen (Sanqi), *Succinum* (Hupo), and *Polygonatum cyrtoneuma* Hua (Huangjing). According to the national pharmacopoeia [17], WXKL mainly contains notoginseng saponin R1 ($\text{C}_{47}\text{H}_{80}\text{O}_{18}$), ginseng saponin Rg1 ($\text{C}_{42}\text{H}_{72}\text{O}_{14}$), and ginseng saponin Rb1 ($\text{C}_{54}\text{H}_{92}\text{O}_{23}$). Figure 1 [18] displays the HPLC chromatograms of the chemical reference substances, WXKL, and negative samples of *Panax notoginseng* and *Codonopsis pilosula*. Previous studies have shown that WXKL may inhibit HF and arrhythmia by regulating the CaMKII signaling pathway [19–23]. WXKL in the treatment of patients with HF or arrhythmia can improve the exercise tolerance and is beneficial for the recovery of cardiac function [24–26]. However, to the best of our knowledge, whether WXKL improves CH via regulating the CaMKII and CnA-NFAT signaling pathways has not been investigated.

Given the pivotal roles of the CaMKII and CaN signaling pathways in the regulation of abnormal hypertrophy, we selected H9c2 cells induced by angiotensin II (Ang II) and used CaMKII silencing and treatment with cyclosporine A (CsA, a CaN inhibitor) to explore the correlation between the CaMKII and CnA-NFAT signaling pathways. Additionally, we sought to determine whether WXKL could improve HF by regulating CaMKII and CnA-NFAT.

2. Materials and Methods

2.1. Construction of Silenced CaMKII δ in H9c2-1632 Cells. H9c2 rat embryonic cardiomyocyte cells were obtained from the Institute of Basic Medical Sciences, Chinese Academy of Medical Sciences (Cell Resource Center, IBMS, CAMS/PUMC, China). First, RNA interference at the site of the target gene, CaMKII δ (Rat), was performed. According to the target gene sequence site, four sequences with the target gene were inserted into the vector pCDNA6.2 emGFP, and miRNA reverse primer was used as the sequencing primer (Table 1). Sequencing results verified that the correct sequence was inserted. Transfection and preparation of plasmids, blasticidin screening, and determination of the concentration of H9c2 cells, and finally cell transfection and screening were performed. Real-time PCR results showed that the relative mRNA expression of H9c2-1141 and H9c2-1632 sites was significantly reduced after RNA interference (Figure S2A), and the inhibition rate of relative mRNA expression after H9c2-1632 site interference was slightly lower than that of H9c2-1141, but the difference was not statistically significant (Table 2). CaMKII δ protein expression was determined by western blot analysis, and the results showed that, after performing RNA interference at four sites, CaMKII δ protein expression was decreased, with the greatest decrease at the H9c2-1632 site (Figure S2B). Combined with real-time PCR, the H9c2-1632 site was finally selected as a target to construct a CaMKII δ (Rat) RNA interference cell line. The H9c2-1632 cells were cultured in an incubator containing 5% CO_2 in high-sugar Dulbecco's modified Eagle's medium containing 10% fetal bovine serum at 37°C.

2.2. Drugs and Solutions. Ang II (A9525, Sigma Co., St. Louis, MO, USA) was dissolved in deionized water at a concentration of 10^{-5} mol/L; 20 μL of this solution was added to the culture medium (2 mL), reaching a final concentration of 10^{-7} mol/L. CsA (Sigma Co.) was dissolved in ethyl alcohol at a concentration of 10^{-4} mol/L; 20 μL of this solution was added to the culture medium (2 mL) at a final concentration of 10^{-6} mol/L. WXKL (1910051, Shandong Buchang Pharmaceuticals Co., Ltd., Shandong, China) was dissolved in saline at a concentration of 5 g/L.

In HPLC, 1 g of finely ground WXKL was added to a conical flask with a stopper, 50 ml of water-saturated *n*-butanol was added, and the flask was tightly stoppered and weighed. After soaking for 12 hours and ultrasonic treatment (power 300 W, frequency 40 kHz) for 1 h, the flask was weighed again after cooling, water-saturated *n*-butanol was added to make up for the lost weight, and the flask was shaken well. After filtration, 25 ml of the filtrate was collected. The *n*-butanol solution was evaporated to dryness, and methanol solution was added to the residue to 10 ml and shaken. According to the proportion of prescription Chinese medicine, *notoginseng* and *Codonopsis* were removed separately to make negative samples of *Panax notoginseng* and *Codonopsis pilosula*, and the negative control solution was prepared according to the previously mentioned methods.

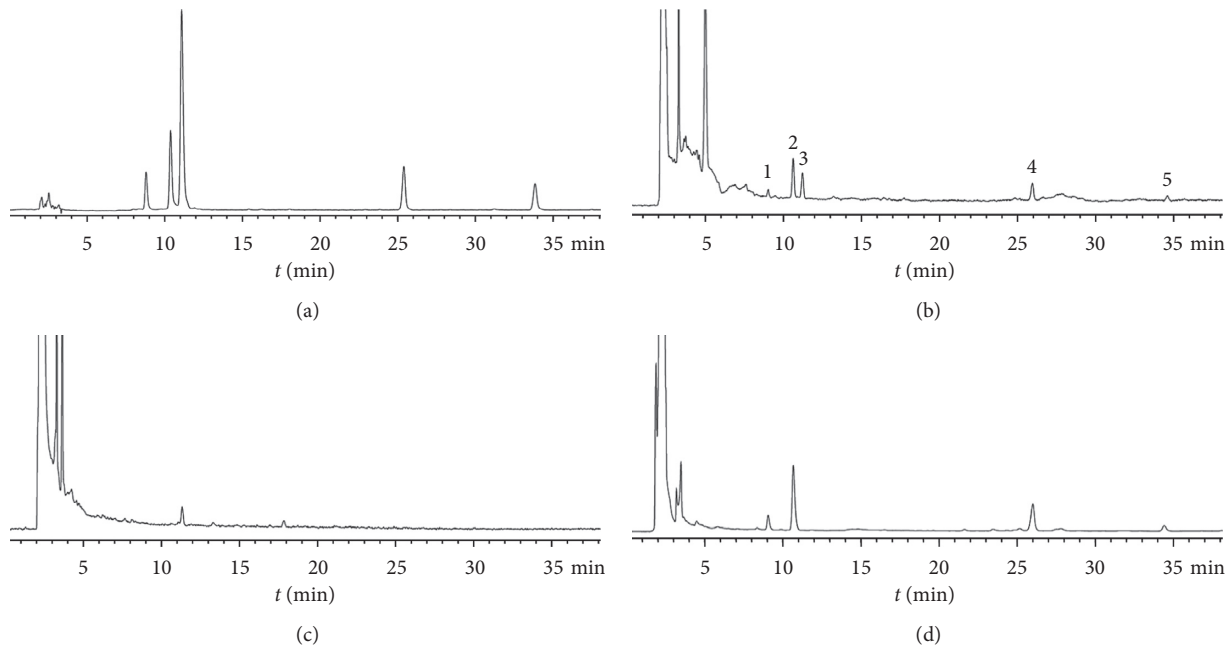


FIGURE 1: The HPLC chromatograms of WXXL. (a) Chemical reference substances, (b) WXXL, (c) negative samples of *Panax notoginseng*, and (d) *Codouopsis pilosula*. (1) notoginsenoside R1; (2) ginsenoside Rg1; (3) obetyolin; (4) ginsenoside Rb1; (5) ginsenoside Rd.

TABLE 1: CaMKII δ (Rat) (NM_012519.2) RNAi site.

	Initiation site	RNAi site sequence
1#	408	TAGAATCTGCCGTCTCTTGAA
2#	754	CCTGGGTATCTTTCTCCAGAA
3#	1141	ACTATGCTGGCTACGAGAAAT
4#	1632	GTACATGGATGGAAATGGAAT

TABLE 2: Inhibition rate of CaMKII δ (rat) H9c2-1141 and H9c2-1632 sites after the RNA interference.

Cells	Relative expression	Inhibition rate of CaMKII δ (rat)
H9c2-NEG	1	0
H9c2-1141	0.1765726	82.34%
H9c2-1632	0.1890273	81.10%

Methanol was added to prepare reference substances containing notoginsenoside R1 0.247 mg, ginsenoside Rg1 0.422 mg, ginsenoside 0.042 mg, ginsenoside Rb1 0.847 mg, and ginsenoside Rd 0.255 mg per 1 mL.

2.3. Chromatographic Conditions. Analyses were performed on an Agilent 1260 HPLC system consisting of a quaternary delivery system, an autosampler, and a DAD detector. All the separations were carried out on Amethyst C₁₈ column (4.6 × 250 mm, 4 μ m). The gradient elution used acetonitrile (A) and water (B) as a mobile phase at a flow rate of 1 mL/min. The gradient program was as follows: 0–14 min, 22%–30%A; 14–35 min, 30%–38%A; 35–45 min, 38%–38%A; 45–47 min, 38%–95%A; 47–62 min, 95%–95%A; 62–65 min, 95%–22%A. The column temperature was maintained at

27°C, and the chromatogram was monitored at a wavelength of 210 nm.

2.4. Cell Grouping and Drug Administration. H9c2 rat embryonic cardiomyocytes were split into 13 different treatment groups: (1) negative control group: only secondary antibody was added to H9c2 cells with no primary antibody; (2) control group: H9c2 cells were cultured for 72 h; (3) control + Ang II group: H9c2 cells were pretreated with Ang II for 48 h and cultured for another 24 h; (4) control + Ang II + WXXL group: H9c2 cells were pretreated with Ang II for 48 h, treated with WXXL, and cultured for another 24 h; (5) control + WXXL group: H9c2 cells were cultured for 48 h, treated with WXXL, and cultured for another 24 h; (6) siCaMKII group: H9c2-1632 cells were cultured for 72 h; (7) siCaMKII + Ang II group: H9c2-1632 cells were pretreated with Ang II for 48 h and cultured for another 24 h; (8) siCaMKII + Ang II + WXXL group: H9c2-1632 cells were pretreated with Ang II for 48 h, treated with WXXL, and cultured for another 24 h; (9) siCaMKII + WXXL group: H9c2-1632 cells were cultured for 48 h, treated with WXXL, and cultured for another 24 h; (10) CsA group: H9c2 cells were pretreated with CsA for 72 h; (11) CsA + Ang II group: H9c2 cells were pretreated with CsA and Ang II for 48 h and cultured for another 24 h; (12) CsA + Ang II + WXXL group: H9c2 cells were pretreated with CsA and Ang II for 48 h, treated with WXXL, and cultured for another 24 h; (13) CsA + WXXL group: H9c2 cells were pretreated with CsA for 48 h, treated with WXXL, and cultured for another 24 h.

2.5. Western Blot Analysis. Proteins were extracted from H9c2 cells, subsequently lysed with lysis buffer containing phenylmethylsulfonyl fluoride in ice for 40 min,

and shaken once every 8 min during this period. The lysates were centrifuged at 1200 rpm for 20 min at 4°C, and the supernatants were collected. Proteins were analyzed by sodium dodecyl sulfate-polyacrylamide gel electrophoresis, transferred onto nitrocellulose membranes, blocked in 5% bovine serum albumin (BSA) or milk, and then incubated with primary antibodies at 4°C overnight. Subsequently, the membranes were washed three times with tris-buffered saline/Tween 20 at the specified time intervals and finally incubated with secondary antibody at room temperature. ECL visualization was performed, and the resulting images were captured using the GeneGnome Gel Imaging System (Syngene Co., Bangalore, India). The gel images were analyzed using ImageJ software (Image-Pro Plus, Media Cybernetics, Rockville, MD, USA). The antibodies used in the present study are listed in Table S1.

2.6. Confocal Imaging. For the cytoskeletal assay, H9c2 cells were cultured in a confocal laser culture dish until reaching a moderate density. Upon reaching 70–80% confluence, the cells were washed with phosphate-buffered saline (PBS) twice, fixed with 4% paraformaldehyde for 15 min, and washed with PBS three times for 5 min each. Cells were incubated with 0.1% Triton X-100 penetrating fluid at room temperature for 5 min and washed thrice with PBS for 5 min each. Rhodamine-phalloidin was diluted with PBS (2.5 μ L) and added to 200 μ L of the working fluid, fixed for 20 min, and washed with PBS three times for 5 min each. Cells were subjected to confocal laser microscopy. The cells of each group were removed and washed with cold PBS (precooled at 4°C) twice, and the residual PBS was aspirated. Each group was fixed with 4% paraformaldehyde for 10 min at –20°C and washed twice with PBS. Cells were permeabilized with 0.25% Triton X-100 for 10 min and washed three times with cold PBS for 5 min each wash and then treated with 1% BSA for 30 min to block nonspecific antigen recognition. Primary antibodies were diluted with 1% BSA in PBS and added at 100 μ L to each group. Cells were plated at 4°C for 12 h and then washed thrice with PBS for 5 min each. The secondary antibody was diluted with 1% BSA in PBS with 100 μ L per sample at room temperature for 60 min away from light. The secondary antibody was removed and cells were washed thrice with PBS for 5 min each. Cells were incubated with DAPI for nuclear staining; finally, an antifluorescence quencher was added. Later, a transparent nail polish seal was used, and cells were observed using a confocal microscope.

For measuring the nuclear translocation of NFATc4, the cell processing method is basically the same as previously mentioned. Images were analyzed using Image-Pro Plus Analysis Software. First, color images were converted to gray images. The ratio of IOD to the area represented by NFATc4 fluorescence was measured. NFATc4 translocation was quantified as the ratio between the number of cells containing nucleus-localized NFATc4 (NFATc4-positive), and the total number of cells was counted.

2.7. Electrophysiological Recording. Using the whole-cell patch clamp technique, the whole-cell Ca^{2+} current was recorded by an Axon-700B amplifier (Axon Instruments, San Jose, CA, USA) with the pCLAMP 9.2 software (Axon Instruments). Borosilicate glass microelectrodes had tip resistances of 3.0–5.0 M Ω , which adjusts the three-dimensional manipulator for G Ω sealing and breaks the membrane absorption in the whole-cell recording mode. The membrane capacitance and $I_{\text{Ca-L}}$ current were recorded after stabilization. To eliminate the errors resulting from cell size, the I value was expressed as the current density (pA/pF). Cells were superfused with extracellular fluid containing (all in mmol/L): 125 NaCl, 10.8 BaCl₂, 1 MgCl₂, 5.4 CsCl, 10 HEPES, and 10 glucose (pH 7.35, adjusted with NaOH). A pipette solution was used containing (mmol/L): 120 CsCl, 3 MgCl₂, 5 Na₂ATP, 10 EGTA, and 5 HEPES (pH 7.3, adjusted with CsOH).

2.8. Statistical Analysis. Data were expressed as mean \pm SD. One-way ANOVA was used to compare multiple groups with a normal distribution. Statistical analysis was performed using the SPSS program (version 20.0). $P < 0.05$ was considered statistically significant, and $P < 0.01$ was considered highly statistically significant. Data acquisition and analysis were performed using pCLAMP 9.2 software (Axon Instruments), Origin 6.1 software (MicroCal Software, Northampton, MA, USA), and GraphPad Prism 5 (GraphPad Software Incorporate, La Jolla, CA, USA).

3. Results

We explored the interaction between CaMKII and CnA-NFAT signaling in CH induced by Ang II and the effect of WXKL. Therefore, we sought to characterize the role of CaMKII and CnA-NFAT signaling in cardiomyocytes using siRNA-mediated silencing (siCaMKII) and CsA. We analyzed the results of cytoskeletal enlargement; L-type Ca^{2+} current ($I_{\text{Ca-L}}$); expression of CaMKII, CnA-NFAT, and inflammatory signaling pathways in cardiomyocytes induced by Ang II; and the protein expression and nuclear transfer of NFATc4.

3.1. Effects of SiCaMKII and CsA on Myocardial Cytoskeletal Protein. We used fluorescence confocal microscopy to observe cytoskeletal enlargement (a direct indicator of hypertrophy in myocardial cells) to assess whether the CH model had been successfully established and ensure the feasibility of the experiment.

Immunofluorescence staining showed that Ang II effectively induced CH, as evidenced by an increase in cell width and length (Figure 2). CsA and siCaMKII prevented an Ang II-stimulated increase in cell size, and the effect was similar in cells treated with WXKL (Figure 2). Taken together, the results revealed that siCaMKII and CsA may inhibit the hypertrophic response to Ang II in H9c2 cells. Moreover, WXKL improved Ang II-induced CH.

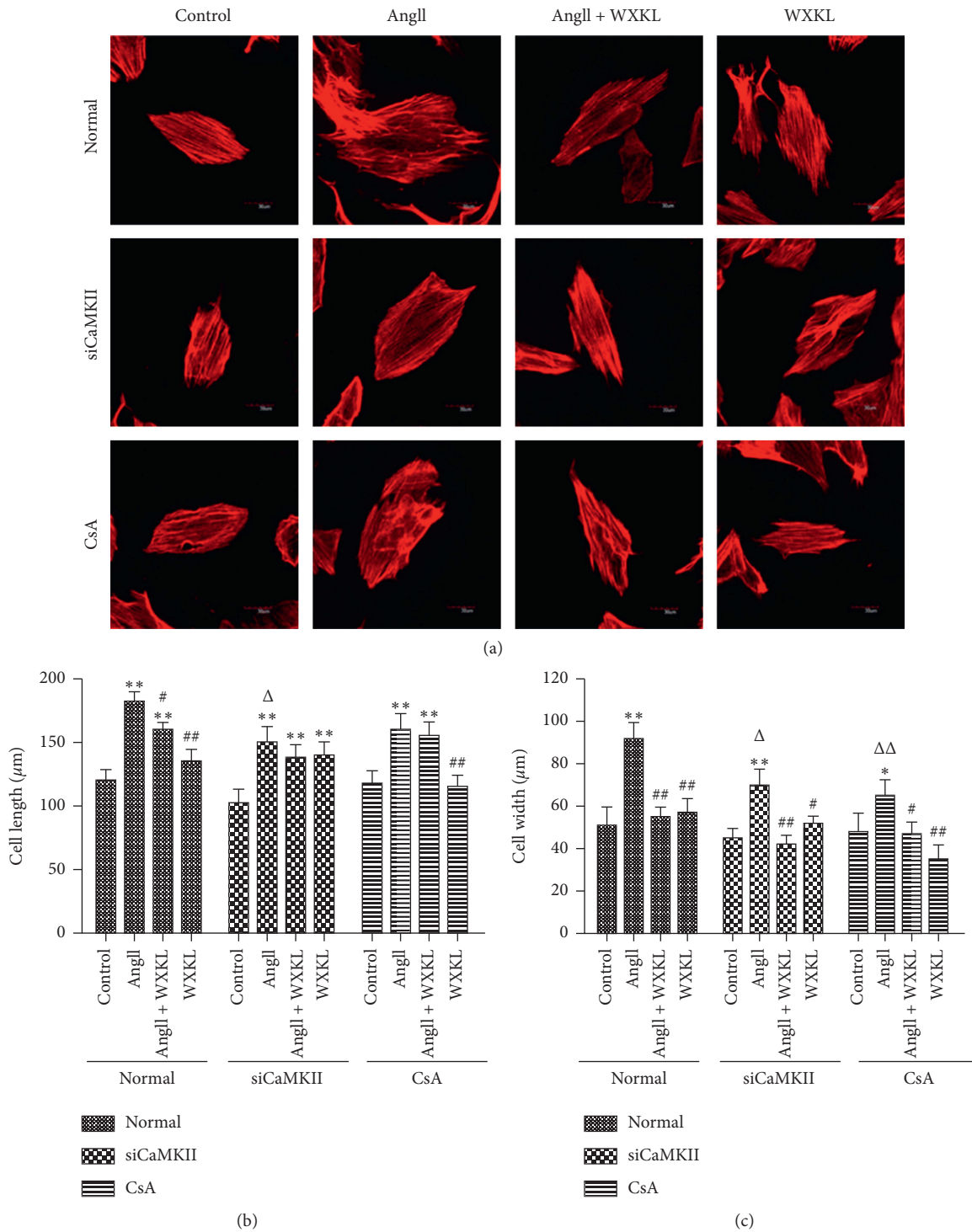


FIGURE 2: SiCaMKII decreases Ang II-induced cell surface area enlargement in H9c2 cells. H9c2 cells were treated with Ang II (10^{-7} M for 48 h). CaMKII was silenced or CsA (10^{-6} M) was added to the culture medium prior to Ang II administration. After administering Ang II, WXKL (5 g/L) was added, and the culture medium was incubated for 24 h. The control cells received no treatment. (a) Representative images of immunofluorescence staining for phalloidin following treatment ($n = 10$ cells per group). Scale bar: $30\ \mu\text{m}$. (b) Mean cell length measurement ($n = 10$ cells per group). (c) Mean cell width measurement ($n = 10$ cells per group). Data are presented as the mean \pm SD. Statistical significance was determined by one-way ANOVA. * $P < 0.05$ and ** $P < 0.01$ vs. the control group. # $P < 0.05$ and ## $P < 0.01$ vs. the Ang II group. ▲ $P < 0.05$ and ▲▲ $P < 0.01$; the control group in SiCaMKII or CsA vs. the control group in normal. △ $P < 0.05$ and △△ $P < 0.01$; the Ang II group in SiCaMKII or CsA vs. the Ang II group in normal.

3.2. I_{Ca-L} Significantly Reduced after CaMKII δ Silencing. I_{Ca-L} is present in many cardiomyocytes, and it plays a key role in the formation of an action potential plateau, intracellular Ca^{2+} elevation, and muscle contraction. CaM, as a Ca^{2+} receptor, plays a major role in Ca^{2+} -dependent inactivation and facilitation of I_{Ca-L} .

Results revealed that compared with control treatment, Ang II significantly increased the amplitude of I_{Ca-L} within the range of -20 mV to $+10$ mV. Pretreatment with siCaMKII reduced the elevated I_{Ca-L} amplitude. Similarly, WXXL decreased the Ang II-induced elevated amplitude of I_{Ca-L} (Figures 3(a) and 3(b)). Interestingly, in the CsA group (Figure 3), I_{Ca-L} was significantly increased, and its steady-state activation and inactivation were increased (Figures 3(c) and 3(d)). These results suggest that siCaMKII and WXXL inhibit the calcium current and impede inactivation. Furthermore, treatment with CsA led to the opposite results. Therefore, we suspected that CaN inhibition may alter other pathways and cause an increase in calcium current.

3.3. Treatment with CsA Activates the CaMKII Signaling Pathway. To further investigate Ang II-induced CaMKII expression in H9c2 cells and the effect of drug intervention on CaMKII protein expression, we measured CaMKII protein levels using laser scanning confocal microscopy. Additionally, CaMKII signaling pathway proteins were subjected to western blotting to explore the mechanism.

The results revealed that Ang II treatment significantly increased the fluorescence intensity of CaMKII in H9c2 cells compared with control treatment (Figure 4(a)). Pretreatment with siCaMKII reduced the Ang II-induced elevation in the fluorescence intensity of CaMKII, and WXXL led to a similar decrease. However, the fluorescence intensity corresponding to the CaMKII protein level was significantly higher in the CsA group than in the normal group (Figure 4(b)) and was observed to decrease after WXXL treatment. Therefore, the results showed that the fluorescence intensity indicating CaMKII protein expression increased after stimulation with Ang II, whereas WXXL treatment significantly reduced this increase. However, treatment with CsA did not inhibit this effect.

The expression of CaMKII, p-CaMKII, RyR2, p-RyR2, PLB, and p-PLB in H9c2 cells after stimulation with Ang II for 48 h was evaluated using western blot analysis. Exposure of H9c2 cells to Ang II resulted in increased expression of CaMKII pathway proteins (Figure 5(a)). Pretreatment with siCaMKII significantly decreased the Ang II-induced elevated expression of p-RyR2 and p-PLB ($P < 0.01$, Figures 5(e) and 5(f)) and reduced that of CaMKII and p-CaMKII ($P < 0.05$, Figures 5(b) and 5(c)). Interestingly, pretreatment with CsA led to significantly upregulated CaMKII expression levels ($P < 0.01$, Figure 5(b)). After treatment with WXXL for 24 h, protein expression was decreased in each group. Therefore, the CaMKII signaling pathway was blocked by silencing CaMKII expression, which reduced the degree of hypertrophy, and WXXL had a similar effect. However, the CaMKII signaling pathway was activated in H9c2 cells treated with CsA.

3.4. CaMKII Controls the CnA-NFAT Pathway. Next, we elucidated the effects of siCaMKII, CsA, and WXXL on the CnA-NFAT signaling pathway.

Treatment with Ang II significantly increased the fluorescence intensity of CnA in both the nucleus and the cytoplasm (Figure S1). The siCaMKII cells showed downregulation of CnA protein levels and lower fluorescence intensities. After treatment with WXXL for 24 h, Ang II-induced CnA protein expression was inhibited, and its fluorescence intensity and nuclear transfer were reduced (Figure S1). These results revealed that the fluorescence intensity and nuclear transfer of CnA in the Ang II-treated group were significantly higher; however, CaMKII silencing as well as treatment with CsA and WXXL suppressed this effect.

As shown in Figure 6(a), the expression of upstream and downstream proteins, including CnA, p-CnA, NFATc4, p-NFATc4, GATA4, p-GATA4, ANP, and BNP, in the CnA-NFAT signaling pathway was detected by western blotting. Exposure of H9c2 cells to Ang II resulted in increased expression of CnA-NFAT signaling pathway proteins (Figure 6). Pretreatment with siCaMKII markedly decreased the Ang II-induced elevated expression of p-CnA ($P < 0.01$, Figure 6(c)) and reduced that of GATA4 and BNP ($P < 0.05$, Figures 6(f) and 6(i)). Interestingly, pretreatment with CsA led to significantly upregulated ANP expression levels ($P < 0.01$, Figure 6(h)). After treatment with WXXL for 24 h, protein expression was decreased in each group. Therefore, the CnA-NFAT signaling pathway was blocked by silencing CaMKII expression, and WXXL played a role in improving the expression of various proteins in CH.

3.5. SiCaMKII Inhibits Nuclear Transfer of NFATc4 in Hypertrophic Cardiomyocytes. Subsequently, we further analyzed CnA-NFAT signaling, and immunofluorescence and western blots were performed to detect NFATc4 nuclear translocation.

The results demonstrated that NFATc4 was translocated to the nucleus in response to Ang II stimulation (Figure 7), whereas pretreatment with siCaMKII or CsA inhibited Ang II-induced nuclear translocation of NFATc4; furthermore, such transfer was inhibited after treatment with WXXL. The data presented in Figures 6 and 7 suggest that inhibition of hypertrophy by siCaMKII and WXXL was mediated, at least in part, by CaMKII and CnA-NFATc4 signaling.

3.6. Effects of SiCaMKII and CsA on the Inflammatory Signaling Pathway (MyD88-TLR4). Finally, to further elucidate the interaction between the CaMKII and CnA-NFAT signaling pathways, western blotting was used to measure the expression of MyD88, NF- κ B, p-NF- κ B, TLR2, and TLR4 in different groups (Figure 8).

The results demonstrated that protein expression was increased in H9c2 cells after Ang II treatment for 48 h. A statistically significant difference was observed in the expression of MyD88, NF- κ B, and p-NF- κ B ($P < 0.01$, Figures 8(b), 8(c), and 8(d)). Compared with that after Ang II treatment in normal H9c2 group, inflammation-related

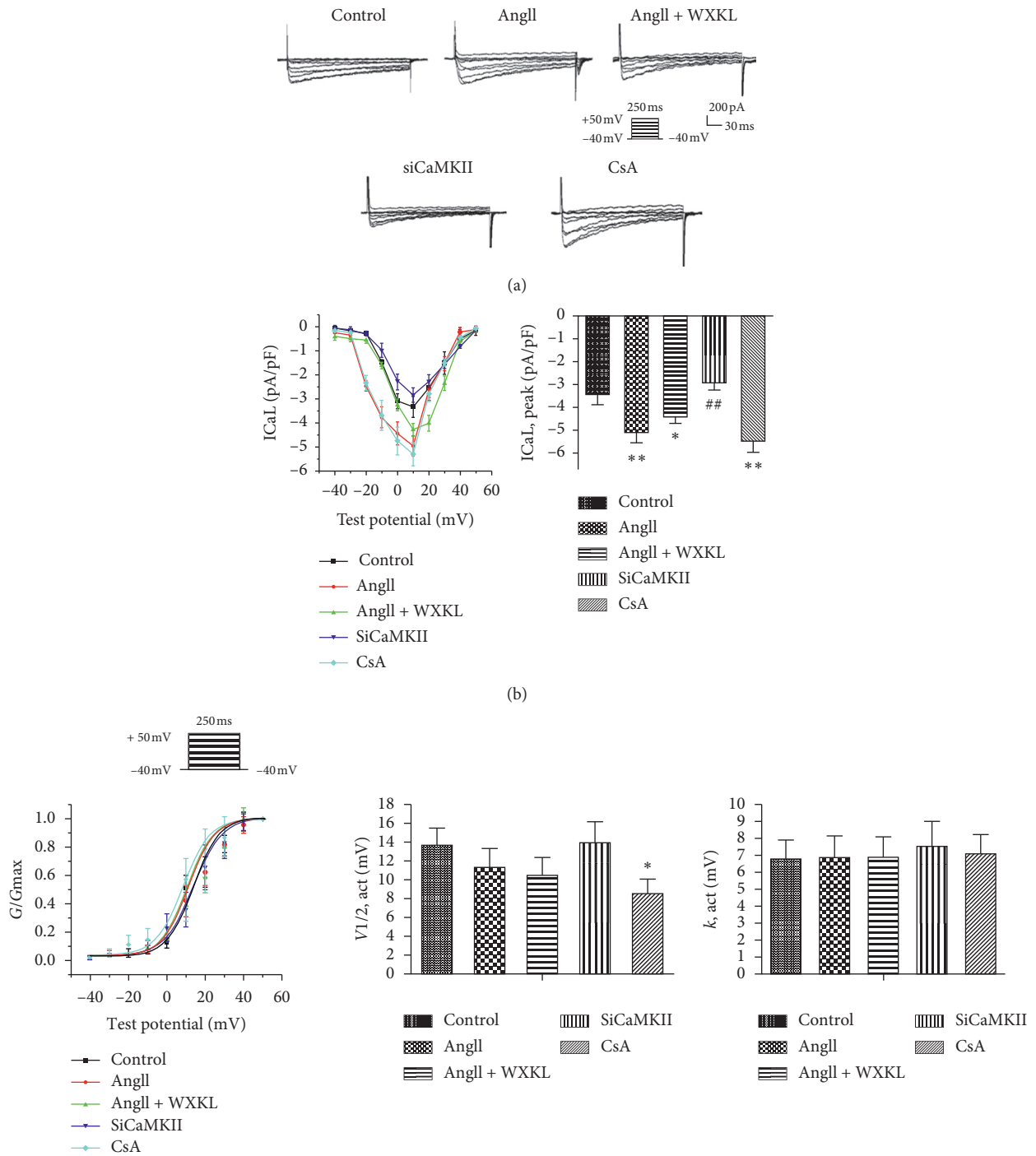


FIGURE 3: Continued.

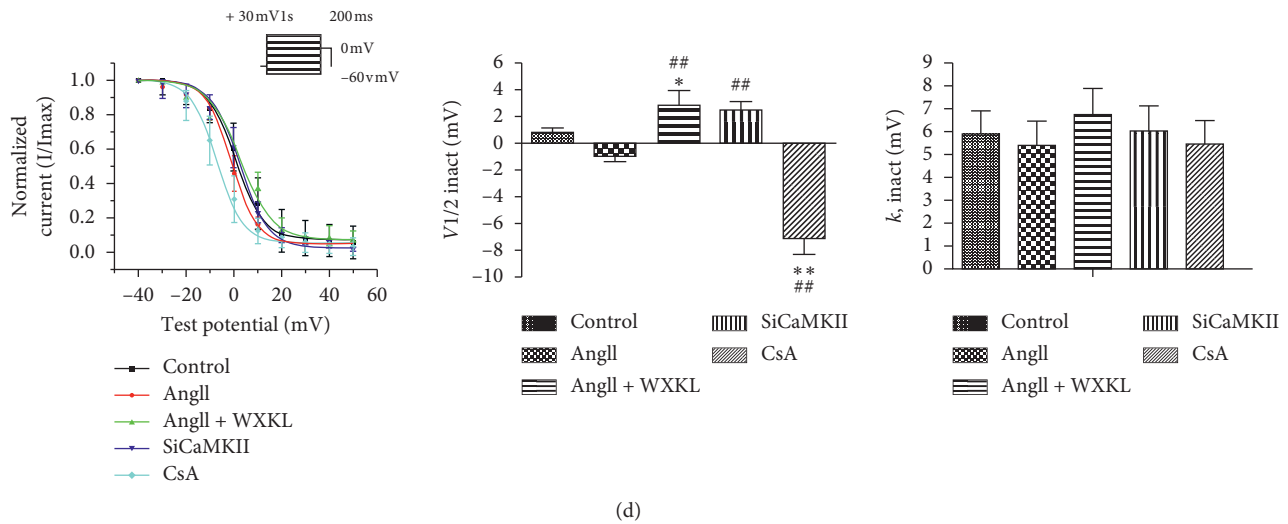


FIGURE 3: Changes in patch clamp inspection. (a) I_{Ca-L} current in the control, Ang II, Ang II + WXKL, siCaMKII, and CsA groups. (b) Effects of siCaMKII and CsA on the I_{Ca-L} current-voltage (I-V) curve in H9c2 cells. I-V curves and peak current density (PA/PF) of each group ($n = 10$ cells per group). (c) Effects of siCaMKII and CsA on I_{Ca-L} steady-state activation (SSA) in H9c2 cells. I_{Ca-L} steady-state activation curves (original data point diagram and curve fit by Boltzmann equation), comparison of semiactivation voltage ($V_{1/2, act}$), and comparison of slope factors (K_{act}) in each group ($n = 10$ cells per group). (d) Effects of siCaMKII and CsA on I_{Ca-L} steady-state inactivation in H9c2 cells. I_{Ca-L} steady-state inactivation curves (original data point diagram and curve fitting by Boltzmann equation); comparison of semi-inactivation voltage ($V_{1/2, inact}$); comparison of slope factors (K_{inact}) in each group ($n = 10$ cells per group). Values are presented as mean \pm SD; Statistical significance was determined by one-way ANOVA. * $P < 0.05$ and ** $P < 0.01$ vs. the control group. # $P < 0.05$ and ## $P < 0.01$ vs. the Ang II group.

protein expression decreased after that in the siCaMKII group. In the CsA group, NF- κ B expression was slightly decreased whereas that of other proteins was increased. After treatment with Ang II for 48 h, the rate of increase of MyD88 and TLR2 was higher in the CsA group than that in H9c2 cells. After administering WXKL, protein expression decreased in each group. The previously mentioned findings indicated that, in the siCaMKII group, protein expression reduced in Ang II-induced cardiomyocytes and the inflammatory pathway was inhibited, but the opposite result was observed in the CsA group. Furthermore, the effect of WXKL was similar to that of siCaMKII.

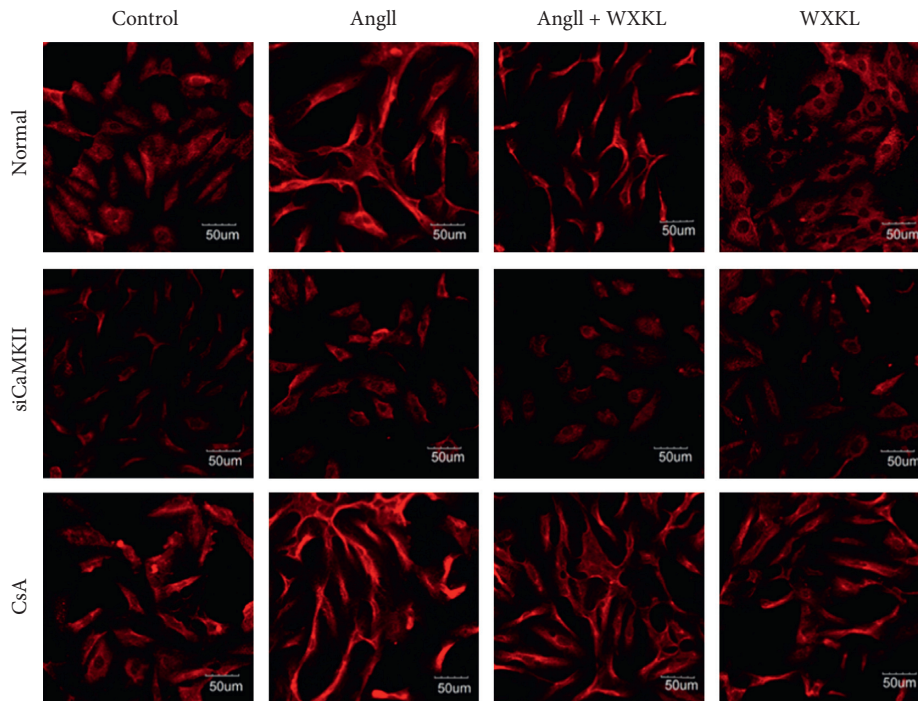
4. Discussion

In the present study, we found that [1] Ang II activated the CaMKII, CnA-NFAT, and MyD88 inflammatory pathways in H9c2 cells and caused myocardial hypertrophy [2]. The siRNA-mediated silencing of CaMKII inhibited protein expression in the CaMKII pathway, further attenuated protein expression in the CnA-NFAT signaling pathway, and inhibited the reduction in NFATc4 nuclear transfer. Moreover, CaMKII silencing played a role in improving Ang II-induced myocardial hypertrophy, and WXKL had a similar effect [3]. CsA, a CaN inhibitor, inhibited expression in the CnA-NFAT pathway but activated the CaMKII and MyD88 signaling pathways.

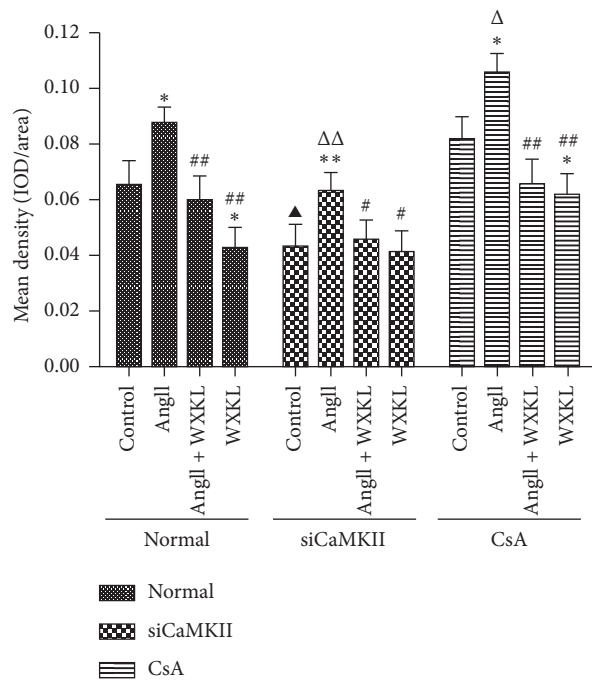
Both physiological and pathological CH are related to the increase in cardiomyocyte Ca^{2+} levels. Ca^{2+} regulates the activity of various Ca^{2+} -dependent signaling pathways, including those of CaMKII and CnA-NFAT [6]

(Figure 9). It is known that CaMKII phosphorylates class II histone deacetylases (HDACs), particularly HDAC4 and HDAC5, by boosting the export of these molecules from the nucleus, resulting in the disinhibition of MEF-2-mediated gene expression and CH [27–30]. CnA can maintain NFAT activity through a noncatalytic mechanism by associating with NFAT, blocking its nuclear export sequence and thereby maintaining its nuclear localization [31]. Once activated by sustained elevation of intracellular calcium, CaN dephosphorylates NFAT, enabling its translocation to the nucleus and consequently activating prohypertrophic target genes [32]. Our data showed that Ang II stimulation results in NFATc4 translocated to the nucleus, whereas pretreatment with siCaMKII or CsA inhibited Ang II-induced nuclear translocation of NFATc4; furthermore, transfer was inhibited after treatment with WXKL.

Previous research has shown that CaMKII inhibition can decrease Ang II-induced cardiac fibroblast proliferation and the secretion of TGF- β 1 and TNF- α . In addition, CaMKII inhibition reversed the upregulation of MMP-1, 2, and 9 and collagen I and III after Ang II intervention [33]. A previous study revealed that treatment with KN-93 (a CaMKII inhibitor) significantly reduced the expression of CH-related proteins, including NFATc3, p-HDAC4, p-HDAC5, GATA-4, and the hypertrophy marker BNP. Furthermore, the combined inhibition of the CaMKII and CaN signaling pathways may obviously relieve CH responses [13]. The results of the current study revealed that siCaMKII inhibited



(a)



(b)

FIGURE 4: Effects of siCaMKII and CsA on the CaMKII signaling cascade. (a) Double immunofluorescence staining to observe the effects of siCaMKII, CsA, and WXKL on CaMKII expression in each group. Scale bar: 50 μ m. (b) Mean density of CaMKII in each group. Data are presented as the mean \pm SD. Statistical significance was determined by one-way ANOVA. * P < 0.05 and ** P < 0.01 vs. the control group. # P < 0.05 and ## P < 0.01 vs. the Ang II group. ▲ P < 0.05 and ▲▲ P < 0.01; the control group in SiCaMKII or CsA vs. the control group in normal. △ P < 0.05 and △△ P < 0.01; the Ang II group in SiCaMKII or CsA vs. the Ang II group in normal.

protein expression in the CaMKII pathway and further reduced that in the CnA-NFAT signal pathway, thereby improving Ang II-induced hypertrophic cardiomyocytes. This was similar to the results of previous studies that

demonstrated that, in the absence of CaMKII signals, CaN does not seem to contribute to abnormal cardiac remodeling, thus highlighting CaMKII and not CaN as a promising drug target to combat HF [16].

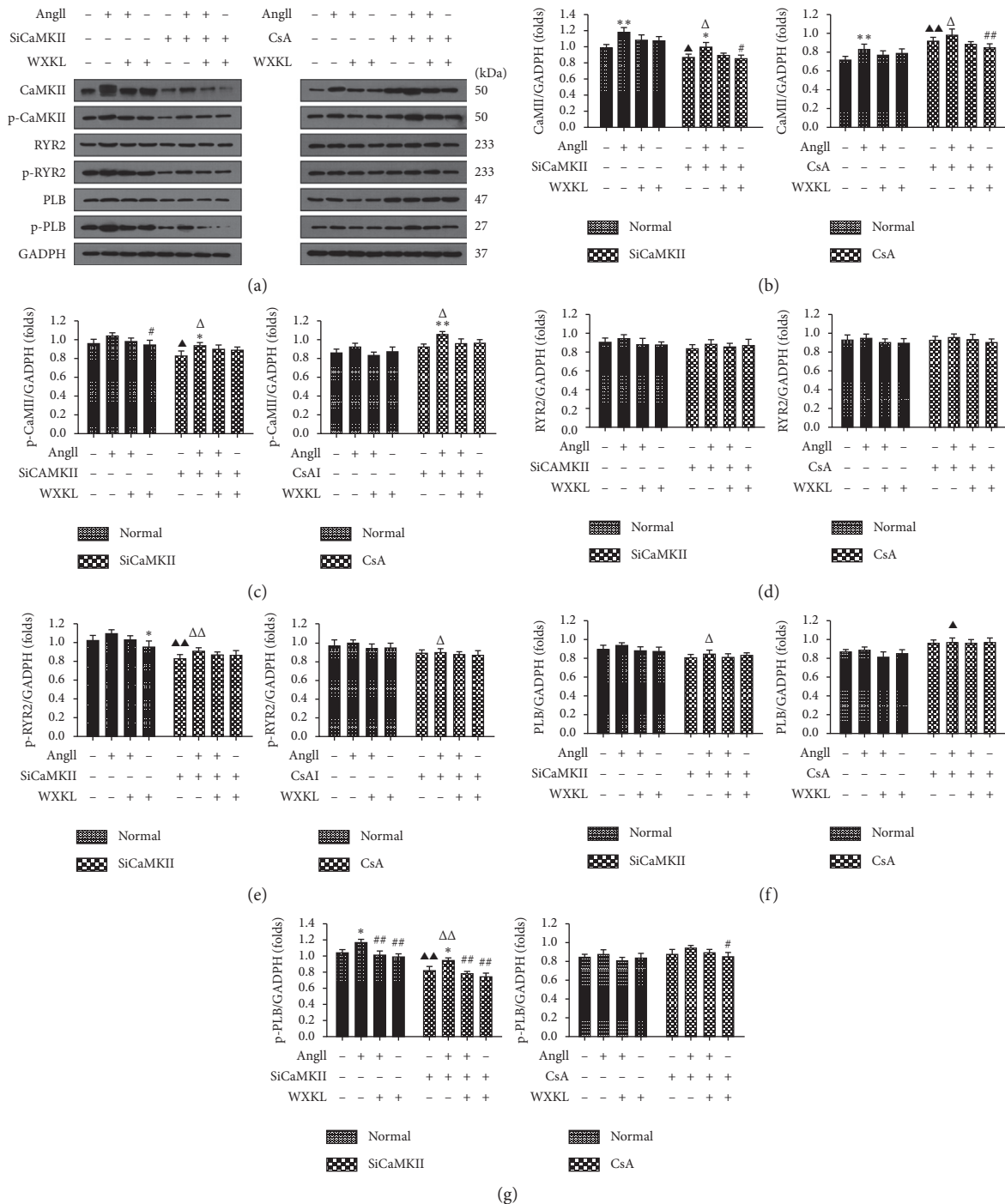


FIGURE 5: Effects of siCaMKII and CsA on Ang II-induced activation of CaMKII signaling in H9c2 cells. (a) Representative western blotting images. Densitometric analysis of (b) CaMKII, (c) p-CaMKII, (d) RyR2, (e) p-RyR2, (f) PLB, and (g) p-PLB expression levels ($n = 3$ cells per group). Data are presented as the mean \pm SD. Statistical significance was determined by one-way ANOVA. * $P < 0.05$ and ** $P < 0.01$ vs. the control group. # $P < 0.05$ and ## $P < 0.01$ vs. the Ang II group. $\Delta P < 0.05$ and $\Delta\Delta P < 0.01$; the control group in SiCaMKII or CsA vs. the control group in normal. $\triangle P < 0.05$ and $\triangle\triangle P < 0.01$; the Ang II group in SiCaMKII or CsA vs. the Ang II group in normal.

Excess CaMKII activity leads to phosphorylation of the L-type Ca^{2+} channel (LTCC), sarcoplasmic-endoplasmic reticulum Ca^{2+} -ATPase, ryanodine receptor 2 (RyR2), and PLB proteins. CaMKII phosphorylates the LTCC that leads to increased $I_{\text{Ca-L}}$ and forms a Ca^{2+} overload in the cell, which causes early afterdepolarizations and triggers

arrhythmia. Hyperphosphorylation of the sarcoplasmic reticulum (SR) results in the consumption of SR Ca^{2+} stores, leading to damaged cytosolic Ca^{2+} transients, which in turn induces systolic and diastolic dysfunction. Moreover, hyperphosphorylation events at RyR2 cause abnormal release of SR Ca^{2+} that activates the electrogenic $\text{Na}^+/\text{Ca}^{2+}$ -

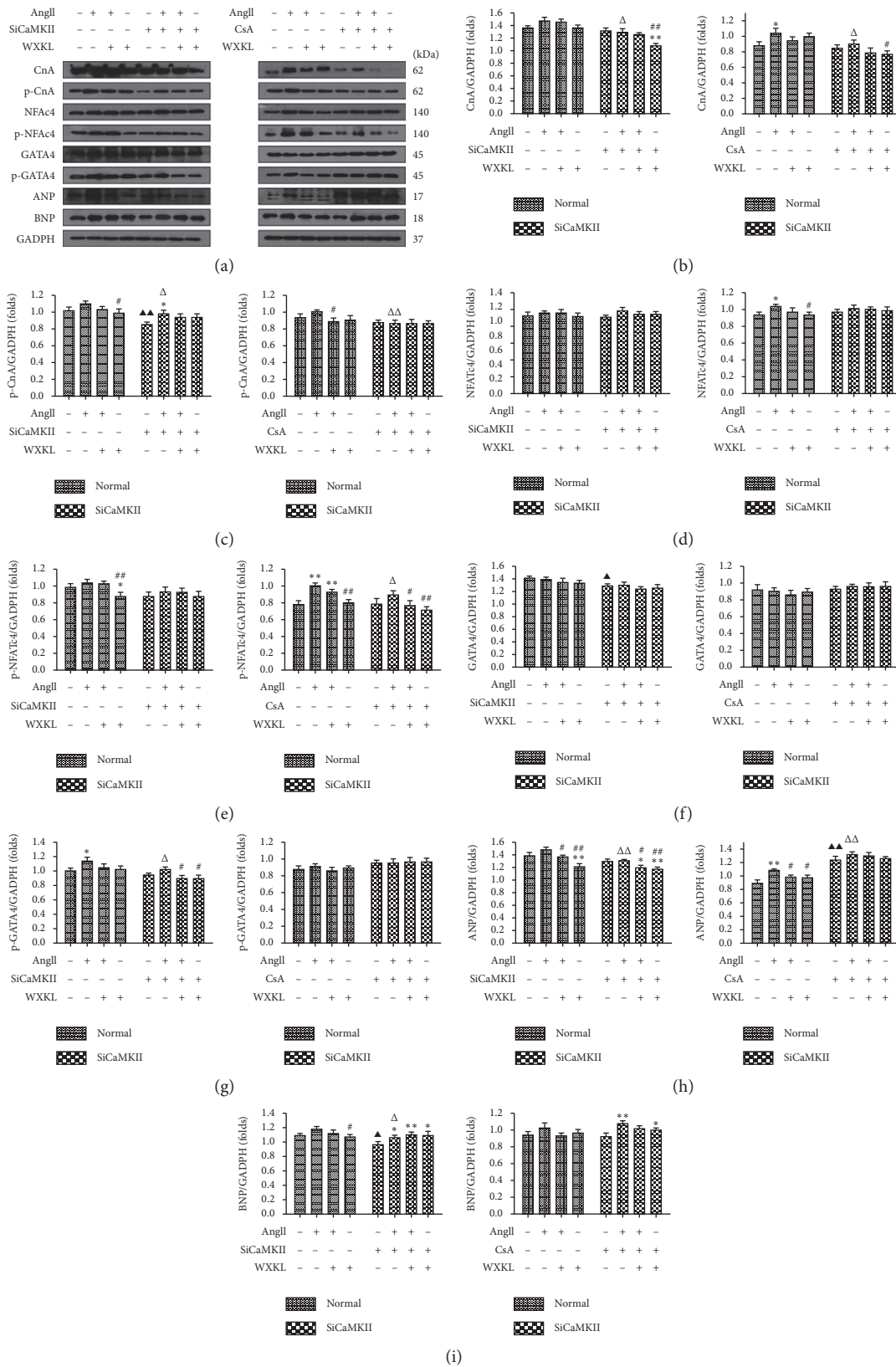


FIGURE 6: Effects of siCaMKII and CsA on Ang II-induced activation of CnA-NAFT signaling in H9c2 cells. (a) Representative western blotting images. Densitometric analysis of (b) CnA, (c) p-CnA, (d) NFATc4, (e) p-NFATc4, (f) GATA4, (g) p-GATA4, (h) ANP, and (i) BNP expression levels ($n = 3$ cells per group). Data are presented as the mean \pm SD. Statistical significance was determined by one-way ANOVA. * $P < 0.05$ and ** $P < 0.01$ vs. the control group. # $P < 0.05$ and ## $P < 0.01$ vs. the Ang II group. $\blacktriangle P < 0.05$ and $\blacktriangle\blacktriangle P < 0.01$; the control group in SiCaMKII or CsA vs. the control group in normal. $\triangle P < 0.05$ and $\triangle\triangle P < 0.01$; the Ang II group in SiCaMKII or CsA vs. the Ang II group in normal.

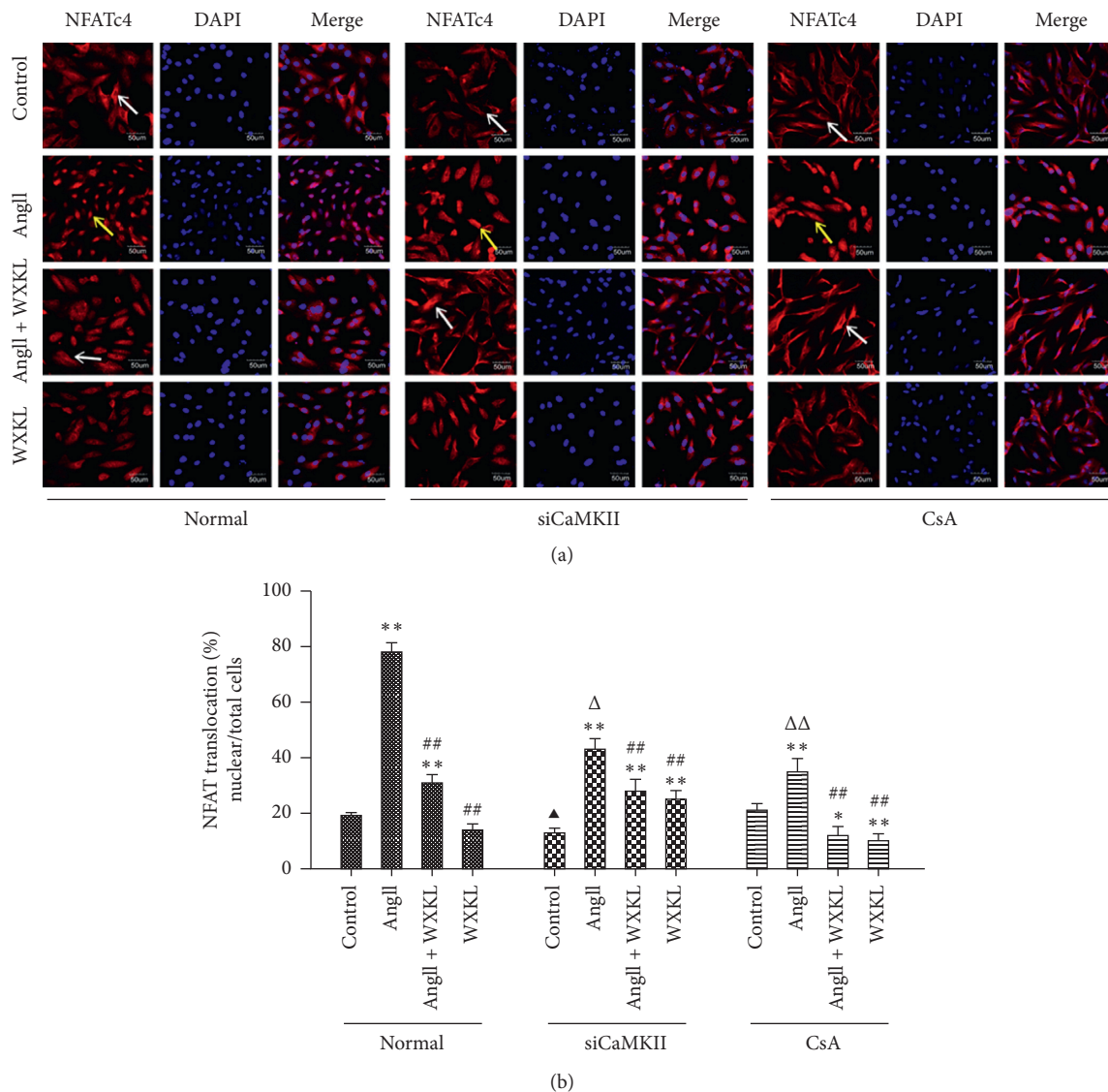


FIGURE 7: Ang II-induced NFATc4 nuclear translocation is inhibited by siCaMKII. H9c2 cells were treated with Ang II (10^{-7} M) for 48 h. CaMKII was silenced or CsA (10^{-6} M) was added to the culture medium prior to Ang II administration. WXKL (5 g/L) was added for 24 h after Ang II administration. The control cells received no treatment. (a) Representative images of immunofluorescence staining of NFATc4. Blue: DAPI staining; red: NFATc4. Scale bar: 50 μ m. Yellow arrow: nuclear translocation; white arrow: no nuclear translocation or nuclear translocation was decreased. (b) Semiquantitative analysis of NFATc4 nuclear translocation. Data are presented as the mean \pm SD. Statistical significance was determined by one-way ANOVA. * $P < 0.05$ and ** $P < 0.01$ vs. the control group. [#] $P < 0.05$ and ^{##} $P < 0.01$ vs. the Ang II group. [▲] $P < 0.05$ and ^{▲▲} $P < 0.01$; the control group in SiCaMKII or CsA vs. the control group in normal. ^Δ $P < 0.05$ and ^{ΔΔ} $P < 0.01$; the Ang II group in SiCaMKII or CsA vs. the Ang II group in normal.

exchanger (NCX), which can cause delayed after-depolarizations [34]. Interestingly, our study revealed that CnA expression was gradually reduced after treatment with CsA, but the CaMKII signaling pathway tended to be activated. This result was consistent with few studies that found either no effect or a deterioration of hypertrophy with CsA or FK506 [35, 36]. Conversely, previous studies have suggested that CaN inhibitors attenuate hypertrophy in a variety of models [37]. These discrepancies may be explained by the inherent differences between the different models. In addition, the inherent nonspecific effects associated with CsA and FK506 are to be considered. FK506 can also directly

alter ryanodine receptor function through its effects on FKBP12 and FKBP12.6, while CsA may influence the leakage of calcium from the sarcoplasmic reticulum through the lipid bilayer [38, 39]. Acute treatment with CsA causes alterations of LTCC activity in dissociated human cardiomyocytes [40]. The current study demonstrated that administration of CsA activated the CaMKII signaling pathway and increased the degree of CH. This is possibly because the specificity of actions by CsA may be associated with their selective interactions with specific CaN subtypes or because of the presence of cell-specific CaN substrates [41].

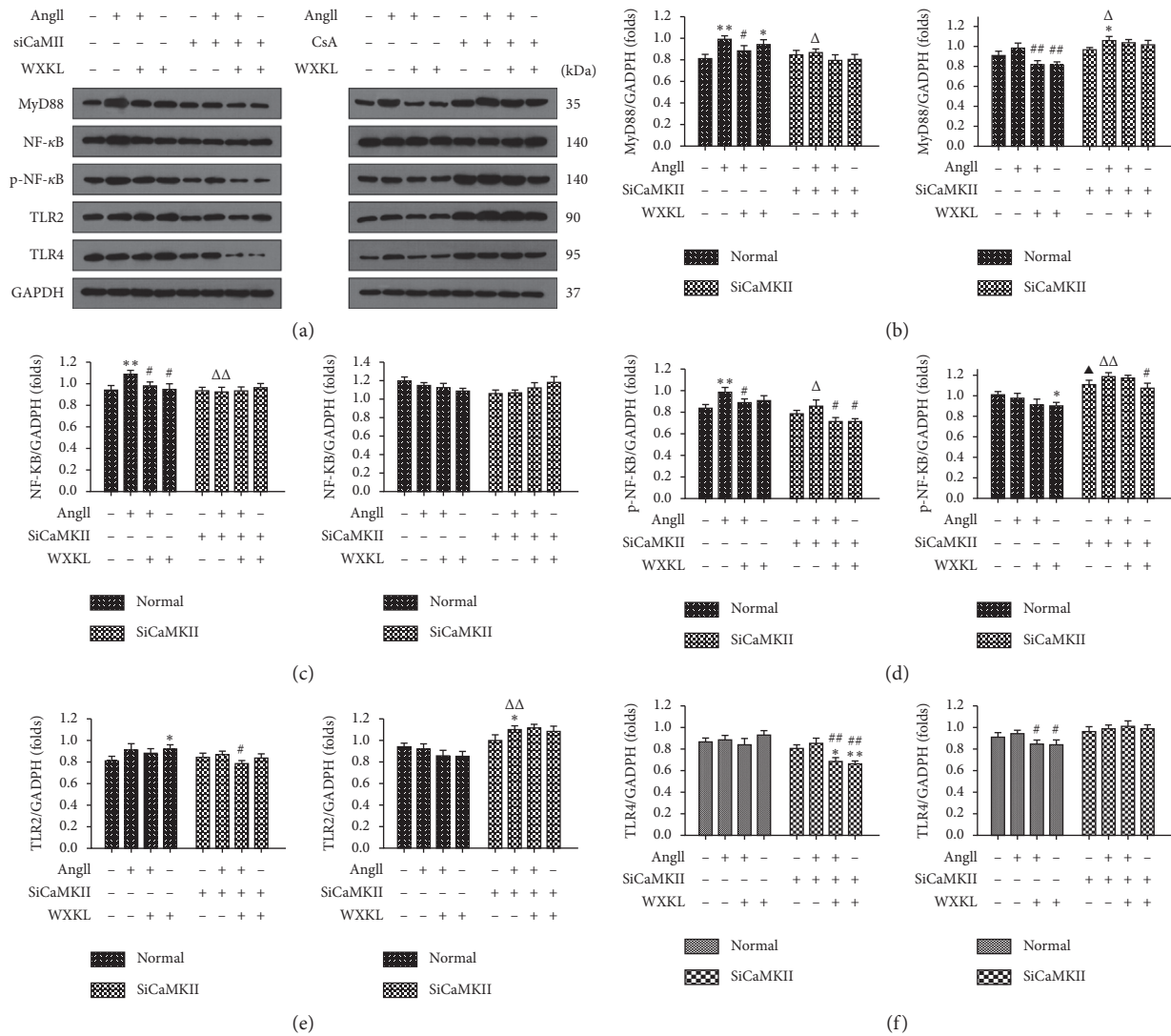


FIGURE 8: Effects of siCaMKII and CsA on Ang II-induced activation of the inflammatory signal transduction pathway in H9c2 cells. (a) Representative western blotting images. Densitometric analysis of (b) MyD88, (c) NF-κB, (d) p-NF-κB, (e) TLR2, and (f) TLR4 expression levels ($n = 3$ cells per group). Data are presented as the mean \pm SD. Statistical significance was determined by one-way ANOVA. * $P < 0.05$ and ** $P < 0.01$ vs. the control group. # $P < 0.05$ and ## $P < 0.01$ vs. the Ang II group. $\blacktriangle P < 0.05$ and $\blacktriangle\blacktriangle P < 0.01$; the control group in SiCaMKII or CsA vs. the control group in normal. $\triangle P < 0.05$ and $\triangle\triangle P < 0.01$; the Ang II group in SiCaMKII or CsA vs. the Ang II group in normal.

Three different CnA subtypes are found in mammals: CnA α and CnA β , which are universally expressed, and CnA γ [9]. Furthermore, it has been reported that CnA β 1 may have a cardioprotective action that decreases inflammation and scar formation [9]. Moreover, mice overexpressing constitutively active CaN show decreased apoptosis after ischemia/reperfusion, whereas deletion of the phosphatase-encoding exon of CnA β leads to increased cell death and reduced cardiac function [42, 43]. In contrast, transgenic mice overexpressing an artificially truncated, constitutively active form of CnA α lacking the auto-inhibitory domain show strong CH and develop HF within the first few weeks of life, which is a response phenocopied by overexpression of a constitutively active form of NFAT [32]. Other studies have suggested that knockout mice

lacking the phosphatase domain of CnA β show smaller hearts at baseline and exhibit reduced hypertrophy in response to pressure overload, Ang II, or isoproterenol [44]. Notably, in the study by Zhang et al. [36], CsA augmented hypertension but did not prevent CH in spontaneously hypertensive rats. CsA is known to cause numerous unwanted side effects. It has been shown that CsA increases Ang II receptors independently from CaN inhibition, which causes vasoconstriction and systemic hypertension and can promote CH [35, 45–47]. This may be due to CsA alleviating the cardioprotective action of CnA β .

There have been some studies on the mechanism of CaMKII and inflammatory pathway regulation [48–53]. Increasing evidence has shown that as a multipurpose kinase, CaMKII plays a pivotal role in many cardiac pathophysiological conditions

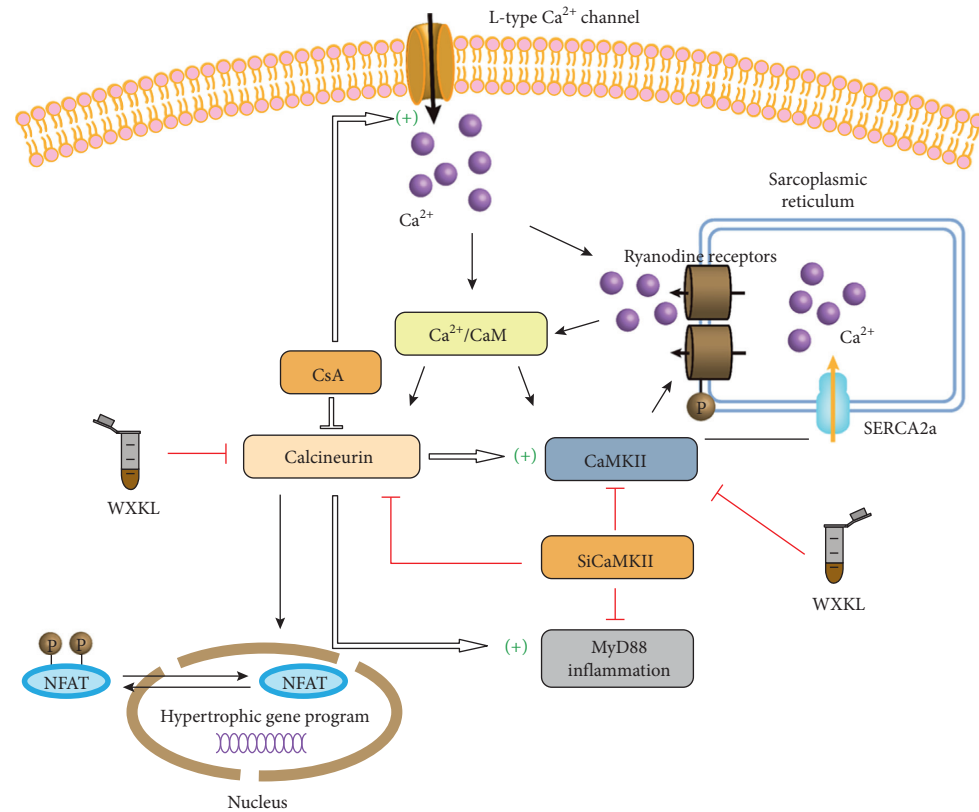


FIGURE 9: Ca²⁺-dependent signaling pathways in cardiac hypertrophy. Upon activation by CaM, CaN dephosphorylates cytoplasmic NFAT, a known hypertrophic transcription factor, and promotes its translocation to the nucleus and subsequent transcriptional activity. After silencing CaMKII, protein expression in the CaMKII and CaN-NFAT signaling pathways was inhibited, and the nuclear transfer of NFATc4 was decreased. CsA, an inhibitor of CaN, inhibits the expression in the CaN-NFAT pathway but activates the CaMKII signaling pathway, MyD88 inflammatory pathway, and I_{Ca-L}. WXXKL improves CH through the CaMKII and CaN-NFAT signaling pathways. CaM: calmodulin; CaN: calcineurin; NFAT: nuclear factor of activated T cells; CaMKII: Ca²⁺/calmodulin-dependent protein kinase II; L-type Ca²⁺ current: I_{Ca-L}; CsA: cyclosporine A; WXXKL: Wenxin Keli; CH: cardiac hypertrophy.

involving inflammation [54]. Previous studies have shown that TLR4 mediates endothelial inflammation, activation, and dysfunction induced by CaN inhibitors, and according to previous observations, MyD88 silencing in endothelial cells prevented the induction of proinflammatory and endothelial activation markers by CsA and tacrolimus [55]. Our data indicate that, after CsA treatment, the expression of MyD88 and TLR2 obviously increased. The activation of MyD88, NF- κ B, TLR2, and TLR4 inflammatory response pathways in pathological states induces an increase in CaMKII protein expression, causes calcium homeostasis, and promotes the occurrence of potentially malignant arrhythmias [56, 57].

WXXL is the first antiarrhythmic Chinese medicine to be approved by the state. Our previous studies indicated that WXXL treatment considerably preserves cardiac function and inhibits arrhythmia by modulating the CaMKII signaling pathway [22, 23]. Moreover, WXXL treats CH and arrhythmia through a mechanism that possibly involves LTCC regulation [20]. We propose a new role for WXXL that may inhibit CH by regulating pathological autophagy [21]. Notably, treatment with WXXL significantly inhibited Ang II-induced hypertrophy in the present study. In addition, WXXL suppressed Ang II-induced elevated expression of CaMKII, CnA, and NFATc4

and prevented Ang II-induced nuclear translocation of NFATc4, suggesting that WXXL attenuated CH by inhibiting the CaMKII and CnA-NFAT signaling pathways. Therefore, owing to its numerous therapeutic benefits, WXXL may be considered as a promising choice for the treatment of CH.

In conclusion, the present study demonstrated that siCaMKII attenuates Ang II-induced CH, which may be partially associated with the downregulation of the CnA-NFAT and MyD88 signaling pathways, and WXXL had a similar effect. Furthermore, siCaMKII may be a promising approach to attenuate the progression of CH and arrhythmia. Our studies define the crosstalk between the CaMKII and CnA-NFAT signaling pathways in vitro, so numerous biological studies are needed for further research in vivo. This will improve the understanding of the mechanisms underlying hypertrophy and may provide evidence for drug application in the treatment of CH.

Abbreviations

CaM:	Calcium/calmodulin
CaMKII:	Calcium-/calmodulin-dependent protein kinase II

CnA-	Calcineurin A-nuclear factor of activated
NFAT:	T cells
CH:	Cardiomyocyte hypertrophy
Ang:	Angiotensin
siCaMKII:	Silenced CaMKII δ
CsA:	Cyclosporine A
WXKL:	Wenxin Keli
I _{Ca-L} :	L-type Ca ²⁺ current
HF:	Heart failure
CaN:	Calcineurin
HDAC:	Histone deacetylase
LTCC:	L-type Ca ²⁺ channel
RyR2:	Ryanodine receptor 2
SR:	Sarcoplasmic reticulum
NCX:	Na ⁺ /Ca ²⁺ -exchanger
BSA:	Bovine serum albumin
PBS:	Phosphate-buffered saline.

Data Availability

The data and materials used in the study are available from the corresponding author upon reasonable request.

Conflicts of Interest

The authors declare that they have no conflicts of interest.

Authors' Contributions

XYW and GYH designed the work. AN wrote the article. CY contributed to cell experiment. XYF and WHH were responsible for critical revision of the article. GXY and CHW searched a lot of literature and revised the manuscript. SK and LYY contributed to the results interpretation. LXY, YF, and PXD analyzed the data. HXF, WX, and LY revised the manuscript.

Acknowledgments

This work was supported by the National Key R&D Program of China (grant nos. 2018YFC1704900 and 2018YFC1704901), National Natural Science Foundation of China (grant nos. 81373835 and 81430098), Scientific Research Program of Outstanding Young Talents in Universities of Fujian Province ([2016] 23), and Scientific Research Startup Funding Project of Fujian Health College (no. 2016-1-2).

Supplementary Materials

Table S1: list of antibodies. Figure S1: effects of siCaMKII and CsA on the CnA-NFAT signaling cascade; double immunofluorescent staining to observe the effects of siCaMKII, CsA and WXKL on expression of CnA in each group. Figure S2: H9c2-1632: validation of CaMKII δ (Rat) 1632 site cell line after RNA interference. (*Supplementary Materials*)

References

- [1] L. Schirone, M. Forte, S. Palmerio et al., "A review of the molecular mechanisms underlying the development and progression of cardiac remodeling," *Oxidative Medicine and Cellular Longevity*, vol. 2017, Article ID 3920195, 9 pages, 2017.
- [2] H.-Y. Fang, M.-Y. Hung, Y.-M. Lin et al., "17 β -Estradiol and/or estrogen receptor alpha signaling blocks protein phosphatase 1 mediated ISO induced cardiac hypertrophy," *PLoS One*, vol. 13, no. 5, Article ID e0196569, 2018.
- [3] C. W. Yancy, M. Jessup, B. Bozkurt et al., "2013 ACCF/AHA guideline for the management of heart failure: executive summary: a report of the American College of cardiology foundation/American heart association task force on practice guidelines," *Circulation*, vol. 128, no. 16, pp. 1810–1852, 2013.
- [4] P. Balakumar and G. Jagadeesh, "Multifarious molecular signaling cascades of cardiac hypertrophy: can the muddy waters be cleared?" *Pharmacological Research*, vol. 62, no. 5, pp. 365–383, 2010.
- [5] M. A. Shibu, C.-H. Kuo, B.-C. Chen et al., "Oolong tea prevents cardiomyocyte loss against hypoxia by attenuating p-JNK mediated hypertrophy and enhancing P-IGF1R, p-akt, and p-Badser136 activity and by fortifying NRF2 anti-oxidation system," *Environmental Toxicology*, vol. 33, no. 2, pp. 220–233, 2018.
- [6] I. Shimizu and T. Minamino, "Physiological and pathological cardiac hypertrophy," *Journal of Molecular and Cellular Cardiology*, vol. 97, pp. 245–262, 2016.
- [7] J. J. Saucerman and D. M. Bers, "Calmodulin mediates differential sensitivity of CaMKII and calcineurin to local Ca²⁺ in cardiac myocytes," *Biophysical Journal*, vol. 95, no. 10, pp. 4597–4612, 2008.
- [8] B. Sanna, O. F. Bueno, Y.-S. Dai, B. J. Wilkins, and J. D. Molkentin, "Direct and indirect interactions between calcineurin-NFAT and MEK1-extracellular signal-regulated kinase 1/2 signaling pathways regulate cardiac gene expression and cellular growth," *Molecular and Cellular Biology*, vol. 25, no. 3, pp. 865–878, 2005.
- [9] L. E. Felkin, T. Narita, R. Germack et al., "Calcineurin splicing variant calcineurin A β 1 improves cardiac function after myocardial infarction without inducing hypertrophy," *Circulation*, vol. 123, no. 24, pp. 2838–2847, 2011.
- [10] J. Heineke and J. D. Molkentin, "Regulation of cardiac hypertrophy by intracellular signalling pathways," *Nature Reviews Molecular Cell Biology*, vol. 7, no. 8, pp. 589–600, 2006.
- [11] B. Fiedler, S. M. Lohmann, A. Smolenski et al., "Inhibition of calcineurin-NFAT hypertrophy signaling by cGMP-dependent protein kinase type I in cardiac myocytes," *Proceedings of the National Academy of Sciences*, vol. 99, no. 17, pp. 11363–11368, 2002.
- [12] Q. Liu, Y. Chen, M. Auger-Messier, and J. D. Molkentin, "Interaction between NF κ B and NFAT coordinates cardiac hypertrophy and pathological remodeling," *Circulation Research*, vol. 110, no. 8, pp. 1077–1086, 2012.
- [13] C. H. Chen, J. W. Lin, C. Y. Huang et al., "The combined inhibition of the CaMKII δ and calcineurin signaling cascade attenuates IGF-IIR-induced cardiac hypertrophy," *Journal of Cellular Physiology*, vol. 235, no. 4, pp. 3539–3547, 2019.
- [14] T. Zhang, E. N. Johnson, Y. Gu et al., "The cardiac-specific nuclear δ B isoform of Ca²⁺/calmodulin-dependent protein kinase II induces hypertrophy and dilated cardiomyopathy associated with increased protein phosphatase 2A activity,"

- Journal of Biological Chemistry*, vol. 277, no. 2, pp. 1261–1267, 2002.
- [15] T. Zhang, L. S. Maier, N. D. Dalton et al., “The δ C isoform of CaMKII is activated in cardiac hypertrophy and induces dilated cardiomyopathy and heart failure,” *Circulation Research*, vol. 92, no. 8, pp. 912–919, 2003.
 - [16] M. M. Kreusser, L. H. Lehmann, S. Keranov et al., “Cardiac CaM kinase II genes δ and γ contribute to adverse remodeling but redundantly inhibit calcineurin-induced myocardial hypertrophy,” *Circulation*, vol. 130, no. 15, pp. 1262–1273, 2014.
 - [17] China Medical Science, *Pharmacopoeia: The Pharmacopoeia Of the People’s Republic of China*, China Medical Science Press, Beijing, China, 2015.
 - [18] G. Nan, C. L. Zhang, C. Wang, C. Wang, Y. F. Zhu, and H. H. Wu, “Determination of notoginsenoside R1, ginsenoside Rg1, Rb1, Rd and lobetyolin in Wenxin Keli by HPLC,” *Tianjin Journal of Traditional Chinese Medicine*, vol. 33, no. 7, pp. 434–436, 2016, in Chinese.
 - [19] Y. Chen, S. Nie, H. Gao et al., “The effects of Wenxin Keli on P-wave dispersion and maintenance of sinus rhythm in patients with paroxysmal atrial fibrillation: a meta-analysis of randomized controlled trials,” *Evidence-Based Complementary and Alternative Medicine*, vol. 2013, Article ID 245958, 9 pages, 2013.
 - [20] Y. Chen, Y. Li, L. Guo et al., “Effects of wenxin keli on the action potential and L-type calcium current in rats with transverse aortic constriction-induced heart failure,” *Evidence-Based Complementary and Alternative Medicine*, vol. 2013, Article ID 572078, 12 pages, 2013.
 - [21] J. Li, Y. Li, Y. Zhang et al., “The inhibitory effect of WenxinKeli on H9c2 cardiomyocytes hypertrophy induced by angiotensin II through regulating autophagy activity,” *Oxidative Medicine and Cellular Longevity*, vol. 2017, Article ID 7042872, 11 pages, 2017.
 - [22] X. Yang, Y. Chen, Y. Li, X. Ren, Y. Xing, and H. Shang, “Effects of Wenxin Keli on cardiac hypertrophy and arrhythmia via regulation of the calcium/calmodulin dependent kinase II signaling pathway,” *BioMed Research International*, vol. 2017, Article ID 1569235, 12 pages, 2017.
 - [23] Y. Xing, Y. Gao, J. Chen et al., “Wenxin-Keli regulates the calcium/calmodulin-dependent protein kinase II signal transduction pathway and inhibits cardiac arrhythmia in rats with myocardial infarction,” *Evidence-Based Complementary and Alternative Medicine*, vol. 2013, Article ID 464508, 15 pages, 2013.
 - [24] A.-M. Sun, “Effect of Wenxin granules combined with metoprolol on cardiac function and exercise tolerance in patients with coronary heart disease tachyarrhythmia,” *Chinese Journal of School Doctor*, vol. 34, no. 7, pp. 502–504, 2020.
 - [25] F. Wang and Z.-Q. Chen, “Treatment effect of wenxin granules on patients with heart failure and atrial fibrillation,” *Practical Clinical Journal of Integrated Traditional Chinese and Western Medicine*, vol. 19, no. 10, pp. 132–133, 2019.
 - [26] H.-E. Liu, “Curative effect of wenxin granule combined with metoprolol on patients with CHD and arrhythmia and its effects on 24 h dynamic electrocardiogram,” *Journal of Rare and Uncommon Diseases*, vol. 27, no. 4, pp. 37–39, 2020.
 - [27] J. Bossuyt, K. Helmstadter, X. Wu et al., “Ca²⁺/Calmodulin-dependent protein kinase II δ and protein kinase D overexpression reinforce the histone deacetylase 5 redistribution in heart failure,” *Circulation Research*, vol. 102, no. 6, pp. 695–702, 2008.
 - [28] J. Backs, K. Song, S. Bezprozvannaya, S. Chang, and E. N. Olson, “CaM kinase II selectively signals to histone deacetylase 4 during cardiomyocyte hypertrophy,” *Journal of Clinical Investigation*, vol. 116, no. 7, pp. 1853–1864, 2006.
 - [29] R. Passier, H. Zeng, N. Frey et al., “CaM kinase signaling induces cardiac hypertrophy and activates the MEF2 transcription factor in vivo,” *Journal of Clinical Investigation*, vol. 105, no. 10, pp. 1395–1406, 2000.
 - [30] C. L. Zhang, T. A. McKinsey, S. Chang, C. L. Antos, J. A. Hill, and E. N. Olson, “Class II histone deacetylases act as signal-responsive repressors of cardiac hypertrophy,” *Cell*, vol. 110, no. 4, pp. 479–488, 2002.
 - [31] D. R. Higazi, C. J. Fearnley, F. M. Drawnel et al., “Endothelin-1-stimulated InsP3-induced Ca²⁺ release is a nexus for hypertrophic signaling in cardiac myocytes,” *Molecular Cell*, vol. 33, no. 4, pp. 472–482, 2009.
 - [32] J. D. Molkenkin, J.-R. Lu, C. L. Antos et al., “A calcineurin-dependent transcriptional pathway for cardiac hypertrophy,” *Cell*, vol. 93, no. 2, pp. 215–228, 1998.
 - [33] W. Zhang, D.-Q. Chen, F. Qi, J. Wang, W.-Y. Xiao, and W.-Z. Zhu, “Inhibition of calcium-calmodulin-dependent kinase II suppresses cardiac fibroblast proliferation and extracellular matrix secretion,” *Journal of Cardiovascular Pharmacology*, vol. 55, no. 1, pp. 96–105, 2010.
 - [34] J. Mustrup, S. Neef, and L. S. Maier, “CaMKII as a target for arrhythmia suppression,” *Pharmacology & Therapeutics*, vol. 176, pp. 22–31, 2017.
 - [35] W. Hayashida, Y. Kihara, A. Yasaka, and S. Sasayama, “Cardiac calcineurin during transition from hypertrophy to heart failure in rats,” *Biochemical and Biophysical Research Communications*, vol. 273, no. 1, pp. 347–351, 2000.
 - [36] W. Zhang, R. C. Kowal, F. Rusnak, R. A. Sikkink, E. N. Olson, and R. G. Victor, “Failure of calcineurin inhibitors to prevent pressure-overload left ventricular hypertrophy in rats,” *Circulation Research*, vol. 84, no. 6, pp. 722–728, 1999.
 - [37] B. J. Wilkins and J. D. Molkenkin, “Calcium-calmodulin signaling in the regulation of cardiac hypertrophy,” *Biochemical and Biophysical Research Communications*, vol. 322, no. 4, pp. 1178–1191, 2004.
 - [38] K. S. Park, T. K. Kim, and D. H. Kim, “Cyclosporin A treatment alters characteristics of Ca²⁺-release channel in cardiac sarcoplasmic reticulum,” *American Journal of Physiology-Heart and Circulatory Physiology*, vol. 276, no. 3, pp. H865–H872, 1999.
 - [39] A. Bandyopadhyay, D. W. Shin, J. O. Ahn, and D. H. Kim, “Calcineurin regulates ryanodine receptor/Ca²⁺-release channels in rat heart,” *Biochemical Journal*, vol. 352, no. 1, pp. 61–70, 2000.
 - [40] J. Matthes, A. Jager, R. Handrock et al., “Ca²⁺-dependent modulation of single human cardiac L-type calcium channels by the calcineurin inhibitor cyclosporine,” *Journal of Molecular and Cellular Cardiology*, vol. 36, no. 2, pp. 241–255, 2004.
 - [41] J. Liu, J. D. Farmer Jr., W. S. Lane, J. Friedman, I. Weissman, and S. L. Schreiber, “Calcineurin is a common target of cyclophilin-cyclosporin A and FKBP-FK506 complexes,” *Cell*, vol. 66, no. 4, pp. 807–815, 1991.
 - [42] L. J. De Windt, H. W. Lim, T. Taigen et al., “Calcineurin-mediated hypertrophy protects cardiomyocytes from apoptosis in vitro and in vivo: an apoptosis-independent model of dilated heart failure,” *Circulation Research*, vol. 86, no. 3, pp. 255–263, 2000.
 - [43] O. F. Bueno, D. J. Lips, R. A. Kaiser et al., “Calcineurin A β gene targeting predisposes the myocardium to acute ischemia-induced apoptosis and dysfunction,” *Circulation Research*, vol. 94, no. 1, pp. 91–99, 2004.

- [44] O. F. Bueno, B. J. Wilkins, K. M. Tymitz et al., "Impaired cardiac hypertrophic response in calcineurin A -deficient mice," *Proceedings of the National Academy of Sciences*, vol. 99, no. 7, pp. 4586–4591, 2002.
- [45] A. D. Kirk, L. M. Jacobson, D. M. Heisey, N. A. Fass, H. W. Sollinger, and J. D. Pirsch, "Posttransplant diastolic hypertension: associations with intragraft transforming growth factor-beta, endothelin, and renin transcription," *Transplantation*, vol. 64, no. 12, pp. 1716–1720, 1997.
- [46] P. V. Avdonin, F. Cottet-Maire, G. V. Afanasjeva, S. A. Loktionova, P. Lhote, and U. T. Ruegg, "Cyclosporine A up-regulates angiotensin II receptors and calcium responses in human vascular smooth muscle cells," *Kidney International*, vol. 55, no. 6, pp. 2407–2414, 1999.
- [47] J. Sadoshima and S. Izumo, "Molecular characterization of angiotensin II--induced hypertrophy of cardiac myocytes and hyperplasia of cardiac fibroblasts: critical role of the AT1 receptor subtype," *Circulation Research*, vol. 73, no. 3, pp. 413–423, 1993.
- [48] K. Kashiwase, Y. Higuchi, S. Hirotsu et al., "CaMKII activates ASK1 and NF- κ B to induce cardiomyocyte hypertrophy," *Biochemical and Biophysical Research Communications*, vol. 327, no. 1, pp. 136–142, 2005.
- [49] G. Liu, J. Zhao, Z. Chang, and G. Guo, "CaMKII activates ASK1 to induce apoptosis of spinal astrocytes under oxygen-glucose deprivation," *Cellular and Molecular Neurobiology*, vol. 33, no. 4, pp. 543–549, 2013.
- [50] J. Backs, T. Backs, S. Neef et al., "The isoform of CaM kinase II is required for pathological cardiac hypertrophy and remodeling after pressure overload," *Proceedings of the National Academy of Sciences*, vol. 106, no. 7, pp. 2342–2347, 2009.
- [51] H. Ling, C. B. B. Gray, A. C. Zambon et al., "Ca²⁺/Calmodulin-dependent protein kinase II δ mediates myocardial ischemia/reperfusion injury through nuclear factor- κ b," *Circulation Research*, vol. 112, no. 6, pp. 935–944, 2013.
- [52] M. V. Singh, A. Kapoun, L. Higgins et al., "Ca²⁺/calmodulin-dependent kinase II triggers cell membrane injury by inducing complement factor B gene expression in the mouse heart," *Journal of Clinical Investigation*, vol. 119, no. 4, pp. 986–996, 2009.
- [53] X. Liu, M. Yao, N. Li, C. Wang, Y. Zheng, and X. Cao, "CaMKII promotes TLR-triggered proinflammatory cytokine and type I interferon production by directly binding and activating TAK1 and IRF3 in macrophages," *Blood*, vol. 112, no. 13, pp. 4961–4970, 2008.
- [54] M. R. Rusciano, E. Sommariva, V. Douin-Echinard, M. Ciccarelli, P. Poggio, and A. S. Maione, "CaMKII activity in the inflammatory response of cardiac diseases," *International Journal of Molecular Sciences*, vol. 20, no. 18, p. 4374, 2019.
- [55] R. Rodrigues-Diez, C. González-Guerrero, C. Ocaña-Salceda et al., "Calcineurin inhibitors cyclosporine A and tacrolimus induce vascular inflammation and endothelial activation through TLR4 signaling," *Scientific Reports*, vol. 6, no. 1, p. 27915, 2016.
- [56] M. V. Singh, P. D. Swaminathan, E. D. Luczak, W. Kutschke, R. M. Weiss, and M. E. Anderson, "MyD88 mediated inflammatory signaling leads to CaMKII oxidation, cardiac hypertrophy and death after myocardial infarction," *Journal of Molecular and Cellular Cardiology*, vol. 52, no. 5, pp. 1135–1144, 2012.
- [57] M. V. Singh and M. E. Anderson, "Is CaMKII a link between inflammation and hypertrophy in heart?" *Journal of Molecular Medicine*, vol. 89, no. 6, pp. 537–543, 2011.

Research Article

Correlation between Mitochondrial Dysfunction, Cardiovascular Diseases, and Traditional Chinese Medicine

Li Zhu,¹ Zhigang Chen,¹ Keli Han,¹ Yilin Zhao,¹ Yan Li,¹ Dongxu Li,^{1,2,3} Xiulong Wang,^{1,2,3} Xuefang Li,^{1,2,3} Siyu Sun,^{1,2,3} Fei Lin,^{1,2,3} and Guoan Zhao ^{1,2,3}

¹The First Affiliated Hospital of Xinxiang Medical University, Xinxiang 453100, Henan, China

²Henan Joint International Research Laboratory of Cardiovascular Injury and Repair, Xinxiang, Henan, China

³Henan Engineering Research Center for Mitochondrion Biomedical of Heart, Xinxiang, Henan, China

Correspondence should be addressed to Guoan Zhao; guoanzhao@xxmu.edu.cn

Received 30 July 2020; Revised 8 September 2020; Accepted 19 September 2020; Published 8 October 2020

Academic Editor: Yong Wang

Copyright © 2020 Li Zhu et al. This is an open access article distributed under the Creative Commons Attribution License, which permits unrestricted use, distribution, and reproduction in any medium, provided the original work is properly cited.

Cardiovascular disease (CVD) is the number one threat that seriously endangers human health. However, the mechanism of their occurrence is not completely clear. Increasing studies showed that mitochondrial dysfunction is closely related to CVD. Possible causes of mitochondrial dysfunction include oxidative stress, Ca²⁺ disorder, mitochondrial DNA mutations, and reduction of mitochondrial biosynthesis, all of which are closely related to the development of CVD. At present, traditional Chinese medicine (TCM) is widely used in the treatment of CVD. TCM has the therapeutic characteristics of multitargets and multipathways. Studies have shown that TCM can treat CVD by protecting mitochondrial function. Via systematic literature review, the results show that the specific mechanisms include antioxidant stress, regulation of calcium homeostasis, antiapoptosis, and regulation of mitochondrial biosynthesis. This article describes the relationship between mitochondrial dysfunction and CVD, summarizes the TCM commonly used for the treatment of CVD in recent years, and focuses on the regulatory effect of TCM on mitochondrial function.

1. Introduction

With the continuous progress in the treatment of infectious diseases and the extension of human life span, the battlefield between humans and diseases has shifted to chronic non-communicable diseases. Among them, cardiovascular disease (CVD) has become the leading cause of death in China and worldwide as its incidence continues to increase, and it poses a serious threat to the safety and quality of life of patients [1, 2]. Atherosclerosis, hypertension, myocardial ischemia-reperfusion injury, and heart failure are common CVDs or pathological processes. However, the mechanism of their occurrence is not completely clear. An increasing number of studies has shown that mitochondrial dysfunction is closely related to CVD. The mechanisms mainly include oxidative stress disorder, calcium disorder, reduction of mitochondrial biosynthesis, transition of mitochondrial permeability, and accumulation of mitochondrial

DNA mutation. At present, TCM, which has the characteristics of multitargets and multipathways, is widely used in the treatment of CVD [3]. Therefore, in this paper, we discuss the relationship between mitochondrial dysfunction and CVD, as well as the therapeutic mechanism of TCM in the treatment of CVD with respect to mitochondrial function.

2. Functional Properties of Mitochondria

Mitochondria are semiautonomous organelles with a unique genetic system that provide the chemical energy required for biosynthesis, respiration, secretion, and mechanical movement in organisms; they are also important organelles that generate intracellular free radicals and regulate apoptosis [4–6]. Mitochondria are known as “capacity factories,” “apoptosis switches,” and “enzyme bags.” They are also called “cellular energy-processing factories” because they

oxidize three major nutrients to provide adenosine triphosphate (ATP), which is required for life activities [4]. In addition to being energy producers, mitochondria are also the main site of reactive oxygen species [6] (ROS) production. Furthermore, mitochondria also play an important role in the regulation of intracellular calcium homeostasis, calcium-sensitive enzyme activity, and signal transduction [7]. In conclusion, mitochondria are central mediators of energy production, signal transduction, oxidative stress, Ca^{2+} homeostasis, and apoptosis regulation. Therefore, the normal function of mitochondria is of great importance in life activities.

3. Mitochondria and Cardiomyocytes

Cardiomyocytes are highly dependent on aerobic oxidation to supply energy. They contain a considerable amount of mitochondria, up to 20–30% of cell capacity, which provide more than 90% of energy to the heart muscle [8, 9]. The sources of myocardial energy include fatty acids, glucose, and other carbohydrates. These substrates are metabolized in mitochondria, providing energy for cardiomyocytes through oxidative phosphorylation. In fact, 60% to 90% of the energy needed by myocardium originates from the ATP produced by aerobic oxidation of fatty acids. Only 10% to 40% of the energy is generated by glucose glycolysis and lactic acid oxidation. In addition, the production and utilization of ketone body, ornithine, heme, cardiolipin, and ubiquinone are all related to mitochondria [10].

As a vital functional organelle in myocardial cells, the function of mitochondria is key to elucidating the physiological and pathological changes in CVD, and mitochondrial homeostasis is the core element for maintaining myocardial metabolism, function, and structure [11].

4. Mitochondrial Homeostasis

Mitochondrial homeostasis is the steady-state balance between mitochondrial biogenesis and degradation. It involves many aspects such as mitochondrial division and fusion [6, 12], mitochondrial crest remodeling [6, 8], mitochondrial biosynthesis [13, 14], mitochondrial autophagy [15, 16], and mitochondrial oxidative stress [9, 17]. Mitochondrial homeostasis refers to the healthy and stable state of mitochondrial content and metabolism for ensuring the stability of cell energy supply and material metabolism. To maintain the integrity of the mitochondrial structure, mitochondrial division and fusion and mitochondrial crest morphology are altered along with changes in intracellular energy supply [12]. Mitochondrial health is maintained through biosynthesis and autophagy degradation to respond to different energy requirements of cells [10, 15]. In addition, ROS in mitochondria can be used as signal molecules to activate redox signal molecules through redox reaction, thus participating in the regulation of intracellular signal transduction [18]. Disruption of mitochondrial homeostasis may cause imbalance of mitochondrial motility, lysis of mitochondrial cristae, disruption of mitochondrial biosynthesis, abnormal degradation of mitochondrial autophagy, and

oxidative stress in mitochondria. Therefore, the stable state of mitochondrial structure and function has very important physiological significance for the growth, metabolism, and heredity of organisms [19].

5. Mitochondria Dysfunction and Cardiovascular Diseases

Mitochondria are the energy factories of cells, and their main function is to consume oxygen and metabolize three major nutrients (sugars, lipids, and amino acids) to produce CO_2 , water, and energy (ATP) [4]. Cells often need to manage their energy expenditure based on the availability of nutrients and their ability to produce ATP [10]. Disrupted mitochondrial homeostasis will lead to abnormal metabolism of these common substances in the body. Higher organisms need to consume larger amount of energy, and the ATP produced by anaerobic glycolysis is only approximately 1/16 of that produced by aerobic oxidation.

Mitochondria are exposed to various physiological or stress signals, and they produce different signal molecules that affect oxidative stress, apoptosis, autophagy, and inflammation, which are closely related to the occurrence of CVD [11, 16, 20]. The pathophysiological processes of abnormal effects of mitochondria on CVD are reflected in the following aspects: (1) because cardiomyocytes rely on fatty acid-driven oxidative phosphorylation to produce ATP, a decline in the biological efficiency of the mitochondrial network may directly harm the contractility of cardiomyocytes; (2) because Ca^{2+} flow is the core of overall cardiac activity, incapability of the mitochondrial network to regulate Ca^{2+} homeostasis can alter cardiac function; (3) physiological inflammatory homeostasis has a certain protective effect not only on cardiac function but also on vascular filling, but the accumulation of damaged mitochondria in the cytoplasm of cardiomyocytes or endothelial cells can cause pathogenic inflammation; and (4) the integrity of the cardiovascular system is essential for cardiac contractile and circulatory functions. Severe mitochondrial dysfunction and accumulation of damaged mitochondria initiate a series of cell death that eventually leads to pathological damage.

6. Mitochondrial Dysfunction and Atherosclerosis

Atherosclerotic (AS) is the main cause of death due to cardiovascular disease. In patients with mitochondrial dysfunction, decreased activity of progressive respiratory chain enzymes, excessive production of ROS, and cumulative mitochondrial DNA (mtDNA) damage or mutations are closely related to the occurrence and development of atherosclerosis [21, 22]. Studies have shown that oxidized low-density lipoprotein (ox-LDL) plays an important role in the occurrence and development of atherosclerosis; ROS produced by mitochondria and its modified ox-LDL are involved in all pathological processes of atherosclerosis [23]. Ox-LDL can slow down the electron transport of mitochondrial respiratory

chain by inhibiting the activity of mitochondrial respiratory enzymes and increasing the formation of ROS, thus forming a vicious circle and promoting endothelial injury and atherosclerosis [23]. It was found that when the activity of Mn-SOD (SOD₂) decreased, mtDNA damage increased in apoE^{-/-} rats, which preceded the formation of atherosclerotic plaques. As oxidative stress in mitochondria increased, atherosclerotic lesions were significantly aggravated [24]. In addition, studies in apoE^{-/-}-SOD₂^{+/-} mice have shown that an increase in mitochondrial ROS not only promoted the formation of atherosclerotic plaques but also increased the susceptibility of the body to atherosclerotic risk factors [25]. Moreover, mtDNA damage caused by DNA repair dysfunction can directly accelerate atherosclerosis in apoE^{-/-} rats and promote diabetic atherosclerotic complications. Furthermore, transient opening of mitochondrial permeability transition pore (mPTP) can depolarize mitochondrial membrane potential, whereas long-term opening of mPTP leads to matrix swelling, rupture of mitochondrial outer membrane, and apoptosis. Both of these changes can promote the occurrence and development of atherosclerosis [21, 22]. In an experiment using wild-type mice, it was found that aging led to increases in IL-6 level and mitochondrial dysfunction. Hyperlipidemia further decreased the mitochondrial function and increased the level of Parkin in the aorta of old mice (16 months of age). Importantly, oral spermidine can enhance the mitotic function of aged hyperlipidemic mice, prevent elevation of aortic IL-6 and Parkin levels, reduce mitochondrial dysfunction, and reduce atherosclerosis formation. Overall, new treatments that improve vascular mitochondrial bioenergetics or reduce inflammation before hyperlipidemia may reduce age-related atherosclerosis [26]. Overall, oxidative stress, inflammatory reaction, and mitochondrial dysfunction play a key role in the formation of atherosclerosis. Mitochondria-targeted antioxidant and anti-inflammatory therapies may have great prospects for the treatment of atherosclerosis [27].

7. Mitochondrial Dysfunction and Hypertension

Hypertension is a common CVD in modern society. Many studies have shown that mitochondrial dysfunction is closely related to hypertension [28]. The superoxide anions produced by mitochondria can oxidize the NO released by endothelial cells, decrease the endothelium-dependent vasodilation function, increase vascular force, and increase blood pressure. Uncoupling of mitochondrial oxidative phosphorylation caused by UCP2 gene polymorphism or altered expression is also associated with high blood pressure [29]. In addition, the lack of mitochondrial productivity, calcium overload, and mitochondrial DNA mutations are all involved in the pathological process of arterial hypertension and hypertensive heart disease. Angiotensin II (Ang II) plays an important role in the development of hypertension. Ang II can also inactivate the NO produced by endothelial cell by stimulating the production of mitochondrial ROS, resulting in vascular endothelial dysfunction [30]. Mitochondrial dysfunction is also related to dysfunction of blood pressure regulation

center [31]. Related research has confirmed that mitochondrial dysfunction caused by maternally inherited mitochondrial transfer ribonucleic acid (tRNA) mutations is associated with the development of essential hypertension [32]. Otherwise, under the conditions of inflammation, Ang II stimulation, and metabolic syndrome, disturbances in mitochondrial biogenesis and mitochondrial bioenergetics in the brain will lead to the accumulation of ROS, which plays an active role in the pathophysiology of ROS-related neurogenic hypertension [33]. Overall, increased ROS production, decreased ATP production, and calcium overload play an important role in the occurrence and development of hypertension. Moreover, mitochondrial gene polymorphism and mitochondrial tRNA gene mutations are also associated with hypertension.

8. Mitochondrial Dysfunction and Myocardial Ischemia-Reperfusion Injury

Myocardial ischemia-reperfusion injury (IR injury) is common in reperfusion therapy after acute myocardial infarction, manifesting as arrhythmia, reduced cardiac systolic function, and other phenomena. Mitochondrial energy metabolism disorder is an important factor causing myocardial IR injury [34]. The main mechanisms include reduced mitochondrial ATP production and excessive ROS production, causing oxidative stress, Ca²⁺ overload, and sustained mPTP opening [18, 35]. Excessive ROS production during ischemic myocardial reperfusion is the main cause of myocardial IR injury, and mitochondria are an important source of ROS. On the one hand, increased ROS can damage the mitochondrial membrane system, which affects the mitochondrial membrane potential and disrupts mitochondrial ATP synthesis. On the other hand, mitochondria produce excessive ROS, which causes peroxidation of proteins and lipids and damage to the mitochondrial membrane, further decreasing the activity of the electron transport chain enzymes, which in turn form a vicious circle that eventually leads to cardiomyocyte apoptosis and necrosis [36]. In addition to excessive ROS, myocardial ischemia-reperfusion-induced cell Ca²⁺ overload is an important cause of myocardial IR injury [18, 35]. Persistent opening of mitochondrial mPTP with high permeability also plays an important role in IR injury. This causes the entrance of numerous small molecules to mitochondria, resulting in the swelling of mitochondria, rupture of the outer membrane, collapse of membrane potential, and release of various pro-apoptotic factors to induce cell apoptosis or death [35]. Taken together, improving mitochondrial function, reducing oxidative stress caused by excessive production of mitochondrial ROS, preventing intracellular calcium overload, and preventing the opening of mitochondrial mPTP are effective measures for the prevention and treatment of IR injury.

9. Mitochondrial Dysfunction and Heart Failure

Heart failure (HF) is the final stage of the development of various CVDs, such as myocardial infarction, hypertension, and cardiomyopathy. The relationship between mitochondrial

TABLE 1: Regulatory effects of active components of TCM on mitochondria.

Category	Chemical components of TCM	Monomer source	Molecular formula	Mechanism of action	Reference
Restoratives for invigorating qi	Ginsenoside compound K	<i>Radix ginseng</i>	C ₃₆ H ₆₂ O ₈	Inhibition of nuclear factor- κ B, p38, and JNK MAPK pathways	Lu et al. [43]
	Astragaloside IV	<i>Radix Astragali</i>	C ₄₁ H ₆₈ O ₁₄	Regulation of NF- κ B/PGC-1 α signaling-mediated energy biosynthesis	Zhang et al. [44]
	Astragalus polysaccharides	<i>Radix Astragali</i>	C ₁₀ H ₇ C ₁ N ₂ O ₂ S	Downregulation of miR-23a and miR-92a-activated PI3K/AKT and MAPK/ERK signaling pathways	Gong et al. [45]
	Salidroside	<i>Rhodiola crenulata</i>	C ₁₄ H ₂₀ O ₇	Stimulation of fatty acid β -oxidation and improvement of mitochondrial function	Dong et al. [46]
Restoratives for nourishing yin				Inhibition of apoptosis	Liu et al. [47]
				Activation of a mitochondria-associated AMPK/PI3K/Akt/GSK3 β pathway	Zheng et al. [48]
Restoratives for nourishing yin	Ophiopogonin D	<i>Radix Ophiopogonis</i>	C ₄₄ H ₇₀ O ₁₆	Antioxidant and antiapoptotic effects	Huang et al. [49]
	Ecliptal	<i>Eclipta alba</i>	—	Activation of the Wnt-pathway and alteration of AKT signaling	Yang et al. [50]
Restoratives for nourishing yang	Velvet antler	<i>Cornu cervi pantotrichum</i>	—	Regulation of the PI3K/Akt signaling pathway and mitochondrial membrane potential	Xiao et al. [51]
	Icariin	<i>Herba Epimedii</i>	C ₃₃ H ₄₀ O ₁₅	Activation of sirtuin-1/FOXO1 signaling and improvement of mitochondrial membrane homeostasis	Wu et al. [52]

dysfunction and HF is mainly reflected as follows: the disturbance of mitochondrial energy metabolism plays an important role in the occurrence and development of HF. During HF, mitochondrial ATP synthesis decreased, and ROS production increased, whereas the disturbance of energy metabolism in myocardial mitochondria aggravated the disruption of cardiac mechanical function and deterioration of cardiac function. ROS modified myofibrillar protein in the myocardium via oxidation, resulting in a progressive decrease in cardiac contractile function and irreversible cardiac injury [37, 38]. Studies in an experimental HF model have shown that the expression of myocardial mitochondrial biosynthesis factor is downregulated, whereas mtDNA content is reduced, which not only results in reduced mitochondrial biosynthesis but also causes mitochondrial oxidative phosphorylation and reduces the ability of mitochondria to oxidize fatty acids, which leads to deficiencies in myocardial energy production and HF development [39]. In patients with congenital heart disease, damage in mtDNA replication leads to the loss of right ventricular mtDNA, resulting in the progression of heart hypertrophy to HF [40, 41]. Therefore, to prevent mitochondrial damage and maintain the integrity of its function, reducing oxidative stress will be an important strategy in the treatment of HF [41].

In summary, the maintenance of mitochondrial homeostasis is very important in life activities, and mitochondrial dysfunction is closely related to the occurrence and development of CVD. TCM is widely applied in the clinical treatment of CVD, and mitochondria are the intracellular targets of many kinds of drugs. Thus, we propose that TCM can treat CVD by affecting mitochondrial homeostasis.

10. Protective Effect of TCM on Myocardial Mitochondria

Mitochondria play a significant role in the regulation of physiological function and pathological process in the cardiovascular system [11]. TCM [42], including the chemical components, single herbs, and compound medicines, can treat CVD by regulating the function of mitochondria, which will be described below.

10.1. Chemical Components of TCM. The chemical components of TCM are the substance bases of its pharmacology. The composition of TCM is extremely complex, as each TCM contains many kinds of chemical components. Components that have biological activity and play a role in the prevention and treatment of diseases are known as effective components. Modern studies have shown that the effective components of TCM can protect cardiomyocyte mitochondria in many ways. Several common drugs are summarized in Tables 1–4.

10.2. Single Herbs of TCM. Single herbs are a type of TCM. Different single herbs have different curative effects, but they may have the same drug action. A single herb can have many different effects. Previous studies have shown that some single-herb medicines can treat coronary heart disease (CHD) by affecting mitochondrial homeostasis. Several common drugs are summarized in Table 5.

TABLE 2: Regulatory effects of the active components of traditional Chinese medicine on mitochondria for promoting blood circulation and removing blood stasis.

Chemical components of TCM	Monomer source	Molecular formula	Mechanism of action	Reference
Panax notoginseng saponins	<i>Radix Notoginseng</i>	C ₄₇ H ₈₀ O ₁₇	Attenuation of oxidative stress and cardiomyocyte apoptosis	Zhang et al. [53] Zhou et al. [54]
Notoginsenoside R1	<i>Radix Notoginseng</i>	C ₅₄ H ₉₂ O ₂₄	Elevation of mitochondrial ATP synthase <i>d</i> -subunits	He et al. [55]
Salvianolic acid A	<i>Radix Salviae Miltiorrhizae</i>	C ₂₆ H ₂₂ O ₁₀	Promotion of myocardial mitochondria biogenesis	Zhang et al. [56]
Salvianolic acid B	<i>Radix Salviae Miltiorrhizae</i>	—	Improvement of mitochondrial biogenesis	Pan et al. [57]
Tanshinone IIA	<i>Radix Salviae Miltiorrhizae</i>	C ₁₉ H ₁₈ O ₃	Upregulation of 14-3-3 η , prevention of mPTP opening, and inhibition of apoptosis	Zhang et al. [58]
Dihydrontanshinone	<i>Radix Salviae Miltiorrhizae</i>	—	Anti-inflammatory effect via the NF- κ B, mitochondrial ROS, and MAPK pathways	Wu et al. [59]
Curcumin	<i>Rhizoma Curcumae Longae</i>	C ₂₁ H ₂₀ O ₆	Antioxidant and anti-inflammatory activities Mitochondrial stress and substrate switching inhibition	Li et al. [60]

TABLE 3: Regulatory effects of the active components of interior warming medicines on mitochondria.

Chemical components of TCM	Monomer source	Molecular formula	Mechanism of action	Reference
Flavonoid glycosides	<i>Fenugreek</i>	—	Regulation of glycolipid metabolism	Luan et al. [61]
	<i>Rhizoma Zingiber</i>	C ₁₇ H ₂₆ O ₄	Improvement of ectopic lipid accumulation, mitochondrial dysfunction, and insulin resistance	Liu et al. [62]

TABLE 4: Regulatory effects of the active components of other traditional Chinese medicines on mitochondria.

Type of TCM	Monomer source	Molecular formula	Mechanism of action	Reference
Triptolide	<i>Tripterygium wilfordii</i>	C ₂₁ H ₂₈ O ₆	Regulation of mitochondrial membrane permeabilization	Xi et al. [63]
Oxymatrine	<i>Radix Sophorae Flavescentis</i>	C ₁₆ H ₂₆ N ₂ O ₂	Inhibition of cardiac apoptosis and oxidative stress	Zhang et al. [64]
Epigallocatechin gallate	<i>Green tea</i>	C ₂₂ H ₁₈ O ₁₁	Inhibition of deterioration of mitochondrial structure and function by OMA1	Nan et al. [65]
Cyclovirobuxine D	<i>Buxus microphylla Sieb</i>	C ₂₆ H ₄₆ N ₂ O	Antioxidant effect and promotion of mitochondrial biogenesis	Guo et al. [66]
Tetrandrine	<i>Radix Stephaniae Tetrandrae</i>	C ₃₈ H ₄₂ N ₂ O ₆	Regulation of glycolysis and energy metabolism	Zhang et al. [67]

10.3. *Compound Prescriptions of TCM.* Compound prescriptions are the main form of clinical TCM. After determining the treatment based on syndrome differentiation, a compound prescription is formulated by selecting the appropriate drug, determining the dosage, and combining two or more medicines according to the requirements of the basic structure of the prescription. The main objectives of these prescriptions are to enhance drug efficacy, produce synergistic drug effects, control the direction of multifunctional single herbs, expand the scope of treatment, improve drug adaptation to complex conditions, and control the toxic and side effects of drugs.

Clinically, most of the drugs used to treat CHD are compound prescriptions. The regulation of CHD by

compound prescriptions involve the whole body, including the heart, brain, liver, kidney, lung, large intestine, muscle, and other viscera, and they improve the structure and quantity of mitochondria in each tissue [39, 74]. In addition, compound prescriptions can treat CHD by protecting mitochondrial function, reducing antioxidant stress, improving mitochondrial lipid metabolism, and exerting anti-inflammatory effect. The compound prescriptions commonly used in TCM are listed in Table 6.

In summary, mitochondria are semiautonomous organelles that integrate the three basic life activities: material metabolism, energy metabolism, and genetic variation; they are also the place for intracellular respiration and energy conversion and participate in various important physiological and biochemical

TABLE 5: Regulatory effects of single-herb traditional Chinese medicines on mitochondria.

Type of TCM	Single herb	Mechanism of action	Reference
Restoratives for invigorating qi	<i>Radix Astragali</i>	Promotion of mitochondrial bioenergetics	Huang et al. [68]
Restoratives for invigorating qi	<i>Rhodiola rosea</i>	Promotion of mitochondrial biogenesis and functions	Zhuang et al. [69]
		Antioxidant and anti-inflammatory activities	Zhou et al. [70]
Heat clearing Chinese medicinal herbs	<i>Silybum marianum</i>	Mitigation of oxidative stress and attenuation of reactive fibrosis via TGF β 1/T β Rs/SMAD2/3 signaling	Vilahir et al. [71]
Invigorating the blood and removing blood stasis	<i>Salviae Miltiorrhizae Radix et Rhizoma</i>	Activation of the Nrf2-mediated antioxidant defense system	Li et al. [72]
The interior warming Chinese medicinal herbs	<i>Cortex Cinnamomi</i>	Upregulation of mitochondrial biogenesis	Song et al. [73]

TABLE 6: Regulatory effects of compound prescriptions on mitochondria.

Name of compound prescription	Components of compound prescription	Mechanism of action	Reference
Shengmai formula (SM)	<i>Radix ginseng</i> and <i>Radix Ophiopogonis</i>	Protection of cardiomyocytes against hypoxia Induction of mitophagy and modulation of mitochondrial dynamics	Wang et al. [75], Yu et al. [76]
Shenxian-Shengmai oral (SXSM)	<i>Red Radix ginseng</i> , <i>Herba Epimedii</i> , <i>Fructus Psoraleae (salted)</i> , <i>Fructus Lycii</i> , <i>Herba Ephedrae</i> , etc.	Antioxidant effect, promotion of SOD activity, elevation of GSH content, and reduction of intracellular ROS levels	Zhao et al. [77]
YiXin-Shu (YXS)	<i>Ginseng</i> , <i>Radix Astragali</i> , <i>Salvia miltiorrhiza</i> , <i>Ophiopogon</i> , <i>Ligusticum</i> , etc.	Upregulation of endogenous nuclear receptors (LXR α , PPAR α , PPAR β , and ER α) as well as suppression of apoptosis and oxidative stress Improvement of mitochondrial lipid metabolism, restoration of mitochondrial structure and function, and promotion of mitochondrial biogenesis via the Sirt1/PGC-1 α pathway	Zhao et al. [78]
Shengmai San (SMS)	<i>Panax ginseng</i> , <i>Ophiopogon japonicus</i> , and <i>Schisandra chinensis</i>	Regulation of energy metabolism and elevation of mitochondrial content and biogenesis via PGC-1 α activation	Tian et al. [79], Lu et al. [80], and Li et al. [81]
QiShenYiQi Pills (QSYQ)	<i>Radix Astragali</i> , <i>Salvia miltiorrhiza</i> , <i>Panax notoginseng</i> , etc.	Anti-inflammatory and antioxidant effects, improvement of lipid metabolism, protection of mitochondrial function, and upregulation of AMPK and PGC-1 α expression	Lin et al. [82], Yu et al. [83], and Lin et al. [84]
Shexiang Baoxin Pill (SBP)	<i>Moschus</i> , <i>Radix Ginseng</i> , <i>Calculus Bovis</i> , <i>Styrax</i> , <i>Cortex Cinnamomi</i> , <i>Venenum Bufonis</i> , and <i>Borneolum Syntheticum</i>	Prevention of sepsis-induced apoptosis	Wei et al. [85]
Qiang-Xin 1 formula	<i>Astragalus</i> , <i>Poria</i> , <i>Schisandra</i> , <i>Salvia miltiorrhiza</i> , etc.	Anti-inflammatory effect and improvement of lipid metabolism	Xu et al. [86]
Tongxinluo capsule (TXL)	<i>Radix ginseng</i> , <i>Hirudo</i> , <i>Scorpio</i> , <i>Radix Paeoniae Rubra</i> , etc.		Zhang et al. [74] Ma et al. [87]

TABLE 7: Action mechanisms of TCM on mitochondria.

Action mechanism	Chemical components of TCM	Single herb	Compound prescription
Mitochondrial structure	Velvet antler, icariin, tanshinone IIA, triptolide, and epigallocatechin gallate	—	Shengmai San
Mitochondria biosynthesis	Ecliptal, salvianolic acid A, salvianolic acid B, and cyclovirobuxine D	<i>Radix Astragali</i> , <i>Rhodiola rosea</i> , <i>Cortex, Cinnamomi</i>	QiShenYiQi pills
Mitochondrial function	Flavonoid glycosides, 6-gingerol, and epigallocatechin gallate	<i>Rhodiola rosea</i>	Shengmai formula, Shengmai San, and Shexiang Baoxin pill
Anti-inflammatory effect	Ginsenoside compound K, astragaloside IV, dihydronortanshinone, and curcumin	<i>Rhodiola rosea</i>	Tongxinluo capsule (TXL), Shexiang Baoxin pill
Inhibit apoptosis	<i>Astragalus polysaccharides</i> , ophiopogonin D, and oxymatrine	—	YiXin-Shu, Qiang-Xin 1 formula
Antioxidation	Ophiopogonin D, panax notoginseng saponins, oxymatrine, cyclovirobuxine D, and curcumin	<i>Rhodiola rosea</i> , <i>Silybum marianum</i> , <i>Salviae, Miltiorrhizae Radix et Rhizoma</i>	Shenxian-Shengmai oral, YiXin-Shu, and Shexiang Baoxin pill
Energy metabolism	Salidroside, notoginsenoside R1, and tetrandrine	<i>Radix Astragali</i>	—

processes. Overall, TCM affects the processes of mitochondrial energy metabolism, apoptosis, and oxidative stress in multi-levels via multitargets, and the same category of drugs has certain commonness and individuality. The mechanisms are summarized in Table 7.

11. Conclusions and Perspectives

CVD is the leading cause of death in China [2]. CHD is a relatively common type of CVD. At present, CHD has become a major global public health problem; although antithrombosis, anti-ischemia, and lipid-regulating interventional therapies and secondary preventions have been used to improve CHD symptoms and reduce the mortality and HF after percutaneous coronary intervention (PCI), no reflow after revascularization, depression after CHD, CHD complications, and antithrombotic drug resistance still persist as clinical problems that need to be solved. At present, syndrome differentiation via a combination of modern medicine and TCM is the main method for treating CVD in China and abroad [88].

Coronary atherosclerosis or vasospasm leads to decreased myocardial blood perfusion and increased ischemic damage of cells. During the ischemic period, hypoxia causes inhibition of mitochondrial ATP synthesis and oxidative phosphorylation, making it difficult for cells to maintain normal ATP content. At the same time, under the condition of ischemia and hypoxia, excessive metabolites, such as lactic acid, pyruvate, phosphate, and other acids, accumulate in the myocardium and produce symptoms such as angina pectoris or chest tiredness. An evidence showed that mitochondrial dysfunction occurs in the early stage of CHD and mitochondrial autophagy occurs in the late stage, which involves the steady-state dynamic balance of mitochondria [89].

A growing number of studies showed that mitochondria play an important role in the cardiovascular system. Mitochondria can be used as targets for the treatment of CVDs [90]. Mutations in mtDNA affect CVD, leading to hypertension, atherosclerosis, and cardiomyopathy. However, TCM can regulate the structure and function of mitochondria by increasing electron transport and oxidative phosphorylation of mitochondria, thus regulating mitochondria-mediated apoptosis and reducing mitochondrial ROS to treat CVD.

At present, there are multiple forms of TCM used in the treatment of CVD, including its active components, single herbs, and compound prescriptions [3, 42]. One review of 68 randomized controlled trials that included a total of 16171 patients revealed that, compared with blank control or placebo, TCM effectively reduces the severity of angina pectoris and MI; it also lowers blood pressure in patients with hypertension and improves cardiac function in patients with HF [91]. In most studies, the frequency of adverse effects was not higher for TCM than for controls or Western medicine [91]. However, the methodological quality of the majority of included studies was low; further studies using strictly designed randomized controlled trials are necessary to provide strong evidence [92]. Owing to the complexity of CVD pathogenesis, the action mechanism of TCM in the treatment of CVD is difficult to clarify. Moreover,

mitochondria are the intracellular targets of many drugs, and there are extensive and complex interactions between mitochondria and related drugs [90].

TCM has the advantages of multitarget and multipathways [42, 93]. A large number of clinical experiences and studies have shown that TCM plays an important role in the prevention, treatment, and prognosis of CVD [93]. Previous studies by our team have shown that circRNAs are closely related to the pathological process of acute coronary syndrome via a mechanism that may be related to the up- or downregulation of circRNAs and miRNAs and the coexpression of circRNA-miRNA [94]. In addition, through literature review, we consider that the circRNA-miRNA-mRNA network may be a new regulatory mechanism for TCM to effectively treat CVD [93]. Besides, TCM has been shown to improve the morphology and structure of mitochondria and participate in a series of metabolic processes, including regulation of energy metabolism, inhibition of apoptosis, and reduction of oxygen free radical production in mitochondria. There is a certain correlation between the intracellular targets of TCM and mitochondria.

Furthermore, we should treat diseases according to syndrome differentiation and reasonably choose TCM based on the basic theory of TCM. Integrating TCM with Western medicine, an unprecedented task in today's world, would provide a new medical model with unique advantages that can play an important role in the treatment of diseases [95]. Some experiments have confirmed the efficacy of combining TCM with Western medicine for the treatment of angina pectoris [96], and evidence for using TCM for the treatment of other CVDs is also increasing [3]. The combination of TCM and Western medicine is an attractive avenue for therapeutic intervention in CVD, and it may be the best scheme for CVD treatment. Thus, developing a strategy for integrating TCM with Western medicine will greatly contribute to human health care [95].

Data Availability

This review article is based on some previous studies of the authors on the relationship between mitochondria and cardiovascular diseases and the role of traditional Chinese medicine in the treatment of cardiovascular diseases. Previously reported studies were used to support this study and are available at doi: 10.1155/2015/143145, doi: 10.1155/2020/1584052, doi: 10.1155/2020/8048691, etc. In addition, the results obtained through extensive literature review provide strong support for the article. These prior studies are cited at relevant places within the text as references.

Conflicts of Interest

The authors declare that they have no conflicts of interest regarding the publication of this paper.

Acknowledgments

This work was supported by the Key Scientific Research Projects of Higher Education Institutions in Henan Province

(nos. 2006320035 and 19A360032) and Scientific and Technological Research Projects in Henan Province (nos. 182102310182 and 192102310319).

References

- [1] K. J. Foreman, N. Marquez, A. Dolgert et al., "Forecasting life expectancy, years of life lost, and all-cause and cause-specific mortality for 250 causes of death: reference and alternative scenarios for 2016-40 for 195 countries and territories," *The Lancet*, vol. 392, no. 10159, pp. 2052-2090, 2018.
- [2] D. Zhao, J. Liu, M. Wang, X. Zhang, and M. Zhou, "Epidemiology of cardiovascular disease in China: current features and implications," *Nature Reviews Cardiology*, vol. 16, no. 4, pp. 203-212, 2019.
- [3] X. Xiong, F. Borrelli, A. de Sá Ferreira, T. Ashfaq, and B. Feng, "Herbal medicines for cardiovascular diseases," *Evidence Based Complementary and Alternative Medicine*, vol. 2014, Article ID 809741, 2014.
- [4] J. B. Spinelli and M. C. Haigis, "The multifaceted contributions of mitochondria to cellular metabolism," *Nature Cell Biology*, vol. 20, no. 7, pp. 745-754, 2018.
- [5] F. J. Bock and S. W. G. Tait, "Mitochondria as multifaceted regulators of cell death," *Nature Reviews Molecular Cell Biology*, vol. 21, no. 2, pp. 85-100, 2020.
- [6] K. Boengler, M. Kosiol, M. Mayr, R. Schulz, and S. Rohrbach, "Mitochondria and ageing: role in heart, skeletal muscle and adipose tissue," *Journal of Cachexia, Sarcopenia and Muscle*, vol. 8, no. 3, pp. 349-369, 2017.
- [7] J. Szymański, J. Janikiewicz, B. Michalska et al., "Interaction of mitochondria with the endoplasmic reticulum and plasma membrane in calcium homeostasis, lipid trafficking and mitochondrial structure," *International Journal of Molecular Sciences*, vol. 18, no. 7, 2017.
- [8] E. J. Lesnefsky, Q. Chen, and C. L. Hoppel, "Mitochondrial metabolism in aging heart," *Circulation Research*, vol. 118, no. 10, pp. 1593-1611, 2016.
- [9] B. Martín-Fernández and R. Gredilla, "Mitochondria and oxidative stress in heart aging," *Age*, vol. 38, no. 4, pp. 225-238, 2016.
- [10] S. Herzig, R. J. Shaw, and R. J. Shaw, "AMPK: guardian of metabolism and mitochondrial homeostasis," *Nature Reviews Molecular Cell Biology*, vol. 19, no. 2, pp. 121-135, 2018.
- [11] G. Siasos, V. Tsigkou, M. Kosmopoulos et al., "Mitochondria and cardiovascular diseases-from pathophysiology to treatment," *Annals of Translational Medicine*, vol. 6, no. 12, p. 256, 2018.
- [12] J. N. Meyer, T. C. Leuthner, and A. L. Luz, "Mitochondrial fusion, fission, and mitochondrial toxicity," *Toxicology*, vol. 293, pp. 42-53, 2017.
- [13] K. Palikaras and N. Tavernarakis, "Mitochondrial homeostasis: the interplay between mitophagy and mitochondrial biogenesis," *Experimental Gerontology*, vol. 56, pp. 182-188, 2014.
- [14] N. Pfanner, B. Warscheid, and N. Wiedemann, "Mitochondrial proteins: from biogenesis to functional networks," *Nature Reviews Molecular Cell Biology*, vol. 20, pp. 267-284, 2019.
- [15] P. E. Morales, C. Arias-Durán, Y. Ávalos-Guajardo et al., "Emerging role of mitophagy in cardiovascular physiology and pathology," *Molecular Aspects of Medicine*, vol. 71, Article ID 100822, 2020.
- [16] C. Vásquez-Trincado, I. García-Carvajal, C. Pennanen et al., "Mitochondrial dynamics, mitophagy and cardiovascular disease," *The Journal of Physiology*, vol. 594, no. 3, pp. 509-525, 2016.
- [17] S. J. Forrester, D. S. Kikuchi, M. S. Hernandez, Q. Xu, and K. K. Griending, "Reactive oxygen species in metabolic and inflammatory signaling," *Circulation Research*, vol. 122, no. 6, pp. 877-902, 2018.
- [18] S. Cadenas, "ROS and redox signaling in myocardial ischemia-reperfusion injury and cardioprotection," *Free Radical Biology & Medicine*, vol. 117, Article ID 76, 89 pages, 2018.
- [19] E. Murphy, H. Ardehali, R. S. Balaban et al., "Mitochondrial function, biology, and role in disease," *Circulation Research*, vol. 118, no. 12, pp. 1960-1991, 2016.
- [20] M. Pecoraro, A. Pinto, and A. Popolo, "Mitochondria and cardiovascular disease: a brief account," *Critical Reviews in Eukaryotic Gene Expression*, vol. 29, no. 4, pp. 295-304, 2019.
- [21] J. R. Mercer, K.-K. Cheng, N. Figg et al., "DNA damage links mitochondrial dysfunction to atherosclerosis and the metabolic syndrome," *Circulation Research*, vol. 107, no. 8, pp. 1021-1031, 2010.
- [22] D. A. Chistiakov, I. A. Sobenin, Y. V. Bobryshev et al., "Mitochondrial dysfunction and mitochondrial DNA mutations in atherosclerotic complications in diabetes," *World Journal of Cardiology*, vol. 4, no. 5, pp. 148-156, 2012.
- [23] S. K. Roy Chowdhury, G. V. Sangle, X. Xie, G. L. Stelmack, A. J. Halayko, and G. X. Shen, "Effects of extensively oxidized low-density lipoprotein on mitochondrial function and reactive oxygen species in porcine aortic endothelial cells," *American Journal of Physiology-Endocrinology and Metabolism*, vol. 298, no. 1, pp. E89-E98, 2010.
- [24] A. Devarajan, N. Bourquard, S. Hama et al., "Paraoxonase 2 deficiency alters mitochondrial function and exacerbates the development of atherosclerosis," *Antioxidants & Redox Signaling*, vol. 14, no. 3, pp. 341-351, 2011.
- [25] C. M. Harrison, M. Pompilius, K. E. Pinkerton, and S. W. Ballinger, "Mitochondrial oxidative stress significantly influences atherogenic risk and cytokine-induced oxidant production," *Environmental Health Perspectives*, vol. 119, no. 5, pp. 676-681, 2011.
- [26] D. J. Tyrrell, M. G. Blin, J. Song et al., "Age-associated mitochondrial dysfunction accelerates atherogenesis," *Circulation Research*, vol. 126, no. 3, pp. 298-314, 2020.
- [27] A. N. Orekhov, A. V. Poznyak, I. A. Sobenin et al., "Mitochondrion as a selective target for treatment of atherosclerosis: role of mitochondrial DNA mutations and defective mitophagy in the pathogenesis of atherosclerosis and chronic inflammation," *Current Neuropharmacology*, vol. 18, 2019.
- [28] V. Lahera, N. de Las Heras, A. López-Farré, W. Manucha, and L. Ferder, "Role of mitochondrial dysfunction in hypertension and obesity," *Current Hypertension Reports*, vol. 19, no. 2, p. 11, 2017.
- [29] S. H. H. Chan, C.-A. Wu, K. L. H. Wu, Y.-H. Ho, A. Y. W. Chang, and J. Y. H. Chan, "Transcriptional upregulation of mitochondrial uncoupling protein 2 protects against oxidative stress-associated neurogenic hypertension," *Circulation Research*, vol. 105, no. 9, pp. 886-896, 2009.
- [30] J. D. Widder, D. Fraccarollo, P. Galuppo et al., "Attenuation of angiotensin II-induced vascular dysfunction and hypertension by overexpression of thioredoxin 2," *Hypertension*, vol. 54, no. 2, pp. 338-344, 2009.
- [31] S. H. H. Chan, K. L. H. Wu, A. Y. W. Chang, M.-H. Tai, and J. Y. H. Chan, "Oxidative impairment of mitochondrial electron transport chain complexes in rostral ventrolateral medulla contributes to neurogenic hypertension," *Hypertension*, vol. 53, no. 2, pp. 217-227, 2009.

- [32] Q. Qiu, R. Li, P. Jiang et al., "Mitochondrial tRNA mutations are associated with maternally inherited hypertension in two Han Chinese pedigrees," *Human Mutation*, vol. 33, no. 8, pp. 1285–1293, 2012.
- [33] M. C. Zimmerman, E. Lazartigues, R. V. Sharma, and R. L. Davisson, "Hypertension caused by angiotensin II infusion involves increased superoxide production in the central nervous system," *Circulation Research*, vol. 95, no. 2, pp. 210–216, 2004.
- [34] M.-G. Perrelli, P. Pagliaro, and C. Penna, "Ischemia/reperfusion injury and cardioprotective mechanisms: role of mitochondria and reactive oxygen species," *World Journal of Cardiology*, vol. 3, no. 6, pp. 186–200, 2011.
- [35] C. Penna, M.-G. Perrelli, and P. Pagliaro, "Mitochondrial pathways, permeability transition pore, and redox signaling in cardioprotection: therapeutic implications," *Antioxidants & Redox Signaling*, vol. 18, no. 5, pp. 556–599, 2013.
- [36] N. Lu, Y. Sun, and X. Zheng, "Orientin-induced cardioprotection against reperfusion is associated with attenuation of mitochondrial permeability transition," *Planta Medica*, vol. 77, no. 10, pp. 984–991, 2011.
- [37] M. G. Rosca, E. J. Vazquez, J. Kerner et al., "Cardiac mitochondria in heart failure: decrease in respirasomes and oxidative phosphorylation," *Cardiovascular Research*, vol. 80, no. 1, pp. 30–39, 2008.
- [38] L. A. Kiyuna, R. P. E. Albuquerque, C. H. Chen et al., "Targeting mitochondrial dysfunction and oxidative stress in heart failure: challenges and opportunities," *Free Radical Biology & Medicine*, vol. 129, pp. 155–168, 2018.
- [39] G. Faerber, F. Barreto-Perreira, M. Schoepe et al., "Induction of heart failure by minimally invasive aortic constriction in mice: reduced peroxisome proliferator-activated receptor γ coactivator levels and mitochondrial dysfunction," *The Journal of Thoracic and Cardiovascular Surgery*, vol. 141, no. 2, pp. 492–500, 2011.
- [40] G. Karamanlidis, V. Bautista-Hernandez, F. Fynn-Thompson, P. del Nido, and R. Tian, "Impaired mitochondrial biogenesis precedes heart failure in right ventricular hypertrophy in congenital heart disease," *Circulation: Heart Failure*, vol. 4, no. 6, pp. 707–713, 2011.
- [41] R. Tian, W. S. Colucci, Z. Arany et al., "Unlocking the secrets of mitochondria in the cardiovascular system," *Circulation*, vol. 140, no. 14, pp. 1205–1216, 2019.
- [42] P. Hao, F. Jiang, J. Cheng, L. Ma, Y. Zhang, and Y. Zhao, "Traditional Chinese medicine for cardiovascular disease," *Journal of the American College of Cardiology*, vol. 69, no. 24, pp. 2952–2966, 2017.
- [43] S. Lu, Y. Luo, P. Zhou, K. Yang, G. Sun, and X. Sun, "Ginsenoside compound K protects human umbilical vein endothelial cells against oxidized low-density lipoprotein-induced injury via inhibition of nuclear factor- κ B, p38, and JNK MAPK pathways," *Journal of Ginseng Research*, vol. 43, no. 1, pp. 95–104, 2019.
- [44] S. Zhang, F. Tang, Y. Yang et al., "Astragaloside IV protects against isoproterenol-induced cardiac hypertrophy by regulating NF- κ B/PGC-1 α signaling mediated energy biosynthesis," *PLoS One*, vol. 10, no. 3, Article ID e0118759, 2015.
- [45] L. Gong, H. Chang, J. Zhang, G. Guo, J. Shi, and H. Xu, "Astragaloside IV protects rat cardiomyocytes from hypoxia-induced injury by down-regulation of miR-23a and miR-92a," *Cellular Physiology and Biochemistry*, vol. 49, no. 6, pp. 2240–2253, 2018.
- [46] Z. Dong, P. Zhao, M. Xu et al., "Astragaloside IV alleviates heart failure via activating PPAR α to switch glycolysis to fatty acid β -oxidation," *Scientific Reports*, vol. 7, p. 2691, 2017.
- [47] D. Liu, L. Chen, J. Zhao, and K. Cui, "Cardioprotection activity and mechanism of Astragalus polysaccharide in vivo and in vitro," *International Journal of Biological Macromolecules*, vol. 111, pp. 947–952, 2018.
- [48] T. Zheng, X. Yang, D. Wu et al., "Salidroside ameliorates insulin resistance through activation of a mitochondria-associated AMPK/PI3K/Akt/GSK3 β pathway," *British Journal of Pharmacology*, vol. 172, no. 13, pp. 3284–3301, 2015.
- [49] X. Huang, Y. Wang, Y. Wang, D. L. Ophiopogonin, J. Wang, and Y. Gao, "Ophiopogonin D reduces myocardial ischemia-reperfusion injury via upregulating CYP2J3/EETs in rats," *Cellular Physiology and Biochemistry*, vol. 49, no. 4, pp. 1646–1658, 2018.
- [50] A. Yang, A. Kumar, D. Kumar et al., "Ecliptal, a promising natural lead isolated from Eclipta alba modulates adipocyte function and ameliorates metabolic syndrome," *Toxicology and Applied Pharmacology*, vol. 338, pp. 134–147, 2018.
- [51] X. Xiao, S. Xu, L. Li et al., "The effect of velvet antler proteins on cardiac microvascular endothelial cells challenged with ischemia-hypoxia," *Frontiers in Pharmacology*, vol. 8, p. 601, 2017.
- [52] B. Wu, J.-Y. Feng, L.-M. Yu et al., "Icariin protects cardiomyocytes against ischaemia/reperfusion injury by attenuating sirtuin 1-dependent mitochondrial oxidative damage," *British Journal of Pharmacology*, vol. 175, no. 21, pp. 4137–4153, 2018.
- [53] M. Zhang, Y. Guan, J. Xu et al., "Evaluating the protective mechanism of panax notoginseng saponins against oxidative stress damage by quantifying the biomechanical properties of single cell," *Analytica Chimica Acta*, vol. 1048, pp. 186–193, 2019.
- [54] Z. Zhou, J. Wang, Y. Song et al., "Panax notoginseng saponins attenuate cardiomyocyte apoptosis through mitochondrial pathway in natural aging rats," *Phytotherapy Research*, vol. 32, no. 2, pp. 243–250, 2018.
- [55] K. He, L. Yan, C.-S. Pan et al., "ROCK-dependent ATP5D modulation contributes to the protection of notoginsenoside NR1 against ischemia-reperfusion-induced myocardial injury," *American Journal of Physiology-Heart and Circulatory Physiology*, vol. 307, no. 12, pp. H1764–H1776, 2014.
- [56] J.-Yi Zhang, M. Wang, R.-Y. Wang et al., "Salvianolic acid A ameliorates arsenic trioxide-induced cardiotoxicity through decreasing cardiac mitochondrial injury and promotes its anticancer activity," *Frontiers in Pharmacology*, vol. 9, p. 487, 2018.
- [57] Y. Pan, W. Zhao, and D. Zhao, "Salvianolic acid B improves mitochondrial function in 3T3-L1 adipocytes through a pathway involving PPAR γ coactivator-1 α (PGC-1 α)," *Frontiers in Pharmacology*, vol. 9, p. 671, 2018.
- [58] Z. Zhang, H. He, and Y. Qiao, "Tanshinone IIA pretreatment protects H9c2 cells against anoxia/reoxygenation injury involvement of the translocation of bcl-2 to mitochondria mediated by 14-3-3 η ," *Oxidative Medicine and Cellular Longevity*, vol. 2018, Article ID 3583921, 2018.
- [59] X. Wu, H. Gao, Y. Hou et al., "Dihydrontanshinone, a natural product, alleviates LPS-induced inflammatory response through NF- κ B, mitochondrial ROS, and MAPK pathways," *Toxicology and Applied Pharmacology*, vol. 355, pp. 1–8, 2018.
- [60] H. Li, A. Sureda, H. P. Devkota et al., "Curcumin, the golden spice in treating cardiovascular diseases," *Biotechnology Advances*, vol. 38, Article ID 107343, 2019.
- [61] G. Luan, Y. Wang, Z. Wang et al., "Flavonoid glycosides from fenugreek seeds regulate glycolipid metabolism by improving

- mitochondrial function in 3T3-L1 adipocytes in vitro,” *Journal of Agricultural and Food Chemistry*, vol. 66, no. 12, pp. 3169–3178, 2018.
- [62] Li Liu, L. Yao, S. Wang et al., “Gingerol improves ectopic lipid accumulation, mitochondrial dysfunction, and insulin resistance in skeletal muscle of ageing rats: dual stimulation of the AMPK/PGC-1 α signaling pathway via plasma adiponectin and muscular AdipoR1,” *Molecular Nutrition and Food Research*, vol. 63, no. 6, Article ID e1800649, 2019.
- [63] Y. Xi, W. Wang, L. Wang et al., “Triptolide induces p53-dependent cardiotoxicity through mitochondrial membrane permeabilization in cardiomyocytes,” *Toxicology and Applied Pharmacology*, vol. 355, pp. 269–285, 2018.
- [64] Y.-Y. Zhang, M. Yi, Y.-P. Huang et al., “Oxymatrine ameliorates doxorubicin-induced cardiotoxicity in rats,” *Cellular Physiology and Biochemistry*, vol. 43, no. 2, pp. 626–635, 2017.
- [65] J. Nan, C. Nan, J. Ye et al., “EGCG protects cardiomyocytes against hypoxia-reperfusion injury through inhibition of OMA1 activation,” *Journal of Cell Science*, vol. 132, 2019.
- [66] Q. Guo, J. Guo, R. Yang et al., “Cycloviobuxine D attenuates doxorubicin-induced cardiomyopathy by suppression of oxidative damage and mitochondrial biogenesis impairment,” *Oxidative Medicine and Cellular Longevity*, vol. 2015, Article ID 151972, 2015.
- [67] T.-J. Zhang, R.-X. Guo, X. Li, Y.-W. Wang, and Y.-J. Li, “Tetrandrine cardioprotection in ischemia-reperfusion (I/R) injury via JAK3/STAT3/Hexokinase II,” *European Journal of Pharmacology*, vol. 813, pp. 153–160, 2017.
- [68] Y. Huang, K. Kwan, K. Leung et al., “The extracts and major compounds derived from astragali radix alter mitochondrial bioenergetics in cultured cardiomyocytes: comparison of various polar solvents and compounds,” *International Journal of Molecular Sciences*, vol. 19, no. 6, p. 1574, 2018.
- [69] W. Zhuang, L. Yue, X. Dang et al., “Rosenroot (rhodiola): potential applications in aging-related diseases,” *Aging and Disease*, vol. 10, no. 1, pp. 134–146, 2019.
- [70] Q. Chen, X. Han, R. Li et al., “Anti-atherosclerosis of oligomeric proanthocyanidins from *Rhodiola rosea* on rat model via hypolipemic, antioxidant, anti-inflammatory activities together with regulation of endothelial function,” *Phytomedicine*, vol. 51, pp. 171–180, 2018.
- [71] G. Vilahur, L. Casan \acute{a} , E. Pe \acute{n} a et al., “Silybum marianum provides cardioprotection and limits adverse remodeling post-myocardial infarction by mitigating oxidative stress and reactive fibrosis,” *International Journal of Cardiology*, vol. 270, no. 270, pp. 28–35, 2018.
- [72] G.-H. Li, Y.-R. Li, and P. Jiao, “Therapeutic potential of *salviae miltiorrhizae radix et rhizoma* against human diseases based on activation of nrf2-mediated antioxidant defense system: bioactive constituents and mechanism of action,” *Oxidative Medicine and Cellular Longevity*, vol. 2018, Article ID 7309073, 2018.
- [73] M. Y. Song, S. Y. Kang, A. Kang, J. H. Hwang, Y.-K. Park, and H. W. Jung, “Cinnamomum cassia prevents high-fat diet-induced obesity in mice through the increase of muscle energy,” *The American Journal of Chinese Medicine*, vol. 45, no. 5, pp. 1017–1031, 2017.
- [74] M. Zhang, Y. Liu, and M. Xu, “Carotid artery plaque intervention with Tongxinluo capsule(CAPITAL): a multicenter randomized double-blind parallel-group placebo-controlled study,” *Science Reports*, vol. 9, no. 1, p. 4545, 2019.
- [75] Y. Wang, Y. Zhao, W. Jiang et al., “iTRAQ-based proteomic analysis reveals recovery of impaired mitochondrial function in ischemic myocardium by shenmai formula,” *Journal of Proteome Research*, vol. 17, no. 2, pp. 794–803, 2018.
- [76] J. Yu, Y. Li, X. Liu et al., “Mitochondrial dynamics modulation as a critical contribution for Shenmai injection in attenuating hypoxia/reoxygenation injury,” *Journal of Ethnopharmacology*, vol. 237, pp. 9–19, 2019.
- [77] Y. Zhao, X. Zhang, J. Luan et al., “Shenxian-shengmai oral liquid reduces myocardial oxidative stress and protects myocardium from ischemia-reperfusion injury,” *Cellular Physiology and Biochemistry*, vol. 48, no. 6, pp. 2503–2516, 2018.
- [78] Y. Zhao, L. Xu, Z. Qiao et al., “YiXin-Shu, a ShengMai-San-based traditional Chinese medicine formula, attenuates myocardial ischemia/reperfusion injury by suppressing mitochondrial mediated apoptosis and upregulating liver-X-receptor α ,” *Science Reports*, vol. 6, p. 23025, 2016.
- [79] J. Tian, W. Tang, M. Xu et al., “Shengmai san alleviates diabetic cardiomyopathy through improvement of mitochondrial lipid metabolic disorder,” *Cellular Physiology and Biochemistry*, vol. 50, no. 5, pp. 1726–1739, 2018.
- [80] X. Lu, Lu Zhang, P. Li et al., “The protective effects of compatibility of *Aconiti Lateralis Radix Praeparata* and *Zingiberis Rhizoma* on rats with heart failure by enhancing mitochondrial biogenesis via Sirt1/PGC-1 α pathway,” *Biomedicine & Pharmacotherapy*, vol. 92, pp. 651–660, 2017.
- [81] F. Li, X.-X. Fan, C. Chu, Y. Zhang, J.-P. Kou, and B.-Y. Yu, “A strategy for optimizing the combination of active components based on Chinese medicinal formula sheng-mai-san for myocardial ischemia,” *Cellular Physiology and Biochemistry*, vol. 45, no. 4, pp. 1455–1471, 2018.
- [82] S.-Q. Lin, X.-H. Wei, P. Huang et al., “QiShenYiQi Pills prevents cardiac ischemia-reperfusion injury via energy modulation,” *International Journal of Cardiology*, vol. 168, no. 2, pp. 967–974, 2013.
- [83] J. Yu, W. Zhang, Y. Zhang et al., “A critical courier role of volatile oils from *Dalbergia odorifera* for cardiac protection in vivo by QiShenYiQi,” *Science Reports*, vol. 7, no. 1, p. 7353, 2017.
- [84] S. Lin, X. Wu, L. Tao et al., “The metabolic effects of traditional Chinese medication qiliqiangxin on H9C2 cardiomyocytes,” *Cellular Physiology and Biochemistry*, vol. 37, no. 6, pp. 2246–2256, 2015.
- [85] D. Wei, N. Zheng, and L. Zheng, “Shexiang baoxin pill corrects metabolic disorders in a rat model of metabolic syndrome by targeting mitochondria,” *Frontiers in Pharmacology*, vol. 9, p. 137, 2018.
- [86] X. Xu, Q. Liu, and S. He, “Qiang-xin 1 formula prevents sepsis-induced apoptosis in murine cardiomyocytes by suppressing endoplasmic reticulum- and mitochondria-associated pathways,” *Frontiers in Pharmacology*, vol. 9, p. 818, 2018.
- [87] J. Ma, L. Qiao, and L. Meng, “Tongxinluo may stabilize atherosclerotic plaque via multiple mechanisms scanning by genechip,” *Biomedicine & Pharmacotherapy*, vol. 113, Article ID 108767, 2019.
- [88] F. Lin, J. Wang, X.-J. Xiong et al., “Chinese medical syndrome distribution laws of mitochondrial diseases based on combination of disease and syndrome,” *Zhongguo Zhong Xi Yi Jie He ZaZhi*, vol. 36, no. 11, pp. 1381–1384, 2016.
- [89] J. Wang, F. Lin, L. L. Guo et al., “Cardiovascular disease, mitochondria, and traditional Chinese medicine,” *Evidence Based Complementary and Alternative Medicine*, vol. 2015, Article ID 143145, 2015.
- [90] M. Bonora, M. R. Wieckowski, D. A. Sinclair, G. Kroemer, P. Pinton, and L. Galluzzi, “Targeting mitochondria for

- cardiovascular disorders: therapeutic potential and obstacles,” *Nature Reviews Cardiology*, vol. 16, no. 1, pp. 33–55, 2019.
- [91] P.-P. Hao, F. Jiang, Y.-G. Chen et al., “Erratum: traditional Chinese medication for cardiovascular disease,” *Nature Reviews Cardiology*, vol. 12, no. 6, p. 318, 2015.
- [92] X. Xiong, “Integrating traditional Chinese medicine into Western cardiovascular medicine: an evidence-based approach,” *Nature Reviews Cardiology*, vol. 12, no. 6, p. 374, 2015.
- [93] F. Lin, Y. Yang, Q. Guo et al., “Analysis of the molecular mechanism of acute coronary syndrome based on circRNA-miRNA network regulation,” *Evidence Based Complementary and Alternative Medicine*, vol. 2020, Article ID 1584052, 2020.
- [94] F. Lin, H. W. Chen, G. A. Zhao et al., “Advances in research on the circRNA-miRNA-mRNA network in coronary heart disease treated with traditional Chinese medicine,” *Evidence Based Complementary and Alternative Medicine*, vol. 2020, Article ID 8048691, 2020.
- [95] J. Wang and X. Xiong, “Current situation and perspectives of clinical study in integrative medicine in China,” *Evidence Based Complementary and Alternative Medicine*, vol. 2012, Article ID 268542, 2012.
- [96] X.-J. Xiong, Z. Wang, and J. Wang, “Innovative strategy in treating angina pectoris with Chinese patent medicines by promoting blood circulation and removing blood stasis: experience from combination therapy in Chinese medicine,” *Current Vascular Pharmacology*, vol. 13, no. 4, pp. 540–553, 2015.

Research Article

Mast Cell Degranulation and Adenosine Release: Acupoint Specificity for Effect of Electroacupuncture on Pituitrin-Induced Acute Heart Bradycardia in Rabbits

Xuezhi Wang,¹ Meng Huang,^{1,2} Hongwei Yang,¹ Di Zhang,^{1,2} Wei Yao,^{1,2} Ying Xia,^{1,2} and Guanghong Ding^{1,2} 

¹Shanghai Key Laboratory of Acupuncture Mechanism and Acupoint Function, Department of Aeronautics and Astronautics, Fudan University, Shanghai 200433, China

²Shanghai Research Center for Acupuncture & Meridian, Shanghai 201203, China

Correspondence should be addressed to Guanghong Ding; ghding@fudan.edu.cn

Received 17 July 2020; Revised 11 September 2020; Accepted 21 September 2020; Published 7 October 2020

Academic Editor: Xiao Ma

Copyright © 2020 Xuezhi Wang et al. This is an open access article distributed under the Creative Commons Attribution License, which permits unrestricted use, distribution, and reproduction in any medium, provided the original work is properly cited.

Acupuncture is a medical modality based on the theory of traditional Chinese medicine, and its effect is relatively dependent on acupoint specificity. However, there is little knowledge on acupoint specificity versus acupuncture outcomes because of the deficiency of rigorous investigation on this topic, which has impeded the growing legitimacy of acupuncture in the mainstream of medicine as an evidence-based therapy. Therefore, it is of utmost importance to clarify this critical issue. The present study aims to verify the phenomenon of acupoint specificity in acupuncture-induced cardiovascular regulation and explore the biological mechanism by measuring mast cells' degranulation and adenosine release. This study was conducted to explore the specificity of acupoints in an acute bradycardia rabbit model. After electroacupuncture (EA) stimulation at PC6, PC control (con) 1, PC con 2, LU7, LI11, and nonacupoint, only the PC6 group showed a significant improvement in relative heart rate as compared to that of the model group. There was no significant difference between the relative heart rate of other EA groups and that of the model group. Historical results also showed that the ratio of degranulated mast cells in PC6 was significantly higher than other acupoints and control points. From the results of high-performance liquid chromatography (HPLC), a transient elevation of adenosine concentration during EA was only observed on acupoints and control points ($P < 0.05$) along the pericardium meridian. The EA-induced adjustment on acute bradycardia exhibits a relative specificity of acupoints, which may be related to mast cell degranulation and adenosine release in local acupoint areas. Increased degranulation of mast cells and augmentation of adenosine release during EA may be the mechanisms for PC6 having significantly better acupuncture effects than other acupoints and nonacupoints.

1. Introduction

This study attempts to observe the acupoint specificity and investigate the biological mechanism behind it from the events of degranulation of mast cells and adenosine release caused by acupuncture. In the past two decades, based on high-quality basic and clinical research, acupuncture research has made considerable progress, and the efficacy of acupuncture has been recognized worldwide [1–9]. However, the acupuncture researchers have always avoided discussing acupoint specificity, the core proposition of

acupuncture theory, hindering the growth of legitimacy in the mainstream of medicine as an evidence-based therapy [10]. There are very few clinical and basic studies discussing acupoint specificity, and the research conclusions are controversial [11–15]. A recent randomized clinical trial on chronic stable angina found that receiving acupuncture on the disease-affected meridian can significantly reduce angina attacks compared to receiving acupuncture on the acupoints on the nonaffected meridian, receiving sham acupuncture, or receiving no acupuncture [16]. The results of two clinical studies in patients with migraine indicate that the brain

glucose metabolism caused by acupuncture at acupoints is pertinent and targeted, and acupuncture at different acupoints can lead to different glucose metabolism levels in pain-related brain regions [17, 18]. However, the application of acupuncture on nonacupoints induced disordered and randomized brain glucose metabolism. A study relying on the lipopolysaccharide-induced endotoxemia mouse model found that EA at ST36 drives the vagal-adrenal axis producing anti-inflammatory effects depending on NPY⁺ adrenal chromaffin cells. EA at ST25 activates NPY⁺ splenic noradrenergic neurons through the spinal-sympathetic axis [19], suggesting that neuronal activation induced by EA at different acupoints is specific. Nevertheless, an individual patient meta-analysis of 17,922 patients with chronic pain in randomized controlled trials showed that there is no evidence that any characteristic of acupuncture modifies the acupuncture analgesic effect, including the style of acupuncture, the number or placement of needles, the number, frequency or duration of sessions, patient-practitioner interactions, and the experience of acupuncturists [20]. Given these controversies, acupuncture specificity and its underlying biological basis must be further elucidated as soon as possible.

2. Materials and Methods

2.1. Animals. One of the selection principles for non-acupoint is to close to the target point and maintain a certain distance from distinction. Therefore, the area of the medial forelimb of the experimental animal selected in this experiment should not be too small. According to this standard, we excluded rats and mice, which are commonly used experimental animals. The distances between PC6 and control points on rabbit medial forelimb are moderate. Besides, the rabbit's ear is quite large, and the blood vessels are manifested, which is convenient for repeated intravenous injection. So, the rabbit is suitable as an experimental animal model of the long-term acute bradycardia model.

Male New Zealand rabbits (2.0 ± 0.2 kg) from Shanghai Shengwang Experimental Animals Ltd. (permit number SCXK(SH)-2012-0007) were housed in cages in a temperature-controlled environment ($22\text{--}25^\circ\text{C}$) with a 12/12-hour light/dark cycle. Food and water were freely available. All animals were handled with care to prevent infection and to minimize stress. Animal experiments were performed between 9 am and 5 pm. For each experimental group, animals were chosen randomly. All animals were housed for at least 2 days before experimentation.

2.2. Anesthesia. After rabbits were prepared, a 20% urethane solution (7.5 ml/kg) was injected into the right ear vein using a venous indwelling needle, and injection duration was controlled to be approximately 60 s. When using urethane anesthesia, the rabbit anesthesia time is more than 2 h, which is enough to support the complete experimental process, and the anesthesia effect is stable. Compared with other anesthetic drugs, the animal mortality rate is low, and the impact on heart rate and intraventricular pressure is small.

2.3. Long-Term Acute Myocardial Ischemia Model. Male New Zealand rabbits weighing 2.0 ± 0.2 kg were used in this study. Anesthesia (7.5 ml/kg) was injected into the ear vein with 20% urethane. Then, the animals were placed on the surgical table in a supine position, and Electrocardiograph (ECG) signals were collected. After resting for 20 min, pituitrin (3 units/ml, 2 units/kg) was injected into the ear vein followed by a low concentration of pituitrin (36 units/L) being administered at a rate of 1 ml/min using a microinjection pump until the end of the experiment. A 30% reduction in heart rate from the baseline 2 min after modeling was considered a sign of successful modeling.

2.4. ECG Recording. After anesthesia, animals were placed on the surgical table, and ECG signals were recorded using a two-lead subcutaneous connection. ECG signals were introduced into the Powerlab multichannel physiological recorder (Powerlab 16/30 AD Instruments) via the ECG module (Powerlab Dual Bio Amp ML135 AD Instruments).

2.5. Groups. 48 rabbits were randomly divided into 8 groups. The blank group (Control) animals were only used to record data and underwent no other procedures. The model group (Model) was placed onto the experimental bench for 20 min to induce a long-term acute myocardial ischemia model. No EA was applied after modeling. The Neiguan group (PC6) was placed onto the experimental bench for 20 min to prepare a long-term acute myocardial ischemia model. After modeling was completed, EA was applied at the PC6 for 5 min. The operation of the pericardium meridian control 1 point group (PC con 1), the pericardium meridian control 2 point group (PC con 2), the Lieque group (LU7), the Quchi group (LI11), and the nonacupoint group (Nonacupoint) were the same as that of the PC6 group. The only difference was the EA stimulation position among these EA groups (the PC6 group, the PC con 1 group, the PC con 2 group, the LU7 group, the LI11 group, and the nonacupoint group). The complete experimental procedure is shown in Figure 1(a). Two rabbits were unsuccessful in modeling, and another rabbit had interference when recording ECG data. These three rabbits were not included in statistical analyses.

Other 48 rabbits were randomly divided into 8 groups. Rabbits in the blank control group (Control) were placed onto the experimental operating table, and only tissue fluid under PC6 was collected. Samples were collected every 30 min, and a total of 5 samples were collected over 2.5 h with no other procedures. Rabbits in the model group were placed onto the surgical table, and tissue fluid under PC6 was collected. Samples were collected every 30 min, and a total of 5 samples were collected. The total length of the experiment was 2.5 h, and the acute myocardial ischemia model lasted 55 min. After modeling, EA treatment was not performed. Rabbits in the Neiguan microdialysis EA group (PC6) were placed on the surgical table, and tissue fluid under PC6 was collected. Samples were collected every 30 min, and a total of 5 samples were collected. The total length of the experiment was 2.5 h, and the acute myocardial ischemia model lasted

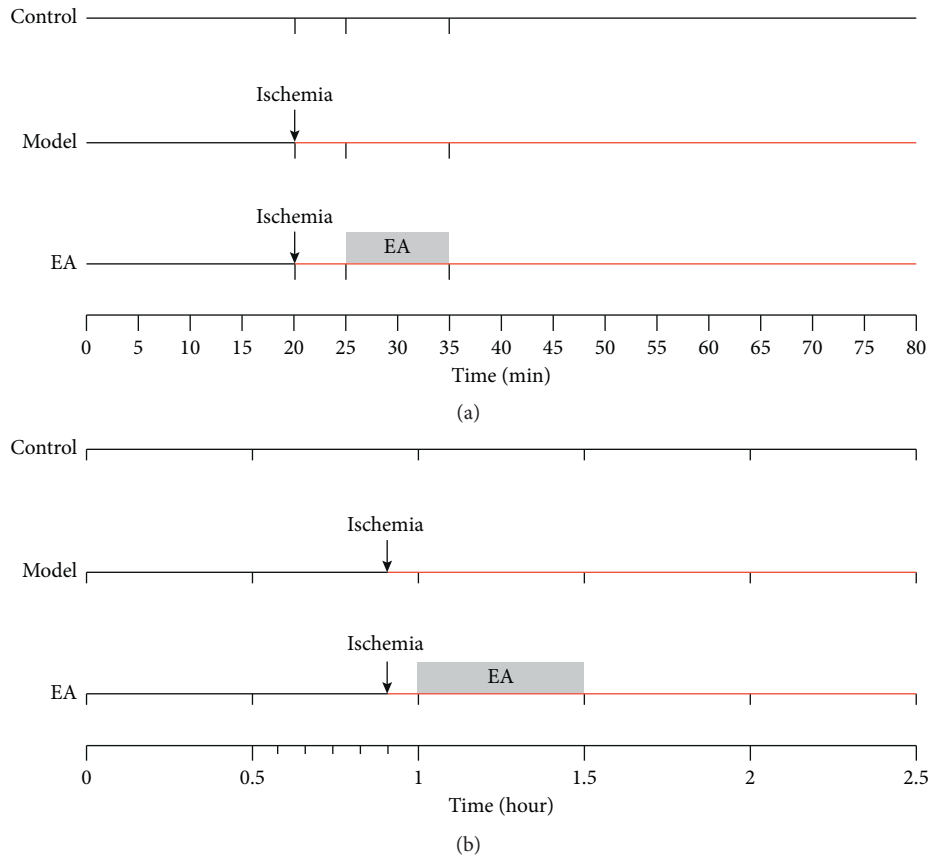


FIGURE 1: Flow chart of experiments. (a) Flow chart of applying acupuncture in the experimental bradycardia model. (b) Flow chart of microdialysis experiments.

55 min. EA was applied at PC6 for 30 min starting at 5 min after the modeling. Procedures for pericardium meridian control 1 point microdialysis EA (PC con 1), pericardium meridian control 2 point microdialysis EA (PC con 2), Lieque microdialysis EA (LU7), Quchi microdialysis EA (LI11), and nonacupoint microdialysis EA (Nonacupoint) groups were the same as those in the Neiguan microdialysis EA group (PC6); only the positions of EA stimulation and microdialysis fluid collection were different. The complete experimental procedure is shown in Figure 1(b). Two rabbits were not included in the statistical analyses due to partial loss.

2.6. Acupoints and Control Acupoints. Figure 2 visually shows the location of acupuncture points and other points on the rabbit's body surface.

PC6 is clinically used to regulate cardiac function [21, 22]. Traditional Chinese medicine has long known that "symptoms of heart and chest should be treated by stimulating PC6." Therefore, we used PC6 as the target point in this study. The anatomical position of PC6 is between the tendons of the palmaris longus and flexor carpi radialis [23], which is the flexor digitorum sublimis, and the deep layer is the flexor digitorum profundus. That location includes the median artery and vein of the forearm, and the deep layer

includes the artery and vein between the bones on the palmar side of the forearm. The medial forearm cutaneous nerve is at this location, and the deep layer is the median nerve palmar branch, with the deepest layer housing the forearm volar interosseous nerve. Clinically, the PC6 acupoint is designated as the point at the middle of the palmar side of the forearm, 2 *cun* above the transverse crease of the wrist, between the tendons of the palmaris longus and flexor carpi radialis [23]. In this experiment, the positioning method for defining PC6 was from the rabbit common acupoint location standard of Experimental Acupuncture [24]. PC6 is designated as the point 1/4 of the anterior forearm length above the transverse crease of the wrist between the ulna and the radius in this experiment.

For PC con 1 and PC con 2, the selection principle of the position of control points on the pericardium meridian includes (1) avoiding acupoints on the same meridian as much as possible and (2) getting as close as possible to PC6 while trying to avoid the difference in acupuncture effect caused by the different segments. As shown in Figure 2, the acupoints are relatively dense at the distal end of the forearm, and there is no acupoint between 5 *cun* above the transverse crease of the wrist and cubital crease. Therefore, the position 9 *cun* above the transverse crease of the wrist is taken as the position of PC con 1 and 7 *cun* as PC con 2 as a compromise. According to the comparative anatomical method, PC con 1 is indicated as the

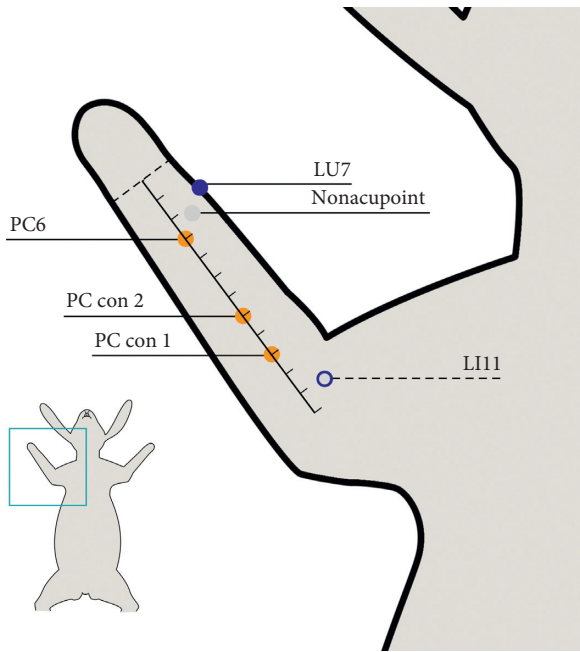


FIGURE 2: Schematic of acupoints and other points on the body surface of a rabbit. The lower left panel shows a schematic of the rabbit in a supine position. The green frame was enlarged to show a detailed forearm partial view on the right side. The dashed line on the wrist is a reference line of the transverse crease of the wrist. According to the rabbit common acupoint location standard in Experimental Acupuncture (29), PC6 is designated as the point at 1/4 of the anterior forearm length above the transverse crease of the wrist between the tendons of the palmaris longus and flexor carpi radialis. On the palmar side of the forearm, between the radius and ulna, the 9 *cun* position above the transverse crease of the wrist is the PC con 1, and the 7 *cun* position is the PC con 2. Since PC6 and all control points are on the pericardium meridian, they are uniformly marked with orange solid dots. LU7 is located on the lateral side of the forearm, on the upper edge of the styloid process of the radius, 1.5 *cun* above the transverse crease of the wrist, between the brachioradialis muscle and the tendon of the long abductor muscle of thumb, represented by a dark blue solid dot. Quchi is designated as the point at the depression on the outer side of the elbow joint. In particular, since its position cannot be observed in the supine position, it is indicated by a dark blue dotted hollow dot. The nonacupoint position is taken from the midpoint of the connection between PC6 and LU7. Since its location is not on any meridian, it is indicated by a solid gray dot.

point 7/12 of the anterior forearm length above the transverse crease of the wrist between the ulna and the radius, and PC con 2 is indicated as the point 3/4 of that length.

For LU7 and LI11, the selection criteria of control acupoints are (1) avoiding acupoints on the pericardium meridian, (2) not including myocardial ischemic disease regions, and (3) getting as close as possible to PC6 at the same level. Therefore, we selected LU7 as a control acupoint on another meridian. LU7 is located on the lateral side of the forearm, on the upper side of the styloid process of the radius, 1.5 *cun* above the transverse crease of the wrist, between the brachioradialis muscle and the tendon of the long abductor muscle of the thumb [23]. LU7 is close to PC6,

but there is a difference in the indications between them, which is a good control point in this experiment. Since LU7 is not a common acupoint in animal experiments, there is little authoritative literature for defining the location of LU7. Therefore, according to the comparative anatomical method, LU7 is located on the lateral side of the forearm, on the upper edge of the styloid process of the radius, 1/8 of the anterior forearm length above the transverse crease of the wrist, between the brachioradialis muscle and the tendon of the long abductor muscle of the thumb. The anatomical position of LI11 is located at the beginning of the extensor carpi radialis longus, where the radial artery and cephalic vein are distributed, as well as the radial nerve and the dorsal cutaneous nerve of the forearm. Clinically, LI11 is located at the lateral end of the transverse cubital crease with the elbow flexed, the midpoint between the connection of LU5 and lateral epicondyle of the humerus [23]. In this experiment, the method of defining LI11 was based on the rabbit common acupoint location standard of Experimental Acupuncture [24]. LI11 is designated as the point at the depression on the outer side of the elbow joint.

For nonacupoint positions, the principles of nonacupoint selection are (1) being close to PC6 while leaving a certain distance to clearly distinguish it from PC6, (2) trying to stay far away from other acupoints, and (3) avoiding the pericardium meridian and other meridians. According to these three principles of selecting nonacupoints, the midpoint of the connection between PC6 and LU7 was taken as the nonacupoint region in this research.

2.7. EA Stimulation. According to the size of the selected experimental animal, the depth of the lesion, and the location of the acupoint, a 0.25×13 mm sterile acupuncture needle was selected as the experimental needle. All acupoints and control acupoints, except LU7, were subjected to perpendicular insertion. The oblique insertion method was used separately at LU7. The depth of needle penetration for all acupoints and control points, which is 7 mm, was referenced to the standard of the rabbit common acupoint location of Experimental Acupuncture [24]. EA stimulation intensity was uniformly 0.4 mA—the minimum current intensity that can be induced by stimulating PC6 to cause slight jitter of the forearm. The output frequency and waveform were 2/100 Hz alternately dense waves with a duration of 10 min. In the microdialysis experiment, the duration of EA was 30 min, while other parameters remain unchanged.

2.8. Microdialysis. This experiment used a linear probe (MD-2005, Basi, USA) with a 5 mm semipermeable membrane. The dialysis solution was Ringer's solution, and 1 mM/L adenosine deaminase inhibitor (EHNA hydrochloride E114, Sigma, USA) was added to Ringer's solution. The dialysis power was supplied by a syringe pump (NE-1000, New Era Pump Systems, USA) with a flow rate of 2 μ l/min. From the beginning of the dialysis process, one sample was collected every 30 min for 2.5 h. A total of 5 samples were collected, each with a volume of 60 μ l. The samples were

immediately placed on ice and then stored at -80°C until HPLC analysis.

2.9. HPLC Detection. An Agilent 1260 HPLC analyzer was used as an analytical device. Chromatographic separation was performed by a reversed-phase column EC-C18. For the measurement of microdialysis fluid, we used a mobile phase containing 215 mM KH_2PO_4 , 2.3 mM tetrabutylammonium bisulfate, and 3.2% acetonitrile (pH 6.2) with a flow rate of 0.3 ml/min. The adenosine standard was separately checked every 5 samples, and the dialysis sample was compared to the standard according to the peak area to calculate actual concentration values.

2.10. Histological Examination. To obtain the number and degranulation ratio of mast cells in acupoints and control acupoints, rabbits were exposed to inhalation carbon dioxide and sacrificed after experiments were completed. Taking the PC6, LU7, nonacupoint, PC con 1, PC con 2, and LI11 of the right forelimb of the rabbit as the center, skin and skeletal muscle tissue samples of $5 \times 5 \times 5 \text{ mm}^3$ around those points were carefully dissected. All tissue samples were immediately soaked in Carnoy's solution for 20 h. After dehydration and waxing, they were trimmed into small pieces of approximately $3 \times 3 \times 3 \text{ mm}^3$ and embedded in paraffin. The sectioning direction was perpendicular to the skin surface, and one sample was taken every 0.15 mm to prepare a paraffin section with a thickness of $5 \mu\text{m}$ and subjected to complex dyeing of toluidine blue and safranin T (0.5 mol/L HCL 5 min, 0.5 mg/ml toluidine blue (PH = 0.5) 45 min, 0.5 mol/L HCl 30 s, 0.25 mg/ml safranin T 30 s) and then sealed.

2.11. Data Analysis and Statistics. ECG was recorded immediately after the completion of the operation, and recording was completed at the end of the experiment. In this experiment, the heart rate was recorded using Lab Chart Pro 7.0 software. The raw data sampling rate was 20 k/s, and 3 Hz high-pass digital filtering was performed during data recording. The original ECG data were extracted and averaged in units of 60 s before statistical analysis. Heart rate was normalized based on the heart rate 5 min before modeling. The relative heart rate of the x -minute is calculated as $R_{\text{HR}}(x) = A_{\text{HR}}(x) / (\sum_{i=15}^{19} A_{\text{HR}}(x) / 5)$, where $A_{\text{HR}}(x)$ represents the x -minute absolute heart rate value. All data were statistically analyzed by F-test, and based on the results of the F-test, a single-tailed T -test was performed for data comparison among groups. All heart rate data processing after extraction from Lab Chart Pro 7.0 was performed in Excel.

Under the $40 \times 10 \times$ light microscope, the diameter of mast cells was approximately $10 \sim 20 \mu\text{m}$. The shape of an intact mast cell is elliptical or fusiform with a clear edge, and the color is a dark brownish purple. Degranulated mast cells are incomplete and elliptical or fusiform with blurred edges or irregularly broken, and their color is light brown. The number of intact mast cells and degranulated mast cells in the field of view of $230 \mu\text{m} \times 310 \mu\text{m}$ was counted under a $40 \times 10 \times$ light microscope. Three sections were taken from

each animal, and 3 fields were observed for each section. The total number of mast cells and the number of degranulated mast cells in each field of view were recorded separately. The ratio of degranulated mast cells = the number of degranulated mast cells/the total number of mast cells $\times 100\%$. The average single visual field degranulation ratio was taken as the tissue degranulation rate at the acupoint or control point. All data were statistically analyzed by F-test, and based on the results of the F-test, a single-tailed T -test was performed for data comparison among groups. All data were processed in Excel.

Five samples were obtained after completion of the microdialysis experiment with a total duration of 2.5 h. To eliminate the influence of microdialysis needle insertion, the concentration of the first sample was not counted. The concentration of the sample collected during the second period (30~60 min) was used as the base concentration. Then, the concentration values of the samples collected at subsequent periods were normalized. The x -minute relative concentration value was calculated as $R_{\text{D}}(x) = A_{\text{D}}(x) / (\sum_{i=2}^5 A_{\text{D}}(x) / A_{\text{D}}(2))$. $A_{\text{D}}(x)$ represents the absolute concentration of adenosine collected from period x . The intragroup comparison data were analyzed using a single-tailed paired T -test. All data were statistically analyzed by F-test, and based on the results of the F-test, a single-tailed T -test was performed for data comparison among groups. All data were processed using Excel.

3. Results

3.1. EA Adjustment of Heart Rate. To determine the existence of acupoint specificity, we tested the acupoint specificity on the pericardium meridian in acute bradycardic rabbits. As shown in Figure 3, pituitrin (2 Unit/kg) was injected into the animals after recording 20 min of heart rate, which caused a sharp drop in heart rate in rabbits. Heart rate dropped to the lowest point at approximately 2 min after the injection. Receiving 10-minute EA treatment starting at 5 min after modeling, heart rate recovery in each group showed distinct trends based on characteristics of acupoints or control points.

Because of variations in basic heart rate ($P < 0.05$), we normalized the heart rate data against the basic heartbeat for better comparison among various groups ($P > 0.05$). The average 5 min basic heart rate before modeling, 15–20 min in Figure 3, was taken as the baseline to recalculate the data. Relative results are shown in Figure 4.

The comparison of the relative heart rate is shown in Figure 5. Compared with the model group, the control group exhibited a significant difference from the beginning of modeling to the end of the experiment. The PC6 group demonstrated a significant advantage from 40 min until the end of the experiment ($P < 0.01$ from 45 to 75 min). The nonacupoint group exhibited a significant disadvantage at 35–45 min and 55 min. Compared to the PC6 group, the nonacupoint group demonstrated a significant disadvantage from 35 min to the end of the experiment. The LU7 group has a significant disadvantage from 55 min until the end of the experiment. The PC con 1 group exhibited a significant

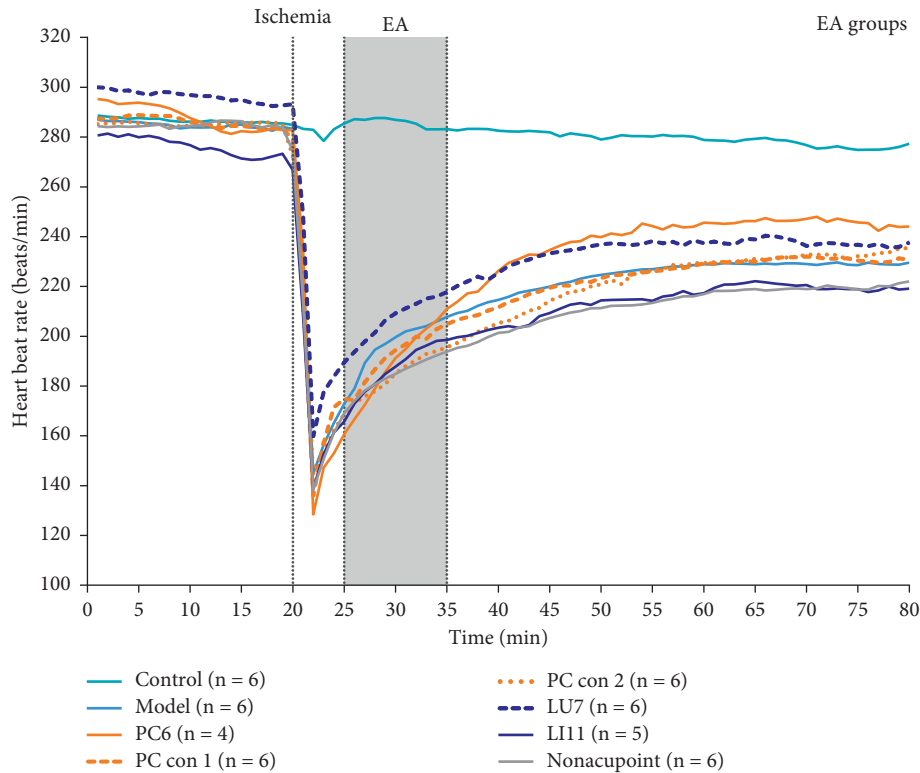


FIGURE 3: Differences in heart rate among different groups. The heart rate of different groups is detected by the Powerlab multichannel physiological recorder (Powerlab 16/30 AD INSTRUMENTS) ($n = 4\sim 6$). The abscissa shows observation time in min. The ordinate is the heart rate in units of beats/min. The green solid line represents the control group (Control), the light blue solid line represents the model group (Model), the orange solid line represents the Neiguan group (PC6), the orange dashed line represents pericardium meridian control point 1 (PC con 1), the orange dotted line represents pericardium meridian control point 2 (PC con 2), the dark blue dashed line represents the Lieque group (LU7), the dark blue solid line represents the Quchi group (LI11), and the gray solid line represents the nonacupoint group (Nonacupoint).

disadvantage from 40 min to 70 min, but there was no significant difference from 75 min to the end of the experiment. The PC con 2 group showed a significant disadvantage from 40 to 60 min. The LI11 group exhibited a significant disadvantage during 45–75 min. Compared to the nonacupoint group, the LU7 group had a significant advantage during 35–65 min. The PC con 1 group displayed a significant disadvantage at 35 min, 45–65 min, and 70 min, while the PC con 2 group demonstrated no significant disadvantage. The LI11 group had a significant advantage at 35–40 min, 50 min, and 65 min.

The above results suggest that acupuncture at PC6 has a comparative advantage, better than other stimulated points. The relative heart rate recovery index in the PC6 group is not only superior to the model group but also better than other EA groups. Similarly, the acupuncture effects of PC con 1, LU7, and LI11 were significantly better than the nonacupoint group.

3.2. Effect of EA on Local Mast Cells in Acupoints. Many recent studies have shown that mast cells play an important role in the activation of acupoints [25–27]. Tissue comprising acupoints and control points were sectioned and stained (Figure 6). Under a $400\times$ upright dissecting microscope, the diameter of mast cells was approximately

$10\sim 20\mu\text{m}$. Intact mast cells were elliptical or fusiform in shape with clear edges and a dark brown-purple color (cells indicated by blue arrows in Figure 6). Degranulated mast cells were elliptical or fusiform with incomplete and blurred edges or irregularly broken sheets, and the color was light brown (cells indicated by white arrows in Figure 6). Mast cell staining results of both acupoints and control points in EA rabbit groups are shown below. The density of mast cells in the acupoints and control acupoints of rabbits in the EA groups is shown in Figure 7. The average number of mast cells ranged from 12 to 44 in the field of view of $230\mu\text{m} \times 310\mu\text{m}$. The PC con 2 group exhibited a maximum mast cell number, and the nonacupoint group possessed the minimum. Compared to the PC6 group, mast cell numbers in the nonacupoint group and the PC con 1 group were significantly lower. Compared to the nonacupoint group, mast cell numbers in the LU7 group and PC con 2 group were significantly higher.

The degranulation ratio of mast cells in acupoints and control acupoints of different rabbit EA groups is shown in Figure 8. The mast cell degranulation ratio in the rabbit EA groups ranged from 22% to approximately 59%. The degranulated mast cell ratio was the highest in the PC6 group and the lowest in the LU7 group. Except for the PC con 1 group, the degranulation ratio of mast cells in the other

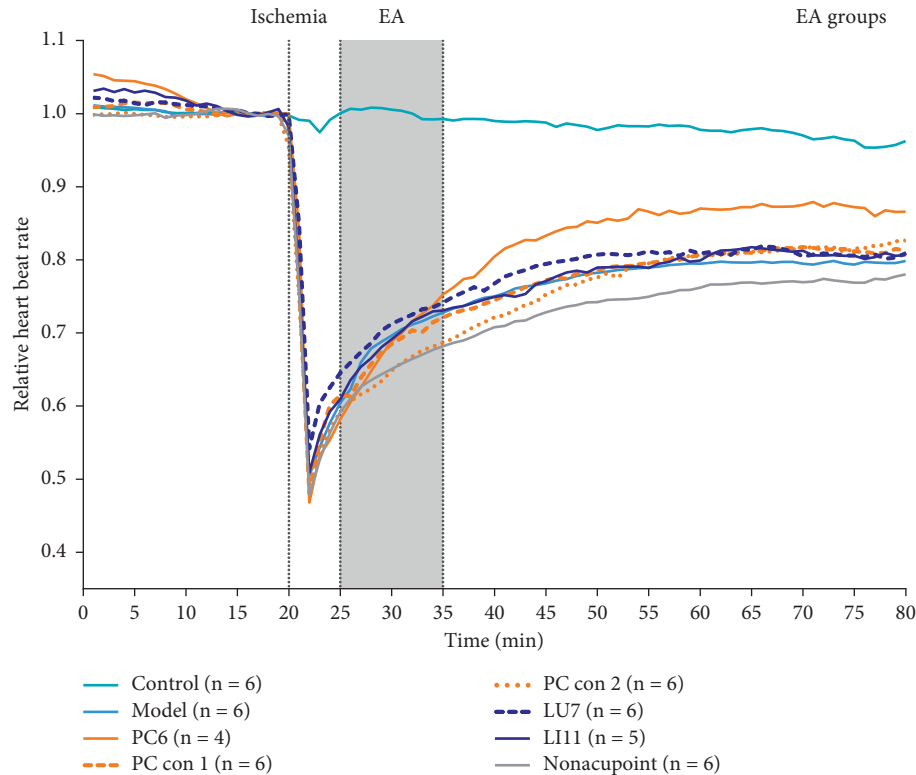


FIGURE 4: Relative heart rate among different groups. The relative heart rate of different groups is calculated against the basic heartbeat ($n = 4\sim 6$). Relative results are shown in Figure 2. The abscissa shows observation time in min. The ordinate is the relative heart rate in units of 1. The green solid line represents the control group (Control), the light blue solid line represents the model group (Model), the orange solid line represents the Neiguan group (PC6), the orange dashed line represents pericardium meridian control point 1 (PC con 1), the orange dotted line represents pericardium meridian control point 2 (PC con 2), the dark blue dashed line represents the Lieque group (LU7), the dark blue solid line represents the Quchi group (LI11), and the gray solid line represents the nonacupoint group (Nonacupoint).

groups was significantly lower than that in the PC6 group. The ratio of degranulated mast cells in the PC con 1 group was significantly higher than that in the nonacupoint group, the LU7 group, and the PC con 2 group.

3.3. Effect of EA on Adenosine Concentration in Acupoints and Control Points. Some studies have indicated that adenosine and A1 receptor are involved in the acupuncture effect [28, 29]. To explore whether adenosine participates in the activation of acupoints in acupoint specificity, we used HPLC to measure the adenosine concentration in acupoints and control acupoints. The original HPLC data of samples from a rabbit in the PC6 groups is shown in Figure 9. Figure 10 shows the absolute adenosine density of acupoints and control acupoints in the resting state. Adenosine samples in the control and model groups were collected from the PC6 acupoint. There was no significant difference between acupoints and control acupoints, except for LU7. Adenosine concentrations in the LU7 group were significantly higher than those in the PC con 1 and LI 11 groups.

Figure 11 shows the changes in adenosine concentrations at different acupoints and control acupoints in the rabbits we studied. As shown in Figure 11, only acupoints and control acupoints on the pericardium meridian caused a short-term increase in the adenosine concentration, which

had a significant advantage compared with that in the $-30\sim 0$ min or $30\sim 60$ min periods. Giving EA stimuli at other body surface points, including other meridians acupoints (LU7, LI11) and nonacupoints, caused no significant differences in adenosine concentration compared with that in the $-30\sim 0$ min or $30\sim 60$ min periods. These results suggest that there is a relative specificity in alterations of adenosine concentration at acupoints and control acupoints along the pericardium meridian in response to EA stimulation in rabbits.

4. Discussion

Acupoint specificity is one of the cores of traditional Chinese medicine acupuncture theory. In the concept of traditional Chinese medicine, acupoints are specific surface points on the human body that show therapeutic effects after stimulation by acupuncture, massage, or moxibustion. The concept of acupoint specificity includes three aspects. The first is the specificity between acupoints of different meridians [30], which means that each meridian has its unique therapeutic effect, while the acupoints on the same meridian have the same main therapeutic effects. The second is the difference between different acupoints of the same meridian [30]; although the same meridian acupoints have similarities in their main therapeutic effects, there are still differences in the

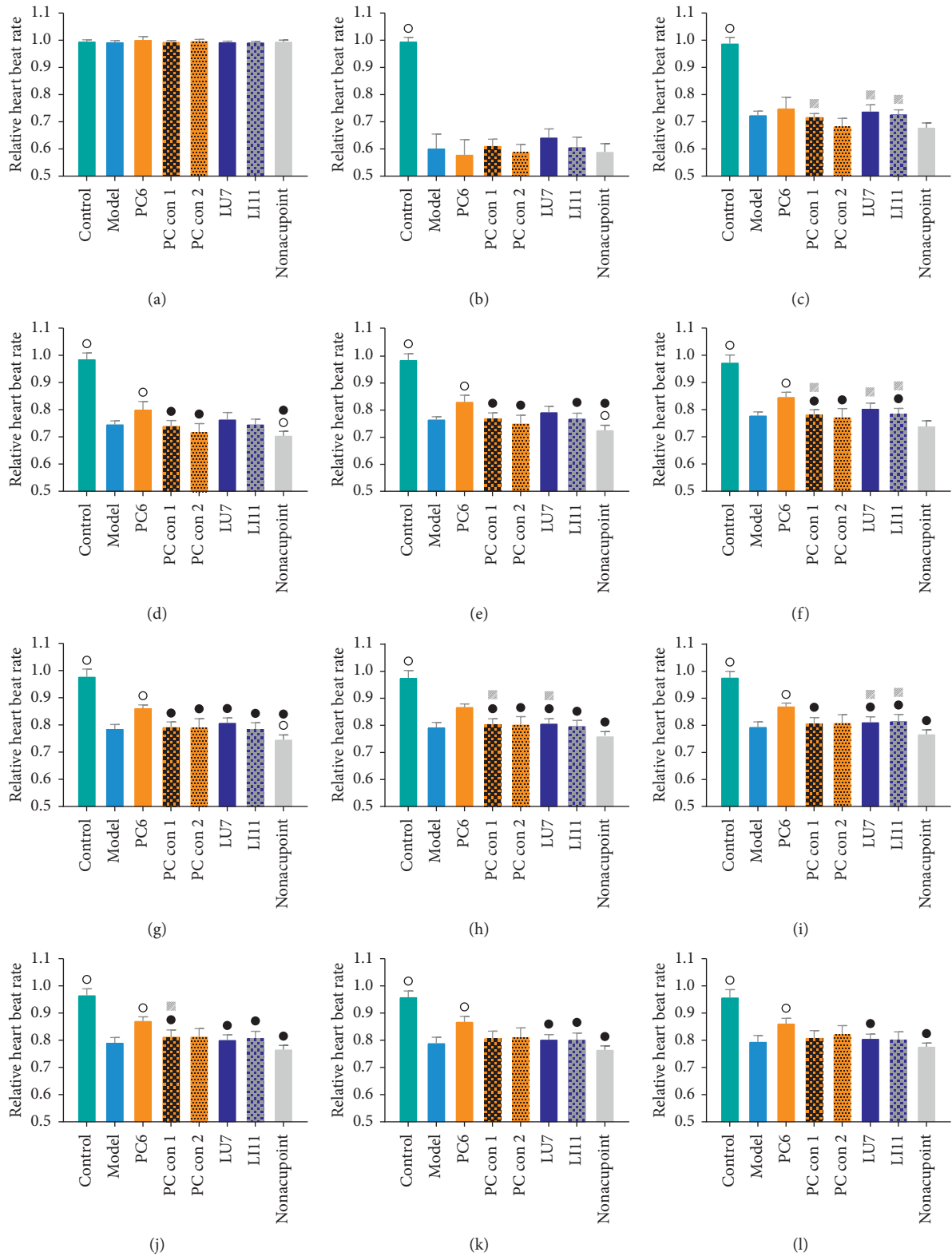


FIGURE 5: Relative heart rate index among different groups. A comparison of the relative heart rate index was made among different groups ($n = 4\sim 6$). ○ indicates a significant difference compared to the model group ($P < 0.05$); ● indicates a significant difference compared to the PC6 group ($P < 0.05$); ■ indicates a significant difference compared to the PC con 1 group ($P < 0.05$); □ indicates a significant difference compared to the PC con 2 group ($P < 0.05$); ▲ indicates a significant difference compared to LU7 group ($P < 0.05$); △ indicates a significant difference compared to Nonacupoint group ($P < 0.05$). (a) 19 min. (b) 25 min. (c) 35 min. (d) 40 min. (e) 45 min. (f) 50 min. (g) 55 min. (h) 60 min. (i) 65 min. (j) 70 min. (k) 75 min. (l) 80 min.

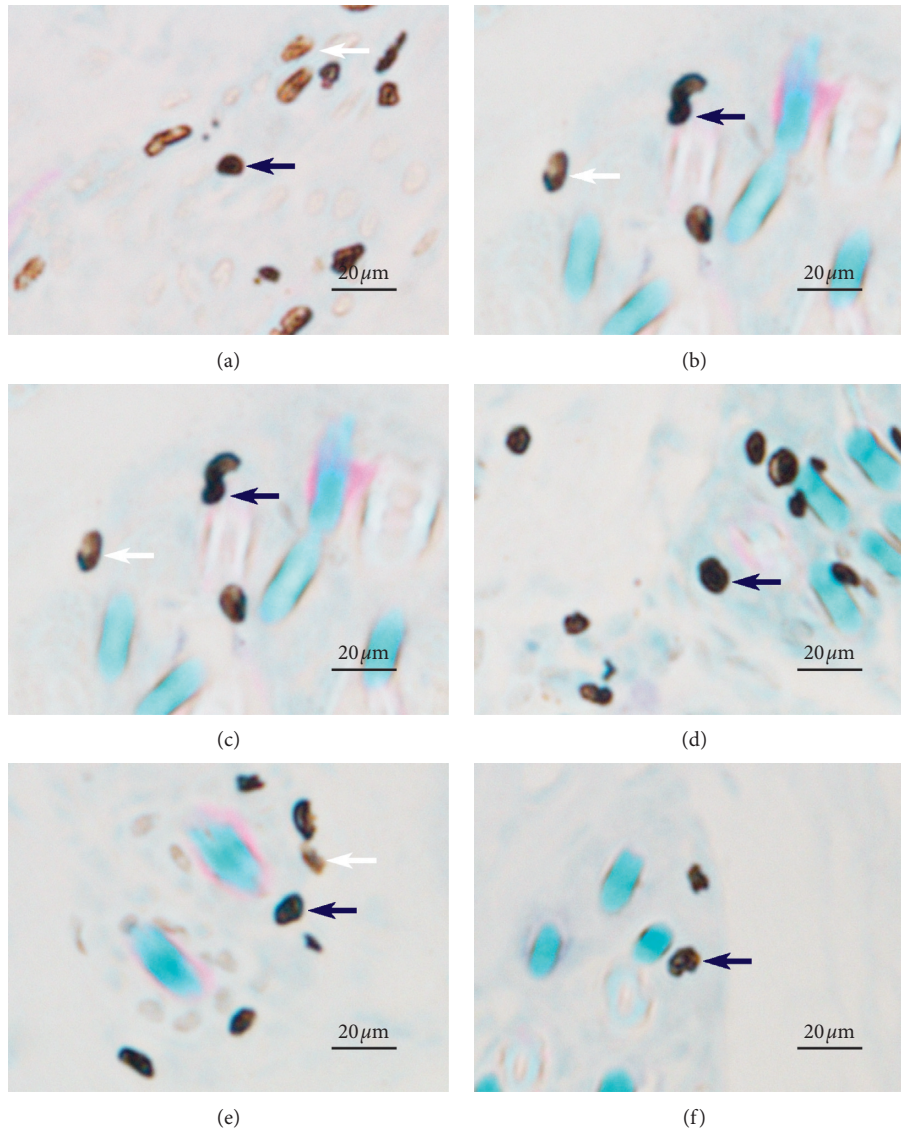


FIGURE 6: The degranulation of mast cells in acupoints and other points after EA. (a) Degranulation of mast cells in PC6 after EA. (b) Degranulation of mast cells in PC con 1 after EA. (c) Degranulation of mast cells in PC con 2 after EA. (d) Degranulation of mast cells in LU7 after EA. (e) Degranulation of mast cells in LI11 after EA. (f) Degranulation of mast cells in nonacupoint after EA.

distribution of these acupoints on the human body, and the main therapeutic effects are not entirely the same. The third is the specificity between acupoints and nonacupoints [30]. Nonacupoints, which refer to body surface points not on the traditional meridian track line or deviate from acupoints, have a further distinct difference compared with acupoints. From a generalized perspective, acupoint specificity can also indicate that an acupoint has a relative specificity in morphology [31–33], biophysical characteristics [34, 35], pathological response [36, 37], or therapeutic effect [16, 19, 26] compared with other acupoints and nonacupoints.

Clinical practice suggests that acupoint specificity plays an important role in guiding clinical treatment [7, 8, 38]. Using the improved rabbit acute bradycardia model, a suitable animal model for the human bradycardia disease [26], we found that stimulating PC6 (the pericardium

meridian, a clinical indicator of angina [39, 40], arrhythmia [41], and gastritis [42]) with EA induced a significant increase in heart rate during bradycardia induced by acute myocardial ischemia in rabbits, and the recovery of relative heart rate was significantly higher than that in the LU7 (the lung meridian, a clinical indicator of cough [43] and headache [44]) and LI11 (the large intestine meridian, a clinical indicator of arm pain [45] and hypertension [46]) groups (Figures 4 and 5). This indicates that the effect of acupuncture cannot be obtained by applying EA stimulation on any random point on the body. As mentioned, in traditional Chinese medicine theory, different acupoints and meridians have different outcome effects, but acupoints on the same meridian may have similar effects. In this study, acupoints and control acupoints on the pericardium meridian show a relative specificity in the response of adenosine

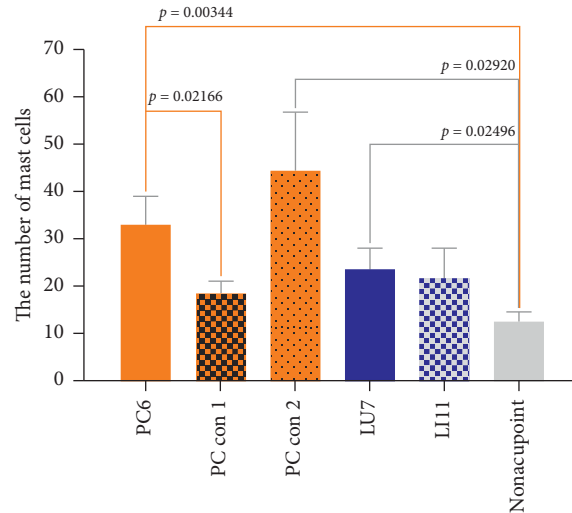


FIGURE 7: Number of mast cells in rabbit acupoints and control acupoints. The density of mast cells was measured from 6 different rabbit groups under $230 \mu\text{m} \times 310 \mu\text{m}$ scope ($n = 4\sim 6$). The graph shows groups of rabbits, and the ordinate is the number of mast cells in units of 1.

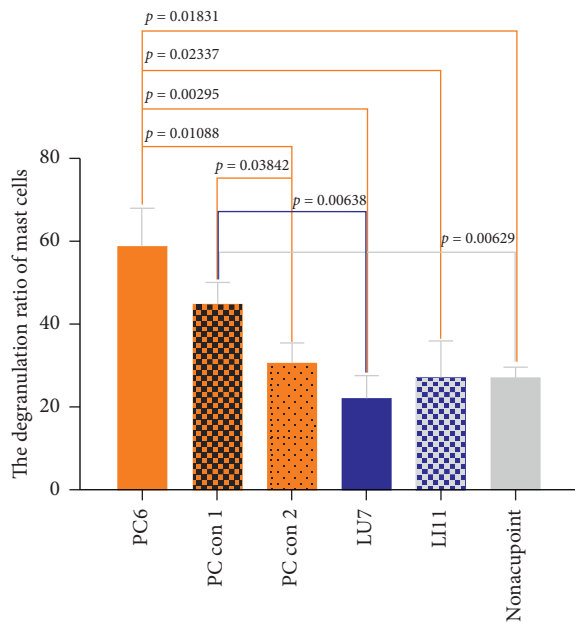


FIGURE 8: Degranulation ratios of mast cells in different EA groups. The degranulation ratio of mast cells at corresponding acupoints and control acupoints of rabbits was measured in 6 EA groups in a scope of $230 \mu\text{m} \times 310 \mu\text{m}$ ($n = 4\sim 6$). The abscissa shows the rabbit group, and the ordinate indicates the ratio of degranulated mast cells as a percent.

to acupoints on other meridians and nonacupoints. However, with respect to the acupuncture effect, we found that only applying EA stimulation at PC6 exerted significant recovery on heart rate. Although the relative heart rate recoveries of control acupoints on the pericardium meridian and acupoints on other meridians were higher than those in the model group, these differences were not statistically significant.

Besides EA, the operation of embedding a linear microdialysis probe can also cause an increase in adenosine

concentration. That is the reason we had to perform EA stimulation one hour after finishing planting the linear microdialysis probe, aiming to reduce the adenosine concentration at the acupoints to a reasonable level. We noticed that the adenosine concentration at LU7 before acupuncture, while showing a descending trend, was significantly higher than that of PC con 1 and LI11 (Figure 10). It may be because of the different directions between the buried linear microdialysis probe and the acupuncture needle to stimulate LU7 during EA. The direction of the buried linear microdialysis probe embedded under the skin of LU7 is perpendicular to the plane of the radius and ulna. Nevertheless, the acupuncture needle stimulating LU7, which forms an acute angle with the line segment between LU7 and radial styloid process, is located on the plane of the radius and the ulna. The LU7 adenosine concentration result may suggest that stimulating LU7 in the direction perpendicular to the radius may be more effective.

To explore differences in the mechanism of acupoint activation, we sectioned tissues from three acupoints and observed the mast cells. The results showed that the density of mast cells in the acupoints on pericardium and lung meridians was higher than that in the nonacupoint, which is consistent with the observation of human anatomy that the densities of cutaneous mast cells are highly relative to the distribution of acupoints (Figure 7) [47]. Differences also could be found in the ratio of degranulated mast cells. The ratio of degranulated mast cells in PC6 was significantly higher than that in LU7 and LI11 (Figure 8). Previous studies have demonstrated that the ratio of degranulated mast cells is closely related to acupuncture's effect [26, 27, 48]. In this work, the acupuncture effect of PC6 was significant, and the ratio of degranulated mast cells in PC6 was also significantly higher than that in the other two acupoints. This suggests that heart rate elevation may be associated with the activation of mast cells. Similarly, the penetration of a needle into the muscle layer under PC6 and electrical stimulation on the needle significantly increases adenosine

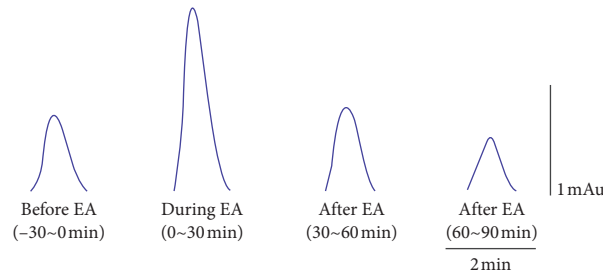


FIGURE 9: Original HPLC data of samples from a rabbit in the PC6 group. From left to right, samples were collected 30 min before EA at PC 6, after 30 min of EA, 30 min after EA, and from 30 min to 60 min from EA. It can be seen that the adenosine concentration rose during the early EA and fell again after stopping EA.

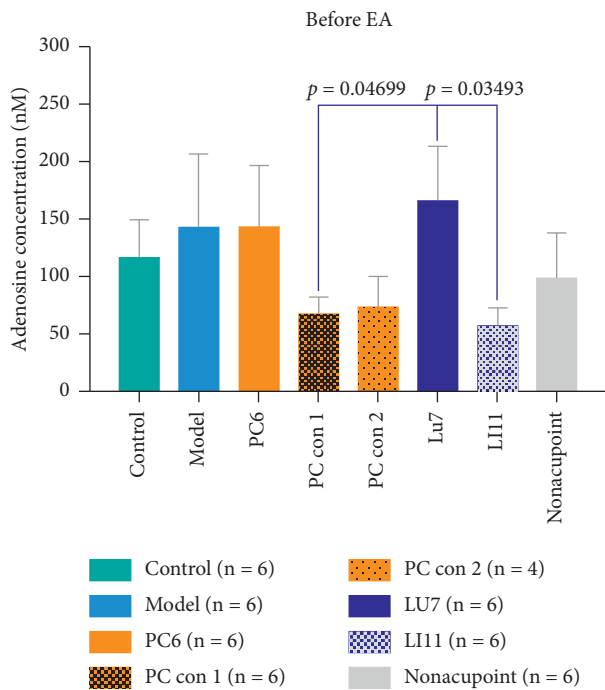


FIGURE 10: Absolute adenosine concentration in the resting state before EA in different groups. The abscissa shows the groups, and the ordinate indicates the adenosine concentration in units of nM.

concentrations in tissue fluid of the superficial fascia under PC6. However, even with the same current stimulation intensity, this phenomenon was not observed in the other two acupoints (Figure 11). When the needle was inserted into the acupoint, the current caused the needle to vibrate, and the mechanical stimulation induced by the needle caused the collagen fibers to be mechanically deformed [49]. Collagen fibers play a role in transmitting mechanical force [50]. Although the goal of mechanical force transferred by collagen fibers is still unclear, there is evidence that the TRPV2 channel on the surface of the mast cell membrane opens when subjected to mechanical stimulation. This behavior causes a large amount of calcium influx, which activates mast cells and releases certain intracellular mediators [51]. Acupuncture can cause a significant increase in adenosine concentration in interstitial fluid [29]. The

adenosine in tissue fluid activates the adenosine A1 receptor on nerve endings to produce the acupuncture signals [28]. Adenosine in tissue fluid may be derived from activated mast cells [52]. One study has shown that injection of sodium cromolyn—a kind of mast cell membrane stabilizer—in acupoints inhibits an increase of adenosine [52]. In addition, mast cell degranulation results in increased extracellular ATP levels [53, 54], and adenosine is a hydrolysate of ATP. Therefore, we have reason to believe that elevated adenosine in the tissue fluid during EA is partly derived from degranulated mast cells. Combined with previous studies about the acupuncture mechanism and the results we report, we present a diagrammatic sketch to show the mechanism of acupoint activation for specific acupoint effects (Figure 12).

Stimulating one or several specific acupoints in a nonspecific way achieves various regulating effects of acupuncture on different diseases. However, the existence of acupoint specificity is still controversial [8, 19, 20]. After observing the contrast of regulations on heart rate induced by acupuncture application on various acupoints and control points based on the rabbit acute bradycardia model, we tried for the first time to explain the physiological mechanism behind it from the view of acupoint activation and thus put forward the hypothesis that differences based on mast cell degranulation and adenosine release may be one potential physiological basis of acupoint specificity. The effect of applying acupuncture at PC6 on the heart rate regulation of acute bradycardia also provides a new perspective for clinical exploration of the treatment of related diseases and contributes a reference for selecting acupoints. Limited by acupuncturists' actual operation levels, not every acupuncture practice can achieve the expected therapeutic effect. However, we can provide targeted suggestions to improve acupuncture efficiency based on probing the acupoint activation mechanism.

It should be noted that acupoint specificity is a comprehensive proposition. In this study, we only observed PC6 and two control points along the pericardium meridian, LU7 on the lung meridian, LI11 on the large intestine meridian, and the nonpoint beside PC6. Limited samples cannot draw a general and universal conclusion, and the mystery of acupoint specificity urgently needs more scientific research to unveil.

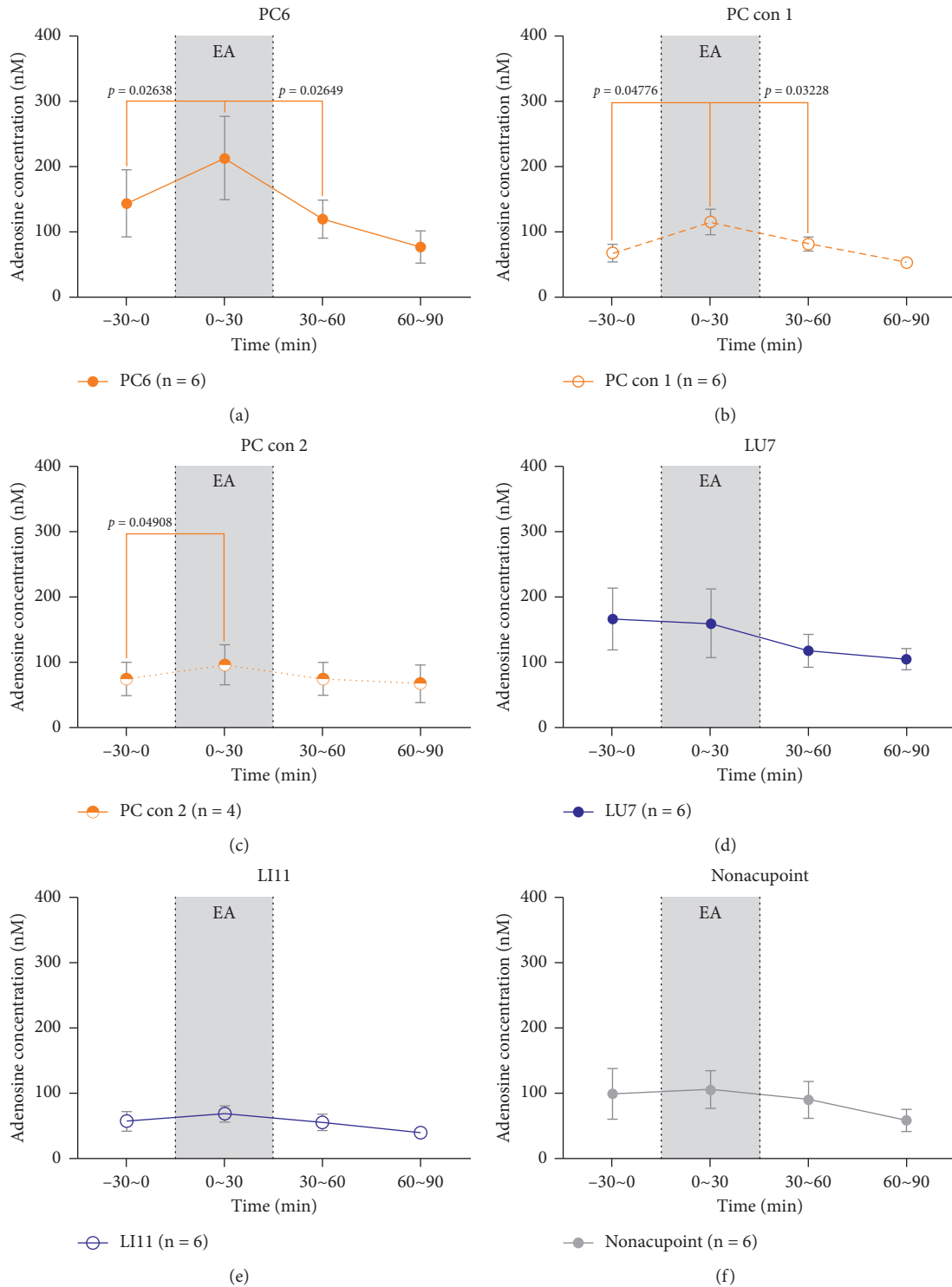


FIGURE 11: The absolute value line chart of adenosine concentrations in different groups. The abscissa shows time in units of min. The ordinate indicates adenosine concentrations in units of nM. From left to right, they are samples collected from 30 min before EA (-30~0 min), samples collected at the time of EA (the time of EA is 30 min), samples collected from 30 to approximately 60 min after EA, and samples collected from 60 to approximately 90 min after EA. (a) PC6 group. EA caused a short-term increase in absolute adenosine concentration in the local area of PC6, which was significantly different from those in the -30~0 min and 30~60 min periods. (b) PC con 1 group. EA caused a short-term increase in absolute adenosine concentration in the local area of PC con 1, which was significant compared to the -30~0 min and 30~60 min periods. (c) PC con 2 group. EA caused a short-term increase in absolute adenosine concentration in the local area of PC con 2; while these levels were significantly different compared to samples collected 30 min before EA, there was a difference compared to samples collected after EA. (d) LU7 group. EA did not cause a short-term increase in adenosine concentrations in the local area of LU7. Rather, it caused a decrease, and there were no significant differences compared to the -30~0 min or 30~60 min periods. (e) LI11 group. EA caused a short-term increase in adenosine concentration but was not significantly different compared to samples collected 30 min before and after EA. (f) Nonacupoint group. EA caused a short-term increase in adenosine concentration, but this increase was not significant compared to the -30~0 min or 30~60 min period.

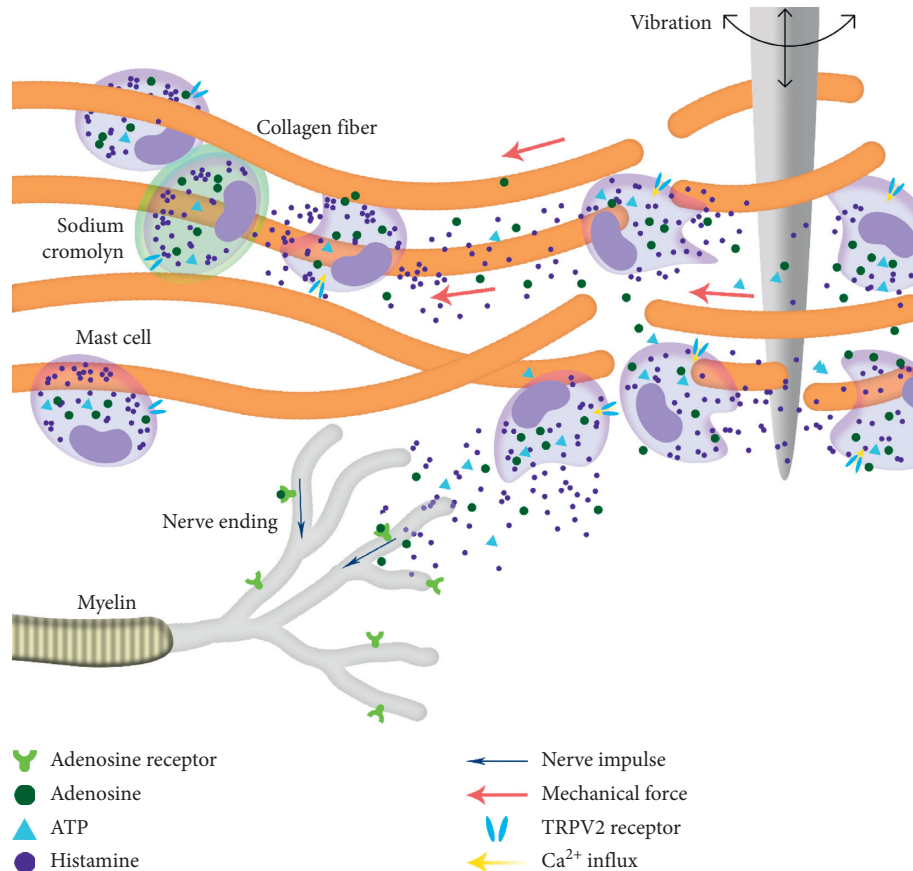


FIGURE 12: The mechanism of acupoint activation for specific acupoint effects. When the needle was inserted into the acupoint, it could induce contraction-relaxation of the skeletal skin muscle, thereby causing local collagen fiber entanglement and deformation. The resulting mechanical force was transmitted to the membrane of the mast cell, inducing the TRPV2 channel on the mast cell membrane to open. It then caused a large amount of calcium influx, activated mast cells, and released intracellular mediators such as histamine, ATP, and adenosine. Adenosine from intracellular and ATP hydrolysis bound to the adenosine A1 receptor on nerve endings to produce a nerve impulse and trigger acupuncture effects. Sodium cromolyn, a mast cell membrane stabilizer, blocks the acupuncture effect by inhibiting the degranulation of mast cells.

5. Conclusions

In summary, our current data led us to speculate that the biological basis of relative acupoint specificity may be based on mast cell degranulation. Acupuncture induces mast cell degranulation to release adenosine, and adenosine activates the A1 receptor on sensory nerves to induce the acupuncture effect in regulating heart rate (Figure 4). Compared to other acupoints, the biological mechanism of the advantage of PC6 in modulating heartbeat is based on differences in the mast cell degranulation ratio and adenosine concentrations in the tissue fluid. Similarly, the difference between PC6, PC con 1, and PC con 2 illustrates that differences between PC6 and nonacupoints in heartbeat modulation are also based on the same basic biological mechanism (Figures 5, 8, and 11). Moreover, we hypothesize that, in an acute myocardial ischemia rabbit model, the reason for the advantage of PC6 in the acupuncture effects compared with other meridian acupoints and control acupoints is the differences in adenosine concentrations in tissue fluid following acupuncture.

Abbreviations

EA: Electroacupuncture
 Con: Control
 HPLC: High-performance liquid chromatography
 ECG: Electrocardiograph.

Data Availability

The datasets used and/or analyzed during the current study are available from the corresponding author on reasonable request.

Ethical Approval

The present study was performed in accordance with the guidelines of the Animal Care and Use Committee of Shanghai Research Center for Acupuncture and Meridian, which are based on the NIH's Guide for the Care and Use of Laboratory Animals. Experimental protocols were approved

by the Animal Care and Use Committee of the Shanghai Research Center for Acupuncture and Meridian.

Conflicts of Interest

The authors declare that they have no conflicts of interest.

Authors' Contributions

XZW, MH, and HWY contributed to the data collection. XZW, MH, and GHD contributed to the data analyses. XZW, MH, WY, YX, and GHD contributed to the writing of the manuscript. DZ contributed to the conceptualization of the experiments and designed the study. GHD contributed to the conceptualization of the experiments and reviewed the data. All authors read and approved the final manuscript. Xuezhi Wang and Meng Huang contributed equally to this study.

Acknowledgments

The authors would like to thank all the subjects participating at the current study. This work was funded by the Ministry of Science and Technology of the People's Republic of China (973 Program, No. 2012CB518502), the National Natural Science Foundation of China (No. 81574053, No. 81590953, No. 81873361), the Shanghai Key Laboratory of Acupuncture Mechanism and Acupoint Function (14DZ2260500), and the Shanghai Association for Science and Technology (Nos. 15441903800 and 18401970100).

References

- [1] W.-T. Zhang, Z. Jin, G.-H. Cui et al., "Relations between brain network activation and analgesic effect induced by low vs. high frequency electrical acupoint stimulation in different subjects: a functional magnetic resonance imaging study," *Brain Research*, vol. 982, no. 2, pp. 168–178, 2003.
- [2] B. Brinkhaus, C. M. Witt, S. Jena et al., "Acupuncture in patients with chronic low back pain," *Archives of Internal Medicine*, vol. 166, no. 4, pp. 450–457, 2006.
- [3] F. Zhou, D. Huang, and Y. Xia, *Acupuncture Therapy for Neurological Diseases: A Neurobiological View*, Y. Xia, X. Cao, G. Wu, and J. Cheng, Eds., pp. 32–80, Springer-Tsinghua Press, New York, NY, USA, 2010.
- [4] G. Ding, D. Zhang, M. Huang, L. Wang, and W. Yao, *Current Research in Acupuncture*, Y. Xia, G. Ding, and G. Wu, Eds., pp. 53–88, Springer, New York, NY, USA, 2012.
- [5] F. Zhou, J. Guo, J. Cheng, G. Wu, and Y. Xia, "Effect of electroacupuncture on rat ischemic brain injury: importance of stimulation duration," *Evidence-Based Complementary and Alternative Medicine*, vol. 2013, Article ID 878521, 12 pages, 2013.
- [6] D. Chao and Y. Xia, *Neural Functions of the Delta-Opioid Receptor*, Y. Xia, Ed., pp. 583–606, Springer, New York, NY, USA, 2015.
- [7] Z. Liu, Y. Liu, H. Xu et al., "Effect of electroacupuncture on urinary leakage among women with stress urinary incontinence," *JAMA*, vol. 317, no. 24, pp. 2493–2501, 2017.
- [8] L. Zhao, J. Chen, Y. Li et al., "The long-term effect of acupuncture for migraine prophylaxis," *JAMA Internal Medicine*, vol. 177, no. 4, pp. 508–515, 2017.
- [9] N. Yin, H. Yang, W. Yao, Y. Xia, and G. Ding, "Mast cells and nerve signal conduction in acupuncture," *Evidence-Based Complementary and Alternative Medicine*, vol. 2018, p. 9, Article ID 3524279, 2018.
- [10] H. M. Langevin and P. M. Wayne, "What is the point? The problem with acupuncture research that no one wants to talk about," *The Journal of Alternative and Complementary Medicine*, vol. 24, no. 3, pp. 200–207, 2018.
- [11] L. Chen, J. Tang, P. F. White et al., "The effect of location of transcutaneous electrical nerve stimulation on postoperative opioid analgesic requirement," *Anesthesia & Analgesia*, vol. 87, no. 5, pp. 1129–1134, 1998.
- [12] M. W. Van Tulder, D. C. Cherkin, B. Berman, L. Lao, and B. W. Koes, "The effectiveness of acupuncture in the management of acute and chronic low back pain. A systematic review within the framework of the Cochrane Collaboration Back Review Group," *Spine*, vol. 24, pp. 1113–1123, 1999.
- [13] N. P. Assefi, K. J. Sherman, C. Jacobsen, J. Goldberg, W. R. Smith, and D. Buchwald, "A randomized clinical trial of acupuncture compared with sham acupuncture in fibromyalgia," *Annals of Internal Medicine*, vol. 143, no. 1, pp. 10–19, 2005.
- [14] K. Linde, A. Streng, S. Jürgens et al., "Acupuncture for patients with migraine," *JAMA*, vol. 293, no. 17, pp. 2118–2125, 2005.
- [15] E. Manheimer, A. White, B. Berman, K. Forys, and E. Ernst, "Meta-analysis: acupuncture for low back pain," *Annals of Internal Medicine*, vol. 142, no. 8, pp. 651–663, 2005.
- [16] L. Zhao, D. Li, H. Zheng et al., "Acupuncture as adjunctive therapy for chronic stable Angina," *JAMA Internal Medicine*, vol. 179, no. 10, p. 1388, 2019.
- [17] J. Yang, F. Zeng, Y. Feng et al., "A PET-CT study on the specificity of acupoints through acupuncture treatment in migraine patients," *BMC Complementary and Alternative Medicine*, vol. 12, no. 1, p. 123, 2012.
- [18] M. Yang, J. Yang, F. Zeng et al., "Electroacupuncture stimulation at sub-specific acupoint and non-acupoint induced distinct brain glucose metabolism change in migraineurs: a PET-CT study," *Journal of Translational Medicine*, vol. 12, no. 1, p. 351, 2014.
- [19] S. Liu, "Somatotopic organization and intensity dependence in driving distinct NPY-expressing sympathetic pathways by electroacupuncture," *Neuron*, 2020.
- [20] H. MacPherson, A. C. Maschino, G. Lewith, N. E. Foster, C. Witt, and A. J. Vickers, "Characteristics of acupuncture treatment associated with outcome: an individual patient meta-analysis of 17,922 patients with chronic pain in randomised controlled trials," *PLoS One*, vol. 8, no. 10, Article ID e77438, 2013.
- [21] Z. Li, C. Wang, A. F. T. Mak, and D. H. K. Chow, "Effects of acupuncture on heart rate variability in normal subjects under fatigue and non-fatigue state," *European Journal of Applied Physiology*, vol. 94, no. 5-6, pp. 633–640, 2005.
- [22] P. Li, S. C. Tjen-A-Looi, L. Cheng et al., "CME article: long-lasting reduction of blood pressure by electroacupuncture in patients with hypertension: randomized controlled trial," *Medical Acupuncture*, vol. 27, no. 4, pp. 253–266, 2015.
- [23] X. Shen and H. Wang, *Acupuncture and Moxibustion*, People's Medical Publishing House, Beijing, China, 2nd edition, 2007.
- [24] Z. Li, *Experimental Acupuncture*, China Press of Traditional Chinese Medicine, Beijing, China, 1st edition, 2007.

- [25] D. Zhang, G. Ding, X. Shen et al., "Role of mast cells in acupuncture effect: a pilot study," *Explore*, vol. 4, no. 3, p. 170, 2008.
- [26] H. Zhu, X. Wang, M. Huang, Y. Jing, D. Zhang, and G. Ding, "Mast cell activation in the acupoint is important for the electroacupuncture effect against pituitrin-induced bradycardia in rabbits," *Scientific Reports*, vol. 7, no. 1, 2017.
- [27] M. Huang, X. Wang, B. Xing et al., "Critical roles of TRPV2 channels, histamine H1 and adenosine A1 receptors in the initiation of acupoint signals for acupuncture analgesia," *Scientific Reports*, vol. 8, no. 1, p. 6523, 2018.
- [28] N. Goldman, M. Chen, T. Fujita et al., "Adenosine A1 receptors mediate local anti-nociceptive effects of acupuncture," *Nature Neuroscience*, vol. 13, no. 7, pp. 883–888, 2010.
- [29] T. Takano, X. Chen, F. Luo et al., "Traditional acupuncture triggers a local increase in adenosine in human subjects," *The Journal of Pain*, vol. 13, no. 12, pp. 1215–1223, 2012.
- [30] F. Liang, *Research and Application of Meridian Acupoint Specificity*, People's Medical Publishing House, Beijing, China, 2014.
- [31] L. Fei, "Experimental exploration and research prospect of meridian material foundation and its functional characteristics," *Chinese Science Bulletin*, vol. 43, no. 15, pp. 658–672, 1998.
- [32] M. Li, "Effects of electroacupuncture on the number of subcutaneous mast cells in and beside the acupoint and the inflammatory pain focus in the rat," *Chinese Acupuncture & Moxibustion*, vol. 23, pp. 33–37, 2003.
- [33] G. Ding, "Dynamic mechanism of directional flow of tissue fluid and human meridian phenomenon," *Progress in Natural Science*, vol. 15, pp. 63–72, 2005.
- [34] X. Shen, "Study on volt-ampere (V-A) characteristics of human acupoints," *Chinese Acupuncture & Moxibustion*, vol. 26, pp. 267–271, 2006.
- [35] Y. Ding, "Observation on the characters of infrared radiation spectrum of acupoints in normal humans and CHD patients," *Journal of Biomedical Engineering*, vol. 23, pp. 309–312, 2006.
- [36] X. Yan, X. Zhang, C. Liu et al., "Do acupuncture points exist?" *Physics in Medicine and Biology*, vol. 54, no. 9, pp. N143–N150, 2009.
- [37] G. M. Khan, S.-R. Chen, and H.-L. Pan, "Role of primary afferent nerves in allodynia caused by diabetic neuropathy in rats," *Neuroscience*, vol. 114, no. 2, pp. 291–299, 2002.
- [38] B. M. Berman, L. Lao, P. Langenberg, W. L. Lee, A. M. K. Gilpin, and M. C. Hochberg, "Effectiveness of acupuncture as adjunctive therapy in osteoarthritis of the knee," *Annals of Internal Medicine*, vol. 141, no. 12, pp. 901–910, 2004.
- [39] Y. Liu, P. Liu, L. Hou et al., "Analysis of the effects of electroacupuncture at the pericardium 6 acupoint on heart function in patients with angina using equilibrium radionuclide angiography quantity analysis technique," *The Journal of Alternative and Complementary Medicine*, vol. 20, no. 6, pp. 466–471, 2014.
- [40] L. Xu, H. Xu, W. Gao, W. Wang, H. Zhang, and D. P. Lu, "Treating angina pectoris by acupuncture therapy," *Acupuncture & Electro-Therapeutics Research*, vol. 38, no. 1, pp. 17–35, 2013.
- [41] M. Zou, "Clinical observation on therapeutic effect of combination of acupuncture and ginger-partition moxibustion for treatment of patients with cardiac arrhythmia," *Chinese Acupuncture & Moxibustion*, vol. 29, pp. 876–878, 2009.
- [42] Y. Liu, H. Gong, J. Liu, and H. Zhang, "Acupoint selection pattern of chronic atrophic gastritis based on data mining methods of latent structure model and frequency item set," *Chinese Acupuncture & Moxibustion*, vol. 38, pp. 667–671, 2018.
- [43] Q. Hu, "Clinical observation of post-infectious cough differentiated as wind-cold retention in the lung treated with scraping therapy and xuanfei zhisou decoction," *Chinese Acupuncture & Moxibustion*, vol. 36, pp. 1257–1262, 2016.
- [44] J. Wu and S. Gu, "Randomized controlled clinical trials for acupuncture treatment of aura-absence migraine patients," *Acupuncture Research*, vol. 36, pp. 128–131, 2011.
- [45] Y.-S. Liu, M. Gadau, G.-X. Zhang et al., "Acupuncture treatment of lateral elbow pain: a nonrandomized pilot study," *Evidence-Based Complementary and Alternative Medicine*, vol. 2016, Article ID 8182071, 8 pages, 2016.
- [46] J. Zhang, N. Marquina, G. Oxinos, A. Sau, and D. Ng, "Effect of laser acupoint treatment on blood pressure and body weight—a pilot study," *Journal of Chiropractic Medicine*, vol. 7, no. 4, pp. 134–139, 2008.
- [47] Y. M. Li, "The neuroimmune basis of acupuncture: correlation of cutaneous mast cell distribution with acupuncture Systems in human," *The American Journal of Chinese Medicine*, vol. 47, no. 8, pp. 1781–1793, 2019.
- [48] M. Huang, D. Zhang, Z.-Y. Sa, Y.-Y. Xie, C.-L. Gu, and G.-H. Ding, "In adjuvant-induced arthritic rats, acupuncture analgesic effects are histamine dependent: potential reasons for acupoint preference in clinical practice," *Evidence-Based Complementary and Alternative Medicine*, vol. 2012, Article ID 810512, 6 pages, 2012.
- [49] H. M. Langevin, D. L. Churchill, and M. J. Cipolla, "Mechanical signaling through connective tissue: a mechanism for the therapeutic effect of acupuncture," *The FASEB Journal*, vol. 15, no. 12, pp. 2275–2282, 2001.
- [50] X. Yu, G. Ding, H. Huang, J. Lin, W. Yao, and R. Zhan, "Role of collagen fibers in acupuncture analgesia therapy on rats," *Connective Tissue Research*, vol. 50, no. 2, pp. 110–120, 2009.
- [51] D. Zhang, A. Spielmann, L. Wang et al., "Mast-cell degranulation induced by physical stimuli involves the activation of transient-receptor-potential channel TRPV2," *Physiological Research*, vol. 61, pp. 113–124, 2012.
- [52] L. Wang, J. Sikora, L. Hu, X. Shen, R. Grygorczyk, and W. Schwarz, "ATP release from mast cells by physical stimulation: a putative early step in activation of acupuncture points," *Evidence-Based Complementary and Alternative Medicine*, vol. 2013, Article ID 350949, 7 pages, 2013.
- [53] L. Wang, D. Zhang, and W. Schwarz, "TRPV channels in mast cells as a target for low-level-laser therapy," *Cells*, vol. 3, no. 3, pp. 662–673, 2014.
- [54] W. Yao, H. Yang, N. Yin, and G. Ding, "Mast cell-nerve cell interaction at acupoint: modeling mechanotransduction pathway induced by acupuncture," *International Journal of Biological Sciences*, vol. 10, no. 5, pp. 511–519, 2014.

Research Article

Molecular Targets and Pathways Contributing to the Effects of Wenxin Keli on Atrial Fibrillation Based on a Network Pharmacology Approach

Yujie Zhang,¹ Xiaolin Zhang,² Xi Zhang,² Yi Cai,² Minghui Cheng,² Chenghui Yan,² and Yaling Han¹ 

¹Liaoning University of Traditional Chinese Medicine, Liaoning, Shenyang 110847, China

²Cardiovascular Research Institute and Department of Cardiology, The General Hospital of Northern Theatre Command, Liaoning, Shenyang 110840, China

Correspondence should be addressed to Yaling Han; yaling.han1953@gmail.com

Received 8 May 2020; Revised 11 September 2020; Accepted 21 September 2020; Published 7 October 2020

Academic Editor: Yong Wang

Copyright © 2020 Yujie Zhang et al. This is an open access article distributed under the Creative Commons Attribution License, which permits unrestricted use, distribution, and reproduction in any medium, provided the original work is properly cited.

Background. Atrial fibrillation (AF) is the most common sustained arrhythmia and is associated with high rates of mortality and morbidity. The traditional Chinese medicine Wenxin Keli (WXKL) can effectively improve clinical symptoms and is safe for the treatment of AF. However, the active substances in WXKL and the molecular mechanisms underlying its effects on AF remain unclear. In this study, the bioactive compounds in WXKL, as well as their molecular targets and associated pathways, were evaluated by systems pharmacology. **Materials and Methods.** Chemical constituents and potential targets of WXKL were obtained via the Traditional Chinese Medicine Systems Pharmacology (TCMSP). The TTD, DrugBank, DisGeNET, and GeneCards databases were used to collect AF-related target genes. Based on common targets related to both AF and WXKL, a protein interaction network was generated using the STRING database. Gene ontology (GO) and Kyoto Encyclopedia of Genes and Genomes (KEGGs) pathway enrichment analyses were performed. Network diagrams of the active component-target and protein-protein interactions (PPIs) were constructed using Cytoscape. **Results.** A total of 30 active ingredients in WXKL and 219 putative target genes were screened, including 83 genes identified as therapeutic targets in AF; these overlapping genes were considered candidate targets for subsequent analyses. The effect of treating AF was mainly correlated with the regulation of target proteins, such as IL-6, TNF, AKT1, VEGFA, CXCL8, TP53, CCL2, MMP9, CASP3, and NOS3. GO and KEGG analyses revealed that these targets are associated with the inflammatory response, oxidative stress reaction, immune regulation, cardiac energy metabolism, serotonergic synapse, and other pathways. **Conclusions.** This study demonstrated the multicomponent, multitarget, and multichannel characteristics of WXKL, providing a basis for further studies of the mechanism underlying the beneficial effects of WXKL in AF.

1. Introduction

Atrial fibrillation (AF) is one of the most common arrhythmias, and its prevalence is increasing [1]. The occurrence of AF can lead to heart failure, embolism, and stroke and significantly increases the rates of disability and death, presenting a serious health issue [2, 3]. Therefore, the prevention and treatment of AF are major concerns.

According to the American Heart Association practice guidelines, current strategies for AF management include

rate control, rhythm control, anticoagulation, lifestyle, and risk factor management [4]. Antiarrhythmic drugs and catheter ablation are the main treatment options. However, available medications for AF are suboptimal based on the high rate of arrhythmia recurrence and the potential proarrhythmic effect [5, 6]. Catheter ablation is also limited by a high rate of recurrence, and patients often require additional surgery [6, 7]. Therefore, researchers, clinicians, and patients seek new effective and safe treatment strategies for AF.

Traditional Chinese medicines (TCMs) have been used for the prevention and treatment of arrhythmias in China for over a thousand years [8]. Wenxin Keli (WXKL), a classical Chinese patent medicine with high efficacy and favorable safety, is useful for the management of patients with AF [9–11]. WXKL is composed of five Chinese herbal extracts: Radix (Dang Shen, DS), Polygonati Rhizoma (Huang Jing, HJ), Notoginseng Radix et Rhizoma (San Qi, SQ), Ambrum (Hu Po, HP), and Nardostachyos Radix et Rhizoma (Gan Song, GS). It is the first Chinese antiarrhythmic medicine approved by the China Food and Drug Administration [11–13].

Recent animal and cell studies [14–16] have demonstrated that WXKL inhibits and prevents atrial arrhythmias via complicated antiarrhythmic mechanisms, but the specific molecular mechanism remains unclear.

Similar to other TCM formulas, WXKL is a multi-component and multitarget agent that achieves its specific therapeutic efficacy via the regulation of molecular networks by active components. In this study, we used a comprehensive network pharmacology-based approach to investigate the mechanisms by which WXKL exerts therapeutic effects in AF. A flowchart of the experimental procedure is shown in Figure 1.

2. Materials and Methods

2.1. Database Building and Active Compound Screening.

All compounds in the five herbal components of WXKL were retrieved from the TCM Systems Pharmacology (TCMSP, <http://lsp.nwu.edu.cn/tcmsp.php>) database and analysis platform, which captures relationships among drugs, targets, and diseases. The database includes chemicals, targets, drug-target networks, and associated drug-target-disease networks, as well as pharmacokinetic properties of natural compounds, such as oral bioavailability (OB), drug-likeness (DL), and blood-brain barrier penetration [17, 18]. Compounds were screened based on absorption, distribution, metabolism, and excretion (ADME), and pharmacokinetic information retrieval filters were used to obtain bioactive compounds for further analysis using the thresholds $OB \geq 30\%$ and $DL \geq 0.18$ [19, 20]. A network was generated using Cytoscape to visualize the complex relationships between active compounds and potential targets [21]. Nodes represent compounds and targets, and edges indicate the intermolecular interactions.

2.2. Identification of Drug Targets. Protein targets of the compounds were retrieved from the TCMSP. Gene names were extracted from UniProtKB (<http://www.uniprot.org>).

2.3. Screening of Potential Targets for AF. AF-associated target genes were obtained from various databases, such as TTD, DrugBank, DisGeNET, and GeneCards. The DrugBank database (<https://www.drugbank.ca/>) is a unique bioinformatics and cheminformatics resource that combines detailed drug data with comprehensive drug target information [22, 23]. The DisGeNET database (

FIGURE 1: Analysis framework based on an integrated network pharmacology strategy.

[disgenet.org/](https://www.disgenet.org/)) includes one of the largest publicly available collections of genes and variants associated with human diseases [24]. The GeneCards database (<https://www.genecards.org/>) is a searchable, integrative database that provides comprehensive, user-friendly information for all annotated and predicted human genes [25]. The term “atrial fibrillation” was used for searches against these four databases to screen targets related to AF.

2.4. Collection of Common Compound-Disease Targets.

The screened chemical targets and disease targets were imported into the ImageGP (<http://www.ehbio.com/ImageGP/index.php>) platform, and common compound-disease targets were obtained as candidates for further analysis [26].

2.5. PPI Network of Compound-Disease Targets.

A protein-protein interaction (PPI) network was generated using the STRING database (<https://string-db.org/>), which covered almost all functional interactions between the expressed proteins [27]. Species was set to “Homo sapiens,” and the target interaction information was obtained. The results were imported into Cytoscape (version 3.6.1; <https://www.cytoscape.org/>) to draw and analyze the interaction network.

The node size reflected the number of combined edges (degree), and nodes with a degree greater than twice the median degree of all nodes were selected as hubs.

2.6. Gene Ontology (GO) and KEGG Pathway Enrichment Analyses. GO analyses based on the three main categories, i.e., biological process (BP), molecular function (MF), and cell component (CC), and a Kyoto Encyclopedia of Genes and Genomes (KEGGs) (<https://www.kegg.jp/>) pathway enrichment analysis were performed using the Metascape system (<http://metascape.org/gp/index.html>) [28] and the ImageGP. A *P* value less than 0.05 indicated significance.

2.7. Pathway Constructions and Analysis. In order to explore the biological effects of cellular targets affecting the diseases through modulating specific pathways, an incorporated “AF pathway” was integrated based on the current understanding of AF pathology [29]. In brief, the obtained target proteins were firstly mapped to KEGG to distribute them to several pathways. Next, pathways closely related to AF were picked out and consolidated into an “AF pathway” under the pathological and clinical data.

3. Results

3.1. Identification of Active Compounds in WXGs. From the TCMSP, 354 total compounds were retrieved, including 134 in Radix (DS), 38 in Rhizoma (HJ), 119 in Notoginseng Radix et Rhizoma (SQ), 6 in Ambrum (HP), and 57 in Nardostachyos Radix et Rhizoma (GS). Among the 354 compounds, 34 satisfied $OB \geq 30\%$ and $DL \geq 0.18$. Finally, 30 compounds were obtained after excluding duplicates (Table 1).

3.2. WXKL Target Identification. In total, 30 compounds in WXKL were associated with 645 target proteins. After eliminating overlapping proteins, 219 proteins were obtained. To further understand the interactions between compounds and targets, we constructed a compound-target network, as shown in Figure 2, by mapping 30 compounds to 219 potential targets associated with inflammation, antioxidant stress, nuclear factor-kappa B, immune regulation, and so on. The network had 253 nodes and 531 edges. Compounds with the most targets in WXKL were quercetin, luteolin, 7-methoxy-2-methyl isoflavone, beta-sitosterol, baicalein, and stigmasterol, with 141, 55, 40, 35, 31, and 28 targets, respectively. These results suggested that the six components are probably related to the therapeutic effects in AF.

3.3. Retrieval of Potential Disease Targets. TTD, DrugBank, DisGeNET, and GeneCards retrieval results were integrated to obtain AF-related disease targets. As shown in Figure 3, the potential targets of WXKL were mapped to the disease targets using the ImageGP platform, and a Venn diagram was drawn. A total of 83 potential targets were obtained

based on the intersection of the two sets of targets. These targets are summarized in Supplementary Table S1.

3.4. Analyses of Candidate Target Proteins. A total of 83 potential genes associated with AF were uploaded to the STRING database for analysis. The systematically selected protein targets with a median confidence score of 0.400 were plotted as a PPI network using the STRING database. A total of 83 nodes and 1253 edges were acquired, and the average node degree was 30.2. Furthermore, using Cytoscape, we constructed a network (Figure 4), in which the edges represent associations between a pair of targets, nodes represent the target, and the degree value represents the intensity. The top ten targets IL-6, TNF, AKT1, VEGFA, CXCL8, TP53, CCL2, MMP9, CASP3, and NOS3 had high degrees in this process, explaining their significance in the network.

3.5. Gene Ontology Enrichment Analysis. We imported the 83 candidate target genes into the Metascape system for a GO analysis.

Based on this analysis, the potential targets were related to many biological processes, molecular functions, and cellular components, including functions that maybe important for the occurrence and development of AF. The top 20 highly enriched BP terms were retained for analysis and included negative regulation of cytokine, reactive oxygen species, and cell migration (Figure 5(c)). Previous study showed that AF targets were the diversity of molecular pathways affecting mechanical stress, sarcomere disarray, chronic inflammation, reactive oxygen species, and activation of atrial fibroblasts, which have collectively emerged from translational research and genome-wide association studies (GWASs) [30]. These results indicated the therapeutic effects of WXKL in AF maybe mediated by its effects on these biological processes. Accordingly, these processes are of great significance for our understanding of the mechanism by which WXKL influences AF.

A total of 119 GO terms in the molecular function category (Figure 5(b)) were enriched, and the top 20 entries were selected for analysis. These terms mainly included cytokine receptor binding, kinase binding, adrenergic receptor activity, phosphatase binding, and antioxidant activity.

In total, 58 GO terms in the cell components category (Figure 5(a)) were enriched, and the top 19 entries were selected for analysis based on $P < 0.01$. The targets were closely related to membrane raft extracellular matrix, RNA polymerase II transcription factor complex, endoplasmic reticulum lumen, neuron projection cytoplasm, mitochondrial outer membrane, perinuclear region of cytoplasm, focal adhesion, and nuclear membrane. Previous study showed interconnectivity of numerous targets functioning in the cardiomyocyte cell membrane, sarcoplasmic reticulum, nucleus, sarcomere, and inflammasome with reported roles in human or preclinical models of AF [31, 32]. Thus, it can be seen that WXKL plays a role in the treatment of AF through these cell components category.

TABLE 1: Basic information for components of WXKL.

MOL ID	Molecule name	OB (%)	DL
MOL008397	Daturilin	50.37	0.77
MOL008393	7-(Beta-xylosyl)cephalomannine_qt	38.33	0.29
MOL007514	Methyl icoso-11,14-dienoate	39.67	0.23
MOL009763	(+)-Syringaresinol-O-beta-D-glucoside	43.35	0.77
MOL008407	(8S, 9S, 10R, 13R, 14S, 17R)-17-[(E, 2R, 5S)-5-Ethyl-6-methylhept-3-en-2-yl]-10,13-dimethyl-1,2,4,7,8,9,11,12,14,15,16,17-dodecahydrocyclopenta[a]phenanthren-3-one	45.4	0.76
MOL006774	Stigmast-7-enol	37.42	0.75
MOL003036	ZINC03978781	43.83	0.76
MOL001006	Poriferasta-7,22E-dien-3-beta-ol	42.98	0.76
MOL004355	Spinasterol	42.98	0.76
MOL002879	Diop	43.59	0.39
MOL000359	Sitosterol	36.91	0.75
MOL001494	Mandenol	42	0.19
MOL008411	11-Hydroxyrankinidine	40	0.66
MOL002140	Perlolyrine	65.95	0.27
MOL006331	4',5-Dihydroxyflavone	48.55	0.19
MOL001040	(2R)-5,7-Dihydroxy-2-(4-hydroxyphenyl)chroman-4-one	42.36	0.21
MOL005344	Ginsenoside rh2	36.32	0.56
MOL005321	Frutinone A	65.9	0.34
MOL000546	Diosgenin	80.88	0.81
MOL007059	3-Beta-hydroxymethyllenetanshiquinone	32.16	0.41
MOL002959	3'-Methoxydaidzein	48.57	0.24
MOL008400	Glycitein	50.48	0.24
MOL001689	Acacetin	34.97	0.24
MOL007088	Cryptotanshinone	52.34	0.4
MOL000449	Stigmasterol	43.83	0.76
MOL002714	Baicalein	33.52	0.21
MOL000358	Beta-sitosterol	36.91	0.75
MOL003896	7-Methoxy-2-methyl isoflavone	42.56	0.2
MOL000006	Luteolin	36.16	0.25
MOL000098	Quercetin	46.43	0.28

3.6. KEGG Pathway Enrichment Analysis. To further reveal the mechanisms underlying the effect of WXKL on AF, we conducted a KEGG pathway enrichment analysis of 83 targets and screened the top 20 pathways based on a threshold value of $P < 0.01$ (Figure 6). Many pathways involving potential target genes were identified, such as the VEGF signaling pathway, HIF-1 signaling pathway, and PI3K-Akt signaling pathway, which are associated with signal transduction. Hepatitis B, TNF signaling pathways, NF-kappa B signaling, cytokine-cytokine receptor interaction, and hepatitis C pathways are related to inflammatory reactions. Moreover, amyotrophic lateral sclerosis, allograft rejection, and allograft rejection are closely related to immunological processes. The calcium signaling pathway modulates intracellular Ca^{2+} levels and a number of Ca^{2+} -dependent intracellular signaling processes. Serotonergic synapses and tryptophan modulate 5-hydroxytryptamine, which is a hormonal trigger for AF. In addition, complement and coagulation cascades revealed that WXKL has a potential role in other related diseases. The AGE-RAGE signaling pathway is highly important in diabetic complications; it elicits the activation of multiple intracellular signaling pathways involving NADPH oxidase, protein kinase C, and MAPKs, thereby resulting in NF-kappa B activity.

Previous study showed that the mechanisms of AF were related to atrial cardiomyopathy, mechanical stress, activation of atrial fibroblasts, fibrofatty infiltrations, inflammation, activation of inflammasomes and macrophages, hypercoagulability and autonomic nervous system dysregulation, sarcoplasmic reticulum Ca^{2+} leak, and so on [30].

The results verified that WXKL alleviates AF by regulating inflammatory, immunity, antioxidant stress, serotonergic synapses, Ca^{2+} levels, and a number of Ca^{2+} -dependent intracellular signaling processes (Figures 7 and 8).

4. Discussion

AF, the most common sustained arrhythmia, currently affects over 33 million individuals worldwide, and its prevalence is expected to be more than double over the next 40 years. AF is associated with a twofold increase in premature mortality and important major adverse cardiovascular events, such as heart failure, severe stroke, and myocardial infarction [33]. AF is not just an atrial disease, with documented associations with systemic inflammation, endothelial dysfunction, cardiometabolic disturbance, and wider abnormalities in myocardial structure and function [34, 35]. In this study, we identified the main active ingredients of WXKL as quercetin, luteolin, 7-methoxy-2-

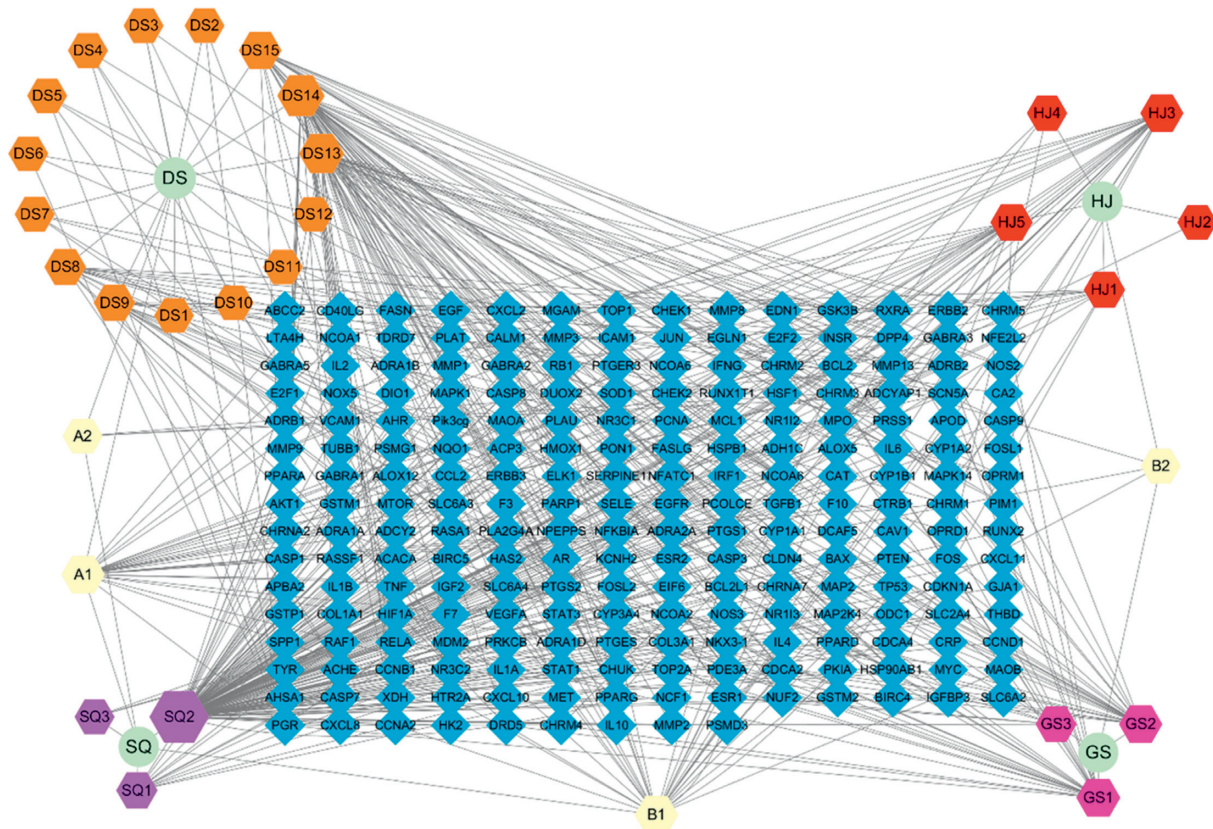


FIGURE 2: Drug-compound-target network of potential targets in WXXL. Blue diamond represents potential active ingredients in WXXL, compounds in WXXL are shown in light yellow, pink, red, orange, and purple, and the herbs are shown in green. Radix (Dang Shen, DS), Polygonati Rhizoma (Huang Jing, HJ), Noto Ginseng Radix et Rhizoma (San Qi, SQ), Ambrum (Hu Po, HP), and Nardostachyos Radix et Rhizoma (Gan Song, GS). A1 represents stigmasterol. A2 represents Diop. B1 represents beta-sitosterol. B2 represents sitosterol. DS1 represents daturinin. DS2 represents (8S, 9S, 10R, 13R, 14S, 17R)-17-[(E, 2R, 5S)-5-ethyl-6-methylhept-3-en-2-yl]-10,13-dimethyl-1,2,4,7,8,9,11,12,14,15,16,17-dodecahydrocyclopenta[a]phenanthren-3-one. DS3 represents ZINC03978781. DS4 represents poriferasta-7,22E-dien-3beta-ol. DS5 represents spinasterol. DS6 represents stigmast-7-enol. DS7 represents 11-hydroxyrankinidine. DS8 represents 3-beta-hydroxymethylenetanshiquinone. DS9 represents frutinone A. DS10 represents 7-(beta-xylosyl)cephalomannine_qt. DS11 represents perlolyrine. DS12 represents methyl icoso-11,14-dienoate. DS13 represents 7-methoxy-2-methyl isoflavone. DS14 represents luteolin. DS15 represents glycitein. GS1 represents cryptotanshinone. GS2 represents acacetin. GS3 represents (2R)-5,7-dihydroxy-2-(4-hydroxyphenyl)chroman-4-one. HJ1 represents diosgenin. HJ2 represents (+)-syringaresinol-O-beta-D-glucoside. HJ3 represents baicalein. HJ4 represents 4',5'-dihydroxyflavone. HJ5 represents 3'-methoxydaidzein. SQ1 represents ginsenoside rh2. SQ2 represents quercetin. SQ3 represents mandenol.

methyl isoflavone, beta-sitosterol, baicalein, and stigmasterol and used network and functional analyses to show that they are potentially valuable for the treatment of AF.

Some compounds detected in this study have reported effects other than anti-inflammatory, anti-immune, and anti-stress activity. Quercetin, a very common flavonoid found in plant foods, prevents arrhythmias and dramatically improves heart muscle function and repair following heart attack. Quercetin has a protective effect against AF, probably by inhibiting platelet aggregation and TXA2 formation, as well as increasing PGI2 generation [35]. Previous studies have suggested that luteolin, a flavonoid, possesses anti-oxidative, anti-tumor, and anti-inflammatory properties. The cardiac protective effects of luteolin have recently been demonstrated *in vitro* and *in vivo* [36].

As illustrated in the compound-target network, many targets could be altered by multiple compounds, such as TNF, IL-6, JUN, and PTGS1. Others, including CRP,

CXCL2, and COL3A1, could only be regulated by quercetin. These results indicated that WXXL has multicomponent and multitarget biological characteristics. A PPI network showed that WXXL could regulate the expression of AF-regulated targets and alleviate AF symptoms. IL-6 (degree = 65), AKT1 (degree = 61), TNF (degree = 61), VEGFA (degree = 56), and TP53 (degree = 53) are potential hub targets in the network.

To predict the mechanisms underlying the therapeutic effects of WXXL in AF, we evaluated the candidate targets by GO enrichment analyses. Based on the top 20 GO terms ($P < 0.01$) in each major category, the major hubs were significantly enriched for multiple biological processes, including negative regulation of cytokine, reactive oxygen species, and cell migration, as shown in Figure 5(c). Furthermore, they were enriched for various molecular functions, including cytokine receptor binding, kinase binding, adrenergic receptor activity, phosphatase binding, and antioxidant activity, as shown in Figure 5(b). The active targets

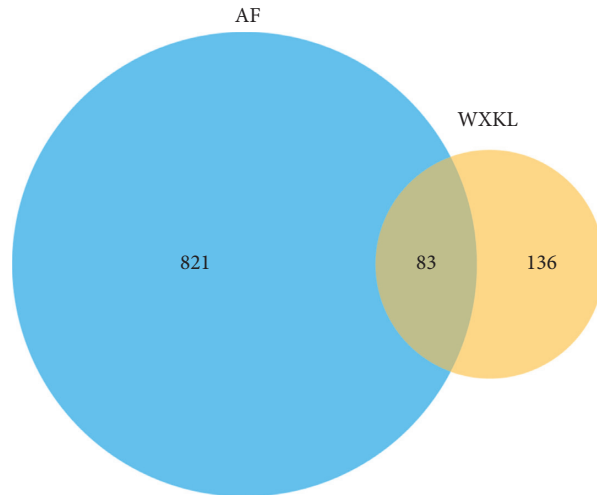


FIGURE 3: Matching of target genes for AF and WXKL.

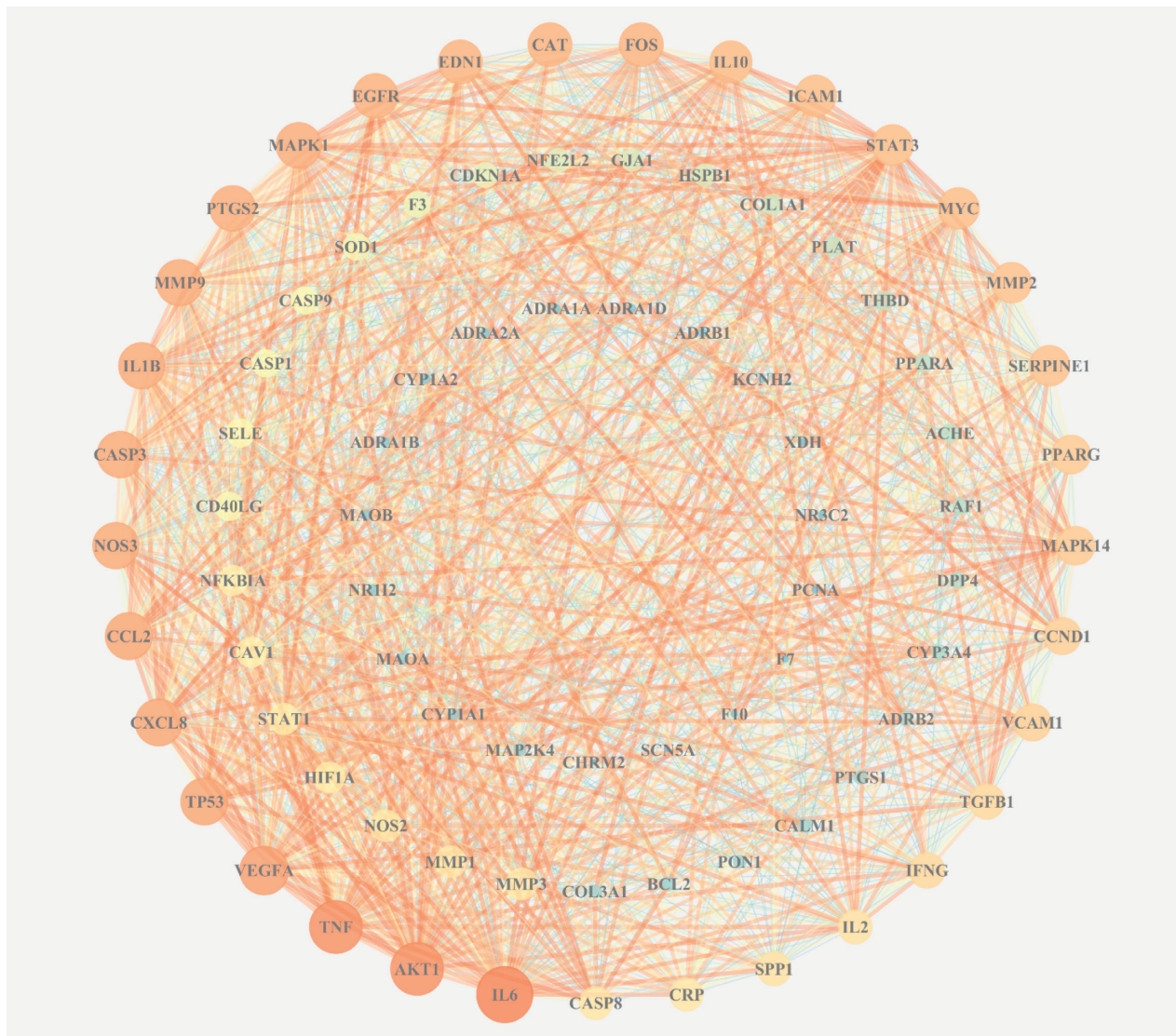
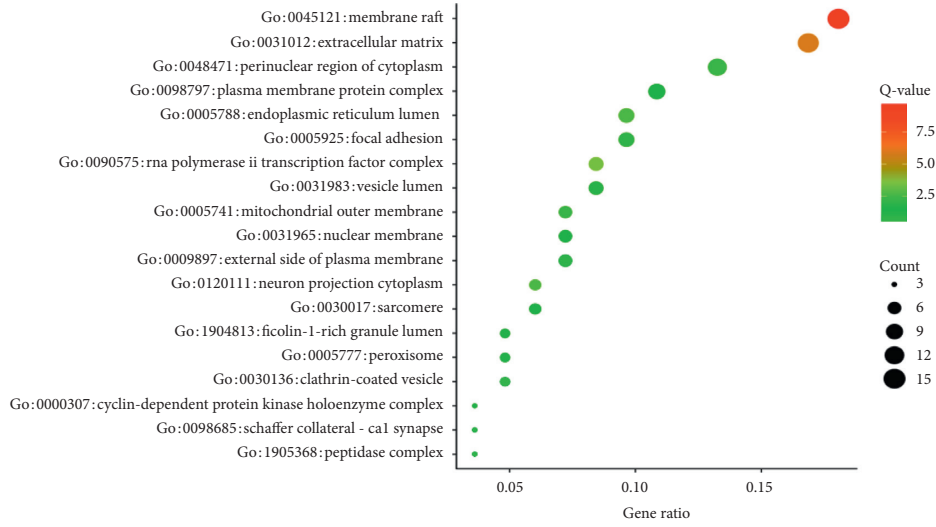
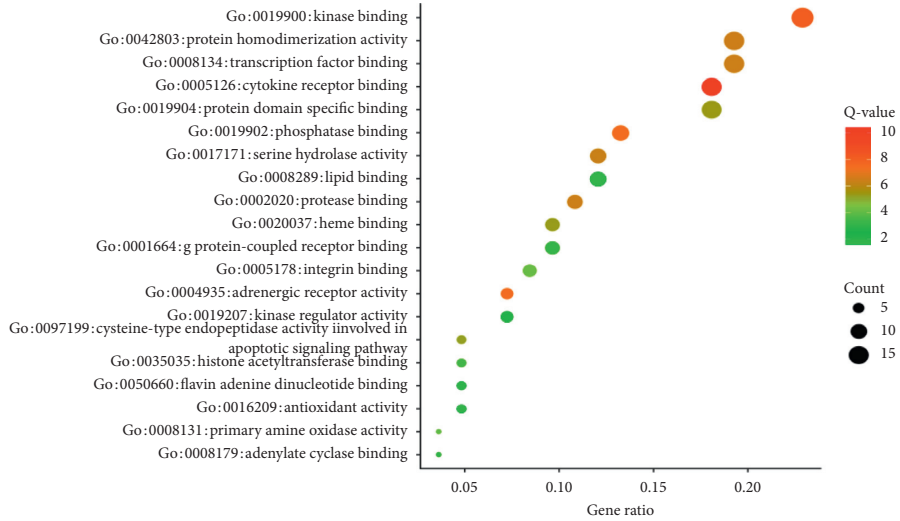


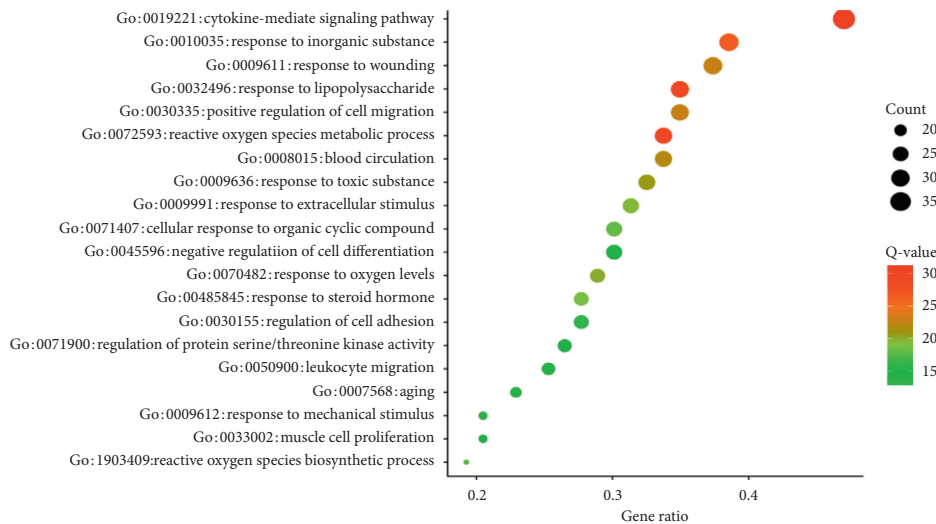
FIGURE 4: PPI network of targets for WXKL in the treatment of AF. Layout of the three rings corresponds to the area and color of nodes. Nodes represent potential targets of WXKL in AF. Node size from large to small indicates a decrease in the degree value. Lines connecting inner nodes indicate relationships between proteins.



(a)



(b)



(c)

FIGURE 5: GO enrichment analyses of potential targets of the main active ingredients of WXKL: (a) cell component (CC); (b) molecular function (MF); (c) biological process (BP). Node colors are shown as a gradient from red to green according to the descending order of *P* values. Node sizes are in the ascending order of the gene count.

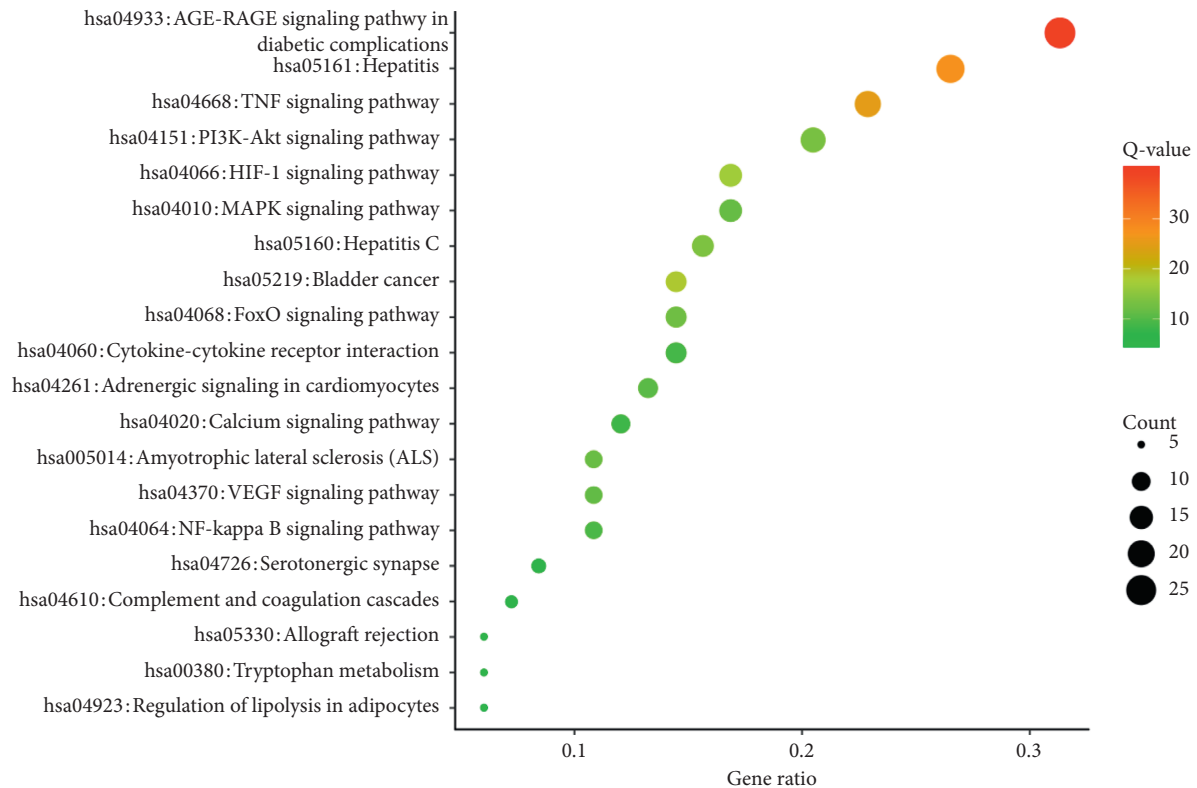


FIGURE 6: KEGG pathway enrichment analyses of potential targets of the main active ingredients of WXKL. Node colors are shown as a gradient from red to green according to the descending order of P values. Node sizes are in the ascending order of the gene count.

IL-6, AKT1, TNF, CCL18, CCL2, and NOS3 were related to various molecular processes, particularly immune regulation, oxidative stress, and inflammatory response. To some extent, these results are consistent with the pathogenesis and clinical features of AF. The key cellular components included membrane raft extracellular matrix, RNA polymerase II transcription factor complex, endoplasmic reticulum lumen, neuron projection cytoplasm, mitochondrial outer membrane, perinuclear region of cytoplasm, focal adhesion, vesicle lumen, cyclin-dependent protein kinase holoenzyme complex, and nuclear membrane, and many targets were highly ranked as potential-related genes. These findings indirectly illustrated the complexity of the pathogenesis of AF and the damage to various cellular components.

It is generally believed that oxidative stress, inflammation, and related processes are important factors for the promotion of apoptosis or myocardial fibrosis, leading to atrial electrical remodeling and structural remodeling and eventually to the occurrence and persistence of AF [37, 38]. The identification of significant leukocyte infiltration in atrial myocardium in AF patients and observed correlation between elevated circulating proinflammatory cytokines and AF severity support this contention [39]. Established inflammatory factors and biomarkers related to AF include tumor necrosis factor α , C-reactive protein, interleukin-2, interleukin-6, interleukin-8, matrix metalloproteinase, endothelin, and myeloperoxidase [34]. Cardiac fibroblasts

which were a highly plastic population of resident cells play an important role in the development of an AF substrate [40]. Activated fibroblasts secrete extracellular matrix proteins and recruit immune cells, leading to dispersion and blockade of conduction in the myocardium. Combined with an already heterogeneous and anisotropic fiber bundle arrangement, focal fibrosis renders the left atrium extremely susceptible to reentrant circuits [40, 41]. VEGF, a pivotal activator of angiogenesis and calcium (Ca^{2+}) signaling in endothelial cells, increases collagen production in atrial fibroblasts [42]. In addition, after treatment, procollagen type I, procollagen type III production, myofibroblast differentiation, and the migratory ability of fibroblasts are reduced in AF. These results further confirm that the targets identified in this study are consistent with previous reports, indicating supporting the therapeutic effects of WXKL.

Obesity is associated with an increased amount of epicardial fat, which is a major mediator of the relationship between obesity and AF [43]. A probable mechanism by which epicardial fat promotes AF is direct adipocyte infiltration into the atrial myocardium, resulting in slow or anisotropic conduction. A second probable mechanism is atrial fibrosis caused by adipokines secreted from epicardial fat. Third, it is possible that epicardial fat contributes to AF by the secretion of proinflammatory factors, such as IL-6, IL-8, and TNF- α . By a KEGG analysis, we found that WXKL can regulate lipolysis in adipocytes (Figures 7 and 8),

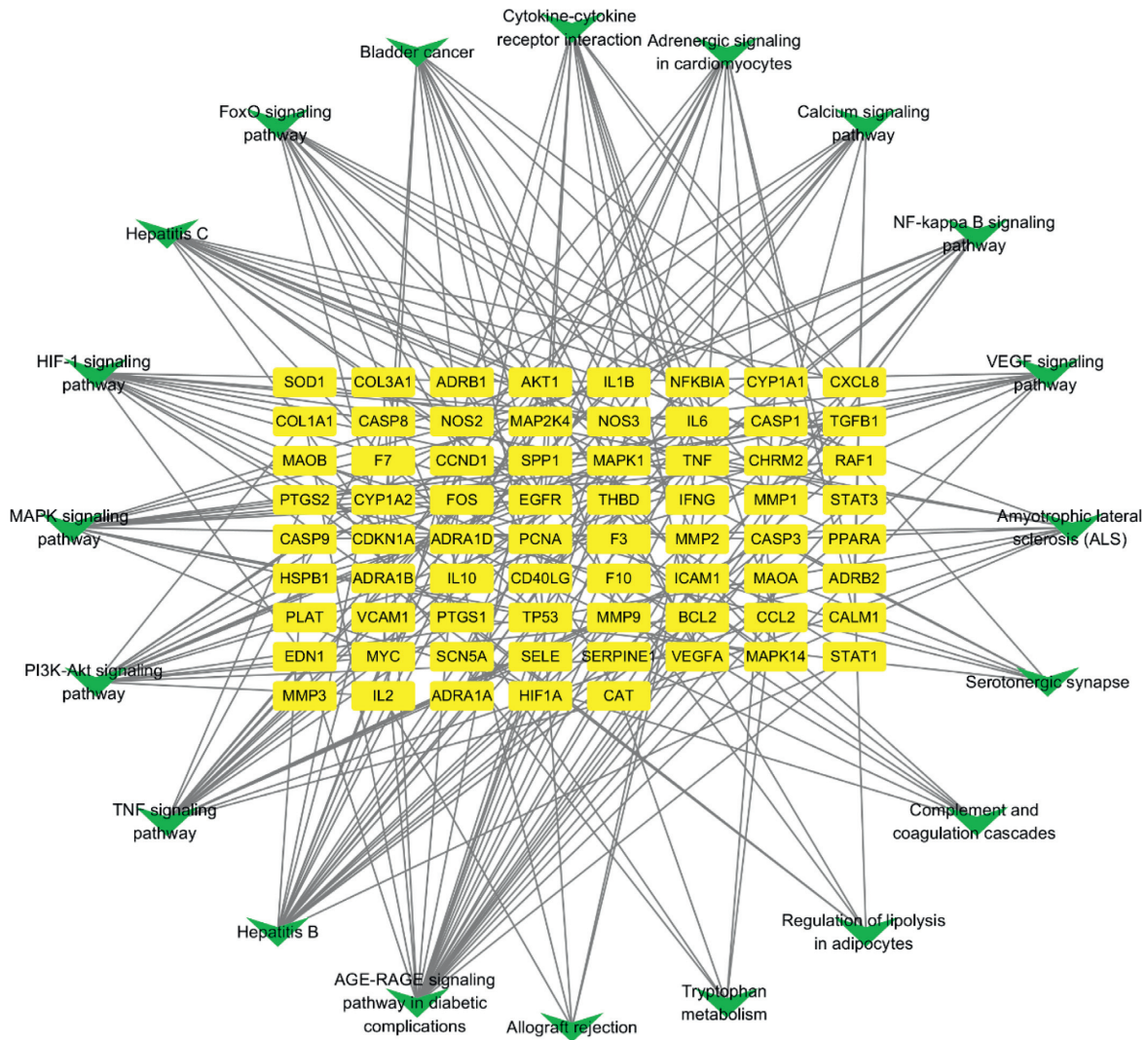


FIGURE 7: Target-pathway network for WXKL. Green and yellow nodes represent pathways and targets, respectively, and edges represent interactions.

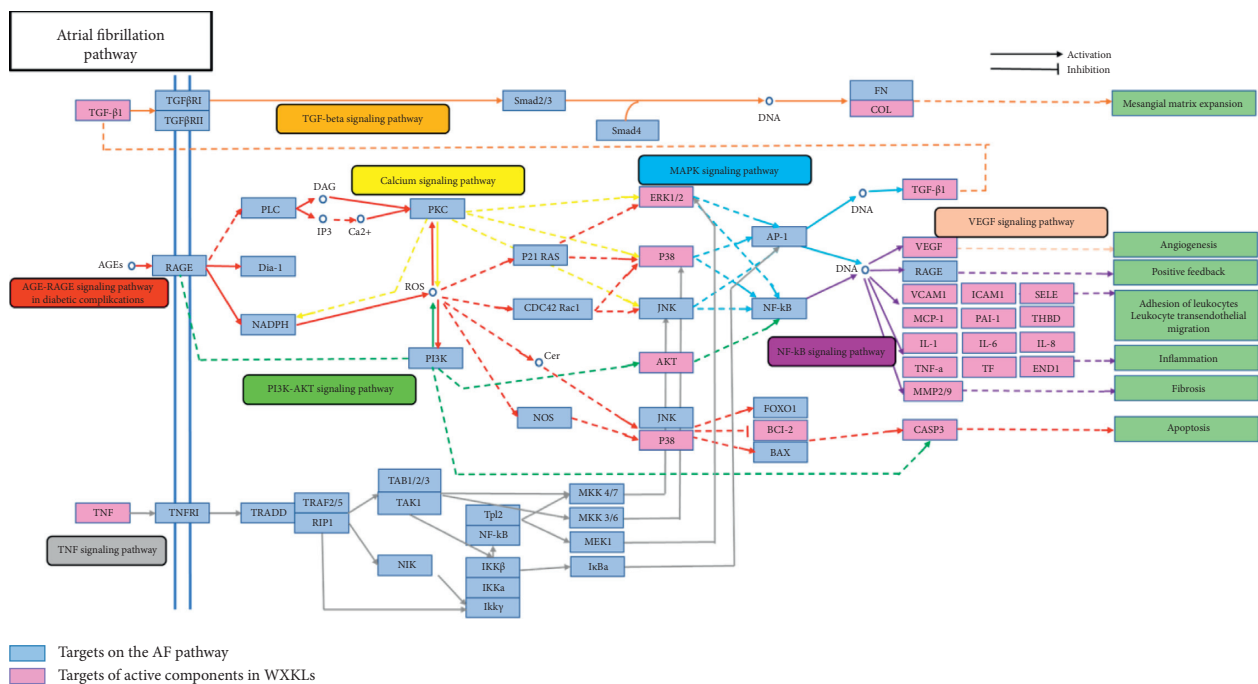


FIGURE 8: Atrial fibrillation pathway and therapeutic modules.

implying that it is a good treatment strategy for patients with obesity and AF.

In 2019, Wang et al. [44] proposed that the relationship between AF and DM is complex and is mediated by structural, electrical, electromechanical, and autonomic changes in the atria, triggered by oxidative stress, inflammation, and glycaemic fluctuations. Glucose-lowering therapies may affect the development of AF. Accordingly, it is important to elucidate the mechanism underlying DM-related AF and to evaluate the best treatment strategy for patients with DM and AF. Our KEGG analysis indicated that the most important pathway by which WXKL effects AF is the AGE-RAGE signaling pathway (Figures 7 and 8), involved in diabetic complications, which elicits the activation of multiple intracellular signaling pathways involving NADPH oxidase, protein kinase C, and MAPKs, resulting in NF-kappa B activity. Combining our KEGG analysis, WXKL maybe is a good treatment strategy for patients with DM and AF.

Serotonin, 5-hydroxytryptamine, is a hormonal trigger for AF [45, 46]. By a KEGG analysis, we found that pathways are related to the role of WXKL in AF including the regulation of serotonergic synapses and tryptophan metabolism.

Accordingly, the targets identified in our study are consistent with previous findings, further supporting the use of WXKL for the treatment of AF by regulating the inflammatory response, oxidative stress reaction, immune regulation, cardiac energy metabolism, tryptophan metabolism, and other pathways.

5. Conclusions

In summary, WXKL is beneficial for the treatment of AF, consistent with previous studies. We further characterized the biological functions of active ingredients in WXKL and their corresponding targets by a network pharmacological approach, improving our understanding of the molecular biological mechanism underlying the effects of WXKL in AF. These findings provide an important theoretical basis for the clinical treatment of AF.

Data Availability

The data used to support the findings of this study are included within the article.

Conflicts of Interest

The authors declare that there are no conflicts of interest regarding the publication of this paper.

Acknowledgments

This research was supported by the Liaoning Science and Technology Project (2015010400-301), National Science Foundation of China (81670340), and Shenyang Science and Technology Project (19-112-4-055). The authors thank all participators in this study.

Supplementary Materials

See Table S1 in the Supplementary Material for information on potential targets and topological attributes. (*Supplementary Materials*)






References

- [1] S. Sumeet, R. Chugh, K. Havmoeller et al., "Worldwide epidemiology of atrial fibrillation: a global burden of disease 2010 study." *Circulation*, vol. 129, no. 8, pp. 837–847, 2014.
- [2] P. A. Wolf, R. D. Abbott, and W. B. Kannel, "Atrial fibrillation as an independent risk factor for stroke: the framingham Study," *Stroke*, vol. 22, no. 8, pp. 983–988, 1991.
- [3] A. Gómez-Outes, J. Lagunar-Ruiz, A.-I. Terleira-Fernández, G. Calvo-Rojas, M. L. Suárez-Gea, and E. Vargas-Castrillón, "Causes of death in anticoagulated patients with atrial fibrillation," *Journal of the American College of Cardiology*, vol. 68, no. 23, pp. 2508–2521, 2016.
- [4] M. K. Chung, L. L. Eckhardt, L. Y. Chen et al., "Lifestyle and risk factor modification for reduction of atrial fibrillation: a scientific statement from the American heart association," *Circulation*, vol. 141, no. 16, 2020.
- [5] A. Verma, C. Jiang, T. R. Betts et al., "Approaches to catheter ablation for persistent atrial fibrillation," *New England Journal of Medicine*, vol. 373, no. 9, pp. 877–878, 2015.
- [6] G. A. Upadhyay and F. J. Alenghat, "Catheter ablation for atrial fibrillation in 2019," *JAMA*, vol. 322, no. 7, pp. 686–687, 2019.
- [7] S. G. Spitzer, L. Károlyi, C. Rämmler et al., "Treatment of recurrent nonparoxysmal atrial fibrillation using focal impulse and rotor mapping (FIRM)-Guided rotor ablation: early recurrence and long-term outcomes," *Journal of Cardiovascular Electrophysiology*, vol. 28, no. 1, pp. 31–38, 2017.
- [8] Z. Wang, W. Z. Tang, and J. L. GeGe, "Efficacy and safety of traditional Chinese medicine on thromboembolic events in patients with atrial fibrillation: a systematic review and meta-analysis," *Complementary Therapies in Medicine*, vol. 32, pp. 1–10, 2017.
- [9] H. Zhuogen, Z. Minan, X. Pingchang, W. Yuanping, Y. Xia, and D. Dingwei, "Wenxin Keli for atrial fibrillation," *Medicine*, vol. 97, no. 17, e0390 pages, 2018.
- [10] N. Zhang, S. G. Tse, M. Y. GongYang et al., "Efficacy of wenxin keli plus amiodarone versus amiodarone monotherapy in treating recent-onset atrial fibrillation," *Cardiology Research and Practice*, vol. 2018, Article ID 6047271, 7 pages, 2018.
- [11] G. Chan, Y. Sun, S. Liu et al., "Therapeutic effects of wenxin keli in cardiovascular diseases: an experimental and mechanism overview," *Frontiers in Pharmacology*, vol. 9, p. 1005, 2018.
- [12] Z. Rui, T. Guihua, Z. Qin et al., "Clinical safety and efficacy of wenxin keli-amiodarone combination on heart failure complicated by ventricular arrhythmia: a systematic review and meta-analysis," *Frontiers in Physiology*, vol. 9, p. 487, 2018.
- [13] Y. Liu, Z. Zhang, Y. N. Yang, G. Li, and T. Liu, "The Chinese herb extract Wenxin Keli: a promising agent for the management of atrial fibrillation," *International Journal of Cardiology*, vol. 203, pp. 614–615, 2016.
- [14] J.-W. Zhang, W. Li, K. Guo et al., "Antiarrhythmic effects and potential mechanism of WenXin KeLi in cardiac purkinje cells," *Heart Rhythm*, vol. 13, no. 4, pp. 973–982, 2016.
- [15] Y. Chen, L. Yang, L. Guo et al., "Effects of wenxin keli on the action potential and L-type calcium current in rats with transverse aortic constriction-induced heart failure,"

- Evidence-Based Complementary and Alternative Medicine*, vol. 2013, Article ID 572078, 12 pages, 2013.
- [16] Y. Minoura, B. K. Panama, and V. V. Nesterenko, et al., "Effect of Wenxin Keli and quinidine to suppress arrhythmogenesis in an experimental model of Brugada syndrome," *Heart Rhythm*, vol. 10, no. 7, pp. 1054–1062, 2013.
- [17] J. Betzenhauser, L. Peng, J. Wang et al., "TCMSP: a database of systems pharmacology for drug discovery from herbal medicines," *Journal of Cheminformatics*, vol. 6, no. 1, p. 13, 2014.
- [18] B. Zhu, W. Zhang, Y. Lu et al., "Network pharmacology-based identification of protective mechanism of Panax Notoginseng Saponins on aspirin induced gastrointestinal injury," *Bio-medicine & Pharmacotherapy*, vol. 105, pp. 159–166, 2018.
- [19] X.-x. Xu, J.-p. Bi, L. Ping, P. Li, and F. Li, "A network pharmacology approach to determine the synergetic mechanisms of herb couple for treating rheumatic arthritis," *Drug Design, Development and Therapy*, vol. 12, pp. 967–979, 2018.
- [20] M.-F. Guo, Y. J. Dai, G. Jia-Rong et al., "Uncovering the mechanism of Astragalus membranaceus in the treatment of diabetic nephropathy based on network pharmacology," *Journal of Diabetes Research*, vol. 2020, Article ID 5947304, 13 pages, 2020.
- [21] T. Qin, L. Wu, Q. Hua, Z. Song, Y. Pan, and T. Liu, "Prediction of the mechanisms of action of Shenkang in chronic kidney disease: a network pharmacology study and experimental validation," *Journal of Ethnopharmacology*, vol. 246, pp. 112–128, 2020.
- [22] Y. Wang, S. Zhang, F. Li et al., "Therapeutic target database 2020: enriched resource for facilitating research and early development of targeted therapeutics," *Nucleic Acids Research*, vol. 48, no. D1, pp. D1031–D1041, 2020.
- [23] D. S. Wishart, Y. D. Feunang, A. C. Guo et al., "DrugBank 5.0: a major update to the DrugBank database for 2018," *Nucleic Acids Research*, vol. 46, no. D1, pp. D1074–D1082, 2018.
- [24] J. Piñero, J. M. Ramirez-Angueta, J. Saüch-Pitarch et al., "The DisGeNET knowledge platform for disease genomics: 2019 update," *Nucleic Acids Research*, vol. 48, no. D1, pp. D845–D855, 2020.
- [25] G. Stelzer, R. Rosen, I. Plaschkes et al., "The GeneCards suite: from gene data mining to disease genome sequence analysis," *Curr Protoc Bioinformatics*, vol. 54, 2016.
- [26] L. Y. Zeng, Q. Wang, L. Y. Han et al., "Mechanism of tripterygium hypoglaucum-leonuri Herba for treating rheumatoid arthritis based on network pharmacology," *Chinese Journal of Experimental Traditional Medical Formulae*, vol. 25, no. 19, pp. 170–181, 2019.
- [27] D. Szklarczyk, A. L. Gable, D. Lyon et al., "STRING v11: protein-protein association networks with increased coverage, supporting functional discovery in genome-wide experimental datasets," *Nucleic Acids Research*, vol. 47, no. D1, pp. D607–D613, 2019.
- [28] Y. Zhou, B. Zhou, L. Pache et al., "Metascape provides a biologist-oriented resource for the analysis of systems-level datasets," *Nature Communications*, vol. 10, no. 1, p. 1523, 2019.
- [29] J. Liu, J. Mu, C. Zheng et al., "Systems-pharmacology dissection of traditional Chinese medicine compound saffron formula reveals multi-scale treatment strategy for cardiovascular diseases," *Entific Reports*, vol. 6, Article ID 19809, 2016.
- [30] Y.-S. Ang, S. Rajamani, and S. M. Haldar, J. Huser, A new therapeutic framework for atrial fibrillation drug development," *Circulation Research*, vol. 127, no. 1, pp. 184–201, 2020.
- [31] N. Hüser, J. J. M. B. Bianca, "Inflammasomes and proteostasis novel molecular mechanisms associated with atrial fibrillation," *Circulation Research*, vol. 127, no. 1, pp. 73–90, 2020.
- [32] S. Nattel, J. Heijman, and L. Zhou, D. Dobromir, "Molecular basis of atrial fibrillation pathophysiology and therapy," *Circulation Research*, vol. 127, no. 1, pp. 51–72, 2020.
- [33] R. S. Dobrev and B. Casadei, "Mechanisms of atrial fibrillation," *Heart*, vol. 105, no. 24, pp. 1860–1867, 2019.
- [34] R. S. Wijesurendra and B. Casadei, "Atrial fibrillation: effects beyond the atrium?" *Cardiovascular Research*, vol. 105, no. 3, pp. 47–238, 2015.
- [35] D. Xiao, Z. L. Gu, and Z. N. Qian, "Effects of quercetin on platelet and reperfusion-induced arrhythmias in rats," *Acta Pharmacologica Sinica*, vol. 14, no. 6, pp. 505–508, 1993.
- [36] Y. Luo, P. Shang, and D. Li, "Luteolin: a flavonoid that has multiple cardio-protective effects and its molecular mechanisms," *Frontiers in Pharmacology*, vol. 8, p. 692, 2017.
- [37] J. Li, J. Solus, Q. Chen et al., "Role of inflammation and oxidative stress in atrial fibrillation," *Heart Rhythm*, vol. 7, no. 4, pp. 438–444, 2010.
- [38] H. A. I Hadi, A. A. Alsheikh-Ali, M. WA, and M. A. S. Jassim, "Inflammatory cytokines and atrial fibrillation: current and prospective views," *Journal of Inflammation Research*, vol. 3, pp. 75–97, 2010.
- [39] U. Schotten, S. Verheule, and P. Kirchhof, A. Goette, "Pathophysiological mechanisms of atrial fibrillation: a translational appraisal," *Physiological Reviews*, vol. 91, no. 1, pp. 265–325, 2011.
- [40] S. Y. Ho, J. A. Cabrera, and S. Q. Damian, "Left atrial anatomy revisited," *Circulation: Arrhythmia and Electrophysiology*, vol. 5, no. 1, pp. 220–228, 2012.
- [41] B. Burstein, E. Libby, and S. Nattel, "Differential behaviors of atrial versus ventricular fibroblasts," *Circulation*, vol. 117, no. 13, pp. 1630–1641, 2008.
- [42] C.-C. Chung, Y.-K. Lin, Y.-C. Chen, Y.-H. Kao, T.-I. Lee, and Y.-J. Chen, "Vascular endothelial growth factor enhances profibrotic activities through modulation of calcium homeostasis in human atrial fibroblasts," *Laboratory Investigation*, vol. 100, no. 2, pp. 285–296, 2020.
- [43] C. X. Wong, A. N. Ganesan, J. B Selvanayagam et al., "Epicardial fat and atrial fibrillation: current evidence, potential mechanisms, clinical implications, and future directions," *European Heart Journal*, vol. 38, no. 17, pp. 1294–1302, 2017.
- [44] A. Wang, J. B. Green, J. L. Halperin, and J. P. Piccini, "Atrial fibrillation and diabetes mellitus," *Journal of the American College of Cardiology*, vol. 74, no. 8, pp. 1107–1115, 2019.
- [45] S. Yusuf, N. Al-Saady, and A. J. Camm, "5-Hydroxytryptamine and atrial fibrillation," *Journal of Cardiovascular Electrophysiology*, vol. 14, no. 2, pp. 209–214, 2003.
- [46] K. T. Murray, L. C. Mace, and Z. Yang, "Nonantiarrhythmic drug therapy for atrial fibrillation," *Heart Rhythm*, vol. 4, no. 3, pp. S88–S90, 2007.

Research Article

Endothelium-Independent Vasodilatory Effect of Sailuotong (SLT) on Rat Isolated Tail Artery

S. Y. Yeon ¹, S. W. Seto ^{1,2}, G. H. H. Chan,³ M. Low ¹, H. Kiat ^{4,5,6}, N. Wang,^{1,7} J. Liu,^{1,8} and D. Chang ¹

¹NICM Health Research Institute, Western Sydney University, Penrith, NSW 2751, Australia

²Department of Applied Biology and Chemical Technology, The Hong Kong Polytechnic University, Hung Hom, Kowloon, Hong Kong SAR, China

³Hong Kong Community College, The Hong Kong Polytechnic University, Hung Hom, Kowloon, Hong Kong

⁴Faculty of Medicine, University of New South Wales, Kensington, NSW 2052, Australia

⁵School of Medicine, Western Sydney University, Penrith, NSW 2571, Australia

⁶Faculty of Medicine and Health Sciences, Macquarie University, Sydney, NSW 2113, Australia

⁷Key Laboratory of Chinese Medicinal Formula of Anhui Province, Anhui University of Chinese Medicine, Hefei 230012, China

⁸Xiyuan Hospital, China Academy of Chinese Medical Sciences, Beijing, China

Correspondence should be addressed to S. W. Seto; saiwang.seto@polyu.edu.hk

Received 15 June 2020; Revised 21 August 2020; Accepted 7 September 2020; Published 22 September 2020

Academic Editor: Silvia Wein

Copyright © 2020 S. Y. Yeon et al. This is an open access article distributed under the Creative Commons Attribution License, which permits unrestricted use, distribution, and reproduction in any medium, provided the original work is properly cited.

Background. Sailuotong (SLT) is a standardized three-herb formulation consisting of extracts of *Panax ginseng*, *Ginkgo biloba*, and *Crocus sativus* for the treatment of vascular dementia (VaD). Although SLT has been shown to increase cerebral blood flow, the direct effects of SLT on vascular reactivity have not been explored. This study aims to examine the vasodilatory effects of SLT and the underlying mechanisms in rat isolated tail artery. **Methods.** Male (250–300 g) Wistar Kyoto (WKY) rat tail artery was isolated for isometric tension measurement. The effects of SLT on the influx of calcium through the cell membrane calcium channels were determined in Ca^{2+} -free solution experiments. **Results.** SLT (0.1–5,000 $\mu\text{g}/\text{mL}$) caused a concentration-dependent relaxation in rat isolated tail artery precontracted by phenylephrine. In the contraction experiments, SLT (500, 1,000, and 5,000 $\mu\text{g}/\text{mL}$) significantly inhibited phenylephrine (0.001 to 10 μM)- and KCl (10–80 mM)-induced contraction, in a concentration-dependent manner. In Ca^{2+} -free solution, SLT (500, 1,000, and 5,000 $\mu\text{g}/\text{mL}$) markedly suppressed Ca^{2+} -induced (0.001–3 mM) vasoconstriction in a concentration-dependent manner in both phenylephrine (10 μM) or KCl (80 mM) stimulated tail arteries. L-type calcium channel blocker nifedipine (10 μM) inhibited PE-induced contraction. Furthermore, SLT significantly reduced phenylephrine-induced transient vasoconstriction in the rat isolated tail artery. **Conclusion.** SLT induces relaxation of rat isolated tail artery through endothelium-independent mechanisms. The SLT-induced vasodilatation appeared to be jointly mediated by blockages of extracellular Ca^{2+} influx via receptor-gated and voltage-gated Ca^{2+} channels and inhibition of the release of Ca^{2+} from the sarcoplasmic reticulum.

1. Background

Cerebrovascular diseases (CVDs), including ischemic stroke and vascular dementia (VaD), are among the major causes of morbidity and mortality in developing and developed countries [1]. CVDs are strongly associated with a number of risk factors, such as hypertension, obesity, aging, diabetes, and hypercholesterolemia [2]. Altered vascular reactivity,

such as impaired vasodilatation or enhanced vasoconstriction, has been considered one of the common characteristics associated with these risk factors [3–5], directly contributing to the development and progression of CVD. For example, impaired vascular relaxation has been shown to play a role in the development of VaD in deoxycorticosterone acetate (DOCA) salt-induced hypertensive rats [6]. Similarly, impaired carotid artery relaxation has been suggested as a

contributor to stroke and dementia in aged mice [7]. Therefore, interventions that can induce vasodilation or suppress vasoconstriction could be useful in reducing the progression of CVD.

Sailuotong (SLT) is a standardized three-herb formula Chinese herbal medicine designed for the management of VaD associated with ischemic stroke [8, 9]. The SLT formula consists of standard extracts of specific dosages of *Panax ginseng* C. A. Meyer (ginseng), *Ginkgo biloba* L. (ginkgo), and *Crocus sativus* L. (saffron). The chemical profile and ratio of the three herbal extracts had been determined and studied in detail previously [10, 11]. The cognitive enhancing effect of SLT has been demonstrated in both preclinical and clinical studies. In a chronic cerebral hypoperfusion model induced by bilateral common carotid artery ligation in rats, eight-week treatment of SLT significantly suppressed hypoperfusion-induced cognitive impairments, and this change is associated with reduction of activity of cholinesterase and increased acetylcholine (ACh) levels and superoxide dismutase (SOD) activity the brain tissue [8]. Our previous work also showed that SLT protected cultured human vascular endothelial cells against hydrogen peroxide-induced injury via increase in SOD activity [12]. The potential beneficial effects of SLT for VaD were demonstrated in two separate phase II randomized, double-blinded, placebo-controlled clinical studies. In these studies, treatment with SLT was shown to significantly improve cognitive function and cerebral blood flow to the inferior frontal and anterior temporal lobes in patients with VaD [11, 13].

Reports from animal and clinical studies have indicated that the clinically beneficial effect of SLT is, at least, partially associated with an increase in cerebral blood flow [14, 15]. However, the underlying mechanism(s) associated with these SLT-mediated cerebral blood flow increase remain to be determined. In this study, we hypothesised that SLT has direct modulatory effects in vascular reactivity. Therefore, this study was aimed to evaluate the vascular effects and the underlying mechanisms of SLT using rat isolated tail artery.

2. Methods

2.1. Chemical and Drugs. SLT extracts were provided in-kind by the Shineway Pharmaceutical Group (Shijiazhuang, China). Acetylcholine (ACh), phenylephrine, calcium chloride (CaCl_2), tetraethylammonium (TEA), clotrimazole, glibenclamide, potassium chloride (KCl), ethylene glycol-bis(β -aminoethyl ether)-*N,N,N',N'*-tetraacetic acid (EGTA), *l*-*N*-nitro arginine methyl ester (L-NAME), and nifedipine were purchased from Sigma-Aldrich (St Louis, MO, USA). All the other reagents were of analytical grade.

2.2. High-Performance Thin-Layer Chromatography (HPLC) Analysis of the SLT Formula. HPLC-PDA was employed to profile the phytochemical composition of the SLT extract used in the study. The HPLC-PDA analysis was performed on a Prominence-I LC-2030 3D Plus Shimadzu HPLC system controlled by Lab Solutions software (Shimadzu, Australia). Separation was achieved using a Shimadzu Shim-

pack GIST (Shimadzu, Australia) reverse phase C18 column (4.6×150 mm I.D., $5 \mu\text{m}$) maintained at 40°C .

The SLT extract was dissolved by sonication in 30% aqueous acetonitrile for 30 min at 5 mg/ml. Individual solutions of standards, crocin, ginsenoside Re, ginsenoside Rg1, ginsenoside Rd, quercetin, kaempferol, and isorhamnetin were prepared to 1 mg/10 ml in 30% aqueous acetonitrile for identification and combined for analysis. The sample and mixed standard were syringe-filtered with $0.45 \mu\text{m}$ PTFE.

The SLT HPLC-PDA profiles were generated by $20 \mu\text{l}$ injection. The mobile phase consisted of 0.1% (v/v) aqueous formic acid (mobile phase A) and 0.1% (v/v) formic acid in acetonitrile (mobile phase B). The gradient program was 10% B for 1 min with a linear increase, to 45% B at 45 min, and then, a wash and re-equilibration. The mobile phase flow rate was maintained at 1.1 ml/min. The PDA was set to acquire absorbance data from 190 to 800 nm.

2.3. Animals. A total of forty 12-week-old, male Wistar Kyoto (WKY) rats weighting 200–250 g were obtained from the Animal Resource Centre (Canning Vale, Western Australia). All experimental animals were housed under a 12:12 hour light-dark cycle (relative humidity: 50–60%; temperature: $22 \pm 1^\circ\text{C}$) and were given standard chow and water *ad libitum* throughout the experimental period. On the day of experiment, the rats were sacrificed by CO_2 asphyxiation, and vascular preparations were isolated under a dissection microscope. All animal protocols conformed to the Guide for the Care and Use of Laboratory Animals by the Australian Code of Practice for the Care and Use of Animals for Scientific Purpose [16]. Institutional ethics approval (Approval number: A12041) was obtained from Western Sydney University prior to commencement of the study.

2.4. Isometric Tension Measurement. Isometric force measurements and experimental protocols were performed on tail artery isolated from the WKY rats as described previously with slight modifications [5, 17]. The isometric force of the arterial ring segments was measured using a multiwire myograph system (Model 620M; Danish Myo Technology, DMT, Denmark). During the isometric tension measurement, the chambers of the myograph were filled with Krebs–Henseleit solution (mmol/L: NaCl 118.0, KCl 4.7, K_3PO_4 1.2, MgSO_4 1.2, NaHCO_3 25.0, CaCl_2 1.8, glucose 11.0), unless stated otherwise. The Krebs–Henseleit solution were prepared and used as follows: All solutions were warmed to 37°C and bubbled with carbogen (95% O_2 and 5% CO_2) before they were added to the myograph chamber. Each chamber containing 5 ml of Krebs buffered solution was bubbled with 95% O_2 and 5% CO_2 and maintained at a pH of 7.4 at 37°C throughout the experiment. Arterial rings (1.5–2.0 mm length) were mounted in the organ chambers, and normalized passive resting force and the corresponding diameter were determined for each preparation from its own length-pressure curve and stretched to their optimal lumen diameter (i.e., ~90% of the diameter which is equivalent to a transmural pressure of 100 mm Hg). The rings were, then,

left for a stabilization period of about 30 minutes until a stable base line tone was obtained before beginning of the experiment. The presence of the endothelium was tested with acetylcholine (1 μ M) after precontraction with phenylephrine (PE) (1 μ M). Tissues which showed a relaxation to acetylcholine of less than 60% of the phenylephrine contraction were not considered with intact endothelium and, therefore, not employed in this study. Responses were recorded using computerized data acquisition and recording software.

2.5. Experimental Protocols of Vascular Tension Studies

2.5.1. Protocol 1: Vasodilatory Effect of the SLT Extract in Rat Isolated Tail Arteries. The acute and direct vasodilatory effect of SLT was evaluated on rat isolated tail artery. PE (1 μ M) was applied to induce a steady contraction. When the contraction reached a plateau, the SLT extract (0.1–5000 μ g/ml) was added cumulatively to the isolated tail artery rings with or without the presence of L-NAME (20 μ M) to obtain a concentration-response curve. The relaxation effect was calculated as the percentage of the contraction in response to PE.

2.5.2. Protocol 2: Effects of Potassium Channel Blockers on SLT-Induced Vasodilation in Rat Isolated Tail Arteries. Rat isolated tail arteries were preincubated with various K⁺ channel blockers: (1) nonselective K⁺ channel blocker, tetraethylammonium (TEA, 1 mM); (2) selective ATP-sensitive K⁺ channel (K_{ATP}) blocker, glibenclamide (3 μ M), and (3) Ca²⁺-dependent K⁺ channel (K_{Ca}) blockers, clotrimazole (5 μ M). Each blocker was allowed to incubate with the preparation for 30 min before the construction of a concentration-response curve.

2.5.3. Protocol 3: Calcium-Induced Vasoconstriction in Rat Isolated Tail Arteries. The effect of SLT on calcium influx induced by two different agents was evaluated. The preparations were initially contracted with either KCl (80 mM) or PE (10 μ M) to determine maximum contraction of each preparation in normal Krebs solution. The preparations were washed with a calcium-free solution (identical concentration of EGTA substituted for Ca²⁺ in a normal Krebs solution) until fully relaxed. To exhaust the intracellular calcium storage, the preparations were stimulated with either PE (10 μ M) or KCl (80 mM) repeatedly, with calcium-free solution wash in between, until any contractile response disappeared. The preparations were, then, incubated with SLT at various concentrations (500, 1,000, and 5,000 μ g/ml) for 30 min. After incubation, a single dose of the contractile agent (either KCl (80 mM) or PE (10 μ M)) was added to the chamber, and calcium (0.001–3 mM)-induced contraction concentration response curves were constructed.

2.5.4. Protocol 4: Phenylephrine- and Potassium Chloride-(KCl-) Induced Vasoconstriction in Rat Isolated Tail Arteries.

In order to assess the effects of SLT on the contraction induced by phenylephrine and potassium chloride (KCl), concentration-response curves of PE and KCl were constructed with or without the presence of SLT at various dosages (500, 1,000, and 5,000 μ g/ml). The arterial preparations were allowed to preincubate with SLT (0, 500, 1,000, and 5,000 μ g/ml) for 30 minutes' prior the construction of the PE or KCl-induced vasoconstriction concentration-response curve.

2.5.5. Protocol 5: Role of Intracellular Calcium-Induced Vasoconstriction in Rat Isolated Tail Arteries. To clarify the role of intracellular Ca²⁺ release from the sarcoplasmic reticulum (SR) in the relaxant effect of SLT, the isolated tail artery rings were exposed to a Ca²⁺-free solution for 15 minutes before the application of 1 μ M of PE to induce the first transient contraction (Con 1). The rings were, then, washed with a normal Krebs solution for three times and incubated in the normal Krebs solution for 45 minutes to allow refill of the intracellular Ca²⁺ storage. After the 45-minute incubation, the medium was rapidly replaced with a Ca²⁺-free solution and allowed to incubate for 15 minutes. The second contraction (Con 2) was induced by 1 μ M of PE with or with the presence of SLT (500, 1,000, or 5,000 μ g/ml). The ratio of Con 2 to Con 1 was calculated.

2.6. Statistical Analysis. Data are expressed as mean \pm S.E.M., and *n* denotes the number of replications for each data point. Relaxation was expressed as the percentage of the contraction elicited by phenylephrine or KCl. Statistical comparisons were performed using the *t*-test or two-way analysis of variance (ANOVA), where appropriate. Differences were considered to be statistically significant at *P* < 0.05. All statistical analyses were performed using GraphPad Prism 5 software (GraphPad Software, Inc., USA).

3. Results

3.1. High-Performance Thin-Layer Chromatography (HPLC) Analysis of the SLT Extract. The active ingredients and contents in SLT have been reported in details previously [10, 11]. Six major bioactive compounds were analyzed using HPLC. Similar to these studies, our results showed that all these major bioactive compounds, including ginsenosides Rg1, ginsenosides Re, ginsenosides Rb1, quercetin, isorhamnetin, and crocin, are present in the SLT extract (Figure 1). The chromatogram is visualized at different wavelengths corresponding to the optimal wavelength to detect the relevant group of markers. SLT is reported to contain ginsengs as ginsenosides Rg1 (2.4 mg/capsule), ginsenosides Re (1.6 mg/capsule), and ginsenosides Rb1 (4.49 mg/capsule). The ginsenosides were confirmed to be present in similar concentrations by matching retention time and the UV spectrum to the reference standards as shown in Figure 1 at 203 nm. The peak size is not reflective of abundance as the different ginsenosides have unique molar absorptivity. SLT is reported to contain *Ginkgo biloba*, with

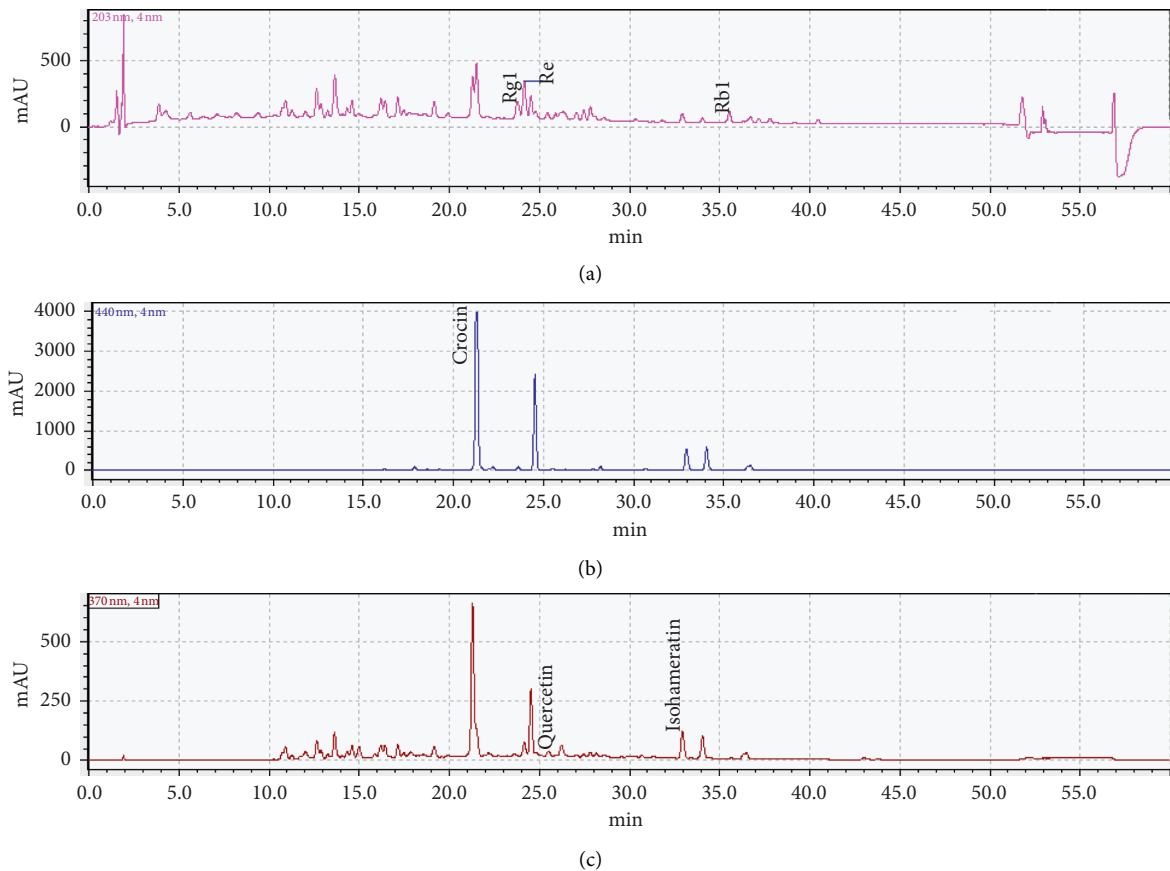


FIGURE 1: HPLC chromatograms of the SLT extract. The chromatogram (a) at 203 nm (pink) shows the ginsenosides Rg1, ginsenosides Re, and ginsenosides. The chromatogram (b) at 440 nm (blue) shows crocin. The chromatogram (c) at 370 nm (maroon) shows quercetin and isorhamnetin.

markers quercetin (2.71 mg/capsule) and isorhamnetin (1.55 mg/capsule). These were identified in the SLT extract used in this study as shown in Figure 1 at 370 nm. SLT is reported to contain saffron, with the marker crocin (1.7 mg/capsule). Crocin was identified in the SLT extract used in this study as shown in Figure 1 at 440 nm. The HPLC analysis of the SLT extract supplied by Shineway was consistent with other reports [10, 11].

3.2. Vasodilatory Effects of the SLT Extract in Rat Isolated Tail Arteries. SLT (0.1–5,000 $\mu\text{g}/\text{ml}$) caused a relaxation in the PE (1 μM)-precontracted rat isolated tail artery in a concentration-dependent manner. The relaxation was initiated at 100 $\mu\text{g}/\text{ml}$ and achieved $80.104 \pm 9.80\%$ at 5,000 $\mu\text{g}/\text{ml}$ ($n=6$) (Figure 2). Preincubation of the isolated tail artery with L-NAME (20 μM) did not significantly alter the SLT-induced relaxation ($n=6$) (Figure 2).

3.3. Effects of Potassium Channel Blockers on SLT-Induced Vasodilatation in Rat Isolated Tail Arteries. Opening of potassium channels plays an important role in vasodilatation. We examined the involvement of potassium channels on the SLT-induced relaxation in the rat isolated tail arteries. Tetraethylammonium (TEA, a nonselective potassium

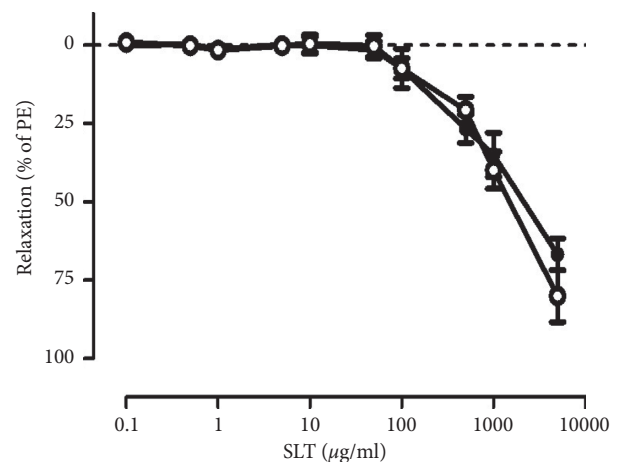


FIGURE 2: Cumulative concentration-response of the SLT extract (0.1–5,000 $\mu\text{g}/\text{ml}$) on phenylephrine (1 μM)-precontracted rat isolated tail artery with (●) or without (○) the presence of L-NAME (20 μM). Values are expressed as mean \pm SEM ($n=6$).

channel blocker) (1 mM), glibenclamide (Glib, an ATP-sensitive potassium channel blocker) (3 μM), and clotrimazole (K_{Ca} , a calcium-activated potassium channel blocker) (5 μM) were tested. As shown in Figure 2, preincubation of potassium channel blockers did not

significantly alter the SLT-induced vasodilatation in PE ($1\ \mu\text{M}$)-precontracted rat isolated tail artery ($n=5-6$) (Figure 3).

3.4. Effects of the SLT Extract on Calcium-Induced Vasoconstriction in Rat Isolated Tail Arteries Stimulated by Phenylephrine or KCl. The effect of the SLT extract on calcium-influx-induced vasoconstriction on rat isolated tail arteries was assessed with two vasoconstrictive stimulants (phenylephrine and KCl) by reintroducing calcium ($0.001-3\ \text{mM}$) into the calcium-free buffer. In the phenylephrine ($10\ \mu\text{M}$)-stimulated tail arteries, cumulative administration of calcium chloride ($0.001-3\ \text{mM}$) induced a vasoconstriction in a concentration-dependent manner, with $29.167 \pm 7.23\%$ contraction observed at $3\ \text{mM}$ ($n=5$). Preincubation of the SLT extract ($500, 1,000, \text{ and } 5,000\ \mu\text{g/ml}$) dose-dependently suppressed the calcium-induced vasoconstriction in the phenylephrine ($10\ \mu\text{M}$)-isolated tail arteries. SLT at $5,000\ \mu\text{g/ml}$ and nifedipine ($10\ \mu\text{M}$) markedly suppressed the calcium-induced vasoconstriction (Figure 4(a)).

Similarly, in the KCl ($80\ \text{mM}$)-stimulated tail arteries, cumulative administration of calcium chloride ($0.001-3\ \text{mM}$) induced a vasoconstriction in the tail artery in a concentration-dependent manner, with $75.460 \pm 14.52\%$ contraction observed at $3\ \text{mM}$ ($n=6$). Preincubation of the SLT extract at $1,000$ and $5,000\ \mu\text{g/ml}$, but not $500\ \mu\text{g/ml}$, markedly inhibited the calcium-induced vasoconstriction in the KCl ($80\ \text{mM}$)-stimulated isolated tail arteries. SLT at $5,000\ \mu\text{g/ml}$ abolished the calcium-induced vasoconstriction ($n=6$) ($P < 0.001$) (Figure 4(b)).

3.5. Effects of the SLT Extract on Phenylephrine- and KCl-Induced Vasoconstriction in Rat Isolated Tail Arteries. The effects of the SLT extract ($500, 1,000, \text{ and } 5,000\ \mu\text{g/ml}$) on phenylephrine-induced vasoconstriction in rat isolated tail arteries were evaluated. Cumulative addition of phenylephrine ($0.0001-10\ \mu\text{M}$) caused a vasoconstriction in the tail arteries in a concentration-dependent manner. Preincubation of the SLT extract at $1,000$ and $5,000\ \mu\text{g/ml}$, but not $500\ \mu\text{g/ml}$, significantly suppressed the phenylephrine-induced vasoconstriction in the isolated tail arteries ($n=5$) ($P < 0.001$). Nifedipine ($10\ \mu\text{M}$) markedly reduced the PE-induced vasoconstriction (Figure 5(a)). The vasoconstriction caused by phenylephrine at $10\ \mu\text{M}$ was markedly suppressed by 67.58% with the presence of the SLT extract at $5,000\ \mu\text{g/ml}$ (control: $16.44 \pm 2.46\ \text{mN}$ vs. SLT: $5.33 \pm 1.02\ \text{mN}$) ($P < 0.05$) ($n=5$) (Figure 5(b)).

The effects of the SLT extract ($500, 1,000, \text{ and } 5,000\ \mu\text{g/ml}$) on KCl-induced vasoconstriction in rat isolated tail arteries were evaluated. Cumulative addition of KCl ($10-80\ \text{mM}$) caused a vasoconstriction in the tail arteries in a concentration-dependent manner. Preincubation of the SLT extract at $500, 1,000, \text{ and } 5,000\ \mu\text{g/ml}$ significantly suppressed the KCl-induced vasoconstriction in the isolated tail arteries in a dose-dependent manner. ($n=3$) ($P < 0.001$) (Figure 5(c)). The vasoconstriction caused by $80\ \text{mM}$ was abolished with the presence of the SLT extract at $5,000\ \mu\text{g/ml}$

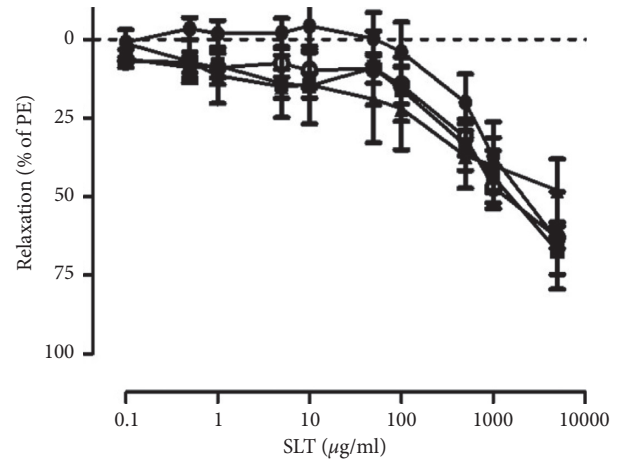


FIGURE 3: Effects of potassium channel blockers on SLT extract-induced relaxation on phenylephrine ($1\ \mu\text{M}$)-precontracted rat isolated tail artery. Tail arteries were preincubated with either vehicle control (\circ), tetraethyl-ammonium (TEA, a nonselective potassium channel blocker) ($1\ \text{mM}$) (\bullet), glibenclamide (Glib, an ATP-sensitive potassium channel blocker) ($3\ \mu\text{M}$) (\blacksquare), or clotrimazole (KCa, a calcium-activated potassium channel blocker) ($5\ \mu\text{M}$) (\blacktriangle) for 30 minutes before construction of the concentration-response curve. Values are expressed as mean \pm SEM ($n=5-6$).

(control: $7.90 \pm 1.75\ \text{mN}$ vs. SLT: $0.54 \pm 0.31\ \text{mN}$) ($P < 0.05$) ($n=3$) (Figure 5(d)).

3.6. Effect of SLT on Intracellular Calcium Release. Phenylephrine (PE) ($1\ \mu\text{M}$) caused a transient contraction in the Ca^{2+} -free solution through a release of intracellular Ca^{2+} from the sarcoplasmic reticulum. A second transient contraction was induced with or without the presence of SLT ($500, 1,000, \text{ and } 5,000\ \mu\text{g/ml}$). SLT significantly suppressed the PE-induced transient contraction ratio (Con 2/Con 1) at $5,000\ \mu\text{g/ml}$ (CLT: 39.12 ± 6.28 vs. SLT $5,000\ \mu\text{g/ml}$: 6.86 ± 1.52) ($P < 0.05$) ($n=6$) (Figure 6).

4. Discussion

Vascular dementia (VaD) is considered to be caused by chronic cerebral ischemia which induces neuronal damage, resulting in a decline in cognitive function eventually. While the development and progression of cognitive impairment and VaD are certainly multifactorial, it has been suggested that cerebrovascular dysfunction leads to reduction of cerebral blood flow which is closely associated with cognitive impairment in diabetes [18, 19]. Sailuotong (SLT) is a standardized three-herb formula designed for the management of VaD. Although data from animal and clinical studies have indicated that the clinically beneficial effect of SLT is closely associated with an increase in cerebral blood flow [11–13], the acute and direct modulatory effects and the underlying mechanisms of actions of SLT in vascular reactivity have not been studied. Results from the current work provide evidence that the SLT extract induces vascular relaxation in rat isolated tail arteries. Furthermore, our results showed that this SLT-induced vasodilatation is mediated *via*

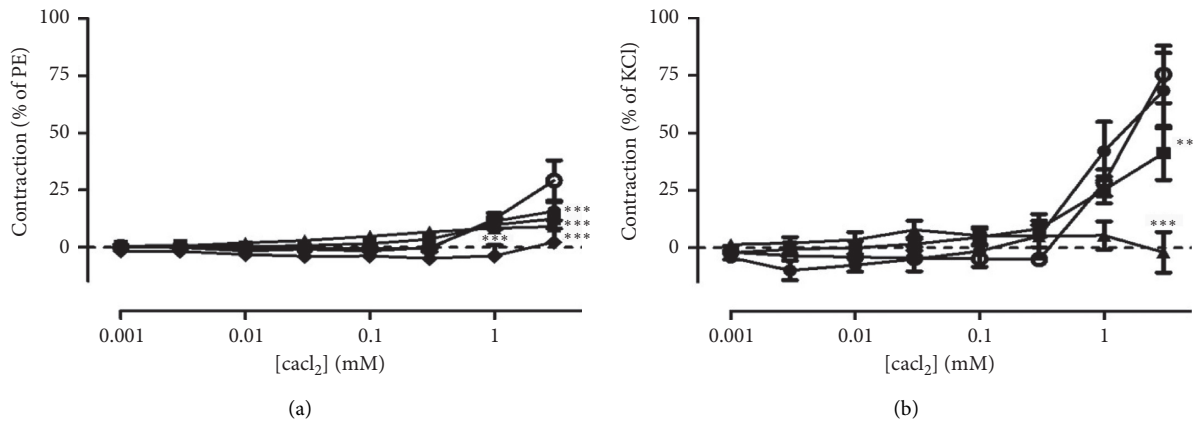


FIGURE 4: (a) Effect of the vehicle control (○), SLT extract (500 (●), 1000 (■), or 5000 (▲) μg/ml), or nifedipine (10 μM) (◆) on Ca²⁺-induced vasoconstriction in phenylephrine (PE) (10 μM)-stimulated rat isolated tail arteries. Values are expressed as mean ± SEM (***P* < 0.001 vs Control) (*n* = 5). (b) Effect of the vehicle control (○) and SLT extract (500 (●), 1,000 (■), or 5,000 (▲) μg/ml) on Ca²⁺-induced vasoconstriction in potassium chloride (KCl) (80 mM)-stimulated rat isolated tail arteries. Values are expressed as mean ± SEM (***P* < 0.01 vs. control ****P* < 0.001 vs. control) (*n* = 5–8).

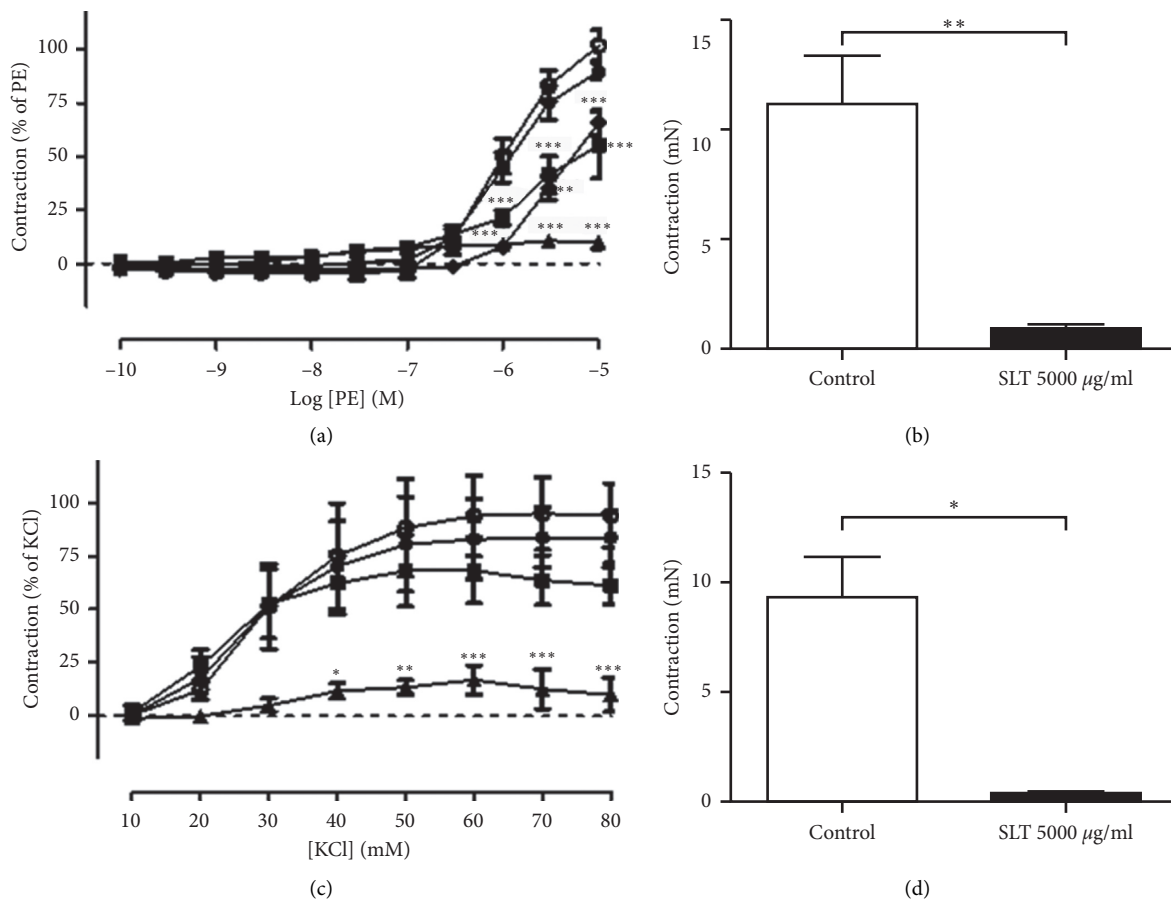


FIGURE 5: (a) Effect of the vehicle control (○), SLT extract (500 (●), 1000 (■), or 5000 (▲) μg/ml), or nifedipine (10 μM) (◆) on phenylephrine-induced vasoconstriction in rat isolated tail arteries. Values are expressed as mean ± SEM (***P* < 0.001 vs. control) (*n* = 5). (b) Isometric tension change of phenylephrine (10 μM)-induced vasoconstriction in rat isolated tail arteries with (closed bar) or without (open bar) the presence of the SLT extract (5000 μg/ml). Values are expressed as mean ± SEM (***P* < 0.01) (*n* = 8). (c) Effect of the vehicle control (○) or SLT extract (500 (●), 1,000 (■), or 5,000 (▲) μg/ml) on potassium chloride (KCl) (80 mM)-induced vasoconstriction in rat isolated tail arteries. Values are expressed as mean ± SEM (**P* < 0.05; ***P* < 0.01; ****P* < 0.001 vs. control) (*n* = 3). (d) Isometric tension change of KCl (80 mM)-induced vasoconstriction in rat isolated tail arteries with (closed bar) or without (open bar) the presence of the SLT extract (5,000 μg/ml). Values are expressed as mean ± SEM (***P* < 0.01) (*n* = 3).

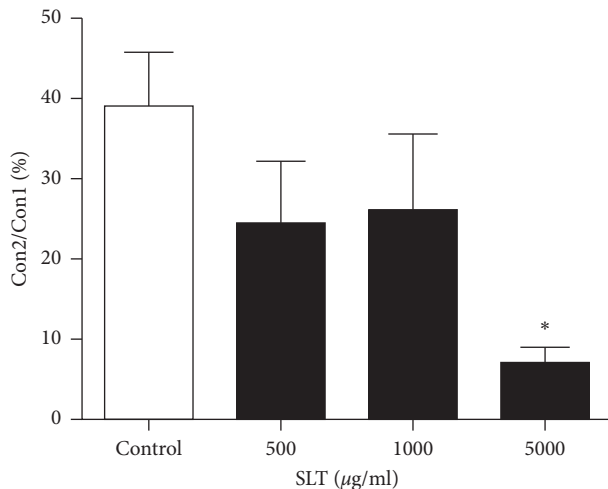


FIGURE 6: Effect of the SLT extract (500, 1,000, and 5,000 µg/ml) on phenylephrine (10 µM)-induced transient vasoconstriction in rat isolated tail arteries. Con2/Con1 (%) refers to the ratio of the second contraction to the first contraction. Values are expressed as mean ± SEM (* $P < 0.05$ vs control) ($n = 6$).

endothelium-independent mechanisms including inhibition of extracellular Ca^{2+} influx and release of Ca^{2+} storage from the sarcoplasmic reticulum.

The individual herb extracts of SLT have been shown to induce vasodilatation *via* endothelium-mediated mechanisms [20]. For example, crocetin, a carotenoid derived from saffron, has been shown to exert vasomodulatory effects via an endothelium-dependent mechanism [21]. Similarly, previous studies have demonstrated that ginseng produces its vasodilatory effect through eNOS activation in the endothelium [22, 23]. In contrast, our results revealed that inhibition of the endothelium by L-NAME failed to suppress the SLT-induced vasodilatation, indicating that the SLT-induced relaxation is largely mediated by an endothelium-independent mechanism. This relaxation was most likely caused by the complex constituents within the SLT extract which acted directly on the vascular smooth muscle cell (VSMC). For instance, the *Ginkgo biloba* extract (GBE) has been shown to induce vasodilation *via* multiple mechanisms, including inhibition of calcium influx through the L-type calcium channel and the activation of NO release in the rat isolated aorta [24]. Indeed, it has been shown that, while all the *Ginkgo* extract constituents, including bilobalide, ginkgolide A, ginkgolide B, ginkgolide C, quercetin, and rutin, have vasodilating action, each of them can contribute to GBE-induced vasorelaxation with different mechanisms and signaling pathways [25].

Since our results indicate that the SLT-induced relaxation was not mediated *via* the endothelium, other endothelium-independent mechanisms were considered. Vascular tone and reactivity regulation are primarily controlled by the changes of intracellular calcium within the vascular smooth muscle cell (VSMC) [26]. A number of calcium channels and mechanisms are responsible for the increase of the intracellular calcium level in VSMC [27–30], and many herbs and their isolated compounds have been

shown to induce vasodilatation *via* inhibition of calcium influx in the VSMC [24]. For instance, the *Ginkgo biloba* extract has been shown to induce aortic relaxation via inhibition of calcium influx through the calcium channel [24]. Similarly, ginsenoside Rg(3), an active ingredient of *Panax ginseng*, has been shown to inhibit the L-type calcium channel in *Xenopus* oocytes in a dose- and voltage-dependent manner [31]. In the current study, reintroduction of calcium to phenylephrine- or KCl-stimulated isolated tail artery bathed in a calcium-free solution caused contractions in a concentration-dependent manner. These results clearly demonstrated the role of calcium influx in vasoconstriction in response to both receptor-mediated (i.e., phenylephrine) and voltage-mediated (KCl) stimulations. SLT dose-dependently inhibited the calcium-influx-induced vessel contraction to both phenylephrine- and KCl-stimulated tail arteries, suggesting SLT was likely to inhibit both receptor- and voltage-mediated calcium influx. In line with this, the ability of SLT to suppress both phenylephrine- and KCl-mediated responses were clearly demonstrated in the phenylephrine- and KCl-induced vasoconstriction experiments, where SLT markedly suppressed the vasoconstriction caused by both agents. Therefore, our results suggested that SLT suppressed calcium influx by inhibition of both the voltage-operated calcium channel (VOCC) and receptor-operated calcium channel (ROCC).

Although the effects of SLT on intracellular calcium storage regulation in VSMC have not been reported previously, the individual components of SLT have been shown to suppress increase of the intracellular calcium level *via* inhibition of both influxes of extracellular Ca^{2+} and release of intracellular Ca^{2+} storage. In our study, SLT inhibited the PE-induced transient contraction in the isolated tail artery, indicating that SLT suppressed the vasoconstriction *via* inhibition of the release of Ca^{2+} from the sarcoplasmic reticulum. Similar to our study, ginsenoside-Rd, a main active constituent of *Panax ginseng*, has been shown to suppress phenylephrine-induced contraction in rat isolated aorta *via* inhibition of both receptor- and store-operated calcium channels in VSMC [22]. Yang et al. [32] have shown that the antiplatelet and antithrombosis properties of saffron were mediated by a mechanism involving inhibition of calcium mobilization via reducing both intracellular calcium release and extracellular calcium influx [32].

Many herbal medicines have been shown to produce their cardiovascular protective effects *via* the opening of potassium channels in VSMCs, such as the ATP-sensitive potassium channel (K_{ATP}) and calcium-activated potassium channel (K_{Ca}) [33, 34]. For example, Li et al. [35] showed that ginsenosides (GS), an extract of *Panax ginseng*, induced aortic relaxation and is, at least, partly mediated by the opening of the K_{Ca} channel in the VSMC [35]. Similarly, activation of the potassium channel has also been demonstrated in ginsenoside Rg3-mediated endothelium-dependent relaxation in rat isolated aorta [36]. The *Ginkgo* extract has been shown to relax smooth muscle cell via a TEA-sensitive (a nonselective potassium channel blocker) mechanism [37] and opening of the K_{Ca} channel [38], while other studies suggested that *Ginkgo* induces vasodilatation

via inhibition of calcium influx [24, 39] and activation of eNOS [40]. In this study, preincubation of TEA (a nonselective potassium channel blocker), glibenclamide (an ATP-sensitive potassium channel blocker), and clotrimazole (a calcium-activated potassium channel blocker) did not have any effects on the SLT-induced relaxation in the rat isolated tail artery, suggesting that the relaxation was independent of potassium channels opening. Although the effects of the individual components of SLT on the potassium channel have been reported previously [36], it is not uncommon that Chinese herbal medicine can induce relaxation independent of potassium channel activation. For example, the Danshen aqueous extract and its active component, Salvianolic acid B, have been shown to produce their vasorelaxant effect independent from potassium channel opening [41].

There are three limitations in the current study. First of all, although numerous studies have demonstrated that the reactivity profile of the rat tail artery resembles the human peripheral arteries [42–44] and have been used as an *ex vivo* model of resistance artery which can be extrapolated to human peripheral vascular disease [45], quantitative measurement of cerebrovascular reactivity should be employed in the future study. In addition, while our current work showed that acute SLT administration did not induce endothelium-dependent vasodilatation in the vessels isolated from a healthy animal, previous work from our group has demonstrated that SLT protected the cultured human endothelial cell from oxidative injury [12], indicating that the endothelium modulatory effects of SLT can only be observed under diseased conditions. Hence, endothelial effects of SLT in disease models should be studied in the future. Finally, while the active components of SLT have been shown to be absorbed into systematic circulation [46], any effects mediated by the metabolites of SLT may be overlooked by the *ex vivo* model used in the current study. A detailed metabolomics study is required to identify and explore the possible contribution of metabolites of SLT on vasculature.

5. Conclusions

In conclusion, we demonstrated that acute administration of the SLT extract induced vasodilatation in rat isolated tail artery. SLT-induced vasodilatation appeared to be principally mediated *via* endothelium-independent mechanisms, including blockage of extracellular Ca^{2+} influx and inhibition of release of Ca^{2+} from the sarcoplasmic reticulum. Results from this work provide direct evidence to explain the beneficial effects of SLT observed in clinical trials.

Abbreviations

SLT:	Sailuotong
VaD:	Vascular dementia
WKY:	Wistar Kyoto
Ca^{2+} :	Calcium ion
K^+ :	Potassium ion
KCl:	Potassium chloride
CaCl_2 :	Calcium chloride
SOD:	Superoxide dismutase

CVD:	Cardiovascular diseases
Ach:	Acetylcholine
TEA:	Tetraethylammonium
EGTA:	Ethylene glycol-bis(β -aminoethyl ether)- <i>N,N,N',N'</i> -tetraacetic acid
PE:	Phenylephrine
L-	<i>N</i> -nitroarginine methyl ester
NAME:	
K_{ATP} :	ATP-sensitive potassium channel
K_{Ca} :	Calcium-dependent potassium channel
SR:	Sarcoplasmic reticulum
VSMC:	Vascular smooth muscle cell
VOCC:	Voltage-operate calcium channel
ROCC:	Receptor-operate calcium channel.

Data Availability

The data that support the findings of this study are available from the corresponding author (SWS) upon reasonable request.

Ethical Approval

All animal protocols conformed to the Guide for the Care and Use of Laboratory Animals by the Australian Code of Practice for the Care and Use of Animals for Scientific Purpose. Institutional ethics approval (Approval number: A12041) was obtained from Western Sydney University prior to commencement of the study.

Conflicts of Interest

As a medical research institute, NICM Health Research Institute receives research grants and donations from foundations, universities, government agencies, individuals, and industry. Sponsors and donors also provide untied funding for work to advance the vision and mission of the institute. The authors declare no conflicts of interest.

Authors' Contributions

Yeon S. Y. and Seto S. W. contributed equally to this work. SWS conceived the study. SWS and CGHH designed the study. SY and NW conducted the experiment. SY and ML performed data analysis. SWS and SY drafted this manuscript. DC, CGHH, HK, NW, and LJ revised the manuscript. All authors read and approved the final manuscript.

Acknowledgments

SY was supported by an International Postgraduate Research Scholarship, Western Sydney University, Australia. SWS was supported in part by a Cardiac Health Institute Research Fellowship. This work was partially supported by a grant (Ref no. CC-CSTH-2017-128(E)) from the College of Professional and Continuing Education, the Hong Kong Polytechnic University.

References

- [1] P. B. Gorelick, A. Scuteri, S. E. Black et al., "Vascular contributions to cognitive impairment and dementia," *Stroke*, vol. 42, no. 9, pp. 2672–2713, 2011.
- [2] C. Y. Santos, P. J. Snyder, W. C. Wu, M. Zhang, A. Echeverria, and J. Alber, "Pathophysiologic relationship between alzheimer's disease, cerebrovascular disease, and cardiovascular risk: a review and synthesis," *Alzheimer's & Dementia: Diagnosis, Assessment & Disease Monitoring*, vol. 7, no. 1, pp. 69–87, 2017.
- [3] S. W. Seto, S. M. Krishna, H. Yu, D. Liu, S. Khosla, and J. Golledge, "Impaired acetylcholine-induced endothelium-dependent aortic relaxation by caveolin-1 in angiotensin II-infused apolipoprotein-E (ApoE^{-/-}) knockout mice," *PLoS One*, vol. 8, no. 3, Article ID e58481, 2013.
- [4] T. Y. Lam, S. W. Seto, Y. M. Lau et al., "Impairment of the vascular relaxation and differential expression of caveolin-1 of the aorta of diabetic +db/+db mice," *European Journal of Pharmacology*, vol. 546, no. 1–3, pp. 134–141, 2006.
- [5] S. W. Seto, S. Bexis, P. Aiden McCormick, and J. R. Docherty, "Actions of thalidomide in producing vascular relaxations," *European Journal of Pharmacology*, vol. 644, no. 1–3, pp. 113–119, 2010.
- [6] B. Sharma and N. Singh, "Defensive effect of natrium diethyldithiocarbamate trihydrate (NDDCT) and lisinopril in DOCA-salt hypertension-induced vascular dementia in rats," *Psychopharmacology*, vol. 223, no. 3, pp. 307–317, 2012.
- [7] M. R. Meyer, N. C. Fredette, M. Barton, and E. R. Prossnitz, "Prostanoid-mediated contractions of the carotid artery become Nox2-independent with aging," *Age*, vol. 37, no. 4, p. 79, 2015.
- [8] D. Chang, J. Liu, K. Bilinski et al., "Herbal medicine for the treatment of vascular dementia: an overview of scientific evidence," *Evidence-Based Complementary and Alternative Medicine*, vol. 2016, Article ID 7293626, 15 pages, 2016.
- [9] X. Zhou, G. Cui, and H. H. Ling Tseng, "Vascular contributions to cognitive impairment and treatments with traditional Chinese medicine," *Evidence-Based Complementary and Alternative Medicine*, vol. 2016, Article ID 9627258, 12 pages, 2016.
- [10] J. Liu, "Development of an evidence-based Chinese herbal medicine for the management of vascular dementia," Western Sydney University, Penrith, Australia, 2008.
- [11] J. Jia, C. Wei, S. Chen et al., "Efficacy and safety of the compound Chinese medicine SaiLuoTong in vascular dementia: a randomized clinical trial," *Alzheimer's & Dementia: Translational Research & Clinical Interventions*, vol. 4, no. 1, pp. 108–117, 2018.
- [12] S. Seto, D. Chang, W. Ko et al., "Sailuotong prevents hydrogen peroxide (H₂O₂)-induced injury in EA.hy926 cells," *International Journal of Molecular Sciences*, vol. 18, no. 1, p. 95, 2017.
- [13] J. Liu, D. Chan, J. Liu, and A. Bensoussan, "A randomised placebo-controlled clinical trial of a Chinese herbal medicine for the treatment of vascular dementia," in *Proceedings of the 2nd International Congress for Complementary Medicine Research*, Munich, Germany, 2007.
- [14] G. Z. Steiner, "The effect of Sailuotong (SLT) on neurocognitive and cardiovascular function in healthy adults: a randomised, double-blind, placebo controlled crossover pilot trial," *BMC Complementary and Alternative Medicine*, vol. 16, no. 1, p. 15, 2015.
- [15] L. Xu and J. X. Liu, "Effect of weinaokang (SLT) on dysmenstric mice model," *Journal of Pharmacological and Clinical Chinese Herbal Medicine*, vol. 23, 2007.
- [16] N. Health, M. R. Council, and A. R. Council, *Australian Code for the Care and Use of Animals for Scientific Purposes*, National Health and Medical Research Council, London, UK, 2013.
- [17] D. M. Andrade, L. L. Borges, I. M. Torres, E. C. Conceição, and M. L. Rocha, "Jabuticaba-induced endothelium-independent vasodilating effect on isolated arteries," *Arquivos Brasileiros de Cardiologia*, vol. 107, no. 3, pp. 223–229, 2016.
- [18] S. Seto, G. Y. Yang, H. Kiat, A. Bensoussan, Y. W. Kwan, and D. Chang, "Diabetes mellitus, cognitive impairment, and traditional Chinese medicine," *International Journal of Endocrinology*, vol. 2015, Article ID 810439, 14 pages, 2015.
- [19] A. Yasir, T. Hardigan, and A. Ergul, "Diabetes-mediated middle cerebral artery remodeling is restored by linagliptin: interaction with the vascular smooth muscle cell endothelin system," *Life Sciences*, vol. 159, pp. 76–82, 2016.
- [20] Y. Kubota, N. Tanaka, S. Kagota et al., "Effects of Ginkgo biloba extract on blood pressure and vascular endothelial response by acetylcholine in spontaneously hypertensive rats," *Journal of Pharmacy and Pharmacology*, vol. 58, no. 2, pp. 243–249, 2006.
- [21] A. Mancini, J. Serrano-Díaz, E. Nava et al., "Crocetin, a carotenoid derived from saffron (*Crocus sativus* L.), improves acetylcholine-induced vascular relaxation in hypertension," *Journal of Vascular Research*, vol. 51, no. 5, pp. 393–404, 2014.
- [22] Y.-Y. Guan, J.-G. Zhou, Z. Zhang et al., "Ginsenoside-Rd from panax notoginseng blocks Ca²⁺ influx through receptor-and store-operated Ca²⁺ channels in vascular smooth muscle cells," *European Journal of Pharmacology*, vol. 548, no. 1–3, pp. 129–136, 2006.
- [23] N. D. Kim, E. M. Kim, K. W. Kang, M. K. Cho, S. Y. Choi, and S. G. Kim, "Ginsenoside Rg3 inhibits phenylephrine-induced vascular contraction through induction of nitric oxide synthase," *British Journal of Pharmacology*, vol. 140, no. 4, pp. 661–670, 2003.
- [24] S. Nishida and H. Satoh, "Mechanisms for the vasodilations induced by Ginkgo biloba extract and its main constituent, bilobalide, in rat aorta," *Life Sciences*, vol. 72, no. 23, pp. 2659–2667, 2003.
- [25] F. Cheung, Y. L. Siow, and O. Karmin, "Inhibition by ginkgolides and bilobalide of the production of nitric oxide in macrophages (THP-1) but not in endothelial cells (HUVEC) 1," *Biochemical Pharmacology*, vol. 61, no. 4, pp. 503–510, 2001.
- [26] T. Akata, "Cellular and molecular mechanisms regulating vascular tone. Part 1: basic mechanisms controlling cytosolic Ca²⁺ concentration and the Ca²⁺-dependent regulation of vascular tone," *Journal of Anesthesia*, vol. 21, no. 2, pp. 220–231, 2007.
- [27] A. P. Somlyo and A. V. Somlyo, "Signal transduction and regulation in smooth muscle," *Nature*, vol. 372, no. 6503, p. 231, 1994.
- [28] A. V. Stanton, "Vascular network changes in the retina with age and hypertension," *Journal of Hypertension*, vol. 13, no. 2, pp. 1724–1728, 1995.
- [29] S. W. Seto, H. Y. Lam, W. S. Lau et al., "Role of monoamine oxidases in the exaggerated 5-hydroxytryptamine-induced tension development of human isolated preeclamptic umbilical artery," *European Journal of Pharmacology*, vol. 605, no. 1, pp. 129–137, 2009.

- [30] H. Karaki and G. B. Weiss, "Calcium release in smooth muscle," *Life Sciences*, vol. 42, no. 2, pp. 111–122, 1988.
- [31] J.-H. Kim, J.-H. Lee, S. M. Jeong et al., "Stereospecific effects of ginsenoside Rg₃ epimers on swine coronary artery contractions," *Biol Pharm Bull*, vol. 29, no. 2, pp. 365–370, 2006.
- [32] L. Yang, Z. Qian, Y. Yang et al., "Involvement of Ca²⁺ in the inhibition by crocetin of platelet activity and thrombosis formation," *Journal of Agricultural and Food Chemistry*, vol. 56, no. 20, pp. 9429–9433, 2008.
- [33] M. G. Campos, M. Oropeza, C. Torres-Sosa, M. Jiménez-Estrada, and R. Reyes-Chilpa, "Sesquiterpenoids from anti-diabetic *Psacalium decompositum* block ATP sensitive potassium channels," *Journal of Ethnopharmacology*, vol. 123, no. 3, pp. 489–493, 2009.
- [34] H.-X. Li, S.-Y. Han, X. Ma et al., "The saponin of red ginseng protects the cardiac myocytes against ischemic injury in vitro and in vivo," *Phytomedicine*, vol. 19, no. 6, pp. 477–483, 2012.
- [35] Z. Li, X. Chen, Y. Niwa, S. Sakamoto, and Y. Nakaya, "Involvement of Ca²⁺-activated K⁺ channels in ginsenosides-induced aortic relaxation in rats," *Journal of Cardiovascular Pharmacology*, vol. 37, no. 1, pp. 41–47, 2001.
- [36] N. D. Kim, S. Y. Kang, J. H. Park, and V. B. Schini-Kerth, "Ginsenoside Rg₃ mediates endothelium-dependent relaxation in response to ginsenosides in rat aorta: role of K⁺ channels," *European Journal of Pharmacology*, vol. 367, no. 1, pp. 41–49, 1999.
- [37] J. J. Kim, D. H. Han, S. H. Lim et al., "Effects of Ginkgo biloba extracts with mirodenafil on the relaxation of corpus cavernosal smooth muscle and the potassium channel activity of corporal smooth muscle cells," *Asian Journal of Andrology*, vol. 13, no. 5, p. 742, 2011.
- [38] M. Mesri, M. Morales-Ruiz, and E. J. Ackermann, "Suppression of vascular endothelial growth factor-mediated endothelial cell protection by survivin targeting," *The American Journal of Pathology*, vol. 158, no. 5, pp. 1757–1765, 2001.
- [39] Y. Wang, J. Cao, and S. Zeng, "Involvement of P-glycoprotein in regulating cellular levels of Ginkgo flavonols: quercetin, kaempferol, and isorhamnetin," *Journal of Pharmacy and Pharmacology*, vol. 57, no. 6, pp. 751–758, 2005.
- [40] A. Koltermann, A. Hartkorn, E. Koch, R. Fürst, A. M. Vollmar, and S. Zahler, "Ginkgo biloba extract EGb® 761 increases endothelial nitric oxide production in vitro and in vivo," *Cellular and Molecular Life Sciences*, vol. 64, no. 13, pp. 1715–1722, 2007.
- [41] F. F. Y. Lam, J. H. Keung Yeung, K. M. Chan, and P. M. Yu Or, "Relaxant effects of danshen aqueous extract and its constituent danshensu on rat coronary artery are mediated by inhibition of calcium channels," *Vascular Pharmacology*, vol. 46, no. 4, pp. 271–277, 2007.
- [42] A. K. Fouda and J. Atkinson, "Sensitivity to noradrenaline and electrical stimulation decreases with age in the rat tail artery," *Naunyn Schmiedebergs Arch Pharmacol*, vol. 334, no. 1, pp. 37–39, 1986.
- [43] F. T. Spradley, J. J. White, W. D. Paulson, D. M. Pollock, and J. S. Pollock, "Differential regulation of nitric oxide synthase function in aorta and tail artery from 5/6 nephrectomized rats," *Physiological Reports*, vol. 1, no. 6, Article ID e00145, 2013.
- [44] L. E. Thompson, G. J. Rinaldi, and D. F. Bohr, "Decreased activity of the sodium-calcium exchanger in tail artery of stroke-prone spontaneously hypertensive rats," *Blood Vessels*, vol. 27, no. 2–5, pp. 197–201, 1990.
- [45] K. Wakitani, T. Takakuwa, M. Sugioka, B. Fujitani, and H. Aishita, "Inhibitory effect of OP-41483.alpha-CD, a prostacyclin analog, on peripheral vascular lesion models in rats," *The Japanese Journal of Pharmacology*, vol. 59, no. 1, pp. 57–63, 1992.
- [46] Y. Zhang, "Pharmacokinetics and brain distribution of ginsenosides after administration of sailuotong," *Zhongguo Zhong Yao Za Zhi*, vol. 39, no. 2, pp. 316–321, 2014.

Research Article

Guanxinshutong Alleviates Atherosclerosis by Suppressing Oxidative Stress and Proinflammation in ApoE^{-/-} Mice

Yingdong Lu ¹, Yuchan Sun,¹ Zhilin Jiang,¹ Dandan Zhang,¹ Hongchen Lin,¹ Yi Qu ¹,
Chang Shang,¹ Mingjing Zhao ², and Xiangning Cui ¹

¹Department of Cardiology, Guang'anmen Hospital, China Academy of Chinese Medical Sciences, Beijing, China

²The Key Laboratory of Chinese Internal Medicine of the Ministry of Education, Dongzhimen Hospital, Beijing University of Chinese Medicine, Beijing, China

Correspondence should be addressed to Xiangning Cui; cuixiangning@126.com

Received 22 June 2020; Revised 20 August 2020; Accepted 8 September 2020; Published 16 September 2020

Academic Editor: Xiao Ma

Copyright © 2020 Yingdong Lu et al. This is an open access article distributed under the Creative Commons Attribution License, which permits unrestricted use, distribution, and reproduction in any medium, provided the original work is properly cited.

Atherosclerosis (AS) is a chronic progressive disease related to dyslipidemia, inflammation, and oxidative stress. Guanxinshutong capsule (GXST), a traditional Chinese medicine, has been widely used in treating coronary atherosclerotic heart disease, while its mechanism actions on AS are still not to be well addressed. Our present study is aimed to examine the effect of GXST on AS and elucidate the multitarget mechanisms of GXST on AS. Network pharmacology analysis was employed to screen the multitarget mechanisms of GXST on AS. ApoE^{-/-} mice were used to validate these effects. Circulating lipid profile and oxidative stress-related factors were measured by the Elisa kit. Furthermore, the aortic trunk and aortic root were excised for oil red O staining, histopathological and immunohistochemical analysis. We first discovered that GXST was clued to exert synergistically anti-atherosclerosis properties including lipid-lowering, anti-inflammation, and antioxidation through the computational prediction based on a network pharmacology simulation. Next, the validation experiments in atherosclerosis mice provided evidence that GXST significantly reduced atherosclerotic lesions, increased collagen deposition, and attenuated LV remodeling to some extent. Mechanistically, GXST modulated lipid profile, downregulated the level of inflammatory cytokines and NF- κ Bp65. GXST also reduced the activity of oxidative parameter MDA and upregulated the activities of antioxidant enzymes (SOD and GSH) compared with the AS model group. In conclusion, GXST intervention might attenuate atherosclerosis by mechanisms involving reducing lipid deposition, modulating oxidative stress and inflammatory responses, but a larger controlled trial is necessary for confirmation.

1. Introduction

Atherosclerosis (AS) is a chronic cardiovascular disease with high incidences of morbidity and mortality characterized by endothelial dysfunction, accumulation of cholesterol, recruitment of macrophage, and foam cells formation [1–3]. The pathophysiology of AS includes inflammatory response and oxidative stress as important factors. In this scenario, attenuating inflammation or ROS could exert a preventive role, thereby delaying or preventing the AS progression [4, 5].

Macrophages are the most prominent cellular contributors to the lesion's physical bulk [6] involved in the

inflammatory response of AS. Decreasing the migration and adhesion of macrophages to the lesion area could effectively increase plaque stability. In addition, previous studies have shown that reducing the production of proinflammatory cytokines, such as IL-6, IL-1 β , and TNF- α , and modulating the activity of nuclear factor kappa B (NF- κ B) could improve cardiovascular outcomes including AS [7, 8]. Moreover, accumulating evidence has demonstrated that oxidative stress caused by excessive reactive oxygen species (ROS) is closely associated with atherosclerosis progression [9, 10]. Previous data showed that patients with atherosclerotic cardiovascular disease (CVD) increased ROS in the vessel wall [11, 12]. The production of ROS by cells, such as

macrophages and endothelial cell, is an important factor that influences smooth muscle cell migration, the homing of macrophage and inflammation, ox-LDL uptake, and fibrous cap stability [13]. Thus, attenuating oxidative stress and inflammation are maybe the critical approaches to improve AS considering their major role involved in AS.

Guanxinshutong capsule (GXST), a traditional Chinese medicine (TCM), is composed of five individual herbs according to the TCM theory of 'Jun-Chen-Zuo-Shi', including Guangzao (*Choerospondiatis Fructus*), Danshen (*Radix Salviae*), Dingxiang (*Caryophylliflos*), Bingpian (*Borneolum Syntheticum*), and Tianzhuhuang (*Bamusae-concretiosilicea*). Guangzao as a 'Jun' (the monarch) herb exerts Qi promoting and blood activating effects; Danshen as a 'Chen' (minister) herb is responsible for invigorating the blood to promote menstruation, dispelling block, and relieving pain; Dingxiang and Bingpian as 'Zuo' (adjuvant) herbs are used for warming spleen and lowering the adverse flow of Qi and regulating the movement of Qi; Tianzhuhuang as a 'Shi' (courier) herb contributes to clearing up the heat and resolving phlegm. In an ischemia and reperfusion (MI/R) injury study, GXST significantly decreased levels of TNF- α , IL-1 β , and IL-6 and obviously inhibited NF- κ B activity in the MI/R model rat [14]. Furthermore, in a randomized clinical trial, GXST capsules are beneficial for the treatment of stable angina pectoris (SAP) patients [15]. It has also been shown that daily oral treatment of MI rats with GXST protects the heart against oxidative stress indicated by the increasing activities of total SOD, CATA, NOS and the levels of NO and GSH [16]. Although several pieces of evidence have supported GXST as anti-inflammation and antioxidant agent in CVD, few reports have evaluated whether those effects could modulate atherogenesis in vivo. Network biology aids the exploration of drug targets and identifies potential active ingredients in TCM research. Integrating network biology and polypharmacology promise an expanded opportunity for druggable targets. In this study, we intended to integrate network pharmacology techniques and pharmacological experiments to systematically identify the active components of GXST and explore potential mechanisms for the treatment of AS.

2. Materials and Methods

2.1. Screening the Effective Components of GXST. The active components of GXST were screened by the Traditional Chinese Medicine System Pharmacology Database (TCMSP, <http://lsp.nwu.edu.cn/browse.php>) and the Encyclopedia of Traditional Chinese Medicine (ETCM, <http://www.nrc.ac.cn:9090/ETCM/>), in which comprehensive information of the herbal ingredients such as components, pharmacokinetic parameter information, candidate target genes, and disease associated with the ingredients were provided [17, 18]. Absorption, distribution, metabolism, and excretion (ADME) are the critical contributors of pharmacokinetic parameters associated with bioactivities. In this study, oral bioavailability (OB, $\geq 30\%$), drug likeness (DL, ≥ 0.18) as suggested by TCMSP [19], and drug likeness grading more

than 0.67 in ETCM were used as the included criteria of bioactive components in GXST [20].

2.2. Compound-Related Targets and AS-Related Targets Fishing. Three public databases including TCMSP, ETCM, and Drugbank [21] were applied to screen the compound-related targets. GeneCards (<https://www.genecards.org/>) and DisGeNET (<https://www.disgenet.org/>) database were used to collect the AS-related targets [22]. The keyword "atherosclerosis" was used, and the targets were human genes/proteins enrolled in our study. The standard gene names and UniProt ID of AS-related targets were obtained from UniprotKB database (<https://www.uniprot.org/>).

2.3. Gene Functions Annotation. Metascape (<http://metascape.org/gp/index.html#/main/step1>) was used to annotate the gene functions of compound-related targets. "*H. sapiens*" was selected for both the input species and the analysis species and $P < 0.01$ was set to analyze the function of the target. The biological processes related to atherosclerosis were screened, and target-functions were visualized and constructed by Cytoscape software.

2.4. Network Construction and Topological Analysis. The protein-protein interactions (PPI) network of the compound and AS-related cotargets were established from the STRING (<https://string-db.org/>) database which provides both experimental and predicted interaction information according to systematic coexpression analysis, detection of shared selective signals across genomes, and automated text-mining of scientific literature [23]. Confidence score ≥ 7 was selected in this study.

The central network analysis was performed by the topological method. Three topological parameters including degree centrality (DC), betweenness centrality (BC), and closeness centrality (CC) were calculated to evaluate the central attributes of the nodes in the network. In the GXST potential target-AS target network, $DC \geq 2 \times \text{median DC}$, $BC \geq \text{median BC}$, and $CC \geq \text{median CC}$ were used as the screening criteria to obtain the key targets.

2.5. GO and KEGG Pathway Enrichment Analysis. The online functional annotation and enrichment tool David (<https://david.ncifcrf.gov/>) was employed to perform the Gene Ontology (GO) and Kyoto Encyclopedia of Genes and Genomes (KEGG) pathway enrichment analysis [24]. P value < 0.05 was considered statistically significant in GO terms and KEGG pathways.

2.6. Validating the GXST Functions by Animal Experiments

2.6.1. Animals. ApoE^{-/-} mice on a C57BL/6 background and their wide-type littermates (male, eight weeks old) were purchased from Peking University School of Medicine (SCXK (Beijing) 2016-0012). Animals were maintained in groups under a 12 h/12 h light-dark cycle in a controlled environment at temperature $20 \pm 2^\circ\text{C}$ and humidity 50–60%

with free access to food and water for 4 weeks. All experiment protocols involving animals were executed conforming to the Laboratory Animals of Institutional Animal Care. The protocol was approved by the Animal Ethics Committee of Guang'anmen Hospital, China Academy of Chinese Medical Sciences.

2.6.2. Drug Administration. GXST capsules were purchased from Shaanxi Buchang Pharmaceutical (Z20020055). The ingredients of GXST capsule are Guangzao, Danshen, Dingxiang, Bingpian, and Tianzhuhuang. Atorvastatin calcium tablets were purchased from Pfizer Ireland Pharmaceuticals (National Drug Standard J20120050).

2.6.3. Experimental Groups, Treatment, and Sample Preparation. After the adaptation period, wide-type mice were fed with a standard chow diet as a sham group ($n = 16$, 21.4 ± 0.3). ApoE^{-/-} mice ($n = 48$, 26.5 ± 0.4) were divided into three groups: (1) Model ($n = 16$), fed with a high-cholesterol diet (76.5% standard feed, 0.5% sodium cholate, 5% white sugar, 3% cholesterol, 10% lard, 5% egg yolk powder, provided by Beijing KeaoXieli Feed Co., Ltd., license number: SCXK (Beijing) 2014-0010.); (2) Atorvastatin ($n = 16$), fed with the above high-cholesterol diet and received atorvastatin treatment ($5 \text{ mg}\cdot\text{kg}^{-1}$) by gavage feeding once daily; (3) GXST ($n = 16$), fed with the above high-cholesterol diet and received GXST treatment ($0.18 \text{ g}\cdot\text{kg}^{-1}$) by gavage feeding once daily. Body weights were measured weekly. Although the study has been designed with equal group sizes, because of technical factors such as fight-related injury resulting in loss of animals, the group sizes become increasingly unequal ($n = 13$ for Sham group, $n = 12$ for Model group, $n = 14$ for Atorvastatin group, $n = 13$ for GXST group).

After 10 weeks and overnight fasting, animals were euthanized for blood and aorta collections. Serum was separated immediately after blood sampling by centrifugation at 3000 rpm for 15 min, and tissues (heart and aorta) were rapidly removed and frozen in liquid nitrogen.

2.6.4. Serum Biochemical Assays. Serum concentrations of total cholesterol (TC), low density lipoprotein cholesterol (LDL-C), high density lipoprotein cholesterol (HDL-C), and triacylglycerols (TG) were determined by enzymatic colorimetric methods using commercially available kits. Murine serum TNF- α , IL-6 and oxidative stress-related factors (SOD, GSH, MDA) were detected by ELISA kits according to the manufacturer's introduction (BD Biosciences).

2.6.5. Hematoxylin and Eosin (HE) and Masson's Trichrome Staining. The top halves of the hearts were obtained under stereoscopic observation, fixed by 4% paraformaldehyde, and embedded in paraffin. Briefly, every consecutive section ($6 \mu\text{m}$ thick) throughout the aortic root area ($300 \mu\text{m}$) was stained with hematoxylin/eosin. One of every five sections (10 sections/mouse) and the leftover sections were stained with Masson's trichrome

staining. The lesion and collagen deposition areas were quantified with Image-Pro Plus 6.0 software (NIH, Bethesda, MD, USA).

2.6.6. Atherosclerotic Lesions Evaluation. Atherosclerotic lesion severity was assessed in the aortas as previously described [25]. In brief, animals were perfused with PBS and 4% paraformaldehyde. Then, the entire mouse aorta was carefully dissected from the arch to the iliac bifurcation to remove adventitious, washed in PBS, and the aorta was opened longitudinally, stained with Oil red O (Sigma-Aldrich, USA), and pinned out under an inverted microscope. Digital images were analyzed with Image-Pro Plus version 6.0 and the extent of the lesion area is expressed as the percentage of the total area of the aorta covered by the lesions.

2.6.7. Immunohistochemistry. The paraffin-embedded aorta sinus sections ($4 \mu\text{m}$) were deparaffinized for citrate or EDTA antigen retrieval according to the manufacturer's instructions, blocked with hydrogen peroxide (H_2O_2 , 3%), and incubated with different primary antibodies: CD68 (Abcam, ab125212, 1:500), TNF- α (Abcam, ab66579, 1:200), IL-6 (Abcam, ab9324, 1:300), NF- κB (Santa Cruz, sc-8414, 1:500), Nrf2 (Abcam, ab137550, 1:300), and HO-1 (Abcam, ab13243, 1:500) for 60-minute incubation at 37°C . Finally, the sections were washed again with PBS for DAB colorimetry. The positive sections were quantified by Image-Pro Plus 6.0 software (NIH, Bethesda, MD, USA).

2.6.8. Western Blots. Total proteins of the aorta were extracted using RIPA agents and quantified with a BCA protein kit to determine protein levels. Briefly, the samples were separated by a 12% sodium dodecylsulfate-polyacrylamide gel electrophoresis and transferred to a poly-vinylidene difluoride filter membrane. Membranes were blocked in Tris-buffered saline (PH7.5) containing 0.05% Tween-20 ($1 \times \text{TBST}$) and 5% skimmed milk for 2 h, then probed overnight at 4°C with an antibody against NF- κB p65, Nrf2, and HO-1, respectively. Membranes were washed with $1 \times \text{TBST}$ for 10 min and incubated for 2 h with horseradish peroxidase-conjugated secondary antibody. Lastly, immunoreactive bands were visualized by chemiluminescence and quantified by densitometry using a Quantity One Analysis Software (Bio-Rad).

2.6.9. Statistical Analysis. All procedures were performed in triplicate. All data were presented as the mean \pm standard deviation (SD). An independent-samples t -test, one-way analysis of variance (ANOVA) was conducted to evaluate the one-way layout data. P values less than 0.05 were considered significant. All analyses were performed using GraphPad Prism6.0 (GraphPad Software, Inc., La Jolla, CA, USA).

3. Results

3.1. Herb-Compound-Target Network of GXST. A total of 49 active compounds and 353 targets after excluding the duplicates were identified in GXST from TCMSP and ETCM database. Ten active compounds, 244 targets from the “monarch herb”, 16 active compounds, 98 targets from the “minister herb” and 27 active components, and 127 targets from the “adjuvant and courier herbs” were identified (Figures 1(a) and 1(b)). The detailed 49 components and 353 targets information are shown in Supplementary Table S1 and Supplementary Table S2. Total of 106 targets for atherosclerosis were acquired from GeneCards and DisGeNET databases after removing redundancies which are shown in Supplementary Table S3. To enrich the biological function of the 353 targets, Metascape (<http://metascape.org/gp/index.html#/main/step1>) was used to annotate gene functions which uncovered that 353 targets were enriched in cellular response to lipid, oxidative stress, lipopolysaccharide, nitrogen compound, metabolic process, and steroid hormone response (Figure 1(c)).

3.2. Pathway Enrichment Analysis. Totally, 38 cotargets were collected as potential therapeutic targets of GXST against AS after 353 potential targets of the 49 compounds in GXST intersected with 106 candidate targets for AS. There were 445 PPIs among these 38 cotargets with high confidence scores (≥ 7) (Figure 2(a)). Topology analysis indicated that TNF- α , IL-1 β , IL-6, IL-10, PTGS2, MMP9, VEGFA, CCL2, CRP, and ICAM1 were the top 10 shared targets based on degree centrality. GO analysis showed that the top 15 biological processes ranked by their LogP were enriched to the regulation of inflammatory response, leukocyte migration, macrophage derived foam cell differentiation, and nitric oxide biosynthetic process (Figure 2(b)). Furthermore, KEGG pathway enrichment analysis showed that 38 cotargets contributed to 158 pathways ($P < 0.05$), and the first 20 pathways were closely related to the pathogenesis of AS (Figure 2(c)).

3.3. Validation the Protective Effects of GXST against AS Progression

3.3.1. GXST Reduces the Lesion Area and Changes the Plaque Composition. ApoE^{-/-} mice were applied as AS model in our study, and the knockdown efficiency of ApoE expression in mice was confirmed by PCR (Supplementary Table S4, Supplementary Figure 1). In order to verify whether GXST has the protective effect against AS progression, we analyzed the lesion area of the aortic trunk by oil red O staining and aortic sinus by HE staining. We also studied the plaque composition including collagen and macrophages via Masson and immunohistochemical staining (CD68). In our study, atherosclerosis in the aorta was reduced in 48% of the GXST group, mainly in the aortic arch (Figures 3(a) and 3(e)). However, the aortic sinus of all groups presented similar lesions in the intermediate stage except the Sham, with the presence of a fibrous cap and areas of deposition of

cholesterol crystals (Figures 3(b) and 3(f)). Although the total lesion in aortic sinus was similar between groups, GXST significantly presented lower macrophage infiltration (CD68) and increased collagen deposition, suggesting a more stable fibrous cap (Figures 3(c), 3(d), 3(g), and 3(h)). In order to further evaluate the therapeutic effects of GXST on AS, we assessed the left ventricular cardiomyocyte morphology and interstitial fibrosis. As shown in the H&E staining image, the GXST group was demonstrated to significantly improve the myocardial shape, arrangement, and nuclear morphology in the LV wall compared to that from the model group mice (Supplementary Figure 4). Meanwhile, the Model group had a significantly higher degree of fibrosis than that of the Sham, while GXST treatment reversed such a trend (Supplementary Figure 4).

3.3.2. GXST Attenuates Plasma Lipid Profiles in ApoE^{-/-} Mice. The results from the network pharmacological analysis suggested that the biological function of GXST on AS was enriched in the cellular response to lipid, oxidative stress, and lipopolysaccharide. Herein, we first evaluated the level of weight gain and plasma lipid profiles. A high-fat diet with 3% cholesterol for 10 weeks in the Model, Atorvastatin, and GXST groups resulted in a significant increase (36.1%, 26.5%, 27.8%) in body weight compared with the Sham group without a high-fat diet (Figure 4(a)). GXST treatment did not significantly inhibit high-fat diet-induced weight gain compared to the Model group after 10 weeks treatment, while GXST prominently induced the loss of weight during from 7 to 9 weeks, and atorvastatin significantly decreased the weight gain from the fifth-week treatment (Figure 4(a)). In addition, serum biochemical parameters of mice including TC, TG, LDL-C, and HDL-C were determined (Figures 4(b)–4(e)). Compared to the Model, GXST markedly decreased the high-fat diet-induced elevation in TC, TG, and LDL-C, whereas it increased the level of HDL-C. As expected, atorvastatin also improved the serum lipid profile.

3.3.3. GXST Attenuates the Inflammatory Response. Topology analysis uncovered the top 10 shared targets between GXST-compounds related and AS targets. Herein, IL-6 and TNF- α concentration in plasma and plaque lesion were significantly decreased in the GXST group (Figures 5(a)–5(d), 5(f), and 5(g)). In addition, consistent with the results of the above proinflammatory factor, the expression level of NF- κ B in the aortic lesion was significantly reduced (Figures 5(e) and 5(h), Supplementary Figure 5).

3.3.4. GXST Attenuated Reactive Oxidative Stress-Associated Factor. According to the GO analysis and KEGG pathway enrichment, the compounds of GXST may also target oxidative stress. Malondialdehyde (MDA), an important ROS marker of lipid peroxidation, increases in AS progression [26]. Glutathione (GSH) and superoxide dismutase (SOD) are important components of the antioxidant defense mechanism that antagonise the effect of oxidative stress [27].

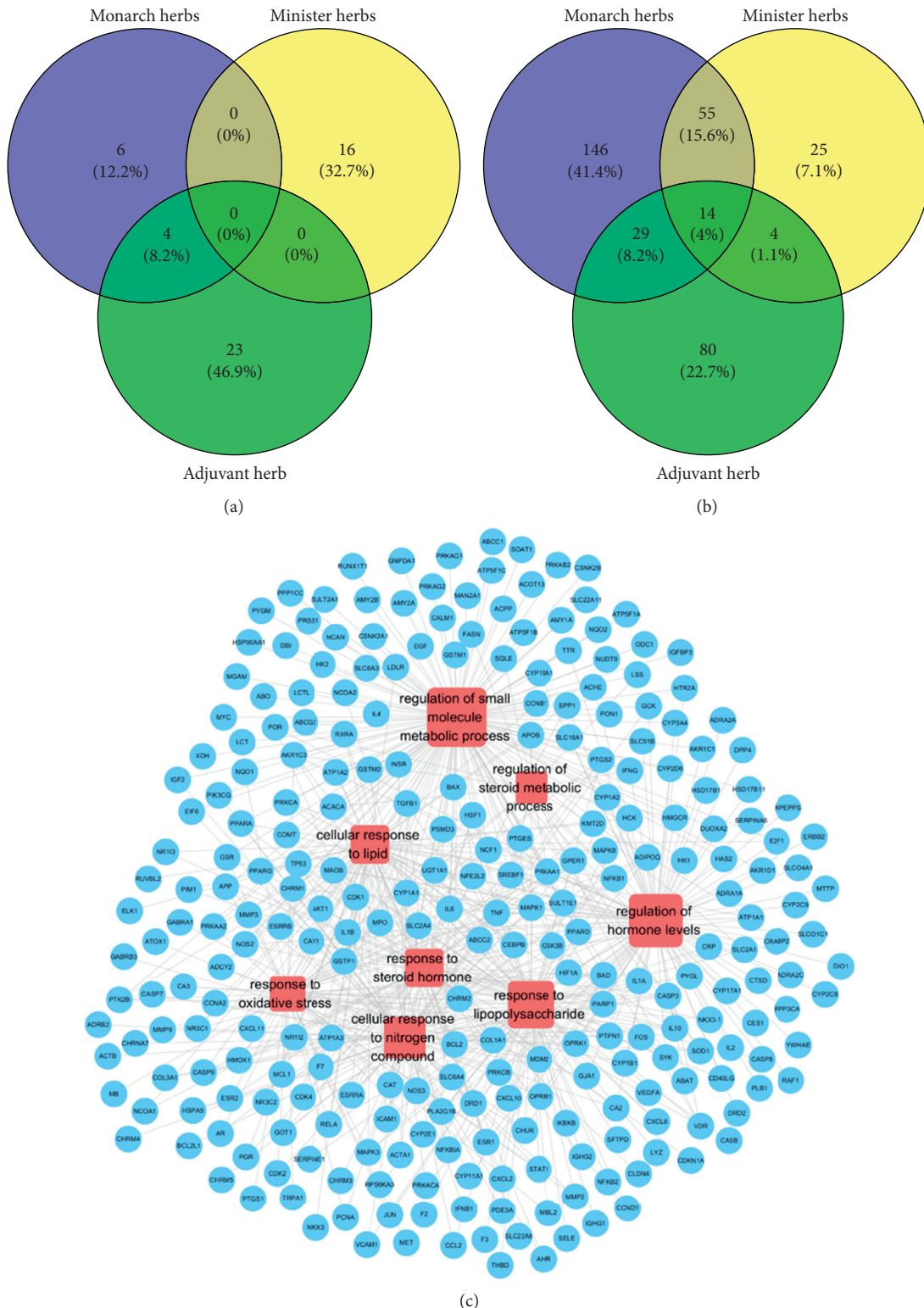


FIGURE 1: Herb-compound-target network of GXST, (a) distribution of active compounds among the herbs, (b) distribution of potential targets among the herbs, (c) network of the herb-compounds targets function. Blue nodes represent targets. Red nodes represent the enrichment of biological function and the size of nodes is proportional to degree centrality by topology analysis.

Analyzing the level of MDA, GSH, and SOD in plasma, we found that GXST significantly decreased MDA while it increased GSH and SOD compared to Model group

(Figures 6(a)–6(c)). Nrf2 is a member of the CNC-b ZIP transcription factor family. On physiological conditions, Nrf2 binds with the negative regulatory factor Keap1 in the

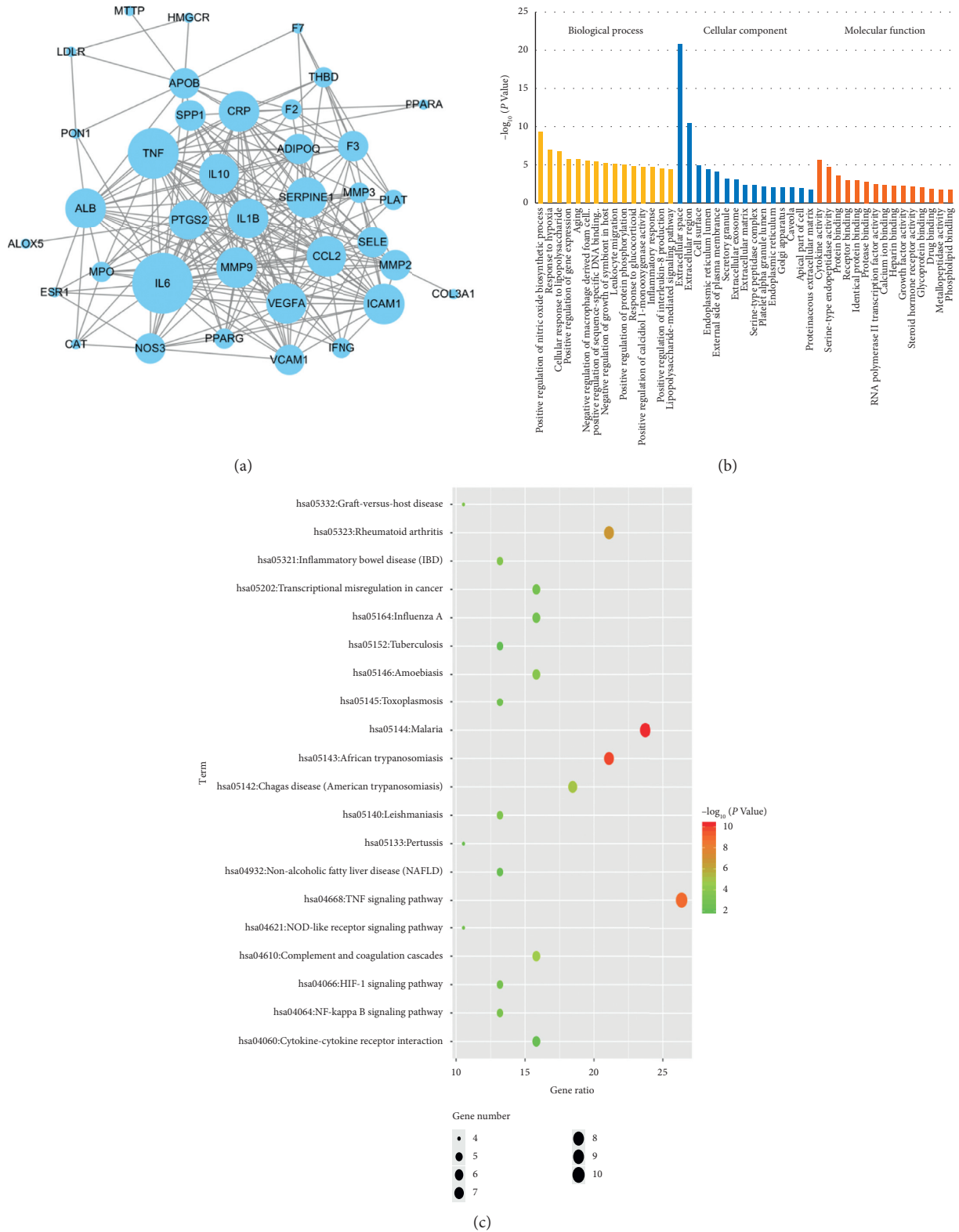


FIGURE 2: Pathway enrichment analysis, (a) network of the 38 shared targets between GXST potential targets and AS targets, (b) GO enrichment analysis for 38 key targets, (c) KEGG enrichment analysis for 38 key targets. Blue nodes represent targets and the size of nodes is proportional to degree centrality by topology analysis.

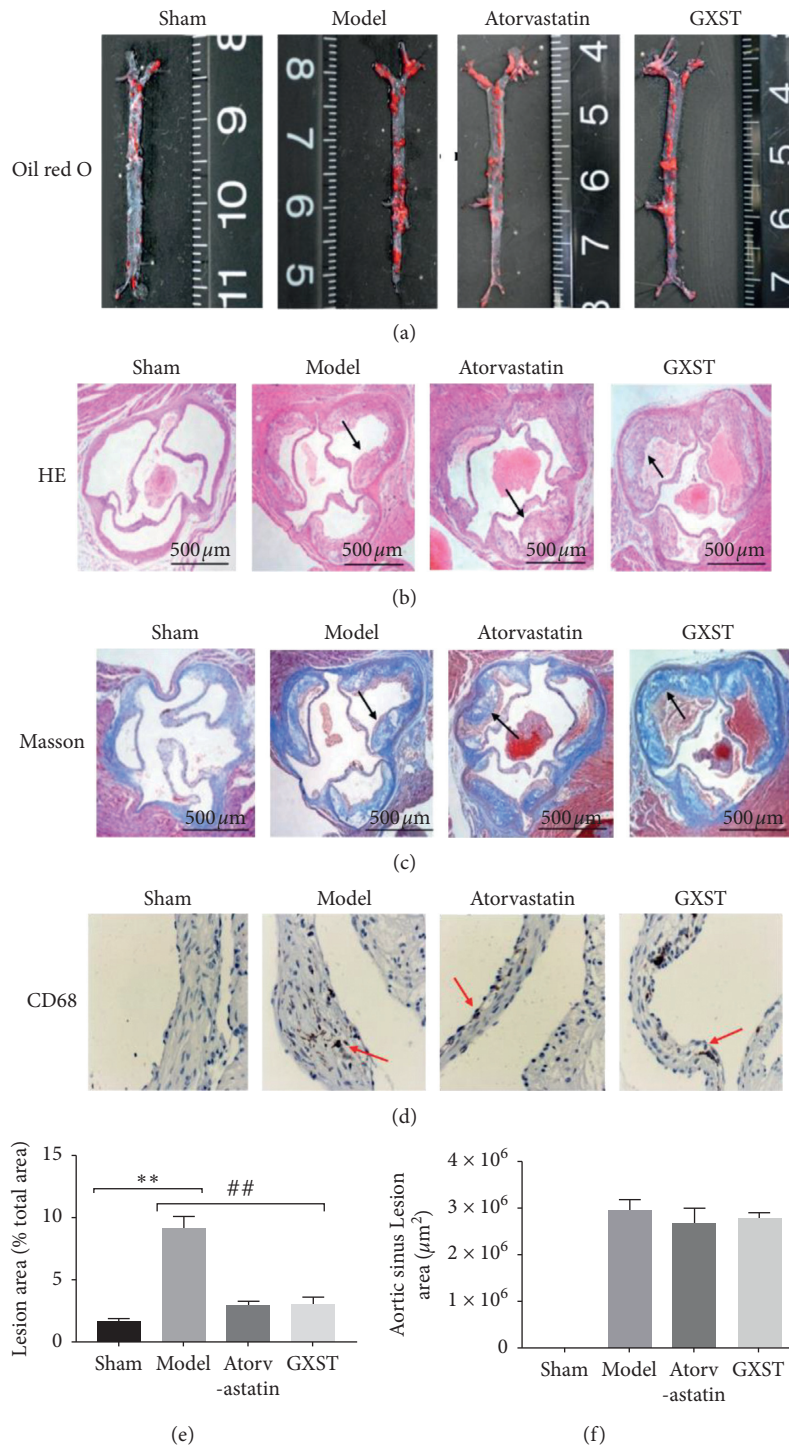


FIGURE 3: Continued.

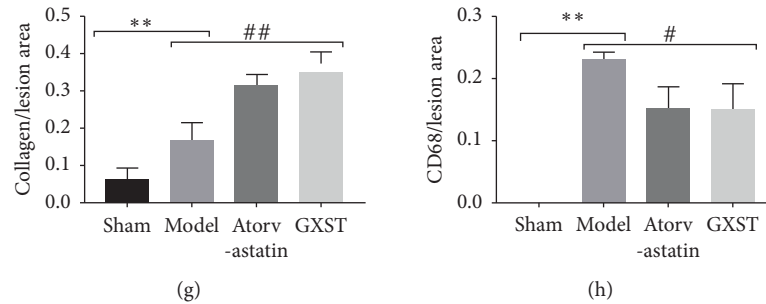


FIGURE 3: GXST reduces the lesion area and plaque composition, (a) representative images of oil red O-stained aortic trunk in each group ($n = 3$), (b) representative images of HE-stained aortic sinus sections from Sham, model, GXST, and atorvastatin ($n = 5$), (c) representative images of Masson-stained aortic sinus sections from Sham, model, GXST, and atorvastatin ($n = 5$), (d) representative photomicrographs images of aortic root sections stained with CD68 in each group ($n = 3$), (e) the size of the aortic trunk lesion was calculated as the percentage of lesion area in each group ($n = 5$), (f) quantitative analysis of the lesion size root in each group ($n = 8$), (g) quantitative analysis of the extracellular matrix in each group ($n = 8$), (h) quantitative analysis of CD68 in each group ($n = 5$). * $P < 0.05$ showed a significant difference compared with the Sham. # $P < 0.05$ showed a significant difference compared with the model, * $P < 0.05$, ** $P < 0.01$, *** $P < 0.001$; # $P < 0.05$, ## $P < 0.01$, ### $P < 0.001$).

cytoplasm. Under ROS stress, Nrf2 decouples with Keap1 enters the nucleus and combines with SOD and detoxification enzyme HO-1 to complete the protective role of antioxidative stress. In our study, the Model group significantly decreased the expression of Nrf2 and HO-1, while GXST restored them (Figures 6(d)–6(g), Supplementary Figure 5).

4. Discussion

AS is a chronic cardiovascular disease whose pathophysiology includes lipid metabolism dysfunction, inflammation, and oxidative stress. The effect of GXST on AS has not been illuminated before the present study. However, its anti-inflammatory, antioxidative effects in other cardiovascular diseases are seen. In this context, a total of 49 active compounds in GXST and 353 compound-related targets, and 106 AS-related targets were identified from the public databases. Among these targets, 38 targets were shared between compound-related and AS-related targets, implicating the possible anti-AS action of GXST. From the PPI network, the top 10 targets were enriched in the inflammatory response and lipid deposition. GO terms and KEGG pathway enriched the function of GXST on cellular response to lipid, inflammation, and oxidative stress. The preventive effect of GXST against AS was verified in ApoE^{-/-} mice. Altogether, these results indicated that GXST modulated atherosclerosis by regulating lipids, inhibiting inflammatory activity, and ROS. The putative active ingredients and multitarget mechanisms of GXST in the treatment of AS were elucidated in the present study for the first time, which provided theoretic evidence for the clinical application of GXST on AS treatment.

ApoE is a glycoprotein with a structural component of all lipoprotein particles except low-density lipoproteins, and it is synthesized mainly in the liver and brain and plays a vital role in lipids metabolism [28]. It has been confirmed that ApoE deficiency contributes to the accumulation of cholesterol-rich remnants in plasma and thus induced AS [29].

ApoE^{-/-} mouse is widely used in the research for AS as it can manifest pathological features of human AS [30–32]. Thus, ApoE knockout mouse was established with high lipid diet in our present study.

From the perspective of traditional Chinese medicine (TCM), the fundamental problem arteriosclerosis caused by hyperlipidemia is the deficiency of Spleen Qi, which leads to the “stagnation” of phlegm. “Stasis” and “Phlegm” block in the vascular wall and these are consistent with the pathology changes of vascular. GXST, a combination of the traditional herb and Mongolian medicine, is well-known to play an important role in promoting blood and QI circulation, removing blood stasis and phlegm, and relieving chest pain.

Analyzing the atherosclerotic lesions of GXST and Sham groups, we noticed that the lesion area in the aorta tree was reduced, while it was not modified in the aortic sinus after GXST treatment. Such discrepancy may reflect the different stages of AS development observed at those sites. As a previous study described, atherosclerotic lesions occur faster in the aortic sinus due to the turbulent blood flow that occurs caused by the faster heart rate in mice [33], while the lesions develop more slowly in the aorta. CD68 is a heavily glycosylated glycoprotein that is highly expressed in macrophages and other mononuclear phagocytes. Traditionally, CD68 is exploited as a valuable cytochemical marker to immune stain monocyte/macrophages in the histochemical analysis. In addition, in the AS progression, monocytes can infiltrate plaques, become activated, and develop into macrophages that can accumulate in the vascular wall. These cells engulf high levels of lipids depending on the variety of scavenger receptors (SR) on the membrane of macrophages such as CD68 and eventually form foam cells that accelerate atherosclerotic plaque formation. In our study, GXST significantly decreased the infiltration of macrophages marked by CD68 in the aortic sinus, although the total lesion in the aortic sinus was similar between GXST and Model groups. Moreover, augmented collagen deposition was indicated by Masson staining. Altogether, GXST treatment changed the plaque composition, presenting lower macrophage

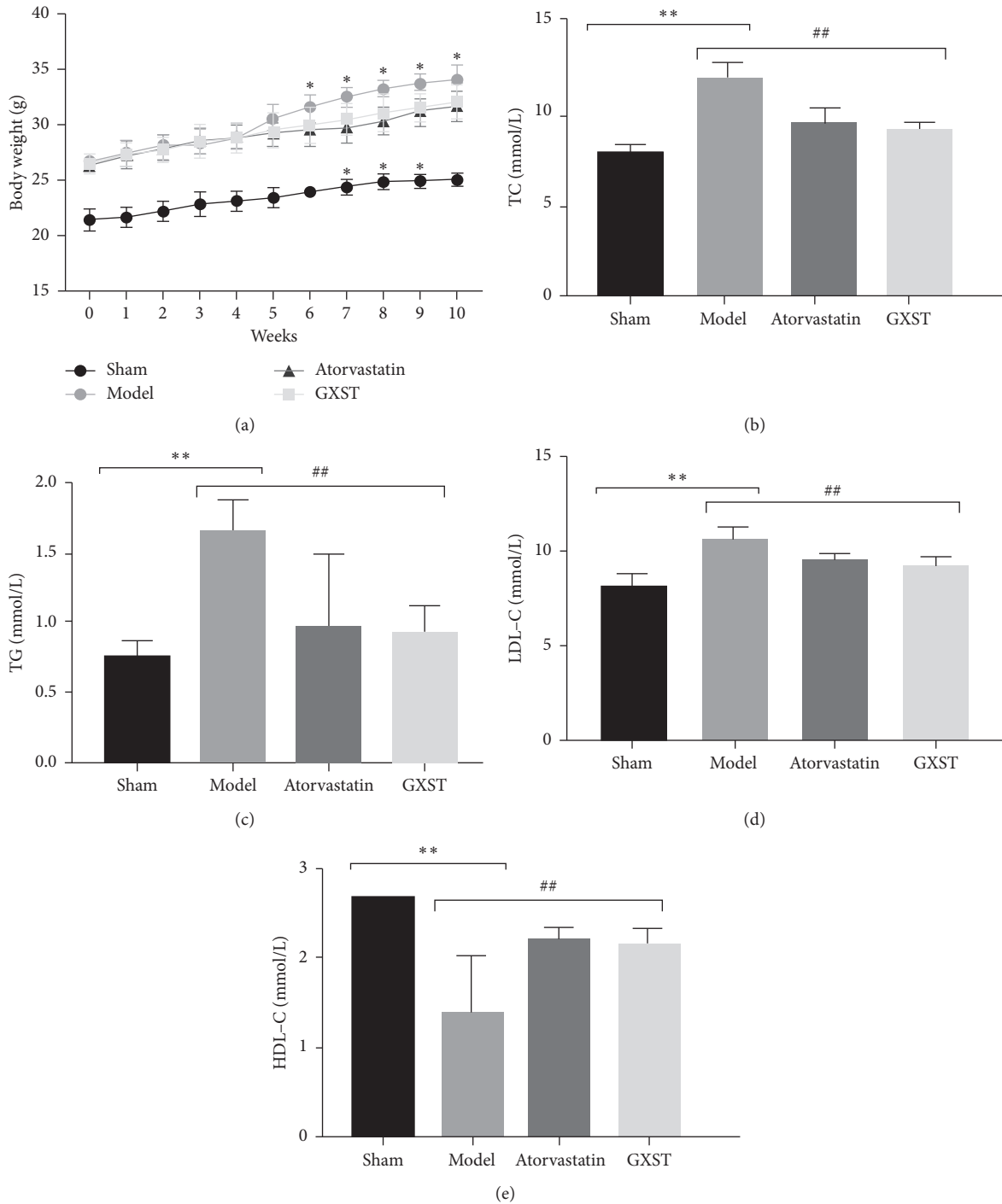


FIGURE 4: Effects of GXST on body weight and serum lipid levels in ApoE^{-/-} mice, (a) body weight in the four groups was compared every week. The effects of GXST treatment on plasma cholesterol levels: TC (b), TG (c), LDL-C (d), and HDL-C (e); Sham (normal saline, *n* = 13); Model (ApoE^{-/-} male mice, *n* = 12); ATF (Model group fed on atorvastatin, *n* = 14); GXST (Model group fed on GXST capsule, *n* = 13). **P* < 0.05 showed a significant difference compared with the Sham. #*P* < 0.05 showed a significant difference compared with the model, **P* < 0.05, ***P* < 0.01, ****P* < 0.001; #*P* < 0.05, ##*P* < 0.01, ###*P* < 0.001.

infiltration and augmented collagen deposition, suggesting a more stable fibrous cap. These results demonstrate the benefits of GXST in stabilizing the fibrous cap and modulating foam cell formation in AS progression. Furthermore, AS is a chronic disease of the arterial wall which is related to

life-threatening complications such as myocardial infarction. Our data demonstrate that, in addition to beneficial stable plaques effects, GXST moderately improves LV remodeling indicated by well-ordered cardiomyocyte and lowered interstitial fibrosis. This kind of target organ

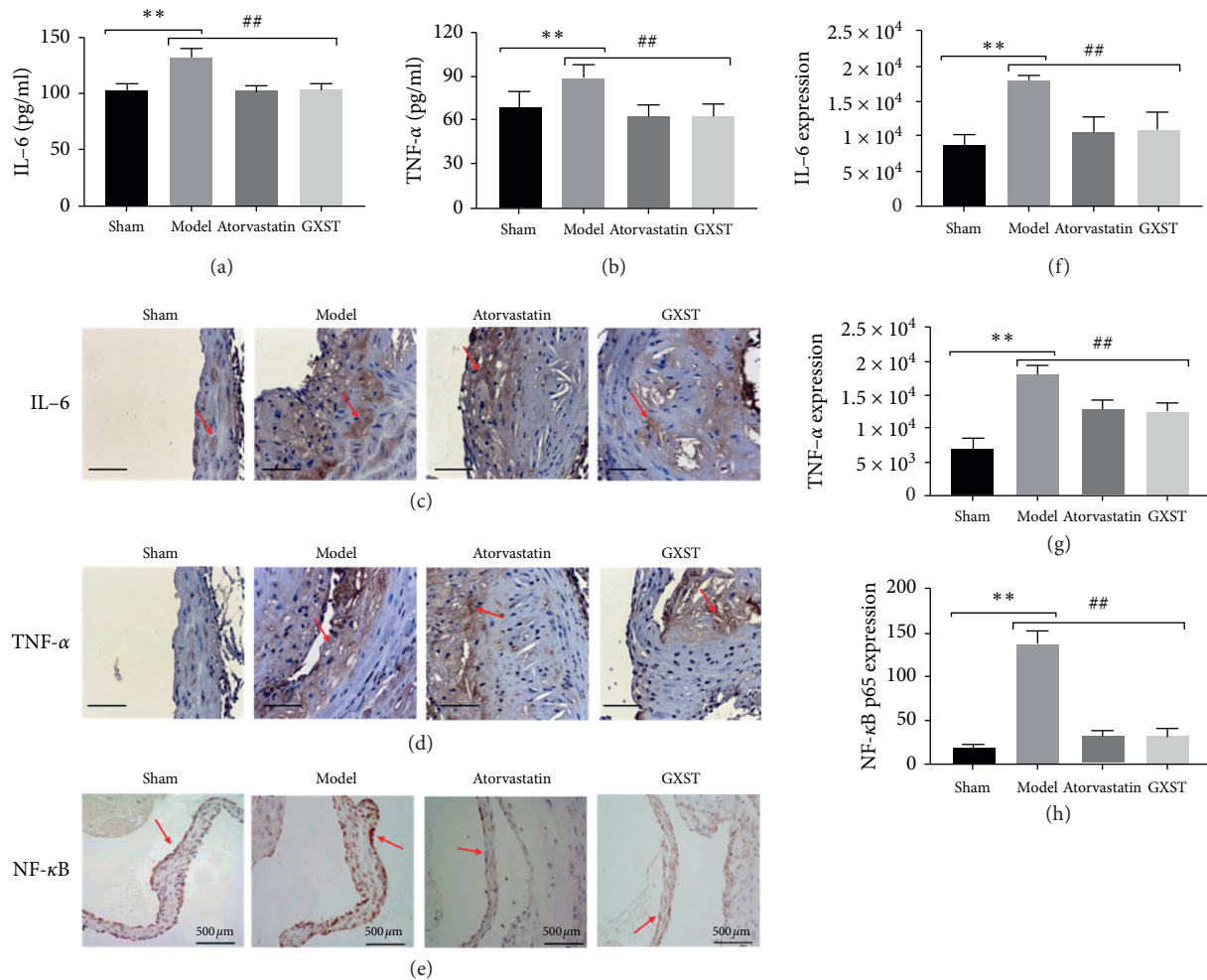


FIGURE 5: GXST attenuates the inflammatory response, (a and b) Blood IL-6 and TNF- α levels ($n = 8$), (c–e) representative images of IL-6, TNF- α , and NF- κ B in the aortic sinus ($n = 3$), (f–h) quantitative analysis of the IL-6, TNF- α , and NF- κ B expression in the aortic sinus ($n = 5$). * $P < 0.05$ showed a significant difference compared with the Sham. # $P < 0.05$ showed a significant difference compared with the model, * $P < 0.05$, ** $P < 0.01$, *** $P < 0.001$; # $P < 0.05$, ## $P < 0.01$, ### $P < 0.001$).

protection by GXST is at least partially dependent on the attenuation of AS in ApoE^{-/-} mice.

Based on our network pharmacology analysis of GXST on AS, diverse underlying mechanisms including lipid-lowering, inflammatory response, and oxidative stress might be associated with the modulation of AS progression. Hypercholesterolemia is being the risk factor sufficiently to cause atherosclerotic, even in the absence of other cardiovascular risk factors [27]. Evidence from clinical trials indicates that a high level of circulating LDL-C level as well as low levels of HDL-C are associated with CVD risk, and the reduction of LDL-C and excessive HDL-C may decrease the incidence of atherosclerotic diseases [34, 35]. In addition, a large number of studies have shown that hypertriglyceridemia contributes to the development and progression of atherosclerosis [36]. Therefore, it is very important to modulate the lipid profile in attenuating AS progression. In our study, we found that GXST treatment markedly reduced the ApoE^{-/-} mice body weight from the 7th to 9th week treatment. Similarly, GXST significantly

decreased the plasma concentration of TG, TC, and LDL-C and increased the HDL-C levels.

For over a decade now, GXST has an anti-inflammatory effect. A recent study reported that GXST decreased levels of TNF- α , IL-1 β , IL-6 and obviously inhibited the NF- κ B pathway [14]. In order to confirm GXST-related anti-inflammatory response associated with reduced atherosclerotic lesions and macrophage infiltration in the aortic sinus, we examined several inflammatory markers of atherosclerosis in plasma and aorta. TNF- α has a central role in controlling inflammatory processes and atherosclerosis development independent of plasma cholesterol levels. Inhibiting TNF- α expression or capturing TNF- α biological action may inhibit advanced lesion formation [37]. IL-6 induced by TNF- α is regarded as a proinflammatory cytokine in AS [38]. Our results showed that GXST treatment reduced the levels of TNF- α and IL-6 in plasma and aortic lesion. Nuclear factor kappa B (NF- κ B), a major transcription factor, regulates the inflammatory response and participates in the AS progression [39, 40]. NF- κ B is a key

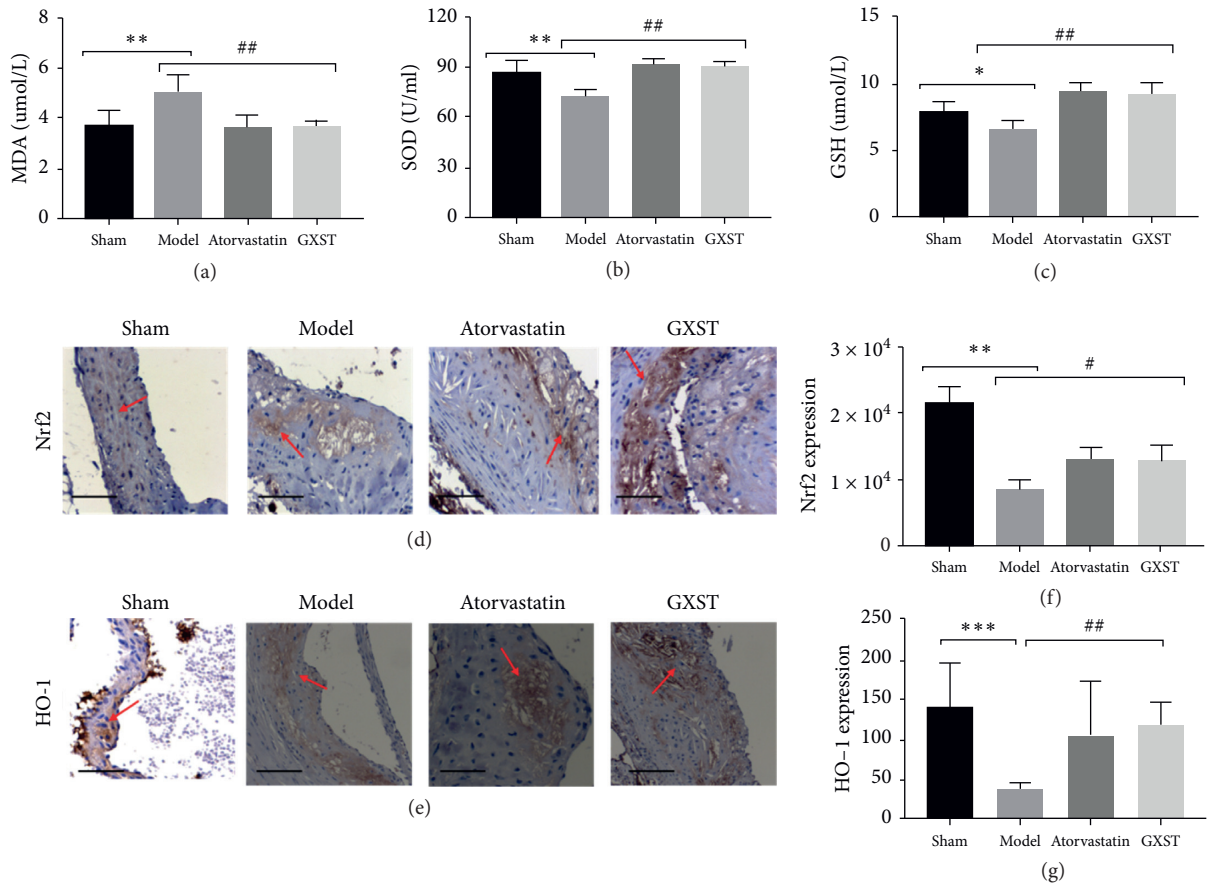


FIGURE 6: GXST attenuated oxidative stress, (a–c) blood MDA, GSH, and SOD levels ($n = 8$), (d–e) representative images of Nrf2 and HO-1 in the aortic sinus ($n = 3$). (f–g) Quantitative analysis of Nrf2 and HO-1 in the aortic sinus ($n = 5$). * $P < 0.05$ showed a significant difference compared with the Sham. # $P < 0.05$ showed a significant difference compared with the model, * $P < 0.05$, ** $P < 0.01$, *** $P < 0.001$; # $P < 0.05$, ## $P < 0.01$, ### $P < 0.001$.

transcription factor induced by oxLDL and inflammatory cytokines, which, in turn, induces the expression of proinflammatory cytokines such as TNF- α and IL-6. The activity of NF- κ B depends on its activation through its translocation into the nucleus. It is well known that oxLDL or proinflammatory cytokine activates the p65/p50 dimer of phosphorylated I κ B which can migrate to the nucleus and induce gene transcription [41]. In our present study, the GXST supplement decreased the expression of NF- κ Bp65 in the aortic sinus indicated by immunohistochemistry staining and western blots. Thus, we suggest that GXST could decrease TNF- α and IL-6 secretion partly by reducing NF- κ B activation. These results implied that GXST could inhibit the inflammatory reaction via downregulating the expression of proinflammatory cytokines including IL-6 and TNF- α mediated by NF- κ B.

Several studies have suggested that oxidative stress also participates in atherosclerotic development and plaque instability [9, 42]. ROS can be generated as metabolic by-products by nearly all cell types. Decreasing ROS levels is a useful strategy for the treatment of AS [43]. GXST has been reported to protect the heart against oxidative stress indicated by the increasing activities of total SOD, NOS and the levels of NO and GSH [16]. The present study found that in

ApoE^{-/-} mice treated with GXST, the SOD (converts the highly reactive ROS to more stable) and GST (reduces the levels of ROS) were increased. Moreover, a defense mechanisms called nuclear erythroid factor 2-related factor 2 (Nrf2)/heme oxygenase-1 (HO-1) pathway was reported to participate in attenuating oxidative stress [44]. Nrf2 could dissociate with kelch-like ECH-associated protein 1 (Keap1, the cytosolic inhibitor of Nrf2), translocate to the nucleus and activate the downstream antioxidant enzymes such as SOD2 and HO-1, and ultimately degrade ROS production and reduce oxidative injury. The present study has indicated that inhibition of HO-1 expression in hyperlipidemic rabbits leads to higher levels of circulating lipid profile and greater atherosclerotic lesions [45]. Herein, GXST treatment was found to increase Nrf2 and HO-1 expression associated with ROS degradation. Overall, these results highlight that GXST ameliorates oxidative stress by decreasing ROS generation and increasing ROS degradation.

5. Conclusions

In conclusion, the present study predicted drug-target-disease interactions and multitarget mechanisms of GXST on AS progression by network pharmacology strategy and

validated the attenuation effect of GXST against AS in vivo. This study showed that the effect of GXST on stabilizing the fibrous cap and modulating foam cell formation was associated with attenuating dyslipidemia, inflammation and oxidative stress.

Data Availability

The data used to support the findings of this study are available from the corresponding author upon request.

Conflicts of Interest

The authors declare no conflicts of interest.

Authors' Contributions

Yingdong Lu, YuchanSun, and Zhilin Jiang contributed equally to this work.

Acknowledgments

This work was supported by the National Natural Science Foundation of China (Gra 81273945).

Supplementary Materials

Supplementary Table S1. Characteristics of active compounds in GXST. This file contains the herbs of GXST and herbs-associated compounds, molecular formula, molecular weight (MW), oral bioavailability (OB), drug-likeness, PubchemID, and SMILES. Supplementary Table S2. The potential targets of the compounds in GXST. This file contains the herbs' compounds and compound-associated targets, Uniprot ID and Gene Code. Supplementary Table S3. AS-related target. This file includes the gene name, target name, Uniprot ID, and the source of the database of AS-related target. Supplementary Table S4. Primer sequences for PCR. Supplementary Figure 1. The knock down efficiency of ApoE expression in mice. Total DNA was extracted from the heart of C57BL/6J wide type (liver) and ApoE^{-/-} mice (liver, brain, heart, and aorta) according to the manufacturers' instructions. The DNA was used as a template to perform PCR with TaKaRa PCR Amplification Kit (TaKaRa Biotechnology) both in wide type (150 bp) and APOE deficiency mice (250 bp). M: DL 2000 marker; N: negative control; P: positive control; 1–8: ApoE^{-/-} mice applied in our study; 9–10: C57BL/6J wide type (liver, liver). Supplementary Figure 2. The lower magnitude for HE, Masson staining (magnification: ×20), and CD68 of the aortic sinus (magnification: ×40). Supplementary Figure 3. The lower magnitude for IL-6, TNF- α and NF- κ B of the aortic sinus (magnification: ×40). Supplementary Figure 4. GXST moderately improves LV remodeling. (A) Representative images of HE staining of left ventricular wall ($n = 3$). (B) Representative images of Masson staining of left ventricular wall ($n = 3$). (C) Quantitative analysis of the extracellular matrix in each group ($n = 5$). * $P < 0.05$ showed a significant difference compared with the Sham. # $P < 0.05$ showed a significant difference compared with the Model, ** $P < 0.01$,

$P < 0.01$. Supplementary Figure 5. The effects of GXST on the protein levels of inflammatory and oxidative stress factors in the aorta. (A) Western blot results of aorta NF- κ Bp65, Nrf2, and HO-1 expression. (B) Quantitative analysis of the expression level in each group ($n = 3$). * $P < 0.05$ showed a significant difference compared with the Sham. # $P < 0.05$ showed a significant difference compared with the Model. ### $P < 0.01$. (Supplementary Materials)


References

- [1] P. Libby, P. M. Ridker, and G. K. Hansson, "Progress and challenges in translating the biology of atherosclerosis," *Nature*, vol. 473, no. 7347, pp. 317–325, 2011.
- [2] H. Kinoshita, T. Matsumura, N. Ishii et al., "Apocynin suppresses the progression of atherosclerosis in ApoE-deficient mice by inactivation of macrophages," *Biochemical and Biophysical Research Communications*, vol. 431, no. 2, pp. 124–130, 2013.
- [3] K. Takeya, R. D. E. Sewell, and M. Rafeian-Kopaei, "Antioxidants and atherosclerosis: mechanistic aspects," *Biomolecules*, vol. 9, no. 8, p. 301, 2019.
- [4] A. C. Kaliora, G. V. Z. Dedoussis, and H. Schmidt, "Dietary antioxidants in preventing atherogenesis," *Atherosclerosis*, vol. 187, no. 1, pp. 1–17, 2006.
- [5] M. Bäck, A. Yurdagul, I. Tabas, K. Öörni, and P. T. Kovanen, "Inflammation and its resolution in atherosclerosis: mediators and therapeutic opportunities," *Nature Reviews Cardiology*, vol. 16, no. 7, pp. 389–406, 2019.
- [6] G. K. Hansson and P. Libby, "The immune response in atherosclerosis: a double-edged sword," *Nature Reviews Immunology*, vol. 6, no. 7, pp. 508–519, 2006.
- [7] P. M. Ridker, "From C-reactive protein to interleukin-6 to interleukin-1," *Circulation Research*, vol. 118, no. 1, pp. 145–156, 2016.
- [8] K. Kojok, A. E.-H. El-Kadiry, and Y. Merhi, "Role of NF- κ B in platelet function," *International Journal of Molecular Sciences*, vol. 20, no. 17, p. 4185, 2019.
- [9] M. Yokoyama, "Oxidant stress and atherosclerosis," *Current Opinion in Pharmacology*, vol. 4, no. 2, pp. 110–115, 2004.
- [10] K. Uno and S. J. Nicholls, "Biomarkers of inflammation and oxidative stress in atherosclerosis," *Biomarkers in Medicine*, vol. 4, no. 3, pp. 361–373, 2010.
- [11] E. Belaidi, J. Morand, E. Gras, J.-L. Pépin, and D. Godin-Ribuot, "Targeting the ROS-HIF-1-endothelin axis as a therapeutic approach for the treatment of obstructive sleep apnea-related cardiovascular complications," *Pharmacology & Therapeutics*, vol. 168, pp. 1–11, 2016.
- [12] P. Marchio, S. Guerra-Ojeda, J. M. Vila, M. Aldasoro, V. M. Victor, and M. D. Mauricio, "Targeting early atherosclerosis: a focus on oxidative stress and inflammation," *Oxidative Medicine and Cellular Longevity*, vol. 2019, Article ID 8563845, 32 pages, 2019.
- [13] I. Perrotta and S. Aquila, "The role of oxidative stress and autophagy in atherosclerosis," *Oxidative Medicine and Cellular Longevity*, vol. 2015, Article ID 130315, 10 pages, 2015.
- [14] L. Zhuo, L. Li-Feng, Y. Tian-Ming, H. Yu, and H. Ya-Ling, "Cardioprotective effects of Guanxinshutong (GXST) against myocardial ischemia/reperfusion injury in rats," *Journal of Geriatric Cardiology: JGC*, vol. 9, no. 2, pp. 130–136, 2012.
- [15] Y. Li, L. Zhang, S. Lv et al., "Efficacy and safety of oral Guanxinshutong capsules in patients with stable angina pectoris in China: a prospective, multicenter, double-blind,

- placebo-controlled, randomized clinical trial," *BMC Complementary and Alternative Medicine*, vol. 19, no. 1, p. 363, 2019.
- [16] Y. Cao, X. He, F. Lui, Z. Huang, and Y. Zhang, "Chinese medicinal formula Guanxin Shutong capsule protects the heart against oxidative stress and apoptosis induced by ischemic myocardial injury in rats," *Experimental and Therapeutic Medicine*, vol. 7, no. 4, pp. 1033–1039, 2014.
- [17] J. Ru, P. Li, J. Wang et al., "TCMSP: a database of systems pharmacology for drug discovery from herbal medicines," *Journal of Cheminformatics*, vol. 6, p. 13, 2014.
- [18] Q. Zeng, L. Li, W. Siu et al., "A combined molecular biology and network pharmacology approach to investigate the multi-target mechanisms of Chaihu Shugan San on Alzheimer's disease," *Biomedicine & Pharmacotherapy*, vol. 120, Article ID 109370, 2019.
- [19] S.-J. Wu, J. Liu, W.-W. Feng et al., "System pharmacology-based dissection of the synergistic mechanism of huangqi and huanglian for diabetes mellitus," *Frontiers in Pharmacology*, vol. 8, p. 694, 2017.
- [20] H.-Y. Xu, Y.-Q. Zhang, Z.-M. Liu et al., "ETCM: an encyclopaedia of traditional Chinese medicine," *Nucleic Acids Research*, vol. 47, no. D1, pp. D976–D982, 2019.
- [21] Y. Yang, F. Ramírez, S.-E. Schelhorn, T. Lengauer, and M. Albrecht, "Computing topological parameters of biological networks," *Bioinformatics*, vol. 24, no. 2, pp. 282–284, 2008.
- [22] J. Pinero, N. Queralt-Rosinach, A. Bravo et al., "DisGeNET: a discovery platform for the dynamical exploration of human diseases and their genes," *Database*, vol. 2015, 2015.
- [23] D. Szklarczyk, J. H. Morris, H. Cook et al., "The STRING database in 2017: quality-controlled protein-protein association networks, made broadly accessible," *Nucleic Acids Research*, vol. 45, no. D1, pp. D362–D368, 2017.
- [24] D. W. Jensen, B. T. Sherman, and R. A. Lempicki, "Systematic and integrative analysis of large gene lists using DAVID bioinformatics resources," *Nature Protocols*, vol. 4, no. 1, pp. 44–57, 2009.
- [25] B. Paigen, A. Morrow, P. A. Holmes, D. Mitchell, and R. A. Williams, "Quantitative assessment of atherosclerotic lesions in mice," *Atherosclerosis*, vol. 68, no. 3, pp. 231–240, 1987.
- [26] A. Schmedes and G. Hölmer, "A new thiobarbituric acid (TBA) method for determining free malondialdehyde (MDA) and hydroperoxides selectively as a measure of lipid peroxidation," *Journal of the American Oil Chemists' Society*, vol. 66, no. 6, pp. 813–817, 1989.
- [27] A. Mizrahi, Y. Berdichevsky, Y. Ugolev et al., "Assembly of the phagocyte NADPH oxidase complex: chimeric constructs derived from the cytosolic components as tools for exploring structure-function relationships," *Journal of Leukocyte Biology*, vol. 79, no. 5, pp. 881–895, 2006.
- [28] E. D. Franca, J. G. B. Alves, and M. H. Hutz, "Apolipoprotein E polymorphism and its association with serum lipid levels in Brazilian children," *Human Biology*, vol. 76, no. 2, pp. 267–275, 2004.
- [29] S. Zhang, R. Reddick, J. Piedrahita, and N. Maeda, "Spontaneous hypercholesterolemia and arterial lesions in mice lacking apolipoprotein E," *Science*, vol. 258, no. 5081, pp. 468–471, 1992.
- [30] J. Feng, Z. Zhang, W. Kong, B. Liu, Q. Xu, and X. Wang, "Regulatory T cells ameliorate hyperhomocysteinaemia-accelerated atherosclerosis in ApoE^{-/-} mice," *Cardiovascular Research*, vol. 84, no. 1, pp. 155–163, 2009.
- [31] C. Li, S. Li, F. Zhang et al., "Endothelial microparticles-mediated transfer of microRNA-19b promotes atherosclerosis via activating perivascular adipose tissue inflammation in ApoE^{-/-} mice," *Biochemical and Biophysical Research Communications*, vol. 495, no. 2, pp. 1922–1929, 2018.
- [32] G. An, B. Li, X. Liu et al., "Overexpression of complement component C5a accelerates the development of atherosclerosis in ApoE-knockout mice," *Oncotarget*, vol. 7, no. 35, pp. 56060–56070, 2016.
- [33] P. A. VanderLaan, C. A. Reardon, and G. S. Getz, "Site specificity of atherosclerosis," *Arteriosclerosis, Thrombosis, and Vascular Biology*, vol. 24, no. 1, pp. 12–22, 2004.
- [34] Z. Zhong, J. Hou, Q. Zhang et al., "Assessment of the LDL-C/HDL-C ratio as a predictor of one year clinical outcomes in patients with acute coronary syndromes after percutaneous coronary intervention and drug-eluting stent implantation," *Lipids in Health and Disease*, vol. 18, no. 1, p. 40, 2019.
- [35] T. Umeda, A. Hayashi, A. Harada et al., "Low-density lipoprotein cholesterol goal attainment rates by initial statin monotherapy among patients with dyslipidemia and high cardiovascular risk in Japan—a retrospective database analysis," *Circulation Journal*, vol. 82, no. 6, pp. 1605–1613, 2018.
- [36] J. Peng, F. Luo, G. Ruan, R. Peng, and X. Li, "Hypertriglyceridemia and atherosclerosis," *Lipids in Health and Disease*, vol. 16, no. 1, p. 233, 2017.
- [37] L. Boesten, A. Zadelaar, A. Vannieuwkoop et al., "Tumor necrosis factor- α promotes atherosclerotic lesion progression in APOE*3-Leiden transgenic mice," *Cardiovascular Research*, vol. 66, no. 1, pp. 179–185, 2005.
- [38] M. Li, B. C. A. M. Van Esch, P. A. J. Henricks, J. Garssen, and G. Folkerts, "Time and concentration dependent effects of short chain fatty acids on lipopolysaccharide- or tumor necrosis factor α -induced endothelial activation," *Frontiers in Pharmacology*, vol. 9, p. 233, 2018.
- [39] M. P. J. De Winther, E. Kanters, G. Kraal, and M. H. Hofker, "Nuclear factor κ B signaling in atherogenesis," *Arteriosclerosis, Thrombosis, and Vascular Biology*, vol. 25, no. 5, pp. 904–914, 2005.
- [40] Z. Liu, S. Xu, X. Huang et al., "Cryptotanshinone, an orally bioactive herbal compound from Danshen, attenuates atherosclerosis in apolipoprotein E-deficient mice: role of lectin-like oxidized LDL receptor-1 (LOX-1)," *British Journal of Pharmacology*, vol. 172, no. 23, pp. 5661–5675, 2015.
- [41] T. Collins and M. I. Cybulsky, "NF- κ B: pivotal mediator or innocent bystander in atherogenesis?," *The Journal of Clinical Investigation*, vol. 107, no. 3, pp. 255–264, 2001.
- [42] T. Morita, "Heme oxygenase and atherosclerosis," *Arteriosclerosis, Thrombosis, and Vascular Biology*, vol. 25, no. 9, pp. 1786–1795, 2005.
- [43] Y.-C. Cheng, J.-M. Sheen, W. L. Hu, and Y.-C. Hung, "Polyphenols and oxidative stress in atherosclerosis-related ischemic heart disease and stroke," *Oxidative Medicine and Cellular Longevity*, vol. 2017, Article ID 8526438, 16 pages, 2017.
- [44] M. Luo, R. Tian, and N. Lu, "Nitric oxide protected against NADPH oxidase-derived superoxide generation in vascular endothelium: critical role for heme oxygenase-1," *International Journal of Biological Macromolecules*, vol. 126, pp. 549–554, 2019.
- [45] X. Liu, A. S. Pachori, C. A. Ward et al., "Heme oxygenase-1 (HO-1) inhibits postmyocardial infarct remodeling and restores ventricular function," *The FASEB Journal*, vol. 20, no. 2, pp. 207–216, 2006.

Research Article

Distribution Analysis of Salvianolic Acids in Myocardial Ischemic Pig Tissues by Automated Liquid Extraction Surface Analysis Coupled with Tandem Mass Spectrometry

Qi Qiu ^{1,2}, Jinglin Cao,¹ Yu Mu,^{1,2} Yang Lin,^{1,2} Yunnan Zhang,^{1,2} Jing Li,¹ and Xiujin Shi¹

¹Department of Pharmacy, Beijing Anzhen Hospital, Capital Medical University, Beijing 100029, China

²School of Pharmaceutical Sciences, Capital Medical University, Beijing 100069, China

Correspondence should be addressed to Qi Qiu; qiuqi8133@163.com

Received 18 June 2020; Revised 11 August 2020; Accepted 31 August 2020; Published 14 September 2020

Academic Editor: Sai-Wang Seto

Copyright © 2020 Qi Qiu et al. This is an open access article distributed under the Creative Commons Attribution License, which permits unrestricted use, distribution, and reproduction in any medium, provided the original work is properly cited.

The distribution of active compounds of traditional Chinese medicine *Salvia miltiorrhiza* Bunge (Chinese name: Danshen) in vivo was determined by establishing a liquid extraction surface analysis coupled with the tandem mass spectrometry (LESA-MS/MS) method. Stability analysis and distribution analysis were designed in the present study using normal animals or a myocardial ischemia model. The model assessment was performed four weeks after surgery, and then three groups were created: a normal-dose group, a model-blank group, and a model-dose group. Meanwhile, Danshen decoction administration began in dose groups and lasted for four weeks. In stability analysis, four salvianolic acids—Danshensu (DSS), caffeic acid (CAA), rosmarinic acid (RA), and salvianolic acid A (SAA)—in kidney tissues from the normal-dose group were detected by LESA-MS/MS under four conditions, and then distribution analysis was conducted in different tissues using the same method. Ejection fraction (EF) and fractional shortening (FS) in animals from two model groups decreased significantly four weeks after surgery ($P < 0.01$) and were improved after four weeks of Danshen decoction administration ($P < 0.01$). Results of stability analysis demonstrated that this method was basically stable since there were no significant differences in signal intensities of DSS, CAA, and SAA under four conditions ($P > 0.05$). Distribution analysis showed the signal intensities of DSS in the liver and kidney and SAA in the heart were higher in the model-dose group than in the normal-dose group ($P < 0.05$ or $P < 0.01$). Signal intensities of RA in the liver and kidney, and SAA in the liver were lower in the model-dose group compared with the normal-dose group ($P < 0.05$ or $P < 0.01$). In conclusion, Danshen decoction has the effect of improving the ischemic condition in a chronic myocardial ischemia model, and the content of two active compounds increased in the targets. These findings contribute to an understanding of the therapeutic role of Danshen in cardiovascular disease.

1. Introduction

Cardiovascular disease (CVD), which is defined as a set of diseases and conditions including coronary heart disease (CHD), cerebrovascular disease, and heart failure, has been the leading cause of mortality across the world [1]. It is estimated that by 2030, 23.6 million people will die each year from CVD. CHD, as the most important disease of CVD, has climbed from the seventh leading cause of death in China in 1990 to the second today [2]. Because of the increasing cost of hospitalization for CHD, it has become one of the largest disease burdens in China.

Traditional Chinese medicine (TCM) is a valuable asset for preventing and treating disease. In China, TCM as a complementary therapy has been widely used for CVD. Recent reviews have also suggested that TCM may be beneficial to patients with CVD. The TCM-Danshen is the dry root and rhizome of *Salvia miltiorrhiza* Bunge and was first recorded in Shennong Herbal Classic. It is commonly used in the treatment of cardiovascular system, digestive system, and nervous system diseases. The theory of TCM considers Danshen an important medicine for expanding blood vessels, promoting blood circulation, eliminating blood stasis, and relieving pain [3]. The main chemical

constituents of Danshen are divided into water- and lip-soluble components [3]. Its water-soluble phenolic acids are salvianolic acids, including Danshensu (DSS), caffeic acid (CAA), rosmarinic acid (RA), and salvianolic acid A (SAA) [4, 5]. These salvianolic acids have pharmacological activities and play a major role in the treatment of CHD [6].

Mapping and quantifying the distribution of drugs in vivo are critical to elucidating their mechanisms of action. The distributions of drugs and their quantities at target sites are closely related to their efficacy and safety. However, analysis of TCMS and their metabolites remains challenging because of the diversity of their compositions, the complexity of biological matrices, and the presence of trace amounts of components and metabolites [7].

In the present study, the distribution of four salvianolic acids (DSS, CAA, RA, and SAA) of Danshen in myocardial ischemic pig tissues was determined using a liquid extraction surface analysis coupled with tandem mass spectrometry (LESA-MS/MS) method which is a fully automated, chip-based method with the characteristics of simplicity and efficiency. An attempt was made to explore the relative amounts and spatial distributions of the target compounds in vivo and the therapeutic effect of Danshen on CHD.

2. Materials and Methods

2.1. Chemicals and Reagents. Standards of CAA (lot no. LL90Q26, 99% purity), DSS sodium salt (lot no. LIA0Q 80, 99% purity), RA (lot no. L970N70, 99% purity), and SAA (lot no. L4B0P55, 99% purity) were purchased from J&K Scientific Ltd (Beijing, China) (Figure 1).

Methanol (CAS no.67-56-1, batch no. 150162, Fisher Scientific UK, Loughborough, UK), ammonium hydroxide (Beijing Chemical Plant, Beijing, China), and high-performance liquid chromatography (HPLC) grade water (CAS no. 7732-18-5, batch no. F8CJ21, DUKSAN, Ansan-si, Korea) were used.

2.2. Drug Preparation. All crude drugs were purchased from Beijing Tongrentang Pharmaceutical Co., Ltd. (Beijing, China), including *Salvia miltiorrhiza* Bunge pieces (lot no. SAA291), *Amomum villosum* Lour pieces (lot no. SA1271), and *Santalum album* L. pieces (lot no. SAA271), and identified at Beijing University of Chinese Medicine. Danshen decoction was prepared as follows: 50 g *Salvia miltiorrhiza* Bunge, 7.5 g *Amomum villosum* Lour, and 7.5 g *Santalum album* L. were decocted with water twice and then were extracted by 95% ethanol. After filtering, recovering ethanol, and decompression drying, the major ingredients of Danshen decoction were obtained. Then, the excipient dextrin was added to form the final product. Analysis of high-performance liquid chromatography-mass spectrometry (HPLC-MS) showed the contents of CAA, RA, SAA, and DSS in the Danshen decoction were 0.08 $\mu\text{g}/\text{mg}$, 2.84 $\mu\text{g}/\text{mg}$, 14.84 $\mu\text{g}/\text{mg}$, and 24.54 $\mu\text{g}/\text{mg}$, respectively (see Figures S1–S5 in the Supplementary Material).

2.3. Animals. 15 male Bama miniature pigs (25 ± 2 kg, 6–10 months, lot no. SCXK2015-0002) were purchased from Tianjin Bainong Laboratory Animal Breeding Technology Co., Ltd. (Tianjin, China). Pigs were housed under standard laboratory conditions, fed twice a day, and given tap water ad libitum. All the animal care and experimental procedures were performed in accordance with the China Physiological Society's "Guiding Principles in the Care and Use of Animals" with the approval from the Animal Care Committee of Beijing Anzhen Hospital, Capital Medical University (no. 0000353).

2.4. Surgical Protocol and Groups. After one week of adaptive feeding, inspection, and quarantine, eleven animals that met test standards were retained. Eight animals were randomly selected to a model building which underwent thoracotomy with an Ameroid constrictor (\varnothing 2.75 mm, Research Instrument SW, USA) placing on the proximal left circumflex artery [8]. Model assessment via coronary angiography (OEC 9900 Elite) and echocardiography (Philips IE33) was performed four weeks after surgery. Six animals which were successfully modelled were randomly divided into a model-blank group ($n=3$) and a model-dose group ($n=3$). The other three animals without undergoing surgery were assigned to the normal-dose group. Then Danshen decoction administration was begun in the model-dose group and normal-dose group with the dose of 0.33 g/kg and lasted for four weeks. This choice of dosage was based on a clinical daily dosage of 20 g/60 kg (Figure 2).

2.5. Evaluation of Danshen Decoction Effect on Heart Function. Echocardiography was assessed four weeks after surgery and four weeks after administration for each animal, and ejection fraction (EF) and fractional shortening (FS) were obtained by the software.

2.6. Tissue Section Preparation. After four weeks of administration, tissues including the kidney, spleen, lung, heart, and liver were harvested from each animal. After washing with PBS, tissues were cut into suitable pieces: kidney ($10 \times 10 \times 8$ mm), spleen ($10 \times 10 \times 5$ mm), lung ($10 \times 10 \times 5$ mm), heart ($10 \times 10 \times 8$ mm), and liver ($10 \times 10 \times 8$ mm) according to their physiological characteristics, and prepared to be sliced. After embedding the tissues in optimal cutting temperature (OCT) compounds, they were sliced to a thickness of 6 μm at -20°C using a cryomicrotome (CM3600, Leica Microsystems GmbH). Five sections of each tissue were sliced for distribution analysis. Five more sections of each kidney tissue from the normal-dose group were sliced for the stability study. All tissue sections were kept frozen at -80°C until analysed.

2.7. Stability Study

2.7.1. Conditions for Stability Study. 12 kidney tissue sections were randomly selected from the -80°C freezer after being frozen for 12 h and then were preprocessed in four

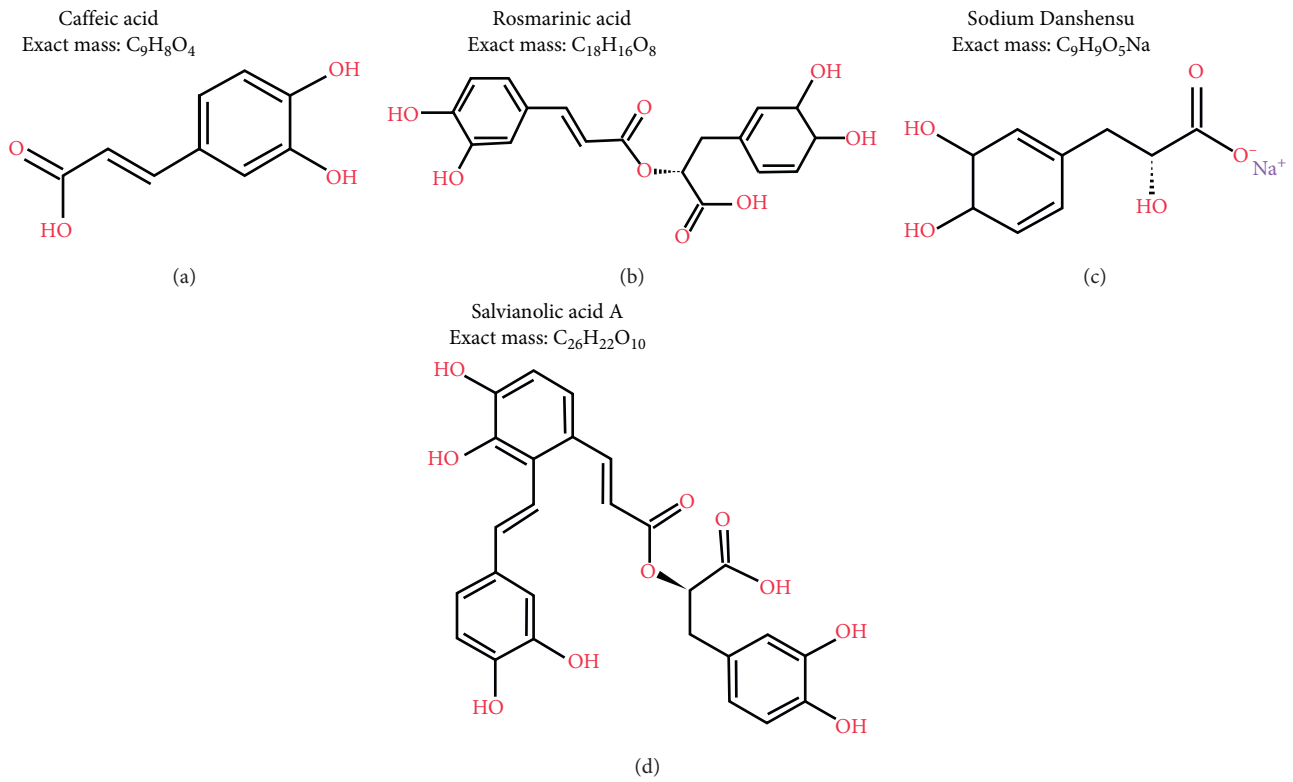


FIGURE 1: Chemical structures of the compounds investigated in this study.

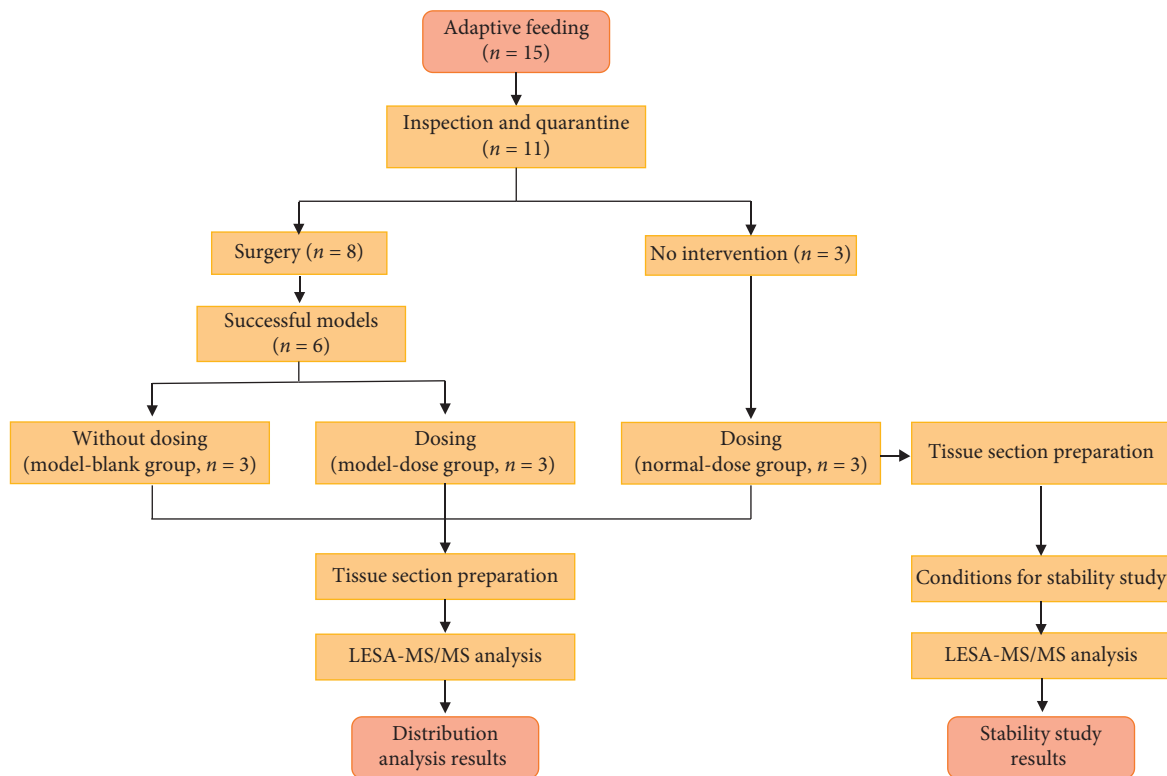


FIGURE 2: Study design and procedures.

conditions as described below. Each condition used three sections to detect.

For normal experimental conditions, three tissue sections were rewarmed at room temperature for 30 min. For a repeated rewarming stability investigation, three tissue sections were rewarmed at room temperature for 30 min, then refrozen at -80°C for 12 h, and rewarmed again. This procedure was repeated three times. The third three tissue sections were used in a long-term frozen stability investigation. Sections were stored in a -80°C freezer for 14 days and rewarmed at room temperature for 30 min. The final three tissue sections were used in a stability study of short-term placement at room temperature for 24 h.

2.7.2. LESA-MS/MS Analysis. Tissue sections were analysed on a TriVersa NanoMate (Advion Inc., Ithaca, NY, USA) with a LESA instrument coupled to a 5500 QTRAP MS (AB Sciex, Concord, Ontario). Three points on the preprocessed tissue section were selected for LESA-MS/MS analysis, and the average signal intensity of these points was taken as the detection result. Tissue sections were fixed on the LESA universal adapter plate and scanned by an Epson Perfection V370 scanner. The pictures were processed further by LESA Points software to generate sampling locations and automatic injection. A conductive pipette tip was picked up by the robotic arm of the TriVersa NanoMate to aspirate $1.7\ \mu\text{L}$ of solvent (80/19.9/0.1 v/v/v, methanol:water:ammonium hydroxide). For salvianolic acids, methanol/formic acid and methanol/ammonium hydroxide combinations with water were investigated. An extraction solution of 80/19.9/0.1 methanol/water/ammonium hydroxide (v/v/v) gave the highest analyte response. Subsequently, the tip was placed over specific sampling locations and $0.7\ \mu\text{L}$ of solvent was dispensed onto the surface of the tissue. The liquid junction between the tissue and the pipette tip was maintained for 2 s for analyte extraction, and then the liquid was aspirated back into the tip. The dispensing/aspirating cycle was repeated two more times. After extraction, the analyte was infused into the MS through a multichannel nanoelectrospray ionization (ESI) chip (Advion Inc., Ithaca, NY, USA). A new pipette tip and chip nozzle were used for every sampling location to eliminate cross-contamination.

ESI flow rate was estimated to be 400–500 nL/min. A spray voltage of 1.7 kV and a gas pressure of 0.7 psi were applied in all experiments. Multiple reaction monitoring (MRM) in negative ion mode was used for transitions at the following m/z values: DSS $196.8 \rightarrow 135.0$, CAA $179.0 \rightarrow 107.0$, RA $359.1 \rightarrow 161.0$, and SAA $493.2 \rightarrow 295.0$ [9, 10]. The MS parameters were as follows: curtain gas pressure, 10 psi; collision gas pressure, medium; delustering potential, 120 V; entrance potential, 10 V; collision energy, 25 eV; collision cell exit potential, 16 V; and dwell time, 50 ms.

2.8. Distribution Analysis. Distribution analysis was performed in the kidney, spleen, lung, heart (ischemic marginal zone of the myocardium), and liver. Three sections of each tissue from each animal were randomly selected for the

detection process. The detection process was consistent with the stability study. The experiment was repeated in three animals in each group, and the average signal intensity was taken as the final detection result.

2.9. Statistical Analysis. Data were collected using Analyst 1.6.2 software (AB Sciex), and statistical analysis was performed with SPSS version 20.0. All data are presented as the mean \pm standard deviation. Statistical analysis was carried out on three or more groups using one-way analysis of variance and Dunnett's test. Statistical analysis of data from repeats was performed by repeated-measures analysis. Values of $P < 0.05$ were considered statistically significant.

3. Results

3.1. Model Assessment. Four weeks after surgery, coronary angiography showed that the rate of coronary artery stenosis in eight miniature pigs was 100% (see Figure S6 in the Supplementary Material). Echocardiography showed that the EF of six animals was less than 60% (see Figure S7 in the Supplementary Material), which supported the diagnosis of myocardial ischemia.

3.2. Effects of Danshen Decoction on Heart Function. Four weeks after surgery, the EF and FS of pigs in the model-blank group and the model-dose group were significantly lower than those in the normal-dose group ($P < 0.01$). There was no significant difference in the EF and FS between the two model groups ($P > 0.05$). After treated with Danshen decoction for four weeks, EF and FS of pigs in the model-dose group were improved significantly than before ($P < 0.05$) and had obvious differences when compared with the model-blank group ($P < 0.01$) (Figure 3).

3.3. Stability Study Results. A sphericity test was performed before analysing the correlation between repeated data. There was no correlation between repeated data in this experiment ($P > 0.05$), and the measured data conformed to the Huynh–Feldt condition. Therefore, one-way analysis of variance was used for statistical analysis. There were no significant differences in signal intensities of DSS, CAA, and SAA under four conditions ($P > 0.05$). RA signal intensity showed lower level after preserving under room temperature for 24 h ($P < 0.05$, $P = 0.047$) compared with normal experimental conditions (Figure 4).

3.4. Distributions of the Four Salvianolic Acids

3.4.1. Distribution of CAA in Different Tissues. The CAA signal intensities in samples from the heart, spleen, kidney, lung, and liver were analysed. Both the model-dose group and normal-dose group showed significantly higher CAA signal intensities than the model-blank group in the heart, spleen, kidney, and lung ($P < 0.05$ or $P < 0.01$). Liver samples from the model-dose group had higher CAA signal intensities than those from the model-blank group ($P < 0.01$), but

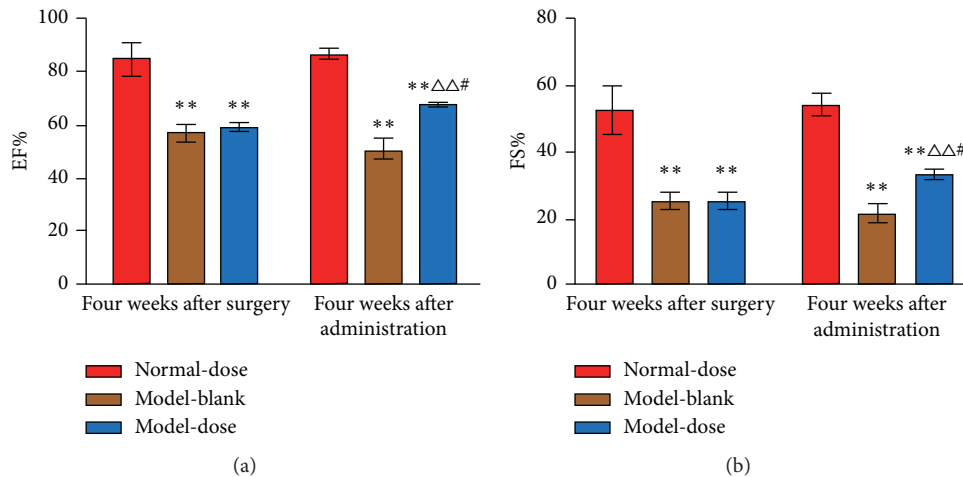


FIGURE 3: Echocardiography results at different time points between groups. (a) Ejection fractions at different time points between groups. (b) Fractional shortening at different time points between groups. EF: ejection fractions; FS: fractional shortening; Normal-dose: normal-dose group; Model-blank: model-blank group; Model-dose: model-dose group. ** $P < 0.01$ vs. normal-dose group. $\Delta P < 0.01$ vs. model-blank group. # $P < 0.05$ vs. model-dose group at four weeks after surgery.

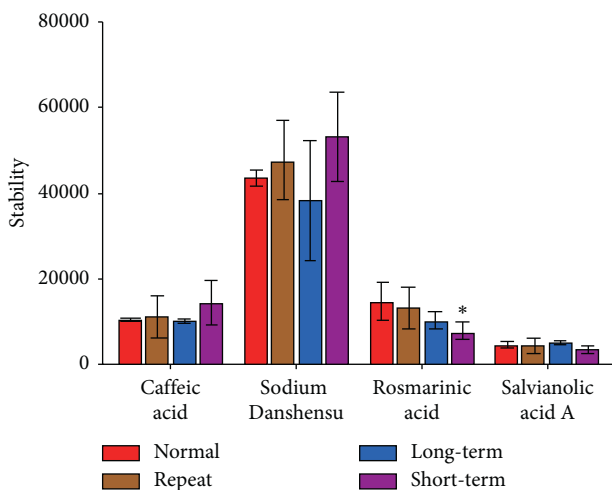


FIGURE 4: Comparison of the signal intensities for the four compounds under different storage conditions. Normal: normal experimental conditions; Repeat: after repeated rewarming for three times; Long-term: after long-term stored in a -80°C freezer; Short-term: after short-term placement at room temperature. * $P < 0.05$ vs. normal experimental conditions.

a significant difference was not observed between the normal-dose group and the model-blank group. There was no statistical difference in CAA signal intensities between the model-dose group and normal-dose group. Moreover, compared with other tissues, the spleen had the highest signal intensity of CAA (Figure 5(a)).

3.4.2. Distribution of DSS in Different Tissues. Kidney, lung, liver, and heart samples from the model-dose group and kidney, liver, spleen samples from the normal-dose group showed higher DSS signal intensities than those from the model-blank group ($P < 0.05$ or $P < 0.01$). Compared with the normal-dose group, the signal intensities of DSS were

significantly higher in the kidney and liver in the model-dose group ($P < 0.01$). Kidney had the highest DSS signal intensity compared with other tissues (Figure 5(b)).

3.4.3. Distribution of RA in Different Tissues. Compared with the model-blank group, both the normal-dose group and model-dose group had higher RA signal intensities in the liver, spleen, kidney, heart, and lung ($P < 0.05$ or $P < 0.01$). Compared with the normal-dose group, liver and kidney samples showed lower signal intensities of RA in the model-dose group ($P < 0.05$ or $P < 0.01$). Samples from the normal-dose group were observed that the liver had the highest RA signal intensity; however, it was not observed in the model-dose group (Figure 5(c)).

3.4.4. Distribution of SAA in Different Tissues. Compared with the model-blank group, liver, kidney, and spleen samples from the normal-dose group and heart, kidney, and spleen samples from the model-dose group showed higher SAA signal intensities ($P < 0.05$ or $P < 0.01$). Significant differences were observed in liver and heart samples between the normal-dose group and model-dose group ($P < 0.05$ or $P < 0.01$). The model-dose group showed higher SAA signal intensities in the heart samples ($P < 0.05$) and lower intensities in liver samples than the normal-dose group ($P < 0.01$). Compared with other tissues, liver tissues had the highest SAA signal intensity (Figure 5(d)).

4. Discussion

The Danshen decoction used in the present study has been reported to commonly use in promoting blood circulation and removing blood stasis [11], with a simple composition as *Salvia miltiorrhiza* Bunge, *Amomum villosum* Lour, and *Santalum album* L. The main chemical components of *Salvia miltiorrhiza* Bunge include lipo- and water-soluble

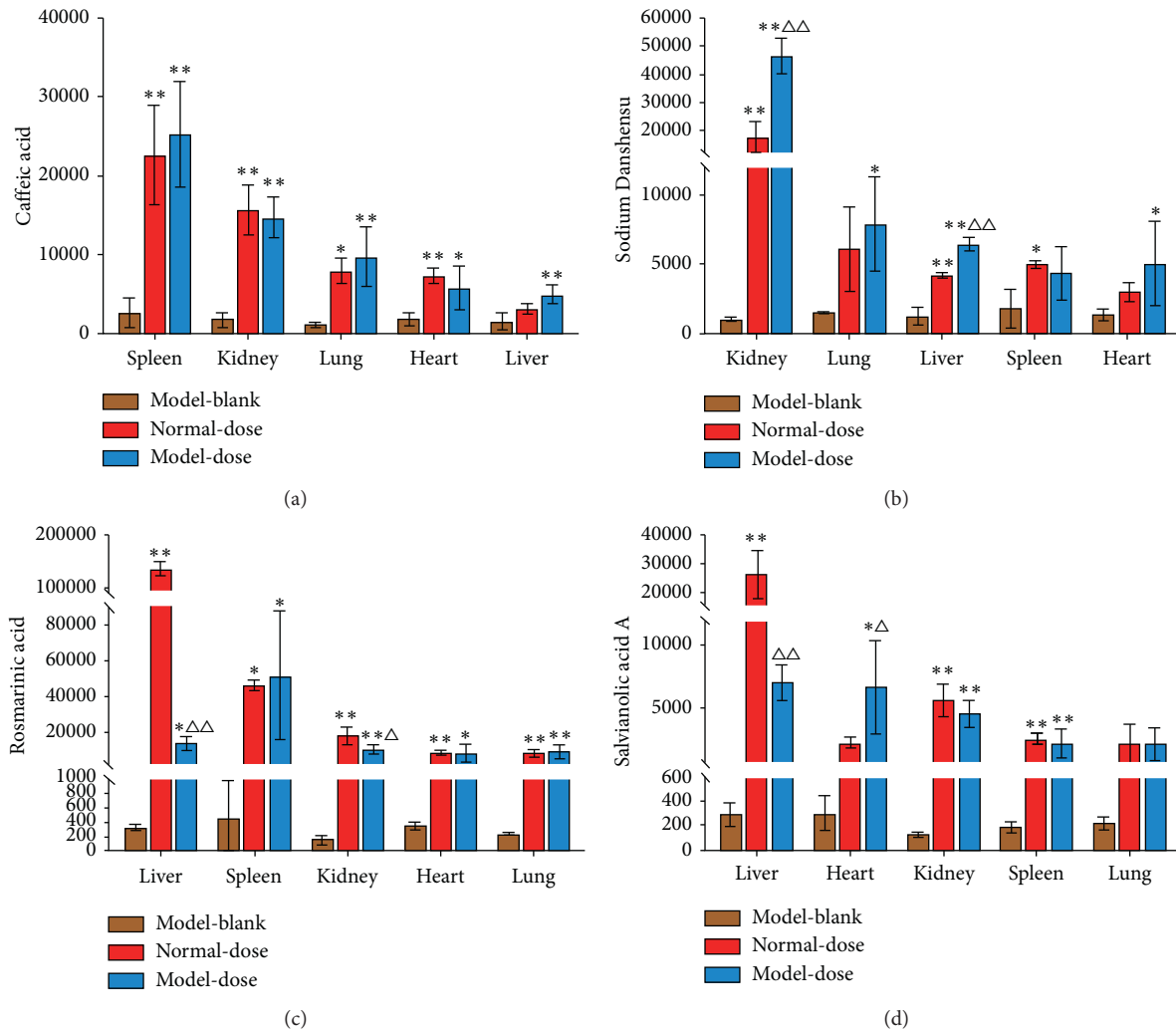


FIGURE 5: Signal intensities of four salvianolic acids in different tissues and groups. (a) Signal intensities of caffeic acid in different tissues and groups. (b) Signal intensities of Danshensu in different tissues and groups. (c) Signal intensities of rosmarinic acid in different tissues and groups. (d) Signal intensities of salvianolic acid A in different tissues and groups. Model-blank: model-blank group; Normal-dose: normal-dose group; Model-dose: model-dose group. * $P < 0.05$, ** $P < 0.01$ vs. model-blank group. $\Delta P < 0.05$, $\Delta\Delta P < 0.01$ vs. normal-dose group.

components. Most of the liposoluble components are conjugated quinones and ketones. The water-soluble components are mainly phenolic acids such as CAA, DSS, RA, and SAA [4, 5]. Pharmacological studies have suggested that there were small quantities of liposoluble components such as tanshinone II-A and cryptotanshinone in *Salvia miltiorrhiza* Bunge [10]. Therefore, we presumed that the liposoluble components of *Salvia miltiorrhiza* Bunge would have little correlation with its traditional therapeutic effects and that the water-soluble components would be the main contributors [12].

Studies have shown that DSS could greatly improve blood rheology, lower lipid levels, inhibit lipid peroxidation, and have antitumour and other pharmacological activities [13]. SAA has protective effects on acute kidney injury induced by ischemia-reperfusion injury [14] and can greatly attenuate monocrotaline-induced hypertrophic damage of the myocardium, parenchymal injury, and collagen deposition in the lungs [15]. RA reportedly has a therapeutic

effect on type 2 diabetes and hyperlipidaemia [16]. Studies have shown that CAA ameliorates cardiac damage in isoproterenol-induced myocardial infarction by maintaining lipid peroxide metabolism because of its free radical scavenging and antioxidant effects [17].

In the present study, after four weeks of administration of Danshen decoction, EF and FS were improved obviously in the model-dose group, which confirmed that Danshen decoction could improve the ischemic condition in a chronic myocardial ischemia model.

In addition, an HPLC-MS/MS method had been established in our previous study to determine the concentration of sodium Danshensu, protocatechualdehyde, caffeic acid, rosmarinic acid, and salvianolic acid A in rat plasma [18]. The results showed that the contents of the five compounds in blood were stable and were sufficient to detect. However, in the preliminary experiment of LESA-MS/MS, the signal intensity of protocatechualdehyde in the tissue was extremely low, so it was not included.

LESA-MS/MS was applied to analyse the distributions of four salvianolic acids. A stability investigation showed that DSS, CAA, and SAA were stable under four experimental conditions, but RA had a poor stability when placed at room temperature for 24 h. However, the samples were usually tested within 2 h of removal from the -80°C freezer. This short time out of the freezer might have little effect on the samples, and the results would be reliable for the distribution study.

Subsequently, distribution analysis showed that the signal intensities of DSS in the liver and kidney and SAA in the heart were higher in the model-dose group than in the normal-dose group. The reason for this might be that DSS has strong water solubility, and the liver and kidney are the main metabolic organs for DSS. It is reported that there is obvious inflammatory cell infiltration and an abnormal increase of vascular permeability in the ischemic zone of the myocardium [19]. The signal intensities of SAA in other organs decreased but increased particularly in the heart, indicating that myocardial ischemia would promote the transfer of SAA from other positions to the heart. The contents of the two salvianolic acids in the targets increased, which is basically consistent with the statement in Ben Cao Zheng that “Danshen is the medicine of heart, spleen, liver, and kidney” and is another proof of the effectiveness of Danshen decoction. These results have been confirmed in other studies. Zhang et al. [20] have found that DSS may have hepatic-protective effects on iron overload mice, and the experiment conducted by Gao et al. [21] suggested that DSS treatment in diabetic mice could help improve the renal clearance. It is reported that SAA protects the myocardium in canine experimental myocardial infarction models. Both oral and intravenous administration of SAA reduced the myocardial infarct area significantly [22]. A meta-analysis including 14 research studies demonstrated that salvianolic acids could exert cardioprotection through promoting angiogenesis in animal models of myocardial infarction [23].

Recently, several studies have analysed salvianolic acids using diverse analytical methods including liquid chromatography with ultraviolet detection (LC-UV), online solid-phase extraction coupled in series to liquid chromatography-tandem mass spectrometry (SPE-LC-MS), high-performance liquid chromatography-diode array detection (HPLC-DAD), HPLC-MS [24], high-speed countercurrent chromatography (HSCCC), and ESI-MS [25]. Although these methods are mature, pretreatment of the samples is always required, which leads to the inevitable loss of spatial information during the homogenization process [26]. LESA-MS/MS is a surface sampling technique that combines extraction of liquid from the tissue surface with nano-ESI-MS which can be used for spatial analysis of drug distributions and has been used historically to describe discrete points on the surfaces of tissue slices [27]. To date, no research has been conducted on salvianolic acids using nano-ESI-MS. Compared with other imaging-capable methods such as quantitative whole-body autoradiography and matrix-assisted laser desorption/ionization-MSI, LESA-MS/MS not only provides spatial distribution information for tissues but also greatly simplifies the pretreatment procedures and shortens the analysis time [26].

As a fully automated, chip-based multichannel MS method, LESA-MS/MS combines microliquid extraction from a solid surface and nano-ESI analysis to obtain information from tissue sections of interest [28]. Studies have shown that the quantitative and spatial distributions of exogenous chloroquine (CHQ) and CHQ metabolites in tissue slices can be rapidly and accurately analysed by LESA-MS/MS without extensive sample preparation such as tissue homogenization or HPLC separation. The results from LESA-MS/MS correlated well with those obtained by LC-MS [29].

5. Conclusions

Danshen decoction has the effect of improving the ischemic condition in a chronic myocardial ischemia model and is basically distributed in the heart, liver, and kidney, which is worth further clinical study. A LESA-MS/MS method was applied for the simultaneous determination of four salvianolic acids (CAA, DSS, RA, and SAA) in animal tissues. The method has characteristics in simple pretreatment of samples, sensitivity, and stability, which showed to be worthy of further application on drug distribution research studies.

Abbreviations

TCM:	Traditional Chinese medicine
LESA-MS/MS:	Liquid extraction surface analysis coupled with tandem mass spectrometry
DSS:	Danshensu
CAA:	Caffeic acid
RA:	Rosmarinic acid
SAA:	Salvianolic acid A
EF:	Ejection fraction
FS:	Fractional shortening
HPLC:	High-performance liquid chromatography
OCT:	Optimal cutting temperature
MRM:	Multiple reaction monitoring
LC-UV:	Liquid chromatography with ultraviolet detection
SPE-LC-MS:	Solid-phase extraction coupled in series to liquid chromatography-tandem mass spectrometry
HPLC-DAD:	High-performance liquid chromatography-diode array detection
HSCCC:	High-speed countercurrent chromatography
MSI:	Mass spectrometry imaging
CHQ:	Chloroquine
LC-MS:	Liquid chromatography coupled with mass spectrometry.

Data Availability

The data used to support the findings of this study are available from the corresponding author upon request.

Conflicts of Interest

The authors declare that there are no conflicts of interest regarding the publication of this paper.

Authors' Contributions

Qi Qiu and Yang Lin conceived and designed the experiments. Qi Qiu, Jinglin Cao, Yu Mu, and Yunnan Zhang performed the experiments. Jinglin Cao and Jing Li analysed the data. Xiujin Shi checked the results. Jinglin Cao, Yu Mu, Qi Qiu, and Yang Lin revised the manuscript. Qi Qiu, Jinglin Cao, Yu Mu, and Yang Lin are joint first authors and contributed equally to this article.

Acknowledgments

This work was supported by the National Major Scientific and Technological Special Project for "Significant New Drugs Development" during the Thirteenth Five-year Plan Period (grant number 2017ZX09304017), the National Natural Science Foundation of China (grant numbers 81403200 and 81541169), and Beijing Hospitals Authority "Qing Miao" Program (grant number QML20150603). The authors are grateful to Yi Tian, from the Department of Nuclear Medicine of Beijing Anzhen Hospital, for establishing animal models in the present study, Mei-Juan Yang, from Beijing University of Chinese Medicine, for preparing the frozen tissue section, and Gabrielle David, PhD, from Liwen Bianji, Edanz Group China (www.liwenbianji.cn/ac), for editing the English text of a draft of this manuscript.

Supplementary Materials

Supplemental Figure 1: the linear graph of salvianolic acids. Supplemental Figure 2: HPLC chromatogram of caffeic acid. Supplemental Figure 3: HPLC chromatogram of rosmarinic acid. Supplemental Figure 4: HPLC chromatogram of salvianolic acid A. Supplemental Figure 5: HPLC chromatogram of Danshensu. Supplemental Figure 6: coronary angiography results four weeks after surgery. Supplemental Figure 7: echocardiography results at different time points. (A) Before left anterior descending ligation. (B) Four weeks after left anterior descending ligation, before administration. (C) Eight weeks after left anterior descending ligation, four weeks after administration. (*Supplementary Materials*)

References

- [1] G. A. Roth, C. Johnson, A. Abajobir, F. Abd-Allah, S. F. Abera, and G. Abyu, "Global, regional, and national burden of cardiovascular diseases for 10 causes, 1990 to 2015," *Journal of the American College of Cardiology*, vol. 70, pp. 1–25, 2017.
- [2] M. Zhou, H. Wang, X. Zeng et al., "Mortality, morbidity, and risk factors in China and its provinces, 1990–2017: a systematic analysis for the Global Burden of Disease Study 2017," *The Lancet*, vol. 394, no. 10204, pp. 1145–1158, 2019.
- [3] D. Y. Kong, "Chemical constituents of salvia miltiorrhiza (dan-shen)," *Chinese Journal of Pharmaceuticals*, vol. 33, pp. 279–285, 1989.
- [4] H. Liu, S. Ma, H. Xia, H. Lou, F. Zhu, and L. Sun, "Anti-inflammatory activities and potential mechanisms of phenolic acids isolated from *Salvia miltiorrhiza* f. *alba* roots in THP-1 macrophages," *Journal of Ethnopharmacology*, vol. 222, pp. 201–207, 2018.
- [5] Y. H. Wang, X. Q. Su, D. K. Li et al., "Study on water-soluble pigments of *salvia miltiorrhiza*," *Research and Practice on Chinese Medicines*, vol. 31, pp. 65–69, 2017.
- [6] F. F. Y. Lam, J. H. K. Yeung, J. H. Y. Cheung, and P. M. Y. Or, "Pharmacological evidence for calcium channel inhibition by danshen (*Salvia miltiorrhiza*) on rat isolated femoral artery," *Journal of Cardiovascular Pharmacology*, vol. 47, no. 1, pp. 139–145, 2006.
- [7] L. Li, B. A. Josef, B. Liu, S. Zheng, L. Huang, and S. Chen, "Three-dimensional evaluation on ecotypic diversity of traditional Chinese medicine: a case study of *Artemisia annua* L.," *Frontiers in Plant Science*, vol. 8, p. 1225, 2017.
- [8] Q. Qiu, Y. Lin, C. Xiao et al., "Time-course of the effects of QSYQ in promoting heart function in ameroid constrictor-induced myocardial ischemia pigs," *Evidence-Based Complementary and Alternative Medicine*, vol. 2014, Article ID 571076, 13 pages, 2014.
- [9] X. F. Lin, L. Li, Y. Zhang, M. Q. Sun, C. Y. Ren, and J. X. Liu, "Methodological study of five kinds of phenolic acids from *salvia miltiorrhiza* extract in rat plasma by LC-MS/MS," *Chinese Journal of Experimental Traditional Medical Formulae*, vol. 21, pp. 93–96, 2015.
- [10] H. Zeng, S. Su, X. Xiang et al., "Comparative analysis of the major chemical constituents in *Salvia miltiorrhiza* roots, stems, leaves and flowers during different growth periods by UPLC-TQ-MS/MS and HPLC-ELSD methods," *Molecules*, vol. 22, no. 5, p. 771, 2017.
- [11] Y.-x. Fei, S.-q. Wang, L.-j. Yang et al., "*Salvia miltiorrhiza* Bunge (Danshen) extract attenuates permanent cerebral ischemia through inhibiting platelet activation in rats," *Journal of Ethnopharmacology*, vol. 207, pp. 57–66, 2017.
- [12] J. Y. Wang, W. Z. Hou, Y. J. Wei et al., "A new method on investigate chemical constituents which have anti-thrombin effect by HPLC," *China Journal of Chinese Materia Medica*, vol. 41, pp. 2855–2860, 2016.
- [13] L. Hua, S. Wang, B. Zhang, Y. Xie, and Q. Yang, "Pharmacological action and pharmacokinetics of danshensu," *Northwest Pharmaceutical Journal*, vol. 26, pp. 310–312, 2011.
- [14] Z. Zhang, D. Qi, X. Wang et al., "Protective effect of Salvianolic acid A on ischaemia-reperfusion acute kidney injury in rats through protecting against peritubular capillary endothelium damages," *Phytotherapy Research*, vol. 32, no. 1, pp. 103–114, 2017.
- [15] Y.-c. Chen, T.-y. Yuan, H.-f. Zhang et al., "Salvianolic acid A attenuates vascular remodeling in a pulmonary arterial hypertension rat model," *Acta Pharmacologica Sinica*, vol. 37, no. 6, pp. 772–782, 2016.
- [16] A. M. Popov, O. N. Krivoshapko, A. A. Klimovich, and A. A. Artyukov, "Biological activity and mechanisms of therapeutic action of rosmarinic acid, luteolin and its sulphated derivatives," *Biomeditsinskaya Khimiya*, vol. 62, no. 1, pp. 22–30, 2016.
- [17] K. S. Kumaran and P. S. M. Prince, "Protective effect of caffeic acid on cardiac markers and lipid peroxide metabolism in cardiotoxic rats: an in vivo and in vitro study," *Metabolism*, vol. 59, no. 8, pp. 1172–1180, 2010.
- [18] Y. M. Zheng, Q. Qiu, S. L. Cao et al., "Simultaneous determination of sodium danshensu, protocatechualdehyde and caffeic acid, rosmarinic acid and salvianolic acid A in the plasma of rats by HPLC—MS/MS method," *Chin J Clin Pharmacol*, vol. 31, pp. 297–299+303, 2015.
- [19] N. G. Frangogiannis, "Pathophysiology of myocardial infarction," *Comprehensive Physiology*, vol. 5, pp. 1841–1875, 2015.

- [20] Y. Zhang, G. Zhang, Y. Liang et al., "Potential mechanisms underlying the hepatic-protective effects of danshensu on iron overload mice," *Biological and Pharmaceutical Bulletin*, vol. 43, no. 6, pp. 968–975, 2020.
- [21] L. Gao, Y. W. Kwan, A. C. Bulmer, and C. W. K. Lai, "Noninvasive real-time characterization of renal clearance kinetics in diabetic mice after receiving danshensu treatment," *Oxidative Medicine and Cellular Longevity*, vol. 2018, Article ID 8267560, 10 pages, 2018.
- [22] L. Li, J. X. Ren, Z. R. Lin, Y. Shi, Y. L. Ma, and J. X. Liu, "Effect of salvianolic acid A on anesthetized canine experimental myocardial infarction," *Zhong Guo Zhong Yao Za Zhi*, vol. 41, pp. 910–916, 2016.
- [23] L. J. Yu, K. J. Zhang, J. Z. Zhu et al., "Salvianolic acid exerts cardioprotection through promoting angiogenesis in animal models of acute myocardial infarction: preclinical evidence," *Oxidative Medicine and Cellular Longevity*, vol. 2017, Article ID 8192383, 11 pages, 2017.
- [24] J. Zhang, Y. He, M. Cui et al., "Metabolic studies on the total phenolic acids from the roots of *Salvia miltiorrhiza* in rats," *Biomedical Chromatography*, vol. 19, no. 1, pp. 51–59, 2005.
- [25] J. Chen, F. Wang, S. C. Lee, X. Wang, and M. Xie, "Separation and identification of water-soluble salvianolic acids from *Salvia miltiorrhiza* Bunge by high-speed counter-current chromatography and ESI-MS analysis," *Talanta*, vol. 69, no. 1, pp. 172–179, 2006.
- [26] J. G. Swales, N. Strittmatter, J. W. Tucker, M. R. Clench, P. J. H. Webborn, and R. J. A. Goodwin, "Spatial quantitation of drugs in tissues using liquid extraction surface analysis mass spectrometry imaging," *Scientific Reports*, vol. 6, Article ID 37648, 2016.
- [27] J. G. Swales, J. W. Tucker, M. J. Spreadborough et al., "Mapping drug distribution in brain tissue using liquid extraction surface analysis mass spectrometry imaging," *Analytical Chemistry*, vol. 87, no. 19, pp. 10146–10152, 2015.
- [28] D. Eikel, M. Vavrek, S. Smith et al., "Liquid extraction surface analysis mass spectrometry (LESA-MS) as a novel profiling tool for drug distribution and metabolism analysis: the terfenadine example," *Rapid Communications in Mass Spectrometry*, vol. 25, no. 23, pp. 3587–3596, 2011.
- [29] W. B. Parson, S. L. Koeniger, R. W. Johnson et al., "Analysis of chloroquine and metabolites directly from whole-body animal tissue sections by liquid extraction surface analysis (LESA) and tandem mass spectrometry," *Journal of Mass Spectrometry*, vol. 47, no. 11, pp. 1420–1428, 2012.

Research Article

Herbal Medicine (Sihogayonggolmoryeo-Tang or Chai-Hu-Jia-Long-Gu-Mu-Li-Tang) for Treating Hypertension: A Systematic Review and Meta-Analysis

Boram Lee ¹ and Chan-Young Kwon ²

¹Clinical Medicine Division, Korea Institute of Oriental Medicine, 1672 Yuseongdae-ro, Yuseong-gu, Daejeon 34054, Republic of Korea

²Department of Oriental Neuropsychiatry, Dong-eui University College of Korean Medicine, 62 Yangjeong-ro, Busanjin-gu, Busan 47227, Republic of Korea

Correspondence should be addressed to Boram Lee; qhfka9357@naver.com

Received 14 July 2020; Accepted 27 August 2020; Published 9 September 2020

Academic Editor: Hong Chang

Copyright © 2020 Boram Lee and Chan-Young Kwon. This is an open access article distributed under the Creative Commons Attribution License, which permits unrestricted use, distribution, and reproduction in any medium, provided the original work is properly cited.

Introduction. For situations in which effective and safe natural-derived products to treat hypertension are needed, recent studies suggest that an herbal medicine, Sihogayonggolmoryeo-tang (SYM), can improve both hypertension and concurrent mood symptoms. We aimed to evaluate the effectiveness and safety of SYM in treating hypertension. **Methods.** Thirteen English, Korean, and Chinese databases were comprehensively searched from their inception to May 2020. Randomized controlled trials (RCTs) using SYM as a monotherapy or adjunctive therapy for hypertension were evaluated. The primary outcome was the systolic and diastolic blood pressure (BP). Descriptive analyses of the relevant data were conducted, and where appropriate data were available, a meta-analysis was performed, and the results were presented as a risk ratio or mean difference with 95% confidence intervals. The risk of bias was assessed using the Cochrane risk of bias tool, and the quality of evidence was evaluated using the Grading of Recommendations, Assessment, Development and Evaluation (GRADE) approach. **Results.** Seven RCTs with 711 participants were included. Compared with placebo, SYM significantly lowered systolic and diastolic BP and concurrent depression. SYM significantly lowered systolic and diastolic BP compared with active controls; however, subgroup analysis revealed no differences between SYM and antihypertensives. In addition, SYM significantly decreased the level of concurrent depression compared with antidepressants. There was no consistent difference in BP reduction between SYM combined with antihypertensives and antihypertensives alone. No serious adverse events were reported following SYM administration. Most of the included studies had an unclear risk of bias, and the quality of evidence was generally rated “low.” **Conclusion.** Current evidence suggests that SYM may have the potential to lower hypertension and concurrent depressive symptoms without serious adverse events. Additional high-quality, placebo-controlled RCTs should be conducted to confirm the efficacy of SYM.

1. Introduction

Hypertension is a major public health challenge worldwide. It is strongly associated with potentially severe conditions including cardiovascular disease and premature death [1]. According to a comprehensive systematic analysis, the proportion of ischemic heart disease disability-adjusted life years attributable to high blood pressure (BP) was 53% in 2010 [2]. In the study, high BP was identified as the leading

risk factor that affects the global disease burden, followed by tobacco smoking and alcohol use [2]. The prevalence of hypertension in adults worldwide in 2010 was estimated at 31.1% [3], but the proportion of patients treated and/or managed with proper medication is still low [4]. In addition, about 1 in 5 patients have apparent treatment-resistant hypertension, which is unresponsive to adequate antihypertensives [5]. More than 20% of hypertension patients taking antihypertensives experience side effects such as

impotence and emotional distress [6], which are the primary determinants of low adherence to antihypertensives [7]. Decreasing sodium intake, weight loss, increasing physical activity, decreasing alcohol intake, and eating a healthy diet including the Dietary Approaches to Stop Hypertension (DASH) diet are healthy lifestyle strategies to reduce the risk of hypertension [8]. However, the development of hypertension due to poor lifestyle habits such as sedentary behavior is still frequently reported [9]. In other words, hypertension remains a major public health issue, and conventional treatment and management strategies still need to be improved.

Some hypertensive patients are interested in complementary and alternative medicine (CAM) modalities. According to the 2012 National Health Interview Survey and the Adult Alternative Medicine supplement, a combination of hypercholesterolemia, hypertension, diabetes, and obesity as dyads and triads was significantly related to the increased use of CAM such as mind-body interventions, manipulative methods, and energy therapies [10]. It has been reported that some supplements/foods including coenzyme Q10, vitamin D, and polyphenol-rich dark chocolate, and mind-body medicine including qigong, breathing, and meditation may be helpful for reducing BP [11]. Herbal medicine (HM) has been used as a treatment approach in East Asian traditional medicine (EATM) to treat various medical conditions including hypertension-related symptoms for thousands of years in East Asia. Today, HM is receiving much attention as an option to replace or supplement conventional medicines, and its effectiveness has already been demonstrated in some diseases including cardiovascular disease and hypertension [12–14].

Sihogayonggolmoryeo-tang (SYM) is a traditional HM used to treat insomnia, anxiety, irritability, and hypertension-related symptoms. In particular, since this HM is well-known for its mood-stabilizing effects [15–17], it may be helpful in improving not only hypertension but also concurrent mood symptoms. In addition, preclinical evidence suggests that SYM can exert a protective effect on the cardiovascular system by enhancing the function of endothelial progenitor cells, inducing antioxidant effects, and inhibiting vasoconstriction [18–20]. However, the efficacy of SYM in the treatment of hypertensive patients has not been systematically summarized and evaluated. Therefore, we aimed to synthesize the available evidence related to the effectiveness and safety of SYM as a monotherapy or adjunctive therapy for patients with hypertension and to assess the methodological quality of these studies to help clinicians establish evidence-based treatment strategies.

2. Materials and Methods

The protocol for this review was registered in the International Prospective Register of Systematic Reviews, PROSPERO (registration number: CRD42020187174). We reported this review in accordance with the Preferred Reporting Items for Systematic Reviews and Meta-Analyses statement [21]. Additionally, we followed the methods of Dr. Lee [22].

2.1. Data Sources and Search Strategy. One researcher (BL) comprehensively searched total 13 electronic databases on May 19, 2020: 5 English databases (Medline (via PubMed), EMBASE (via Elsevier), the Cochrane Central Register of Controlled Trials (CENTRAL), the Allied and Complementary Medicine Database (AMED) (via EBSCO), and the Cumulative Index to Nursing and Allied Health Literature (CINAHL) (via EBSCO)), five Korean databases (Oriental Medicine Advanced Searching Integrated System (OASIS), Korean studies Information Service System (KISS), Research Information Service System (RISS), Korean Medical Database (KMBase), and Korea Citation Index (KCI)), and three Chinese databases (China National Knowledge Infrastructure (CNKI), Wanfang data, and VIP). We also searched the reference lists of included studies and Google Scholar to identify additional eligible studies. Grey literature such as degree theses was also included. No language, publication date, and publication status restrictions were imposed. The following search terms were used in PubMed: Hypertension [MH] OR hypertens * [TIAB] OR “blood pressure” [MH] OR “blood pressure” [TIAB] OR blood pressure [TIAB] AND Chai-Hu-Jia-Long-Gu-Mu-Li-Tang [TIAB] OR Chai-Hu-Jia-Long-Gu-Mu-Li-Wan [TIAB] OR Chai-Hu-Jia-Long-Gu-Mu-Li-Pian [TIAB] OR Saiko-ka-ryukotsu-borei-to [TIAB] OR Saiko-ka-ryukotsu-borei-to [TIAB] OR Sihogayonggolmoryeo-tang [TIAB] (Supplement 1).

2.2. Inclusion Criteria

2.2.1. Types of Studies. We included only randomized controlled trials (RCTs). We also included RCTs using the expression “randomization” without descriptions of the randomization methods. We excluded RCTs in which a quasirandom method was used for the allocation of treatments such as using alternate allocation or allocation by birth date.

2.2.2. Types of Participants. Studies on hypertension patients, diagnosed according to the international hypertension criteria, were included. There was no restriction on age, sex, race, or comorbidity of participants. We excluded trials that included patients suffering from other serious medical conditions such as cancer, liver disease, or kidney disease.

2.2.3. Types of Interventions. We included studies on SYM as a treatment intervention. HMs are known as “modified HMs” when the components are altered to achieve increased efficacy [23, 24]. Thus, we also included studies in which modified forms of SYM, described as “modified SYM” and containing more than 50% of the components of the original prescription, were used as treatment interventions. Modified SYM in the included studies must contain *Bupleuri Radix*, *Fossilia Osis Mastodi*, and *Ostreae Testa*, one of the most critical herbal components of SYM. For the dosage form, we considered only oral administration of SYM. Placebo, no treatment, and active controls such as conventional

medication were included as control interventions. Studies involving SYM combined with other therapies as treatment interventions were also included if the other therapies were equally used in both the treatment and control groups. However, we excluded studies comparing different types of HM. There was no restriction on the treatment duration of SYM.

2.2.4. Types of Outcome Measures. The primary outcome was the systolic BP (SBP) and diastolic BP (DBP) measured after treatment. The secondary outcomes included (1) symptoms associated with hypertension such as insomnia and anxiety after treatment, (2) total effective rate (TER), calculated secondarily based on improvements in BP or other clinical symptoms, (3) the incidence of adverse events during the study period, and (4) quality of life after treatment.

2.3. Study Selection and Data Extraction. We removed duplicates in the search results obtained from the databases and additional sources and screened the titles and abstracts for eligibility using EndNote X8. Afterward, we evaluated the full texts of the eligible articles for final inclusion. For the included studies, we extracted information related to the study characteristics (author, publication year, country, and study design); approval from institutional review boards; informed consent; sample size and the number of dropouts; details about the participants, intervention, and comparisons; duration of the intervention and follow-up; outcome measures; results; and adverse events using a standardized data collection form (Excel 2016, Microsoft, Redmond, WA, USA). We also extracted the components, dosage form, and administration duration and frequency of SYM. The corresponding authors of the included studies were contacted via e-mail if there were insufficient data.

One researcher (BL) performed the abovementioned study selection and data extraction procedures, and another researcher (CYK) cross-checked the process. Any disagreement was resolved through discussion between the researchers.

2.4. Quality Assessment. We evaluated the risk of bias for the included RCTs using the Cochrane Collaboration's risk of bias tool [25]. The studies were classified as "low risk," "unclear," or "high risk" for each of the following domains: random sequence generation, allocation concealment, blinding of participants and personnel, blinding of outcome assessments, completeness of outcome data, selective reporting, and other potential bias. We evaluated the other potential bias domain with an emphasis on possible baseline imbalances between the treatment and control groups, such as the baseline BP level.

Using the Grading of Recommendations, Assessment, Development and Evaluation (GRADE) approach, we evaluated the quality of evidence for major findings with the online program GRADEpro (<https://gradepro.org/>) [26]. The risk of bias, inconsistency, indirectness, and imprecision

of the results and the probability of publication bias were evaluated, and we classified the results into one of four groups: "very low," "low," "moderate," or "high."

One researcher (BL) conducted the abovementioned quality assessment, while another researcher (CYK) cross-checked the data. Any discrepancy was resolved through discussion between them.

2.5. Data Synthesis and Analysis. We conducted a narrative synthesis of the details of the participants, interventions, comparators, and outcomes for all included studies. In the case of primary or secondary outcome of this review, we quantitatively pooled the results using the Review Manager software, version 5.3 (Cochrane, London, UK). Continuous or dichotomous variables were pooled using mean differences (MD) or risk ratios (RRs), with 95% confidence intervals (CIs). We evaluated heterogeneity between the studies included in each meta-analysis in terms of the effect measures using both the χ^2 test and the I^2 statistic. I^2 values $\geq 50\%$ and $\geq 75\%$ were considered indicative of substantial and considerable heterogeneity. The meta-analyzed results were pooled using a random-effect model if the included studies had significant heterogeneity (an I^2 value $\geq 50\%$). A fixed-effect model was used when the heterogeneity was not significant or the number of studies included in the meta-analysis was very small, which leads to poor precision for the estimate of between-study variance [27, 28]. Subgroup analysis was conducted according to the type of active controls used. Sensitivity analyses were planned to identify the robustness of meta-analysis results by excluding [1] studies with high risks of bias and [2] outliers. We also planned to assess the evidence of publication bias using a funnel plot if there were enough studies.

3. Results

3.1. Description of Studies. A total of 104 articles were identified from searching 13 databases, and no records were identified through other sources. After removing 37 duplicates, 49 articles were excluded based on screening the titles and abstracts. Through the full-text evaluation, 11 articles, specifically five case reports, one review article, two non-RCTs, two non-SYM-related articles, and one article comparing two different HMs, were excluded. Therefore, seven articles [29–35] with 711 participants were included in the qualitative and quantitative synthesis (Figure 1).

3.2. Characteristics of Studies. All studies were conducted in China. One article was a thesis [29], and the rest were journal articles. The included studies were as follows: one study comparing SYM with placebo [33], two studies comparing SYM with active controls [30, 35], and three studies comparing SYM plus active controls with active controls only [29, 32, 34]. One study was a three-arm parallel study comparing SYM, active controls, and SYM plus active controls [31]. For the active controls, antihypertensives including captopril, amlodipine besylate, and benazepril were used in four studies [29, 31, 32, 34] and antidepressants

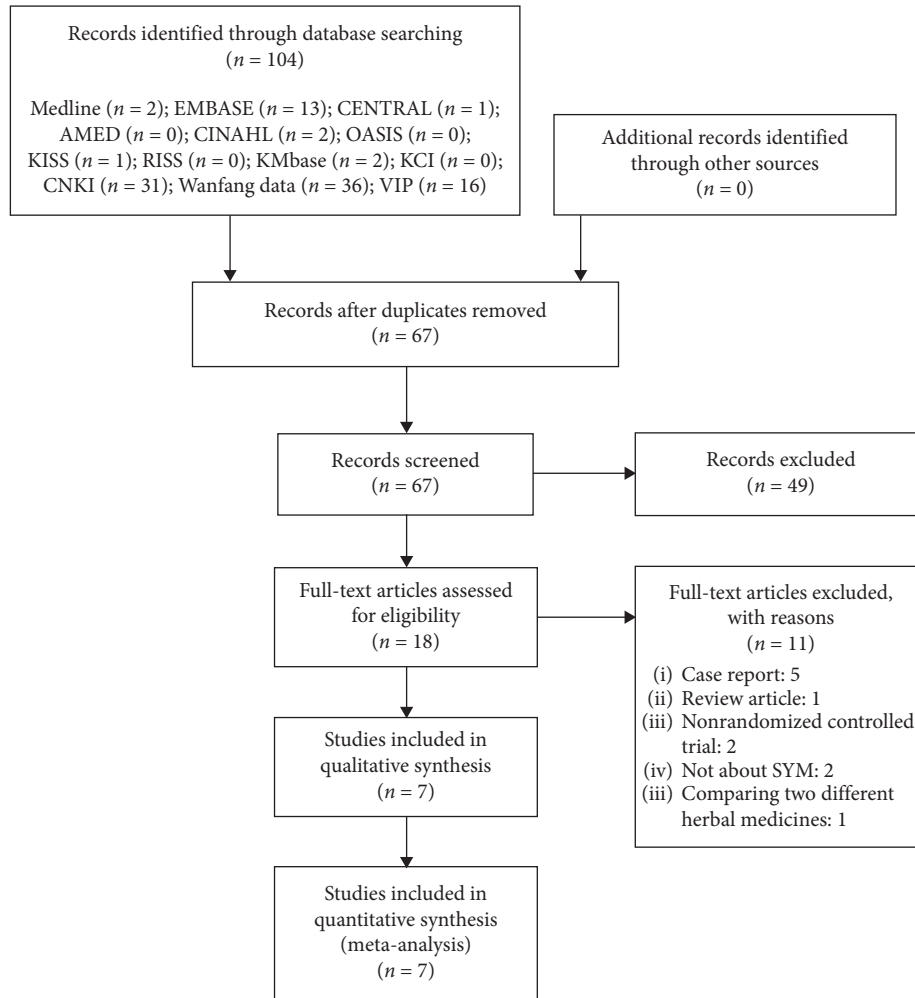


FIGURE 1: A PRISMA flow diagram of the literature screening and selection process. AMED, Allied and Complementary Medicine Database; CENTRAL, Cochrane Central Register of Controlled Trials; CINAHL, Cumulative Index to Nursing and Allied Health Literature; CNKI, China National Knowledge Infrastructure; KCI, Korea Citation Index; KISS, Korean studies Information Service System; KMbase, Korean Medical Database; OASIS, Oriental Medicine Advanced Searching Integrated System; RISS, Research Information Service System; SYM, Sihogayonggolmoryeo-tang.

including Deanxit (flupentixol and melitracen) were used in two studies [30, 35]. Four studies included participants with hypertension [29, 31, 32, 34], two studies included participants with both hypertension and anxiety [30, 35], and one study included participants with both hypertension and depression [33]. One study targeted participants with isolated nocturnal hypertension [32]. Regarding the criteria for diagnosing hypertension, six studies were based on the Chinese Hypertension Prevention Guidelines [29–33, 35], and one study was based on the 2018 European guidelines for the prevention and treatment of hypertension [33]. The diagnosis criteria were not listed for one study [34]. Participants were recruited for four studies [29, 32, 33, 35] according to specific pattern identification: three [29, 32, 33] were for ascendant hyperactivity of liver yang, and the remaining study [35] was for yin deficiency with yang hyperactivity. Daytime SBP and DBP were evaluated in five studies [28–30, 32, 34], and nighttime SBP and DBP were measured in two studies [28, 31]. As symptoms are related to

hypertension, anxiety was assessed in two studies using the Zung self-rating anxiety score (SAS) [30] and Hamilton anxiety rating scale (HAMA) [35]. Depression was assessed in two studies using the Zung self-rating depression scale (SDS) [30] and patient health questionnaire-9 (PHQ-9) [33], respectively. TER calculated based on BP was evaluated in three studies [29, 32, 34], and TER calculated based on the traditional Chinese medicine (TCM) syndrome score was evaluated in four studies [29, 32, 33, 35]. The incidence of adverse events was reported in three studies [29, 33, 35], and quality of life was assessed in one study [29] using Du's hypertension quality of life scale (Table 1). Two articles [30, 33] reported that the studies had been approved by an institutional review board, and three articles [29, 30, 33] reported that the researchers had received consent from the participants.

Regarding the dosage form, a decoction was used in six studies [29–34], and granules were used in the remaining study [35]. At least one of the original components of SYM,

TABLE 1: General characteristics of the included studies.

Study ID	Sample size (A): (B)	Mean age (range) (yr)	Population	(A) treatment group	(B) control group	Treatment period	Outcome	Results reported
Han [29]	60 (30:30)	56.4 (43-75)	(i) SBP \geq 140 mmHg and/or DBP \geq 90 mmHg (ii) Pattern identification*: ascendant hyperactivity of liver yang	SYM + (B)	Captopril 12.5 mg bid + amlodipine besylate 5 mg qd (if there was a severe cough caused by captopril, switch to amlodipine besylate 5 mg qd + furosemide 20 mg qd)	8 wks	(1) Daytime SBP (2) Daytime DBP (3) Nighttime SBP (4) Nighttime DBP (5) TER (BP) (6) TCM syndrome score (7) TER (TCM syndrome score) (8) Du's hypertension quality of life scale	(1) N.S (2) N.S (3) N.S (4) N.S (5) N.S (6) (A) < (B)+ (7) (A) > (B) (P value was not presented) (8) (A) < (B)+ (total score, physiological symptoms, somatization symptoms, and obsessive-compulsive conditions), (A) < (B)* (sleep status, anger and vitality, anxiety, hostility, depression, and interpersonal sensitivity)
Huang [30]	176 (88:88)	(A) 35.51 \pm 3.56 (18-65) (B) 34.89 \pm 3.41 (18-65)	(i) Essential hypertension (ii) Anxiety (CCMD)	SYM + amlodipine besylate 5 mg 1T qd	Deanaxit (flupentixol and melfitracen) 0.5 mg 1T bid + amlodipine besylate 5 mg 1T qd	1 mo	(1) Daytime SBP (2) Daytime DBP (3) SAS (4) SDS	(1) (A) < (B)+ (2) (A) < (B)+ (3) (A) < (B)+ (4) (A) < (B)+
Li [31]	80 (27:26:27)	(A1) 60.7 (42-78) (A2) 59.7 (39-72) (B) 58.7 (38-74)	(i) Grade 1 or 2 hypertension* (ii) Isolated nocturnal hypertension (iii) Depression (PHQ-9>4)	(A1) SYM (A2) SYM + (B)	Benazepril 10 mg qd	6 mo	(1) Daytime SBP (2) Daytime DBP (3) Serum PCIII	(1) (A1) > (B)*, (A2) < (B)*, (A1) > (A2)* (2) N.S (3) (A1) > (A2)*, (A2) < (B)*
Song [32]	94 (47:47)	46.4 \pm 9.3 (31-64)	(i) Isolated nocturnal hypertension (ii) Daytime BP < 135/85 mmHg; nighttime BP \geq 120/70 mmHg (iii) Pattern identification: ascendant hyperactivity of liver yang	SYM + (B)	Amlodipine besylate 2.5 mg	2 wks	(1) Nighttime SBP (2) Nighttime DBP (3) TER (BP) (4) TER (TCM syndrome score)	(1) N.S (2) (A) < (B)* (3) (A) > (B)* (4) (A) > (B)*
Tang [33]	121 (60:61)	(A) 54.18 \pm 9.79 (B) 53.84 \pm 10.28	(i) Grade 1 or 2 hypertension (ii) Depression (PHQ-9>4) (iii) Pattern identification: ascendant hyperactivity of liver yang	SYM + amlodipine besylate 5 mg qd	SYM placebo + amlodipine besylate 5 mg qd	4 wks	(1) Daytime SBP (2) Daytime DBP (3) PHQ-9 (4) TER (TCM syndrome score) (5) CRP (mg/L) (6) Inner diameter of brachial artery (mm) (7) Endothelium-dependent flow-mediated dilation (%) (8) Endothelium-independent response to glyceryl trinitrate (%)	(1) (A) < (B)* (2) (A) < (B)* (3) (A) < (B)* (4) (A) > (B)* (5) (A) > (B)* (6) N.S (7) (A) > (B)* (8) (A) > (B)*
Wang [34]	100 (50:50)	56.21 \pm 3.72 (42-61)	(i) Essential hypertension	SYM + (B)	Amlodipine besylate 5 mg qd	NR	(1) TER (BP)	(1) (A) > (B)*
Wu [35]	80 (40:40)	(A) 48.12 \pm 8.25 (B) 50.12 \pm 2.13	(i) Grade 1 or 2 hypertension (ii) Anxiety (HAMA > 14, CCMD) (iii) Pattern identification: yin deficiency with yang hyperactivity	SYM + Amlodipine besylate 5 mg qd	Deanaxit (flupentixol and melfitracen) bid + amlodipine besylate 5 mg qd	4 wks	(1) Daytime SBP (2) Daytime DBP (3) HAMA (4) TER (TCM syndrome score)	(1) (A) < (B)* (2) N.S (3) (A) < (B)* (4) (A) > (B)* (head distension, profuse dreaming, vexing heat in the chest, palms, and soles, and dry mouth and throat), N.S (dizziness, headache, constipation, insomnia, inability to sleep, tinnitus, eye redness, impatience and irritability, and lumbar aching and knee flaccidity)

An approach in some East Asian traditional medicines that enables individual treatment by categorizing the signs and symptoms of patients into a series of syndrome concepts. * and + mean significant differences between two groups, $P < 0.05$ and $P < 0.01$. N.S means no significant difference between two groups, $P > 0.05$. * An approach in some East Asian traditional medicines that enables individual treatment by categorizing the signs and symptoms of patients into a series of syndrome concepts. # grade 1: SBP 140-159 mmHg and/or DBP 90-99 mmHg/grade 2: SBP 160-179 mmHg and/or DBP 100-109 mmHg. BP, blood pressure; CCMD, Chinese classification of mental disorders; CRP, C-reactive protein; DBP, diastolic blood pressure; HAMA, Hamilton anxiety rating scale; PCIII, procollagen III; PHQ-9, patient health questionnaire-9; SAS, Zung self-rating anxiety scale; SBP, systolic blood pressure; SDS, Zung self-rating depression scale; SYM, Sihogayongmoryeo-tang; TCM, traditional Chinese medicine; TER, total effective rate.

Bupleuri Radix, *Fossilia Ossis Mastodi*, *Ostreae Testa*, *Scutellariae Radix*, *Pinelliae Tuber*, *Poria Sclerotium*, and *Cinnamomi Ramulus*, was used in all studies (each 100%). Additionally, *Rhei Radix et Rhizoma* was used in six studies (85.7%) [29–31, 33–35], followed by *Ginseng Radix* or *Codonopsis Pilosulae Radix* [29–31, 33, 35] and *Zingiberis Rhizoma Recens* [29, 30, 33–35] in five studies (71.4%) each. The administration duration varied from 2 weeks to 7 months, with 4 weeks being the most (Table 2).

3.3. Risk of Bias Assessment. For the random sequence generation domain, four studies [30, 32, 33, 35] were evaluated as having a low risk of bias because they used a random number table, and the remaining three studies [29, 31, 34] were evaluated as having an unclear risk of bias because the relevant information was not provided. None of the articles provided information on allocation concealment and the blinding of outcome assessment; hence, the risk of bias was assessed as unclear. For the blinding of participants and personnel, one study [33] using placebo as a control was judged to have a low risk of bias, and the remaining studies [29–32, 34, 35] without any related information were judged to have a high risk of performance bias given the nature of the interventions used. For the incomplete outcome data domain, one study [30] was determined to have an unclear risk of attrition bias because the related information was not provided, and two studies [33, 35] were judged to have a high risk of bias due to analysis of the results using a per-protocol analysis method. One study [34] that reported only the TER calculated based on BP without reporting the raw data was evaluated to have a high risk of reporting bias. All studies were assessed to have a low risk of bias in other bias domains because they had demographic and clinical homogeneity at the baseline between the treatment and control groups (Figure 2).

3.4. Efficacy

3.4.1. SYM versus Placebo. Compared with placebo, SYM resulted in significantly lower daytime SBP and DBP (SBP: one study [33], MD -8.84 mmHg, 95% CI -15.36 to -2.32 ; and DBP: one study [33], MD -9.11 mmHg, 95% CI -12.03 to -6.19). Additionally, depression measured with PHQ-9 was significantly lower in the SYM group (one study [33], MD -3.52 , 95% CI -4.40 to -2.64). TER based on the TCM syndrome score after treatment was significantly higher in the SYM group than in the placebo group (one study [33], RR 1.21, 95% CI 1.01 to 1.45) (Table 3).

3.4.2. SYM versus Active Controls. The SYM group showed significantly lower daytime SBP and DBP compared with the active control group (SBP: three studies [30, 31, 35], MD -2.54 mmHg, 95% CI -4.18 to -0.89 , $I^2 = 83\%$; and DBP: three studies [30, 31, 35], MD -2.67 , 95% CI -3.73 to -1.60 , $I^2 = 56\%$). However, subgroup analysis according to the type of active controls used to resolve considerable heterogeneity showed that daytime SBP was higher with SYM than with

	Random sequence generation (selection bias)	Allocation concealment (selection bias)	Blinding of participants and personnel (performance bias)	Blinding of outcome assessment (detection bias)	Incomplete outcome data (attrition bias)	Selective reporting (reporting bias)	Other bias
Han [29]	?	?	-	?	+	+	+
Huang [30]	+	?	-	?	?	+	+
Li [31]	?	?	-	?	+	+	+
Song [32]	+	?	-	?	+	+	+
Tang [33]	+	?	+	?	-	+	+
Wang [34]	?	?	-	?	+	-	+
Wu [35]	+	?	-	?	-	+	+

FIGURE 2: Risk of bias summary for all included studies. Low, unclear, and high risk, respectively, are represented with the following symbols: “+,” “?,” and “-.”

antihypertensives (one study [31]; MD 5.00 mmHg, 95% CI 0.16 to 9.84), and daytime DBP showed no significant difference between the SYM and antihypertensives groups (one study [31]; MD 2.20 mmHg, 95% CI -2.73 to 7.13). The degree of anxiety measured using SAS and HAMA showed no consistent results between the SYM and antidepressants groups (SAS: one study [30], MD -10.58 , 95% CI -11.57 to -9.59 ; and HAMA: one study [35]; MD -0.28 , 95% CI -0.95 to 0.39). The degree of depression measured with SDS showed significant results in favor of the SYM group (one study [30], MD -10.94 , 95% CI -12.17 to -9.71) (Table 3).

3.4.3. SYM plus Active Controls versus Active Controls Alone. Antihypertensives were used as the active controls in all three studies included in this comparison. SYM plus antihypertensives resulted in significantly lower daytime SBP than antihypertensives alone (two studies [29, 31], MD -3.22 mmHg, 95% CI -6.15 to -0.29 , $I^2 = 0\%$). However, there were no significant differences between these two groups in daytime DBP, nighttime SBP, and nighttime DBP (daytime DBP: two studies [29, 31], MD -2.46 mmHg, 95% CI -5.09 to 0.18, $I^2 = 72\%$; nighttime SBP: two studies [29, 32], MD -1.79 mmHg, 95% CI -3.81 to 0.23, $I^2 = 0\%$; and nighttime DBP: two studies [29, 32], MD 0.35 mmHg, 95% CI -1.78 to 2.48, $I^2 = 0\%$). The results were significant in

TABLE 2: Details of Sihogayongmoryeo-tang in the included studies.

Study ID	Dosage form	Administration duration and frequency	Doses of components per day (g)																					
			Bupleuri Radix	Fossilia Ossa Mastodi	Ostreae Testa	Scutellariae Radix	Ginseng Radix or Codonopsis Pilosulae Radix	Pineellae Tuber	Poria Sclerotium	Cinnamomi Ramulus	Zingiberis Rhizoma Recens	Zizyphi Fructus	Rhei Radix et Rhizoma	Mintium	Nardolidis seu Sulfurii Concha	Margaritifera Usta Concha	Pseudostellariae Radix	Paeoniae Radix	Glycyrrhizae Radix et Rhizoma	Prunellae Spica	Castrogliae Rhizoma	Uncariae Ramulus cum Uncus	Pterariae Radix	
Han [29]	Decoction	8 wks, bid	15	20	20	9	10	10	10	9	6 pieces	6			10									
Huang [30]	Decoction	1 mo, bid	15	20	20	20	10	10	20	5	6 pieces	3			30									
Li [31]	Decoction	6 mo, bid	NR	NR	NR	NR	NR	NR	NR	NR	NR	NR	NR	NR										
Song [32]	Decoction	2 wks, bid	10	15	15	10	10	10	30	10					15			10						
Tang [33]	Decoction	4 wks, bid	15	30	30	10	10	10	30	10	15	3						10	15	15	10		30	
Wang [34]	Decoction	NR, bid	12	30	30	6	6	3	18	3		6												
Wu [35]	Granule	4 wks, bid	NR	NR	NR	NR	NR	NR	NR	NR	NR	NR	NR	NR										
Frequency (%)			7 (100)	7 (100)	7 (100)	7 (100)	7 (100)	5 (71.4)	7 (100)	7 (100)	7 (100)	6 (85.7)	1 (14.3)	1 (14.3)	1 (14.3)	1 (14.3)	1 (14.3)	1 (14.3)	1 (14.3)	1 (14.3)	1 (14.3)	1 (14.3)	1 (14.3)	1 (14.3)

NR, not reported.

TABLE 3: Summary of findings.

Outcomes		No. of Participants (RCTs)	Anticipated absolute effects (95% CI)		Relative effect (95% CI)	I^2 value	Quality of evidence (Grade)	Comments
			Risk with control group	Risk with SYM group				
<i>SYM versus placebo</i>								
Daytime SBP (mmHg)	Total	113 (1)	—	MD 8.84 lower (15.36–2.32 lower)	—	Not applicable	⊕⊕⊕○ Moderate	Risk of bias (–1)
Daytime DBP (mmHg)	Total	113 (1)	—	MD 9.11 lower (12.03–6.19 lower)	—	Not applicable	⊕⊕⊕○ Moderate	Risk of bias (–1)
PHQ-9	Total	113 (1)	—	MD 3.52 lower (4.40–2.64 lower)	—	Not applicable	⊕⊕⊕○ Moderate	Risk of bias (–1)
TER (TCM syndrome score)	Total	113 (1)	737 per 1,000	892 per 1,000 (744–1,000)	RR 1.21 (1.01–1.45)	Not applicable	⊕○○○ Very low	Risk of bias (–1) Indirectness (–1) Imprecision (–1)
Adverse event	Total	113 (1)	88 per 1,000	71 per 1,000 (20–253)	RR 0.81 (0.23–2.88)	Not applicable	⊕○○○ Very low	Risk of bias (–1) Imprecision (–2)
<i>SYM versus active controls</i>								
	Total	305 (3)	—	MD 2.54 lower (4.18–0.89 lower)	—	83%	⊕○○○ Very low	Risk of bias (–1) Inconsistency (–2)
Daytime SBP (mmHg)	Versus antihypertensives	54 (1)	—	MD 5.00 higher (0.16–9.84 higher)	—	Not applicable	⊕⊕○○ Low	Risk of bias (–1) Imprecision (–1)
	Versus antidepressants	251 (2)	—	MD 3.52 lower (5.26–1.77 lower)	—	15%	⊕⊕⊕○ Moderate	Risk of bias (–1)
	Total	305 (3)	—	MD 2.67 lower (3.73–1.60 lower)	—	56%	⊕⊕○○ Low	Risk of bias (–1) Inconsistency (–1)
Daytime DBP (mmHg)	Versus antihypertensives	54 (1)	—	MD 2.20 higher (2.73 lower–7.13 higher)	—	Not applicable	⊕○○○ Very low	Risk of bias (–1) Imprecision (–2)
	Versus antidepressants	251 (2)	—	MD 2.90 lower (4.00–1.81 lower)	—	0%	⊕⊕⊕○ Moderate	Risk of bias (–1)
SAS	Total (antidepressants)	176 (1)	—	MD 10.58 lower (11.57–9.59 lower)	—	Not applicable	⊕⊕⊕○ Moderate	Risk of bias (–1)
SDS	Total (antidepressants)	176 (1)	—	MD 10.94 lower (12.17–9.71 lower)	—	Not applicable	⊕⊕⊕○ Moderate	Risk of bias (–1)
HAMA	Total (antidepressants)	75 (1)	—	MD 0.28 lower (0.95 lower–0.39 higher)	—	Not applicable	⊕○○○ Very low	Risk of bias (–1) Imprecision (–2)

TABLE 3: Continued.

Outcomes	No. of Participants (RCTs)	Anticipated absolute effects (95% CI)		Relative effect (95% CI)	I^2 value	Quality of evidence (Grade)	Comments
		Risk with control group	Risk with SYM group				
Adverse event	Total (antidepressants)	75 (1)	0 per 1,000	0 per 1,000 (0–0)	Not estimable	Not applicable	⊕⊕○○ Low Risk of bias (–1) Imprecision (–1)
<i>SYM plus active controls versus active controls</i>							
Daytime SBP (mmHg)	Total (antihypertensives)	113 (2)	—	MD 3.22 lower (6.15–0.29 lower)	—	0%	⊕⊕⊕○ Moderate Risk of bias (–1)
Daytime DBP (mmHg)	Total (antihypertensives)	113 (2)	—	MD 2.46 lower (5.09 lower–0.18 higher)	—	72%	⊕○○○ Very low Inconsistency (–1) Imprecision (–1)
Nighttime SBP (mmHg)	Total (antihypertensives)	154 (2)	—	MD 1.79 lower (3.81 lower–0.23 higher)	—	0%	⊕⊕○○ Low Risk of bias (–1) Imprecision (–1)
Nighttime DBP (mmHg)	Total (antihypertensives)	154 (2)	—	MD 0.35 higher (1.78 lower–2.48 higher)	—	0%	⊕⊕○○ Low Risk of bias (–1) Imprecision (–1)
TER (BP)	Total (antihypertensives)	254 (3)	740 per 1,000	903 per 1,000 (807–1,000)	RR 1.22 (1.09 to 1.37)	61%	⊕○○○ Very low Risk of bias (–1) Indirectness (–1) Imprecision (–1)
TER (TCM syndrome)	Total (antihypertensives)	154 (2)	688 per 1,000	881 per 1,000 (743–1,000)	RR 1.28 (1.08 to 1.52)	0%	⊕⊕○○ Low Risk of bias (–1) Indirectness (–1)
Du's hypertension quality of life scale	Total (antihypertensives)	60 (1)	—	MD 9.85 lower (15.87–3.83 lower)	—	Not applicable	⊕⊕○○ Low Risk of bias (–1) Imprecision (–1)
Adverse event	Total (antihypertensives)	60 (1)	33 per 1,000	11 per 1,000 (0–262)	RR 0.33 (0.01 to 7.87)	Not applicable	⊕○○○ Very low Risk of bias (–1) Imprecision (–2)

BP, blood pressure; CI, confidence interval; DBP, diastolic blood pressure; HAMA, Hamilton anxiety rating scale; MD, mean difference; PHQ-9, patient health questionnaire-9; RCT, randomized controlled trial; RR, risk ratio; SAS, Zung self-rating anxiety scale; SBP, systolic blood pressure; SDS, Zung self-rating depression scale; SYM, Sihogayonggolmoryeo-tang; TCM, traditional Chinese medicine; TER, total effective rate.

favor of the SYM group for TER calculated based on BP (three studies [29, 32, 34], RR 1.22, 95% CI 1.09 to 1.37, $I^2 = 61%$) and the TCM syndrome score (two studies [29, 32], RR 1.28, 95% CI 1.08 to 1.52, $I^2 = 0%$). The quality of life measured based on Du's hypertension quality of life scale was significantly improved in the SYM plus antihypertensives group compared with the antihypertensives-alone group (one study [29], MD -9.85 , 95% CI -15.87 to -3.83) (Table 3).

3.4.4. Other Results. In one study [31], serum procollagen III, a biomarker of myocardial fibrosis, was significantly lower in the SYM plus benazepril group compared with the SYM alone or benazepril alone group (all, $P < 0.05$). Tang et al. [33] reported that C-reactive protein was significantly lower in the SYM group than in the placebo group ($P < 0.05$). In addition, they reported that endothelium-dependent vasodilation was significantly improved in the SYM group compared with the placebo group ($P < 0.05$) (Table 1).

3.5. Safety. Of the seven studies, only three studies (42.86%) [29, 33, 35] reported adverse events. Tang et al. [33] reported two cases of blushing and two cases of constipation in the SYM group, with one case of ankle edema and four cases of constipation in the placebo group (RR 0.81, 95% CI 0.23–2.88). Han [29] reported no adverse events in the SYM group and one case of dry cough in the SYM plus antihypertensives group (RR 0.33, 95% CI 0.01–7.87). Wu et al. [35] reported no adverse events in the SYM and antidepressants groups (Table 3).

3.6. Quality of Evidence. In the comparison of SYM with placebo, the quality of evidence for daytime SBP, daytime DBP, and PHQ-9 was graded as “Moderate.” However, TER calculated based on the TCM syndrome score and adverse events was graded as “Very Low.” In the comparison of SYM with active controls and SYM plus active controls with active controls alone, the quality of evidence was graded as “Very Low” to “Moderate” (Table 3). The main reason for the downgrade was the high risk of bias for the included RCTs and the imprecision of the results due to the small sample size and wide CIs. Additionally, when TER was used, the indirectness of the outcome measure also lowered the quality of evidence.

3.7. Publication Bias. Because the number of studies included in each meta-analysis was less than 10, the assessment of publication bias through a funnel plot was not conducted.

4. Discussion

The aim of this study was to present evidence regarding the effect and safety of SYM for the treatment of hypertension through a comprehensive and systematic search, and seven studies [29–35] were included in the analysis. According to the study results, SYM significantly lowered BP and depressive symptoms in hypertensive patients compared with placebo. However, only one study [33] with an unclear risk of bias was included in this comparison, and no definite evidence could be obtained. SYM significantly lowered daytime BP compared to active control with considerable heterogeneity. Subgroup analysis according to the type of active controls used to resolve significant statistical and clinical heterogeneity revealed a significant decrease in the I^2 value. Interestingly, daytime SBP was significantly higher in the SYM group than in the antihypertensives group, but daytime DBP was not significantly different between the two groups. However, compared to the antidepressants group, daytime SBP and DBP were significantly lower in the SYM group. There was no significant difference in the concurrent anxiety symptoms when comparing SYM and antidepressants, but depression symptoms decreased significantly in the SYM group compared with that in the antidepressants group. When SYM plus antihypertensives was compared with antihypertensives alone, daytime SBP was significantly lower. However, daytime DBP and nighttime SBP showed borderline significance, and nighttime DBP had no significant difference between the two groups. However, TER

calculated based on BP and quality of life was significantly higher in the SYM plus antihypertensives group. SYM showed no difference in the incidence of adverse events compared to placebo or active control, and the reported adverse reactions were mild and disappeared spontaneously. Most studies included had an unclear risk of bias, and the quality of evidence for the main findings was generally low.

Although hypertension itself is not a life-threatening problem, it can increase the risk of major medical conditions including cardiovascular and cerebrovascular diseases [36]. In addition, hypertension is reported to be associated with anxiety, depression, and insomnia [37–39], and the prevalence of depression among hypertensive patients is known to be moderate, at about 27% [37]. According to the study results, SYM significantly improved the biomarkers of cardiovascular disease including serum procollagen III and C-reactive protein. In addition, given the increased demand for natural products that can control BP [10], the results of this study suggest the potential of SYM as a treatment option especially for hypertension and concurrent depressive symptoms. Modern pharmacological studies of SYM have shown that this HM can exert antidepressant effects by preventing the collapse of the hypothalamopituitary-adrenal (HPA) axis, including dysfunction in the glucocorticoid negative feedback system [16]. Dysfunction in the HPA axis is associated with negative cardiovascular outcomes, including hypertension, and is speculated to link hypertension and psychological stress [40]. Therefore, SYM can be assumed to have a beneficial effect on both hypertension and depression by restoring stress-related dysfunction in the HPA axis. Interestingly, among the studies included in this review, all studies using pattern identification [29, 32, 34, 35] recruited patients with yang hyperactivity, a concept related to psychological stress [41]. These findings support our hypothesis that the therapeutic effects of SYM may be involved in psychological stress and the HPA axis as a mediator for treating high BP and depression. However, the underlying mechanism of SYM on these conditions needs to be further elucidated.

According to previous studies [14], the pattern identification categories for hypertension are fire syndrome, phlegm-fluid retention syndrome, and deficiency syndrome. Among them, fire syndrome can be classified as a syndrome related to the liver, heart, stomach, and intestine. Based on the included studies using pattern identification and our previous study [42], the treatment principles for SYM were aimed at calming the liver and suppressing liver yang hyperactivity. Therefore, it can be assumed that SYM is used by some researchers under the category of fire syndrome, which mainly includes liver qi or liver yang abnormalities. However, only four of the studies included in this review [29, 32, 34, 35] recruited hypertensive patients with specific patterns, and we could not assess the effects of SYM in hypertensive patients according to specific patterns. Therefore, further study is needed to confirm whether SYM is more effective in hypertensive patients with a certain pattern.

There are some limitations to consider when interpreting the results. First, though we could not assess publication bias

because less than 10 studies were included in this review, all included studies were conducted in China, suggesting potential reporting bias. Second, the risk of bias in all included studies was generally unclear; thus, the planned sensitivity analysis to identify the robustness of the meta-analysis results could not be conducted. Third, the incidence of cardiovascular and cerebrovascular events is an important outcome in hypertensive patients; however, none of the included studies conducted follow-up assessment after SYM administration. Nevertheless, some observational studies have reported the potential impact of HM on these outcomes. For example, in a previous cohort study [43], it was reported that HM improved the overall survival rate of hypertensive patients with type 2 diabetes. Long-term clinical trials or large-scale cohort studies are needed to evaluate the effects of SYM on cardiovascular and cerebrovascular events or mortality in hypertensive patients. Finally, although fatal adverse events induced by SYM were not observed in the included studies or in our previous study [42], only three studies (42.86%) [29, 33, 35] reported the incidence of adverse events, and therefore, the safety profile of SYM remains unclear. Especially, although there was no age limit in the inclusion criteria for our study, and none of the included studies targeted children or pregnant women. Children may be even more susceptible to the adverse effects of HM because of their immature metabolic enzyme systems and an inappropriate dose per body weight. HMs also have the potential to cause adverse pregnancy outcomes and affect embryonic and fetal development in pregnant women, similar to conventional medication [44]. In this review, we could not find any evidence for the safety of SYM administration in this population, and further studies on the safety of SYM administration in this vulnerable population are needed. Moreover, due to concerns about potential adverse herb-drug interactions [45], the safety of HM in the treatment of hypertension should still be validated in well-designed clinical trials.

However, to the best of our knowledge, this is the first systematic review that comprehensively evaluated the effectiveness and safety of SYM for treating hypertensive patients. In addition, we significantly limited the statistical heterogeneity through subgroup analysis. Additional high-quality RCTs with placebo control and large sample sizes should be conducted to provide conclusive evidence on SYM for hypertensive patients. In particular, to generalize the results, relevant studies should be conducted in other East Asian countries besides China. In addition, there is a need for further experimental studies on the mechanism of SYM in the treatment of hypertension.

5. Conclusions

Current evidence suggests that SYM may have positive effects on hypertension and concurrent depressive symptoms, especially compared with placebo or antidepressants, without serious adverse events. However, due to the unclear risk of bias in the included studies and low quality of

evidence for the key findings, additional high-quality and placebo-controlled RCTs are needed to draw a definite conclusion.

Data Availability

The data used to support the findings of this study are included within the article.

Disclosure

Boram Lee and Chan-Young Kwon are co-first authors.

Conflicts of Interest

The authors have no conflicts of interest to declare.

Authors' Contributions

Boram Lee and Chan-Young Kwon contributed equally to this work. This study was conceptualized by BL. The study search, screening, data extraction, and quality assessment were conducted by BL, and CYK cross-checked it. The manuscript was drafted and revised by BL and CYK. All authors have read and approved the final manuscript.

Acknowledgments

This work was supported by the Korea Institute of Oriental Medicine (KSN2013210).

Supplementary Materials

Supplement 1. Search terms used in each database. Supplement 2. PRISMA 2009 checklists. (*Supplementary Materials*)

References

- [1] WHO, *Global Health Risks: Mortality and Burden of Disease Attributable to Selected Major Risks*, World Health Organization, Geneva, Switzerland, 2009.
- [2] S. S. Lim, T. Vos, A. D. Flaxman et al., "A comparative risk assessment of burden of disease and injury attributable to 67 risk factors and risk factor clusters in 21 regions, 1990–2010: a systematic analysis for the Global Burden of Disease Study 2010," *Lancet (London, England)*, vol. 380, no. 9859, pp. 2224–2260, 2012.
- [3] K. T. Mills, J. D. Bundy, T. N. Kelly et al., "Global disparities of hypertension prevalence and control," *Circulation*, vol. 134, no. 6, pp. 441–450, 2016.
- [4] N. Ikeda, D. Sapienza, R. Guerrero et al., "Control of hypertension with medication: a comparative analysis of national surveys in 20 countries," *Bulletin of the World Health Organization*, vol. 92, no. 1, pp. 10–9c, 2014.
- [5] R. M. Carey, S. Sakhuja, D. A. Calhoun, P. K. Whelton, and P. Muntner, "Prevalence of apparent treatment-resistant hypertension in the United States," *Hypertension (Dallas, Texas)*, vol. 73, no. 2, pp. 424–431, 1979.
- [6] C. Bardage and D. G. Isacson, "Self-reported side-effects of antihypertensive drugs: an epidemiological study on

- prevalence and impact on health-state utility," *Blood Pressure*, vol. 9, no. 6, pp. 328–334, 2000.
- [7] M. Morgado, S. Rolo, A. F. Macedo, L. Pereira, and M. Castelo-Branco, "Predictors of uncontrolled hypertension and antihypertensive medication nonadherence," *Journal of Cardiovascular Disease Research*, vol. 1, no. 4, pp. 196–202, 2010.
- [8] W. S. Aronow, "Lifestyle measures for treating hypertension," *Archives of Medical Science*, vol. 5, no. 5, pp. 1241–1243, 2017.
- [9] J. J. Beunza, M. A. Martínez-González, S. Ebrahim et al., "Sedentary behaviors and the risk of incident hypertension: the SUN Cohort," *American Journal of Hypertension*, vol. 20, no. 11, pp. 1156–1162, 2007.
- [10] J. Mbizo, A. Okafor, M. A. Sutton, B. Leyva, L. M. Stone, and O. Olaku, "Complementary and alternative medicine use among persons with multiple chronic conditions: results from the 2012 National Health Interview Survey," *BMC Complementary and Alternative Medicine*, vol. 18, no. 1, p. 281, 2018.
- [11] R. Nahas, "Complementary and alternative medicine approaches to blood pressure reduction: an evidence-based review," *Canadian family physician Medecin de famille canadien*, vol. 54, no. 11, pp. 1529–1533, 2008.
- [12] C.-h. Han, M. Kim, S.-Y. Cho et al., "Adjunctive herbal medicine treatment for patients with acute ischemic stroke: a systematic review and meta-analysis," *Complementary Therapies in Clinical Practice*, vol. 33, pp. 124–137, 2018.
- [13] L. Yu, Y. Qin, Q. Wang et al., "The efficacy and safety of Chinese herbal medicine, Rhodiola formulation in treating ischemic heart disease: a systematic review and meta-analysis of randomized controlled trials," *Complementary Therapies in Medicine*, vol. 22, no. 4, pp. 814–825, 2014.
- [14] J. Wang and X. Xiong, "Evidence-based Chinese medicine for hypertension," *Evidence-Based Complementary and Alternative Medicine*, vol. 2013, p. 97, 2013.
- [15] K. Mizoguchi, R. Ikeda, H. Shoji et al., "Saikokaryukotsuboreito, a herbal medicine, prevents chronic stress-induced anxiety in rats: comparison with diazepam," *Journal of Natural Medicines*, vol. 63, no. 1, pp. 69–74, 2009.
- [16] K. Mizoguchi, N. Sun, X.-L. Jin et al., "Saikokaryukotsuboreito, a herbal medicine, prevents chronic stress-induced dysfunction of glucocorticoid negative feedback system in rat brain," *Pharmacology Biochemistry and Behavior*, vol. 86, no. 1, pp. 55–61, 2007.
- [17] K. Mizoguchi, M. Yuzurihara, A. Ishige, M. Aburada, and T. Tabira, "Saiko-ka-ryukotsu-borei-to, a herbal medicine, ameliorates chronic stress-induced depressive state in rotarod performance," *Pharmacology Biochemistry and Behavior*, vol. 75, no. 2, pp. 419–425, 2003.
- [18] H. Iijima, A. Daikonya, S. Takamatsu et al., "Effects of the herbal medicine composition "Saiko-ka-ryukotsu-borei-To" on the function of endothelial progenitor cells in hypertensive rats," *Phytomedicine: International Journal of Phytotherapy and Phytopharmacology*, vol. 20, no. 3-4, pp. 196–201, 2013.
- [19] H. Okano and C. Ohkubo, "Anti-pressor effect of a Chinese-Japanese herbal medicine, saiko-ka-ryukotsu-borei-to on hemodynamics in rabbits," *Vivo (Athens, Greece)*, vol. 13, no. 4, pp. 333–337, 1999.
- [20] M. Wei, F. Shintani, S. Kanba et al., "Endothelium-dependent and-independent vasoactive actions of a Japanese kampo medicine, saiko-ka-ryukotsu-borei-to," *Biomedicine & Pharmacotherapy*, vol. 51, no. 1, pp. 38–43, 1997.
- [21] D. Moher, A. Liberati, J. Tetzlaff, and D. G. Altman, "Preferred reporting items for systematic reviews and meta-analyses: the PRISMA statement," *PLoS Medicine*, vol. 6, no. 7, 2009.
- [22] B. Lee, C.-Y. Kwon, and G. T. Chang, "Acupoint herbal patching for children with recurrent respiratory tract infection: a systematic review and meta-analysis," *Complementary Therapies in Clinical Practice*, vol. 40, p. 101209, 2020.
- [23] S. S. K. Durairajan, A. Iyaswamy, S. G. Shetty et al., "A modified formulation of Huanglian-Jie-Du-Tang reduces memory impairments and beta-amyloid plaques in a triple transgenic mouse model of Alzheimer's disease," *Scientific Reports*, vol. 7, no. 1, p. 6238, 2017.
- [24] T. Yamada, T. Wajima, H. Nakaminami, K. Kobayashi, H. Ikoshi, and N. Noguchi, "The modified Gingyo-san, a Chinese herbal medicine, has direct antibacterial effects against respiratory pathogens," *BMC Complementary and Alternative Medicine*, vol. 16, no. 1, p. 463, 2016.
- [25] J. P. T. Higgins, D. G. Altman, P. C. Gøtzsche et al., "The Cochrane Collaboration's tool for assessing risk of bias in randomised trials," *Bmj*, vol. 343, no. 2, p. d5928, 2011.
- [26] H. Balshem, M. Helfand, H. J. Schünemann et al., "GRADE guidelines: 3. Rating the quality of evidence," *Journal of Clinical Epidemiology*, vol. 64, no. 4, pp. 401–406, 2011.
- [27] G. C. de Souza, A. C. Matias Pereira, M. D. Viana et al., "Acmella oleracea (L) R. K. Jansen reproductive toxicity in zebrafish: an in vivo and in silico assessment," *Evidence-Based Complementary and Alternative Medicine*, vol. 2019, 2019.
- [28] M. Borenstein, L. V. Hedges, J. P. T. Higgins, and H. R. Rothstein, "A basic introduction to fixed-effect and random-effects models for meta-analysis," *Research Synthesis Methods*, vol. 1, no. 2, pp. 97–111, 2010.
- [29] M. Han, *The Therapeut Effect of Longgu Muli Decoction on Quality of Life of Patients with Hypertension*, Shandong University of Traditional Chinese Medicine, Berlin, Germany, 2013.
- [30] W. M. Huang, "Effect comparison of Amlodipine Besylate combined with Chaihu plusing Longgu Oyster decoction or Flupentixol and Melitracen treating primary hypertension complicated with anxiety," *China Modern Medicine*, vol. 24, no. 14, pp. 122–124, 2017.
- [31] X. Q. Li and Y. K. Li, "Effect of chaihu jia longgu muli decoction on serum PCIII in patients with hypertension," *Seek Medical And Ask The Medicine*, vol. 10, no. 3, p. 491, 2012.
- [32] X. X. Song, C. H. Yan, X. T. Zhang, and A. M. Liu, "Clinical observation of Caihulonggumuli decoction in adjuvant treatment of isolated nocturnal hypertension with hyperactivity of liver yang," *Hubei Journal of TCM*, vol. 38, no. 5, pp. 7–8, 2016.
- [33] Y. L. Tang, J. M. Wang, T. Y. Zhuang, C. Yang, and J. P. Fu, "Efficacy and safety of modified Chaihu Jia Longgu Muli tang in treating mild to moderate essential hypertension complicated with depression and liver-yang hyperactivity syndrome," *Chinese Journal of Experimental Traditional Medical Formulae*, vol. 38, pp. 1–7, 2020.
- [34] X. F. Wang, "Clinical observation of Chaihu Jia Longgu Muli decoction in treating essential hypertension," *Journal of Medical Aesthetics and Cosmetology*, vol. 28, no. 23, p. 65, 2019.
- [35] X. F. Wu, X. Z. Xie, G. L. Xu, and J. Y. Wang, "Clinical observation of Chaihu Jia Longgu Muli decoction in the treatment of essential hypertension with anxiety," *World Journal of Integrated Traditional and Western Medicine*, vol. 11, no. 11, pp. 1497–1499, 2016.
- [36] B. C. Bansal, A. K. Agarwal, and B. B. Rewari, "Hypertension and cerebrovascular disease," *Journal of the Indian Medical Association*, vol. 97, no. 6, pp. 226–232, 1999.

- [37] Z. Li, Y. Li, L. Chen, P. Chen, and Y. Hu, "Prevalence of depression in patients with hypertension," *Medicine*, vol. 94, no. 31, p. e1317, 2015.
- [38] Y. Pan, W. Cai, Q. Cheng, W. Dong, T. An, and J. Yan, "Association between anxiety and hypertension: a systematic review and meta-analysis of epidemiological studies," *Neuropsychiatric Disease and Treatment*, vol. 11, pp. 1121–1130, 2015.
- [39] A. N. Vgontzas, D. Liao, E. O. Bixler, G. P. Chrousos, and A. Vela-Bueno, "Insomnia with objective short sleep duration is associated with a high risk for hypertension," *Sleep*, vol. 32, no. 4, pp. 491–497, 2009.
- [40] N. Burford, N. Webster, and D. Cruz-Topete, "Hypothalamic-pituitary-adrenal Axis modulation of glucocorticoids in the cardiovascular system," *International Journal of Molecular Sciences*, vol. 18, no. 10, p. 2150, 2017.
- [41] Q. Yan, "Neuroimmune imbalances and yin-yang dynamics in stress, anxiety, and depression," *Methods in Molecular Biology*, vol. 1781, pp. 77–85, 2018.
- [42] C. Y. Kwon, B. Lee, S. Y. Chung et al., "Efficacy and safety of Sihogayonggolmoryeo-tang (Saikokaryukotsuboreito, Chai-Hu-Jia-Long-Gu-Mu-Li-Tang) for post-stroke depression: a systematic review and meta-analysis," *Scientific Reports*, vol. 9, no. 1, p. 146, 2019.
- [43] Y. J. Lin, T. J. Ho, Y. C. Yeh et al., "Chinese herbal medicine treatment improves the overall survival rate of individuals with hypertension among type 2 diabetes patients and modulates in vitro smooth muscle cell contractility," *PLoS One*, vol. 10, no. 12, 2015.
- [44] C. C. Wang, L. Li, C. B. San Lau, P. C. Leung, and K. P. Fung, "Pregnancy outcomes, embryonic and fetal development in maternal exposure to Chinese medicines," *Birth Defects Research Part C: Embryo Today: Reviews*, vol. 99, no. 4, pp. 275–291, 2013.
- [45] A. Tachjian, V. Maria, and A. Jahangir, "Use of herbal products and potential interactions in patients with cardiovascular diseases," *Journal of the American College of Cardiology*, vol. 55, no. 6, pp. 515–525, 2010.

Review Article

Yiqi Fumai Injection as an Adjuvant Therapy in Treating Chronic Heart Failure: A Meta-Analysis of 33 Randomized Controlled Trials

Heyun Nie, Shuqing Li, Meilu Liu, Weifeng Zhu , Xu Zhou , and Dongmei Yan 

Evidence-based Medicine Research Center, Jiangxi University of Traditional Chinese Medicine, Nanchang, Jiangxi, China

Correspondence should be addressed to Xu Zhou; zhouxu_ebm@hotmail.com and Dongmei Yan; yandongmeiebm@163.com

Received 16 May 2020; Revised 7 July 2020; Accepted 24 July 2020; Published 19 August 2020

Guest Editor: Xiao Ma

Copyright © 2020 Heyun Nie et al. This is an open access article distributed under the Creative Commons Attribution License, which permits unrestricted use, distribution, and reproduction in any medium, provided the original work is properly cited.

Background. Yiqi Fumai injection (YQFM) is a traditional Chinese medicine widely used for cardiovascular diseases in China. This systematic review aimed to evaluate whether YQFM could be an effective and safe complementary therapy for chronic heart failure (CHF). **Methods.** Eight electronic literature databases were searched up to March 31, 2020. Randomized controlled trials (RCTs) comparing YQFM + conventional treatment with conventional treatment alone for CHF were included. The primary outcome was response to treatment, which was graded by improvements in heart function based on the New York Heart Association (NYHA) criteria, while the secondary outcomes included the left ventricular ejection fraction (LVEF), cardiac output, left ventricular end-systolic diameter (LVESD), amino-terminal pro-brain natriuretic peptide (NT-proBNP), 6-minute walk test performance (6MWT), quality of life (QoL) as assessed by the Minnesota Living with Heart Failure questionnaire, and adverse reactions. Data from individual RCTs were pooled by a random-effects meta-analysis with effect measures of proportional odds ratios (pORs) and 95% confidence intervals (95% CIs) for the ordinal outcomes and the mean difference (MD) and 95% CI for the continuous outcomes. **Results.** In total, 33 RCTs involving 3070 patients with an overall moderate-to-high risk of bias were selected. The meta-analysis showed that compared with conventional treatment alone, YQFM plus conventional treatment had a significantly higher likelihood of improving the response to treatment (pOR 1.88, 95% CI 1.47 to 2.42, $I^2 = 0\%$). YQFM also significantly improved the LVEF (MD 5.53%, 95% CI 4.73 to 6.33, $I^2 = 82\%$), cardiac output (MD 0.32 L/min, 95% CI 0.19 to 0.45, $I^2 = 47\%$), and LVESD (MD -3.73 mm, 95% CI -5.51 to -1.95, $I^2 = 22\%$), reduced the NT-proBNP levels (MD -341.83 pg/mL, 95% CI -417.89 to -265.77, $I^2 = 88\%$), and improved the 6MWT (MD 61.86 m, 95% CI 45.05 to 78.67, $I^2 = 64\%$) and QoL (MD -9.82, 95% CI -14.17 to -5.46, $I^2 = 81\%$). No serious adverse events related to YQFM were reported. **Conclusion.** Although limited by a moderate-to-high risk of bias, the current evidence suggests that YQFM as a complementary treatment significantly improves heart function and related indicators in patients with CHF. The clinical use of YQFM needs careful safety monitoring. Well-designed studies are still required to further evaluate the efficacy and safety of YQFM for CHF.

1. Introduction

Chronic heart failure (CHF) is a major cardiovascular disease that manifests as myocardial structural and functional damage and persistent left ventricular systolic dysfunction [1]. With the ageing of the population and changes in people's lifestyle, the incidences of the primary diseases of CHF, such as hypertension, diabetes, and coronary heart disease, are rapidly increasing, and the global burden of CHF is rising annually. In the United States, the annual incidence of CHF among people aged over 65 is 19.3 per 1,000 people, and the annual direct and indirect costs of treating CHF exceed 39

billion dollars [2]. In 2015, the prevalence of CHF in the Chinese population aged over 65 years reached 10% [3]. CHF patients have a poor prognosis and a high mortality rate. The one-year hospitalization rates of inpatients and stable CHF patients were 44% and 32%, respectively [4]. The five-year mortality rate of CHF is as high as 60%–80%, which is similar to that of malignant tumours, such as breast cancer and colorectal cancer [3]. Sudden cardiac death, which is the main cause of death (40.2%), is difficult to prevent and rescue [5].

Currently, the drugs recommended in clinical practice guidelines for CHF mainly include diuretics, angiotensin-converting enzyme inhibitor, β -receptor blocker,

aldosterone receptor antagonists, and digitalis [1], all of which are limited by contraindications and adverse effects. For example, diuretics can result in hypovolemia associated with hypotension, renal function deterioration, and electrolyte imbalance [4]; digoxin can easily cause poisoning manifested as gastrointestinal adverse reactions, visual disturbances, and arrhythmias [6]. In addition, these drugs are expensive, causing a tremendous economic burden for patients and medical care systems. It is expected that, by 2030, the annual total medical expenses for CHF patients could increase to \$53 billion [7]. Therefore, there is a need for more CHF treatment choices.

In China, traditional Chinese medicine (TCM) as a complementary therapy has been widely used for cardiovascular diseases. In particular, innovative TCM injections, such as Yiqi Fumai injections (YQFM), provide new options for CHF treatment. The compounds of YQFM include the active ingredients of the following three herbs: total saponins panax ginseng from red ginseng, ophiopogonin from *Radix Ophiopogonis*, and schizandrol from *Schisandra chinensis*; these compounds are finally prepared in a freeze-dried powder injection. This preparation can overcome the storage and transportation inconveniences related to the instability of TCM injections [8]. YQFM can be easily dissolved in normal saline for an intravenous drip and has the advantages of rapid action, a high concentration of active ingredients, and accurate dosing. Pharmacological studies have demonstrated the cardioprotective effects of YQFM, including reducing myocardial ischaemia and hypoxia injury, enhancing the systolic function of the heart, delaying ventricular remodelling, inhibiting cardiomyocyte apoptosis, and ultimately improving cardiac function [9].

Since its approval for marketing in 2007, the efficacy and safety of YQFM for CHF have been assessed in many RCTs. However, the results are inconsistent likely due to the insufficient sample sizes. For example, Zhang [10] and Yu et al. [11] found that YQFM injection significantly improved both the response to treatment and left ventricular ejection fraction (LVEF) in patients with CHF, but the findings reported in the RCTs of Zhai and Hui [12] and Xue et al. [13] suggested negative results. Therefore, we systematically reviewed currently available RCTs of YQFM as a complementary therapy for CHF and aimed to provide more compelling evidence by pooling individual RCT data using meta-analytic methods.

2. Methods

The reporting of this study was guided by the Preferred Reporting Items for Systematic Reviews and Meta-analyses checklist.

2.1. Eligibility Criteria. Eligible RCTs compared YQFM+conventional treatment with the same conventional treatment alone for the treatment of patients with CHF and reported any outcomes of interest. Patients should be diagnosed with CHF by any recognized criteria such as the New York Heart Association (NYHA) criteria, the

Chinese Medical Association criteria, the Framingham criteria, or the World Health Organization criteria, with no limitations on age, sex, and disease course. Studies enrolling patients with other heart diseases, such as acute heart failure, obstructive cardiomyopathy, hypertrophic cardiomyopathy, and atrial fibrillation, were excluded. Eligible conventional treatment could include diuretics, angiotensin-converting enzyme inhibitor, β -receptor blocker, digitalis preparation, and aldosterone receptor antagonists. Other TCM preparations and ingredients that were the same as those found in YQFM were not allowed in either the YQFM group or the control group.

2.2. Literature Search. Four Chinese databases (Chinese National Knowledge Infrastructure, Wanfang Data, CQVIP, and the Chinese Biomedical Literature Database) and four English databases (PubMed, EMBASE, the Cochrane Library, and Clinicaltrials.gov) were searched. The keywords used in the search included “Yiqi Fumai,” “heart failure,” and “cardiac insufficiency.” For example, the search strategy for PubMed is as follows: (Yiqifumai[tw] OR Yiqi Fumai[tw] OR Yi qi Fu mai[tw]) AND (heart failure[mh] OR heart failure[tw] OR heart insufficiency[tw] OR heart decompensation[tw] OR cardiac failure[tw] OR cardiac insufficiency[tw] OR cardiac decompensation[tw]). Additionally, the major cardiovascular journals and the references of the included studies and related reviews were manually searched. The search was conducted from the inception of each database to March 31, 2020. There was no limitation on the publication language.

2.3. Literature Screening. Two reviewers performed an independent, repeated screening of the retrieved papers. The titles and abstracts were first read to exclude studies that did not meet the inclusion criteria, and then, the full text was read and rescreened to determine the RCTs that would be finally included. Disputes were settled through discussion with a third researcher.

2.4. Data Extraction. Two reviewers independently and repeatedly extracted the data from the included literature and cross-checked them. Disputes were settled through discussion with a third researcher. The extracted data included the baseline characteristics and outcomes of interest of each study. The former included the first author’s name, publication year, sample size, patient characteristics, diagnostic criteria, NYHA class of cardiac function, interventional and control measures, dose and course of treatments, and length of follow-up. The latter included the number or percentage of events, mean, and standard deviation for analysis.

2.5. Outcomes

2.5.1. Primary Outcome. The primary outcome was response to treatment, which was categorized into the following three groups according to the NYHA cardiac function

classification: (1) marked response: achievement of class I heart function or improvement in heart function by more than two classes; (2) moderate response: improvement in heart function by one class; and (3) no response: no improvement or deterioration in heart function.

2.5.2. Secondary Outcomes. The secondary outcomes included the LVEF, cardiac output, left ventricular end-systolic diameter (LVESD), N-terminal pro-brain natriuretic peptide (NT-proBNP), 6-minute walk test (6MWT), quality of life (QoL) as assessed by the Minnesota Living with Heart Failure questionnaire, and adverse events (AEs).

2.6. Risk of Bias Assessment. The Cochrane risk of bias assessment tool was used to assess the level of the risk of bias for each included RCT, which was assessed for seven items: random assignment methods, allocation concealment, investigator and patient blindness, blind evaluation of outcomes, data completeness, selective reporting, and other sources of bias risk. Each item was rated as “low risk,” “unclear,” or “high risk”. We finally judged the overall risk of bias of each RCT based on the following criteria [14]: (1) overall low risk of bias: no items suffer a risk of bias; (2) overall moderate risk of bias: 1–3 items have an unclear risk of bias; and (3) overall high risk of bias: ≥ 1 item suffer a high risk of bias or ≥ 4 items have an unclear risk of bias. Two reviewers working independently performed the assessments. Disputes were settled through discussion with a third researcher.

2.7. Statistical Analysis. The meta-analysis was performed using Review Manager 5.3. Mean differences (MDs) were used as the effect measures for continuous variables, and proportional odds ratios (pORs) were used as the effect measures for ordinal variables and their 95% confidence intervals (CIs) were also calculated. In this meta-analysis, data from the individual studies were pooled by the inverse variance method with a random-effects model. Heterogeneity was assessed using the Chi-square test and I^2 statistic; $p > 0.1$ or $I^2 \leq 50\%$ were considered indicative of nonsignificant heterogeneity among studies, and other values were considered indicative of significant heterogeneity. Additionally, subgroup analyses stratified by the daily dose of YQFM (low dose: ≤ 2.6 g; medium dose: 3.9 g; and high dose: ≥ 5.2 g), patients’ average age (< 60 vs ≥ 60 years), and level of overall risk of bias (moderate vs. high) were performed to explore the source of heterogeneity. If, at least, 10 studies were included in the meta-analysis, funnel plots, Egger’s test, and Begg’s test were used to evaluate publication bias.

3. Results

3.1. Screening Results. A total of 617 publications were obtained in the initial screening. After reading the titles, abstracts, and full texts, 33 RCTs [10–13, 15–43] with a total of 3070 patients were eventually included. All RCTs were from China. The selection process is shown in Figure 1.

3.2. Characteristics of the Included RCTs. Among the 3070 patients, the male to female ratio was approximately 3 : 2. The course of the YQFM treatment was two weeks or less in most RCTs (31, 93.9%); only two RCTs had a four-week course of treatment. The daily dose of YQFM was ≤ 2.6 g in nine (27.3%) RCTs; 3.9 g in five (15.2%) RCTs; and ≥ 5.2 g in 18 (54.5%) RCTs. Conventional treatment mainly included diuretics (furosemide, spironolactone), angiotensin-converting enzyme inhibitors (ramipril, captopril, and enalapril), β -blockers (metoprolol), and digitalis preparation (digoxin). The baseline NYHA class of the CHF patients was reported in 20 RCTs, of which a total of 336 (23.0%) patients were class II, 852 (58.3%) were class III, and 274 (18.7%) were class IV. The length of the follow-up was the same as the course of treatment in all RCTs. The baseline characteristics are presented in detail in Table 1.

3.3. Risk of Bias Assessment. The detailed random sequence generation method was reported in 13 of the RCTs, of which six used the random number table method and one used the random lottery method (low risk), but six used an inappropriate distribution method such as order of admission (high risk). The allocation concealment method was not mentioned in any of the RCTs. None of the RCTs mentioned the blinding method for patients and clinicians (unclear risk), except for one RCT [36], which claimed that a random single-blinded method was used, which was also rated as “high risk” because there was no placebo group to allow blinding. Although none of the RCTs mentioned whether the outcome assessors were blinded, the RCTs with no subjective outcomes were considered to have a low risk of bias for this item. Three RCTs lacked data and did not mention the reasons for loss to follow-up, and thus, the item “data completeness” was rated as “high risk” for those studies. Eight RCTs did not report the important outcomes for CHF, and thus, the item “selective reporting” was rated as “high risk”. Overall, 17 (51.5%) RCTs were judged to have a moderate risk of bias, 16 (48.5%) RCTs had a high risk of bias, and no RCTs were at a low risk of bias. The details of the risk of bias assessment are shown in Figures S1–S2 in the supplementary files.

3.4. Evaluation of Outcomes

3.4.1. Response to Treatment. Eleven RCTs ($n = 969$) [10–12, 15, 17, 27, 31, 35, 39, 41, 43] evaluated response to treatment. After treatment, 194 (39.8%), 245 (50.3%), and 48 (9.9%) patients in the YQFM group and 130 (27.0%), 248 (51.4%), and 104 (21.6%) patients in the control group had a significant, moderate, and no response to treatment, respectively. As Figure 2 indicates, the possibility of improving by more than one class of clinical efficacy was significantly higher in the YQFM group than in the control group (pOR 1.88, 95% CI 1.47 to 2.42, $p < 0.00001$), with no significant statistical heterogeneity ($I^2 = 0\%$; $p = 0.79$) among the RCTs.

3.4.2. LVEF. Twenty-six RCTs ($n = 2488$) [10–13, 15, 17–19, 21–23, 26–34, 36, 37, 40–43] reported LVEF data. The random-effects meta-analysis found that the increase in

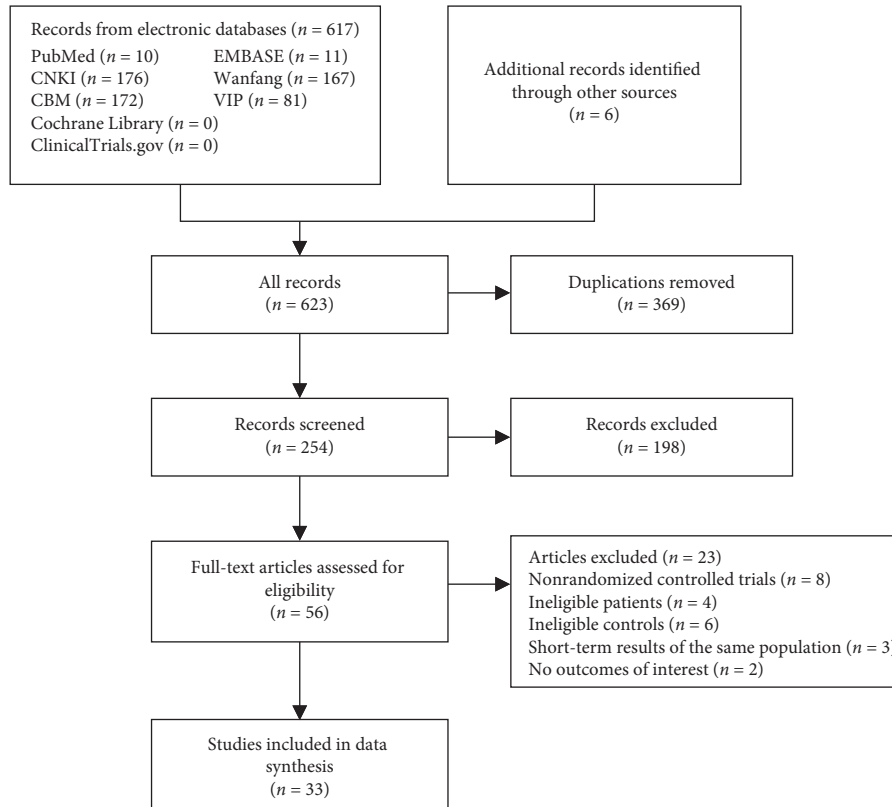


FIGURE 1: Flowchart of the selection process.

TABLE 1: Baseline characteristics of included studies.

Study	Sample size (T/C)	Male (T/C)	Mean age (T/C)	Cardiac function (T/C)			Interventions in both Yiqi Fumai injection and control group	Dose of Yiqi Fumai injection	Treatment period (weeks)	Outcomes
				NYHA II	NYHA III	NYHA IV				
Aunt and Nurbia [15]	60/60	—	55.4 (total)	—	—	—	Furosemide, metoprolol	5.2 g	2	a, b, f
Diao [16]	43/43	22/21	60.3/60.5	—	—	—	Spironolactone, digoxin	—	4	b
Dong and Liu [17]	60/60	38/35	56.4/56.1	—	—	—	Enalapril, metoprolol	5.2 g	2	a, b, e
Feng [18]	27/24	—	56.0~86.0	12/10	12/12	3/2	Spironolactone, metoprolol	5.2 g	—	b, d
Li [19]	30/30	14/17	67.5/64.7	16/18	14/12	—	Furosemide, metoprolol	1.3 g	2	b
Li et al. [20]	30/30	15/15	71.1/70.9	—	—	—	Ramipril, furosemide	5.2 g	1.5	e, f
Li [21]	30/30	—	64.3 (total)	—	—	—	Furosemide, captopril	2.6 g	4	b, f, g
Li et al. [22]	59/59	35/34	68.5/68.3	—	—	—	Atorvastatin	5.2 g	2	b, e, h
Liu [23]	45/45	24/25	56.7/55.2	/	19/18	26/27	Dobutamine hydrochloride	5.2 g	2	b, e, d, h
Lv [24]	43/40	30/28	62.7/61.5	17/16	14/13	12/11	Furosemide, metoprolol	2.6 g	2	h
Mao and Song [25]	30/30	17/18	58.5/58.6	—	—	—	Spironolactone, metoprolol	2.6 g	2	b, e
Ren [26]	44/44	—	55.0 (total)	—	—	—	Trimetazidine	5.2 g	2	b, e, h

TABLE 1: Continued.

Study	Sample size (T/C)	Male (T/C)	Mean age (T/C)	Cardiac function (T/C)			Interventions in both Yiqi Fumai injection and control group	Dose of Yiqi Fumai injection	Treatment period (weeks)	Outcomes
				NYHA II	NYHA III	NYHA IV				
Sun [27]	30/30	11/10	76.0/74.0	6/5	15/17	9/8	Enalapril, metoprolol	3.9 g	2	a, b, e, f, c, g
Sun [28]	60/60	43/44	58.4/58.2	16/17	26/27	18/16	Captopril, metoprolol	5.2 g	2	b, e, h
Wang and He [29]	35/29	19/16	54.9/52.5	9/7	20/18	6/4	Furosemide, digoxin	3.9 g	2	b, c, d, h
Wang [30]	50/50	32/30	70.0/69.5	—	—	—	Aspirin, spironolactone	5.2 g	2	b, e, h
Wang et al. [31]	33/32	19/18	64.3/63.8	—	—	—	Milrinone	5.2 g	1	a, b, e, c
Wang [32]	49/49	32/33	76.0/79.0	—	—	—	Metoprololsuccinate	5.2 g	2	b
Wang and Niu [33]	35/35	21/22	58.0/59.0	10/10	18/19	7/6	Isosorbide dinitrate	3.9 g	2	b, c, h
Wu [34]	32/30	19/17	60.3/62.4	—	—	—	Enalapril	2.1 g	2	b, c
Xi [35]	79/79	39/36	56.0/56.0	—	—	—	Amiodarone, furosemide	2.6 g	2	a
Xue et al. [13]	44/43	28/25	55.3/55.5	7/6	28/28	9/9	Captopril, metoprolol	2.6 g	2	a, b
Yang and Liu [36]	60/60	—	72.2/73.1	6/8	54/52	—	Enalapril, metoprolol	5.8 g	2	b, e
Yang [37]	150/150	89/87	57.2/56.4	29/28	96/97	25/25	Captopril, digoxin	5.2 g	2	b, e, f, h
Yang et al. [38]	30/30	22/23	70.7/70.8	8/5	18/18	4/7	Enalapril, metoprolol	5.2 g	2	b, e
Yang [39]	30/30	16/15	69.0/67.8	6/6	16/18	8/7	Furosemide, metoprolol	2.6 g	2	a
Yu and Wang [40]	30/30	15/16	66.0/65.0	6/6	21/20	3/4	Furosemide, spironolactone	3.9 g	2	b, h
Yu et al. [11]	45/45	25/23	51.5/52.0	—	—	—	Spironolactone, metoprolol	2.6 g	2	a, b
Zhai and Hui [12]	30/30	—	63.0 (total)	20	36	4	Ramipril, furosemide	5.2 g	2	a, b, e, h
Zhang [41]	30/30	—	70.0 (total)	26	20	14	Enalapril, metoprolol	5.2 g	2	a, b, e, f, h
Zhang [10]	40/40	23/24	56.3/55.9	—	—	—	Furosemide, captopril	3.9 g	2	a, b, e
Zhu [42]	100/100	66/66	63.7/63.2	—	—	—	Atorvastatin	5.2 g	2	b, d, h
Zhu and Han [43]	50/50	31/28	66.2/69.0	—	—	—	Aspirin, spironolactone	5.2 g	2	a, b, c, d, g

Notes. Both groups received the same basic treatment; “—” = not reported; T = trial group; C = control group; NYHA = New York Heart Association. Outcomes: a = response rate; b = left ventricular ejection fraction; c = cardiac output; d = left ventricular end-systolic diameter; e = N-terminal pro-brain natriuretic peptide; f = 6-minute walk test; g = quality of life; h = adverse reaction.

LVEF in the YQFM group was significantly higher than that in the control group (MD 5.53%, 95% CI 4.73 to 6.33, $p < 0.00001$; Figure 3). Heterogeneity was high ($I^2 = 82\%$).

3.4.3. Cardiac Output. Six RCTs ($n = 421$) [27, 29, 31, 33, 34, 43] evaluated the cardiac output of CHF patients. Cardiac output relative to baseline improved significantly more in the YQFM group than in the control group (MD 0.32 L/min, 95% CI 0.19 to 0.45, $p < 0.00001$; Figure 4), with relatively low statistical heterogeneity among the RCTs ($I^2 = 47\%$).

3.4.4. LVESD. Four RCTs ($n = 305$) [18, 23, 29, 43] reported LVESD data. The YQFM group had a higher reduction in LVESD than the control group (MD -3.73 mm, 95% CI -5.51 to -1.95, $p < 0.00001$; $I^2 = 22\%$; Figure 5).

3.4.5. NT-proBNP. Fourteen RCTs ($n = 1368$) [10, 12, 13, 17, 20, 23, 26–28, 31, 36–38, 41] reported the evaluation results of NT-proBNP. The YQFM group had a significantly greater reduction in NT-proBNP than the control group (MD -341.83 pg/mL, 95% CI -417.89 to -265.77, $p < 0.00001$; Figure 6), and there was considerable heterogeneity ($I^2 = 88\%$) among the RCTs.

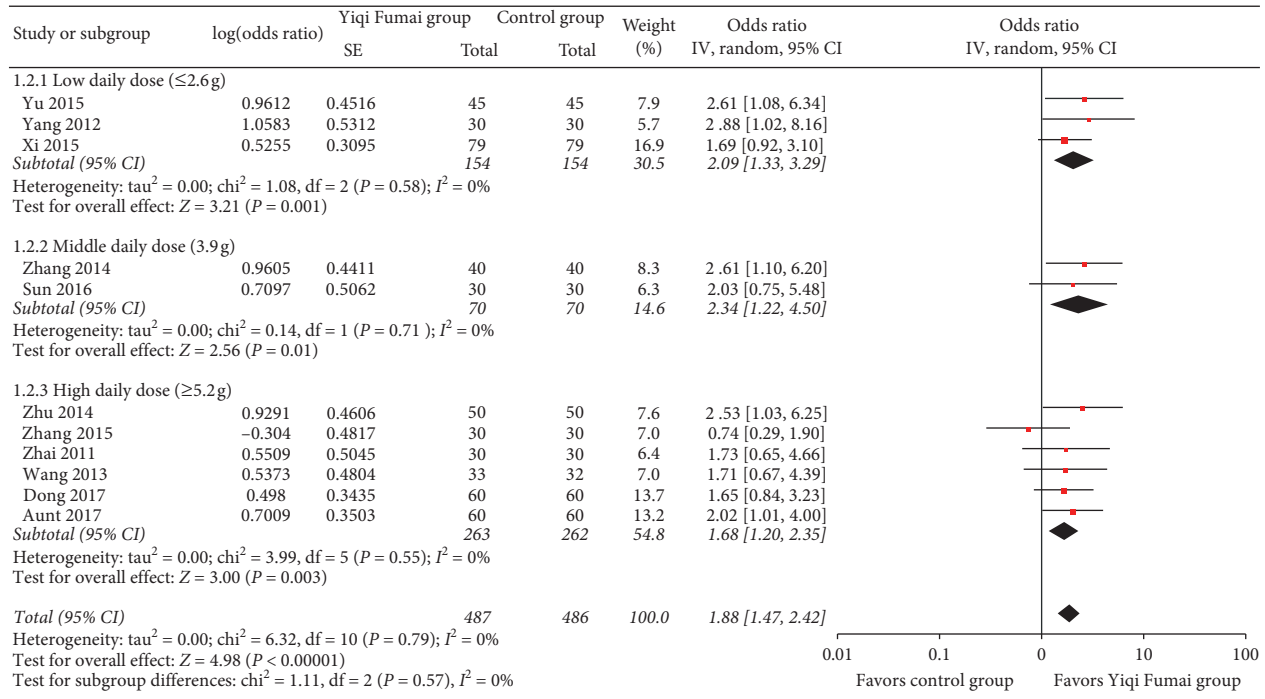


FIGURE 2: Meta-analysis of the response to treatment.

3.4.6. *6MWT*. Six RCTs ($n = 660$) [15, 20, 21, 27, 37, 41] reported changes in the patients' exercise capacity as assessed by the 6MWT. The patients in the YQFM group displayed significantly greater improvement in the 6MWT than those in the control group (MD 61.86 m, 95% CI 45.05 to 78.67, $p < 0.00001$; Figure 7). The heterogeneity was moderate ($I^2 = 64\%$).

3.4.7. *QoL*. Three RCTs ($n = 220$) [21, 27, 43] assessed the QoL using the Minnesota Living with Heart Failure questionnaire. After the treatments, the magnitude of reduction (improvement) in the questionnaire scores in the YQFM group was significantly greater than that in the control group (MD -9.82, 95% CI -14.17 to -5.46, $p < 0.00001$; $I^2 = 81\%$; Figure 8).

3.5. *Subgroup Analysis*. The subgroup analyses showed a statistically significant increased tendency in the LVEF along with an increase in the YQFM daily dose (low vs. medium vs. high: MD 3.92% vs. 5.18% vs. 6.09%, interaction $p = 0.03$; Figure 2), a significantly higher increase in cardiac output in patients with an average age < 60 years (< 60 versus ≥ 60 years: 0.51 L/min vs. 0.26 L/min, interaction $p = 0.003$), and a significant higher improvement in the 6MWT in patients with an average age < 60 years (< 60 versus ≥ 60 years: 0.51 L/min vs. 0.26 L/min, interaction $p = 0.03$) and in RCTs with a moderate overall risk of bias (moderate vs. high: MD 83.90 m vs. 52.56 m, interaction $p = 0.0010$). The other subgroup analyses showed no significant subgroup differences (all interactions $p > 0.05$). Subgroup analyses of the LVESD and QoL were not

performed because there were too few RCTs. The details of the subgroup analyses are shown in Tables S1–S3 in the supplementary files.

3.6. *Safety*. Thirteen [12, 22–24, 26, 28–30, 33, 37, 40–42] of the 35 RCTs reported AEs during treatment, including 11 RCTs that reported no AEs in either group and two RCTs [30, 42] that reported AEs in detail. One RCT [30] reported that 0 (0.0%), 2 (3.39%), 1 (1.69%), and 1 (1.69%) patients in the YQFM group and 4 (6.78%), 2 (3.39%), 2 (3.39%), and 4 (6.78%) patients in the control group had gastrointestinal reactions, nausea, vomiting, and upper abdominal discomfort, respectively, and the incidence of these AEs did not significantly differ between the two groups. Whether these AEs were associated with YQFM was uncertain. Another RCT [42] reported one (10%) case of dry mouth in the control group and one (10%) case of nausea and vomiting in the YQFM group. The correlation between nausea or vomiting and YQFM was also not reported.

3.7. *Publication Bias*. According to the funnel plots (Figures S3–S5 in supplementary files), the effect estimates of the response to treatment, LVEF, and NT-proBNP were distributed symmetrically, indicating that the possibility of publication bias was small. This finding is consistent with the results of Egger's tests (response to treatment: $p = 0.687$; LVEF: $p = 0.527$; NT-proBNP: $p = 0.062$) and Begg's tests (response to treatment: $p = 0.533$; LVEF: $p = 0.355$; NT-proBNP: $p = 0.063$). The other outcomes were not tested because of insufficient data.

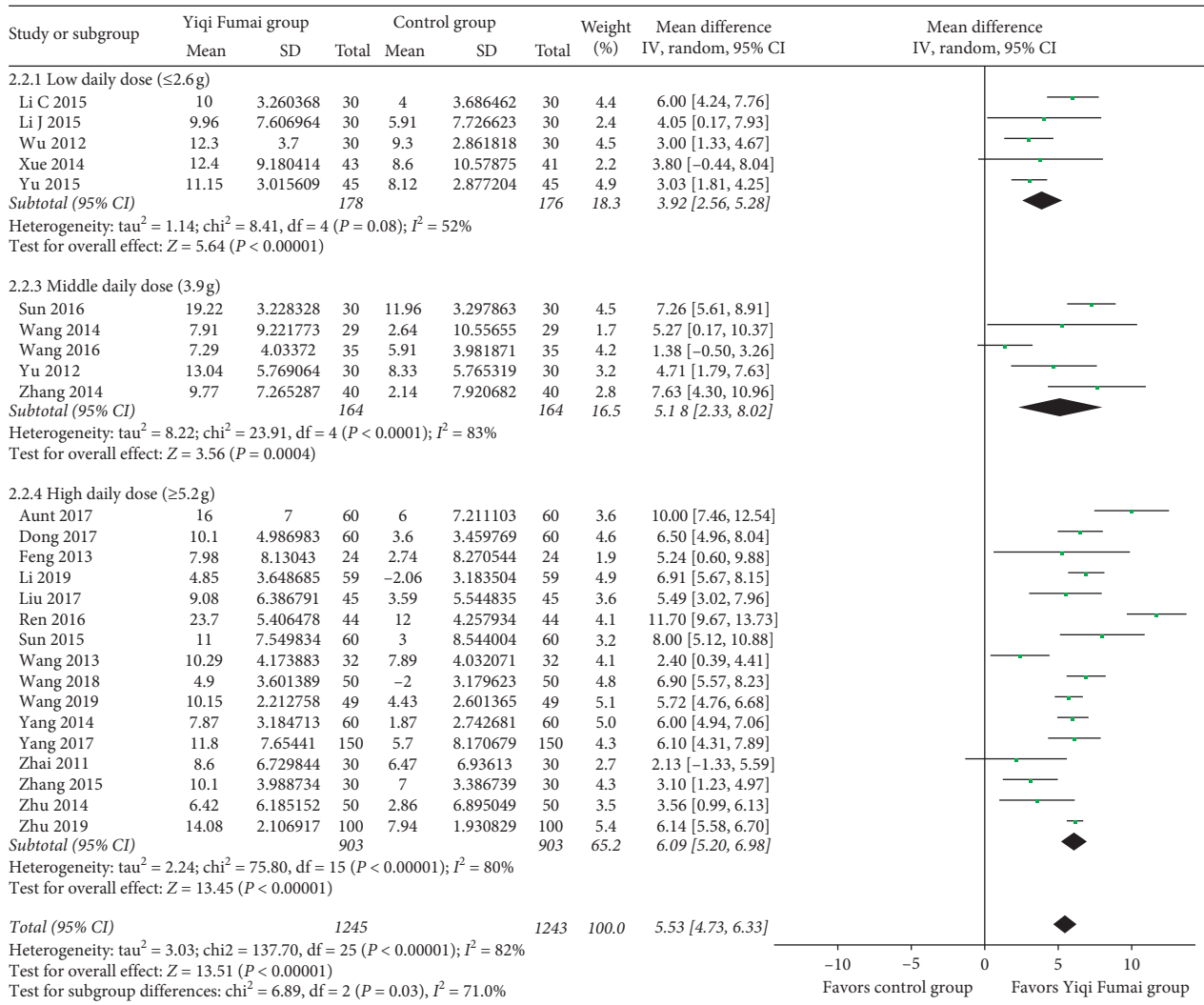


FIGURE 3: Meta-analysis of the left ventricular ejection fraction (%).

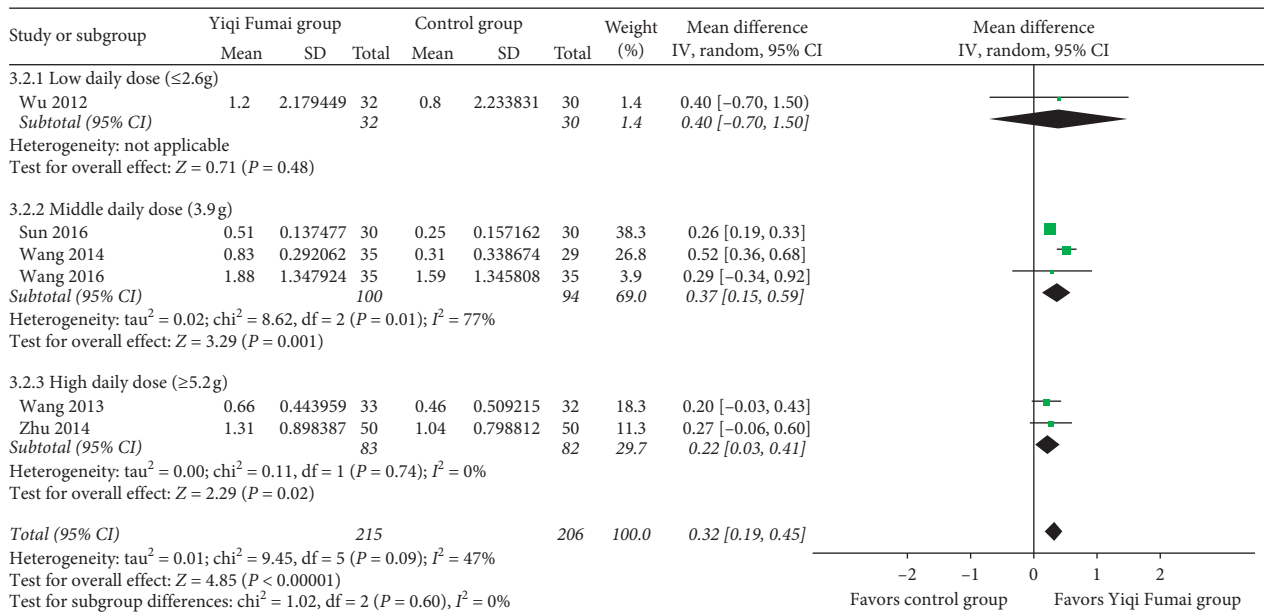


FIGURE 4: Meta-analysis of the cardiac output (L/min).

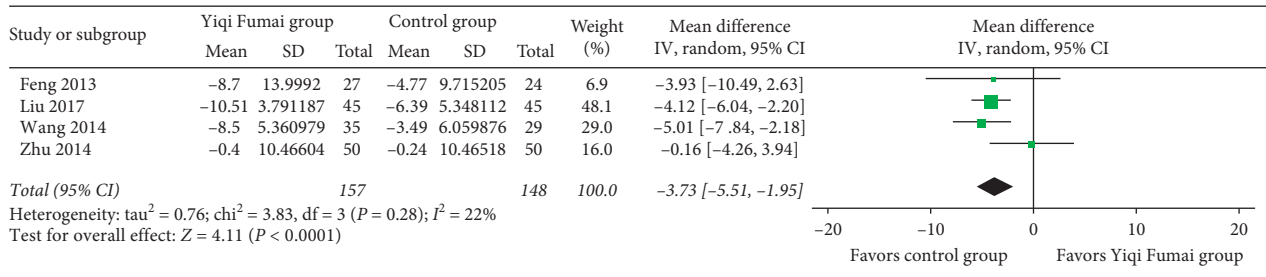


FIGURE 5: Meta-analysis of the left ventricular end-systolic diameter (mm).

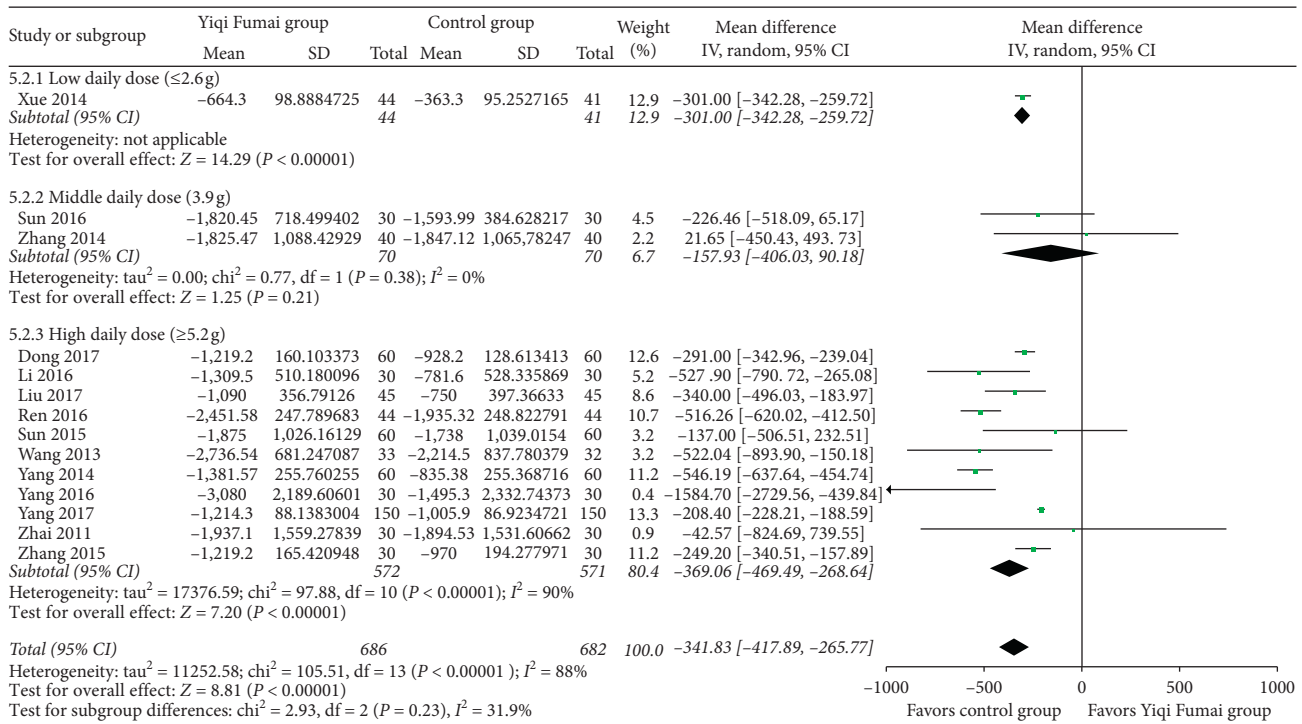


FIGURE 6: Meta-analysis of N-terminal pro-brain natriuretic peptide (pg/mL).

4. Discussion

To the best of our knowledge, this study is the first systematic review to assess YQFM for CHF. The findings showed that as a complementary therapy, YQFM combined with conventional treatment presented a remarkably improved efficacy in the primary outcome compared with the control group as the YQFM group had a 12.8% higher probability of having a marked response rate and an 88% higher probability of improving by one class in response to treatment. YQFM also significantly improved all secondary outcomes, including the LVEF, cardiac output, LVESD, NT-proBNP, 6MWT, and QoL, in CHF patients. There was a dose-response effect on the LVEF in which a high YQFM dose provided significantly better improvement than a low dose.

The response to treatment is based on an evaluation of the NYHA cardiac function classification, which mainly reflects cardiac function in terms of the intensity of the physical activity that patients can perform. Therefore, the effects of YQFM on the response to treatment can be verified

by the results of another physical test, i.e., the 6MWT, and both tests ultimately reveal significant improvements in the QoL. YQFM also increased the LVEF, a percentage of stroke volume of the end-diastolic volume of the ventricle that is positively associated with cardiac output and inversely associated with the LVESD; these outcomes can all predict the prognosis of CHF patients. Based on the effect size, 12.8% of the patients eventually achieved class I heart function or improvement in heart function by ≥ 2 classes and a 5.15% increase in the LVEF, and these results are even better than the average efficacy of Western medicines [44]; thus, we believe that the additional improvements in the cardiac function indices provided by YQFM have a promising clinical value. The NT-proBNP level is also an independent factor predicting a poor prognosis of CHF, such as all-cause death and cardiovascular disease/heart failure hospitalization. Although the cut-off value used to evaluate prognosis is not completely clear, a decrease of -341.83 pg/mL can be considered meaningful for improving the prognosis of CHF patients. Overall, YQFM is clinically effective in treating

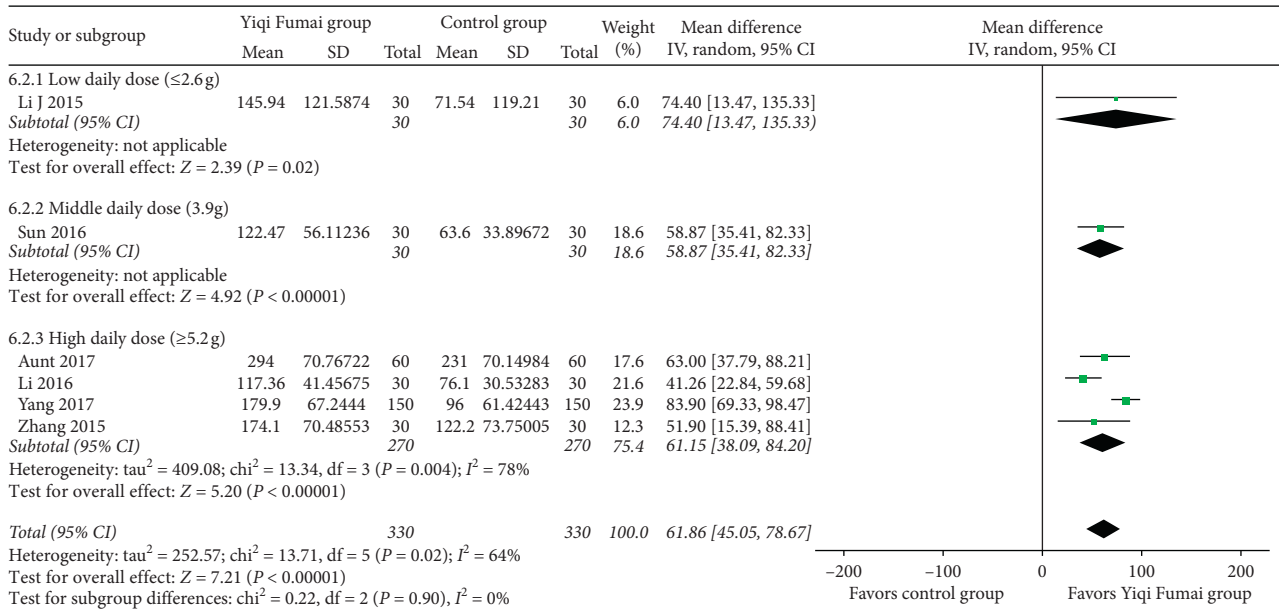


FIGURE 7: Meta-analysis of the 6-minute walk test performance m.

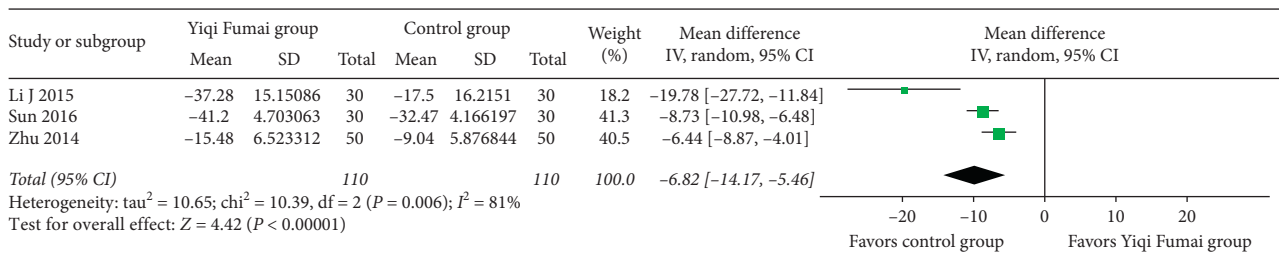


FIGURE 8: Meta-analysis of the Minnesota Living with Heart Failure questionnaire.

CHF patients based on the findings of this systematic review. According to the results of the subgroup analysis, YQFM is effective for CHF patients of all ages, and the daily dose of YQFM could be increased to 5.2 g/day to ensure safety and further improve the efficacy.

A few studies have investigated the mechanism of the entire formula of YQFM in the treatment of CHF. Therefore, we attempt to discuss the underlying mechanism of each component of YQFM. Ophiopogonin, the active component of Radix Ophiopogonis, is the largest component (54.5%) of YQFM; it has been demonstrated to be effective in inhibiting endoplasmic reticulum stress and reducing myocardial cell apoptosis by upregulating cytochrome P450 2J2 and epoxyeicosatrienoic acids, which can further inhibit myocardial hypertrophy, stabilize myocardial cell membrane, and improve positive inotropic action [45]. An important cause of CHF is myocardial ischaemia/reperfusion injury, which leads to the highly sensitive state of mitochondrial permeability caused by Ca²⁺ stimulation. Schizandrol, the second active component (27.3%), can reduce mitochondrial sensitivity; it therefore, plays a role in protection against myocardial ischaemia/reperfusion injury and has cardiovascular protection effects such as controlling the ventricular rate, anti-inflammation, and anti-cell apoptosis [46]. Total

saponins panax ginseng, the third ingredient (18.2%) of YQFM, can inhibit myocardial cell apoptosis by down-regulating caspases in apoptotic signal transduction, improving myocardial remodelling caused by CHF, enhancing myocardial contractility, and finally, recovering myocardium damage after ischaemia and hypoxia [47]. Although all single components have been proven to be beneficial for CHF, the abovementioned mechanism evidence was all based on animal experiments. The specific mechanism in humans and whether the three TCMs have synergistic effects remain unclear.

YQFM appears to be relatively safe because only two of the 33 included RCTs reported mild gastrointestinal side effects in the YQFM group. However, observational safety monitoring data show that YQFM is not completely safe. For instance, a retrospective study [48] of 2476 patients receiving YQFM reported 31 AEs after YQFM (incidence: 1.25%), including 26 common AEs and five serious AEs; most of the AEs were systemic damages and allergic reactions on the skin, and all of them were remitted after treatment. Another study [49] summarized 42 AEs after YQFM treatment from 2007 to 2014; of these AEs, palpitations (16.3%), drowsiness (10.2%), and rashes (10.2%) were the most common. However, the degree of the association between YQFM and

AEs was unclear in both studies. In any case, the clinical use of YQFM requires careful monitoring of adverse reactions and prompt treatment. The drip rate of YQFM is recommended to be lower than 40 drops per minute based on the results of a study investigating the risk factors of adverse reactions to YQFM [50].

This study has some limitations. First, due to methodological flaws such as inappropriate randomization methods and the lack of reporting allocation concealment and blinding methods, the included RCTs had an overall moderate-to-high risk of bias. Second, the residual heterogeneity in the LVEF, NT-proBNP, and QoL remained high after the explanation of the subgroup analyses, which may impact the accuracy of the effect estimates. We cannot perform subgroup analyses of the two suspected sources of heterogeneity, different baseline NYHA cardiac functions and different types of cointerventions, since the subgroup data were not separately reported in the primary studies. Nevertheless, regarding these outcomes, most results of individual RCTs are positive, and the negative individual results were generally marginally significant and/or had a small weight; thus, we believe that the high heterogeneity is unlikely to distort the direction of the results favouring the YQFM group. The meta-analytic estimates averaged by a random-effects model are still clinically meaningful. Third, because all included RCTs had short follow-up periods, this study was unable to evaluate the effects of YQFM on long-term CHF endpoints (e.g., mortality).

5. Conclusions

Our findings suggest that YQFM is an effective complementary treatment for CHF that can significantly improve the response to treatment, LVEF, cardiac output, LVESD, NT-proBNP, 6MWT, and QoL. YQFM dose-dependently improves the LVEF. Although the RCT evidence shows that YQFM is relatively safe, data from retrospective studies suggest that the clinical use of YQFM still needs careful safety monitoring. Due to the limitations of the risk of bias and heterogeneity, more high-quality studies are necessary to further verify the efficacy and safety of YQFM for CHF.

Abbreviations

CI:	Confidence interval
MD:	Mean difference
pOR:	Proportional odds ratio
RCT:	Randomized controlled trial
CHF:	Chronic heart failure
YQFM:	Yiqi Fumai injection
NYHA:	New York Heart Association
LVEF:	Left ventricular ejection fraction
LVESD:	Left ventricular end-systolic diameter
NT-proBNP:	N-terminal pro-brain natriuretic peptide
6MWT:	6-minute walk test
QoL:	Quality of life
TCM:	Traditional Chinese medicine
AEs:	Adverse events.

Data Availability

The datasets used and/or analyzed during the current study are available from the corresponding author on reasonable request.

Conflicts of Interest

The authors declare that they have no conflicts of interest.

Authors' Contributions

Heyun Nie and Shuqing Li contributed equally to this work and are the co-first authors. HN and SL designed the study, screened articles, extracted data, assessed risk of bias, performed data analysis, and drafted the manuscript. ML and WZ provided critical methodological advice and revised the manuscript. XZ and DY conceived and designed the study, conducted the search, developed the manuscript, and act as guarantors. All authors read and approved the final manuscript.

Acknowledgments

This research was supported by the National Natural Science Foundation of China (Nos. 81202911 and 81360509), Degree and Postgraduate Education Reform Project of Jiangxi University of Jiangxi Province (No. JXYJG-2018-108), Education Science 13th Five-Year Plan Project of Jiangxi Province (No. 20YB148), Teaching Reform Project of Colleges and Universities in Jiangxi Province (JXJG-19-12-14), Degree and Postgraduate Education Reform Project of Jiangxi University of Traditional Chinese Medicine (jzyjg-2019-05), Science and Technology Project of Department of Education of Jiangxi Province (GJJ190662), and Jiangxi University of Traditional Chinese Medicine 1050 Youth Talent Project (5142001011). All funders had no role during the entire process of this study.

Supplementary Materials

Figures S1-S2: results of the risk of bias assessment. Figures S3-S5: funnel plots. Table S1-S3: results of the subgroup analyses. (*Supplementary Materials*)

References

- [1] Chinese society of cardiology, "Chinese heart failure diagnosis and treatment guide 2018," *Chinese Journal of Heart Failure and Cardiomyopathy*, vol. 2, no. 4, pp. 196–225, 2018.
- [2] C. Rogers and N. Bush, "Heart failure," *Nursing Clinics of North America*, vol. 50, no. 4, pp. 787–799, 2015.
- [3] J. Huang, "Epidemiological characteristics and prevention strategies of heart failure in China," *Chinese Journal of Heart and Heart Rhythm*, vol. 3, no. 2, pp. 81–82, 2015.
- [4] Committee of experts on rational drug use, "Guidelines for the rational use of heart failure," *Chinese Journal of the Frontiers of Medical Science*, vol. 117, pp. 1–78, 2nd edition, 2019.

- [5] F. Orso, G. Fabbri, and A. P. Maggioni, "Epidemiology of heart failure," *Handbook of Experimental Pharmacology*, vol. 243, pp. 15–33, 2017.
- [6] S. Angraal, S. V. Nuti, F. A. Masoudi et al., "Digoxin use and associated adverse events among older adults," *The American Journal of Medicine*, vol. 132, no. 10, pp. 1191–1198, 2019.
- [7] C. Albert and J. D. Estep, "Economic impact of chronic heart failure management in today's cost-conscious environment," *Cardiac Electrophysiology Clinics*, vol. 11, no. 1, pp. 1–9, 2019.
- [8] A. Ju, R. Luo, and X. Su, "Research progress on chemical composition and quality control of Yiqi Fumai lyophilized injection," *Drug Evaluation Research*, vol. 41, no. 3, pp. 365–371, 2018.
- [9] A. Ju, R. Luo, and X. Qin, "Pharmacological effects and clinical research progress of Yiqi Fumai lyophilized injection," *Drug Evaluation Research*, vol. 41, no. 3, pp. 354–364, 2018.
- [10] Y. Zhang, "Efficacy of Yiqi Fumai injection in the treatment of chronic heart failure," *Medicine & people*, vol. 27, no. 9, p. 112, 2014.
- [11] Z. Yu, L. Zhang, T. Hu, L. Wang, and C. Zheng, "Clinical study of Yiqi Fumai (lyophilized) for injection in treating coronary heart disease with heart failure," *China Health Care Nutrition*, vol. 25, no. 17, p. 246, 2015.
- [12] X. Zhai and X. Hui, "Clinical observation on Yiqi Fumai injection for heart failure," *Chinese Journal of Integrative Medicine on Cardio-/Cerebrovascular Disease*, vol. 9, no. 8, pp. 899–900, 2011.
- [13] L. Xue, H. Wang, X. Lei, and L. Feng, "Effects of Yiqi Fumai injection on cardiac function and plasma BNP in chronic heart failure," *Chinese Journal of Integrative Medicine on Cardio-/Cerebrovascular Disease*, vol. 12, no. 3, pp. 279–280, 2014.
- [14] J. Chen, D. Chen, and Q. Ren, *Acupuncture and Related Techniques for Obesity and Cardiovascular Risk Factors: A Systematic Review and Meta-Regression Analysis*, Acupuncture in Medicine, London, UK, 2020.
- [15] A. Aunt and Y. Nurbia, "120 cases of chronic congestive heart failure with injection of yiqi-doumai (lyophilization)," *Medical Frontier*, vol. 7, no. 26, pp. 227–228, 2017.
- [16] Y. Diao, "Effect evaluation of Yiqi Fumai injection combined with western medicine in the treatment of chronic heart failure," *Cardiovascular Disease Journal of Integrated Traditional Chinese and Western Medicine*, vol. 6, no. 1, pp. 163–164, 2018.
- [17] X. Dong and J. Liu, "Clinical trial on the treatment of chronic heart failure with Yiqi Fumai injection," *China Health Care Nutrition*, vol. 27, no. 21, pp. 284–285, 2017.
- [18] C. Feng, "Clinical trial on the treatment of chronic heart failure with injection of Yiqi and lyophilization," *Guangming Journal of Chinese Medicine*, vol. 28, no. 8, pp. 1607–1608, 2013.
- [19] C. Li and X. Fan, "Clinical effect of Yiqi Fumai lyophilization on chronic heart failure," *Practical Clinical Journal of Integrated Traditional Chinese and Western Medicine*, vol. 15, no. 8, pp. 75–76, 2015.
- [20] H. Li, A. Guan, and S. Liu, "Effect of Yiqi Fumai for injection combined with western medicine on patients with refractory end-stage heart failure," *Shanxi Journal of Traditional Chinese Medicine*, vol. 37, no. 8, pp. 989–990, 2016.
- [21] J. Li, "Clinical observation of Yiqi Fumai injection combined with western medicine in treating chronic heart failure," *Chinese Journal of Modern Drug Application*, vol. 9, no. 16, pp. 167–169, 2015.
- [22] Y. Li, X. Jia, S. Liu, C. Feng, and H. Feng, "Effect of Yiqi Fumai Injection combined with atorvastatin on chronic heart failure of patients with coronary heart disease and its effects on sCD40, sCD146 and PAPP-A," *Chinese Archives of Traditional Chinese Medicine*, vol. 37, no. 5, pp. 1225–1228, 2019.
- [23] B. Liu, "Clinical observation of Yiqi Fumai injection combined with western medicine for heart failure," *Journal of New Chinese Medicine*, vol. 49, no. 8, pp. 23–25, 2017.
- [24] Y. Lv, "Clinical effect of Yiqi Fumai injection in elderly patients with chronic heart failure," *Journal of Anhui Health Vocational & Technical College*, vol. 16, no. 1, pp. 34–35, 2017.
- [25] J. Mao and Y. Song, "Clinical observation on Yiqi Fumai injection in treating chronic heart failure of coronary heart disease," *China Health Care Nutrition*, vol. 28, no. 31, pp. 70–71, 2018.
- [26] H. Ren, "Clinical effect of Yiqi Fumai (lyophilized) for injection combined with trimetazidine on chronic heart failure," *The World Clinical Medicine*, vol. 10, no. 8, pp. 4–7, 2016.
- [27] H. Sun, *Yiqifumai Frozen Powder Injection Agent in Treatment of Chronic Heart Failure (Two Gas Yin Deficiency Syndrome) Clinical Observation*, Shandong University of Traditional Chinese Medicine, Jinan, China, 2016.
- [28] J. Sun, "Clinical efficacy of Yiqi Fumai (lyophilized) for injection in the treatment of chronic heart failure in elderly patients with coronary heart disease," *Journal of Clinical Rational Drug Use*, vol. 8, no. 18, pp. 114–115, 2015.
- [29] H. Wang and Z. He, "Clinical observation of digoxin tablet combined with Yiqi Fumai in treatment of chronic heart failure," *Journal of Clinical Rational Drug Use*, vol. 29, no. 5, pp. 532–535, 2014.
- [30] J. Wang, "Safety evaluation of Yiqi Fumai injection in the treatment of senile coronary heart disease with chronic heart failure," *Chinese Journal of Convalescent Medicine*, vol. 27, no. 3, pp. 276–277, 2018.
- [31] J. Wang, L. Zhang, and S. Zhang, "Clinical observation of Yiqi Fumai for injection combined with milrinone in treatment of refractory heart failure," *Journal of Emergency in Traditional Chinese Medicine*, vol. 22, no. 7, pp. 1234–1235, 2013.
- [32] S. Wang, "Effect of Yiqi Fumai injection and metoprolol succinate sustained release tablets in coronary heart disease complicated with heart failure," *Clinical Medicine*, vol. 4, no. 18, pp. 22–23, 2019.
- [33] S. Wang and J. Niu, "Efficacy of Yiqi Fumai (lyophilization) on coronary heart disease and heart failure," *Health Way*, vol. 15, no. 11, pp. 239–240, 2016.
- [34] H. Wu, "Clinical study of Yiqi Fumai injection on chronic congestive heart failure," *Chinese Remedies & Clinics*, vol. 12, no. 3, pp. 396–397, 2012.
- [35] K. Xi, "Clinical effect of amiodarone combined with Yiqi Fumai injection in treatment of chronic heart failure complicated with ventricular arrhythmia," *China Modern Medicine*, vol. 22, no. 26, pp. 161–165, 2015.
- [36] C. Yang and Z. Liu, "Clinical study of Yiqi Fumai (lyophilization) for injection in the treatment of chronic heart failure in elderly patients with coronary heart disease," *Practical Geriatrics*, vol. 28, no. 7, pp. 607–608, 2014.
- [37] L. Yang, "Effect of Yiqi Fumai (lyophilized) for injection on cardiac function and plasma brain natriuretic peptide in patients with chronic heart failure," *Modern Journal of Integrated Traditional Chinese and Western Medicine*, vol. 26, no. 4, pp. 391–393, 2017.
- [38] Y. Yang, Y. Zhang, J. Lu, K. Xing, and G. Tian, "Clinical effect of Yiqi Fumai injection on chronic heart failure elder patients

- with coronary heart disease,” *Shanxi Journal of Traditional Chinese Medicine*, vol. 37, no. 10, pp. 1325-1326, 2016.
- [39] Z. Yang, *The Yiqi Fumai Injection Qi and Yin Deficiency Failure before and after Treatment and its Effect with Chronic Heart on the BNP*, Fujian University of Traditional Chinese Medicine, Fuzhou, China, 2012.
- [40] D. Yu and T. Wang, “Yiqi Fumai injection for the treatment of 30 cases of chronic heart failure,” *Shanxi Journal of Traditional Chinese Medicine*, vol. 33, no. 6, pp. 655-656, 2012.
- [41] R. Zhang, “Efficacy of Yiqi Fumai injection in the treatment of elderly patients with chronic heart failure,” *Chinese Journal of Integrative Medicine on Cardio-/Cerebrovascular Disease*, vol. 13, no. 14, pp. 1647-1648, 2015.
- [42] H. Zhu, “Effect of Yiqi Fumai injection combined with atorvastatin calcium on coronary heart disease and heart failure,” *China Practical Medicine*, vol. 14, no. 36, pp. 114-116, 2019.
- [43] R. Zhu and Q. Han, “Clinical observation on Yiqi Fumai for injection in treating coronary heart disease with heart failure,” *Chinese Journal of Integrative Medicine on Cardio/Cerebrovascular Disease*, vol. 12, no. 6, pp. 669-671, 2014.
- [44] H. Li, Y. Duan, and B. Chen, “New pharmacological treatments for heart failure with reduced ejection fraction (HFrEF): a Bayesian network meta-analysis,” *Medicine (Baltimore)*, vol. 99, no. 5, Article ID e18341, 2020.
- [45] X. Sun, “Research progress on modern application of ophiopogonis Radix,” *Modern Chinese Medicine*, vol. 20, no. 11, pp. 1462-1464, 2018.
- [46] X. Zhang, “Research progress on modern application of schisandra chinensis,” *Heilongjiang Medicine Journal*, vol. 28, no. 6, pp. 1259-1260, 2015.
- [47] W. Wang, “Research progress in pharmacological effects of ginsenoside on cardiovascular diseases in last decade,” *Chinese Traditional and Herbal Drugs*, vol. 47, no. 20, pp. 3736-3739, 2016.
- [48] J. Sun, X. Qi, L. Zhang, X. Chen, and P. Ma, “A post-marketing surveillance study on patients using Yiqi Fumai injection (freeze-dried) in a hospital,” *Chinese Journal of Hospital Pharmacy*, vol. 39, no. 1, pp. 97-100, 2019.
- [49] N. Ma, Y. Hou, X. Wang, and J. Mao, “Literature-based study of adverse effects of Yi-Qi--Fu-Mai sterile powde,” *Chinese Journal of New Drugs*, vol. 24, no. 10, pp. 1197-1200, 2015.
- [50] H. Cao, C. Hao, and J. Bi, “Clinical safety monitoring study of Yiqi Fumai lyophilized injection,” *Drug Evaluation Research*, vol. 42, no. 3, pp. 467-471, 2019.

Research Article

Five-Animal Frolics Exercise Improves Anxiety and Depression Outcomes in Patients with Coronary Heart Disease: A Single-Blind Randomized Controlled Trial

Jun Jiang,¹ Qingbao Chi,² Yuting Wang,¹ Xue Jin ,¹ and Shui Yu ¹

¹Department of Cardiovascular, The First Hospital of Jilin University, Changchun 130021, China

²Department of Spine Surgery, The First Hospital of Jilin University, Changchun 130021, China

Correspondence should be addressed to Xue Jin; jinxue18@126.com and Shui Yu; yushuijl@126.com

Received 13 May 2020; Accepted 8 July 2020; Published 7 August 2020

Guest Editor: Mingjun Zhu

Copyright © 2020 Jun Jiang et al. This is an open access article distributed under the Creative Commons Attribution License, which permits unrestricted use, distribution, and reproduction in any medium, provided the original work is properly cited.

Introduction. The patients with coronary heart disease (CHD) always have emotional implications. As the branch of traditional Chinese medicine, Five-Animal Frolics Exercise (FAE) is a popular mind-body exercise in China and shown to improve emotional wellbeing. **Aim.** We aimed to explore the effects of FAE on the emotional disorders of CHD patients. **Methods.** CHD patients were assigned into an experiment group (EG, FAE) and a control group (CG, routine nursing care). We measured serum levels of miR-124 and miR-135 and scores of the Hamilton Depression/Anxiety scale (HAMD/HAMA), Self-Rating Anxiety Scale (SAS), the Self-Rating Depression Scale (SDS), Short Form 36 Health Survey Questionnaire (SF-36), and Pittsburgh Sleep Quality Index (PSQI). **Results.** After a 3-month FAE intervention, serum levels of miR-124 and miR-135 and the scores of HAMD/HAMA, SAS, SDS, and PSQI in the EG group were lower than those in the CG group, while SF-36 scores in the EG group were higher than those in the CG group ($p < 0.05$). Serum levels of miR-124 and miR-135 had a strong relationship with SAS and SDS scores ($p < 0.05$). **Discussion/Implications for Practice.** The study suggests that FAE intervention controls anxiety and depression outcomes and improves life quality in CHD patients by affecting serum levels of miR-124 and miR-135.

1. Introduction

As a traditional medical model shifts to a social-psychological-biological model of modern medicine, much attention is paid to the effects of psychological stress and mental disorders on coronary heart disease (CHD) [1, 2]. Psychological stress affects the neuroendocrine system and immune system, which in turn acts on the nervous system, causing anxiety and depression-like behaviors [3]. Psychological intervention has become the focus in the prevention of emotional disorders in heart disease patients [4]. Aerobic exercise can reduce the risk of adverse cardiovascular events in CHD patients and reduce the severity of anxiety and depression [5]. Exercise therapy can effectively improve anxiety, depression, and life quality. Furthermore, exercise therapy can reduce the levels of various inflammatory and cardiovascular indicators, and some scholars believe that

exercise therapy also has a certain beneficial effect on neuroimmune [6].

As a branch of traditional Chinese medicine, Five-Animal Frolics Exercise (FAE) follows the social-psychological-biological model of modern medicine and coordinates the limbs and body by imitating animal gait [7]. It mainly prevents the progression of cardiovascular diseases by paying much attention to patients' mental and psychological problems and subjective feelings, emphasizing comprehensive treatment, and treating patients from multilevel and multiangle cooperation. The mind-body exercise is performed in a comprehensive and harmonious way. FAE not only treats patients with exercise treatment [8] but also pays attention to the changes of patients' psychological state and the negative effects caused by psychosocial situation [9]. miRNAs play a crucial role in the regulation of psychological stress reaction [10]. Exercise has been found to show a

positive impact on psychological stress by decreasing miR-124 [11]. MiR-124 has been observed to play important roles in the etiology of depression [12]. MiR-135 is involved with NMDA receptor-dependent long-term depression [13] and a kind of anxiety-regulating microRNAs [14]. In this study, the effects of FAE on depression and anxiety of CHD patients were explored, and the changes of serum levels of miR-124 and miR-135 were investigated.

2. Patients and Methods

2.1. Design. This study belongs to a single-blind randomized trial. All procedures were approved by human research ethics committee of our hospital and conform to the provisions of the Declaration of Helsinki [15]. Informed consent to participate in the study was obtained from all participants.

2.2. Subjects and Recruitment. The cases included in this study were the patients who were discharged at our hospital from March 1, 2017, to March 1, 2018.

2.2.1. Inclusion Criteria. The patients who met diagnostic criteria for CHD, anxiety, and depression were included. CHD was diagnosed according to the “Diagnostic Criteria for Coronary Atherosclerotic Heart Disease” issued by the Ministry of Health of the People’s Republic of China in 2010; the diagnostic criteria for anxiety and depression refers to the Chinese Classification of Mental Disorders (Revision 3, CCMD-3) [16]. Anxiety and depression were measured based on the Hamilton Depression Rating Scale (HAMD) and the Hamilton Anxiety Scale (HAMA). They met the diagnostic criteria of anxiety and depression according to the HAMD, HAMA, Self-Rating Anxiety Scale (SAS), and Self-Rating Depression Scale (SDS).

2.2.2. Exclusion Criteria. The patients who could not take some exercise and did not provide consent written form or history clinical data were excluded.

2.3. Sample Size Calculation. The sample size estimation of this study was due to the fact that there are few clinical studies on the therapy based on a FAE. Therefore, considering the sample size of each group, 100 cases of the lowest sample size of clinical research were the initial targets. Based on the actual situation, two aspects were considered. According to the estimated number of inpatients in our hospital, it was estimated that the number of patients who were diagnosed with CHD and met the inclusion and exclusion criteria in the annual inpatients was more than 100. The subjects who voluntarily joined the clinical study may be lower than the 100 cases. According to the period of the clinical study, the total duration was one year, and the follow-up period was 3 months; the shedding rate was set at 20%. Therefore, the final sample size of each group was 60, and the final number of total sample size was 120.

2.4. Randomization. A total of 120 patients were assigned into the control group (CG, normal nursing care) and the experimental group (EG, FAE intervention), and the allocation ratio was 1:1 according to a random number produced by computer (Figure 1). Random allocation sequence was not concealed until interventions were assigned. Two investigators enrolled participants, and two statistical experts assigned participants to interventions. The exercise trainers were blinded after assignment to interventions. After admission, CHD patients were given conventional treatment in the CG group, such as the use of nitrates, anticoagulants, receptor blockers, vasoconstrictase inhibitors, calcium antagonists, statins, and other drugs. Patient’s psychological state should be understood, and negative mood was eliminated to avoid all kinds of incentives. The following items were observed: heart rate and pain location. After the pain of CDH patients was stable, appropriate physical exercise could be performed safely.

The therapy was performed in the EG group based on conventional treatment of the CG group. FAE were trained as follows: training time was selected at 4 pm daily during the patient’s hospital stay. The location was selected in the open space of ward corridor. The exercise video was provided by our hospital for Loop Playback. The patients in the EG group were guided by five presentational trainers to learn FAE and mimic the movements of five different animals (tiger, deer, bear, monkey, and bird) and focused on massaging and strengthening specific internal organs. The patient’s breath required a nasal suction, when the inhalation touched the upper tip of the tongue, the tongue tip was flat when exhaling, and the respiratory rate was 8–10 beats/min. The patients were practiced regularly, and meditation time was 30–60 min at one time with low-decibel meditation light music background and professional guidance.

2.5. Test Cycle and Visit Point. The test periods were 3 months in total, including 1 month of treatment and 3 months of observation. Follow-up was performed at 1 month and 3 months after the enrollment. Weekly telephone follow-up was performed to strengthen the subject’s compliance and minimize the subject. The rate of dropout of the tester was also promptly excluded from subjects with poor compliance. There were 4 on-site visits at the month 0, 1, and 3. The telephone interviews determined the number of monthly telephone follow-ups based on the subject’s compliance at our hospital.

2.6. Observation Index. General conditions included the current medical therapy, history, diagnosis, vital signs, physical examination, and the type, amount, and start and end time of the combined medication. Safety indicators included blood routine, urine routine, liver and kidney functions, blood lipids, blood sugar, BNP, 6-minute walk test, and Brog sensor score. Disease evaluation indicators included the HAMD, HAMA, Self-Rating Anxiety Scale (SAS), the Self-Rating Depression Scale (SDS), Short Form 36 Health Survey Questionnaire (SF-36), and Pittsburgh Sleep Quality Index (PSQI).

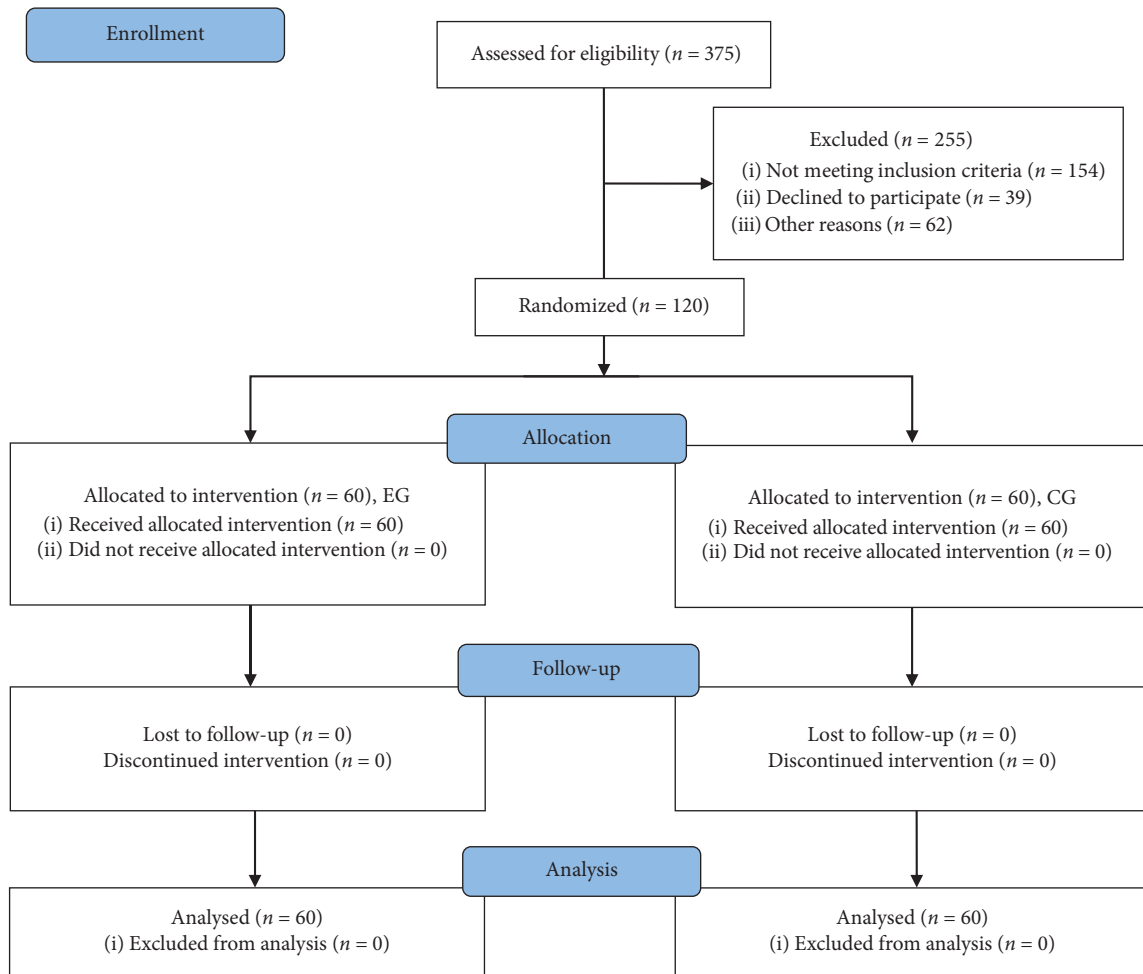


FIGURE 1: CONSORT flow diagram. EG, the patients received FAE. CG, the patients received routine nursing care. The follow-up was three months.

The statistical scale was measured at baseline and after 1 month and 3 months of treatment, and the amount of change in the score and the improvement rate were calculated; the improvement rate was given as (pretreatment score–treatment score)/pretreatment score \times 100%; total effective rate = cure rate + significant efficiency + effective. The following criteria were used: recovery, improvement rate of 75%; markedly effective, 50% < improvement rate < 75%; effective, 25% < improvement rate < 50%; and invalid, improvement rate < 25%.

2.7. Adverse Events. If an adverse event occurred, it should be recorded in time, and the corresponding method was taken according to the severity of the adverse event. The final result was recorded and analyzed if the adverse event disappeared. They should be reported to the responsible person for discussion and treatment if serious adverse events occurred.

2.8. Quantitative Real-Time PCR (qRT-PCR) Analysis. 5 mL blood was obtained from each participant, and serum was prepared via centrifugation at $2000 \times g$ for 10 min. Total RNA

was obtained by using the RNA purification kit (Epicenter, Chicago, IL, USA). 2 μ g of RNA from each person was reversely transcribed by using the cDNA Reverse Transcription Kit (Applied Biosystems, Foster City, CA, USA). The following primers were used for real-time PCR and synthesized by TaKaRa (Dalian, China), miR-124 (forward primer: 5'-CTAGTCTAGAGTCGCTGTTATCTCATTG. TCTG-3' and reverse primer: 5'-CGCGGATCCTCT GCTTCTGTCACAGAATC-3'), miR-135 (forward primer: 5'-AGCATAATACAGCAGGCACAGAC-3' and reverse primer: 5'-AAAGGTTGTTCTCCACTCTCTCAC-3'), and U6 snRNA (5'-CTCGCTTCGGCAGCACA-3') as an internal control. The qRT-PCR reaction was performed using the following condition: 1 cycle of 95°C for 40 s, followed by 45 cycles of 95°C for 10 s, 60°C for 20 s, and 1 cycle of 60°C for 50 s, and maintained at 4°C. Relative gene levels were normalized to the level of U6 snRNA and calculated by using the $2^{-\Delta\Delta CT}$ method.

2.9. Statistical Analysis. The data were analyzed by using SPSS 20.0 statistical software. Count data were examined by using the Pearson 2 test. The two groups were compared by the LSD method if the data were in accordance with the normal

distribution and expressed by the mean standard deviation (S.D.); they were represented by median (P25 and P75) and analyzed by a nonparametric test if they were not normally distributed. The data were compared in a single group before and after treatment, and a paired sample *t*-test was used if the normal distribution was consistent. The Wilcoxon signed rank sum test was used if it was not normally distributed. The Pearson correlation coefficient test was used to explore the relationship between the relative levels of miR-124 or miR-135 and/or SAS and SDS scores. The primary outcomes included anxiety and depression scores at 1 month. Secondary outcomes were measured after a 3-month follow-up. The statistically significant test level was set at $p < 0.05$, and the confidence interval of the parameter was 95%.

3. Results

3.1. Baseline Characteristics. In this study, no subjects were excluded from the study, and 120 subjects finished the present experiment, and the follow-up was 3 months (Figure 1). There was no significant difference in the baseline level between the two groups, including gender, age, combined disease (including hypertension, diabetes, and hyperlipidemia), blood lipids test (total cholesterol, glycerol triglyceride, and low-density lipoprotein), fasting blood glucose, electrocardiogram, BNP, the 6-minute walk test, and the Brog sensory score (Table 1, $p > 0.05$).

3.2. Anxiety and Depression Scale. HAMD, HAMA, SAS, and SDS were measured in the two groups. The anxiety and depression scales were scored at baseline (month 0), the first follow-up (month 1, primary outcomes), and the last follow-up (month 3, secondary outcomes). The first follow-up and baseline were calculated as the amount of change (I). The change in the final follow-up from the baseline was calculated as the amount of change (II).

Before intervention, the statistical difference for HAMD, HAMA, SAS, and SDS was insignificant between the two groups ($p > 0.05$, Table 2). After FAE intervention, the scores for HAMD, HAMA, SAS, and SDS in the EG group were lower than those in the CG group ($p < 0.05$, Table 2). The comparison of the amounts of changes (I) and (II) showed that the changes for the scores of HAMD, HAMA, SDS, and SAS in the EG group were higher than that in the CG group at baseline (month 0), the first follow-up (month 1), and the last follow-up (month 3) (Table 2, $p < 0.05$).

3.3. PSQI. The PSQI scores of the two groups were recorded at baseline (month 0), the first follow-up (month 1), and the last follow-up (month 3). The statistical difference for PSQI scores at baseline was insignificant between the two groups (Table 3, $p > 0.05$). After FAE intervention, the changes in PSQI scores were significantly different when compared with before intervention (Table 3, $p < 0.05$). The sleep quality of both groups was significantly improved. Baseline changes were compared between the groups and showed that the statistical differences were significant for the PSQI in amounts of changes (I) and (II) (Table 3, $p < 0.05$).

TABLE 1: Clinical baseline characteristics between two groups.

Parameters	EG ($n = 60$)	CG ($n = 60$)	<i>P</i> values
Gender (male)	24 (40%)	24 (40%)	—
Age (yr)	61.00 ± 8.93	63.10 ± 10.04	0.763
Combined with hypertension	45 (75%)	42 (70%)	0.816
Combined with diabetes	24 (40%)	24 (40%)	—
Combined with tuberculosis	57 (95%)	51 (85%)	0.615
Abnormal ECG check	33 (55%)	36 (60%)	0.805
Total cholesterol	3.89 ± 1.32	3.82 ± 1.03	0.965
Triglyceride	1.50 ± 0.92	1.82 ± 0.78	0.328
Low-density lipoprotein	2.04 ± 1.06	1.91 ± 0.63	0.877
Fasting blood sugar	6.60 ± 1.40	7.28 ± 2.62	0.372
BNP	87.02 ± 79.40	99.96 ± 138.24	0.868
6-minute walk test	527.78 ± 49, 77	539.25 ± 57.59	0.135
Brog feels the score	11.89 ± 1.61	11.25 ± 1.68	0.409

3.4. Comparison of Curative Effects. The percentage of total effectiveness of the PSQI efficacy of the two groups is described in Table 4. After FAE intervention, the EG group had a total effective rate of 100%, and the CG group had a total effective rate of 45% ($p < 0.05$). Comparing the total efficiency and inefficiency of the two groups, the statistical difference for the efficacy of PSQI was significant between the two groups.

3.5. Quality of Life Scale (SF-36). The scores of the simple quality of life scale (SF-36) of the two groups were measured at baseline (month 0), the first follow-up (month 1), and the last follow-up (month 3). Except for body pain, the scores of the other factors were insignificant before intervention (Table 5, $p > 0.05$). The baselines of change (I) were statistically different for physical role functioning, vitality, emotional wellbeing, and mental health between the two groups (Table 5, $p < 0.05$) but not for other factors (Table 5, $p > 0.05$). The baselines of change (II) were statistically different for physical functioning, physical role functioning, emotional wellbeing, and perception of changes in health between the two groups (Table 5, $p < 0.05$) but not for other factors (Table 5, $p > 0.05$).

3.6. Laboratory Inspection and Other Indicators. All subjects had no abnormalities in both groups during blood tests, urine routine, and liver and kidney function tests during the clinical study. Combined with BNP, the 6-minute walk test, and Brog sensory score at baseline (month 0), the subjects of two groups had better cardiac function and performed the exercises or regular exercise (walking, cycling, and jogging.).

3.7. Number of Adverse Events and Treatment. During the 0-week period, the number of adverse events was two, the symptom was diarrhea, one was from the EG group, and the other occurred during the taking medicine. The tester did not have any further adverse events. There were no serious adverse events between the two groups.

TABLE 2: Comparison of four anxiety depression scales between two groups.

Parameters and time points		EG	CG	<i>p</i>
HAMD	0 month	12.0 (10.0, 14.0)	11.5 (8.3, 14.8)	0.908
	1 month	7.5 (5.3, 10.0)	9.5 (7.0, 12.0)	
	3 months	5.0 (4.0, 6.0)	8.0 (5.3, 10.0) [#]	
	Amounts of change (I)	4.0 (2.3, 6.8) [#]	2.0 (0.3, 3.8)	0.015*
	Amounts of change (II)	7.0 (5.3, 8.8) [#]	3.0 (2.3, 5.8)	0.002*
HAMA	0 month	17.0 (15.0, 19.0)	15.0 (12.0, 17.0)	0.095
	1 month	10.0 (7.0, 12.0)	12.0 (10.0, 14.0)	
	3 months	5.5 (5.0, 7.8) [#]	9.0 (7.0, 12.0) [#]	
	Amounts of change (I)	8.0 (5.3, 9.0) [#]	2.0 (2.0, 4.0)	<0.001*
	Amounts of change (II)	11.0 (9.0, 12.0) [#]	5.0 (4.0, 7.8)	<0.001*
SDS	0 month	41.0 (39.3, 47.5)	40.5 (35.3, 49.0)	0.770
	1 month	34.0 (31.0, 36.0)	35.0 (32.0, 44.3)	
	3 months	30.0 (29.3, 32.0) [#]	34.0 (30.3, 40.8) [#]	
	Amounts of change (I)	7.0 (5.0, 10.0) [#]	3.0 (1.0, 6.8)	0.012*
	Amounts of change (II)	10.0 (8.3, 14.8) [#]	5.5 (3.3, 8.0)	0.005*
SAS	0 month	50.0 (51.0, 55.5)	50.0 (50.0, 52.0)	0.106
	1 month	41.0 (34.0, 43.5)	45.0 (39.5, 48.8)	
	3 months	32.0 (31.0, 37.5) [#]	40.0 (32.8, 44.3) [#]	
	Amounts of change (I)	14.5 (10.3, 18.0) [#]	4.5 (3.0, 8.8)	<0.001*
	Amounts of change (II)	20.0 (15.3, 22.8) [#]	8.5 (6.3, 17.0) [#]	<0.001*

Note. Amounts of change (I) is the comparison between 1 month and 0 month, and the amounts of change (II) is the comparison between 3 months and 0 month. *The comparison between the test group and the control group is statistically significant ($p < 0.05$). [#]There were significant differences between the two groups before and after treatment ($p < 0.05$).

TABLE 3: Comparison of PSQI between two groups.

	EG	CG	<i>p</i> values
0 month	14.0 (10.3, 15.0)	11.0 (9.0, 13.8)	0.100
1 month	9.0 (6.5, 11.8)	9.0 (7.3, 12.0)	
3 months	7.0 (5.0, 7.8) [#]	8.0 (6.0, 11.5) [#]	
Amounts of change (I)	3.0 (1.3, 6.8) [#]	1.0 (0.0, 1.8)	0.003*
Amounts of change (II)	6.0 (4.0, 8.0)	2.5 (1.0, 4.0) [#]	0.001*

Note. Amounts of change (I) is the comparison between 1 month and 0 month, and the amounts of change (II) is the comparison between 3 months and 0 month. *The comparison between the test group and the control group is statistically significant ($p < 0.05$). [#]There were significant differences between the two groups before and after treatment ($p < 0.05$).

TABLE 4: Comparison of curative effect of PSQI.

Groups	Therapeutic results				Total effective	<i>p</i> values
	Healing	Significant effective	Effective	Invalid		
EG		7 (35%)	13 (65%)		100% [#]	<0.001*
CG	1 (5%)	2 (10%)	6 (30%)	11 (55%)	45%	

Note. *The comparison between the test group and the control group is statistically significant ($p < 0.05$). [#]There were significant differences between the two groups before and after treatment ($p < 0.05$).

3.8. FAE Reduced Serum Levels of miR-124 and miR-135 in CHD Patients. Before FAE intervention, the statistical difference for miR-124 (Figure 2(a)) and miR-135 (Figure 2(b)) was insignificant between the two groups ($p > 0.05$). After a 3-month intervention, the levels for miR-124 (Figure 2(a)) and miR-135 (Figure 2(b)) in the TG group were lower than those in the CG group ($p < 0.05$). The results suggest that FAE reduced serum levels of miR-124 and miR-135 in CHD patients.

3.9. Serum Levels of miR-124 and miR-135 had a Strong Relationship with SAS and SDS. The Pearson correlation coefficient test showed that the increase in the levels of miR-124

and miR-135 would result in the increase in the scores of SAS (Figures 3(a) and 3(b)), SDS (Figures 3(c) and 3(d), $p < 0.05$). The results suggest that serum levels of miR-124 and miR-135 have a strong positive relationship with SAS and SDS scores ($p < 0.05$).

4. Discussion

The differences for the changes of HAMD, HAMA, SDS, SAS, and PSQI scores were significant between the two groups ($p < 0.05$). The improvement in the EG group was better than that in the CG group. The results

TABLE 5: The comparison of life quality of SF-36 between two groups.

Parameters and time points	EG	CG	<i>p</i>	
Physical functioning	0 month	88.0 (84.0, 100.0)	85.0 (85.0, 95.0)	0.430
	1 month	94.0 (88.0, 100.0)	85.0 (80.0, 95.0)	
	3 months	100.0 (100.0, 100.0) [#]	87.5 (81.3, 95.0) [#]	
	Amounts of change (I)	3.8 (0.0, 5.0) [#]	0.0 (0.0, 0.0)	0.295
	Amounts of change (II)	5.0 (0.0, 10.0)	0.2 (0.0, 5.0)	0.003*
Physical role functioning	0 month	12.9 (0.0, 18.8)	11.3 (0.0, 75.0)	0.925
	1 month	25.0 (25.0, 50.0)	0.0 (0.0, 87.5)	
	3 months	50.0 (50.0, 100.0) [#]	37.5 (6.3, 100.0) [#]	
	Amounts of change (I)	21.0 (0.0, 25.0) [#]	0.0 (0.0, 0.0)	0.049*
	Amounts of change (II)	50.0 (25.0, 50.0) [#]	12.5 (0.0, 43.8)	0.003*
Body pain	0 month	84.0 (75.0, 100.0)	79.0 (74.0, 100.0)	0.042*
	1 month	95.0 (88.0, 100.0)	84.0 (74.0, 100.0)	
	3 months	92.0 (74.0, 100.0) [#]	89.0 (76.5, 100.0) [#]	
	Amounts of change (I)	2.0 (0.0, 9.0)	0.0 (0.0, 0.0)	0.109
	Amounts of change (II)	3.1 (0.0, 15.0)	3.3 (0.0, 26.0)	0.274
General health perceptions	0 month	30.0 (25.0, 45.0)	32.5 (20.0, 40.0)	0.579
	1 month	45.0 (26.8, 53.8)	32.5 (25.0, 45.0)	
	3 months	56.0 (45.0, 70.3) [#]	52.5 (35.0, 67.0) [#]	
	Amounts of change (I)	3.6 (0.0, 13.8)	1.2 (0.0, 3.8)	0.637
	Amounts of change (II)	20.0 (5.5, 30.0)	17.0 (5.0, 30.3)	0.949
Vitality	0 month	45.0 (41.0, 50.0)	55.0 (45.0, 65.0)	0.117
	1 month	55.0 (50.0, 68.8)	55.0 (45.0, 65.0)	
	3 months	62.5 (55.0, 70.0) [#]	57.5 (51.3, 73.8) [#]	
	Amounts of change (I)	10.0 (0.0, 18.8)	0.0 (0.0, 0.0)	≤0.001*
	Amounts of change (II)	15.0 (5.3, 23.8)	5.0 (0.0, 10.0)	0.073
Social functioning	0 month	88.0 (75.0, 100.0)	88.0 (65.3, 100.0)	0.610
	1 month	88.0 (88.0, 100.0)	88.0 (78.3, 100.0)	
	3 months	100.0 (100.0, 100.0) [#]	100.0 (100.0, 100.0) [#]	
	Amounts of change (I)	5.0 (0.0, 12.8)	0.0 (0.0, 0.0)	0.172
	Amounts of change (II)	12.0 (0.0, 13.0)	12.0 (0.0, 34.0)	0.728
Emotional wellbeing	0 month	0.0 (0.0, 91.8)	0.0 (0.0, 100.0)	0.942
	1 month	50.0 (33.0, 100.0)	0.0 (0.0, 100.0)	
	3 months	100.0 (67.0, 100.0) [#]	33.0 (8.3, 100.0) [#]	
	Amounts of change (I)	23.0 (0.0, 33.0) [#]	0.0 (0.0, 0.0)	0.012*
	Amounts of change (II)	67.0 (8.3, 100.0) [#]	0.0 (0.0, 33.0)	0.003*
Mental health	0 month	50.0 (42.0, 60.0)	48.0 (42.5, 56.0)	0.073
	1 month	60.0 (49.0, 68.0)	48.0 (42.5, 55.8)	
	3 months	68.0 (60.0, 72.0) [#]	56.0 (48.0, 64.0) [#]	
	Amounts of change (I)	8.0 (0.0, 18.5) [#]	0.0 (0.0, 0.0)	0.001*
	Amounts of change (II)	17.0 (1.0, 24.0)	4 (-0.8, 13.5)	0.062
Perception of changes in health	0 month	25.0 (25.0, 25.0)	25.0 (25.0, 50.0)	0.666
	1 month	37.5 (25.0, 50.0)	25.0 (25.0, 50.0)	
	3 months	50.0 (25.0, 50.0) [#]	50.0 (25.0, 50.0)	
	Amounts of change (I)	0.0 (0.0, 25.0)	0.0 (0.0, 0.0)	0.322
	Amounts of change (II)	15.0 (0.0, 25.0)	0.0 (0.0, 25.0)	0.002*

Note. Amounts of change (I) is the comparison between 1 month and 0 month, and the amounts of change (II) is the comparison between 3 months and 0 month. *The comparison between the test group and the control group is statistically significant ($p < 0.05$). [#]There were significant differences between the two groups before and after treatment ($p < 0.05$).

demonstrated that FAE had high efficacy for controlling the symptoms related to depression and anxiety in CHD patients. It may be a potential approach in the prevention of the progression of anxiety and depression in CHD patients.

After a 3-month intervention, serum levels of miR-124 and miR-135 and the scores of the HAMD/HAMA, SAS, SDS, and PSQI in the EG group were lower than those in the CG group, while SF-36 scores in the EG group were higher

than those in the CG group. Serum levels of miR-124 and miR-135 had a strong positive relationship with SAS and SDS. The results suggest that miR-124 and miR-135 may be candidate biomarkers in the diagnosis of the CHD patients with depression and anxiety. The study suggests that FAE can control the symptoms related to anxiety and depression and improve sleep quality and life quality in CHD patients by affecting serum levels of miR-124 and miR-135. The results were consistent with a previous report that FAE

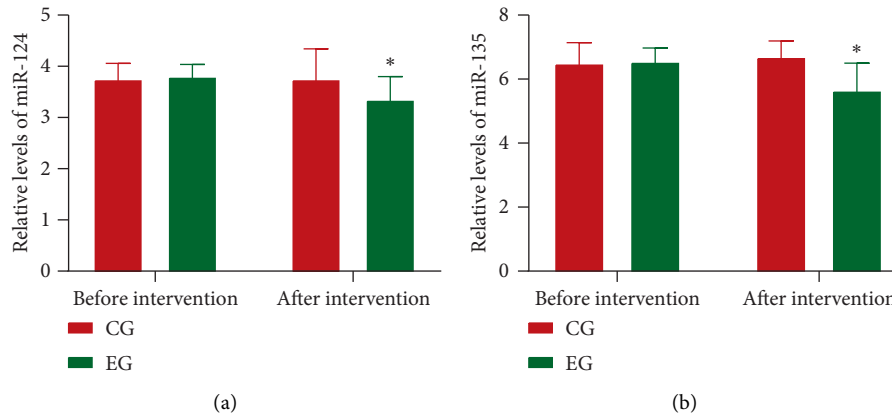


FIGURE 2: Relative levels of miR-124 and miR-135 in the patients with coronary heart disease. EG and FAE were used. CG, a control group. $n=20$ for each group. The statistical different was significant if $p < 0.05$.

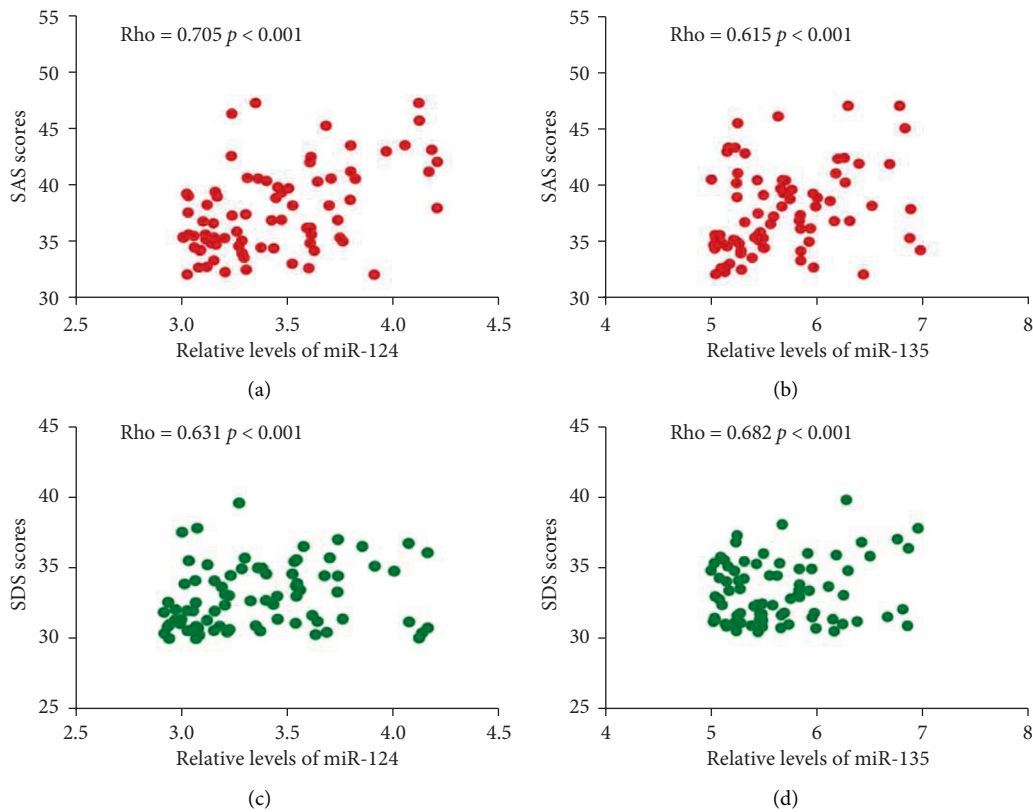


FIGURE 3: Pearson correlation coefficient analysis of the relationship between relative levels of miR-124 and miR-135 and the values of SAS and SDS. (a) The relationship between relative levels of miR-124 and the scores of SAS. (b) The relationship between relative levels of miR-135 and the scores of SAS. (c) The relationship between relative levels of miR-124 and the scores of SDS. (d) The relationship between relative levels of miR-135 and the scores of SDS. There is a strong positive relationship if rho value falls within 0.5 and 1. There is a strong negative relationship if rho value falls within -0.5 and -1 .

intervention improved anxiety and emotional disorders in the patients [17].

According to the anxiety and depression scores, the patients had different degrees of mild-to-moderate anxiety and depression before the intervention. After the implementation of FAE, the anxiety and depression of

patients were alleviated and improved, further demonstrating that psychological intervention promoted the mental health of patients. The number of anxiety and depression in the two groups decreased after intervention, but the number of anxiety and depression in the EG group was significantly lower than that in the CG group

($p < 0.05$), indicating that the implementation of the FAE reduces more anxiety and depression than normal physical exercise.

There is increasing strong evidence supporting the integrated effectiveness of mind-body treatments (non-pharmacological interventions) for heart disease [18]. Mindfulness-based meditation can attenuate the severity of depression and anxiety symptoms among heart disease patients and improve depression and anxiety clinical outcomes. FAE is a Chinese traditional Qigong, which focuses on mind-body integration, and thought to be effective in improving physical and mental wellbeing. FAE has been found to be effective in the prevention of the progression of anxiety and depression in chronic obstructive pulmonary disease (COPD) patients [19]. FAE is figuratively known as the “five animals” exercise, which is the most interesting activity for most CHD patients. CHD patients will be glad to participate in the activities, which show the moderating effect of mindfulness and benefits on multidimensional mental health [20]. FAE maintains single-minded status and effectively eliminates the distractions, which are harmful to mental health [21]. All these properties of FAE may contribute to alleviate the pathogenesis of emotion disorders of CHD patients.

4.1. Study Limitations. There were some limitations in the present work. The subjects were only included at our hospital, which had certain geographical restrictions, which led to some selection biases. The four anxiety scales used in this study were credible in the psychiatric reliability. However, for nonpsychiatric diseases and non-psychiatric physicians, their reliability may be affected because they were not analyzed by psychiatrists, and the diagnosis of emotional disorders only included anxiety and depression. FAE is only popular in China and seldom known in other countries. The detailed molecular mechanism on how FAE can affect miRNA remains unclear. In the comparison of life quality of SF-36 between two groups, the difference of the amounts of change (I) of vitality and mental health was statistically significant between the EG group and the CG group. But the difference of the amounts of change (II) of vitality and mental health between the EG group and the CG group was statistically insignificant. The reasons may be caused by the following reasons: (1) the study was performed in the small population, and some bias will be induced ($n = 60$ in each group); (2) one and three months of intervention still belongs to a short-term study. A long-term study, such as one-year term, may be necessary to find the stable results for mental health [22]. A short-term intervention may lead to a significant variety of mental health issue, just as the outcome of one month of intervention may be occasionally better than that of three months of intervention in the present result. Vitality is closely associated with mental health and can be defined by using mental wellbeing [23], and a short-term study will cause the results in a significant variety. Therefore, a long-term study in a larger population is possibly also needed to find the stable results.

5. Conclusions

The EG group has better improvement in the anxiety and depression scale (HAMD, HAMA, SAS, and JDS), PSQI, curative effects, and SF-36. Serum levels of miR-24 and miR-135 had a strong positive relationship with SAS and SDS scores. The study suggests that FAE inhibits the risk of anxiety and depression and improves sleep quality and life quality in CHD patients by affecting serum levels of miR-24 and miR-135. We recommend that the CHD patients should insist on practicing FAE to prevent the risk of mental diseases, such as depression and anxiety. On the other hand, a long-term study in a larger population is needed to confirm the present conclusion.

Data Availability

The data for the current study are available from the corresponding author upon reasonable request.

Conflicts of Interest

The authors declare that there are no conflicts of interest.

Authors' Contributions

Jun Jiang, Qingbao Chi, Yuting Wang, and Xue Jin designed and performed the present experiments and analyzed all data. Shui Yu developed the overview and involved in writing the article. All authors agreed the final submission.

Acknowledgments

The authors are very grateful to all the patients in the study. The authors also thank Professor Qi Song and Chun Sun for supporting technique help. The study was performed by using the financial support from the Talent Creative Projects of the First Hospital of Jilin University (grant no. JLU2019CC).

References

- [1] C. D. Spielberger, “8 effects of stress, emotion, and type-A behavior on heart disease and psychological disorders,” in *Proceedings of the 28th International Congress of Psychology*, Beijing, China, 2019.
- [2] P. Pimple, B. B. Lima, M. Hammadah et al., “Psychological distress and subsequent cardiovascular events in individuals with coronary artery disease,” *Journal of the American Heart Association*, vol. 8, no. 9, Article ID e011866, 2019.
- [3] M. H. Antoni and F. S. Dhabhar, “The impact of psychosocial stress and stress management on immune responses in patients with cancer,” *Cancer*, vol. 125, no. 9, pp. 1417–1431, 2019.
- [4] Y. Wu, B. Zhu, Z. Chen et al., “New insights into the comorbidity of coronary heart disease and depression,” *Current Problems in Cardiology*, Article ID 100413, pp. 1–31, 2019.
- [5] T. Liu, A. W. Chan, Y. H. Liu, and R. E. Taylor-Piliae, “Effects of Tai Chi-based cardiac rehabilitation on aerobic endurance, psychosocial well-being, and cardiovascular risk reduction among patients with coronary heart disease: a systematic

- review and meta-analysis," *European Journal of Cardiovascular Nursing*, vol. 17, no. 4, pp. 368–383, 2018.
- [6] J. F. Machi, R. Schmidt, L. M. Salgueiro et al., "Exercise benefits the cardiac, autonomic and inflammatory responses to organophosphate toxicity," *Toxicology Reports*, vol. 6, pp. 666–673, 2019.
- [7] J. Zhang and S.-n. Shen, "On the source of traditional philosophy and five-animal exercises led by TCM," *Journal of Nanjing University of Traditional Chinese Medicine (Social Science Edition)*, vol. 1, 2011.
- [8] Z. Li and L. Zhou, "Observation on patients with dyslipidemia treated by five-animal exercises," *Journal of Guangzhou Sport University*, vol. 29, no. 4, pp. 97–103, 2009.
- [9] L. Cui-lian, "Research on the effects of five-animal exercise training to college students' mental health," *Journal of Gansu Lianhe University (Natural Science Edition)*, vol. 2, 2010.
- [10] C. Wiegand, A. Savelsbergh, and P. Heusser, "MicroRNAs in psychological stress reactions and their use as stress-associated biomarkers, especially in human saliva," *Biomedicine Hub*, vol. 2, no. 3, pp. 1–15, 2017.
- [11] A. Pan-Vazquez, N. Rye, M. Ameri et al., "Impact of voluntary exercise and housing conditions on hippocampal glucocorticoid receptor, miR-124 and anxiety," *Molecular Brain*, vol. 8, p. 40, 2015.
- [12] Z. Gu, J. Pan, and L. Chen, "MiR-124 suppression in the prefrontal cortex reduces depression-like behavior in mice," *Bioscience Reports*, vol. 39, no. 9, 2019.
- [13] Z. Hu, D. Yu, Q. H. Gu et al., "miR-191 and miR-135 are required for long-lasting spine remodelling associated with synaptic long-term depression," *Nature Communications*, vol. 5, p. 3263, 2014.
- [14] C. P. Murphy and N. Singewald, "Role of microRNAs in anxiety and anxiety-related disorders," *Current Topics in Behavioral Neurosciences*, Springer, Berlin, Germany, 2019.
- [15] F. Rosmini, "Points of view in comparison on the 5th revision of the declaration of Helsinki," *Annali Dell'istituto Superiore di Sanita*, vol. 38, no. 2, pp. 169–174, 2002.
- [16] Y. F. Chen, "Chinese classification of mental disorders (CCMD-3): towards integration in international classification," *Psychopathology*, vol. 35, no. 2-3, pp. 171–175, 2002.
- [17] T. Chun-lan, "Effect of health Qigong Wuqinxi on middle-aged and elderly people's level of anxiety," *Shandong Sports Science & Technology*, vol. 6, 2011.
- [18] A. Rao, M. DiGiacomo, P. J. Newton, J. L. Phillips, and L. D. Hickman, "Meditation and secondary prevention of depression and anxiety in heart disease: a systematic review," *Mindfulness*, vol. 10, no. 1, pp. 1–14, 2019.
- [19] Z. Li, S. Liu, L. Wang, and L. Smith, "Mind-body exercise for anxiety and depression in COPD patients: a systematic review and meta-analysis," *International Journal of Environmental Research and Public Health*, vol. 17, no. 1, p. 22, 2020.
- [20] B. Zhang and M. Zhang, "Practicing Wuqinxi style on environment and psychological effects," *Journal of Anyang Normal University*, vol. 5, 2012.
- [21] Y. Zhong, "The analysis of the adjustment mechanism of health-care Qigong to human emotion based on the theory of mental energy," in *Proceedings of the 3rd International Conference on Science and Social Research (ICSSR 2014)*, Tianjin, China, 2014.
- [22] I. Arends, J. Almansa, S. A. Stansfeld, B. C. Amick, J. J. L. Van Der Klink, and U. Bültmann, "One-year trajectories of mental health and work outcomes post return to work in patients with common mental disorders," *Journal of Affective Disorders*, vol. 257, pp. 263–270, 2019.
- [23] E. Masciocchi, M. Maltais, K. El Haddad et al., "Defining vitality using physical and mental well-being measures in nursing homes: a prospective study," *The Journal of Nutrition, Health & Aging*, vol. 24, no. 1, pp. 37–42, 2020.

Review Article

Qiju Dihuang Decoction for Hypertension: A Systematic Review and Meta-Analysis

Shuo Zhang,¹ Xue Bai,² Zhen-Lin Chen,³ Jia-Jia Li,² Yan-Yan Chen ,² and Yu-Ping Tang ²

¹School of Traditional Chinese Medicine, Beijing University of Chinese Medicine, Beijing 100029, China

²Key Laboratory of Shaanxi Administration of Traditional Chinese Medicine for TCM Compatibility, Shaanxi University of Chinese Medicine, Xi'an 712046, Shaanxi, China

³Graduate School, Shaanxi University of Chinese Medicine, Xi'an 712046, Shaanxi, China

Correspondence should be addressed to Yu-Ping Tang; yupingtang@sntcm.edu.cn

Received 14 May 2020; Revised 26 June 2020; Accepted 8 July 2020; Published 31 July 2020

Guest Editor: Mingjun Zhu

Copyright © 2020 Shuo Zhang et al. This is an open access article distributed under the Creative Commons Attribution License, which permits unrestricted use, distribution, and reproduction in any medium, provided the original work is properly cited.

Objective. To systematically evaluate the efficacy of Chinese herbal medicine Qiju Dihuang Decoction (QDD) for hypertension. **Methods.** A comprehensive literature search of randomized controlled trials using QDD to treat hypertension was conducted in 7 electronic databases, including Chinese databases. Subjects and abstracts of the trials were read in NoteExpress for preliminary screening, and the full text was read for further screening. The data extraction table was made for the selected 19 trials, and risk of bias was assessed by using the Cochrane collaboration tool, followed by data analysis using Rev Man 5.3. **Results.** The antihypertensive efficacy of QDD is 1.45 times that of antihypertensive drugs and 1.56 times that of conventional therapies, which can also reduce the endothelin level. QPAD exhibits an antihypertensive effect, and its clinical efficacy is 1.34 times and 1.61 times that of antihypertensive drugs, which can not only significantly lower the diastolic blood pressure but also reduce the 24 h mean ambulate blood pressure. At the same time, it can decrease the TCM syndrome score, inhibit the inflammation, protect the renal function, reduce the insulin resistance, and improve the life quality of patients. **Conclusion.** QDD can effectively reduce blood pressure and improve the life quality of patients with hypertension, which plays a certain role in preventing hypertension complications. However, due to the methodological deficiencies, more rigorous randomized controlled trials will be needed in the future to provide stronger evidence.

1. Introduction

Hypertension is a common clinical cardiovascular disease with systemic arterial pressure increase as the main sign, which not only causes headache, dizziness, and other clinical symptoms but also damages important organs such as the heart, brain, kidney and eyes, and it further produces multiple system lesions or dysfunction [1]. Its high morbidity and mortality bring physical and mental suffering to patients [2]. In recent years, hypertension has become a global public health problem involving over one billion people worldwide [3, 4]. Patients with hypertension require a long-term medication with diuretics, angiotensin-converting enzyme inhibitors, and calcium antagonists that are widely used. However, they frequently cause some

contraindications and adverse reactions, such as irritant dry cough, hyperkalemia, sexual dysfunction, and renal deterioration, which seriously affects the life quality of many patients. And after using these drugs, about half of patients cannot effectively control their blood pressure [5]. Traditional Chinese medicine (TCM) is often used to treat patients with hypertension [6, 7], which can not only achieve good clinical efficacy but also may reduce the adverse reactions. Moreover, there are also certain advantages that TCM is applied for treating the complications of hypertension. Hypertension belongs to vertigo or headache in TCM. The first treatises on “vertigo” and “headache” appeared in *Inner Canon of Yellow Emperor* (Huang Di Nei Jing in Chinese). TCM believes that the onset of hypertension is mainly due to wind, phlegm, deficiency, blood

stasis, and other diseases caused by the wind dizzy internal movement, phlegm and blood stasis, and Qi and blood block or Qing-qiao loss of nourishing, which results in the imbalance between Qi and blood and Yin and Yang. Therefore, the nature of hypertension is usually described as deficiency in origin and excess in superficiality.

Qiju Dihuang Decoction (QDD), recorded in the Qing Dynasty *Measles Complete Book* (Ma Zhen Quan Shu in Chinese), is one of the most commonly used TCM formulae for the syndrome of “liver and kidney Yin deficiency,” mainly used for vertigo, tinnitus, eyes acerbity photophobia, and vision dim [8, 9]. QDD is composed by 8 kinds of herbs, including Lycii Fructus (Gouqizi, fruit from *Lycium barbarum* L.), Chrysanthemi Flos (Juhua, inflorescence from *Chrysanthemum morifolium* Ramat.), Rehmanniae Radix Praeparata (Shudihuang, root tuber from *Rehmannia glutinosa* Libosch.), Dioscoreae Rhizoma (Shanyao, rhizome from *Dioscorea opposita* Thunb.), Corni Fructus (Shanzhuyu, pulp from *Cornus officinalis* Sieb. et Zucc.), Moutan Cortex (Mudanpi, velamen from *Paeonia suffruticosa* Andr.), Poria (Fuling, sclerotium from *Poria cocos* Schw. Wolf), and Alismatis Rhizoma (Zexie, tuber from *Alisma orientale* Sam. Juzep.). Gouqizi and Shudihuang can benefit the kidney Yang and nourish essence, Juhua can clear the liver and improve the vision, Shanyao can tonify the spleen and nourish the kidney, Shanzhuyu can nourish the kidney and liver, Mudanpi can clear away the liver-fire, Fuling can induce diuresis with bland drug, and Zexie can infiltrate to remove dampness and turbidity. Pharmacological studies have found that QDD can improve the liver fat metabolism, reduce the capillary permeability, enhance the immunity, diminish the inflammation, delay the senility, and decrease the alloxan caused by high blood glucose. QDD contains many chemical components such as cycloene terpenes, flavones, cholines, and vitamin [10, 11]. As an effective drug, QDD is widely used for the treatment of hypertension and related complications by combining with other Chinese herbal medicines. Some animal experiments proved that QDD could not only reduce blood pressure and blood lipids [12] but also lowers the ratio of middle level of renal arteriolus and lumen diameter in spontaneously hypertensive rats [13], so as to regulate renal vascular remodeling and to improve renal blood flow [14], which plays a protective role in the kidney. At the same time, by improving the ultrastructure of endothelial cells, it can regulate the mitochondrial membrane potential and calcium ion concentration of cells, affect the proliferation of endothelial cells [15], regulate the NO-NOS system, and reduce the damage of vascular endothelial cells [16]. Although there are some systematic reviews and meta-analyses on Chinese herbal medicines for the treatment of hypertension, most of them only reported the antihypertensive effect of Chinese herbal medicines and the changes in blood pressure before and after treatment and did not touch upon the life quality of patients and the prevention of complications. So far, only some studies have shown that QDD can be used alone or in combination with other TCM formulae to treat hypertension and other related diseases, but the clinical indicators and antihypertensive effects in these studies are different. In

addition, the efficacy of QDD in the treatment of hypertension has not been systematically assessed. Therefore, this study was designed to evaluate the effect of QDD on hypertension patients' blood pressure, life quality, renal function, and insulin resistance as well as the potential mechanism of lowering blood pressure.

2. Data and Methods

This study was conducted following the Preferred Reporting Items for Systematic Reviews and Meta-analyses (PRISMA) [17].

2.1. Literature Search. Randomized controlled trials (RCTs) that evaluated the effect of QDD for hypertension were searched in the following 7 electronic databases: the Chinese National Knowledge Infrastructure (CNKI, from 1980 to 2020), Chinese Biomedical Literature Database (CBM, from 1978 to 2020), Wanfang Database (from 1998 to 2020), Weipu Database (from 1989 to 2020), PubMed (from 1959 to 2020), and Web of Science (from 1986 to 2020) and Springerlink (from 1996 to 2020). We used the following terms “blood pressure” OR “high blood pressure” OR “hypertension” OR “essential hypertension” OR “primary hypertension” OR “gao xue ya” OR “xue ya” AND (“Qiju Dihuang decoction” OR “Qijudihuang decoction” OR “Qi ju di huang decoction” OR “Qijudihuang tang” OR “Qiju dihuang tang” OR “Qi ju di huang tang” OR “Qijudihuangtang” AND “clinical trial” OR “randomized controlled trial” OR “randomized controlled trial” OR “lin chuang yan jiu” OR “lin chuang shi yan”). No restriction on language was applied.

2.2. Criteria for Literature Inclusion

2.2.1. Patients. Trials were considered eligible for inclusion if the diagnosis of hypertension in the patients conformed to the diagnostic criteria established by the World Health Organization or International Hypertension Federation or the guidelines for the prevention and treatment of hypertension in China. And patients were not restricted by age, gender, or nationality. Studies were excluded if (a) the diagnostic criteria of the study object were unclear; (b) the patient had secondary hypertension; (c) the patient was accompanied by other adverse states (such as depression, insomnia, and perimenopause); (d) the patient was pregnant.

2.2.2. Intervention and Control Measures. The intervention measures in the treatment group should be QDD alone or in combination with other antihypertensive treatments. And, the control group should be other antihypertensive treatments or placebo, such as conventional therapy, conventional antihypertensive drugs, and lifestyle interventions (CADLI). However, trials involving qigong, TAI Chi, acupuncture, moxibustion, massage, and cupping as common interventions will be excluded.

2.2.3. Outcomes. The primary outcome was defined as blood pressure, which included antihypertensive effects, systolic blood pressure (SBP), and diastolic blood pressure (DBP). The secondary outcomes included clinical effects, TCM syndrome score, life quality, 24 h ambulatory blood pressure, angiotensin II (Ang II), endothelin (ET), insulin sensitivity index (ISI), insulin (INS), mA1b, β_2 -microglobulin (β_2 -MG), *N*-acetyl- β -glucosidase (NAG), high sensitivity C-reactive protein (HsCRP), and adverse reactions.

2.2.4. Studies. This study included a randomized controlled trial using QDD to treat hypertension in the experimental group. Studies were excluded if (a) they were not random; (b) no control group was used; (c) the experimental design was not rigorous and statistical methods are inappropriate; (d) it was on the indeterminacy of measurement index outcome criterion; (e) they failed to obtain effective analysis data; (f) they were animal experiments; (g) they were plagiarized.

2.3. Data Extraction. Two researchers independently screened the titles and abstracts of potential eligible studies, and then they retrieved and reviewed the full text of the possible studies based on the inclusion and exclusion criteria and extracted the data. If there was disagreement, they agreed through discussion or submitted it to a third party for evaluation. Data extraction table mainly included the basic information of the study (author's name, title of the study, year of publication, country/region, and publication status), study characteristics (sample size, source of cases, age, gender distribution, diagnostic criteria, and inclusion and exclusion criteria), intervention and control measures (dosage form, dose, and duration), research methodology (random scheme generation, allocation hiding, blind method, incomplete result data, selective reporting, other biases, and loss of follow-up), and outcome measures.

2.4. Assessment of Literature Quality. According to the Cochrane collaboration tool, two reviewers independently evaluated the methodological quality of each included study. It comprised the following seven aspects: random sequence generation, allocation concealment, blind method, incomplete result data, selective reporting, and other biases [18]. The quality evaluation results of each item can be divided into three grades: "low risk," "high risk," and "unclear." When necessary, the consensus on this issue was studied with the help of a third party.

2.5. Statistical Analysis. Statistical analysis was performed using Rev Man 5.3 software. The results of a single study were firstly described. The binomial variables were described by using relative risk (RR) and 95% confidence interval (CI), and the continuous variables were described by mean difference (MD) and 95% CI to describe the effect value of the intergroup comparison. Heterogeneity was judged on the basis of the results of I^2 test. $I^2 > 50\%$ indicated that the heterogeneity of inter-study was significant, and the random

effect model was adopted. And, the fixed effect model was adopted when $I^2 < 50\%$ [19]. Subgroup analysis was conducted by different treatment methods in the control group. Inverted funnel plots were used to determine potential publication bias when more than 10 studies were included in the meta-analysis.

3. Results

3.1. Results of Our Literature Search. Based on the retrieval strategy, 383 potential relevant literatures on the treatment of hypertension by QDD were preliminarily searched in 7 databases, and 244 literatures were retrieved after 139 copies were removed. After reviewing the titles and abstracts, 189 articles were excluded because they did not comply with the inclusion criteria and 55 articles initially met the intended criteria. After reading the full text, 19 eligible studies were included for meta-analysis [20–38]. The flow chart of literature retrieval and screening is shown in Figure 1.

3.2. Basic Characteristics of the Included Studies. Table 1 summarizes the basic characteristics of the 19 trials. All the trials were conducted in China. A total of 2043 patients with hypertension were included. Sample sizes ranged from 60 to 333. In the treatment group, QDD alone was used in 7 trials, then QDD plus antihypertensive drugs (QPAD) was used in 11 trials, and QDD plus CADLI (QPCADLI) was used in 1 trial. Table 2 lists the detailed information of QDD ingredients used in 19 trials. For control conditions, 16 trials were treated with antihypertensive drugs, and conventional therapy was used in 2 trials; additionally, CADLI was used in 1 trial. All 19 included trials reported the efficacy of QDD in the treatment of hypertension. Antihypertensive effects and blood pressure were the primary outcomes. 14 trials reported antihypertensive effects [21–25, 27–29, 32, 34–38], and 11 reported blood pressure [20–23, 26, 29–31, 33, 37, 38]. In terms of secondary outcome indicators, clinical effects were described in 2 trials [26, 31] and TCM syndrome score was described in 1 trial [31]; furthermore, life quality was described in 2 trials [26, 31], and 24 h ambulatory blood pressure was described in 1 trial [34]. The change of Ang II was described in 2 trials [20, 36], and ET was described in 1 trial [20]; in addition, ISI and INS were described in 1 trial [30]. The changes of mA1b, β_2 -MG, and NAG were described in 1 trial [33], and HsCRP was described in 1 trial [36]. All included trials reported treatment duration ranging from 1 to 6 months.

3.3. Risk of Bias Assessment of the Literature Included in the Study. Table 3 summarizes the methodological quality of the 19 included trials. The risk of bias in the trials was assessed by using the criteria in the Cochrane Handbook for Systematic Reviews of Interventions [18]. Although randomization was announced in all of the included trials, 6 trials reported random sequence generation methods, including random number table [20, 28, 29, 32, 35] and the order of treatment [23]. However, no details were found in the domains of random allocation concealment, blinding of

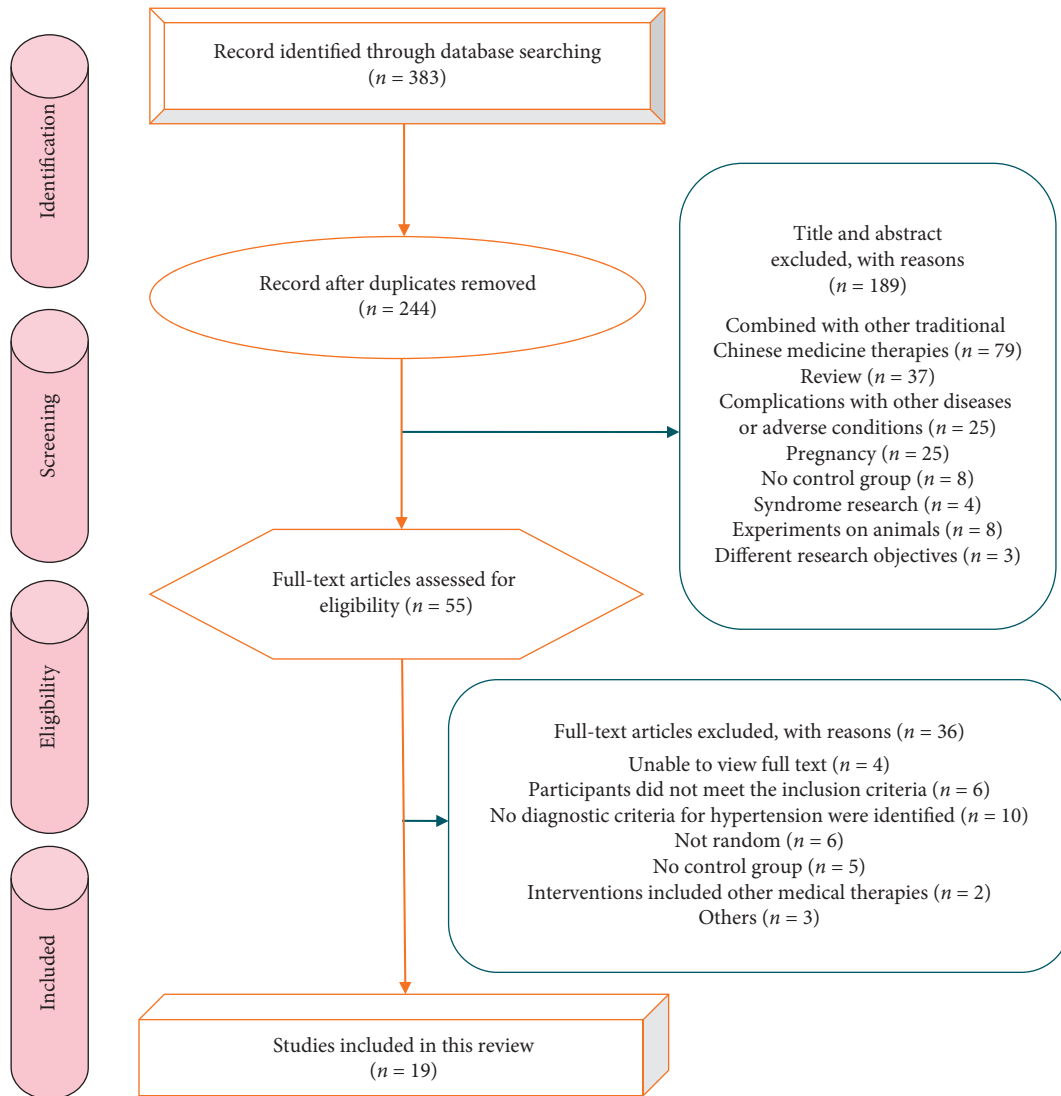


FIGURE 1: Flow diagram of literature selection.

participants, personnel and outcome assessors, and selective outcome reporting.

3.4. Blood Pressure. The antihypertensive effect was formulated in accordance with the criteria for the diagnosis and efficacy of TCM diseases [39]. We used obvious effect as the index of antihypertensive effect, which was reported in 14 trials [21–25, 27–29, 32, 34–38]. 3 trials evaluated the antihypertensive effect of QDD compared with antihypertensive drugs, revealing that QDD antihypertensive efficiency was 1.45 times that of antihypertensive drugs (3 trials, $n = 146$; RR: 1.45; 95% CI: 1.03 to 2.05; $p = 0.03$; Figure 2(a)). Meta-analysis of 8 trials comparing QPAD with antihypertensive drugs showed that QPAD antihypertensive efficiency was 1.34 times that of antihypertensive drugs (8 trials, $n = 623$; RR: 1.34; 95% CI: 1.14 to 1.58; $p = 0.0005$; Figure 2(b)). QDD was compared with conventional therapy in 2 trials. According to QDD, antihypertensive efficiency was 1.56 times that of conventional therapy (2 trials, $n = 230$;

RR: 1.56; 95% CI: 1.26 to 1.95; $p < 0.0001$; Figure 2(c)). However, there is no obvious difference between QPCADLI and CADLI on antihypertensive effect (1 trial, $n = 193$; RR: 1.09; 95% CI: 0.94 to 1.26; $p = 0.25$).

Meta-analysis of 11 trials reported the changes in blood pressure levels before and after treatment [20–23, 26, 29–31, 33, 37, 38]. 4 trials comparing QDD with antihypertensive drugs exhibited a significant lowering effect of QDD in DBP (4 trials, $n = 400$; MD: -5.55 ; 95% CI: -7.19 to -3.19 ; $p < 0.00001$; Figure 3(a)), but had no obvious difference in SBP (4 trials, $n = 400$; MD: -2.63 ; 95% CI: -8.06 to 2.81 ; $p = 0.34$; Figure 3(b)). QPAD and antihypertensive drugs were compared in 7 trials, and it was found that QPAD could remarkably reduce DBP (7 trials, $n = 562$; MD: -8.24 ; 95% CI: -10.04 to -6.45 ; $p < 0.00001$; Figure 3(c)), while SBP was not significantly different from that of antihypertensive drugs (7 trials, $n = 562$; MD: -2.22 ; 95% CI: -19.37 to 14.94 ; $p = 0.80$; Figure 3(d)). However, after excluding [30], combined with the results of the other 6 trials, meta-analysis identified an obvious lowering effect of QPAD in SBP (6

TABLE 1: Characteristic of the 19 trials included in the meta-analysis.

Author(s)	Sample size (experimental/control)	Gender (male/female)	Diagnostic criteria	Experimental	Control	Duration	Outcome measures
Du et al. [20]	60/60	66/54	WHO-ISHNGMH-1999	QDD (6 g, tid) + C	Felodipine sustained release tablet (5 mg, qd)	1 month	BP, Ang II, ET
Du et al. [21]	30/30	31/29	DCPTHC	QDD (9 g, bid) + C	Nifedipine delayed-release tablet (30 mg, qd)	1 month	AE, BP
Guo and Li [22]	40/40	46/34	DCPTHC	Modified QDD (1 dose/d) + C	Nifedipine delayed-release tablet (10 mg, bid), captopril tablet (25 mg, bid)	1 month	AE, BP
Huang [23]	40/40	NR	DCPTHC	QDD (9 g, bid) + C	Nifedipine tablet (30 mg, qd)	1 month	AE, BP
Liang [24]	133/132	128/137	WHO-ISHNGMH-1999	QDD (6 g, bid) + C	CADLI	6 months	AE
Li et al. [25]	50/50	49/51	WHO-ISHNGMH-1999	Modified QDD (1 dose/d)	Conventional treatment (nao liqing, luo buma tablet, and dihydrochlorothiazide)	3 months	AE
Liu [26]	50/50	47/53	WHO-ISHNGMH-1999	Modified QDD (1 dose/d) + C	Amlodipine besylate tablet (5 mg, qd)	1 month	BP, CE, QL
Liu et al. [27]	219/114	159/174	GDTCDIMCM	Modified QDD (1 dose/d)	Conventional treatment (nao liqing, luo buma tablet, and dihydrochlorothiazide)	3 months	AE
Lu [28]	40/40	48/32	WHO-ISHNGMH-1999	Modified QDD (1 dose/d)	Captopril tablet (25 mg, tid)	NR	AE
Luo and Luo [29]	60/60	65/55	WHO-ISHNGMH-1999	Modified QDD (1 dose/d)	Nitrendipine tablet (10 mg, tid)	2 months	AE, BP
Peng et al. [30]	30/30	34/26	WHO-ISHNGMH-1999	QDD (1 dose/d)	Losartan potassium tablet (50 mg, qd)	2 months	BP, ISI, INS
Song [31]	36/36	42/30	WHO-ISHNGMH-1999	Modified QDD (1 dose/d) + C	Amlodipine besylate tablet (5 mg, qd)	1 month	BP, CE, TCMSS, QL
Sun et al. [32]	32/31	26/37	WHO-ISHNGMH-1999	QDD (1.5 g, tid) + C	Telmisartan tablet (40 mg, qd)	1 month	AE
Wang [33]	60/30	48/42	WHO-ISHNGMH-1999	Modified QDD (1 dose/d) + C	Irbesartan tablet (150 mg, qd)	2 months	BP, mA1b β_2 -MG, NAG
Wang et al. [34]	40/40	41/39	DCPTHC	QDD (9 g, bid) + C	Enalapril maleate and folic acid tablet (0.8 mg, qd)	1 month	AE, 24 h ABP
Yang and He [35]	40/40	46/34	DCPTHC	Modified QDD (1 dose/d) + C	Enalapril maleate capsules (5 mg, bid)	3 months	AE
Yu [36]	50/50	68/32	DCPTHC	QDD (1 dose/d) + C	Conventional antihypertensive drugs (ACEI, ARB, CCB, and diuretic)	1 month	AE, Ang II, HsCRP
Zhang [37]	34/34	30/32	WHO-ISHNGMH-1999	QDD (1 dose/d) + C	Amlodipine besylate tablet (5 mg, qd)	1 month	AE, BP
Zhu [38]	46/46	49/43	DCPTHC	QDD (9 g, bid) + C	Nifedipine controlled release tablet (30 mg, qd)	2 months	AE, BP

Abbreviations. ABP: ambulatory blood pressure; ACEI: angiotensin-converting enzyme inhibitors; AE: antihypertensive effect; Ang II: angiotensin II; ARB: angiotensin receptor blockers; BP: blood pressure; β_2 -MG: β_2 -microglobulin; CADLI: conventional antihypertensive drugs and lifestyle interventions; CCB: calcium channel blocker; CE: clinical effects; DCPTHC: diagnostic criteria for the prevention and treatment of hypertension in China; ET: endothelin; GDTCDIMCM: guide to diagnosis and treatment of common diseases in internal medicine of Chinese medicine; HsCRP: high-sensitivity C-reactive protein; INS: insulin; ISI: insulin sensitivity index; NAG: *N*-acetyl- β -glucosidase; NR: not reported; QDD: Qiju Dihuang decoction; QL: quality of life; TCMSS: TCM syndrome score; WHO-ISH GMH: World Health Organization-International Society of Hypertension Guidelines for the Management of Hypertension.

TABLE 2: The ingredients of Qiju Dihuang Decoction used in the 19 trials.

References	TCM	Ingredients of QDD
Du et al. [20]	QDD (6 g, tid)	Rehmanniae Radix Praeparata (Shudihuang), Corni Fructus (Shanzhuyu), Dioscoreae Rhizoma (Shanyao), Poria (Fuling), Moutan Cortex (Mudanpi), Alismatis Rhizoma (Zexie), Lycii Fructus (Gouqizi), Chrysanthemi Flos (Juhua)
Du et al. [21]	QDD (9 g, bid)	Rehmanniae Radix Praeparata (Shudihuang), Corni Fructus (Shanzhuyu), Dioscoreae Rhizoma (Shanyao), Poria (Fuling), Moutan Cortex (Mudanpi), Alismatis Rhizoma (Zexie), Lycii Fructus (Gouqizi), Chrysanthemi Flos (Juhua)
Guo and Li [22]	Modified QDD (1 dose/d)	Rehmanniae Radix (Shengdi) 12 g, Corni Fructus (Shanzhuyu) 9 g, Dioscoreae Rhizoma (Shanyao) 9 g, Poria (Fuling) 6 g, Moutan Cortex (Mudanpi) 6 g, Alismatis Rhizoma (Zexie) 6 g, Lycii Fructus (Gouqizi) 9 g, White Chrysanthemi Flos (Baijuehua) 12 g, Gastrodiae Rhizoma (Tianma) 9 g, Uncariae Ramulus Cum Uncis (Gouteng) 9 g, Haliotidis Concha (Shijueiming) 15 g
Huang [23]	QDD (9 g, bid)	Rehmanniae Radix Praeparata (Shudihuang), Corni Fructus (Shanzhuyu), Dioscoreae Rhizoma (Shanyao), Poria (Fuling), Moutan Cortex (Mudanpi), Alismatis Rhizoma (Zexie), Lycii Fructus (Gouqizi), Chrysanthemi Flos (Juhua)
Liang [24]	QDD (6 g, bid)	Rehmanniae Radix Praeparata (Shudihuang), Corni Fructus (Shanzhuyu), Dioscoreae Rhizoma (Shanyao), Poria (Fuling), Moutan Cortex (Mudanpi), Alismatis Rhizoma (Zexie), Lycii Fructus (Gouqizi), Chrysanthemi Flos (Juhua)
Li et al. [25]	Modified QDD (1 dose/d)	Lycii Fructus (Gouqizi) 15 g, Hordei Fructus Germinatus (Shengmaiya) 15 g, Chrysanthemi Flos (Juhua) 15 g, Poria (Fuling) 15 g, Rehmanniae Radix Praeparata (Shudihuang) 15 g, Alismatis Rhizoma (Zexie) 10 g, Corni Fructus (Shanzhuyu) 15 g, Dioscoreae Rhizoma (Shanyao) 15 g, Moutan Cortex (Mudanpi) 10 g, Glehniae Radix (Beishashen) 30 g, Cyathulae Radix (Chuanniuxi) 30 g, Haliotidis Concha (Shijueiming) 30 g, Ostreae Concha (Shengmuli) 30 g, Raw keel (Shenglonggu) 30 g, Glycyrrhizae Radix et Rhizoma (Gancao) 6 g
Liu [26]	Modified QDD (1 dose/d)	Rehmanniae Radix Praeparata (Shudihuang) 10 g, White Chrysanthemi Flos (Baijuehua) 12 g, Lycii Fructus (Gouqizi) 15 g, Poria (Fuling) 15 g, Chinese yam (Shanyao) 15 g, Moutan Cortex (Mudanpi) 12 g, Corni Fructus (Shanzhuyu) 12 g, Alismatis Rhizoma (Zexie) 12 g, Cyathulae Radix (Niuxi) 12 g, Uncariae Ramulus Cum Uncis (Gouteng) 12 g, Gastrodiae Rhizoma (Tianma) 10 g, Magnetitum (Cishi) 30 g
Liu et al. [27]	Modified QDD (1 dose/d)	Lycii Fructus (Gouqizi) 15 g, Chrysanthemi Flos (Juhua) 15 g, Rehmanniae Radix Praeparata (Shudihuang) 15 g, Corni Fructus (Shanzhuyu) 15 g, Dioscoreae Rhizoma (Shanyao) 15 g, Radix glehniae (Beishashen) 30 g, Haliotidis Concha (Shijueiming) 30 g, Raw keel (Shenglonggu) 30 g, Ostreae Concha (Shengmuli) 30 g, Cyathulae Radix (Chuanniuxi) 30 g, Moutan Cortex (Mudanpi) 10 g, Alismatis Rhizoma (Zexie) 10 g, Poria (Fuling) 15 g, Hordei Fructus Germinatus (Shengmaiya) 15 g, Glycyrrhizae Radix et Rhizoma (Gancao) 6 g
Lu [28]	Modified QDD (1 dose/d)	Lycii Fructus (Gouqizi) 25 g, Chrysanthemi Flos (Juhua) 15 g, Rehmanniae Radix Praeparata (Shudihuang) 15 g, Taxilli Herba (Sangjisheng) 15 g, Tortoise plastron (Guiban) 15 g, Cyathulae Radix (Niuxi) 15 g, Dioscoreae Rhizoma (Shanyao) 15 g, Poria (Fuling) 15 g, Corni Fructus (Shanzhuyu) 10 g, Moutan Cortex (Mudanpi) 10 g, Haliotidis Concha (Shijueiming) 20 g
Luo and Luo [29]	Modified QDD (1 dose/d)	Rehmanniae Radix Praeparata (Shudihuang) 15 g, Corni Fructus (Shanzhuyu) 12 g, Dioscoreae Rhizoma (Shanyao) 15 g, Poria (Fuling) 10 g, Moutan Cortex (Mudanpi) 10 g, Alismatis Rhizoma (Zexie) 10 g, Lycii Fructus (Gouqizi) 15 g, White Chrysanthemi Flos (Baijuehua) 10 g, Ostreae Concha (Shengmuli) 15 g, Raw keel (Shenglonggu) 15 g, Haliotidis Concha (Shijueiming) 10 g, Maybush (Shanzha) 15 g
Peng et al. [30]	QDD (1 dose/d)	Rehmanniae Radix Praeparata (Shudihuang), Corni Fructus (Shanzhuyu), Dioscoreae Rhizoma (Shanyao), Poria (Fuling), Moutan Cortex (Mudanpi), Alismatis Rhizoma (Zexie), Lycii Fructus (Gouqizi), Chrysanthemi Flos (Juhua)
Song [31]	Modified QDD (1 dose/d)	Rehmanniae Radix Praeparata (Shudihuang) 10 g, White Chrysanthemi Flos (Baijuehua) 12 g, Lycii Fructus (Gouqizi) 15 g, Poria (Fuling) 15 g, Dioscoreae Rhizoma (Shanyao) 15 g, Moutan Cortex (Mudanpi) 12 g, Corni Fructus (Shanzhuyu) 12 g, Alismatis Rhizoma (Zexie) 12 g, Cyathulae Radix (Niuxi) 12 g, Gastrodiae Rhizoma (Tianma) 10 g, Uncariae Ramulus Cum Uncis (Gouteng) 12 g, Magnetitum (Cishi) 30 g
Sun et al. [32]	QDD (1.5 g, tid)	Rehmanniae Radix Praeparata (Shudihuang), Corni Fructus (Shanzhuyu), Dioscoreae Rhizoma (Shanyao), Poria (Fuling), Moutan Cortex (Mudanpi), Alismatis Rhizoma (Zexie), Lycii Fructus (Gouqizi), Chrysanthemi Flos (Juhua)
Wang [33]	Modified QDD (1 dose/d)	Rehmanniae Radix Praeparata (Shudihuang) 10 g, White Chrysanthemi Flos (Baijuehua) 15 g, Lycii Fructus (Gouqizi) 15 g, Poria (Fuling) 15 g, Dioscoreae Rhizoma (Shanyao) 30 g, Moutan Cortex (Mudanpi) 15 g, Corni Fructus (Shanzhuyu) 30 g, Alismatis Rhizoma (Zexie) 15 g, Cyathulae Radix (Niuxi) 15 g, Gastrodiae Rhizoma (Tianma) 10 g, Tortoise plastron (Guiban) 15 g
Wang et al. [34]	QDD (9 g, bid)	Rehmanniae Radix Praeparata (Shudihuang), Corni Fructus (Shanzhuyu), Dioscoreae Rhizoma (Shanyao), Poria (Fuling), Moutan Cortex (Mudanpi), Alismatis Rhizoma (Zexie), Lycii Fructus (Gouqizi), Chrysanthemi Flos (Juhua)

TABLE 2: Continued.

References	TCM	Ingredients of QDD
Yang and He [35]	Modified QDD (1 dose/d)	Rehmanniae Radix (Shengdi) 12 g, Corni Fructus (Shanzhuyu) 9 g, Dioscoreae Rhizoma (Shanyao) 9 g, Poria (Fuling) 6 g, Moutan Cortex (Mudanpi) 6 g, Alismatis Rhizoma (Zexie) 6 g, Lycii Fructus (Gouqizi) 9 g, White Chrysanthemi Flos (Baijuehua) 12 g, Gastrodiae Rhizoma (Tianma) 9 g, Uncariae Ramulus Cum Uncis (Gouteng) 9 g, Haliotidis Concha (Shijuejing) 15 g, Paeoniae Radix Rubra (Chishao) 9 g, Salviae Miltiorrhizae Radix et Rhizoma (Danshen) 30 g
Yu [36]	QDD (1 dose/d)	Rehmanniae Radix Praeparata (Shudihuang), Corni Fructus (Shanzhuyu), Dioscoreae Rhizoma (Shanyao), Poria (Fuling), Moutan Cortex (Mudanpi), Alismatis Rhizoma (Zexie), Lycii Fructus (Gouqizi), Chrysanthemi Flos (Juhua)
Zhang [37]	QDD (1 dose/d)	Rehmanniae Radix Praeparata (Shudihuang), Corni Fructus (Shanzhuyu), Dioscoreae Rhizoma (Shanyao), Poria (Fuling), Moutan Cortex (Mudanpi), Alismatis Rhizoma (Zexie), Lycii Fructus (Gouqizi), Chrysanthemi Flos (Juhua)
Zhu [38]	QDD (9 g, bid)	Rehmanniae Radix Praeparata (Shudihuang), Corni Fructus (Shanzhuyu), Dioscoreae Rhizoma (Shanyao), Poria (Fuling), Moutan Cortex (Mudanpi), Alismatis Rhizoma (Zexie), Lycii Fructus (Gouqizi), Chrysanthemi Flos (Juhua)

Abbreviations. QDD: Qiju Dihuang decoction.

TABLE 3: Methodology quality of the 19 studies according to the Cochrane handbook.

References	A	B	C	D	E	F	G	H
Du et al. [20]	+	?	?	?	?	+	?	?
Du et al. [21]	?	?	?	?	?	+	?	?
Guo and Li [22]	?	?	?	?	?	+	?	?
Huang [23]	-	?	?	?	?	+	?	?
Liang [24]	?	?	?	?	?	+	?	?
Li et al. [25]	?	?	?	?	?	+	?	?
Liu [26]	?	?	?	?	?	+	?	?
Liu et al. [27]	?	?	?	?	?	+	?	?
Lu [28]	+	?	?	?	?	+	?	?
Luo and Luo [29]	+	?	?	?	?	+	?	?
Peng et al. [30]	?	?	?	?	?	+	?	?
Song [31]	?	?	?	?	?	+	?	?
Sun et al. [32]	+	?	?	?	?	+	?	?
Wang [33]	?	?	?	?	?	+	?	?
Wang et al. [34]	?	?	?	?	?	+	?	?
Yang and He [35]	+	?	?	?	?	+	?	?
Yu [36]	?	?	?	?	?	+	?	?
Zhang [37]	?	?	?	?	?	+	?	?
Zhu [38]	?	?	?	?	?	+	?	?

Abbreviations. A: adequate sequence generation; B: allocation concealment; C: blinding patient; D: blinding personnel; E: blinding assessor; F: incomplete outcome data; G: selective reporting; H: other bias; +: low risk; -: high risk; ?: unclear.

trials, $n = 490$; MD: -12.53 ; 95% CI: -15.79 to -9.28 ; $p < 0.00001$; Figure 3(e)).

3.5. Clinical Effects. Clinical effect was determined by the TCM syndrome score. The clinical symptoms were significantly alleviated, and the TCM syndrome score was decreased by $> 70\%$ after treatment, indicating an obvious effect. At the same time, the TCM syndrome score was decreased by 50~70% for improvement. No improvement or aggravation of symptoms and a reduction of TCM syndrome score below 50% is invalid. Obvious effect was used as an indicator of clinical efficacy. Two trials [26, 31] described clinical effects, and meta-analysis revealed that QPAD was 1.61 times higher than antihypertensive drugs in clinical

efficacy of hypertension (2 trials, $n = 172$; RR: 1.61; 95% CI: 1.12 to 2.31; $p = 0.01$; Figure 4).

3.6. TCM Syndrome Score. The scoring method of TCM syndromes refers to the guiding principles for clinical research of new Chinese medicine [40]. According to the degree of clinical manifestations, the scores are zero, one, two, and three points respectively; moreover, the lower the score, the better the effect. Only one trial [31] reported TCM syndrome scores before and after treatment, suggesting that QPAD significantly reduced the scores in patients compared with antihypertensive drugs (1 trial, $n = 72$; MD: -3.00 ; 95% CI: -3.61 to -2.39 ; $p < 0.00001$).

3.7. Life Quality. SF-36 was used to evaluate the life quality of patients. And, the higher the score, the higher the life quality.

2 trials reported changes in patients' life quality before and after treatment [26, 31]. Compared with antihypertensive drugs, QPAD can remarkably improve the life quality of patients (2 trials, $n = 172$; MD: 9.12; 95% CI: 8.27 to 9.98; $p < 0.00001$; Figure 5).

3.8. 24 h Ambulatory Blood Pressure. 24 h ambulatory blood pressure was only reported in one trial [34]. Compared with antihypertensive drugs, QPAD can significantly reduce mean systolic blood pressure (1 trial, $n = 80$; MD: -13.30 ; 95% CI: -16.84 to -9.76 ; $p < 0.00001$) and diastolic blood pressure (1 trial, $n = 80$; MD: -6.25 ; 95% CI: -8.69 to -3.81 ; $p < 0.00001$) as well as the standard deviation of systolic blood pressure (1 trial, $n = 80$; MD: -2.06 ; 95% CI: -3.90 to -0.22 ; $p = 0.03$). However, there is no obvious difference between QPAD and antihypertensive drugs in the standard deviation of diastolic blood pressure (1 trial, $n = 80$; MD: -0.49 ; 95% CI: -2.30 to 1.32; $p = 0.60$).

3.9. Ang II and ET. Ang II at baseline and after intervention was reported by 2 trials [20, 36]. Compared with antihypertensive drugs, QPAD can significantly reduce huge

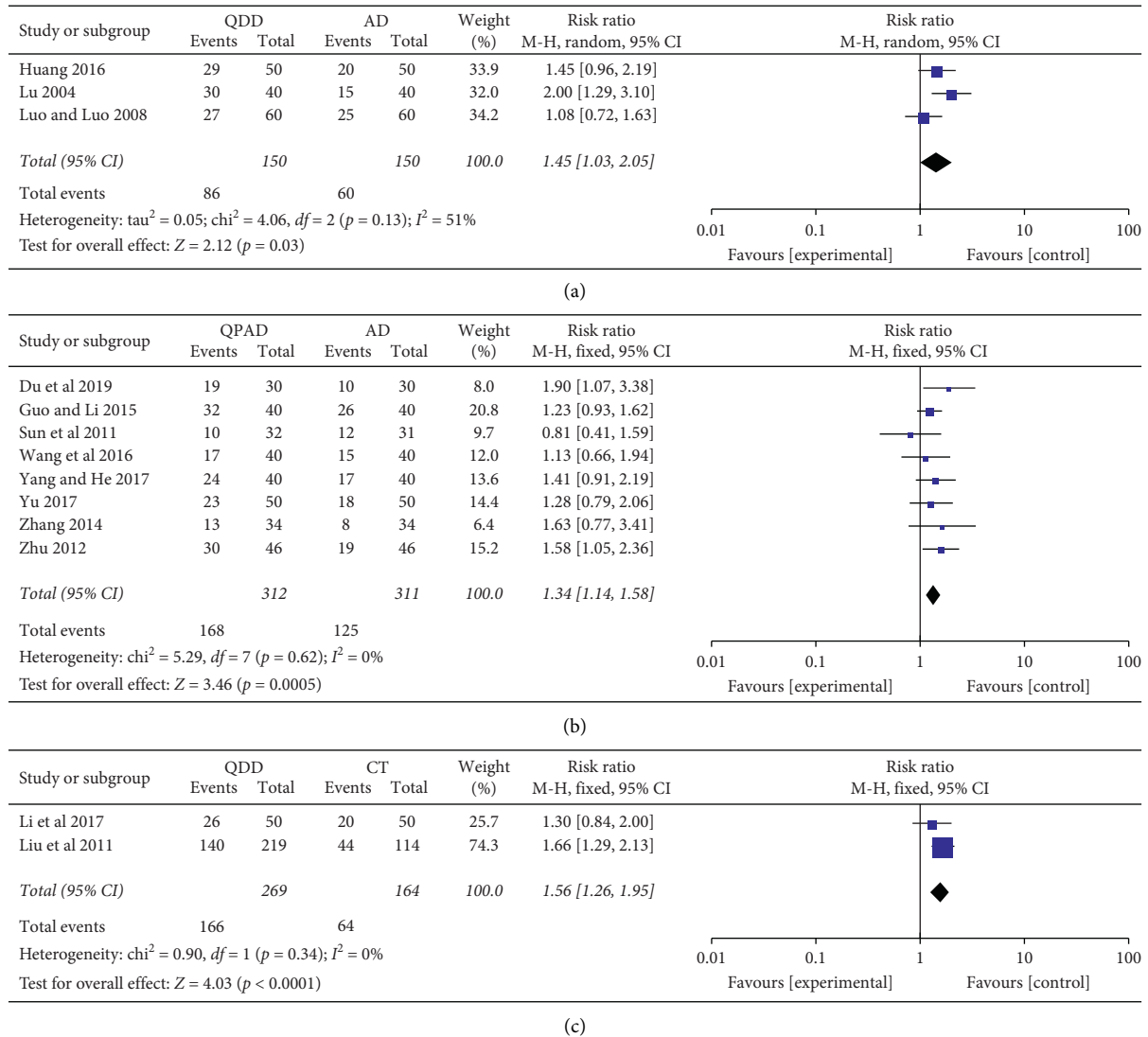


FIGURE 2: Forest plot of the trials showed antihypertensive effects in different interventions for (a) QDD vs. AD, (b) QPAD vs. AD, and (c) QDD vs. CT; abbreviations: AD: antihypertensive drugs; CT: conventional therapy; QDD: Qiju Dihuang decoction; QPAD: Qiju Dihuang decoction plus antihypertensive drugs.

quantities of Ang II levels and inhibit the activity of it (1 trial, $n = 100$; MD: -76.00 ; 95% CI: -98.83 to -53.17 ; $p < 0.00001$). However, there was no remarkable difference between QDD and antihypertensive drugs (1 trial, $n = 72$; MD: -10.86 ; 95% CI: -24.29 to 2.57 ; $p = 0.11$).

Only 1 trial described ET [20], and a significant inhibition of ET bioactivity by QDD was exhibited compared with antihypertensive drugs (1 trial, $n = 72$; MD: -9.12 ; 95% CI: -15.18 to -3.06 ; $p = 0.003$).

3.10. ISI and INS. Only one trial reported ISI at baseline and after intervention [30], and the results identified that QPAD significantly increased ISI and decreased insulin resistance (1 trial, $n = 60$; MD: 1.13 ; 95% CI: 0.89 to 1.37 ; $p < 0.00001$).

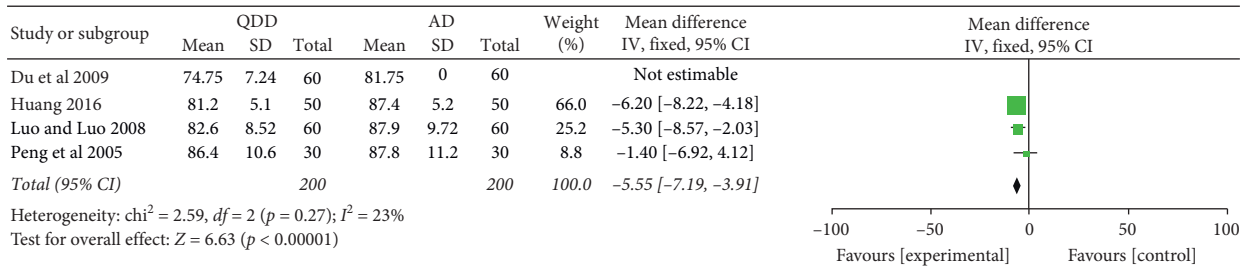
INS level was also reported by the same trial as ISI, revealing that the reduction in INS was obviously greater for

QPAD than that of antihypertensive drugs alone (1 trial, $n = 60$; MD: -2.30 ; 95% CI: -3.23 to -1.37 ; $p < 0.00001$).

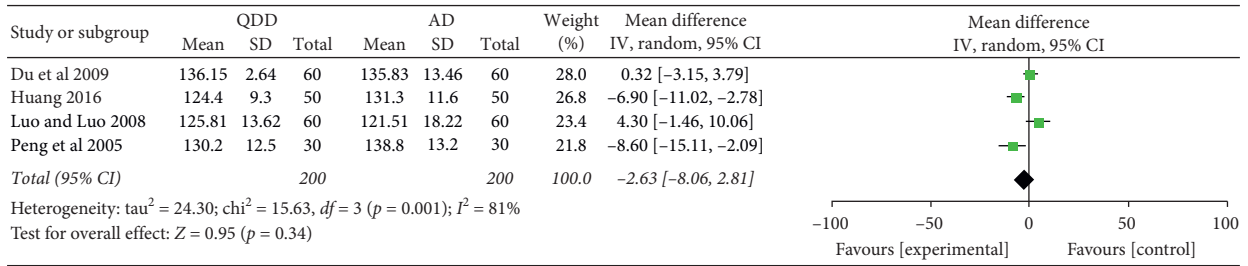
3.11. mA1b, β_2 -MG, and NAG. Only 1 trial reported mA1b at baseline and after intervention [33]. A remarkable reduction in mA1b with QPAD was evaluated, comparing with antihypertensive drugs (1 trial, $n = 90$; MD: -8.33 ; 95% CI: -14.72 to -1.94 ; $p = 0.01$).

The effect of QPAD on β_2 -MG level was reported in the same trial as mA1b. Compared with antihypertensive drugs, QPAD can lower the level of β_2 -MG better (1 trial, $n = 90$; MD: -0.09 ; 95% CI: -0.13 to -0.05 ; $p < 0.0001$).

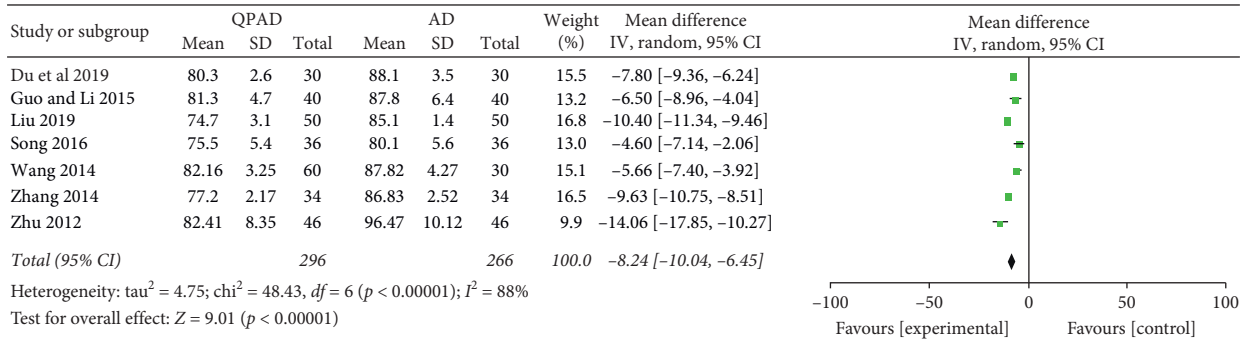
The same trial also reported the NAG level, in which QPAD was compared with antihypertensive drugs, and it was found to have a significant lowering effect in NAG (1 trial, $n = 90$; MD: -4.97 ; 95% CI: -9.92 to -0.02 ; $p = 0.05$).



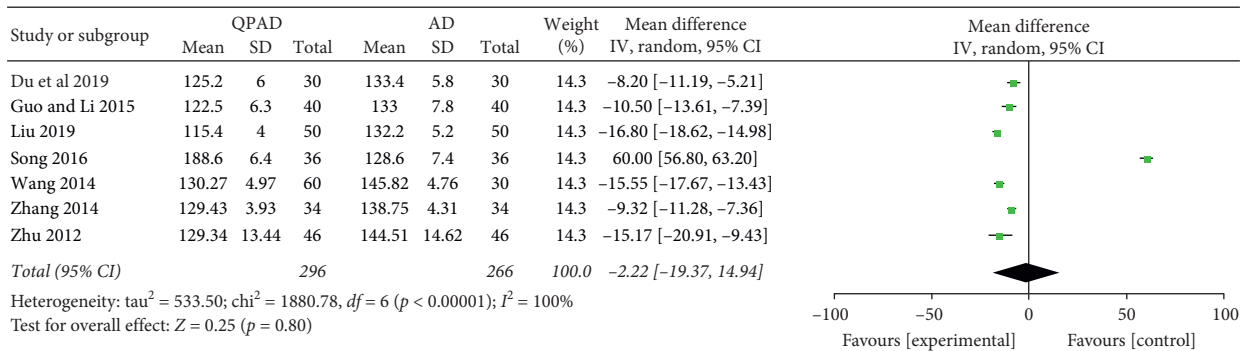
(a)



(b)

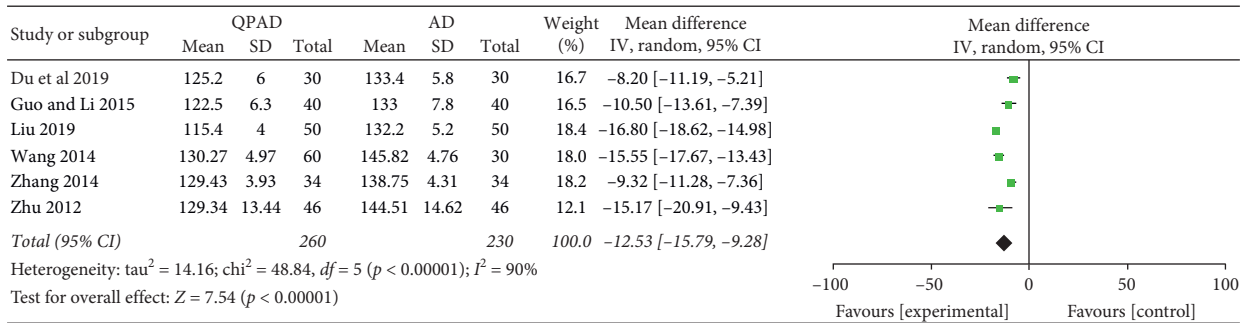


(c)



(d)

FIGURE 3: Continued.



(e)

FIGURE 3: Forest plot of the trials showed blood pressure in different interventions for (a) DBP, QDD vs. AD, (b) SBP, QDD vs. AD, (c) DBP, QPAD vs. AD, (d) SBP, QPAD vs. AD, and (e) SBP, QPAD vs. AD; Abbreviations: AD: antihypertensive drugs; DBP: diastolic blood pressure; QDD: Qiju Dihuang decoction; QPAD: Qiju Dihuang decoction plus antihypertensive drugs; SBP: systolic blood pressure.

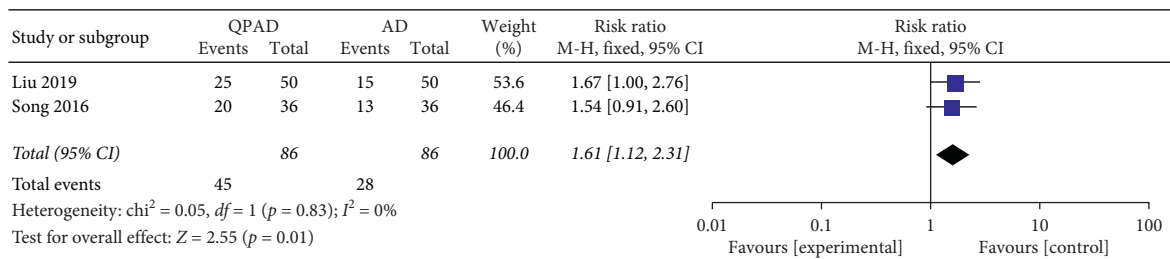


FIGURE 4: Forest plot of the trials showed clinical effects in QPAD vs. AD; Abbreviations: AD: antihypertensive drugs; QPAD: Qiju Dihuang decoction plus antihypertensive drugs.

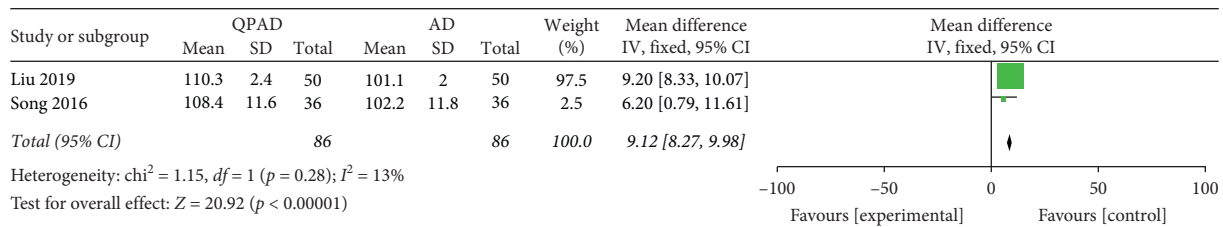


FIGURE 5: Forest plot of the trials showed life quality in QPAD vs. AD. Abbreviations: AD: antihypertensive drugs; QPAD: Qiju Dihuang decoction plus antihypertensive drugs.

3.12. *HsCRP Level.* The HsCRP level at baseline and post-intervention was reported by 1 trial that compared QPAD with antihypertensive drugs [36]. The meta-analysis exhibited an obvious lowering effect by QPAD in HsCRP (1 trial, n = 100; MD: -0.50; 95% CI: -0.74 to -0.26; p < 0.0001).

3.13. *Adverse Reactions.* No adverse reactions were reported in all trials.

3.14. *Evaluation of Publication Bias.* Since fewer than 10 trials were included in each subgroup, publication bias could not be adequately analyzed.

4. Discussion

TCM has certain advantages and characteristics in the treatment of hypertension. In recent years, the classic TCM

formulae for treating hypertension have attracted much attention [41–43]. However, most studies only reported the antihypertensive effect but did not concern the effect of TCM on the life quality of patients and the prevention of complications. Therefore, our study aimed to systematically evaluate the efficacy of QDD on blood pressure, life quality, renal function, insulin resistance, and other aspects of patients with hypertension as well as the potential hypertensive mechanism. And, it would provide a better evidence for hypertensive patients, policymakers, and clinicians.

This systematic review and meta-analysis contained 19 trials and 2043 patients with hypertension, which evaluated the efficacy of QDD in the treatment of hypertension, including QDD vs. antihypertensive drugs, QDD vs. conventional therapy, QPAD vs. antihypertensive drugs, and QPCADLI vs. CADLI. In summary, this study has identified that QDD can significantly reduce the blood pressure, improve the antihypertensive efficiency, show an obvious

lowering effect on TCM syndrome score, inhibit the inflammation, protect the kidney function, reduce the insulin resistance, and improve the life quality of patients. And, reduction of Ang II and ET levels is possibly one potential antihypertensive mechanism of QDD.

Patients with long-term hypertension will lead to a variety of pathophysiological changes, which will not only cause headache, chest tightness, palpitations, and other symptoms but also may involve various organs and cause different complications. Therefore, hypertension is a major predisposing factor for many high-risk diseases. Many studies have also showed that the treatment of hypertension can play a preventive role in the occurrence of cardiovascular and cerebrovascular diseases [44]. Effective and stable control of blood pressure can significantly reduce the incidence of coronary heart disease by around 20–25%, 35–45% lower incidence of cerebral apoplexy, and heart failure in lower rates up to 50% [45]. Compared with the current prevalence trend of hypertension, if hypertension can be effectively controlled, the number of deaths from cardiovascular and cerebrovascular diseases in adults will be decreased by 564 100 until 2030 [46]. Controlling blood pressure to target levels is the basis of preventing cardiovascular and cerebrovascular diseases in patients with hypertension, so effectively lowering blood pressure is the most critical task for treatment of hypertension. All the trials included in the meta-analysis involved measures of the antihypertensive effect of QDD. We found that both QDD alone and in combination with antihypertensive drugs can remarkably reduce diastolic blood pressure and improved the antihypertensive effect. And, the choice of QDD treatment is one of the effective ways for patients with “liver and kidney Yin deficiency” hypertension. In addition, compared with antihypertensive drugs, QPAD can significantly reduce the mean systolic blood pressure and diastolic blood pressure at 24 h as well as the standard deviation of systolic blood pressure, which suggested that the combination of QDD and antihypertensive drugs is a more optimal choice for patients who cannot effectively improve the fluctuation of blood pressure by only taking antihypertensive drugs.

This study also discovered the potential mechanism of QDD for the reduction of blood pressure and the prevention of complications. Ang II vascular remodeling is one of the important pathological changes in the pathogenesis of hypertension, such as vascular smooth muscle proliferation, apoptosis, and other lesions, which will damage vascular walls, decrease vascular compliance, and lead to the imbalance of vascular active substances and disorder hemodynamic, all of which will lead to increase blood pressure. And, it was also reported to regulate the constriction of arterioles throughout the body and increase blood pressure [47]. In addition, when vascular endothelial cells are dysfunctional, vasomotor substances (such as ET) and growth-promoting factors are released abnormally, then blood vessel will narrow and peripheral resistance will increase, which also can promote blood pressure of patients [48]. The results of our study showed that QDD could significantly inhibit ET and also has an obvious lowering effect on Ang II when being combined with antihypertensive drugs.

Therefore, antihypertensive effect of QDD might attribute to inhibit the Ang II and ET release, protect the vascular endothelial cell function, and reduce the vascular remodeling. Insulin resistance was the pathophysiological basis of multiple complications in some patients with hypertension [49]. And, there was a significant correlation between insulin resistance and essential hypertension, which is one of the important causes of primary hypertension. Therefore, the current hot issue in hypertension field is how to reasonably lower blood pressure and improve insulin resistance [50]. In our systematic review, QPAD can not only increase ISI and decrease insulin resistance but also significantly reduce the INS, which provides a reliable evidence for the prevention of hypertension complications. In addition, the kidney is an organ which can expel excess metabolites through the urine and prevent proteins and blood cells from leaking out of the blood vessels. However, chronic high blood pressure may cause the protein to leak into the urine, which can damage the filter system of kidney. If the blood pressure has not been well controlled for a long time, an irreversible structural damage will be caused, which may give rise to renal impairment and even chronic renal failure. The main renal complication of hypertension is renal arteriosclerosis [51]. Therefore, the treatment of hypertension should also pay attention to the changes in renal function. In our meta-analysis, QDD showed a significant lowering effect on mA1b, β_2 -MG, and NAG, which proved that QDD could certainly prevent renal complications of hypertension.

QDD contains 8 single TCMs, including Lycii Fructus (Gouqizi), Chrysanthemi Flos (Juhua), Rehmanniae Radix Praeparata (Shudihuang), Dioscoreae Rhizoma (Shanyao), Corni Fructus (Shanzhuyu), Moutan Cortex (Mudanpi), Poria (Fuling), and Alismatis Rhizoma (Zexie). Anthocyanins from Gouqi (Figure 6(a)) can not only reduce blood lipid but also protect vascular endothelium, thus they may prevent atherosclerosis [52]. Total flavonoids from Juhua (Figure 6(b)) can protect the vasodilation and dilate blood vessels by controlling calcium and potassium channels, which shows that they can reduce blood pressure [53, 54]. Shudihuang has a strong effect on the cardiovascular system, and it can improve hemorheology [55]. The Shudihuang extract has a bilateral effect on blood pressure [56]. Diosgenin from Shanyao (Figure 6(c)) has obvious effects on reducing the occurrence of cardiovascular and cerebrovascular diseases because it can effectively decrease calcium overload in cardiomyocytes and regulate related signaling pathways [57]. Water extract of Shanzhuyu has an antihypertensive effect [58]. Total iridoid glycosides have a certain protective effect on the vascular endothelium of the heart and thoracic aorta, and its active component morroniside (Figure 6(d)) can prevent the injury of vascular endothelial cells by increasing the activity of SOD [59]. Paeonol from Mudanpi (Figure 6(e)) has obvious protective effect on blood vessels, which is mainly related to lowering blood lipid and inhibiting atherosclerosis. Paeonol can also significantly increase serum NO level and decrease plasma ET content [60]. Furthermore, Zexie water extract can reduce blood pressure by dilating blood vessels. Zexie terpenoids can not only inhibit the release of norepinephrine by the sympathetic

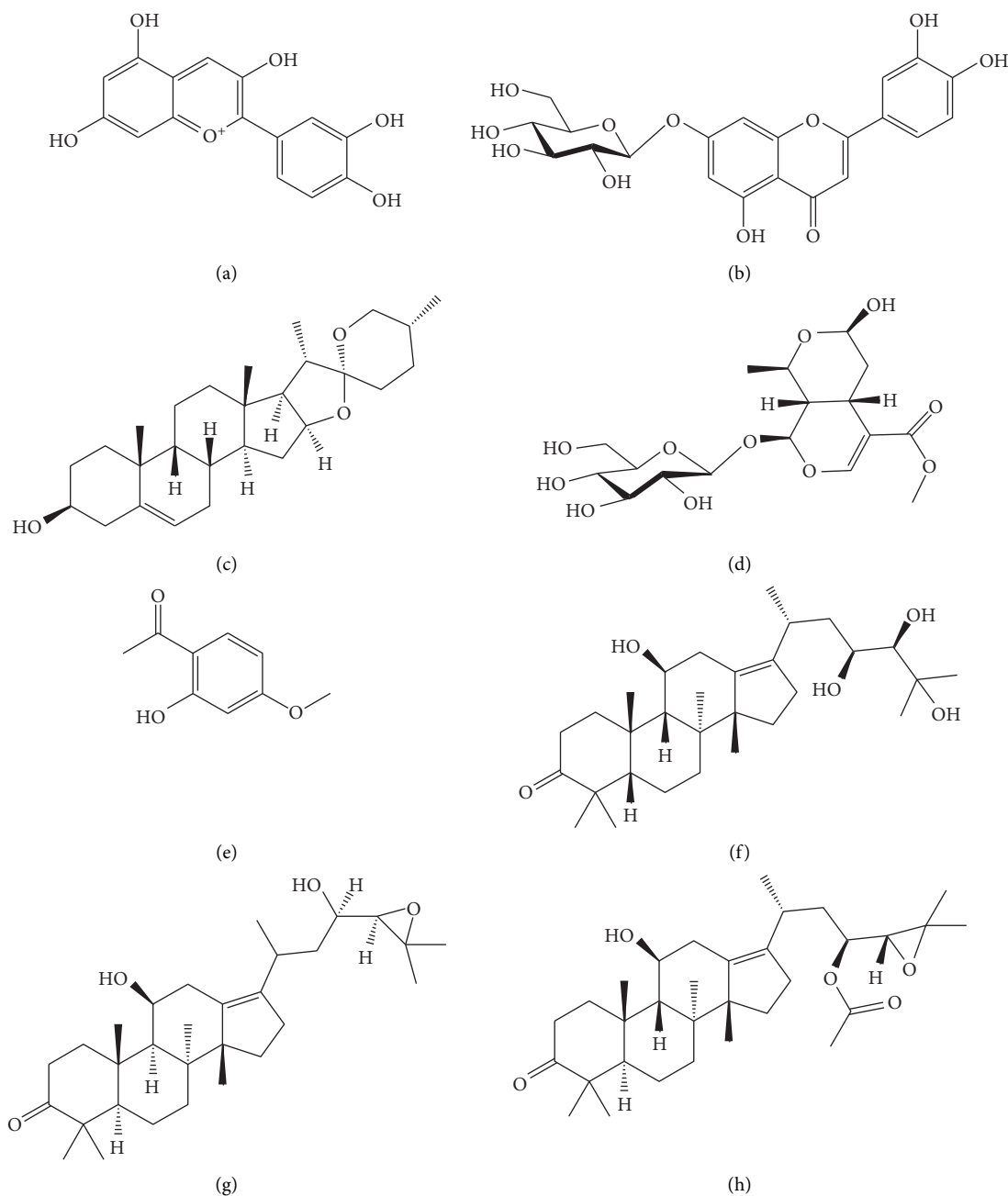


FIGURE 6: Chemical structures of the main active ingredients of QDD. (a) Anthocyanins from Gouqi, (b) cynaroside from Juhua, (c) diosgenin from Shanyao, (d) morroniside from Shanzhuyu, (e) paeonol from Mudanpi, (f) alisol A from Zexie, (g) alisol B from Zexie, and (h) alisol B 23-acetat from Zexie; abbreviations: QDD: Qiju Dihuang decoction.

nerve but also block Ca^{2+} , so it can significantly lower the blood pressure [61]. Alisol A (Figure 6(f)), alisol B (Figure 6(g)), and alisol B 23-acetat (Figure 6(h)) can inhibit Ang II and reduce blood pressure [62]. In addition, the increase in blood pressure caused by the constriction of the aorta via the adrenal glands in the body can be offset by their vasodilation effect [63], and elevated blood pressure caused by the secretion of angiotensin can also be inhibited by alisol [61].

Hypertension belongs to vertigo or headache in TCM, and it often follows other symptoms according to its

complex etiology. So, its treatment should consider the alleviation of some relative symptoms. Our research results showed that QPAD could significantly decrease the TCM syndrome score of patients and improve the life quality of patients. So, it has an obvious effect on reducing the clinical symptoms.

With the accelerating pace of our life, the incidence of hypertensive patients increases year by year and shows a trend of becoming younger [64]. Therefore, in addition to providing low-salt and low-fat diet, regular work, rest, and other health guidance to patients, it is particularly important

to find appropriate drugs and optimized therapeutic scheme. Although antihypertensive drugs have been improved continuously in recent years, their adverse reactions cannot be avoided till now. There are various ways of treating hypertension by TCM, such as herbs, acupuncture, acupoint application, cupping, and foot bath. The multitarget of TCM exactly reflects the characteristics and advantages of integrated intervention. In recent years, many formulae have shown good antihypertensive effect [65–69]. Since hypertension has a very complicated pathological process, integrated TCM and chemical medicine treatment may be a better choice [70]. Our research results showed that QDD alone can significantly reduce the blood pressure, improve the antihypertensive effect, and inhibit the ET biological activity. Moreover, when combined with chemical medicine, QDD can also stabilize blood pressure fluctuations, decrease TCM syndrome score, inhibit inflammation, protect kidney function, reduce insulin resistance, and improve life quality of patients. Therefore, QDD combined with antihypertensive drugs is recommended to treat patients with hypertension of “liver and kidney Yin deficiency.”

Although the effects of QDD on hypertension were evaluated using a meta-analysis, there were some limitations. Firstly, though all of 19 included trials reported randomization, only 6 trials had the random number table. In 19 trials, one used a medical order and the rest of the test randomness was not clear. However, all trials had some deficiencies such as random allocation concealment, blinding of participants, personnel and outcome assessors, or selective outcome reporting. Secondly, no publication bias had been evaluated, because the number of trials included in each subgroup was too small (no more than 10). And, regarding the efficacy of QPAD for SBP, there was a greater heterogeneity among the 7 included trials. Thirdly, there are still 9 trials using modified QDD that does not exactly reflect the effect of QDD. Fourthly, QDD is widely used in the treatment of ophthalmic diseases in the clinic [8], but no outcome indicators related to ophthalmology have been reported in the included trials, so the efficacy of prevention and treatment of hypertensive ophthalmic complications remains unclear. Fifthly, the adverse reactions of QDD on hypertension are unknown, because it is not shown in the included trials.

5. Conclusion

In summary, this study identified that QDD can significantly reduce the blood pressure of hypertension patients and improve the antihypertensive effects; furthermore, it shows a significant ET-lowering effect. Combining with antihypertensive drugs, it can also exhibit an obvious reduction on TCM syndrome score and average blood pressure of 24 h, Ang II, INI, mA1b, β_2 -MG, NAG, and HsCRP level. At the same time, QDD can improve the effect of insulin resistance and patients' life quality. However, due to some less standard design of the included randomized controlled trials, more long-term, randomized and double-blind clinical trials will be needed in the future to provide stronger evidence for the treatment of hypertension with QDD.

Abbreviations

Ang II:	Angiotensin II
β_2 -MG:	β_2 -Microglobulin
CADLI:	Conventional antihypertensive drugs and lifestyle interventions
CI:	Confidence interval
DBP:	Diastolic blood pressure
ET:	Endothelin
HsCRP:	High-sensitivity C-reactive protein
INS:	Insulin
ISI:	Insulin sensitivity index
MD:	Mean difference
NAG:	N-acetyl- β -glucosidase
QDD:	Qiju Dihuang Decoction
QPAD:	Qiju Dihuang Decoction plus antihypertensive drugs
QPCADLI:	Qiju Dihuang Decoction plus conventional antihypertensive drugs and lifestyle interventions
RCTs:	Randomized controlled trials
RR:	Relative risk
SBP:	Systolic blood pressure
TCM:	Traditional Chinese medicine.

Data Availability

The data used to support the findings of this study are available from the corresponding author upon request.

Conflicts of Interest

The authors declare that they have no conflicts of interest.

Authors' Contributions

Shuo Zhang and Xue Bai designed the study, conducted the statistical analysis, drew the tables and pictures, and drafted the full text; Zhen-lin Chen, Jia-jia Li, Yan-yan Chen, and Yu-ping Tang helped to retrieve the database, screen the trials, extract the data, and modify the text.

Acknowledgments

This study was funded by the National Natural Science Foundation of China (81773882 and 81974584) and Key Research and Development Program of Shaanxi Province (2019ZDLSF04-05 and 2019SF-295). This research was also financially supported by Subject Innovation Team of Shaanxi University of Chinese Medicine (2019-YL10).

References

- [1] B. Lu, “Correlation between traditional Chinese medicine syndromes and target organ damage in patients with central obesity hypertension,” *Chinese Journal of Integrative Medicine on Cardio/Cerebrovascular Disease*, vol. 15, pp. 1–5, 2017.
- [2] J. Wang and X. J. Xiong, “Evidence-based Chinese medicine for hypertension,” *Evidence-Based Complementary and Alternative Medicine*, vol. 2013, Article ID 978398, 12 pages, 2013.

- [3] T. Unger, "Decade in review-hypertension: the past decade in hypertension-facts, hopes, and hypes," *Nature Reviews Cardiology*, vol. 11, no. 5, pp. 633–635, 2014.
- [4] F. Guo, D. He, W. Zhang, and R. G. Walton, "Trends in prevalence, awareness, management, and control of hypertension among United States adults, 1999 to 2010," *Journal of the American College of Cardiology*, vol. 60, no. 7, pp. 599–606, 2012.
- [5] E. A. Gebreyohannes, A. S. Bhagavathula, T. B. Abebe, Y. G. Tefera, and T. M. Abegaz, "In-hospital mortality among ischemic stroke patients in Gondar University Hospital: a retrospective cohort study," *Stroke Research and Treatment*, vol. 2019, no. 12, pp. 1–7, 2019.
- [6] J. Seid and X. J. Xiong, "Current situation and perspectives of clinical study in integrative medicine in China," *Evidence-Based Complementary and Alternative Medicine*, vol. 2012, Article ID 268542, 11 pages, 2012.
- [7] X. J. Xiong, F. Borrelli, A. D. Ferreira et al., "Herbal medicines for cardiovascular diseases," *Evidence-Based Complementary and Alternative Medicine*, vol. 2014, Article ID 809741, 2 pages, 2014.
- [8] X. L. Xiao and J. Li, "Meta analysis of the efficacy and safety of Qiju Dihuang pill in the treatment of dry eye," *International Eye Science*, vol. 20, no. 1, pp. 96–102, 2020.
- [9] S. Li and D. Li, "Clinical application and discrimination of Qiju Dihuang Wan and Mingmu Dihuang Wan," *China Journal of Traditional Chinese Medicine and Pharmacy*, vol. 28, no. 7, pp. 2186–2188, 2013.
- [10] G. X. Sun, B. Wu, and K. S. Bi, "Quantitative identification qijudi huang pill by integrating overall information method based on parallel five wavelength high performance liquid chromatographic fingerprints," *Chinese Journal of Chromatography*, vol. 28, no. 9, pp. 877–884, 2010.
- [11] J. H. Zhou, T. Hong, K. Y. Zhang et al., "Study on quality standard improvement of Qiju Dihuang oral liquid," *Chinese Pharmaceutical Journal*, vol. 30, no. 13, pp. 1796–1800, 2019.
- [12] J. Y. Dan, *A Comparative Study on the Intervention of Shenmai Oral Liquid and Qiju Rehmannia Pill on Insulin Resistance in Rats*, Hubei University of Chinese Medicine, Wuhan, China, 2000.
- [13] Z. J. Yue and D. H. Li, "Method of PE kidney spontaneously hypertensive rats vascular remodeling kidney influence," *Guiding Journal of Traditional Chinese Medicine and Pharmacology*, vol. 17, no. 9, pp. 63–65, 2011.
- [14] Z. J. Yue, D. H. Li, and Z. D. Zou, "The research on the protection of kidney of spontaneous hypertension rat by kidney improvement," *Chinese Journal of Experimental Traditional Medical Formulae*, vol. 15, no. 8, pp. 63–65, 2009.
- [15] F. F. Duo, *Kidney Method Intervention Angiotensin II Induced Experimental Studies of Human Umbilical Vein Endothelial Cells Damage*, Capital Medical University, Beijing, China, 2011.
- [16] C. R. Jia and W. J. Wang, "Effect of kidney-tonifying therapy on vec NO-NOS system in patient with primary hypertension," *Hebei Journal of Traditional Chinese Medicine*, vol. 31, no. 2, pp. 9–10, 2016.
- [17] D. Moher, A. Liberati, J. Tetzlaff et al., "Preferred reporting items for systematic reviews and meta-analyses: the PRISMA statement," *PLoS Medicine*, vol. 6, no. 7, Article ID e1000097, 2009.
- [18] J. P. T. Higgins and S. Green, *Cochrane Reviewers' Handbook 5.3.0*, Cochrane, London, UK, 2014, <http://www.cochrane-handbook.org>.
- [19] J. P. T. Higgins, S. G. Thompson, J. J. SG et al., "Measuring inconsistency in meta-analyses," *BMJ*, vol. 327, no. 7414, pp. 557–560, 2003.
- [20] B. J. Du, Z. F. Huang, and X. C. Kong, "The influence of plasma Ang II, ET and CGRP levels of patients with hypertension using Qiju Dihuang pill combined plendil," *Journal of Traditional Chinese Medicine*, vol. 26, no. 4, pp. 53–54, 2009.
- [21] J. Y. Du, H. J. Zhou, and Y. L. Lin, "Clinical efficacy observation of combination of Qiju Dihuang pill and sustained-release nifedipine on hypertension of liver-kidney yin deficiency type," *Liaoning Journal of Traditional Chinese Medicine*, vol. 21, no. 6, pp. 47–49, 2019.
- [22] M. R. Guo and J. Li, "Treating 40 cases of hypertension of liver-kidney yin deficiency pattern by integrative medicine," *Chinese Medical Journal*, vol. 28, no. 6, pp. 112–113, 2015.
- [23] Q. T. Huang, "Qiju Dihuang wan combined with nifedipine in the treatment of liver and kidney yin deficiency hypertension randomized controlled study," *Journal of Traditional Chinese Medicine*, vol. 30, no. 11, pp. 61–63, 2016.
- [24] T. Liang, "Clinical study of Qiju Dihuang pill for liver and kidney yin deficiency hypertension," *MedForum*, vol. 34, no. 1, pp. 122–123, 2013.
- [25] Z. Y. Li, L. J. He, and Q. F. Che, "Improvement effect of modified Qiju Dihuang decoction for clinical symptoms of elderly refractory hypertension disease," *International Journal of Medical Informatics*, vol. 7, no. 17, pp. 11–12, 2017.
- [26] L. P. Liu, "A study on treating the YinXu Yangkang type of hypertension with the Qiju Dihuang decoction," *Chinese Journal of Medical Research*, vol. 11, no. 4, pp. 75–77, 2019.
- [27] S. C. Liu, H. X. Wang, Z. M. Hou et al., "Clinical study of modified Qiju Dihuang decoction in the treatment of senile refractory hypertension," *JETCM*, vol. 20, no. 11, pp. 1729–1730, 2011.
- [28] X. Lu, "Clinical study of modified Qiju Dihuang decoction in the treatment of liver and kidney yin deficiency hypertension," *Xinjiang Journal of Traditional Chinese Medicine*, vol. 22, no. 5, pp. 19–20, 2011.
- [29] D. H. Luo and C. C. Luo, "Clinical observation on the treatment of hypertension with Qiju Dihuang decoction," *JETCM*, vol. 17, no. 3, pp. 296–300, 2008.
- [30] M. Peng, P. Yang, and P. Z. Liu, "Qiju Dihuang decoction improves insulin resistance in patients with hypertension," *Chinese Medicine Modern Distance Education of China*, vol. 3, no. 9, pp. 44–45, 2005.
- [31] Y. Q. Song, "Effect observation of modified Qiju Dihuang decoction combined with western medicine treatment of hypertension of hyperactivity of yang due to yin deficiency," *Liaoning Journal of Traditional Chinese Medicine*, vol. 43, no. 2, pp. 296–298, 2016.
- [32] W. B. Sun, "Clinical study of Qiju Dihuang capsule combined with western medicine in the treatment of liver and kidney yin deficiency hypertension," *Chinese Communications*, vol. 13, no. 33, pp. 152–153, 2011.
- [33] Y. C. Wang, "Protective effect of Qiju Dihuang decoction on renal damage in early hypertension," *Journal of Changchun University of Traditional Chinese Medicine*, vol. 30, no. 1, pp. 107–108, 2014.
- [34] X. M. Wang, X. P. Wei, and J. Y. Jiao, "Observation on the curative effect of Qiju Dihuang pill combined with enalapril maleate capsules on patients with H type hypertension," *Chin. Baby*, no. 6, pp. 115–116, 2016.
- [35] X. X. Yang and X. S. He, "Clinical observation on the treatment of essential hypertension with Qiju Dihuang

- decoction and irapril maleate," *Scientific and Technical Information Processing*, vol. 46, no. 12, pp. 90–92, 2017.
- [36] L. M. Yu, "Study on the therapeutic effect of Qiju Dihuang decoction and western medicine on senile hypertension," *Journal of Imaging*, vol. 1, no. 13, pp. 240–241, 2017.
- [37] J. Zhang, "Clinical study on the treatment of essential hypertension with Chinese and western medicine," *The Journal of Medical Practice Management*, vol. 20, no. 9, pp. 830–831, 2014.
- [38] C. Q. Zhu, "Efficacy analysis of Qiju Dihuang pill combined with nifedipine controlled-release tablet in the treatment of senile hypertension," *Chinese Medicine and Pharmacy*, vol. 2, no. 3, pp. 119–121, 2012.
- [39] G. R. Li, "Standards for the diagnosis and treatment of TCM diseases were introduced," *Standardized Information*, vol. 5, 1995.
- [40] N. Shi, X. Han, W. Yu, and A. Lu, "Adoption in China of clinical practice guidelines for hypertension using traditional Chinese medical approaches: a literature review based on clinical studies," *The Journal of Alternative and Complementary Medicine*, vol. 19, no. 1, pp. 1–8, 2013.
- [41] J. Wang and X. J. Xiong, "Control strategy on hypertension in Chinese medicine," *Evidence-Based Complementary and Alternative Medicine*, vol. 2012, Article ID e284847, 6 pages, 2012.
- [42] X. J. Xiong, X. C. Yang, L. Duan et al., "Traditional Chinese medicine suppresses left ventricular hypertrophy by targeting extracellular signal-regulated kinases signaling pathway in spontaneously hypertensive rats," *Scientific Reports*, vol. 7, Article ID e42965, 2017.
- [43] X.-j. Xiong, X.-c. Yang, W. Liu et al., "Therapeutic efficacy and safety of traditional Chinese medicine classic herbal formula Longdanxiegan Decoction for hypertension: a systematic review and meta-analysis," *Frontiers in Pharmacology*, vol. 9, p. e466, 2018.
- [44] J. L. Duan, R. D. Sheng, H. Liao et al., "Advances in the treatment of hypertension with hyperlipidemia by traditional Chinese medicine," *Hunan Journal of Traditional Chinese Medicine*, vol. 34, no. 10, pp. 180–182, 2018.
- [45] R. Hao, "On the research progress of refractory hypertension (review)," *Chinese Journal of Urban Rural Industrial Hygiene*, vol. 29, no. 1, pp. 25–27, 2014.
- [46] Y. C. Li, X. Y. Zeng, J. M. Liu et al., "Can China achieve a one-hird reduction in premature mortality from noncommunicable diseases by 2030?," *BMC Medicine*, vol. 15, p. 132, 2017.
- [47] Y. M. Zhao, L. N. Xia, X. M. Zhou et al., "Research development of Chinese and western medicine treatment for hypertension," *Journal of Traditional Chinese Medicine*, vol. 37, no. 11, pp. 2690–2693, 2019.
- [48] X. Meng and X. J. Xiong, "Traditional Chinese medicine insights of newly-diagnosed and young hypertension and clinical practice of tianma gouteng decoction for hypertension treatment," *Journal of Chinese Medicine & Traditional Chinese*, pp. 1–10, 2020.
- [49] G. M. Reaven and Y.-D. I. Chen, "Role of insulin in regulation of lipoprotein metabolism in diabetes," *Diabetes/Metabolism Reviews*, vol. 4, no. 7, pp. 639–652, 1988.
- [50] X. Lu, "An overview of insulin resistance and its mechanism in hypertension treated with traditional Chinese medicine," *Journal of Integrated Traditional Chinese and Western Medicine*, vol. 28, no. 31, pp. 3531–3534, 2019.
- [51] W. B. Yao, "Talk about hypertension," *Journal of Hubei Water Resources Technical College*, vol. 15, no. 4, pp. 66–69, 2019.
- [52] X. Liu, Y. Zhou, S. J. Zou et al., "Research progress of Chinese herb Gouqi," *Science, Technology and Innovation*, no. 2, pp. 45–46, 2019.
- [53] D. He, X. Ru, L. Wen et al., "Total flavonoids of Flos Chrysanthemi protect arterial endothelial cells against oxidative stress," *Journal of Ethnopharmacology*, vol. 139, no. 1, pp. 68–73, 2012.
- [54] H.-D. Wen, J. Cai, J.-H. Xu, X.-M. Zhou, and Q. Xia, "Endothelium-dependent and direct relaxation induced by ethyl acetate extract from Flos Chrysanthemi in rat thoracic aorta," *Journal of Ethnopharmacology*, vol. 101, no. 1–3, pp. 221–226, 2005.
- [55] K. Zhou, T. Asano, H. Shiomoto et al., "Studies on Rehmanniae Radix. I. effect of 50% ethanolic extract from steamed and dried Rehmanniae Radix on hemorheology in arthritic and thrombotic rats," *Biological and Pharmaceutical Bulletin*, vol. 17, no. 9, pp. 1282–1286, 1994.
- [56] S. Q. Chen, J. X. Li, X. Y. Wu et al., "Advances in pharmacology of rehmanniaglucoside," *Chemical Engineering Journal*, vol. 33, no. 11, pp. 46–50, 2019.
- [57] K. Liu, W. Zhao, X. Gao, J. Kou, and B. Liu, "Diosgenin ameliorates palmitate-induced endothelial dysfunction and insulin resistance via blocking IKK β and IRS-1 pathways," *Atherosclerosis*, vol. 223, no. 2, pp. 350–358, 2012.
- [58] Y. M. Huang, H. Li, and C. R. Li, "Advance on chemical compositions and pharmacology of cornus officinalis," *Acta Medica Academica*, vol. 19, no. 6, pp. 500–502, 2010.
- [59] C. R. Zhang, G. Cao, Y. Zhang et al., "Research progress on chemical constituents, pharmacological activities and processing history of Fructus Corni," *Journal of Traditional Chinese Medicine*, vol. 29, no. 9, pp. 2002–2005, 2011.
- [60] M. Dai, Q. Y. Liu, and X. M. Zi, "Protective effective of paeonol on artery Endothelial cells of the hyperlipidaemia rats," *Chinese Journal of Basic Medicine in Traditional Chinese Medicine*, vol. 7, no. 2, pp. 38–40, 2001.
- [61] Z. Z. Xing, W. Chen, and N. Zeng, "Research progress on chemical constituents and pharmacological effects of Zexie (*Alisma orientalis*)," *Guiding Journal of Traditional Chinese Medicine and Pharmacology*, vol. 23, no. 15, pp. 75–78, 2017.
- [62] B. Makino, M. Kobayashi, K. Kimura et al., "Local variation in the content of angiotensin II and arginine vasopressin receptor antagonistic terpenoids in the rhizomes of *Alisma orientale*," *Planta Medica*, vol. 68, no. 3, pp. 226–231, 2002.
- [63] J. T. Ishimatsu and S. W. Li, "The development of alisma on cardiovascular system," *Chinese Foreign Medical Treatment*, vol. 31, no. 20, p. 191, 2012.
- [64] P. K. Whelton, R. M. Carey, W. S. Aronow et al., "2017 ACC/AHA/AAPA/ABC/ACPM/AGS/APhA/ASH/ASPC/NMA/PCNA guideline for the prevention, detection, evaluation and management of high blood pressure in adults: executive summary: a report of the American College of Cardiology/American Heart Association Task Force on clinical practice guidelines," *Circulation*, vol. 138, no. 17, 2018.
- [65] Y. Cao, L.-t. Liu, and M. Wu, "Is Chinese herbal medicine effective for elderly isolated systolic hypertension? A systematic review and meta-analysis," *Chinese Journal of Integrative Medicine*, vol. 23, no. 4, pp. 298–305, 2017.
- [66] X. J. Xiong, P. Q. Wang, X. K. Li et al., "The effect of Chinese herbal medicine jian ling decoction for the treatment of essential hypertension: a systematic review," *BMJ Open*, vol. 5, no. 2, Article ID e006502, 2015.
- [67] X. J. Xiong, P. Q. Wang, L. Duan et al., "Efficacy and safety of Chinese herbal medicine xiao yao san in hypertension: a

- systematic review and meta-analysis," *Phytomedicine*, vol. 61, Article ID UNSP 152849, 2019.
- [68] X. Xiong, X. Yang, X. Li, G. Yue, Y. Xing, and W. C. Cho, "Efficacy and safety of Chinese herbal medicine for patients with postmenopausal hypertension: a systematic review and meta-analysis," *Pharmacological Research*, vol. 141, pp. 481–500, 2019.
- [69] H. Wang, C. Liu, J. Zhai, and H. Shang, "Niu Huang Jiangya Preparation (a traditional Chinese patent medicine) for essential hypertension: a systematic review," *Complementary Therapies in Medicine*, vol. 31, pp. 90–99, 2017.
- [70] Y. Shang, X.-j. Han, W.-l. Weng et al., "Appraisal of the quality and contents of clinical practice guidelines for hypertension management in Chinese medicine: a systematic review," *Chinese Journal of Integrative Medicine*, vol. 24, no. 7, pp. 545–550, 2018.

Research Article

Network Pharmacology-Based Strategy to Investigate the Pharmacological Mechanisms of *Ginkgo biloba* Extract for Aging

Yanfei Liu ^{1,2}, Yue Liu ³, Wantong Zhang,² Mingyue Sun,² Weiliang Weng ²,
and Rui Gao ²

¹Graduate School of Beijing University of Chinese Medicine, Beijing 100029, China

²Institute of Clinical Pharmacology of Xiyuan Hospital, China Academy of Chinese Medical Sciences, Beijing 100091, China

³Cardiovascular Diseases Center, Xiyuan Hospital of China Academy of Chinese Medical Sciences, Beijing 100091, China

Correspondence should be addressed to Weiliang Weng; wengweiliangtcm@163.com and Rui Gao; ruigao@126.com

Received 15 May 2020; Accepted 26 June 2020; Published 27 July 2020

Guest Editor: Hong Chang

Copyright © 2020 Yanfei Liu et al. This is an open access article distributed under the Creative Commons Attribution License, which permits unrestricted use, distribution, and reproduction in any medium, provided the original work is properly cited.

Aging is a main risk factor for a number of debilitating diseases and contributes to an increase in mortality. Previous studies have shown that *Ginkgo biloba* extract (EGb) can prevent and treat aging-related diseases, but its pharmacological effects need to be further clarified. This study aimed to propose a network pharmacology-based method to identify the therapeutic pathways of EGb for aging. The active components of EGb and targets of sample chemicals were obtained from the Traditional Chinese Medicine Systems Pharmacology Database and Analysis Platform (TCMSP) database. Information on aging-related genes was obtained from the Human Ageing Genomic Resources database and JenAge Ageing Factor Database. Subsequently, a network containing the interactions between the putative targets of EGb and known therapeutic targets of aging was established, which was used to investigate the pharmacological mechanisms of EGb for aging. A total of 24 active components, 154 targets of active components of EGb, and 308 targets of aging were obtained. Network construction and pathway enrichment were conducted after data integration. The study found that flavonoids (quercetin, luteolin, and kaempferol) and beta-sitosterol may be the main active components of EGb. The top eight candidate targets, namely, PTGS2, PPARG, DPP4, GSK3B, CCNA2, AR, MAPK14, and ESR1, were selected as the main therapeutic targets of EGb. Pathway enrichment results in various pathways were associated with inhibition of oxidative stress, inhibition of inflammation, amelioration of insulin resistance, and regulation of cellular biological processes. Molecular docking results showed that PPARG had better binding capacity with beta-sitosterol, and PTGS2 had better binding capacity with kaempferol and quercetin. The main components of EGb may act on multiple targets, such as PTGS2, PPARG, DPP4, and GSK3B, to regulate multiple pathways, and play an antiaging role by inhibiting oxidative stress, inhibiting inflammation, and ameliorating insulin resistance.

1. Introduction

Aging is inevitable, but pathological aging poses a serious threat to human health, reduces the quality of life of elderly individuals, and promotes the development of related diseases [1, 2]. Aging is an extremely important factor that induces many types of cardiovascular and cerebrovascular diseases, such as atherosclerosis, myocardial infarction, stroke, and heart failure [3, 4]. Among them, vascular aging plays a central role in morbidity and mortality [5]. After years of research, researchers have put forward many

hypotheses regarding aging mechanisms, such as oxidative stress, genetic determination theory, free radical theory, neuroendocrine theory, and mitochondrial damage theory [4, 6, 7]. Most importantly, increasing oxidative stress, a major characteristic of aging, has been implicated in various age-related diseases [8]. The biological mechanisms of aging are still being explored. As fertility declines and life expectancy increases, the proportion of the aging global population is increasing, and the presence of age-related diseases increases the socioeconomic burden. Therefore, it has become one of the most important issues in studying the

biological mechanisms of aging and exploring effective drugs that can delay or reduce the development of age-related diseases and clarify the mechanism. It is believed that many medicinal herbs have antiaging properties, but the mechanisms remain unclear.

The extract of *Ginkgo biloba* (EGb), a well-known medicinal plant, is used to treat many aging-related diseases, such as cardiovascular and neurodegenerative aging-related diseases [9]. Due to its medicinal value, increasing attention has been paid to the basic research and clinical application of EGb. A study found that the chemical composition of EGb is complex, including flavonoids, lactones, polyphenols, alkyl phenolic acids, organic acids, steroids, and trace elements [10]. EGb preparation is a relatively successful case of plant medicine developed by modern science and technology and occupies an important position in the field of antiaging and clinical medication for cardiovascular and cerebrovascular diseases [9, 11]. Previous studies have shown that EGb has certain efficacy in the prevention and treatment of age-related diseases [9, 12–14]. However, the pharmacologic profiles of EGb for aging remain unclear. Therefore, in this study, a network pharmacology method was used to preliminarily explore the molecular mechanism of EGb in aging.

2. Materials and Methods

2.1. Identification and Screening of Candidate Compounds. The active constituents of EGb were obtained from the Traditional Chinese Medicine Systems Pharmacology Database and Analysis Platform (TCMSP) database (<http://lsp.nwsuaf.edu.cn/tcmsp.php>). TCMSP is an integrated systems pharmacology platform of Chinese herbal medicines that covers chemicals, targets, and drug targets and pharmacokinetic properties for compounds involving oral bioavailability (OB), drug likeness (DL), blood-brain barrier, intestinal epithelial permeability, and aqueous solubility [15]. In this study, OB and DL were utilized to screen the chemical constituents with $OB \geq 30\%$ and $DL \geq 0.18$ simultaneously [16]. In addition, active ingredients with low OB and remarkable efficacy reported in the literature were included.

2.2. Potential Targets of Active Components. The validated target proteins of the active components were obtained from the TCMSP database. The target protein name of the active ingredient was converted to the standard target gene name through the UniProt Knowledge Base (UniProtKB, <http://www.uniprot.org/>). The UniProtKB is the central hub for the collection of functional information on proteins, with accurate, consistent, and rich annotation. The target protein names were inputted into UniProtKB, with the organism restricted to “Homo sapiens,” eventually gaining the official symbol.

2.3. Search of Aging-Related Targets and Genes. Aging-related genes were obtained by retrieving data from the Human Ageing Genomic Resources (HAGR) database (<http://genomics.senescence.info/>) and JenAge Ageing

Factor Database (AgeFactDB, <http://agefactdb.jenage.de>). HAGR is a collection of databases and tools for studying human aging through modern approaches, such as functional genomics, network analysis, systems biology, and evolutionary analysis [17]. The purpose of the AgeFactDB is to collect and integrate aging phenotype and longevity data, and it also includes genes that are homologous to known aging-related genes [18]. The target matching analysis of aging-related genes and EGb was conducted to select the target of EGb acting on aging.

2.4. Construction of Networks and Analyses. The Cytoscape software was adopted to visually display and analyze the network structure. It is an open source software platform for visualizing molecular interaction networks and biological pathways and integrating these networks with annotations, gene expression profiles, and other state data [19]. Two networks were constructed in this study as follows. (1) A component-component target network was established by joining the active components of herbs and their corresponding components. (2) Based on the component-component target network, the core network was screened according to the degree value.

2.5. Gene Ontology (GO) and Pathway Enrichment Analysis. The Database for Annotation, Visualization, and Integrated Discovery (DAVID) provided a comprehensive set of functional annotation tools to understand the biological meaning behind a large list of genes. DAVID tools were able to identify enriched biological themes, particularly GO terms that involved biological process (BP), cell component (CC), and molecular functions (MFs) and visualized genes on KEGG pathway maps [20]. The target of EGb acting on aging was inputted into the DAVID database with the organism limited to “Homo sapiens.” The dividing value of recognized GO terms was set to $FDR < 0.05$, and KEGG pathways were set to $P < 0.05$ [21, 22].

2.6. Molecular Docking. In the analysis of the component-target action network, it is generally believed that a node with greater degree is the pivot node in the whole network. Therefore, the components of the core network were molecularly docked with the target. The 3D structure of the core components was obtained using PubChem (<https://pubchem.ncbi.nlm.nih.gov/>), and target proteins were retrieved from the Protein Data Bank (<http://www.rcsb.org/pdb>). The main pharmacodynamic components of *Ginkgo biloba* were docked with the core target gene by AutoDock. PyMOL was used to display the interaction diagram between receptor proteins and ligand small molecules.

3. Results

3.1. Identification of the Active Compounds in EGb. A total of 24 active ingredients of EGb were included according to the OB and DL values in the TCMSP database and reported in

the literature. The results are shown in Additional file 1. The OB of ginkgolide A was <30%, but it was a common compound in EGb and was shown to prevent and treat Alzheimer's disease, a disease associated with aging [14, 23]. Hence, ginkgolide A was also considered a candidate compound.

3.2. Identification of Targets in EGb. By searching the abovementioned databases, 154 targets of active ingredients of EGb (Additional file 2: targets of active ingredients) and 308 targets of aging (Additional file 3: targets of aging) were obtained. Moreover, 28 targets of active components of EGb for antiaging were obtained by integrating the intersection of targets of active ingredients and aging (Additional file 4: potential targets of EGb for antiaging).

3.3. Component-Component Target Network Analysis. The 24 active ingredients of EGb and 28 targets of the active components of EGb for antiaging were retrieved. We constructed networks to present the relationship among EGb components and component targets with therapeutic effects against aging. The network consists of 52 nodes and 164 edges (Figure 1(a)). Based on the component-target network, the core network was screened according to the degree. The screening condition was a degree >10. Four compounds, including quercetin (MOL000098), luteolin (MOL000006), kaempferol (MOL000422), and beta-sitosterol (MOL000358), and eight targets, including PTGS2, PPARG, GSK3B, DPP4, CCNA2, AR, MAPK14, and ESR1, had a degree >10 (Figure 1(b)). The results indicated that these four components might play a vital role in the antiaging network of EGb through the abovementioned target genes.

3.4. GO and KEGG Pathway Enrichment Analysis. To illustrate the mechanism of EGb in aging, we performed GO and KEGG pathway enrichment analysis for 27 putative therapeutic targets. We identified enrichment results in the related items: 195 BPs, 42 MFs, and 25 CCs. Subsequently, 21 significantly enriched GO terms with FDR <0.05 were determined, including 13 BPs, 2 CCs, and 6 MFs (Figure 2). For BPs, these putative therapeutic targets were mainly enriched in positive regulation of transcription from RNA polymerase II promoter (GO:0045944), positive regulation of nitric oxide biosynthetic process (GO:0045429), positive regulation of transcription, DNA-templated (GO:0045893), positive regulation of superoxide anion generation (GO:0032930), negative regulation of apoptotic process (GO:0043066), peptidyl-serine phosphorylation (GO:0018105), positive regulation of smooth muscle cell proliferation (GO:0048661), Ras protein signal transduction (GO:0007265), response to drug (GO:0042493), positive regulation of extracellular signal-regulated kinase (ERK) 1 and 2 cascade (GO:0070374), cellular response to estradiol stimulus (GO:0071392), cellular response to lipopolysaccharide (GO:0071222), and peptidyl-threonine phosphorylation (GO:

0018107). For CCs, the targets were enriched in the nucleoplasm (GO:0005654) and nucleus (GO:0005634). For MFs, the targets were enriched with enzyme binding (GO:0019899), identical protein binding (GO:0042802), transcription factor binding (GO:0008134), protein binding (GO:0005515), chromatin binding (GO:0003682), and core promoter sequence-specific DNA binding (GO:0001046). Therefore, the results indicated that EGb mainly exerted antiaging therapeutic effects by regulating these BPs, MFs, and CCs.

The X-axis shows the counts of target genes, and the Y-axis shows significantly enriched GO categories of the target genes (FDR <0.05).

We performed KEGG pathway enrichment analysis to examine the pathways for 27 putative therapeutic targets of EGb for antiaging. The top 20 pathways were determined (Figure 3), mainly including pathways in cancer (hsa05200), neurotrophin signaling pathway (hsa04722), proteoglycans in cancer (hsa05205), gonadotropin-releasing hormone (GnRH) signaling pathway (hsa04912), PI3K-Akt signaling pathway (hsa04151), the tumor necrosis factor (TNF) signaling pathway (hsa04668), insulin resistance (hsa04931), sphingolipid signaling pathway (hsa04071), focal adhesion (hsa04510), nonalcoholic fatty liver disease (hsa04932), MAPK signaling pathway (hsa04010), ErbB signaling pathway (hsa04012), HIF-1 signaling pathway (hsa04066), T cell receptor signaling pathway (hsa04660), Toll-like receptor signaling pathway (hsa04620), type II diabetes mellitus (hsa04930), NOD-like receptor signaling pathway (hsa04621), FOXO signaling pathway (hsa04068), VEGF signaling pathway (hsa04370), and Wnt signaling pathway (hsa04310). The results indicate that these pathways might play an important role in the antiaging effect of EGb. It provided research ideas for exploring the targets of EGb for antiaging.

The Y-axis represents significant pathways of the target genes, and the X-axis shows the rich factor. The rich factor represents the ratio of the number of target genes belonging to a pathway to the number of all annotated genes located in the pathway. A higher rich factor represents a higher enrichment level. The color of the dot corresponds to different P values, and the size of the dot reflects the number of target genes expressed in the pathway.

3.5. Molecular Docking. Eight proteins were docked with four components using AutoDock, and 20 conformations were obtained. The binding energy scoring and docking parameters are shown in Table 1. A low binding score is prone to interaction. Therefore, the three groups with the lowest scores were selected for composition analysis. The conformations of receptor protein PPARG and beta-sitosterol ligand small molecules, receptor protein PTGS2 and kaempferol ligand small molecules, and receptor protein PTGS2 and quercetin ligand small molecules were constructed.

The binding pattern between receptor protein PPARG and beta-sitosterol ligand small molecules is presented in Figure 4(a). Amino acid residues Glu343 and beta-sitosterol

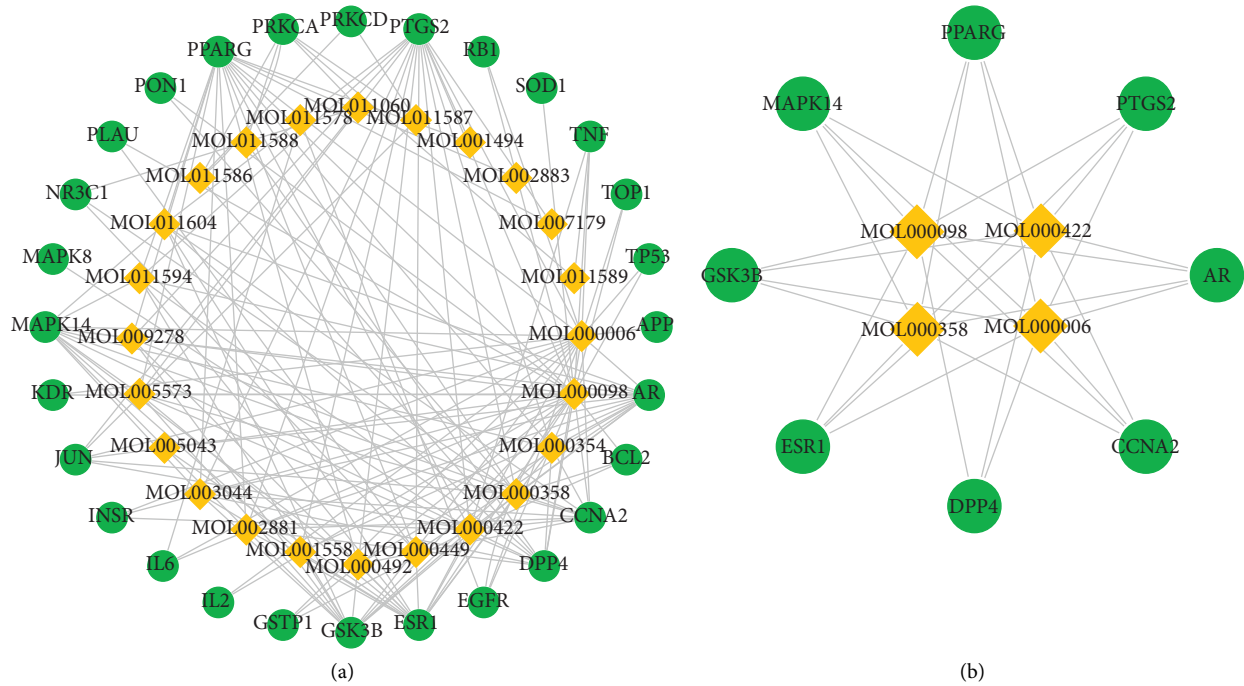


FIGURE 1: Component-component target network. (a) The network of EGb components and component targets with therapeutic effects against aging. (b) Filter the core network with a degree >10 based on component-component target network. The diamond shape represents the components, and the ellipse represents the target gene.

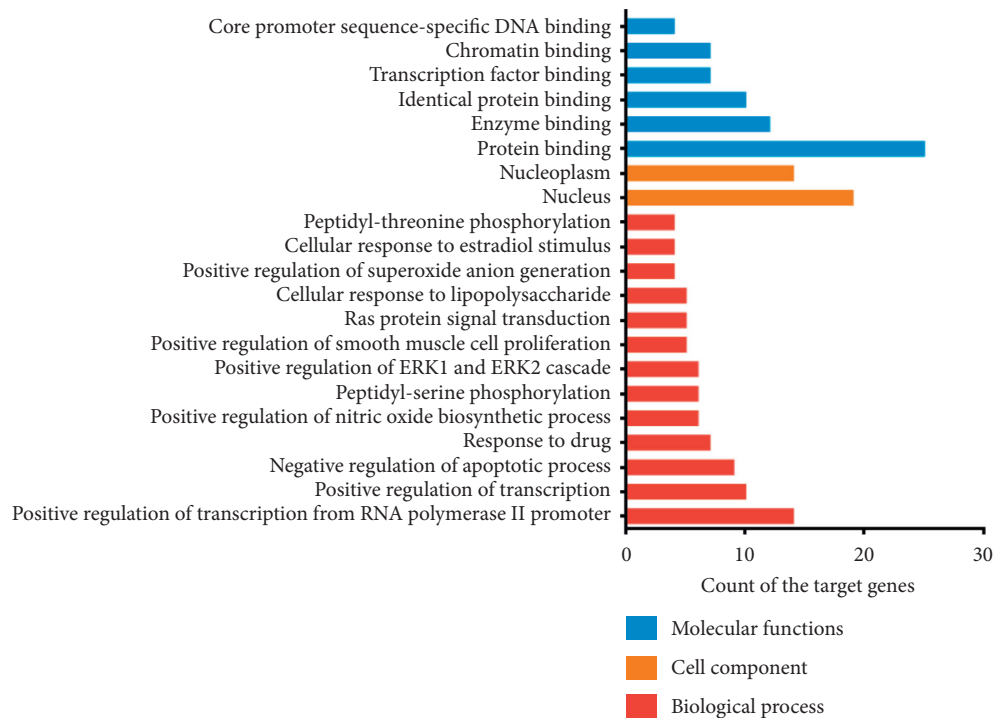


FIGURE 2: GO enrichment analysis of putative therapeutic targets.

ligand small molecules formed hydrogen bond interactions, and amino acid residues Tyr473, Phe264, His266, Lys265, Ile262, Gly284, Ser342, Arg288, Glu291, Tyr477, and Phe287 and beta-sitosterol ligand small molecules formed hydrophobic interactions.

The binding pattern between the receptor protein PTGS2 and kaempferol ligand small molecules is shown in Figure 4(b). Amino acid residues Thr206, His207, and His386 and kaempferol ligand small molecules formed hydrogen bond interactions, and amino acid residues

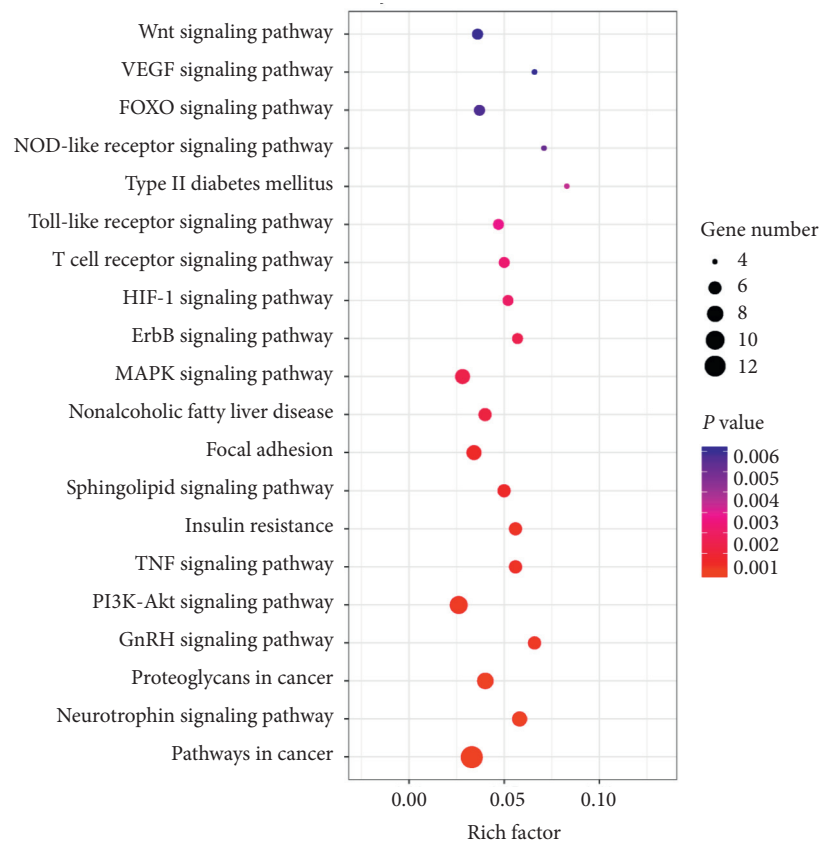


FIGURE 3: KEGG pathway enrichment analyses of putative therapeutic targets.

TABLE 1: Molecular docking of eight proteins and four components.

Protein	Grid size	Docking score (kcal/mol)			
		Quercetin	Luteolin	Kaempferol	Beta-sitosterol
GSK3B	40 × 40 × 40	-8.1	-8.5	-8.5	-9.0
DPP4	60 × 58 × 48	-8.6	-8.2	-8.2	-8.4
PPARG	40 × 40 × 40	-8.3	-8.3	-8.3	-9.7
CCNA2	40 × 40 × 40	-7.6	-7.7	-7.7	-7.4
AR	40 × 40 × 40	-8.8	-8.7	-8.7	-8.9
PTGS2	40 × 40 × 40	-9.6	-9.4	-9.5	-8.5
ESR1	42 × 44 × 44	-9.2	-9.0	-9.0	-7.9
MAPK14	40 × 40 × 40	-8.4	-8.6	-8.5	-8.3

Ala202, Ala199, Gln203, Leu391, Leu390, Asn382, Tyr385, and Phe210 and kaempferol ligand small molecules formed hydrophobic interactions.

The binding pattern between the receptor protein PTGS2 and quercetin ligand small molecules is shown in Figure 4(c). Amino acid residues Glu465, His39, Arg44, and Asp125 and quercetin ligand small molecules formed hydrogen bond interactions, and amino acid residues Cys41, Gly45, Val46, Arg469, Tyr130, Leu152, Pro153, and Gln461 and quercetin ligand small molecules formed hydrophobic interactions.

4. Discussion

Previous studies have shown that EGb is effective in the prevention and treatment of aging-related diseases [12–14].

However, the mechanism of its antiaging action needs to be further explored. Therefore, the network pharmacology method was used to predict the possible mechanism and main active components of EGb in delaying aging to provide an innovative idea for further animal experiments. The possible mechanism of EGb for aging is shown in Figure 5. The results of this study also show that various compounds of EGb have antiaging effects. Quercetin, luteolin, kaempferol, and beta-sitosterol may play vital roles in the antiaging network of EGb based on the prediction method of network pharmacology. Quercetin, a polyphenol widely present in nature, has received the most attention in antiaging. Studies have shown that quercetin exerts neuroprotective actions in the aging nervous system by stimulating cellular defenses against oxidative stress, activating sirtuin 1 (SIRT1), and

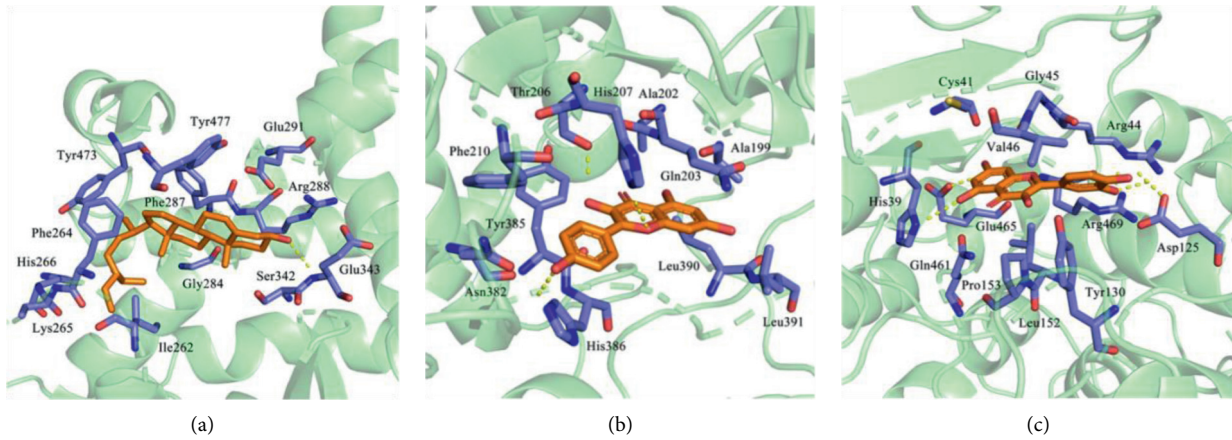


FIGURE 4: Docking diagram of components and protein molecules. (a) The binding pattern between receptor protein PPARG and beta-sitosterol ligand small molecules. (b) The binding pattern between receptor protein PTGS2 and kaempferol ligand small molecules. (c) The binding pattern between receptor protein PTGS2 and quercetin ligand small molecules.

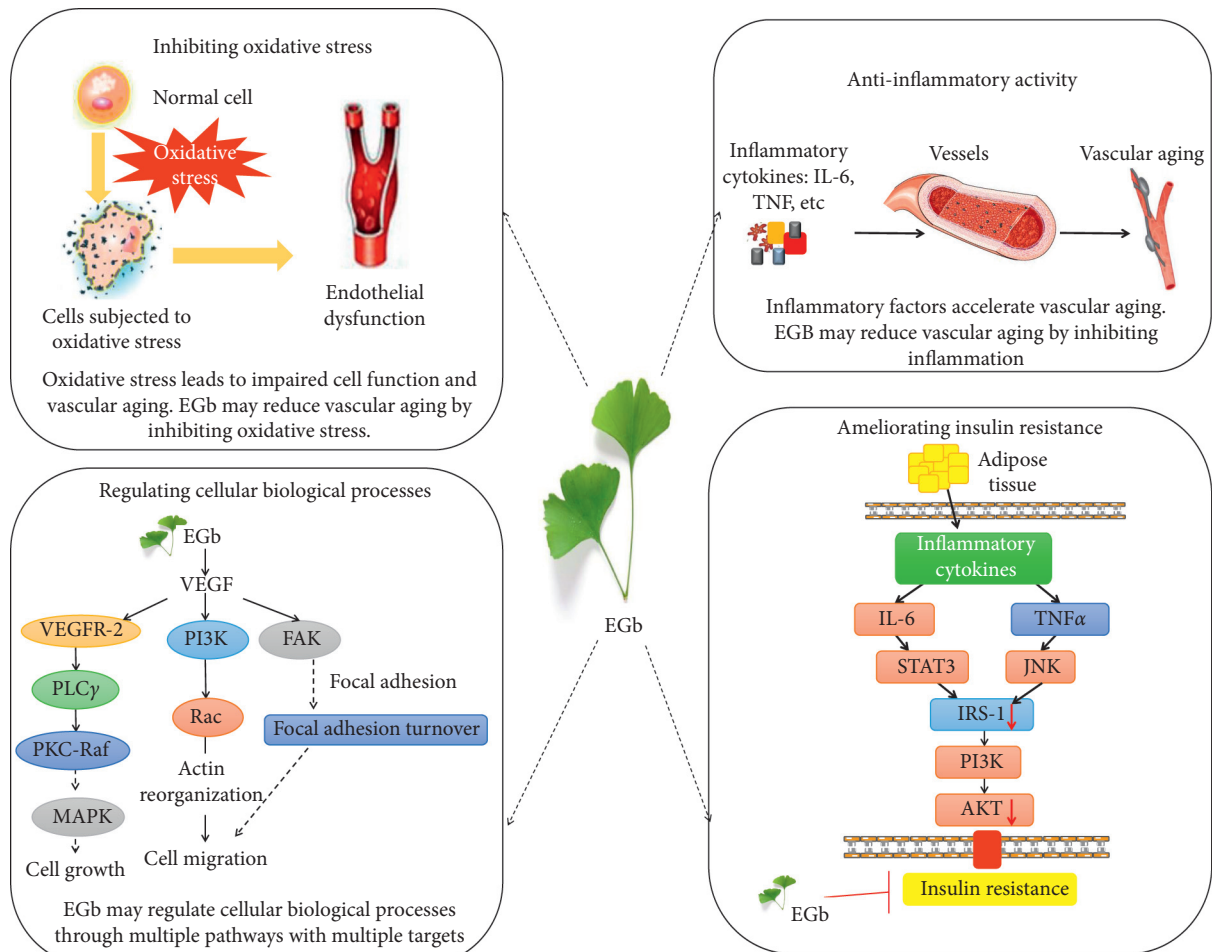


FIGURE 5: Possible mechanism of EGb for aging.

inducing autophagy [24]. Quercetin plays an antiaging role via enhancement of cell proliferation and restoration of heterochromatin architecture [25]. In addition, several evidence-based studies suggest that quercetin is a significant research prospect in the prevention and treatment of

vascular aging-related diseases [26, 27]. Luteolin has the potential for antioxidative activity. Luteolin, as an anti-inflammatory and neuroprotective agent, can inhibit the generation of reactive oxygen species via modulation of the AMPK-SIRT1 pathway to prevent the development of age-

related disorders [28]. The study also found that luteolin may improve cognitive performance in older mice by inhibiting microglial activation and neuroinflammation [29]. Luteolin may be potentially useful in the prevention of skin aging by inhibiting the UVA-induced production of collagen MMP-1 [30]. A prospective study showed that vegetables and foods rich in kaempferol, lutein, and folate may slow cognitive decline with aging [31]. Kaempferol is an antioxidant and anti-inflammatory agent that regulates the NF-kappaB signaling cascade and inhibits NADPH oxidase activation; hence, it is considered as a potential antiaging agent [32]. Beta-sitosterol may increase the proliferation and stimulate the differentiation of embryonic neural stem cells to prevent neurodevelopmental syndromes and cognitive decline during aging [33]. Beta-sitosterol can extend the lifespan of adult flies, possibly by activating AMP-activated protein kinase (AMPK) [34].

These eight targets, namely, DPP4, GSK3B, CCNA2, AR, ESR1, PTGS2, PPARC, and MAPK14, may play a crucial role in the antiaging network of EGb. DPP4 and GLP-1 had been found to play important roles in oxidative stress, lipid metabolism, insulin resistance, and inflammation. Recently, a study found that the balance between DPP4 and GLP-1 might be a therapeutic target for the management of vascular aging and atherosclerosis in animals [35]. Studies have shown that GSK3B, which acts as a negative regulator in the hormonal control of glucose homeostasis, Wnt signaling, and regulation of transcription factors and microtubules, is closely related to the Healthy Aging Index [36]. Silencing of CCNA2, which controls both the G1/S and G2/M transition phases of the cell cycle, remarkably triggered cellular aging, while CCNA2 overexpression delayed cellular aging [37]. The expression of PTGS, with a particular role in the inflammatory response, was upregulated in diseases related to brain aging [38]. PPARC, a key regulator of adipocyte differentiation and glucose homeostasis, is associated with inflammation [39]. MAPK14 plays important roles in cell proliferation, differentiation, migration, transformation, and programmed cell death [40].

In the GO enrichment analysis, the targets were closely related to positive regulation of transcription from RNA polymerase II promoter, nitric oxide biosynthetic process, smooth muscle cell proliferation, and negative regulation of the apoptotic process. CCs involve the nucleoplasm nucleus. MFs involve the binding of enzymes, proteins, and transcription factors. According to a study by Nakazawa et al., RNA polymerase II ubiquitination provides a two-tier protection mechanism by activating transcription-coupled nucleotide excision repair and, in parallel, processing of DNA damage-stalled RNA polymerase II, which together prevent prolonged transcription arrest and protect against neurodegeneration [41]. Nitric oxide generated through endothelial nitric oxide synthase acts as a gas signaling mediator to promote mitochondrial biogenesis and bioenergetics, with a favorable impact on chronic age-related diseases [42]. There is evidence suggesting that vascular smooth muscle cells accelerate aging and increase the incidence of age-related diseases, such as obesity, diabetes, and atherosclerosis [43, 44]. According to a study by Zhan et al.

[45], vascular smooth muscle cells pretreated with the AMPK activator and mammalian target of rapamycin inhibitor could reduce the replication aging of cells. The apoptotic process plays an important role in the aging process [46]. Moorefield et al. [47] used histological methods to detect the morphology, cell composition, and apoptosis of cryptovilli in old (18–22 months) and young (2–4 months) Sox9-EGFP IESC reporter mice, and cleaved caspase-3 staining showed increased apoptotic cells in the crypt and villi of older mice. The study found that some conserved transcription factors, such as the helix-loop-helix transcription factor and forkhead transcription factor (FOXO), control the expression of many autophagy-related genes and have important implications for longevity [48]. A study by Alvarez-Garcia et al. [49] found that the Col2a1Cre and AcanCreER mouse lacking all FOXO isoforms (FOXO 1, 3, and 4) led to severe cell loss in the nucleus pulposus and cartilage endplates, leading to spontaneous degeneration of the intervertebral disk (IVD), which is a prevalent age-associated musculoskeletal disorder, and the findings demonstrate that FOXOs are critical regulators of IVD homeostasis during aging and suggest that maintaining or restoring FOXO expression can delay the onset of IVD degeneration.

KEGG pathway enrichment analyses demonstrated that EGb is involved in the regulation of multiple pathways. Increased oxidative stress and inflammation, including the HIF-1 and TNF signaling pathways, play significant roles in aging, especially vascular aging [50]. The neurotrophin signaling pathway plays an important role in higher-order activities, such as neural development, learning, and memory, and several genes in the pathway are closely related to brain aging [51]. Insulin resistance is strongly associated with type II diabetes and nonalcoholic fatty liver disease, and the elderly population often develops insulin resistance [52]. Oxidative stress, mitochondrial dysfunction, accumulation of intracellular lipid derivatives, and inflammation (via IL-6 and TNF α) contribute to decreased activation of signaling molecules, including PI3K and AKT, leading to insulin resistance [53–55]. The absence of sphingomyelin, a second messenger that functions in a variety of cellular signaling pathways, leads to a shortened lifespan in animals, suggesting that sphingolipid signaling may play a role in neuronal function and animal stress response during aging [56]. Focal adhesion, mitogen-activated protein kinase (MAPK) signaling pathway, and ErbB signaling pathway are modules that are involved in cell proliferation, differentiation, and migration [57–59]. Focal adhesion, a signaling molecule associated with cell survival, relies on the interaction between integrins and actin to connect cells to the extracellular matrix [58]. Studies have shown that extracellular matrix protein-cell interactions give rise to target organ damage and inflammatory pathways, leading to calcification or atherosclerosis [1, 60]. The MAPK signaling pathway, including ERK1/2, c-Jun N-terminal kinase, and p38, is closely related to the BP of aging, and the progression of the inflammatory process leads to dysregulation of MAPK, which accelerates cell aging [61]. Inactivation of the ErbB signaling pathway leads to a loss of myocardial

protective function during cardiac hypertrophy and onset of early failure [59]. The T cell receptor signaling pathway, Toll-like receptor (TLR) signaling pathway, and NOD-like receptor signaling pathway are responsible for generating innate immune responses and play a critical role in inflammation. Toll-like receptors play a significant role in promoting aging adipose tissue inflammation, and the study showed that old TLR4-deficient mice have improved glucose tolerance compared to age-matched wild-type mice [62]. A different set of NOD-like receptors induces caspase-1 activation, and the activated caspase-1 regulates the maturation of the proinflammatory cytokines IL-1B and IL-18 and drives pyroptosis [63]. The FOXO family regulates the expression of genes involved in apoptosis, cell-cycle control, glucose metabolism, oxidative stress resistance, and longevity. Recent evidence indicates that the FOXO family plays a key role in the self-renewal of adult and embryonic stem cells, which could contribute to tissue regeneration [64]. Vascular endothelial growth factor (VEGF) can stimulate endothelial cell growth, promote angiogenesis, and increase vascular permeability. The decreased angiogenesis associated with the aging of the body is related to the decreased expression of VEGF, and the proliferation ability of vascular endothelial cells in elderly animals is weakened. The addition of VEGF can help restore the proliferation ability of vascular endothelial cells, leading to delayed vascular aging [65]. Wnt proteins are secreted morphogens that are required for basic developmental processes. Overactivation of the Wnt/ β -catenin signaling pathway is closely related to stem cell aging [66].

5. Conclusions

In this study, the active components and mechanism of EGb for aging were analyzed based on network pharmacology. Four compounds, eight targets, and 20 significant pathways in EGb were identified by network analysis, which explained the mechanism of EGb for aging by multiple components, targets, and pathways. Our study found that flavonoids (quercetin, luteolin, and kaempferol) and beta-sitosterol, the main active components of EGb, might slow aging by inhibiting oxidative stress, inhibiting inflammation, ameliorating insulin resistance, and regulating BPs (cell proliferation, differentiation, and migration). Molecular docking results showed that PPARG had better binding capacity with beta-sitosterol, and PTGS2 had better binding capacity with kaempferol and quercetin. However, additional experiments must be conducted to verify these results for more evidence in the future.

Data Availability

The data used to support the study are available from the corresponding author upon request.

Conflicts of Interest

The authors declare that they have no conflicts of interest.

Authors' Contributions

Weiliang Weng and Rui Gao contributed to the topic conception, manuscript revision, and decision to submit for publication and are the cocorresponding authors. Wantong Zhang and Mingyue Sun helped in data analysis and revision of the manuscript. All authors discussed the results and wrote the manuscript. Yanfei Liu and Yue Liu performed the network pharmacology analysis and writing of the manuscript together, contributed equally to this work, and are the co-first authors.

Acknowledgments

The authors would like to thank *Editage* (<http://www.editage.cn>) for English language editing. This study was supported by the Fundamental Research Funds for the Central Public Welfare Research Institutes of China Academy of Chinese Medical Sciences (ZZ13-YQ-001), National Major Scientific and Technological Special Project for "National New Drug Innovation Program" during the Thirteenth Five-Year Plan Period (2017ZX09304003), and National Key R&D Program of China (2019YFC1709300).

Supplementary Materials

Additional file 1: chemical information of main compounds in EGb. Additional file 2: targets of active ingredients. Additional file 3: target of aging. Additional file 4: potential targets of EGb for antiaging. (*Supplementary Materials*)

References

- [1] P. Lacolley, V. Regnault, P. Segers, and S. Laurent, "Vascular smooth muscle cells and arterial stiffening: relevance in development, aging, and disease," *Physiological Reviews*, vol. 97, no. 4, pp. 1555–1617, 2017.
- [2] C. Cleeland, A. Pipingas, A. Scholey, and D. White, "Neurochemical changes in the aging brain: a systematic review," *Neuroscience & Biobehavioral Reviews*, vol. 98, pp. 306–319, 2019.
- [3] A. De Almeida, T. P. Ribeiro, and I. A. De Medeiros, "Aging: molecular pathways and implications on the cardiovascular system," *Oxidative Medicine and Cellular Longevity*, vol. 2017, Article ID 7941563, 19 pages, 2017.
- [4] A.-J. Ding, S.-Q. Zheng, X.-B. Huang et al., "Current perspective in the discovery of anti-aging agents from natural products," *Natural Products and Bioprospecting*, vol. 7, no. 5, pp. 335–404, 2017.
- [5] Z. Ungvari, S. Tarantini, A. J. Donato et al., "Mechanisms of vascular aging," *Circulation Research*, vol. 123, no. 7, pp. 849–867, 2012.
- [6] M. P. Hamon, E. K. Ahmed, M. A. Baraibar et al., "Proteome oxidative modifications and impairment of specific metabolic pathways during cellular senescence and aging," *Proteomics*, vol. 20, no. 5–6, Article ID 1800421, 2019.
- [7] O. Moltedo, P. Remondelli, and G. Amodio, "The mitochondria-endoplasmic reticulum contacts and their critical role in aging and age-associated diseases," *Frontiers in Cell and Developmental Biology*, vol. 7, p. 172, 2019.

- [8] H. Zhang, K. J. A. Davies, and H. J. Forman, "Oxidative stress response and Nrf₂ signaling in aging," *Free Radical Biology and Medicine*, vol. 88, no. Pt B, pp. 314–336, 2015.
- [9] W. Zuo, F. Yan, B. Zhang, J. Li, and D. Mei, "Advances in the studies of Ginkgo biloba leaves extract on aging-related diseases," *Aging and Disease*, vol. 8, no. 6, pp. 812–826, 2017.
- [10] C. Ude, M. Schubert-Zsilavec, and M. Wurglics, "Ginkgo biloba extracts: a review of the pharmacokinetics of the active ingredients," *Clinical Pharmacokinetics*, vol. 52, no. 9, pp. 727–749, 2013.
- [11] Y. Liu, W. Weng, R. Gao et al., "New insights for cellular and molecular mechanisms of aging and aging-related diseases: herbal medicine as potential therapeutic approach," *Oxidative Medicine and Cellular Longevity*, vol. 2019, Article ID 4598167, 25 pages, 2019.
- [12] H. T. Phu, D. T. B. Thuan, T. H. D. Nguyen, A. M. Posadino, A. H. Eid, and G. Pintus, "Herbal medicine for slowing aging and aging-associated conditions: efficacy, mechanisms and safety," *Current Vascular Pharmacology*, vol. 18, no. 4, pp. 369–393, 2020.
- [13] O. Thancharoen, C. Limwattananon, O. Waleekhachonloet, T. Rattanachotphanit, P. Limwattananon, and P. Limpawattana, "Ginkgo biloba extract (EGB761), cholinesterase inhibitors, and memantine for the treatment of mild-to-moderate Alzheimer's disease: a network meta-analysis," *Drugs & Aging*, vol. 36, no. 5, pp. 435–452, 2019.
- [14] L.-C. Kuo, Y.-Q. Song, C.-A. Yao et al., "Ginkgolide A prevents the amyloid- β -induced depolarization of cortical neurons," *Journal of Agricultural and Food Chemistry*, vol. 67, no. 1, pp. 81–89, 2019.
- [15] J. Ru, P. Li, J. Wang et al., "TCMSP: a database of systems pharmacology for drug discovery from herbal medicines," *Journal of Cheminformatics*, vol. 6, no. 13, 2014.
- [16] J. Huang, L. Li, F. Cheung et al., "Network pharmacology-based approach to investigate the analgesic efficacy and molecular targets of xuangui dropping pill for treating primary dysmenorrhea," *Evidence-Based Complementary and Alternative Medicine*, vol. 2017, Article ID 7525179, 12 pages, 2017.
- [17] R. Tacutu, T. Craig, A. Budovsky et al., "Human ageing genomic resources: integrated databases and tools for the biology and genetics of ageing," *Nucleic Acids Research*, vol. 41, pp. D1027–D1033, 2013.
- [18] R. Hühne, T. Thalheim, and J. Sühnel, "AgeFactDB—the JenAge ageing factor database—towards data integration in ageing research," *Nucleic Acids Research*, vol. 42, no. D1, pp. D892–D896, 2014.
- [19] N. T. Doncheva, J. H. Morris, J. Gorodkin, and L. J. Jensen, "Cytoscape StringApp: network analysis and visualization of proteomics data," *Journal of Proteome Research*, vol. 18, no. 2, pp. 623–632, 2019.
- [20] D. W. Huang, B. T. Sherman, and R. A. Lempicki, "Systematic and integrative analysis of large gene lists using DAVID bioinformatics resources," *Nature Protocols*, vol. 4, no. 1, pp. 44–57, 2009.
- [21] M. Gorski, P. J. Van Der Most, A. Teumer et al., "1000 Genomes-based meta-analysis identifies 10 novel loci for kidney function," *Scientific Reports*, vol. 7, p. 45040, 2017.
- [22] Y. Li, Y. Li, W. Lu et al., "Integrated network pharmacology and metabolomics analysis of the therapeutic effects of Zi Dian Fang on immune thrombocytopenic purpura," *Frontiers in Pharmacology*, vol. 9, p. 597, 2018.
- [23] Y. Chen, C. Wang, M. Hu et al., "Effects of ginkgolide A on okadaic acid-induced tau hyperphosphorylation and the PI3K-Akt signaling pathway in N2a cells," *Planta Medica*, vol. 78, no. 12, pp. 1337–1341, 2012.
- [24] L. G. Costa, J. M. Garrick, P. J. Roquè et al., "Mechanisms of neuroprotection by quercetin: counteracting oxidative stress and more," *Oxidative Medicine and Cellular Longevity*, vol. 2016, Article ID 2986796, 10 pages, 2016.
- [25] L. Geng, Z. Liu, W. Zhang et al., "Chemical screen identifies a geroprotective role of quercetin in premature aging," *Protein & Cell*, vol. 10, no. 6, pp. 417–435, 2019.
- [26] S. G. Kim, J. Y. Sung, J.-R. Kim, and H. C. Choi, "Quercetin-induced apoptosis ameliorates vascular smooth muscle cell senescence through AMP-activated protein kinase signaling pathway," *The Korean Journal of Physiology & Pharmacology*, vol. 24, no. 1, pp. 69–79, 2020.
- [27] R. V. Patel, B. M. Mistry, S. K. Shinde, R. Syed, V. Singh, and H.-S. Shin, "Therapeutic potential of quercetin as a cardiovascular agent," *European Journal of Medicinal Chemistry*, vol. 155, pp. 889–904, 2018.
- [28] B. Sung, J. W. Chung, H. R. Bae, J. S. Choi, C. M. Kim, and N. D. Kim, "Humulus japonicus extract exhibits antioxidative and anti-aging effects via modulation of the AMPK-SIRT1 pathway," *Experimental and Therapeutic Medicine*, vol. 9, no. 5, pp. 1819–1826, 2015.
- [29] M. D. Burton, J. L. Rytych, R. Amin, and R. W. Johnson, "Dietary luteolin reduces proinflammatory microglia in the brain of senescent mice," *Rejuvenation Research*, vol. 19, no. 4, pp. 286–292, 2016.
- [30] Y. P. Hwang, K. N. Oh, H. J. Yun, and H. G. Jeong, "The flavonoids apigenin and luteolin suppress ultraviolet A-induced matrix metalloproteinase-1 expression via MAPKs and AP-1-dependent signaling in HaCaT cells," *Journal of Dermatological Science*, vol. 61, no. 1, pp. 23–31, 2011.
- [31] M. C. Morris, Y. Wang, L. L. Barnes, D. A. Bennett, B. Dawson-Hughes, and S. L. Booth, "Nutrients and bioactives in green leafy vegetables and cognitive decline," *Neurology*, vol. 90, no. 3, pp. e214–e222, 2018.
- [32] J. M. Kim, E. K. Lee, D. H. Kim, B. P. Yu, and H. Y. Chung, "Kaempferol modulates pro-inflammatory NF- κ B activation by suppressing advanced glycation endproducts-induced NADPH oxidase," *Age*, vol. 32, no. 2, pp. 197–208, 2010.
- [33] R. Mahmoudi, M. Ghareghani, K. Zibara et al., "Alyssum homolocarpum seed oil (AHSO), containing natural alpha linolenic acid, stearic acid, myristic acid and β -sitosterol, increases proliferation and differentiation of neural stem cells in vitro," *BMC Complementary and Alternative Medicine*, vol. 19, no. 1, p. 113, 2019.
- [34] W.-S. Lin, J.-Y. Chen, J.-C. Wang et al., "The anti-aging effects of *Ludwigia octovalvis* on *Drosophila melanogaster* and SAMP8 mice," *Age*, vol. 36, no. 2, pp. 689–703, 2014.
- [35] X. W. Cheng, M. Narisawa, E. Jin, C. Yu, W. Xu, and L. Piao, "Dose rectification of an imbalance between DPP4 and GLP-1 ameliorates chronic stress-related vascular aging and atherosclerosis?" *Clinical and Experimental Pharmacology and Physiology*, vol. 45, no. 5, pp. 467–470, 2018.
- [36] T. E. Druley, L. Wang, S. J. Lin et al., "Candidate gene resequencing to identify rare, pedigree-specific variants influencing healthy aging phenotypes in the long life family study," *BMC Geriatr*, vol. 16, p. 80, 2016.
- [37] S. Xu, W. Wu, H. Huang et al., "The p53/miRNAs/Ccna2 pathway serves as a novel regulator of cellular senescence: complement of the canonical p53/p21 pathway," *Aging Cell*, vol. 18, no. 3, Article ID e12918, 2019.
- [38] V. H. Ryan, C. T. Primiani, J. S. Rao et al., "Coordination of gene expression of arachidonic and docosahexaenoic acid

- cascade enzymes during human brain development and aging," *PLoS One*, vol. 9, no. 6, Article ID e100858, 2014.
- [39] D. Castellano-Castillo, P. D. Denechaud, L. Fajas et al., "Human adipose tissue H3K4me3 histone mark in adipogenic, lipid metabolite and inflammatory genes is positively associated with BMI and HOMA-IR," *PLoS One*, vol. 14, no. 4, Article ID e0215083, 2019.
- [40] W. Wu, W. Zhang, M. Choi et al., "Vascular smooth muscle-MAPK14 is required for neointimal hyperplasia by suppressing VSMC differentiation and inducing proliferation and inflammation," *Redox Biology*, vol. 22, Article ID 101137, 2019.
- [41] Y. Nakazawa, Y. Hara, Y. Oka et al., "Ubiquitination of DNA damage-stalled RNAPII promotes transcription-coupled repair," *Cell*, vol. 180, no. 6, pp. 1228–1244, 2020.
- [42] A. Valerio and E. Nisoli, "Nitric oxide, interorganelle communication, and energy flow: a novel route to slow aging," *Frontiers in Cell and Developmental Biology*, vol. 3, p. 6, 2015.
- [43] B. A. Monk and S. J. George, "The effect of ageing on vascular smooth muscle cell behaviour—a mini-review," *Gerontology*, vol. 61, no. 5, pp. 416–426, 2015.
- [44] Y. Yin, Z. Zhou, W. Liu, Q. Chang, G. Sun, and Y. Dai, "Vascular endothelial cells senescence is associated with NOD-like receptor family pyrin domain-containing 3 (NLRP3) inflammasome activation via reactive oxygen species (ROS)/thioredoxin-interacting protein (TXNIP) pathway," *The International Journal of Biochemistry & Cell Biology*, vol. 84, pp. 22–34, 2017.
- [45] J. K. Zhan, Y. J. Wang, S. Li et al., "AMPK/TSC2/mTOR pathway regulates replicative senescence of human vascular smooth muscle cells," *Experimental and Therapeutic Medicine*, vol. 16, no. 6, pp. 4853–4858, 2018.
- [46] Y. Wu, M. Chen, and J. Jiang, "Mitochondrial dysfunction in neurodegenerative diseases and drug targets via apoptotic signaling," *Mitochondrion*, vol. 49, pp. 35–45, 2019.
- [47] E. C. Moorefield, S. F. Andres, R. E. Blue et al., "Aging effects on intestinal homeostasis associated with expansion and dysfunction of intestinal epithelial stem cells," *Aging*, vol. 9, no. 8, pp. 1898–1915, 2017.
- [48] L. R. Lapierre, C. Kumsta, M. Sandri, A. Ballabio, and M. Hansen, "Transcriptional and epigenetic regulation of autophagy in aging," *Autophagy*, vol. 11, no. 6, pp. 867–880, 2015.
- [49] O. Alvarez-Garcia, T. Matsuzaki, M. Olmer et al., "FOXO are required for intervertebral disk homeostasis during aging and their deficiency promotes disk degeneration," *Aging Cell*, vol. 17, no. 5, Article ID e12800, 2018.
- [50] M. P. Lisanti, U. E. Martinez-Outschoorn, S. Pavlides et al., "Accelerated aging in the tumor microenvironment," *Cell Cycle*, vol. 10, no. 13, pp. 2059–2063, 2011.
- [51] J. Li, Y. Zhou, G. Du, X. Qin, and L. Gao, "Bioinformatic analysis reveals key genes and pathways in aging brain of senescence-accelerated mouse P8 (SAMP8)," *CNS & Neurological Disorders-Drug Targets*, vol. 17, no. 9, pp. 712–722, 2018.
- [52] T. Su, Y. Xiao, Y. Xiao et al., "Bone marrow mesenchymal stem cells-derived exosomal MiR-29b-3p regulates aging-associated insulin resistance," *ACS Nano*, vol. 13, no. 2, pp. 2450–2462, 2019.
- [53] A. R. Martins, R. T. Nachbar, R. Gorjao et al., "Mechanisms underlying skeletal muscle insulin resistance induced by fatty acids: importance of the mitochondrial function," *Lipids in Health and Disease*, vol. 11, no. 1, p. 30, 2012.
- [54] K. Bouzakri, M. Roques, P. Gual et al., "Reduced activation of phosphatidylinositol-3 kinase and increased serine 636 phosphorylation of insulin receptor substrate-1 in primary culture of skeletal muscle cells from patients with type 2 diabetes," *Diabetes*, vol. 52, no. 6, pp. 1319–1325, 2003.
- [55] K. Morino, K. F. Petersen, and G. I. Shulman, "Molecular mechanisms of insulin resistance in humans and their potential links with mitochondrial dysfunction," *Diabetes*, vol. 55, no. Suppl 2, pp. S9–S15, 2006.
- [56] J. P. Chan, J. Brown, B. Hark et al., "Loss of sphingosine kinase alters life history traits and locomotor function in *Caenorhabditis elegans*," *Frontiers in Genetics*, vol. 8, no. 132, 2017.
- [57] Q. Peng, Z. Deng, H. Pan, L. Gu, O. Liu, and Z. Tang, "Mitogen-activated protein kinase signaling pathway in oral cancer," *Oncology Letters*, vol. 15, no. 2, pp. 1379–1388, 2018.
- [58] M. F. Mian, C. Kang, S. Lee et al., "Cleavage of focal adhesion kinase is an early marker and modulator of oxidative stress-induced apoptosis," *Chemico-Biological Interactions*, vol. 171, no. 1, pp. 57–66, 2008.
- [59] J. Wang, J. Zhang, X. Ding et al., "Differential microRNA expression profiles and bioinformatics analysis between young and aging spontaneously hypertensive rats," *International Journal of Molecular Medicine*, vol. 41, no. 3, pp. 1584–1594, 2018.
- [60] M. H. Ben Mahdi, V. Andrieu, and C. Pasquier, "Focal adhesion kinase regulation by oxidative stress in different cell types," *IUBMB Life*, vol. 50, no. 4-5, pp. 291–299, 2000.
- [61] M. Cano, A. Guerrero-Castilla, S. M. Nabavi, A. Ayala, and S. Argüelles, "Targeting pro-senescence mitogen activated protein kinase (Mapk) enzymes with bioactive natural compounds," *Food and Chemical Toxicology*, vol. 131, Article ID 110544, 2019.
- [62] A. K. Ghosh, M. O'Brien, T. Mau, and R. Yung, "Toll-like receptor 4 (TLR4) deficient mice are protected from adipose tissue inflammation in aging," *Aging*, vol. 9, no. 9, pp. 1971–1982, 2017.
- [63] F. Song, Y. Ma, X.-Y. Bai, and X. Chen, "The expression changes of inflammasomes in the aging rat kidneys," *The Journals of Gerontology Series A: Biological Sciences and Medical Sciences*, vol. 71, no. 6, pp. 747–756, 2016.
- [64] M. K. Lehtinen, Z. Yuan, P. R. Boag et al., "A conserved MST-FOXO signaling pathway mediates oxidative-stress responses and extends life span," *Cell*, vol. 125, no. 5, pp. 987–1001, 2006.
- [65] G. G. Camici, G. Savarese, A. Akhmedov, and T. F. Lüscher, "Molecular mechanism of endothelial and vascular aging: implications for cardiovascular disease," *European Heart Journal*, vol. 36, no. 48, pp. 3392–3403, 2015.
- [66] A. S. Brack, M. J. Conboy, S. Roy et al., "Increased Wnt signaling during aging alters muscle stem cell fate and increases fibrosis," *Science*, vol. 317, no. 5839, pp. 807–810, 2007.